Insight into the Role of Bipyridine Ligands in Palladium-Catalyzed Aerobic Oxidation

Reactions

by

Paul B. White

A dissertation submitted in partial fulfillment of

the requirements for the degree of

Doctor of Philosophy

(Chemistry)

at the

UNIVERSITY OF WISCONSIN–MADISON

2013

Date of the final oral examination: 09/17/13

The dissertation is approved by the following members of the Final Oral Committee:
     Shannon S. Stahl, Professor, Chemistry
     Hans J. Reich, Professor, Chemistry
     Clark R. Landis, Professor, Chemistry
     John F. Berry, Associate Professor, Chemistry
     Thomas C. Brunold, Professor, Chemistry

Insight into the Role of Bipyridine Ligands in Palladium-Catalyzed Aerobic Oxidation Reactions

Paul White

Under the supervision of Professor Shannon S. Stahl

At the University of Wisconsin–Madison

ABSTRACT: Pd-catalyzed oxidative transformations provide a direct means to increase the functional group complexity of an organic molecule. These reactions require a stoichiometric oxidant to turnover the reduced palladium catalyst (Pd^0), and our group has invested significant effort in developing methods that use O_2 as the terminal oxidant. Pd^0 will often aggregate even in the presence of oxidant to form catalytically inactive Pd-black, which effectively terminates the reaction. Oxidatively stable ligands such as pyridines and sulfoxides were observed early on to stabilize Pd^0 and promote reoxidation and increase catalyst longevity.

Since then, the field of oxidative Pd catalysis has seen remarkable growth in the development of new and diverse ligands that not only promote catalyst reoxidation but also enable novel reactivity and selectivity. The majority of examples have used monodentate ligands because their labile nature allows for facile substrate oxidation while still effectively stabilizing Pd^0. Bidentate ligands have been generally avoided because the strong metal-ligand complexes that are formed often inhibit substrate oxidation. However, bidentate ligands have certain advantages that arise from controlling the coordination environment. The most notable advantage is the facile access to enantioselective methods, but achiral stereoselective methods have also seen significant development. The premier bidentate ligand classes that support substrate oxidation are 1) 3,3'-annulated-2,2'-bipyridine ligands such as 4,5-diazafluorenone (DAF), 2) bipyridine and

phenanthrolines that are substituted *ortho* to the nitrogen and 3) mixed heterocycles such as pyridine-oxazolines. Despite the increasing number of reports that use these ligand classes, little is known about how they interact with the Pd^{II} salt or their role in catalysis. This thesis describes experimental and computational mechanistic studies that were carried out to interrogate why these ligands are so unique and how they affect catalysis.

Solution-phase interactions between DAF and $Pd(OAc)_2$ were investigated by NMR spectroscopy in order to identify a precatalyst structure. Multiple DAF-$Pd(OAc)_2$ complexes were observed rather than the anticipated 1:1 ligand:Pd that forms with other bidentate ligands. Subsequent rigorous NMR spectroscopic experiments revealed that these complexes consisted of monomeric and dimeric Pd complexes where the DAF ligand was either bridging (μ), monodentate (κ^1) or chelating (κ^2). Multiple crystal structures were obtained that complemented the NMR spectroscopic characterization. A catalytic cycle where monodentate DAF-Pd complexes were present in substrate oxidation was proposed to explain the catalytic activity observed with DAF compared to other bidentate ligands.

The effect of nucleophile electronics on the amidopalladation and β-hydride elimination steps within the aza-Wacker reaction was investigated with a well-defined bipyridine-$PdCl_2$. Amidopalladation occurred via alkene insertion into a Pd–amidate bond and was found to be an equilibrium process, which favored electron-rich sulfonamides. β-Hydride elimination also favored electron-rich sulfonamides and was the rate-determining step. Both processes were proposed to occur via an intermediate cationic Pd complex, which was supported by an observed Cl^- inhibition and the necessity of polar, coordination solvents for reactivity to occur. The cationic process highlighted how typical chelating ligands inhibit substrate oxidation by forming rigid metal-ligand complexes that require a challenging anion ligand dissociation step prior to substrate oxidation.

The viability of monodentate DAF intermediates was investigated within the context of the aerobic Pd-catalyzed aza-Wacker cyclization. DAF was found to yield superior rates and yields compared to previously reported catalyst systems that used monodentate ligands. Pyridine

titration experiments revealed that the ligand was weakly coordinating to $Pd(OAc)_2$ and formed a *trans*-$Pd(\kappa^1$-DAF)(pyridine)$(OAc)_2$ complex en route to complete ligand dissociation. This species was characterized by both NMR spectroscopy and X-ray crystallography. A reaction coordinate was calculated with DFT methods for the aza-Wacker reaction whereby the DAF ligand partially dissociates during substrate oxidation. The computational and experimental reaction barriers were in agreement, which provided support for this mechanism. The experimental and computational investigation was extended to the 6,6'-dimethyl-2,2'-bipyridine (6,6'-Me_2bpy) ligand, which was found to behave similarly.

Substituted pyridine-oxazoline (pyrox) ligands have been used in asymmetric aerobic Pd-catalyzed oxidation reactions and contain many of the same structural features of 6,6'-Me_2bpy. The origin of enantioselectivity for the $Pd(TFA)_2$/pyrox-catalyzed aza-Wacker cyclization was investigated by DFT methods. Both *cis*- and *trans*-amidopalladation pathways were calculated to give high enantioselectivity when substrate oxidation took place from a cationic pyrox-Pd complex. The *trans*-amidopalladation was found to be the lower energy pathway, which agreed with experimental observations. The $Pd(OAc)_2$/pyrox catalyst system had been previously observed to perform the oxidative cyclization albeit with lower yield and enantioselectivity. This switch in enantioselectivity was proposed to originate from the pyrox ligand partially dissociating during substrate oxidation steps, similar to DAF and 6,6'-Me_2bpy.

REFLECTIONS AND ACKNOWLEDGEMENTS

Writing these acknowledgements fills me with a sense of impending nostalgia. The past five years have been some of the greatest in my life. I have grown as an individual and a scientist, met the love of my life, and developed treasured relationships with coworkers and colleagues. There is a strange sense of continuity or permanence that I've experienced during my time here. As a first year, I was always in awe of and inspired by the older generation (Xuan, Nicky, Rick, Nattawan and Tianning) who permeated an element of greatness, intellect and friendliness about them and were excellent mentors. As I've progressed through this group, I've had the joy of seeing my current and younger coworkers come into their own as scientists and walk the same path I have traveled. I have been fortunate enough to lend a helping hand in some of my coworkers' growth and for that I am truly grateful at the opportunity.

I would like to thank Shannon who has been an outstanding mentor and boss. You have taught me so much from understanding science to presenting science. Thank you for pitching such interesting mechanistic projects and allowing me the opportunity to pursue NMR spectroscopy during my time here. Your enthusiasm for science has been infectious and I'm glad that I got for work for someone as excited as you are.

I must especially thank Charlie Fry, whose summer NMR spectroscopy course flipped a switch in my head and made me fall head over heels in love with NMR spectroscopy. Thank you for your time, enthusiasm, advice and all the great discussions we've had in the past. You have been like a second PI to me and I appreciate your guiding hand in choosing my postdoctoral advisor. I will treasure my first CANMR and ENC conferences that you took me on and look forward to seeing you there in the future.

I would like to thank my past mentors, Rick, Nattawan and Xuan, who all had hands in developing my skillset from synthesis and screening to computational chemistry and NMR kinetics to experimental design for investigating reaction mechanisms. Your time, patience and enthusiasm have made a lasting impression on me.

I would also like to express my gratitude to all the students I have mentored. Dian, Jon and Harry, thank you for letting me improve my teaching skills through my interactions with you. Working with you all has been rewarding and I appreciate you asking questions that make me reconsider my own understanding of our science. I am truly proud at what you have accomplished and I look forward to seeing what cool things you will do.

I'd like to also thank Jamie for letting me sleep on your futon for the past month and a half during which I was homeless and finishing my thesis. Thank you for your friendship and all the great conversations we've had.

A great thank you, Stahl group, for making this a wonderful place to work and live. I have enjoyed the combination of intellectual stimulation and camaraderie that lies at the heart of what makes the Stahl group so amazing. Keep up the hard work!

I certainly wouldn't be here without my loving parents, who have selflessly provided me with opportunities to better myself. I look up to you two constantly and hope one day to be as amazing teachers, counselors and parents as you one day.

Lastly, but far from least, I would like to thank my beautiful and wonderful wife Teresa. You have been a source of constant joy for me. Never in a million years did I think I would find someone with so many shared interests as me, and I am incredibly grateful to the University that I was able to meet someone as amazing as you. You have been a pillar to lean on when times are hard and the icing on the gluten-free cake when things are great. I appreciate your patience and

understanding of my drive to constantly do the best I can in the pursuit science, which has lead to long hours in lab or sitting in front of the spectrometer. I love you and can't wait to see what our future holds.

I would like to impart some words of wisdom: Although we earn an individual degree in the end, no graduate student is an island. I am a product of all the people who have helped me a along in graduate school. So, be there for your fellow coworkers and do not be afraid to ask for help or guidance when you need it. Be patient, be persistent and always keep a flexible mind.

As I leave Madison, enriched by my experiences and memories, I look forward to my postdoctoral position and future place in the scientific community with the same eager eyes that I had when I joined this truly amazing group, and I can't wait to begin. Thank you everyone for positively contributing to my life.

TABLE OF CONTENTS

LIST OF FIGURES

LIST OF SCHEMES

LIST OF TABLES

ABBREVIATIONS AND ACRONYMS

AP – amidopalladation

Bpy – 2,2'-bipyridine

DAF – 4,5-diazafluorenone

DFT – density functional theory

DMF – dimethylformamide

DMSO – dimethylsulfoxide

EXSY – exchange spectroscopy

HMBC – Heteronuclear Multiple-Bond Correlation

HSQC – Heteronuclear Single Quantum Coherence

Me – methyl

Ms, mesyl – methanesulfonyl

Neocuproine – 2,9-dimethyl-1,10-phenanthroline

NMR – Nuclear Magnetic Resonance

NOESY – Nuclear Overhauser effect spectroscopy

PCM – polarizable-continuum model

Phen – 1,10-phenanthroline

PhTMS – trimethyl(phenyl)silane

Pyr – pyridine

Pyrox – 2-(2-pyridyl)oxazoline

ROESY – Rotating-frame Nuclear Overhauser Effect Spectroscopy

TFA – trifluoroacetate

THF – tetrahydrofuran

TOCSY – Total Correlation Spectroscopy

Ts, tosyl – toluenesulfonyl

Chapter 1.

Survey of Mono- and Bidentate Ligands Employed in Aerobic

Pd-Catalyzed Oxidation Reactions

1.1 Introduction

The development of transition-metal catalyzed alkene functionalization methods in the past 50 years has revolutionized the way chemists transform simple and available starting materials into value-added products. Representative transformations include polymerization, hydroformylation, hydrogenation and oxidation. Oxidation reactions are intriguing because they provide a direct means of increasing the complexity of the substrate through the use of a sacrificial oxidant such as Cu^{II}, quinones, iodine(III) reagents and dioxygen. Dioxygen represents an ideal oxidant because the reduction product is water, which is easily removed from the reaction mixture.[1] The most prominent early example of an aerobic Pd-catalyzed oxidation is the Wacker oxidation, which couples ethylene and water to form acetaldehyde (eq 1.1).[2]

$$H_2C{=}CH_2 \;+\; 1/2\,O_2 \quad \xrightarrow[\;H_2O\;]{[Pd]/[Cu]} \quad \underset{H}{\overset{O}{\parallel}}\!\!\diagup\!\!\diagdown \qquad\qquad (1.1)$$

Although the specific details of the mechanism are controversial, the formation of the C–O bond is agreed to occur from attack of a water nucleophile on a Pd-coordinated alkene (Scheme 1.1).[3] This step, defined as "nucleopalladation", has sparked enormous efforts to develop methods for making C–C, C–N and other C–O bonds with different nucleophiles.[4] The resulting Pd–alkyl terminates in formation of acetaldehyde and a Pd^0 species. Additionally, numerous groups have explored different oxidative and non-oxidative ways to functionalize the resulting Pd–C bond to afford a variety of products. Catalyst reoxidation occurs from reaction of Pd^0 with $CuCl_2$ to regenerate the Pd^{II} catalyst (Scheme 1.1). The reduced CuCl co-oxidant reacts with dioxygen and acid produced during substrate oxidation to regenerate $CuCl_2$ and H_2O.

Scheme 1.1. Generic Catalytic Cycle for the Wacker Reaction
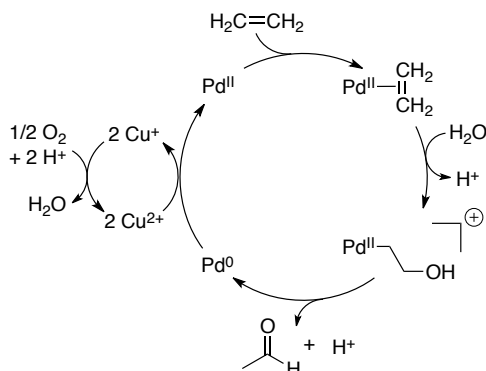
The Wacker oxidation is performed under aqueous conditions; however many substrates are not water-soluble, which has driven the development of alternative catalysts that operate in organic solvents. Unfortunately, simple palladium salts alone are often insufficient to ensure long-lived activity in organic solvents due to decomposition of the catalyst. As a result, heteroatom-containing organic molecules called "ligands" were added to stabilize Pd^0 and hinder decomposition. Ligands represent a powerful means to enable new reactivity, alter selectivity and improve catalyst longevity. In addition to Wacker oxidations, ligands have been employed in other aerobic Pd-catalyzed oxidations including alcohol oxidation, C–C coupling of alkenes and arenes, and dehydrogenation, which will be elaborated upon throughout this chapter (Scheme 1.2).

Scheme 1.2. Additional Examples of Aerobic Pd-Catalyzed Oxidation Reactions
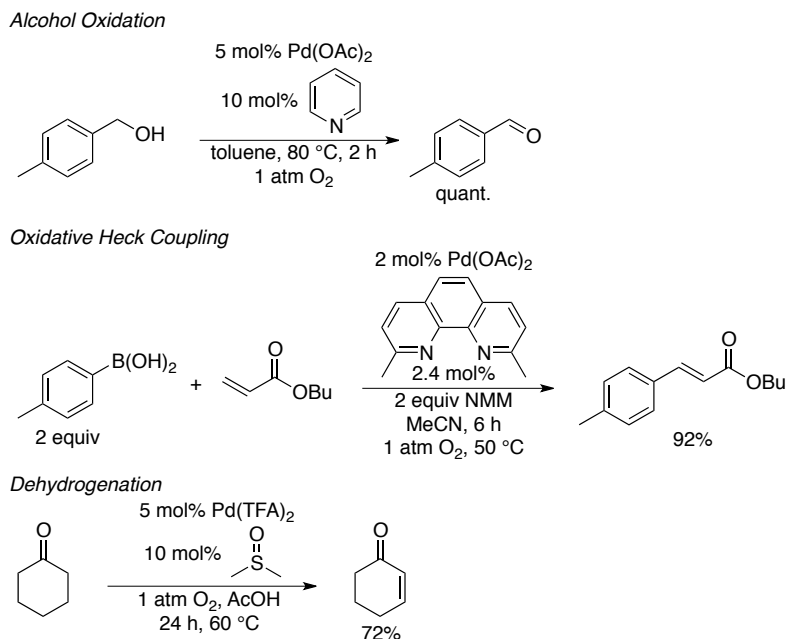
The general catalytic cycle for aerobic Pd^{II}-catalyzed oxidations is essentially identical to the Wacker oxidation: a substrate (SubH$_2$) interacts with and is oxidized by a Pd^{II} center, which produces the desired product (Sub^{ox}) and Pd^0 (Scheme 1.3). The Pd^0 catalyst is subsequently reoxidized by dioxygen to regenerate the active Pd^{II} catalyst. Similarly, there is also a competing pathway for catalyst decomposition from Pd^0.

Ligands (L) play a critical role in all aspects of the catalytic cycle in different and sometimes contradictory ways (Scheme 1.3). For example, electron-rich ligands promote Pd^0 reoxidation but inhibit substrate oxidation by making the Pd^{II} center less oxidizing. Additionally, coordinatively saturated Pd^0 complexes are more resistant to aggregation and decomposition, but unsaturated Pd^{II} complexes facilitate substrate coordination and oxidation (Scheme 1.3). Each of these facets of catalyst reactivity and stability must be carefully considered and balanced when designing a catalyst system. Unfortunately, a predictive model to guide future catalyst and ligand design has yet to become available despite the numerous catalyst systems and empirical observations reported in the literature.

Scheme 1.3. Influence of Ligands in Aerobic Pd-Catalyzed Oxidation Reactions

Substrate Oxidation
*favors electron-deficient Pd^{II}
*requires open coordination site

L_nPdX_2

H_2O

SubH$_2$

$1/2\ O_2$
$2\ HX$

$2\ HX$
Sub^{ox}

L_nPd^0

Catalyst Reoxidation
*favors electron-rich Pd^0
*promoted by ligands

-L

$[Pd^0]_n$
"Pd-black"

Catalyst Decomposition
*bimolecular
*disfavored with strongly
coordinating ligands
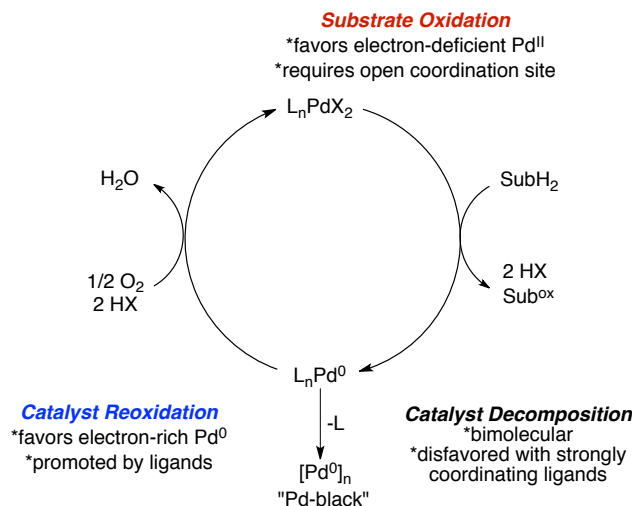
This chapter will survey prominent examples where mono- and bidentate ligands have been used in aerobic Pd-catalyzed oxidation reactions. Mechanistic insight into the role of the ligand will be discussed where available. At the end, observations will be summarized in an attempt to provide a series of guidelines when considering ligands for future catalyst design.

1.2 Monodentate Ligands

1.2.1 Dimethylsulfoxide (DMSO) as a Solvento Ligand.[5]

1.2.1.1 Wacker-type Oxidations

Early examples by Larock, Hiemstra and Andersson introduced the utility of $Pd(OAc)_2$ in DMSO as a catalyst/solvent system for aerobic Wacker-type Pd-catalyzed oxidation reactions.[6] A variety of carboxylic acid, oxygen and nitrogen nucleophiles reacted with simple 1,2-disubstituted alkenes to form five- and six-membered heterocycles in high yields (Scheme 1.4). Originally, this catalyst system used a co-oxidant such as $Cu(OAc)_2$ or 1,4-benzoquinone in addition to O_2, however subsequent screening revealed that O_2 alone was sufficient to reoxidize

the catalyst. The catalysts were found to be reactive at room temperature but optimal rates were obtained at elevated temperature (~65-80 °C).

Scheme 1.4. Representative Examples of Aerobic Pd-Catalyzed Wacker-type Oxidations using DMSO as a Solvent.
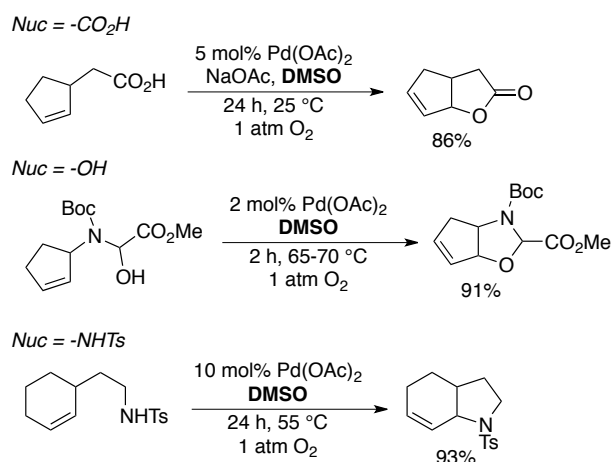
Hiemstra noted several key observations in the optimization of the aminoalcohol synthesis.[6b] Most solvents other than DMSO would support one turnover and then precipitate Pd^0, and attempts to use DMSO in catalytic quantities proved equally unsuccessful. These observations spoke to the necessity of using solvent-quantities of DMSO to stabilize Pd^0. Other polar, coordinating solvents such as DMA and DMF facilitated a few turnovers but precipitated Pd^0 over time, thus demonstrating an inferior ability to stabilize Pd^0 than DMSO.

1.2.1.2 Alcohol Oxidation

Larock later applied the $Pd(OAc)_2$ in DMSO system to the aerobic Pd-catalyzed oxidation of alcohols (eq 1.2).[7] Primary and secondary benzylic and allylic alcohols were oxidized in modest to excellent yield. A significant drawback was the variable and often lengthy reaction time (1-3 days). Attempts to perform the reaction with less solvent (i.e. more concentrated) shifted the reaction from homogenous to heterogeneous and reduced the catalyst efficiency.

(1.2)

1.2.1.3 Mechanistic Studies for Alcohol Oxidation

The success of $Pd(OAc)_2$ in DMSO in aerobic Pd-catalyzed oxidation reactions prompted the Stahl group to probe the mechanism of the alcohol oxidation reaction reported by Larock. Early mechanistic studies revealed a zero-order dependence on substrate and first-order dependence on O_2 dependence in the initial rates.[8] A nonlinear (saturation-like) $Pd(OAc)_2$ dependence was also observed where the rate leveled out at high [Pd] due to competitive, binuclear catalyst decomposition. These results pointed towards a fast alcohol oxidation step, which had been observed previously in stoichiometric studies, and a rate-limiting Pd^0 reoxidation (Scheme 1.5).

Scheme 1.5. Summary of Mechanistic Work for Aerobic Pd-Catalyzed Alcohol Oxidation in DMSO.
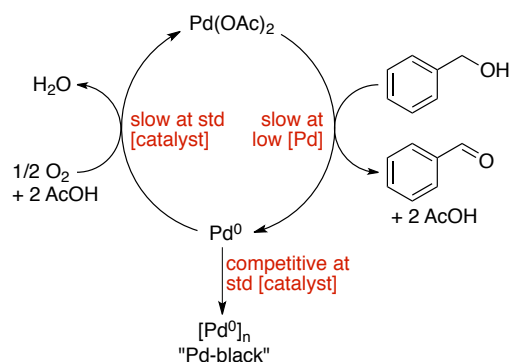
A follow-up study revealed that the rate-determining step changed from Pd^0 reoxidation to alcohol oxidation if a sufficient supply of O_2 is present in solution (Scheme 1.5).[9] Subsequent experiments revealed that the Pd^0 reoxidation step was slow because O_2 is poorly soluble in DMSO (3.2 mM/atm at 80 °C). In other words, the dissolved O_2 was consumed faster than it was replenished, which meant that the reaction was controlled by mass-transport-limited kinetics. As

a consequence, catalyst decomposition becomes a significant concern since Pd^0 is inherently unstable.

1.2.1.4 Conclusions

The $Pd(OAc)_2$ in DMSO catalyst system represented a significant advancement for aerobic Pd-catalyzed oxidation reactions. The vastly improved substrate scope, owing to the use of an organic solvent, enabled the development of new catalytic transformations. However, as described above, $Pd(OAc)_2$ in DMSO had significant limitations, which restricted its application. The eventual precipitation of Pd^0 in DMSO as a solvent is reflective both of the inability of DMSO to sufficiently stabilize Pd^0 as a ligand at elevated temperature (i.e. DMSO is a weakly coordinating) and poor O_2 solubility resulting in slow reoxidation kinetics. Using a catalytic quantity of DMSO in a solvent with much higher O_2 solubility could mitigate the O_2 solubility problem; however, Hiemstra observed that Pd/DMSO catalysts rapidly precipitated Pd^0 at elevated temperatures. The challenge of catalyst instability with Pd/DMSO would be addressed in by performing the reaction at ambient temperature, using high pressures of O_2 or acidic solvents that stabilize Pd^0.

1.2.2 DMSO as a Stoichiometric Ligand.

1.2.2.1 Directed C–C Coupling of Anilides and Arenes

In 2008, Buchwald reported the aerobic, directed coupling of anilides and arenes using a $Pd(OAc)_2$/DMSO catalyst in a solvent system consisting of trifluoroacetic acid (TFAH) and an arene (eq 1.3).[10] The reaction conditions initially used a $Pd(OAc)_2$ catalyst in AcOH, but substitution of AcOH with TFAH resulted in a significant improvement in conversion although Pd-black was still observed (Table 1.1). Catalyst decomposition was hindered by the introduction

of catalytic quantities of DMSO, which supported the efficient coupling of various electron-rich and -deficient anilides and arenes (Table 1.1).

$$(1.3)$$
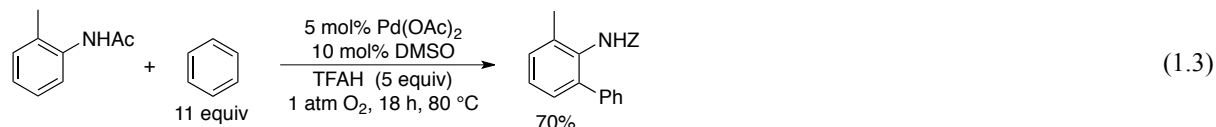
Table 1.1. Optimization of the Catalyst System

Additive	Conv (%)	Yield (%)
5 equiv AcOH	11	3
5 equiv TFAH	66	64
5 equiv TFAH, 10 mol% DMSO	91	87
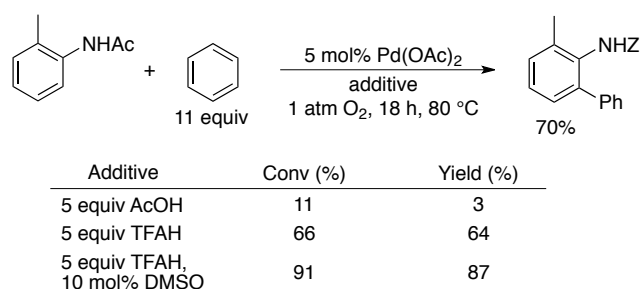
1.2.2.2 Oxidative Amidation ("aza-Wacker")

In 2010, Stahl reported a convenient aerobic Pd-catalyzed synthesis of 1,2-diamines via the oxidative cyclization of sulfamides derived from allylic amines (eq 1.4).[11] The oxidative amidation of alkenes is strikingly similar to the Wacker oxidation but with a nitrogen nucleophile rather than water. As such, this reaction has also been called the "aza-Wacker" reaction. Initial catalyst optimization was performed at 80 °C, which resulted in Pd-black observed in the reactions. The Pd(TFA)$_2$/DMSO catalyst was found to be significantly more stable at ambient temperatures and efficiently cyclized a variety of *N,N′*-diaryl sulfamides in good to excellent yields.

$$(1.4)$$
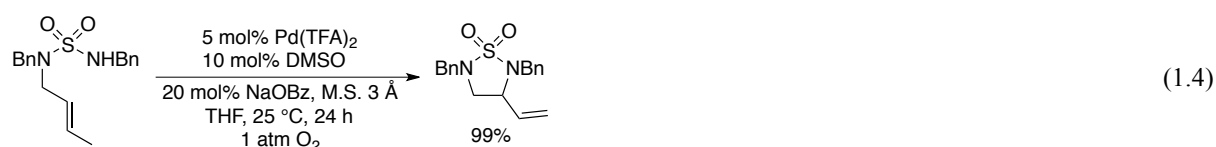
The Pd(TFA)$_2$/DMSO catalyst later expanded the aza-Wacker method to six- and seven-membered heterocycles (eq 1.5).[12] This reaction was significantly more challenging than forming the five-membered rings previously reported. As a result, the reaction required elevated temperatures (60 °C) in order to effectively transform the substrate into the six-membered heterocycle. In order to mitigate the formation of Pd-black due to the high temperature, the reaction was performed using 60 psi (~4 atm) of O$_2$, which increased the relative rate of reoxidation over decomposition.

$$(1.5)$$

1.2.2.3 Dehydrogenation of Cyclic Ketones

In 2011, Stahl reported the application of the Pd(TFA)$_2$/DMSO catalyst system to the aerobic dehydrogenation of cyclic ketones.[13] The catalyst oxidized 2-, 3- and 4-substituted cyclohexanones selectively to the enone in high yield (eq 1.6). The observed selectivity was highly dependent on the solvent and ligand. Pd(TFA)$_2$ in DMSO produced an active catalyst, however the selectivity for the enone was poor and large quantities of phenol were produced. Changing the solvent to acetic acid resulted in enhanced selectivity but poor yields, which were improved upon by the addition of DMSO in catalytic quantities. Interestingly, the reaction was performed at 80 °C without the need for high pO$_2$, indicating that acetic acid could play a role in accelerating catalyst reoxidation.

$$(1.6)$$

5 mol% Pd(TFA)$_2$, DMSO	34%	56%
5 mol% Pd(TFA)$_2$, 10 mol% DMSO, AcOH	91%	8%

1.2.2.4 Mechanistic Studies for Dehydrogenation of Cyclic Ketones

Analysis of the reaction rate data revealed that the first oxidation to the enone was 33x faster than the second oxidation to the phenol eq 1.7).

$$(1.7)$$
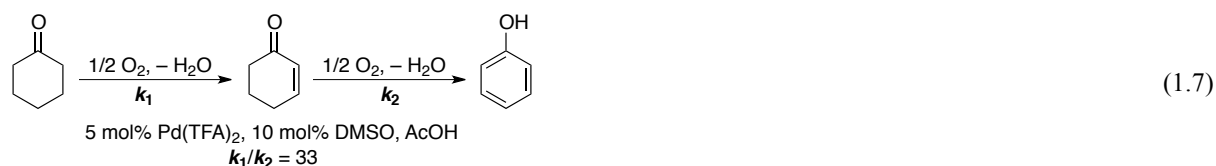
A first order dependence on both the catalyst and substrate was observed. Increasing [DMSO] only slightly inhibited the rate; however significant quantities of Pd-black were produced in the absence of DMSO. Furthermore, a zero-order dependence on O_2 was observed. Together, these results indicated that the slow step in cyclohexanone-to-cyclohexenone dehydrogenation was substrate oxidation and that the role of DMSO was to stabilize any transient Pd^0 (Scheme 1.6).

Scheme 1.6. Summary of Mechanistic Observations for the Aerobic Dehydrogenation of Cyclohexanone
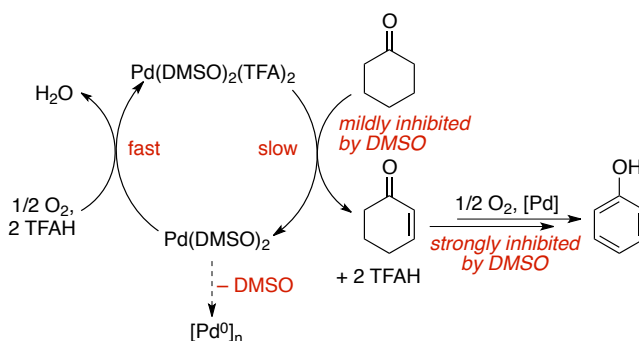
Next, the oxidation of cyclohexenone to phenol was investigated in order to understand the origin of chemoselectivity. DMSO was found to strongly inhibit the initial rate of cyclohexenone oxidation compared to the ligand-free condition. An induction period was observed at the start of the reaction when DMSO was present but was absent for the ligand-free condition. The induction

period was directly dependent on [DMSO], with higher [DMSO] increasing the length. Induction periods indicate a change in catalyst identity during the reaction. Stahl has reported a thorough mechanistic study for a separate aerobic Pd-catalyzed dehydrogenation method that oxidizes cyclohexanones to phenols where a similar induction period was observed and attributed to the formation of Pd nanoparticles that catalyze the oxidation to the phenol.[14] These results further support the role of DMSO to stabilize Pd^0 by hindering the formation of unselective but active meta-stable nanoparticles.

1.2.2.5 Characterization of Pd^{II} Coordination Complexes with DMSO Ligands

The role of DMSO for stabilizing Pd^0 has been discussed above, but its interaction with Pd^{II} and its role in substrate oxidation has received less attention in the literature. DMSO is a unique ligand because it is ambidentate and has been observed to coordinate to transition metals through either the *S*- or *O*-lonepair (or both at once).[15] Early solid-state characterization of $Pd(DMSO)_2(TFA)_2$ revealed a *trans*-Pd(*S*-DMSO)(*O*-DMSO)(TFA)_2 complex, though the solution phase identity was not known for several decades.[16]

The titration of DMSO into a solution containing $Pd(TFA)_2$ revealed several *mono*- and *bis*-DMSO-ligated $Pd(TFA)_2$ adducts at -60 °C in THF and EtOAc by ^1H and ^{19}F NMR spectroscopy.[17] At 0.5 equiv DMSO to $Pd(TFA)_2$, the Pd(*S*-DMSO)(TFA)_2 (eq 1.8, **1**) complex was dominant. Addition of more DMSO resulted in the growth of the Pd(*S*-DMSO)_2(TFA)_2 (**2**) and Pd(*O*-DMSO)(*S*-DMSO)(TFA)_2 (**3**) complexes. Unbound DMSO was not present until >2 equiv DMSO were added, reflecting the thermodynamic driving force for ligand coordination. Chemical exchange (EXSY) experiments revealed that free DMSO exchanged with the *O*-DMSO of **3**, which suggested that the Pd–O bond was more labile than the Pd–S bond (eq 1.8). This hypothesis was further supported by variable temperature studies that showed the *O*-bound resonances coalesced at -40 °C followed by the *S*-bound resonances at +40 °C.[11] These studies

concluded that DMSO is a very labile ligand for Pd^{II} at standard reaction temperatures (50 – 80 °C).

$$(1.8)$$
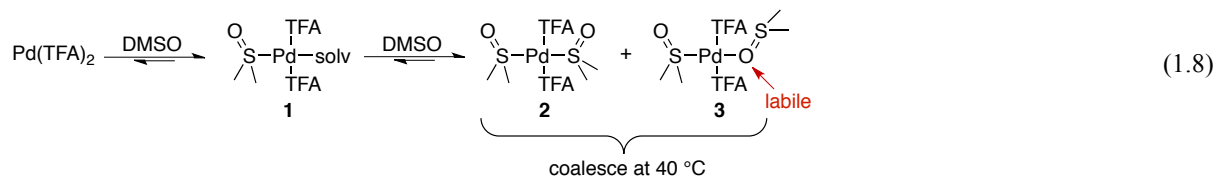
1.2.2.6 Conclusions

The Pd(TFA)$_2$/DMSO system represents an improvement over Pd(OAc)$_2$ in DMSO because the reoxidation of Pd^0 was found to be kinetically superior. The challenges associated with catalyst in the previous system were met by performing the reaction at milder temperatures where DMSO would be less labile or using high pO_2 to accelerate reoxidation. Additionally, the use of acidic solvents (AcOH or TFAH) enabled the operation of the Pd(TFA)$_2$/DMSO catalyst system at high temperature without resorting to high pO_2 and suggesting a role of the solvent in stabilizing Pd^0 or accelerating reoxidation. NMR spectroscopic studies revealed that DMSO is a moderately weak ligand for Pd(TFA)$_2$. *The labile coordination of DMSO to Pd(TFA)$_2$ contributes to rapid substrate oxidation by facilitating substrate coordination to the catalyst.* Overall, the Pd(TFA)$_2$/DMSO system is a versatile oxidation catalyst but requires careful manipulation of the conditions to suppress catalyst decomposition.

1.2.3 Triethylamine (NEt$_3$).

In 2002, Sigman reported a convenient, room-temperature catalytic method to aerobically oxidize benzylic, allylic and aliphatic alcohols to the aldehyde or ketone (eq 1.9).[18] This method represented an improvement over the current methods at the time, which were performed at 80 °C. The catalyst system consisted of Pd(OAc)$_2$ and NEt$_3$ as a ligand in dichloroethane. Measuring the initial rate as a function of [NEt$_3$] revealed that stoichiometries $\leq 1.5:1$

NEt$_3$:Pd(OAc)$_2$ promoted the substrate oxidation step while >1.5:1 inhibited the rate. NMR spectroscopic studies revealed that solutions of NEt$_3$ and Pd(OAc)$_2$ produced an equilibrium between free Pd(OAc)$_2$, free NEt$_3$ and the *mono-* and *bis*-NEt$_3$-ligated Pd(OAc)$_2$ complexes (eq 1.10). The incomplete formation of the saturated Pd(NEt$_3$)$_2$(OAc)$_2$ complex demonstrated that NEt$_3$ was more labile than DMSO as a ligand for Pd^{II}. Taken together with the initial rate data, Sigman proposed that the active catalyst species was the unsaturated Pd(NEt$_3$)(OAc)$_2$ species, which can readily facilitate substrate coordination.

$$(1.9)$$

$$(1.10)$$
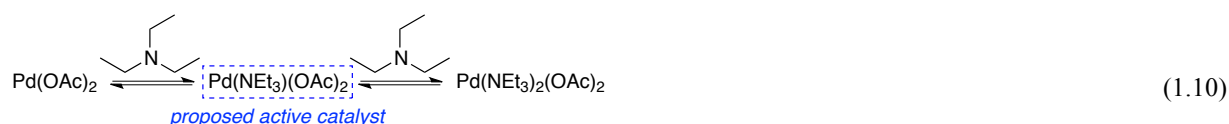
1.2.4 Pyridine (pyr)

1.2.4.1 Alcohol Oxidation

In 1998, Uemura reported a Pd(OAc)$_2$/pyridine catalyst as a competitive alcohol oxidation method to the Pd(OAc)$_2$ in DMSO system.[19] The reaction cleanly oxidized primary and secondary benzylic and aliphatic alcohols to the corresponding aldehyde or ketone (eq 1.11). Other nitrogen-containing ligands such as 2,6-lutidine and NEt$_3$ also worked, however pyridine was shown to be superior at elevated temperature (80 °C), which was necessary for smooth substrate oxidation. At ambient temperature, pyridine was found to inhibit the reaction similar to Sigman's observations that pyridine inhibited reactivity at room temperature during his development of the Pd/NEt$_3$ system.[18]

R$_1$ = benzylic, alkyl
R$_2$ = H or alkyl

(1.11)
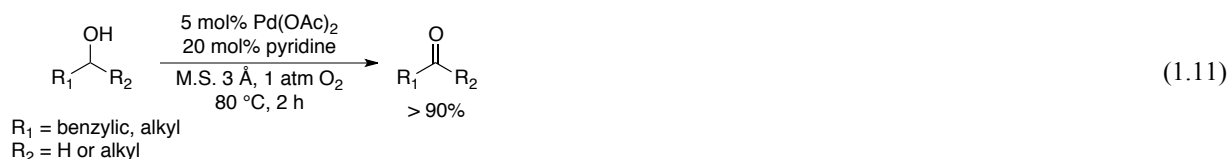
1.2.4.2 Mechanism Studies for Alcohol Oxidation

A follow-up study by Uemura expanded the scope of oxidized alcohols and provided preliminary mechanistic insights.[20] Alkenic alcohols were identified as problematic because the oxidized product would inhibit catalyst turnover and precipitate Pd^0. This could be abated by the addition of excess pyridine (25x relative to Pd), suggesting that pyridine could aid in the dissociation of chelating products. Modifying the reaction conditions by either increasing the temperature (110 °C) or performing the reaction with less solvent resulted in the precipitation of Pd^0.

In 2002, Stahl reported a rigorous mechanistic study of Uemura's catalyst system.[21] The catalyst and substrate displayed saturation kinetics, and a kinetic isotope effect (KIE) was evident for a PhCD$_2$OH substrate (Table 1.2). The initial rate of the reaction was also observed to be independent of the oxygen pressure. Together, these data supported a catalytic cycle where substrate oxidation was the limiting half-reaction (Scheme 1.7).

Table 1.2. Summary of Kinetic Orders for Alcohol Oxidation

R$_1$ = H, Me

Component	Kinetic Order
O$_2$	zero
catalyst	saturation
ROH	saturation, KIE = 1.3-1.8
pyr	≤1:1 pyr:Pd promotes; >1:1 pyr:Pd inhibits

Pyridine was found to influence both the substrate oxidation and catalyst reoxidation half-reactions. In the absence of pyridine, the catalyst performed a stoichiometric oxidation of the substrate followed by the immediate precipitation of Pd^0. Upon the addition of pyridine to the system, the initial rate increased until a 1:1 pyr:Pd stoichiometry was reached, after which pyridine inhibited the reaction (Table 1.2). NMR spectroscopic investigations revealed that a 2:1 pyr:Pd(OAc)$_2$ mixture forms the well-defined Pd(pyr)$_2$(OAc)$_2$ (eq 1.12, **5**) complex in solution and, in the presence of excess ligand, there is no observable exchange between bound and unbound pyridine. These results indicated that pyridine formed a stronger complex with Pd^{II} than the DMSO or NEt$_3$ ligands.[18]

(1.12)
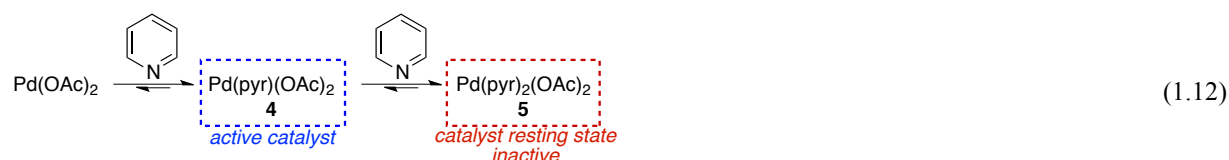
The saturation behavior of the catalyst indicated the presence of an off-cycle catalyst resting state in equilibrium with the active catalyst species. The peak in the initial rate at 1:1 pyr:Pd suggested that the active catalyst species could be a three-coordinate Pd(pyr)(OAc)$_2$ complex (eq 1.12, **4**), which would facilitate substrate coordination. Under catalytic conditions (i.e. 4:1 pyr:Pd(OAc)$_2$), the formation of **4** would require the unfavorable dissociation of a pyridine ligand from **5** and explained the inhibitory effect of >1:1 pyr:Pd. The necessity for an unsaturated catalyst demonstrated that substrate coordination was challenging as well as inhibited by the presence of strongly coordinating ligands. In summary, catalyst reactivity was favored at low [pyr], whereas catalyst stability required higher [pyr] (Scheme 1.7).

Scheme 1.7. Summary of Mechanistic Observations for Pd(OAc)$_2$/Pyridine Alcohol Oxidation
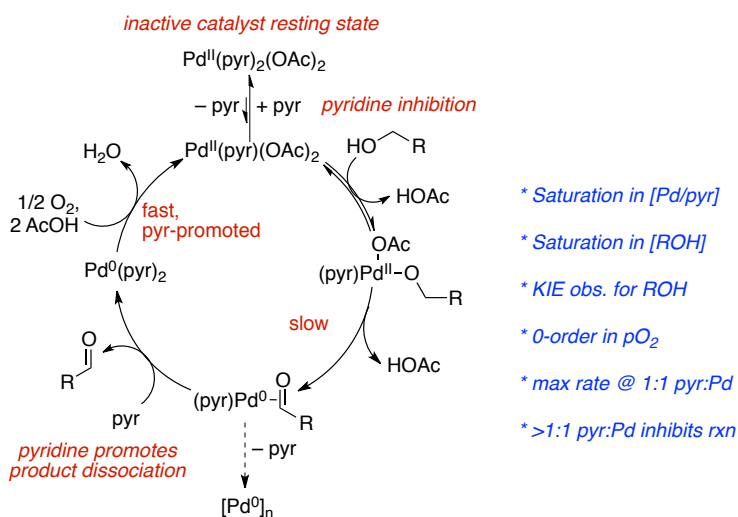
1.2.4.3 Aza-Wacker

In 2002, Stahl reported the application of the Pd(OAc)$_2$/pyridine catalyst to the aerobic oxidative amidation of alkenes.[22] The catalyst smoothly cyclized aliphatic and aromatic sulfonamides into the corresponding substituted pyrrolidine or indoline in high yield (eq 1.13). The optimal catalyst consisted of a 2:1 pyridine:Pd(OAc)$_2$ stoichiometry rather than the 4:1 stoichiometry used in the Uemura alcohol oxidation conditions.

$$(1.13)$$
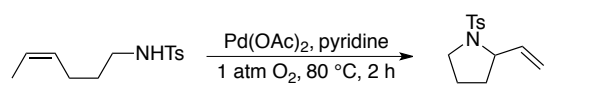
1.2.4.4 Mechanism of the Aza-Wacker Oxidation

A combined experimental and theoretical mechanistic study investigated the catalyst resting state, turnover-limiting step, and role of pyridine in the above reaction.[23] The investigation was performed using a 4:1 pyr:Pd(OAc)$_2$ stoichiometry (Uemura conditions) as the standard conditions rather than the reported 2:1 stoichiometry in order to avoid catalyst decomposition.

Under these conditions, a zero-order dependence was observed on the pO_2 (Table 1.3). The catalyst and amide both demonstrated saturation kinetics. A promoting effect of pyridine was observed up to a 1:1 - 1.5:1 pyr:Pd stoichiometry, after which the ligand inhibited the reaction (Table 1.3). Exogenous AcOH also had a significant inhibitory effect on the initial rate. Lastly, *in situ* NMR spectroscopic studies of the reaction revealed that the catalyst resting state was the $Pd(pyr)_2(OAc)_2$ complex.

Table 1.3. Summary of Kinetic Orders for aza-Wacker Oxidation

Component	Kinetic Order
O_2	zero (4:1 pyr:Pd); first (2:1 pyr:Pd)
catalyst	saturation
amide	saturation
pyr	≤1:1 pyr:Pd promotes; >1:1 pyr:Pd inhibits
AcOH	inhibts

The interpretation of these experiments was very similar to the Uemura alcohol oxidation study (cf Scheme 1.7). The zero-order dependence on pO_2, Pd^{II} resting state and kinetic dependence on both [catalyst] and [amide] confirmed that the rate-determining step involved substrate oxidation (Scheme 1.8). The saturation behavior for [catalyst] combined with the inhibitory effect of pyridine with >1:1 pyr:Pd stoichiometries suggested that substrate coordination required dissociation of a pyridine ligand from $Pd(pyr)_2(OAc)_2$. Additionally, the inhibitory effect of AcOH demonstrated that formation of the Pd–N is reversible and likely not the rate-determining step. A Hammett correlation with *para*-substituted sulfonamides revealed that electron-rich substrates promoted the reaction, which suggested that the rate-determining step was alkene insertion into the Pd–N$_{amidate}$ bond. DFT studies supported these experimental

conclusions but also proposed that dissociation of a second pyridine ligand prior to alkene insertion could also be the rate-determining step (Scheme 1.8).

Scheme 1.8. Proposed Catalytic Cycle for Pd(OAc)$_2$/Pyridine-Catalyzed Aza-Wacker Cyclization
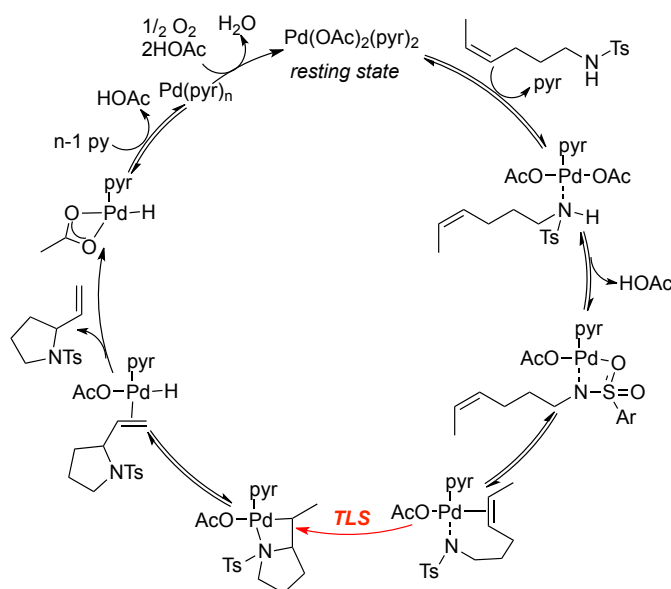
1.2.4.5 Conclusions

The Pd(OAc)$_2$/pyridine catalyst system provided a more robust alternative to the previous catalyst systems for high-temperature Pd-catalyzed aerobic oxidations. Pyridine was observed to more effectively stabilize Pd^0 and promote catalyst reoxidation than DMSO or NEt$_3$ because it formed stronger metal-ligand bonds. In turn, substrate oxidation became more challenging because ligand dissociation was required for the substrate coordination to Pd^{II}. The "volcano"-like dependence of the initial rates on [pyridine] speaks to these contradictory roles as *the "sweet spot" for substrate oxidation was found to be 1:1 pyr:Pd, however >2:1 pyr:Pd stoichiometries were necessary to effectively stabilize Pd^0*. As a result, the Pd(OAc)$_2$/pyridine catalyst is limited to high-temperature reactions where there is sufficient thermal energy to labilize the metal-ligand
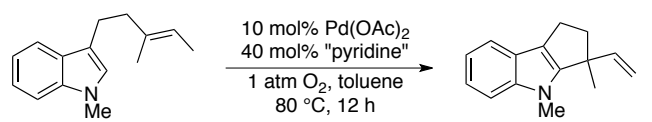
bonds. Future efforts would rely upon making alterations to the pyridine ligand to make it more labile at Pd^{II} while retaining its effectiveness at stabilizing Pd^0.

1.2.5 Derivatives of Pyridine

1.2.5.1 Ethyl Nicotinate

Stoltz reported an aerobic $Pd(OAc)_2$-catalyzed oxidative annulation of indoles that was promoted by ethyl nicotinate ligands (4:1 L:Pd).[24] Substituted pyridines with electron-donating and -withdrawing functional groups were screened during the catalyst optimization. Stoltz observed a correlation between the pK_a of the pyridinium ($pyrH^+$) ligand and the conversion of substrate (Table 1.4). Increasingly acidic pyridine ligands were found to promote substrate oxidation until the ligand became so acidic ($pK_a < 3.35$) that it insufficiently stabilized Pd^0, resulting in Pd-black. Ethyl nicotinate ($pK_a = 3.35$) was found to provide the ideal balance between catalyst reactivity and longevity: sufficiently labile to promote substrate oxidation but sufficiently coordinating to stabilize Pd^0.

Table 1.4. Effect of Pyridine Electronics on Oxidative Annulation of Indoles

pyridine ligand	pK_a ($pyrH^\pm$)	Conversion (%)
4-MeO	6.47	3
unsubstituted	5.25	23
3-CO$_2$Et	3.35	76
3-CN	1.39	55
3,5-di-Cl	0.90	22

1.2.5.2 2-fluoropyridine (2-Fpy)

The application of electron-deficient pyridine ligands to generate reactive Pd catalysts was also investigated by Stahl for the aerobic, oxidative homocoupling of *o*-xylene.[25] The catalyst system consisted of Pd(OAc)$_2$/Cu(OTf)$_2$ catalyst with 2-fluoropyridine (2-Fpyr) as a ligand (2:1 L:Pd) and catalytic TFAH in acetic acid as the solvent (Scheme 1.9). A series of electron-rich and -deficient pyridine ligands were screened during catalyst optimization and a similar trend to Stoltz's oxidative annulation was observed: increasingly acidic ligands promoted substrate oxidation until the ligand was too electron-deficient to coordinate to Pd, after which the promoting effect was attenuated. For this reaction, 2-Fpyr (pKa = -0.44) was found to be the ideal medium between catalyst reactivity and longevity.

Scheme 1.9. Effect of Pyridinium pK_a on the Rate of Oxidative Coupling
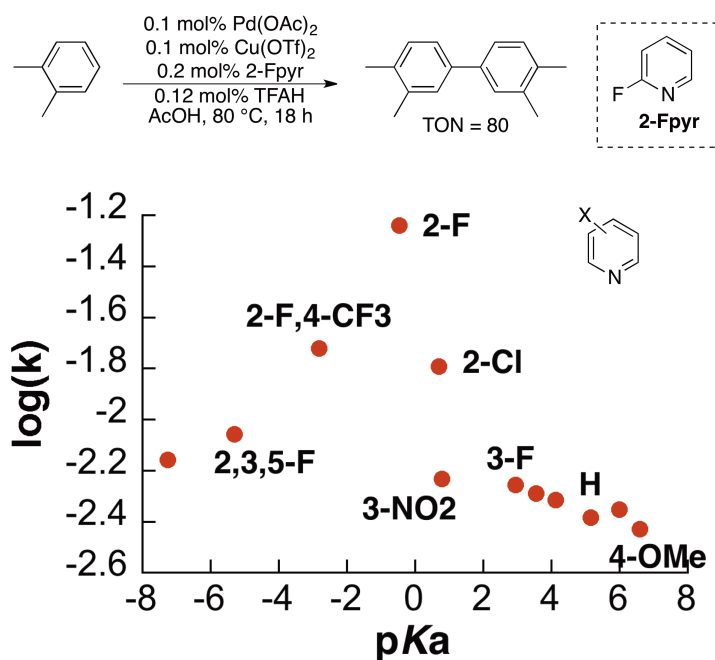
NMR spectroscopic investigations into the catalyst mixture in C$_6$D$_6$ revealed multiple 2-Fpyr-coordinated Pd species in equilibrium (eq 1.14). Free 2-Fpyr ligand was also observed. The

major ligated Pd species was Pd(2-Fpyr)$_2$(TFA)$_2$, which was generated from the protonolysis of Pd(OAc)$_2$ by TFAH to generate Pd(TFA)$_2$ and AcOH (eq 1.14). Two other minor species were identified to be the mixed carboxylate monomer and dimer, Pd(2-Fpyr)$_2$(OAc)(TFA) and [Pd(2-Fpyr)(OAc)(TFA)]$_2$ (eq 1.14).[26] NMR spectroscopic analysis of solutions containing 2-Fpyr and Pd(OAc)$_2$ in the absence of TFAH revealed that 2-Fpyr does not form any identifiable complex with Pd(OAc)$_2$ (eq 1.15). These results indicated that the promoting effect of the ligand was dependent on the electrophilicity of the Pd^{II} salt. Furthermore, pyridines that are more acidic (i.e. more electron-deficient) than 2-Fpyr, such as 2,4,6-trifluoropyridine, were observed to not coordinate to Pd(TFA)$_2$ or Pd(OAc)$_2$ (eq 1.16).

Pd(OAc)$_2$ + TFAH + 2 2-Fpyr ⇌   (1.14)

Pd(2-Fpyr)$_2$(TFA)$_2$ + Pd(2-Fpyr)$_2$(OAc)(TFA) + [Pd(2-Fpyr)(OAc)(TFA)]$_2$ + AcOH
major species

Pd(OAc)$_2$ + 2 2-Fpyr ⟶ no reaction   (1.15)
not electrophlic enough

PdX$_2$ + 2 2,4,6-tri-Fpyr $\xrightarrow{\text{X = OAc, TFA}}$ no reaction   (1.16)
too electron-deficient
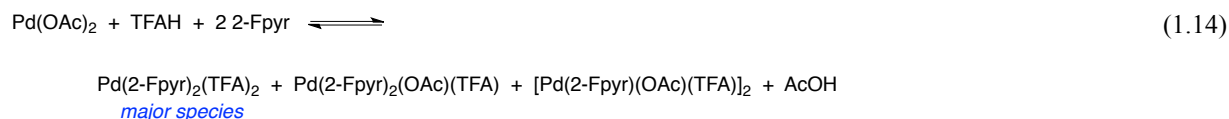
1.2.5.3 Bulky 2,6-disubstuted Pyridines

In 2009, Yu reported an aerobic Pd-catalyzed method for the *meta*-selective olefination of electron-deficient arenes in modest yields.[27] A series of 2,6-dialkyl-substituted pyridine ligands were screened. The catalyst activity was sensitive to the size of the alkyl group: unhindered pyridine ligands inhibited the reaction while excessively bulky ligands did not bind to Pd^{II} or Pd^0, which resulted in the formation of Pd-black (Scheme 1.10). The highest reactivity was achieved with a substitution pattern consisting of a methylene alpha to the pyridine and a methine beta to the pyridine. X-ray crystallographic characterization of a Pd and ligand mixture revealed a *bis*-

ligated Pd(OAc)$_2$ monomer (eq 1.17, **6**). Subsequent NMR spectroscopic analysis revealed that this monomer rapidly dissociated an equivalent of the ligand to form a *mono*-ligated Pd(OAc)$_2$ complex that was consistent with a dimeric structure (eq 1.17, **7**). Yu described these ligands as "mutually" repulsive meaning that in solution the formation of a mono-"pyridine" complex is preferred, which is more reactive towards substrate. The ligand likely sufficiently stabilizes Pd^0 by forming the *bis*-"pyridine" adduct due to the reduced coordination sphere and longer Pd– ligand bonds for Pd^0.

Scheme 1.10. Optimization of Ligand Structure for Olefination of Electron-Deficient Arenes

(1.17)
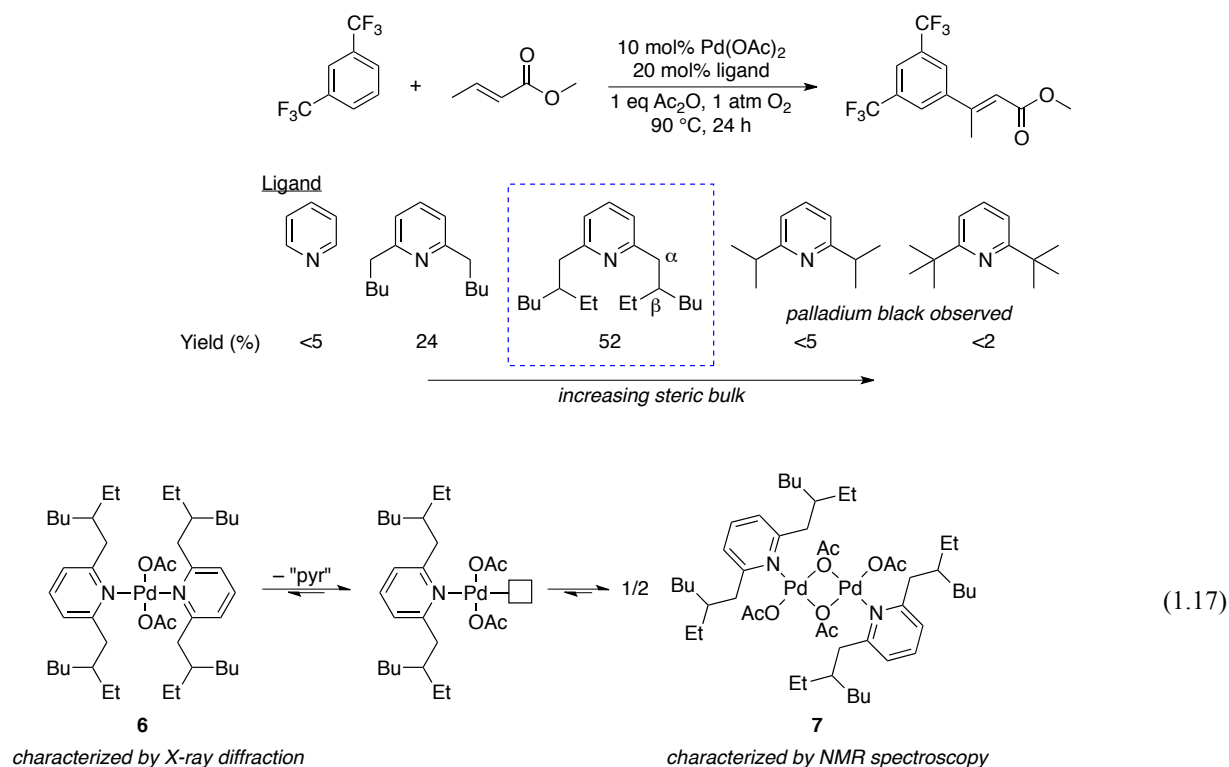
1.2.6 Monodentate Ligand Summary

The above examples represent a historical as well as conceptual evolution of aerobic Pd-catalyzed oxidation reactions. A significant challenge in oxidative catalysis is the stabilization and reoxidation of the reduced catalyst, Pd^0. Early examples used polar, coordinating solvents

such as water or DMSO where Pd^0 would be stabilized by an "ocean of ligand." Catalytic methods using these conditions could often be performed at elevated temperature but, in the case of DMSO, suffered from an unstable Pd^0 resting state due to low O_2 solubility hampering catalyst reoxidation.

The movement away from polar, coordinating solvents required the use ancillary ligands that could sufficiently stabilize Pd^0, which would be bolstered by solvents with higher O_2 solubility. Catalyst systems using monodentate ligands attracted the most attention with the most prominent early example being the $Pd(TFA)_2$/DMSO catalyst. While this catalyst was stable under ambient conditions, reactions necessitating higher temperatures required modifications such as high pressures of O_2 or acid solvents in order to sufficiently promote catalyst reoxidation. A key feature of this catalyst system was the change from a Pd^0 catalyst resting state to an innately more stable Pd^{II} complex.

The growing need for a general, thermally-stable catalyst resulted in the development of the $Pd(OAc)_2$/pyridine system. Pyridine, unlike DMSO and NEt_3, formed strong metal-ligand bonds to Pd^0 as well as Pd^{II}. As a consequence, catalyst reoxidation was greatly enhanced but at the cost of slower substrate oxidation rates. The $Pd(OAc)_2$/pyridine catalyst system was thus limited to elevated temperatures where labilization of a pyridine ligand from Pd^{II} in the presence of substrate was facile.

Subsequent modifications to the $Pd(OAc)_2$/pyridine system resulted in more active catalysts while retaining pyridine's superior ability to stabilize Pd^0. The addition of electron-deficient groups to the pyridine ligand weakened the Pd^{II}-"pyridine" bonds, which allowed weakly coordinating substrates such as arenes to more effectively interact with Pd^{II} (Scheme 1.11). Furthermore, electron-deficient pyridines created a more-oxidizing Pd^{II} center, which made difficult transformations like oxidative C–C couplings more accessible. Alternatively, sterically crowded pyridine ligands were applied to promote substrate coordination by generating an unsaturated catalyst. The large substituents on pyridine were proposed to favor the formation of a reactive *mono*-ligated three-coordinate Pd^{II} complex over the commonly observed *bis*-ligated

four-coordinate Pd^{II} complex (Scheme 1.11). As a result, substrate coordination to the metal center became more facile. However, these modifications required extensive screening since extremely acidic or excessively bulky pyridine ligands would insufficiently stabilize Pd^0.

Scheme 1.11. Effect of Modified Pyridine Ligands on Substrate Coordination

Standard Pyridine - Substrate Coordination is Difficult
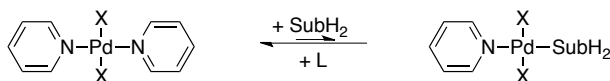
Electron-Deficient Pyridine - Weak Pd^{II}-Pyr Bonds Faciltate SubH$_2$ Coordination
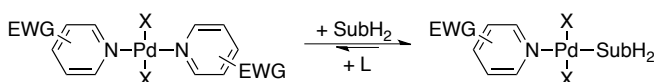
Bulky Pyridine - Favors Three-Coordinate Pd^{II} with Open Coordination Site
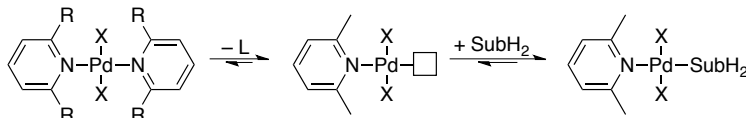
1.3 Bidentate Ligands

Bidentate ligands have been observed to generally inhibit aerobic Pd-catalyzed oxidation reactions.[13,14a,19,20,22,25] Typical bidentate ligands, such as 2,2-bipyridine (bpy) or 1,10-phenanthroline (phen), form stronger metal-ligand bonds than their monodentate ligand counterparts (pyridine) due to the chelate effect. Therefore, substrate coordination to the metal becomes increasingly challenging since partial ligand dissociation is disfavored but can occur via anionic (X-type) ligand dissociation. Ionization of a ligand to form a charge-separated Pd complex is sensitive to the polarity of the solvent, and catalytic methods that successfully employed bpy or phen use polar, coordinating solvents or high-temperatures,[28] which will be briefly discussed in two case studies.

Scheme 1.12. Mechanism for Substrate Coordination to Bidentate Ligands
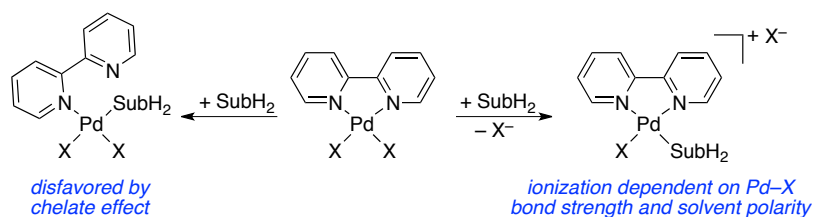
On the other hand, the chelate effect exhibited by these bidentate ligands excels at stabilizing Pd^0. Development and application of bidentate ligands that promote substrate oxidation while harnessing their innate ability to stabilize Pd^0 has been the subject of recent catalyst development. Catalysts consisting of sterically crowded or wide bite-angle bidentate ligands have begun to receive increasing attention as they are often used in nonpolar solvents and/or at modest temperatures (<80 °C). The first section will discuss Sheldon's thorough study of water-soluble phenanthroline ligands in the modern Wacker oxidation and alcohol oxidations. Subsequent sections will introduce recent applications of bidentate ligands for diverse Pd-catalyzed oxidation reactions.

1.3.1 Bathophenanthroline Disulfonate (PhenS*)

1.3.1.1 Wacker Oxidation of Olefins

In the traditional Wacker process, the high concentrations of Cu co-oxidant needed to rapidly reoxidize Pd^0 and the insolubility of larger olefins in water are among the most significant disadvantages. Sheldon addressed these concerns through the development of a water-soluble catalyst consisting of Pd(OAc)$_2$ with a bathophenanthroline disulfonate ligand (PhenS*) to help stabilize Pd^0 (eq 1.18).[29] The catalyst effectively converts terminal olefins to the corresponding methyl ketone without isomerization of the alkene. The catalyst could be recycled; however addition of NaOAc was necessary to maintain catalyst activity between cycles. In the absence of

NaOAc, brown-black solutions indicative of cluster or colloidal Pd^0 formed upon heating and the catalyst became inactive.

(1.18)
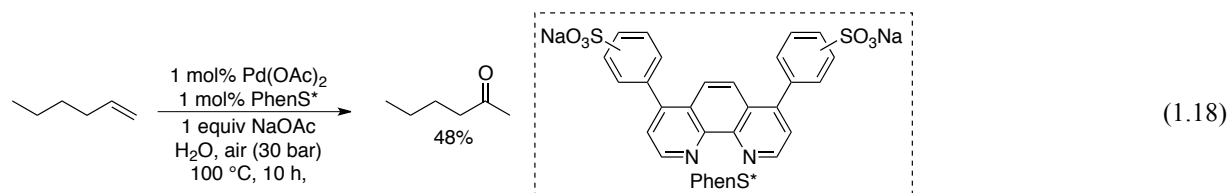
1.3.1.2 Mechanistic Study of the PhenS*-Promoted Wacker Oxidation

A follow-up report by Sheldon investigated the mechanism the $Pd(PhenS*)(OAc)_2$ catalyst system. A water-soluble olefin was employed for the study in lieu of the previously reported organic-soluble olefins in order to simplify interpretation of data by avoiding substrate solubility issues. The reaction was zero-order in substrate until 50% conversion and then became first order for subsequent conversion. This observation indicated a saturation dependence on [substrate] due to solubility limitations. Additionally, a half-order dependence on [catalyst] was observed. The half-order dependence suggested the presence of an inactive dimeric catalyst resting state in equilibrium with an active monomeric catalyst. Sheldon proposes the catalyst resting state to be a $[Pd(PhenS*)(OH)]^{2+}$ dimer, of which phen analogs have been characterized and found to be stable in aqueous conditions (Scheme 1.13).[30] The olefin substrate breaks up the dimer by coordinating to Pd and then undergoes *cis*-hydroxypalladation to afford the Pd-alkyl, which subsequently forms acetaldehyde and Pd^0. The Pd^0 species is stabilized by PhenS* and reoxidized by dioxygen to form the peroxo species. The $Pd(PhenS*)(O_2)$ complex serves to oxidize an equivalent of $Pd^0(PhenS*)$ in the presence of acid to regenerate the $[Pd(PhenS*)(OH)]^{2+}$ dimer.

Scheme 1.13. Proposed Catalytic Cycle for Aerobc Pd/PhenS*-Catalyzed Wacker Oxidation
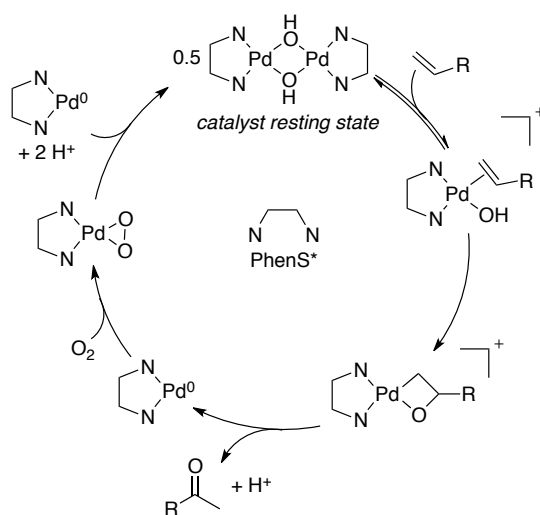
1.3.1.2.1 Alcohol Oxidation

In 2000, Sheldon applied the Pd(OAc)$_2$/PhenS* catalyst system to the aqueous oxidation of primary and secondary aliphatic and benzylic alcohols (Scheme 1.14).[31] The catalyst loadings were remarkably low compared to other reported Pd-catalyzed alcohol oxidations. Initial turnover frequencies were largest for small alcohols since they were more soluble in water; however the addition of surfactants improved the rate by increasing the solubility of alcohols in general. The addition of NaOAc was found to improve the reaction rate as well as the catalyst stability. For aliphatic alcohols, over-oxidation to the carboxylic acid occurred but could be inhibited by the addition of catalytic quantities of TEMPO.

Scheme 1.14. Substrate Scope for Pd(PhenS*)(OAc)$_2$-Catalyzed Alcohol Oxidation
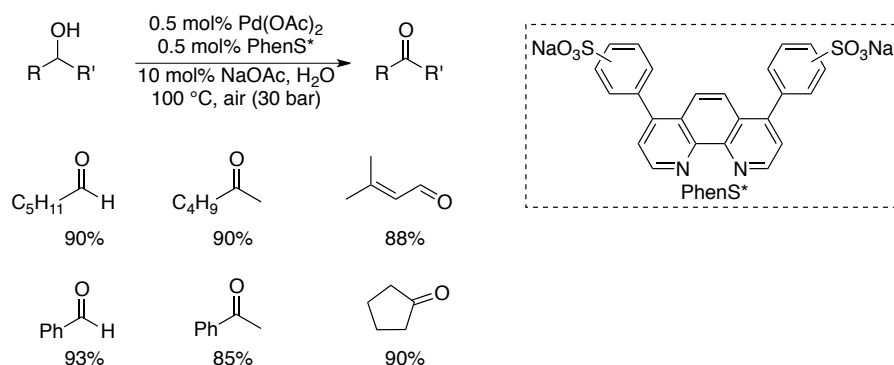
1.3.1.2.2 Mechanistic Study of the PhenS*-Promoted Alcohol Oxidation
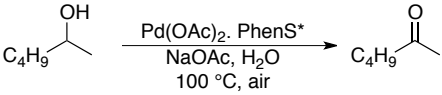
In 2002, Sheldon explored the role of each of the components in the Pd(PhenS*)(OAc)$_2$-catalyzed alcohol oxidation reaction.[32] Mono-, bi- and tridentate pyridine ligands were explored to better understand the role of ligand lability on the reaction. Monodentate ligands were found to be too labile and ineffectively stabilized Pd^0 (Scheme 1.15). Higher yields were obtained with bipyridine and bipyrimidine but they also resulted in the eventual formation of Pd-black. Only the rigid phenanthroline structure of PhenS* was found to effectively promote substrate oxidation and catalyst reoxidation. The tridentate terpyridine ligand was too coordinating and inhibited substrate oxidation. The ideal L:Pd stoichiometry was found to be 1:1 L:Pd: <1:1 was ineffective at stabilizing Pd^0 while >1:1 inhibited substrate coordination.

Scheme 1.15. Investigation of Ligands on Catalyst Activity and Stability
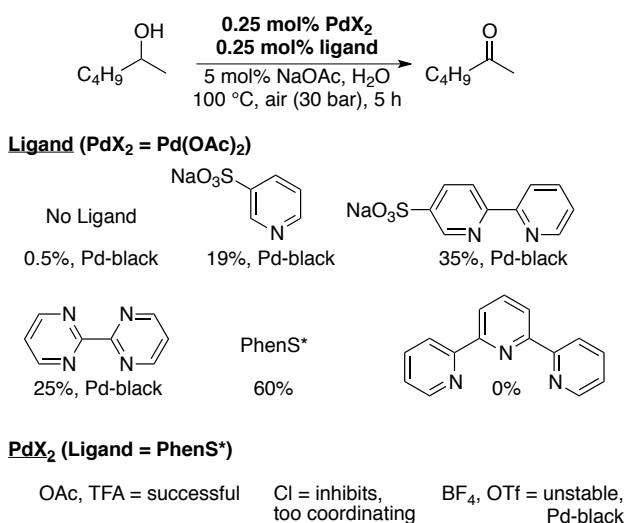
The counter anion of the palladium salt also played a critical role. Acetate and trifluoroacetate promoted the reaction while strongly coordinating anions such as chloride inhibited substrate oxidation (Scheme 1.15). In the presence of non-coordinating anions such as tetrafluoroborate, the entirety of the Pd catalyst decomposed into Pd-black. These observations described the role of both L- and X-type ligands in managing the balance between promoting substrate oxidation and effectively stabilizing Pd^0.

The identity of the catalyst resting state and rate-determining step was determined by investigating the kinetic orders of the alcohol, catalyst and pO_2. The rate of the reaction was limited by the solubility of the alcohol, which resulted in pseudo-zero order dependence; however at low [alcohol] a first order dependence was observed (Table 1.5). A half-order dependence on [catalyst] was observed, which indicated that the catalyst resting state was a dimeric structure that dissociated into an active monomeric catalyst. The reaction was found to be insensitive to the pO_2. Lastly, an inter- and intramolecular KIE of 1.4-1.8 was observed for an alcohol deuterated at the α-position (Table 1.5). These observations revealed substrate oxidation to be the turnover-limiting half-reaction with β-hydride elimination as the slow step.

Table 1.5. Summary of Mechanistic Observations

Component	Kinetic Order
O_2	zero
catalyst	half
ROH	saturation, KIE = 1.4-1.8
Ligand	≤1:1 PhenS*:Pd promotes; >1:1 PhenS*:Pd inhibits

With these observations in hand, Sheldon proposed a catalytic cycle that started with a hydroxide-bridged $[Pd(PhenS*)(OH)]^{2+}$ dimer (Scheme 1.16). The alcohol breaks up the dimer into reactive, cationic monomers. The Pd-bound hydroxide facilitates inner-sphere deprotonation of the alcohol to form the Pd-alkoxide and water, which subsequently dissociates. The three-coordinate Pd-alkoxide then undergoes rate-limiting β-hydride elimination to form the aldehyde and a Pd–H complex. The Pd–H reductively eliminates to generate a proton and Pd^0, which is stabilized by PhenS*. Two equivalents of the Pd(PhenS*) complex react with an equivalent of O_2 and two equivalents of acid to regenerate the dimeric catalyst resting state (Scheme 1.16). This proposed catalytic cycle is very similar to the proposed cycle for Sheldon's Pd(PhenS*)(OAc)$_2$-catalyzed Wacker oxidation of olefins (cf. Scheme 1.13).

Scheme 1.16. Proposed Catalytic Cycle for Pd/PhenS*-Catalyzed Oxidation of Alcohols
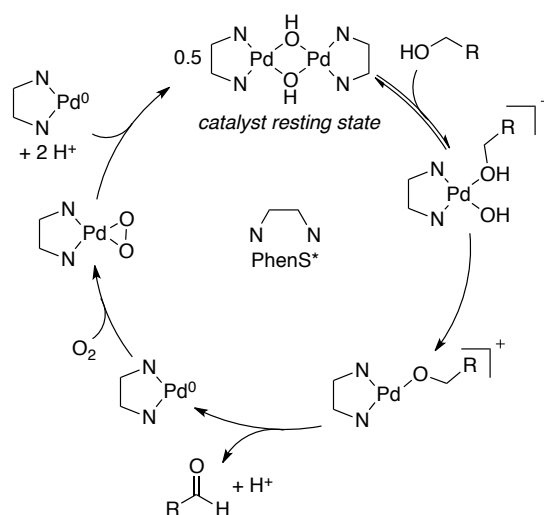
1.3.2 2,9-Dimethyl-1,10-Phenanthroline (dmphen, neocuproine)

1.3.2.1 Oxidative Heck Method for Aryl/Vinyl Coupling

In 2004, Larhed reported the first ligand-modulated Pd-catalyzed oxidative Heck arylation of olefins (eq 1.19).[33] Pyridine, bipyridine and phosphine ligands were found to inhibit the reaction. However 2,9-dimethyl-1,10-phenanthroline (dmphen) was found to accelerate the substrate oxidation step, which allowed significantly reduced catalyst loadings (1 mol%) to be used. Arylboronic acids reacted with electron-deficient alkenes to selectively form 1,2-substituted (β-substituted) olefins whereas electron-rich alkenes selectively formed 1,1-disubstituted (α-substituted) olefins.[34] In the absence of dmphen, the reactions displayed poor selectivity or did not proceed at all.

$$(1.19)$$
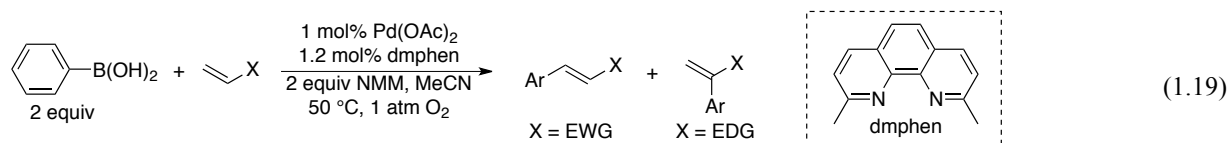
1.3.2.2 Mechanistic Studies into Aryl/Vinyl Oxidative Heck Coupling

Larhed later reported a computational investigation into the selectivity for the coupling of electron-rich olefins and arylboronic acids. The dmphen ligand was abbreviated with a *N,N'-*dimethylethanediimine ligand. The stereodetermining step was alkene insertion in the Pd–C bond (carbopalladation), which occurred from a cationic Pd complex. The barriers for carbopalladation to generate both the α- and β-substituted products were calculated for a variety of electron-rich and -deficient arenes. Electron-rich arenes were found to generate the highest selectivity for the α-substituted olefin, with more electron-deficient arenes degrading the selectivity (Table 1.6). These results mirrored the experimental observations that electron-deficient arylboronic acids yielded slightly lower selectivities for the α-substituted olefins than electron-rich arylboronic acids.

Table 1.6. Comparison of Activation Energies for Substituted Arylboronic Acids
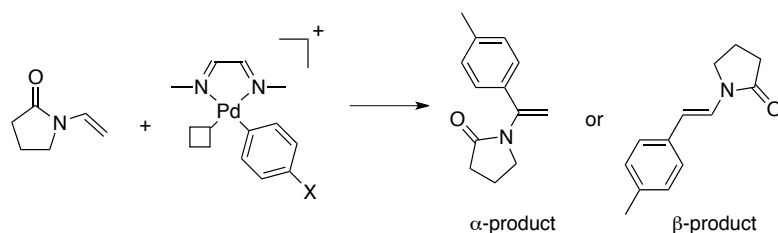
X	$\Delta E_\alpha^\ddagger$	$\Delta E_\beta^\ddagger$	$\Delta\Delta E^\ddagger$
OMe	9.8	13.5	-3.7
Me	12.4	14.8	-2.4
H	13.9	15.3	-1.4
CF$_3$	15.3	16.4	-1.1

all values are in kcal/mol

The likelihood of a highly stereoselective cationic pathway was further bolstered by comparing the results and selectivity obtained through a neutral pathway. They proposed that the addition of LiCl would partially dissociate the dmphen ligand and coordinate to Pd *trans* to the aryl group. The olefin would then coordinate *trans* to the dmphen ligand and be poised for

carbopalladation. Experimentally, the reaction was slowed and the stereoselectivity was destroyed (Scheme 1.17). Similarly, the computed neutral pathway (i.e. partial diimine ligand dissociation) also demonstrated lower selectivity and higher calculated barriers than the cationic path (Scheme 1.17). These results provided tentative evidence for a cationic pathway where the chelating dmphen ligand promotes substrate oxidation and enhances selectivity. Subsequent method development focused on replacing O_2 with air and using a microwave reactor.[35]

Scheme 1.17. Comparison of Neutral and Cationic Carbopalladation Pathways
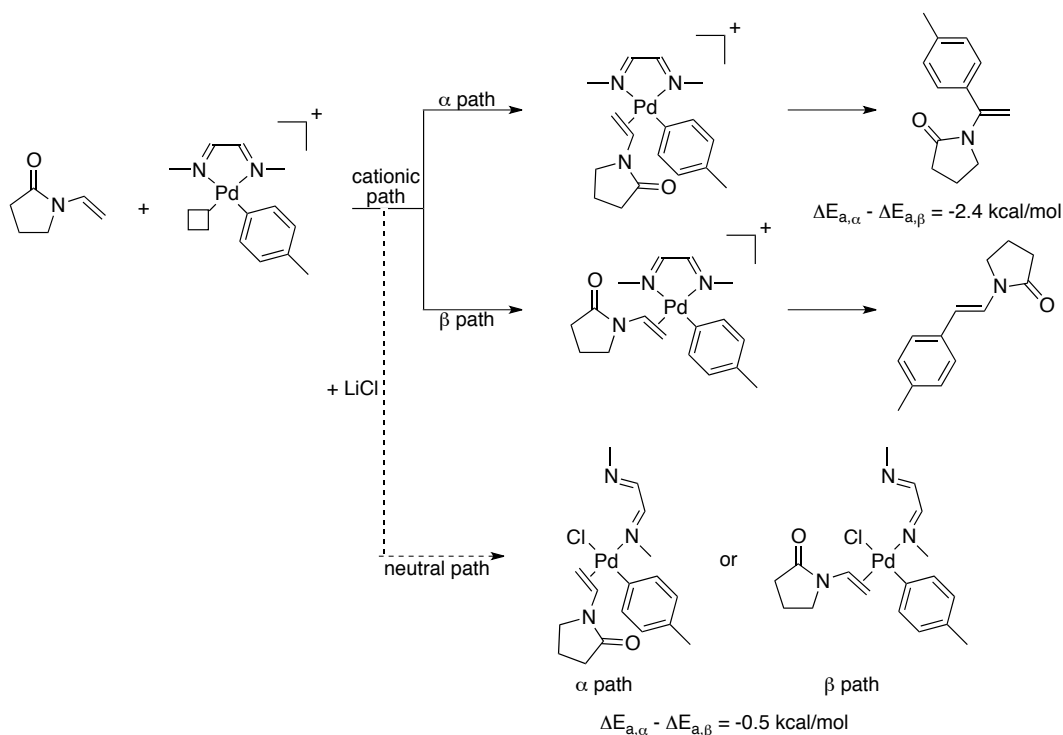
1.3.2.3 Oxidative Heck Method for Vinyl/Vinyl Coupling

In 2012, Stahl reported an aerobic Pd(TFA)$_2$/dmphen-catalyzed oxidative Heck method that coupled vinylboronic acids and terminal olefins.[36] For the majority of olefins, carbopalladation occurred selectively at the α-position of olefin to form the 1,3-disubstituted diene (Scheme 1.18).

Dmphen was found to be most active ligand and enforced the highest selectivity. Other ligands such as pyr, bpy and phen were found to inhibit the reaction and favored the formation of the linear diene product (Scheme 1.18). The reaction did not proceed past one turnover in the absence of ligand. β-styrenylboronic acids gave the highest yields, however other vinylboronic acids were also tolerated but with typically lower yields. A large range of functionalized olefins was successful, including those with silyl, carbonyl, phthalimide and alcohol groups.

Scheme 1.18. Influence of Ligands on Catalyst Activity and Selectivity
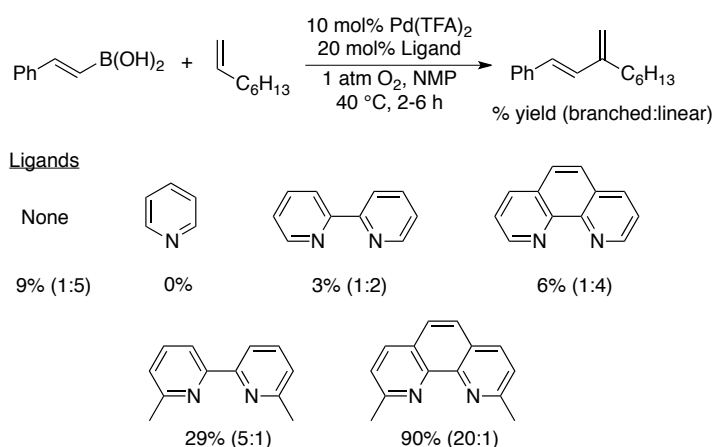
Preliminary mechanistic insight into the origin of the high regioselectivity was obtained with DFT methods. A cationic reaction coordinate was proposed on the basis of studies by Larhed. The stereodetermining step was found to be carbopalladation of the terminal olefin from the cationic [Pd(dmphen)(vinyl)(olefin)]+ complex (Scheme 1.19). The linear (β-substituted) product is disfavored due to the steric interactions between the R-group on the olefin and the methyl groups on the dmphen ligand. This steric interaction would be minimized by binding the opposite face of the olefin, which would produce the branched (α-substituted) product (Scheme 1.19).

Scheme 1.19. Origin of the Observed Selectivity for the Branched Product

Vi = vinyl group

Linear products   **Branched products**

$\Delta\Delta G^{\ddagger}_{\text{branched-linear}}$ = -2.3 kcal/mol
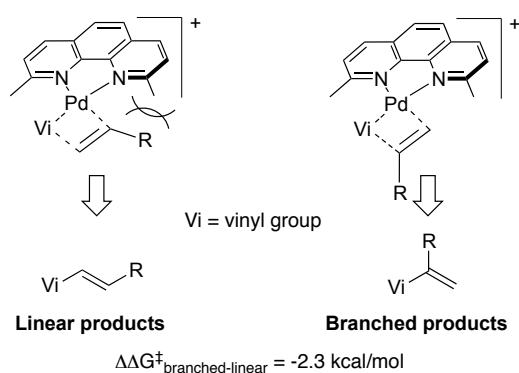
1.3.2.4 Conclusions

The dmphen represented an early important example of how modifications to the bpy and phen framework could result in the emergence of catalytic activity. The methyl groups that project into the square plane were critical in enforcing the selectivity for Heck reactions. This steric motif would later be found in the development of sterically crowded bipyridine and pyridyloxazoline ligands for other Pd-catalyzed transformations, including asymmetric catalysis.

1.3.3 6,6'-dimethyl-2,2'-bipyridine (6,6'-Me$_2$bpy)

In instances where dmphen has been used as a ligand for oxidative Pd-catalyzed transformations, 6,6'-Me$_2$bpy has also been observed to be moderately effective but often with lower yields or selectivity.[37] In the reaction reported below by Stahl, 6,6'-Me$_2$bpy was found to be superior to dmphen for both the oxidative Heck and dehydrogenation reactions. Chapter 4 will briefly touch upon the differences between dmphen and 6,6'-Me$_2$bpy that give rise to differences in reactivity.

1.3.3.1 Tandem Oxidative Heck-Dehydrogenation

Stahl reported a tandem oxidative Heck-dehydrogenation method using a [Pd(CH$_3$CN)$_4$](BF$_4$)$_2$/6,6'-Me$_2$bpy catalyst to couple cyclohexenones and arylboronic acids followed by dehydrogenation to the phenol.[38] The reaction produced stoichiometric Pd-black in the absence of ligands and the addition of most pyridine and bipyridine ligands inhibited the reaction. 6,6'-Me$_2$bpy was found to be uniquely active at promoting both the oxidative Heck coupling and dehydrogenation steps. The Heck coupling proceeded first in DMA at 50 °C, and the dehydrogenation could be triggered by adding DMSO and performing the reaction 80 °C. Using this catalyst, a number of *meta*-substituted phenols were synthesized with both electron-rich and -deficient arylboronic acids in modest to good yield (eq 1.20).

$$(1.20)$$
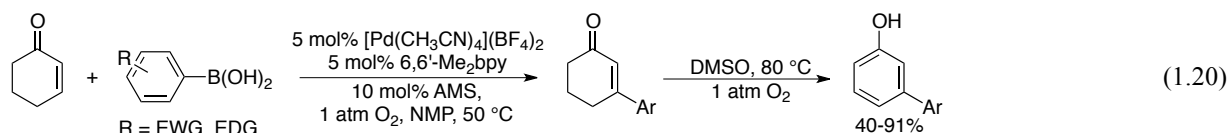
1.3.4 Quinoline/Pyridine-Oxazolines

1.3.4.1 Asymmetric Heck

In 2007, Jung reported an aerobic Pd-catalyzed asymmetric Heck coupling between arylboronic acids and electron-deficient olefins.[39] This reaction was a non-typical Heck coupling because the stereocenter formed upon carbopalladation was retained due to β-hydride elimination occurring distal to the site of nucleophilic attack (Scheme 1.20). Dmphen was found to promote this reaction in good yield, which encouraged the authors to pursue an enantioselective method by using chiral *bis*-oxazoline (box) and pyridine-oxazoline (pyrox) ligands (Scheme 1.20). The yield was relatively insensitive to the identity of the ligand, however the highest enantioselectivities (~42% ee) were obtained with the pyrox ligands.

Scheme 1.20. Comparison of Yield and Enantioselectivity as a Function of Ligand Identity

PhB(OH)$_2$ + [olefin]CHO → (5 mol% Pd(OAc)$_2$, 5.5 mol% ligand, 1 atm O$_2$, DMF, 24 °C, 16 h) → product CHO, Ph
(% yield, % ee)

Ligand

dmphen
85%, 0% ee

box
^{i}Pr, ^{i}Pr
71%, 16% ee

pyrox
R = ^{i}Pr; 71%, 25% ee
Ph; 69%, 21% ee
^{t}Bu; 76%, 42% ee
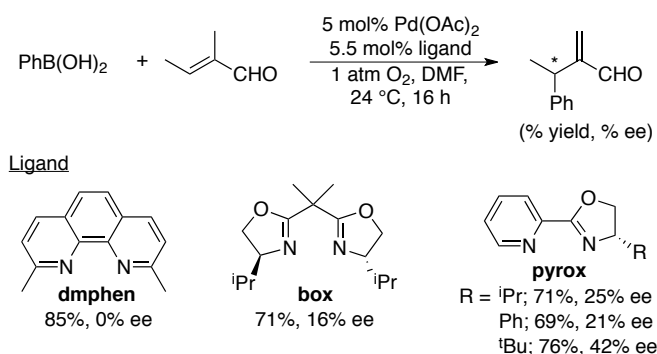
The authors noted that the moderately low observed ee could be due to the inefficient complexation of the ligand and metal prior to the reaction. As a result, the unligated Pd(OAc)$_2$ catalyst would be active and produce an achiral mixture, thus lowering the overall ee. This complication was partly solved by preforming the ligated catalyst, which allowed ee's >70% to be obtained for a variety of substrates (Scheme 1.21). The carbopalladation transition state was proposed to occur from a cationic Pd complex with a rigid bidentate ligand. The authors ascribed the observed enantioselectivity to the steric interaction between the olefin and the chiral group on the oxazoline.

Scheme 1.21. Improved Enantioselectivity from a Well-Defined Catalyst and Model for Enantioselectivity
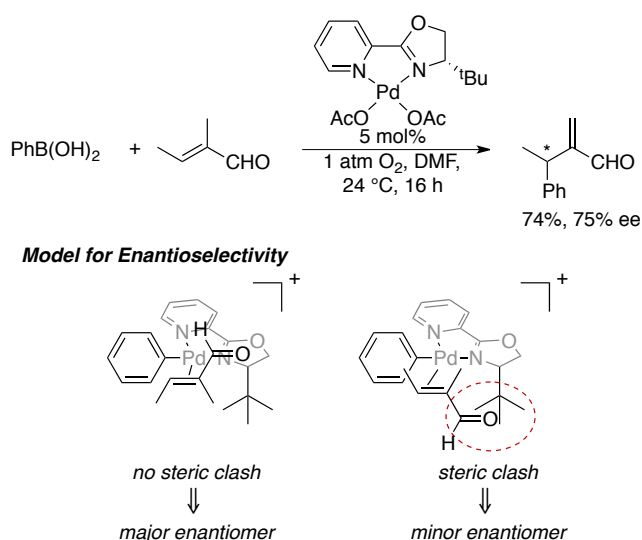
1.3.4.2 Asymmetric Dialkoxylation

Sigman reported an asymmetric, aerobic Pd-catalyzed dialkoxylation of *ortho*-vinyl phenols.[40] A previous investigation revealed that addition of the two nucleophiles does not involve a β-hydride elimination step but rather reductive elimination.[41] A quinone methide is formed after the first alkoxylation, which is activated towards nucleophilic attack by a second equivalent of alcohol (eq 1.21).

(1.21)
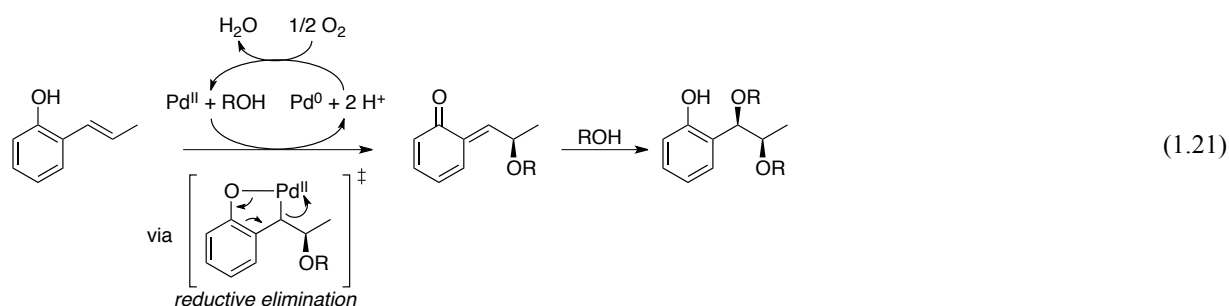
An enantioselective variant of this reaction was accessed by using a quinoline-oxazoline (quinox) ligand. Other ligands including various bioxazoline (biox), box and pyrox ligands were

also screened, however either low yields or poor enantioselectivity removed them from contention (Scheme 1.22). Addition of Cu salts eroded the enantioselectivity by exchanging ligands with the Pd catalyst.

Scheme 1.22. Influence of Ligands on the Yield and Enantioselectivity for Dialkoxylation
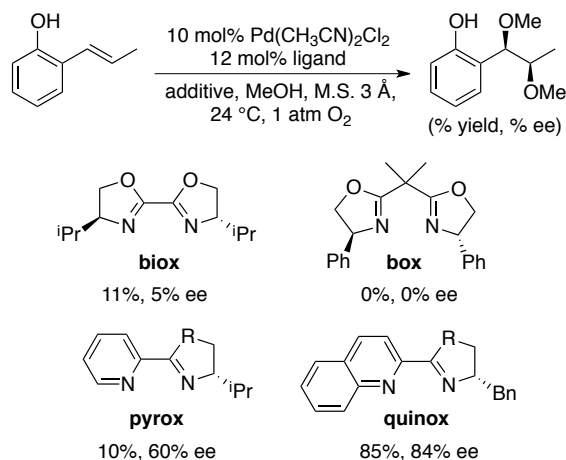
Using the Pd(OAc)$_2$/quinox catalyst system, a variety of substituted phenols and alcohols could be transformed to form the dialkoxylated product in good yields and enantioselectivity (Scheme 1.23). Additionally, a 1,4-dioxane moiety could be installed by using 1,2-ethanediol as a nucleophile. A follow-up paper applied this catalyst system using two different alcohol nucelophiles via an intra/intermolecular dialkoxylation.[42]

Scheme 1.23. Substrate Scope for the Asymmetric Dialkoxylation Reaction
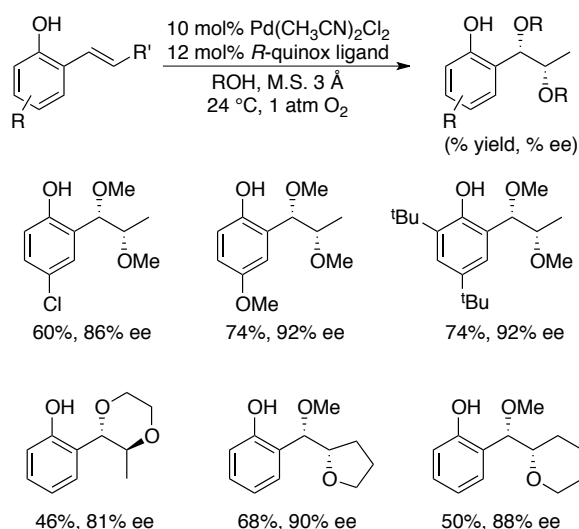
1.3.4.3 Asymmetric Aza-Wacker

In 2009, Yang reported an aerobic asymmetric Pd-catalyzed tandem C–N and C–C bond cyclization of *ortho*-allyl anilides.[43] A series of chiral diimine ligands, such as (–)-sparteine, box and pyrox, were screened but demonstrated either low yield or enantioselectivity (Scheme 1.24). Quinox ligands were found to be the most active ligands with the highest enantioselectivity. The ideal reaction conditions were found to employ a Pd(OAc)$_2$/quinox catalyst with TfNH and 2,6-lutidine as an acid/base mixture in toluene (Scheme 1.24).

Scheme 1.24. Influence of Ligands on the Yield and Enantioselectivity for the Tandem Cyclization
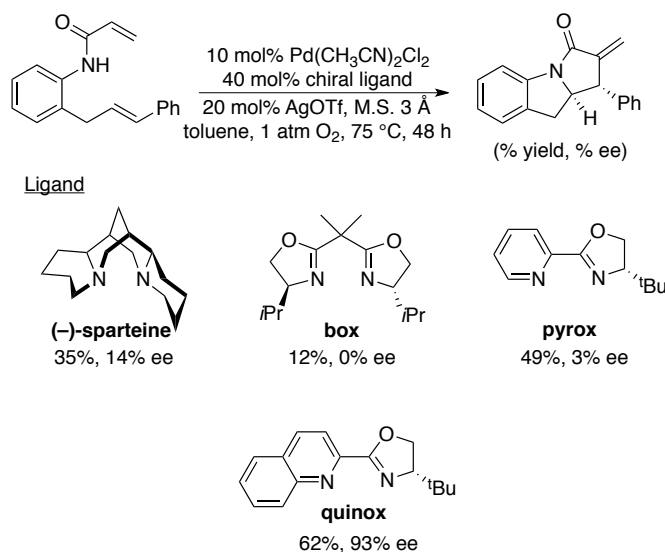
A small variety of substrates were investigated and each product exhibited modest to good yields and ≥80% ee despite the high reaction temperature (75 °C). The absolute configuration of one of the products was determined by X-ray crystallography to be *R* for the C–N center and *S* for the C–C center (Scheme 1.25). The combination of these two stereocenters necessarily arises from a tandem *cis*-amidopalldation (alkene insertion into the Pd–N bond) and *cis*-carbopalladation (alkene insertion into the Pd–C bond) mechanism. A stereochemical model was proposed where the alkene coordinates *trans* to the quinoline moiety and therefore experiences the full effect of the chiral steric group on the oxazoline ligand (Scheme 1.25). This steric interaction favors one of four possible alkene orientations, which undergoes amidopalladation and produces the correct enantiomer.

Scheme 1.25. Stereochemical Model for Observed Enantioselectivity in the Tandem Cyclization Reaction

Major Enantiomer
Favored TS

Minor Enantiomer
Disfavored TS

Minor Enantiomer
Disfavored TS

Major Enantiomer
Disfavored TS
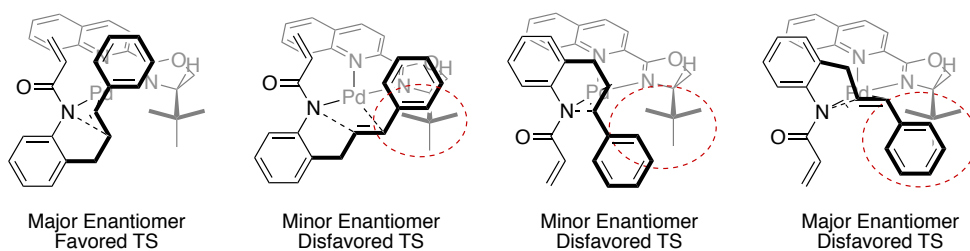
Stahl reported a comparable aerobic asymmetric Pd-catalyzed cyclization of aliphatic sulfonamides to produce chiral pyrrolidines.[44] Similar to Yang, biox and (–)-sparteine ligands resulted in poor yield and enantioselectivity (Scheme 1.26). Pyrox ligands were found to be slightly superior to the quinox ligands, giving >95% ee and modest to excellent yields. The catalyst system used a Pd(TFA)$_2$ salt with an excess of the chiral ligand in toluene at 50 °C (Scheme 1.26). The reaction temperature could be lowered to room temperature without any loss in yield by using a 24 h reaction time. The substrate scope was tolerant of simple substitution patterns along the alkyl chain. Replacement of the terminal methyl group with a benzyl group gave high yields and enantioselectivity.

Scheme 1.26. Influence of Ligands on the Yield and Enantioselectivity for the Aza-Wacker Cyclization
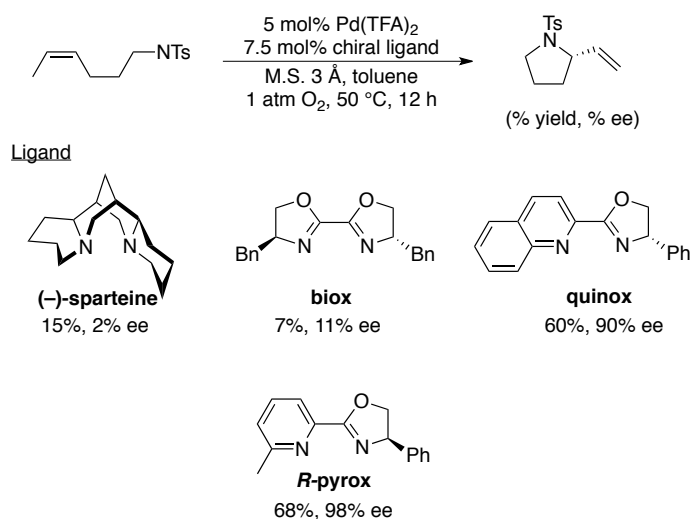
The mechanism of C–N bond formation was assumed to be alkene insertion into the Pd–N bond (*cis*-amidopalladation) due to the large precedent for this pathway in the aza-Wacker reaction. The reaction coordinate was calculated from the ligated-Pd catalyst through the amidopalladation step using DFT methods. Analysis of the data revealed that the origin of enantioselectivity was the steric interaction between the terminal methyl group and the phenyl group on the chiral oxazoline ligand (Scheme 1.27). Although these computations rationalized the observed enantioselectivity, a subsequent experimental mechanistic paper revealed that the C–N bond was formed via alkene activation by Pd[II] followed by nucleophilic attack of the sulfonamide (*trans*-amidopalladation).

Scheme 1.27. Proposed Origin of Enantioselectivity for the Aza-Wacker Cyclization Reaction
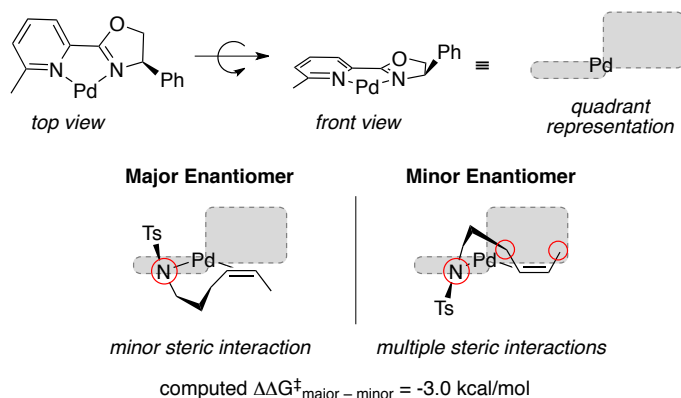
1.3.4.4 Mechanistic Studies of the Pd(TFA)₂/Pyrox-Catalyzed Aza-Wacker Cyclization

In 2012, Stahl reported the mechanism of amidopalladation for the Pd(TFA)$_2$/pyrox-catalyzed aza-Wacker cyclization.[45] The stereoforming step was investigated by using a stereolabeled deuterated substrate and the cyclized products were analyzed by chiral HPLC and ^{1}H/^{2}H NMR spectroscopy (Table 1.7). Rather than the assumed *cis*-amidopalladation (*cis*-AP) pathway, the reaction was observed to proceed exclusively through *trans*-amidopalladation (*trans*-AP). Furthermore, when Pd(OAc)$_2$ was used as the Pd salt, the mechanism switched to

cis-amidopalladation with concomitant erosion of the yield and enantioselectivity (Table 1.7). This reaction was a rare example of an aza-Wacker cyclization that proceeded through *trans*-AP and the origin of enantioselectivity was not obvious. A subsequent computational investigation that discusses the origin of enantioselectivity as a function of Pd^{II} salt as well as amidopalladation pathway is the subject of Chapter 5.

Table 1.7. Determining the Mechanism of Amidopalladation with a Stereolabeled Deuterated Substrate
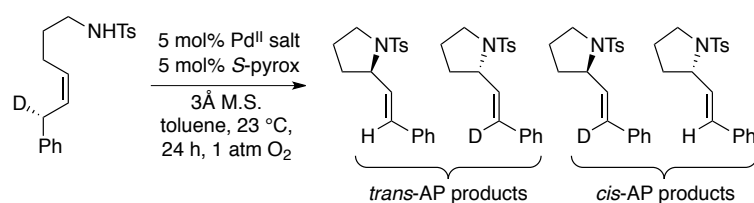
PdX$_2$	% yield	% ee	*trans*-:*cis*-AP
Pd(TFA)$_2$	90	96	>9:1
Pd(OAc)$_2$	48	20	1:9

1.3.4.5 Conclusions

The quinoline- and pyridine-oxazolines represent the primary class of ligands used for aerobic asymmetric Pd-catalyzed transformations. Despite the growing number of examples and transformations, there have been very few mechanistic investigations that probe the origin of enantioselectivity. Furthermore, it is intriguing that the quinox and pyrox ligand class support Pd-catalyzed oxidations when the majority of other chelating ligands inhibit reactivity. A possible explanation is the feature that dmphen, quinox and pyrox all have in common: a substituent *ortho* to the nitrogen of the pyridine ligand. For dmphen and pyrox, this is a methyl group whereas for quinox it is the quinoline methine. These steric groups have been shown to create distorted square-planar Pd^{II} complexes, which would be more reactive compared to typical bpy- or phen-ligated structures (Scheme 1.28).[46]

Scheme 1.28. Possible Origins for Enhanced Reactivity Observed for Quinox and Pyrox Ligands
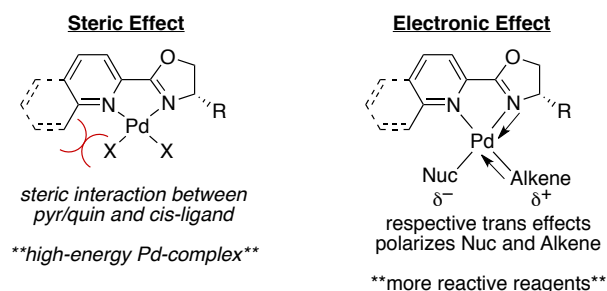
Additionally, the quinox and pyrox ligands consist of two different nitrogen heterocycles, which creates an electronically asymmetric coordination environment (Scheme 1.28). This allows for the opportunity to form an ideal arrangement of ligands based on their respective *trans* effect. The nucleophile has been proposed to coordinate *trans* to the oxazoline, which is a stronger *trans* donor than pyridine. The alkene electrophile then coordinates *trans* to pyridine, which is a weaker *trans* donor than an alkene. As a result, the nucleophile and electrophile become polarized (i.e. more anionic or cationic) as the nucleophile feels the effect of the *trans* influence from the oxazoline and the alkene exerts its *trans* influence on the pyridine. This process could effectively form more activated coupling partners and promote reactivity. Furthermore, these preferred binding positions permit the greatest stereocontrol to be obtained as the electrophile sits closest to the chiral functional group of the oxazoline. Chapter 5 will discuss some of these principles.

1.3.5 4,5-Diazafluoren-9-one (DAF)

1.3.5.1 Allylic Acetoxylation

The first application of DAF for aerobic Pd catalysis was reported by Stahl in the allylic acetoxylation of terminal olefins.[47] DAF was unique since it was the only ligand among mono- and bidentate ligands screened that promoted the acetoxylation reaction (Scheme 1.29). The reaction was tolerant of a variety of functional groups such as amides, esters and protected

alcohols, and aliphatic and benzylic substrates worked equally well. In glacial acetic acid, the product of aliphatic allylic acetoxylation was susceptible to alkene isomerization, which was inhibited by the introduction of a 3:1 dioxane:AcOH solvent system.

Scheme 1.29. Effect of Ligands on Aerobic Pd-Catalyzed Allylic Acetoxylation Reaction
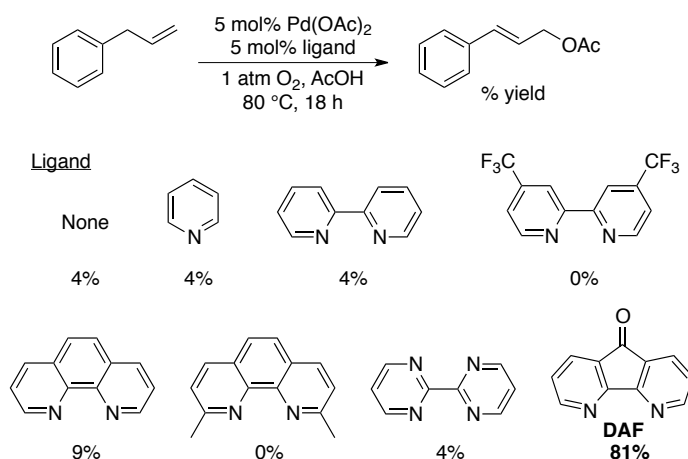
The ligand was initially conceived to create a more activated "Pd^{II}" by enabling a resonance structure with a formal Pd^{IV} oxidation state (Scheme 1.30). This concept was later questioned when dipyridyl ketone, which would have a similar resonance structure, was found to inhibit the reaction. Additionally, 9,9'-dimethyl-4,5-diazafluorene (Me$_2$DAF) was found to promote the reaction, albeit not as well as DAF, even though a resonance structure with Pd^{IV} does not exist for that ligand.

Scheme 1.30. Accessibility of an Activated Pd^{II} through Resonance with Pd^{IV}
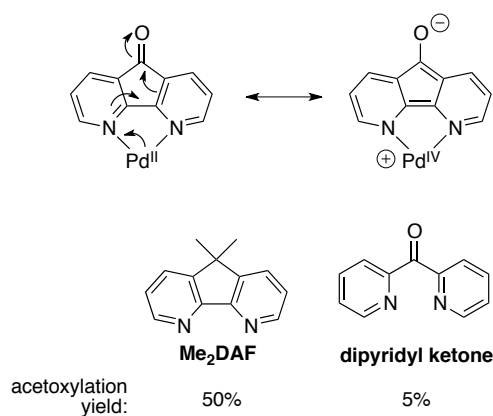
Preliminary mechanistic investigations revealed that C–H activation was an irreversible step. DAF promoted reductive elimination from a well-defined Pd(π-allyl) in the presence of O$_2$, whereas the bipyridine ligand was found to be unreactive. Furthermore, reductive elimination was found to be reversible and required O$_2$ to effectively trap the Pd^0-alkene adduct. Stahl proposed a catalytic cycle where a Pd(OAc)$_2$/DAF catalyst engages the allyl substrate in C–H activation (Scheme 1.31). The resulting cationic Pd(DAF)(π-allyl) undergoes a reversible reductive elimination step. The reaction of Pd^0 and dioxygen regenerates the catalyst and releases the allylic acetate product. Ongoing efforts in the Stahl lab are focused on understanding this mechanism further.

Scheme 1.31. Proposed Catalytic Cycle for the Pd(OAc)$_2$/DAF-Catalyzed Allylic Acetoxylation Reaction
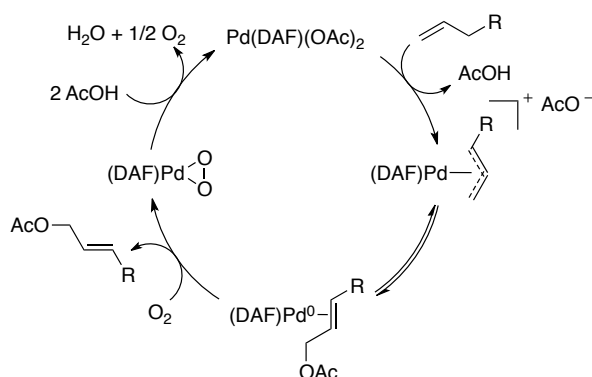
1.3.5.2 C–C Coupling of Indoles and Benzene

Shortly after publishing the Pd(OAc)$_2$/DAF-catalyzed allylic acetoxylation reaction, Stahl reported an aerobic Pd-catalyzed C–C coupling method of indoles and benzene using DAF and Me$_2$DAF as ligands.[48] The diazafluorene motif was found to be the most active catalyst among mono- and bidentate ligands screened (Scheme 1.32). Furthermore, the stereoselectivity of the reaction was governed by the identity of the Pd^{II} salt and ligand (Scheme 1.32).

Scheme 1.32. Effect of Ligand and Catalyst on Stereoselectivity for C–C Coupling
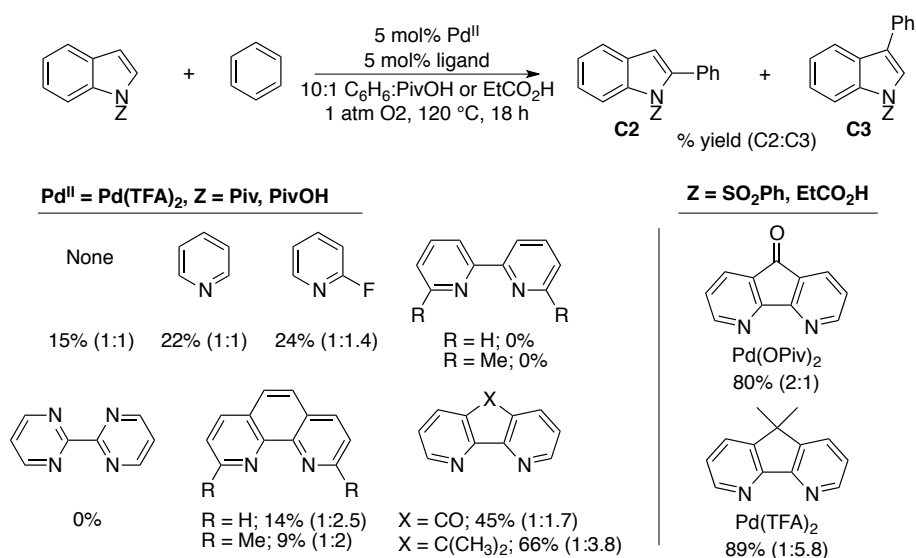
A preliminary mechanistic investigation revealed that C–H activation was a reversible process. H/D exchange was observed to occur exclusively at the C3 position in the presence of CD_3CO_2D and Pd^{II}/ligand, irrespective of the catalyst system used. A KIE of 2.8-3.8 was measured using the one-pot C_6H_6/C_6D_6 method, which was consistent with concerted metalation-deprotonation as the operative C–H activation method. These results provided circumstantial support for a transmetalation mechanism where two Pd^{II} catalysts separately activate the indole and benzene followed by arene transfer from one Pd to another.

1.3.5.3 Dehydrogenation of Linear Aldehydes and Ketones

The groups of Stahl[49] and Huang[50] reported back to back an aerobic Pd^{II}/DAF catalyst system that dehydrogenated the α,β-position of linear (and cyclic) ketones and aldehydes. In each of the methods, other mono- and bidentate ligands were found to inhibit the reaction or be inferior to DAF. The Stahl method used a $Pd(TFA)_2$ salt, which dehydrogenated dihydrocinnamaldehyde as well as linear and cyclic ketones equally in DMSO at 80 °C. The scope for linear substrates was limited by the necessity to have an aryl group in the β-position in order to prevent alkene isomerization (Scheme 1.33). Cyclic substrates were tolerated as long as only one location could be dehydrogenated. This was successfully applied to the synthesis of chromones and flavones. Cyclohexanone substrates underwent further dehydrogenation to afford the phenol.

Scheme 1.33. Substrate Scope for the Stahl Dehydrogenation Method
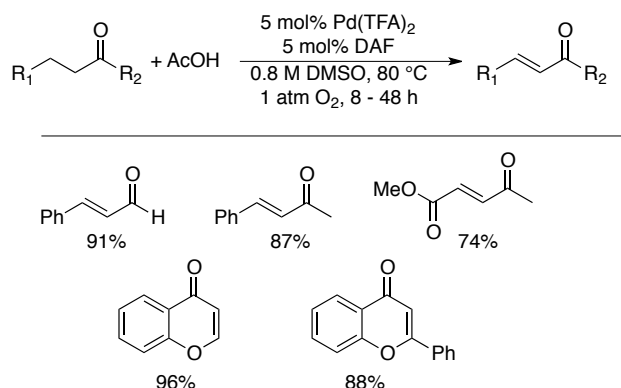
The Huang method used a Pd(OAc)$_2$ salt with catalytic K$_2$CO$_3$ in DMF at 30 °C. This method was milder than the Stahl method; however it was limited to only hydrocinnamyl aldehydes (Scheme 1.34). The conditions were not suitable for the dehydrogenation of ketones; however good yields could be obtained by performing the reaction at elevated temperature in the absence of DAF.

Scheme 1.34. Substrate Scope for the Huang Dehydrogenation Method
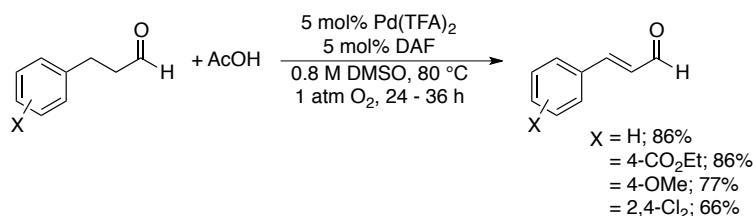
Selectively deuterated substrates at either the α- or β-positions were used to probe the rate-limiting step. A primary KIE of 2.6 was measured at the α-position whereas the KIE measured at the β-position was negligible. This indicated that C–H activation to form the Pd-enolate was rate-limiting followed by rapid β-hydride elimination and reoxidation (Scheme 1.35).

Scheme 1.35. Summary of Mechanistic Details for Pd/DAF-Catalyzed Dehydrogenation

1.3.5.4 Conclusions

The diazafluorene framework has proven to be a versatile ligand class that is able to promote a variety of Pd-catalyzed transformations. These ligands significantly differ geometrically from the traditional bpy framework. For example, DAF has a carbonyl group that bridges the 3,3' positions of bpy, which increases the distance between the two nitrogen atoms and shifts the orientation of the nitrogen lone pairs (Scheme 1.36). As a result, the DAF ligand would coordinate to a metal much more weakly than the bpy analog. Chapters 2 and 4 of this thesis are dedicated to understanding DAF's interaction with Pd^{II} and the role it plays in catalysis.

Scheme 1.36. Geometric Differences Between DAF and Bpy
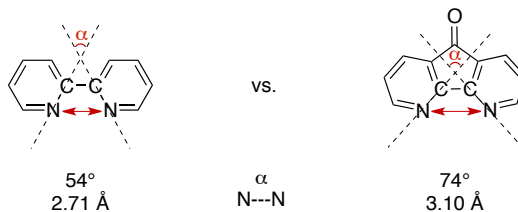
1.3.6 Summary of Bidentate Ligands

A common theme in the above sections is how substitution on the bipyridine ring can give rise to catalytic activity. The substitution has been particularly localized to the 3,3'- and 6,6'-positions (or 2,9-positions for phen). The diazafluorene ligands have functional groups that tie the 3,3'-carbons together and pinch the ligand back. The increased distance between the nitrogens results in forming weak complexes with transition metals. This phenomenon effectively overcomes, or at least lessens, the chelate effect, which is one of the greatest challenges when using bidentate ligands (Scheme 1.37).

Scheme 1.37. Mechanisms by which Substituted Bidentate Ligands Could Promote Reactivity
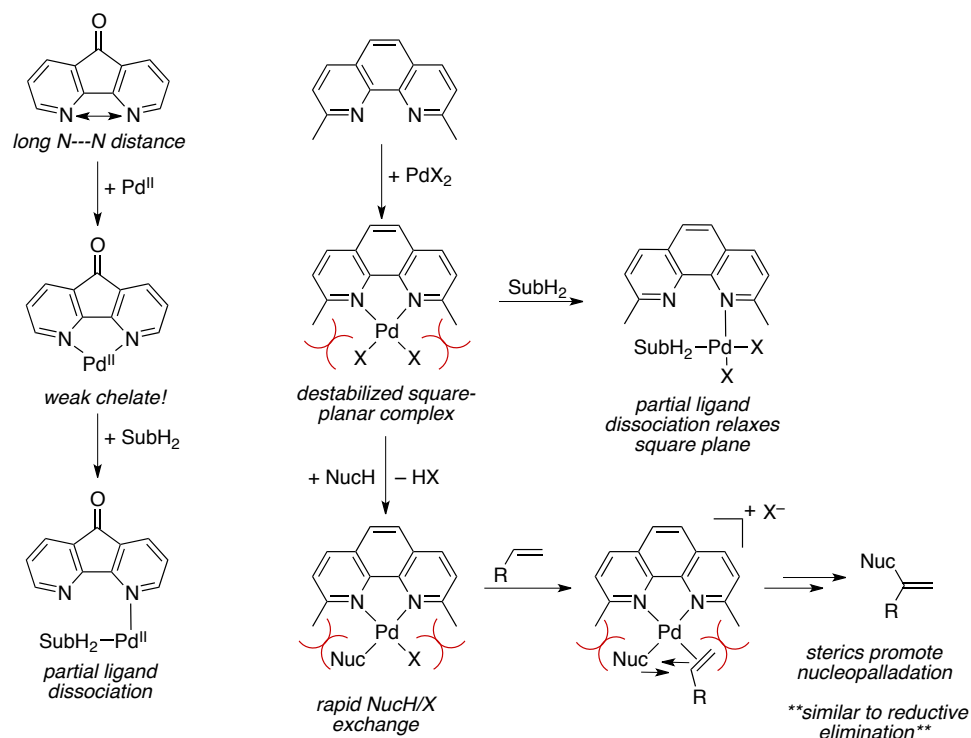
Alternatively, the dmphen, 6,6'-Me$_2$bpy, quinox and pyrox ligands all have substituents that project into the square plane. The resulting ligated Pd complex is distinctly more distorted than the standard bpy- or phen-ligated Pd^{II} complexes. The influence of these substituents would be

ubiquitous in the catalytic cycle. For example, they could help labilize counter-anions in order to readily accommodate a nucleophile such as an arene or amidate. These steric groups could also promote nucleopalladation similar to how bulky ligands promote reductive elimination in traditional Pd^0 chemistry. Or, the destabilized complex could have weak Pd–N bonds that would be readily displaced by an incoming substrate, which essentially overcomes the chelate effect challenge.

These are all interesting and valid explanations for the emergence of catalytic activity in substituted bidentate ligands. The literature currently lacks thorough mechanistic studies to understand the role of these ligands in catalysis. The work contained within this thesis aims to provide insight into the mechanism of how many of these bidentate ligands operate in catalysis. Chapter 2 focuses on DAF-Pd(OAc)$_2$ interactions in solution and describes potential intermediates that could exist along a catalytic cycle. Chapter 3 provides insight into how the electronics of the nitrogen nucleophile influence the amidopalladation and β-hydride elimination steps and highlights the challenges of using typical bipyridine ligands in Pd-catalyzed aza-Wacker reactions. Chapter 4 explores DAF and 6,6'-Me$_2$bpy as ligands for the Pd-catalyzed aza-Wacker cyclization reaction and investigates how they operate within the catalytic cycle. Chapter 5 provides a model for the observed enantioselectivity in the Pd(TFA)$_2$/pyrox-catalyzed asymmetric aza-Wacker cyclization and proposes an explanation for the loss of enantioselectivity when Pd(OAc)$_2$ is used as the Pd^{II} salt.

1.4 References

1. Stahl, S. S., *Angew. Chem. Int. Ed.* **2004,** *43*, 3400-3420.

2. For recent reviews, see: (a) Takacs, J. M.; Jiang, X. *Curr. Org. Chem.* **2003**, *7*, 369. (b) Cornell, C. N.; Sigman, M. S., *Inorg. Chem.* **2007,** *46*, 1903-1909. (c) Muzart, J., *Tetrahedron* **2007,** *63*, 7505-7521.

3. Keith, J. A.; Henry, P. M., *Angew. Chem. Int. Ed.* **2009,** *48*, 9038-9049.

4. McDonald, R. I.; Liu, G. S.; Stahl, S. S., *Chem. Rev.* **2011,** *111*, 2981-3019.

5. Several applications of this catalyst system to C–C coupling have been published but will not be discussed. See (a) Bee, C.; Leclerc, E.; Tius, M. A., *Org. Lett.* **2003,** *5*, 4927-4930. (b) Hibi, A.; Toyota, M., *Tetrahedron Lett.* **2009,** *50*, 4888-4891. (c) Feng, C.; Loh, T.-P., *J. Am. Chem. Soc.* **2010,** *132*, 17710-17712.

6. (a) Larock, R. C.; Hightower, T. R., *J. Org. Chem.* **1993,** *58*, 5298-5300. (b) Van Benthem, R. A. T. M.; Hiemstra, H.; Michels, J. J.; Speckamp, W. N., *J. Chem. Soc. Chem. Comm.* **1994**, 357-359. (c) Vanbenthem, R. A. T. M.; Hiemstra, H.; Longarela, G. R.; Speckamp, W. N., *Tetrahedron Letters* **1994,** *35*, 9281-9284. (d) Ronn, M.; Backvall, J. E.; Andersson, P. G., *Tetrahedron Lett.* **1995,** *36*, 7749-7752. (e) Larock, R. C.; Hightower, T. R.; Hasvold, L. A.; Peterson, K. P., **1996,** *61*, 3584-3585.

7. Peterson, K. P.; Larock, R. C., *J. Org. Chem.* **1998,** *63*, 3185-3189.

8. Steinhoff, B. A.; Fix, S. R.; Stahl, S. S., *J. Am. Chem. Soc.* **2002,** *124*, 766-767.

9. Steinhoff, B. A.; Stahl, S. S., *J. Am. Chem. Soc.* **2006,** *128*, 4348-4355.

10. Brasche, G.; Garcia-Fortanet, J.; Buchwald, S. L., *Org. Lett.* **2008,** *10*, 2207-2210.

11. McDonald, R. I.; Stahl, S. S., *Angew. Chem. Int. Ed.* **2010,** *49*, 5529-5532.

12. Lu, Z.; Stahl, S. S., *Org. Lett.* **2012,** *14*, 1234-1237.

13. Diao, T. N.; Stahl, S. S., *J. Am. Chem. Soc.* **2011,** *133*, 14566-14569.

14. (a) Izawa, Y.; Pun, D.; Stahl, S. S., *Science* **2011,** *333*, 209-213. (b) Pun, D.; Diao, T. N.; Stahl, S. S., *J. Am. Chem. Soc.* **2013,** *135*, 8213-8221.

15. For comprehensive reviews, see: (a) Calligaris, M.; Carugo, O. *Coord. Chem. Rev.* **1996**, *153*, 83-154. (b) Calligaris, M. *Coord. Chem. Rev.* **2004**, *248*, 351-375.

16. Bancroft, D. P.; Cotton, F. A.; Verbruggen, M. *Acta Crystallogr., Sect. C* **1989**, *45*, 1289-1292

17. Diao, T. N.; White, P.; Guzei, I.; Stahl, S. S., *Inorg. Chem.* **2012,** *51*, 11898-11909.

18. Schultz, M. J.; Park, C. C.; Sigman, M. S., *Chem. Commun.* **2002,** 3034-3035.

19. Nishimura, T.; Onoue, T.; Ohe, K.; Uemura, S., *Tetrahedron Lett.* **1998,** *39*, 6011-6014.

20. Nishimura, T.; Onoue, T.; Ohe, K.; Uemura, S., *J. Org. Chem.* **1999,** *64*, 6750-6755.

21. Steinhoff, B. A.; Stahl, S. S., *Org. Lett.* **2002,** *4*, 4179-4181.

22. Fix, S. R.; Brice, J. L.; Stahl, S. S., *Angew. Chem. Int. Ed.* **2002,** *41*, 164-166.

23. Ye, X. A.; Liu, G. S.; Popp, B. V.; Stahl, S. S., *J. Org. Chem.* **2011,** *76*, 1031-1044.

24. Ferreira, E. M.; Stoltz, B. M., *J. Am. Chem. Soc.* **2003,** *125*, 9578-9579.

25. Izawa, Y.; Stahl, S. S., *Adv. Synth. Catal.* **2010,** *352*, 3223-3229.

26. Unpublished work contributed by Dian Wang, who has given permission for its inclusion in this work.

27. Zhang, Y. H.; Shi, B. F.; Yu, J. Q., *J. Am. Chem. Soc.* **2009,** *131*, 5072-5074.

28. (a) Shiotani, A.; Itatani, H.; Inagaki, T., *J. Mol. Catal.* **1986,** *34*, 57-66. (b) Yoo, K. S.; Yoon, C. H.; Jung, K. W., *J. Am. Chem. Soc.* **2006,** *128*, 16384-16393. (c) Gasperini, M.; Ragaini, F.; Cenini, S.; Gallo, E.; Fantauzzi, S., *Applied Organomet. Chem.* **2007**, *21*, 782-787. (d) Hu, J.; Gu, Y.; Guan, Z.; Li, J.; Mo, W.; Li, T.; Li, G., *Chem. Sus. Chem.* **2011**, *4*, 1767-1772. (e) Ye, M.; Gao, G.-L.; Yu, J.-Q., *J. Am. Chem. Soc.* **2011**, *133*, 6964-6967. (f) Ben-Yahia, A.; Naas, M.; Kazzouli, S. E.; Essassi, E. M.; Guillaumet, G., *Eur. J. Org. Chem.* **2012**, 7075-7081.

29. Brink, G. J. t.; Arends, I. W. C. E.; Papadogianakis, G.; Sheldon, R. A., *Chem. Commun.* **1998,** 2359-2360.

30. (a) Wimmer, S.; Castan, P.; Wimmer, F. L.; Johnson, N. P., *Inorg. Chim. Acta* **1988,** *142*, 13-15. (b) Wimmer, S.; Castan, P.; Wimmer, F. L.; Johnson, N. P., *J. Chem. Soc. Dalton Trans.* **1989,** 403-412.

31. Brink, G.-J. t.; Arends, I. W. C. E.; Sheldon, R. A., *Science* **2000,** *287*, 1636-1639.

32. Brink, G.-J. t.; Arends, I. W. C. E.; Sheldon, R. A., *Adv. Synth. Catal.* **2002,** *344*, 355-369.

33. Andappan, M. M. S.; Nilsson, P.; Larhed, M., *Chem. Commun.* **2004,** 218-219.

34. Andappan, M. M. S.; Nilsson, P.; Schenck, H. v.; Larhed, M., *J. Org. Chem.* **2004,** *69*, 5212-5218.

35. Lindh, J.; Enquist, P. A.; Pilotti, A.; Nilsson, P.; Larhed, M., *J. Org. Chem.* **2007,** *72*, 7957-62.

36. Zheng, C. W.; Wang, D.; Stahl, S. S., *J. Am. Chem. Soc.* **2012,** *134*, 16496-16499.

37. Ref [36], see also: (a) Yasuda, H.; Watarai, K.; Choi, J. C.; Sakakura, T., *J. Mol. Catal. A: Chem.* **2005,** *236*, 149-155. (b) Qiu, S. F.; Xu, T.; Zhou, J.; Guo, Y. L.; Liu, G. S., *J. Am. Chem. Soc.* **2010,** *132*, 2856-2857. (c) Ragaini, F.; Larici, H.; Rimoldi, M.; Caselli, A.; Ferretti, F.; Macchi, P.; Casati, N., *Organometallics* **2011,** *30*, 2385-2393.

38. Izawa, Y.; Zheng, C. W.; Stahl, S. S., *Angew. Chem. Int. Ed.* **2013,** *52*, 3672-3675.

39. Yoo, K. S.; Park, C. P.; Yoon, C. H.; Sakaguchi, S.; O'Neil, J.; Jung, K. W., *Org. Lett.* **2007,** *9*, 3933-3935.

40. Zhang, Y.; Sigman, M. S., *J. Am. Chem. Soc.* **2007,** *129*, 3076-3077.

41. Schultz, M. J.; Sigman, M. S., *J. Am. Chem. Soc.* **2006,** *128*, 1460-1461.

42. Jensen, K. H.; Pathak, T. P.; Zhang, Y.; Sigman, M. S., *J. Am. Chem. Soc.* **2009,** *131*, 17074-17075.

43. He, W.; Yip, K.-T.; Zhu, N.-Y.; Yang, D., *Org. Lett.* **2009,** *11*, 5626-5628.

44. McDonald, R. I.; White, P. B.; Weinstein, A. B.; Tam, C. P.; Stahl, S. S., *Org. Lett.* **2011,** *13*, 2830-2833.

45. Weinstein, A. B.; Stahl, S. S., *Angew. Chem. Int. Ed.* **2012,** *51*, 11505-11509.

46. Ref [43]. See also (a) Newkome, G. R.; Fronczek, F. R.; Gupta, V. K.; Puckett, W. E.; Pantaleo, D. C.; Kiefer, G. E., *J. Am. Chem. Soc.* **1982,** *104*, 1782-1783. (b) Canty, A. J.; Skelton, B. W.; Traill, P. R.; White, A. H., *Aust. J. Chem.* **1992,** *45*, 417-422. (c) Milani, B.; Alessio, E.;

Mestroni, G.; Sommazzi, A.; Garbassi, F.; Zangrando, E.; Brescianipahor, N.; Randaccio, L., *J. Chem. Soc. Dalton Trans.* **1994,** 1903-1911.

47. Campbell, A. N.; White, P. B.; Guzei, I. A.; Stahl, S. S., *J. Am. Chem. Soc.* **2010,** *132*, 15116-15119.

48. Campbell, A. N.; Meyer, E. B.; Stahl, S. S., *Chem. Commun.* **2011,** *47*, 10257-10259.

49. Diao, T.; Wadzinski, T. J.; Stahl, S. S., *Chem. Sci.* **2012,** *3*, 887-891.

50. Gao, W. M.; He, Z. Q.; Qian, Y.; Zhao, J.; Huang, Y., *Chem. Sci.* **2012,** *3*, 883-886.

Chapter 2.

Structurally Diverse Diazafluorenone (DAF)-Palladium(II)

Complexes: Insights into the Utility of DAF as a Ligand in

Aerobic Oxidation Reactions

This work was done in collaboration with Dr. Charles Fry, Dr. Ilia Guzei and Brian Dolinar at

the University of Wisconsin–Madison

This work has been submitted for publication

2.1 Introduction

The renewed interest in Pd-catalyzed aerobic oxidation reactions over the past 10 to 15 years can be attributed, at least in part, to the identification of ancillary ligands that have enabled new synthetic transformations and support improved catalyst activity, selectivity, and stability.[1] The ligands tune catalyst sterics and electronics, thereby influencing elementary steps, such as ligand substitution, oxidative addition, reductive elimination and β-hydride elimination, and provide the basis for catalyst-controlled regio- and stereoselective transformations. Continued development and identification of new ligands remains an important goal to reduce catalyst loadings, enhance catalyst lifetimes and promote the discovery of novel transformations.

Pd-catalyzed aerobic oxidation reactions require the use of oxidatively stable ligands. Monodentate pyridine derivatives are especially common;[2] however, catalysts containing these ligands become increasingly susceptible to decomposition at elevated temperatures.[3] Catalyst stability can be enhanced through the use of bidentate ligands, such as 2,2'-bipyridine (bpy) and 1,10-phenanthroline (phen) derivatives, and such ligands have been used effectively in Pd-catalyzed aerobic oxidation reactions, typically in polar solvents (e.g., H_2O, DMSO, DMF)[4] or at high temperatures (120-200 °C).[5] These conditions are often needed to promote anionic ligand dissociation from (N~N)PdX$_2$ species to provide open coordination sites for substrate oxidation steps. Under mild conditions and/or in non-polar solvents, bidentate ligands such as bpy and phen often strongly inhibit Pd-catalyzed aerobic oxidation reactions.[6]

4,5-Diazafluoren-9-one (DAF) is a rare exception to the above observations. This ligand was identified as a uniquely active bipyridine-type ligand in Pd-catalyzed allylic acetoxylation of terminal olefins;[6b] other bidentate ligands, such as bpy and phen, inhibited the reaction (Scheme 2.1A). DAF was then found to be effective in several other Pd-catalyzed reactions, including oxidative C–C and C–O coupling of arenes,[7] dehydrogenation of cyclic ketones[8] and oxidative Heck reactions (Scheme 2.1).[9]

Scheme 2.1. Representative Pd-Catalyzed Aerobic Oxidation Reactions Promoted by DAF

Reaction	DAF	bpy	phen
A	81%	0%	9%
B	80%	0%	14%
C	87%	33%	36%
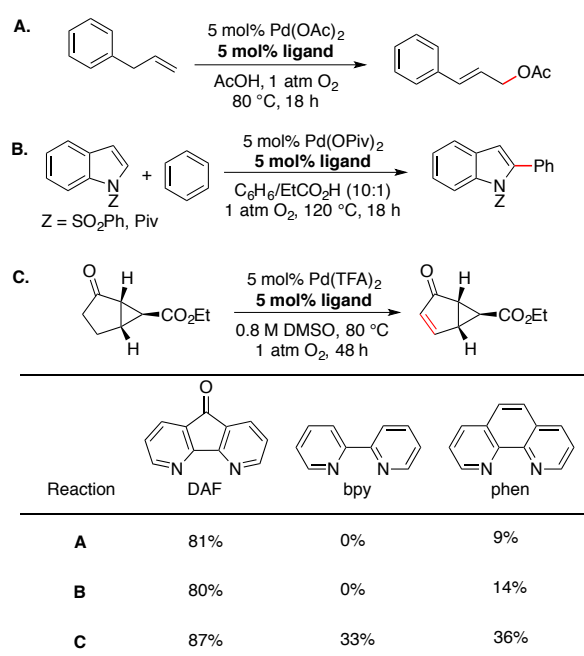
The beneficial effect of DAF in these reactions could arise from its unique coordination properties relative to more-traditional bidentate nitrogen ligands. Hints of unusual DAF coordination chemistry are evident from previously reported complexes with first-row transition metals[10] and palladium(0),[11] in which pentahapto (η^5), bridging (μ) and mondentate (κ^1) coordination modes have been identified, in addition to the traditional bidentate binding mode. On the other hand, previously characterized DAF-Pd^{II} complexes are limited to two examples (Scheme 2.2),[12] and both exhibit the canonical bidentate coordination mode.

Scheme 2.2. Previously Characterized DAF-Pd^{II} Coordination Complexes

ref 12   ref 6b
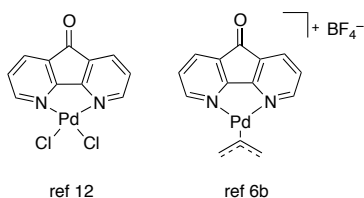
Here we show that the DAF-Pd^{II} coordination chemistry is much richer and more complex than the structures in Scheme 2.2 suggest. Through the use of multinuclear NMR spectroscopy, X-ray crystallography and density functional theory (DFT) calculations, we have identified and characterized six independent coordination complexes that arise from the combination of DAF and Pd(OAc)$_2$. These complexes include both monomeric and dimeric structures, in which DAF exhibits κ^1, κ^2, and μ coordination modes. These results are considered within the context of Pd^{II}-catalyzed oxidation reactions in which the unique coordination properties of DAF could facilitate substrate access to and activation by the Pd^{II} center.

2.2 Results

2.2.1 DAF:Pd(OAc)$_2$ Titration Experiments

^{1}H NMR spectroscopic analysis of a 1:1 mixture of DAF and Pd(OAc)$_2$ in CDCl$_3$ reveals the presence of a complex mixture of species (Figure 2.1). This spectrum contrasts the spectra obtained upon mixing more typical bidentate nitrogen ligands, such as 4,4'-^{t}Bu$_2$bpy and neocuproine (Figure 2.1). The latter solutions feature single Pd(κ^2-N~N)(OAc)$_2$ species, which have been described previously in the literature.[13]
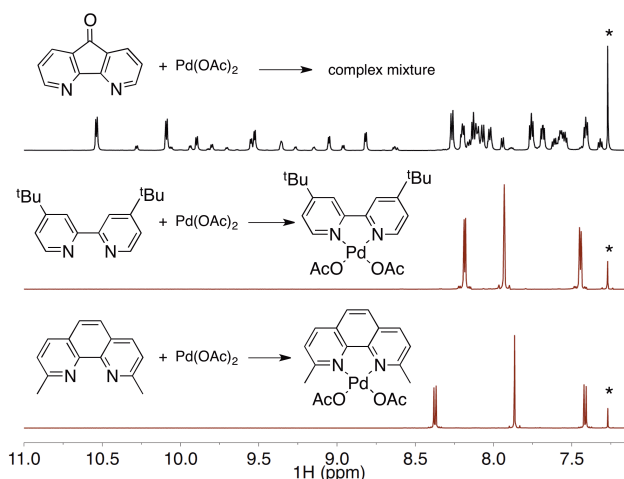
Figure 2.1. ^{1}H NMR spectra of 1:1 solutions of Pd(OAc)$_2$ and three different bidentate nitrogen ligands highlighting the unusual complexity of the DAF-Pd(OAc)$_2$ mixture. [Pd(OAc)$_2$] = 40 mM, [Ligand] = 40 mM, T = -45 °C (top) and 24 °C (middle and bottom), solvent = CDCl$_3$ (0.5 mL); The " * " corresponds to the CHCl$_3$ solvent peak.

In light of the complexity of the 1:1 DAF:Pd(OAc)$_2$ ^{1}H NMR spectrum, we performed a titration experiment in which different quantities of DAF were added to a solution of Pd(OAc)$_2$ (Figure 2.2A). The most diagnostic region of the ^{1}H NMR spectrum is from 8.6–10.9 ppm, where the *ortho* protons of the DAF ligand appear. With 0.5 equiv of DAF, a single peak assigned to species **A** predominates in this region of the spectrum. At 1 equiv of DAF, several pairs of resonances are evident, with the major pair assigned to species **B**. The pairs of resonances are attributed to Pd^{II} complexes with unsymmetrically coordinated DAF ligands. Free DAF is also present in this spectrum. When ≥ 2 equiv of DAF are added, only small quantities of **A** and **B** are present, and the spectra reveal four new species, three with unsymmetrical DAF ligands, **C**–**E**, and one with a symmetrical DAF ligand, **F**. The growth and/or decay of each of these species were tracked as a function of DAF equivalents (Figure 2.2C). This plot provided the conditions under which the concentration of individual species could be maximized to facilitate more thorough structural characterization.

The nomenclature employed for the spectral assignments is presented in Figure 2.2B. Within a given complex, protons belonging to each DAF ligand are labeled with the lower-case letter of the complex name, **a**–**f**. A superscript "0" is used to designate resonances associated with a symmetrical DAF ligand in which both pyridyl rings are coordinated to Pd. For complexes with monodentate (κ^1) DAF ligands, a superscript "1" is used to designate the coordinated ring, and a superscript "2" for the uncoordinated ring. Finally, subscripts *o*, *m*, and *p* are used to designate the *ortho*, *meta*, and *para* protons.

A) NMR Titration of DAF with Pd(OAc)$_2$

B) Nomenclature for Spectral Assignment

C) [Species] vs Equivalents DAF
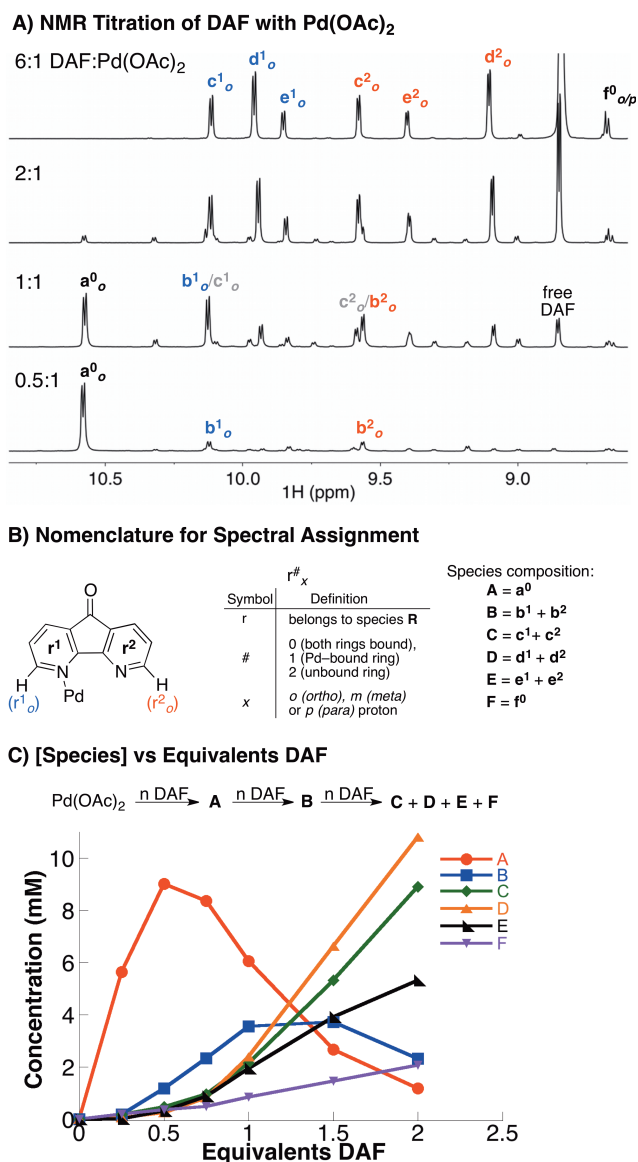
Figure 2.2. ^{1}H NMR spectra obtained from the titration of DAF with Pd(OAc)$_2$ at -45 °C (A). Description of the nomenclature used to assign resonances in the NMR spectra (B). Speciation plot associated with the six DAF-Pd(OAc)$_2$ complexes identified in the titration experiments (C).

2.2.2 Overview of Methods Used to Characterize DAF-Pd(OAc)$_2$ Complexes

The integration of the ^{1}H NMR peaks together with selective 1D TOCSY,[14] 1D and 2D ROESY[15] and ^{1}H-^{15}N HMBC[16] experiments provided key insights into the identity of complexes **A**–**F** (Scheme 2.3). The 1D TOCSY experiments enabled assignment of the *ortho*, *meta*, and *para* protons within individual rings of the DAF ligand, even when significant overlap was

present among resonances from different complexes. The ROESY experiments revealed through-space interactions between ligands within the Pd coordination sphere, including DAF↔DAF and DAF↔OAc interactions. ROESY experiments were used in place of NOESY experiments because the NOE sign and intensity depend on temperature and molecular size and can lead to false-negative results. These data, together with integration of the DAF and OAc resonances, were used to determine the DAF:OAc:Pd stoichiometry for each of the complexes **A**–**F**.

Scheme 2.3. Application of NMR Techniques for Structure Assignment
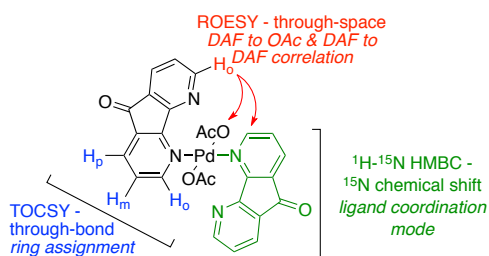
The ^{1}H-^{15}N HMBC experiment provided a means to determine the ^{15}N chemical shift of the DAF nitrogen atoms without isotopic enrichment, and this experiment clearly distinguished between coordinated and uncoordinated nitrogen atoms. Uncoordinated pyridine ligands exhibit ^{15}N chemical shifts at ~300 ppm, whereas Pd^{II}-coordinated pyridine ligands appear at ~200 ppm (Scheme 2.4).[17] These differences allowed distinction between monodentate and bidentate DAF coordination modes.

Scheme 2.4. Effect of Coordination on ^{15}N Chemical Shift

^{15}N Chemical Shift of Free and Coordinated Bpy

δ(^{15}N) = 307 ppm   δ(^{15}N) = 217 ppm

Application of ^{15}N Chemical Shift to DAF Coordination

δ(^{15}N) near 200 ppm   δ(^{15}N) near 200 and 300 ppm
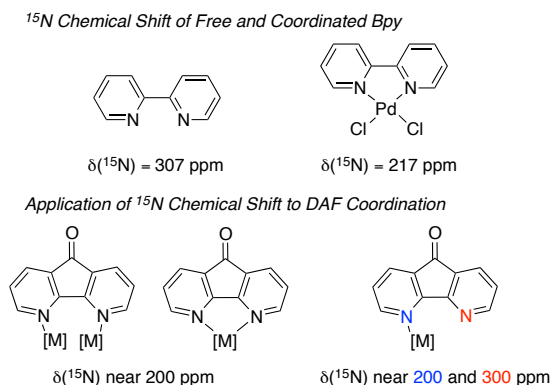
The NMR spectroscopic data was complemented by X-ray crystallography, which provided solid-state structural data that was compared to the solution-phase NMR data. Finally, DFT calculations facilitated structural assignment of the closely related structures **C–E**. Application of these techniques to determine the identity of complexes **A–F** is elaborated below.

2.2.3 Structural Assignment of A

The first species evident in the ligand titration is complex **A**. As mentioned previously, **A** grows to its maximum concentration at 0.5 equiv DAF, relative to Pd(OAc)$_2$. The TOCSY experiment correlates the three major ^{1}H resonances to the same DAF ring (Figure A2.2). The observation of only three DAF resonances indicates that the two DAF pyridyl rings are equivalent in **A** (Figure 2.3A). The ^{1}H-^{15}N HMBC spectrum reveals a single ^{15}N resonance at 204 ppm, indicating that $\mathbf{a^0}_o$ is associated with a coordinated pyridyl ligand (Figure 2.3B). The presence of both $^2J_{NH}$ and $^3J_{NH}$ cross-peaks in the HMBC spectrum complements the results from the TOCSY experiment and confirms that the resonances belong to the same complex.
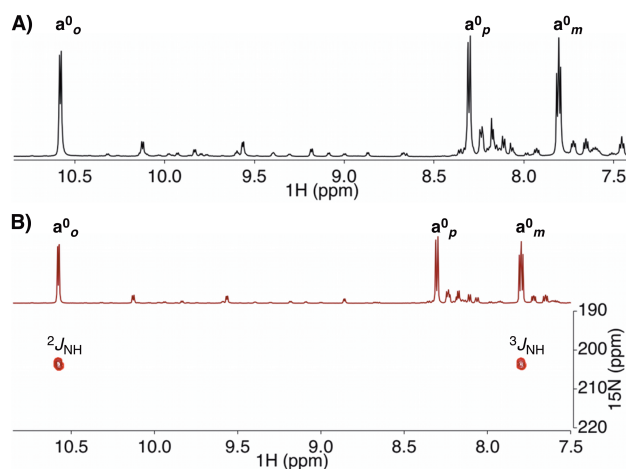
Figure 2.3. 1D ^{1}H (A) and ^{1}H-^{15}N HMBC spectra (B) of a solution of Pd(OAc)$_2$ and 0.5 equiv of DAF in CDCl$_3$, focusing on the aromatic spectral region. Cross-peaks for both 2- and 3-bond N–H coupling are observed. [Pd(OAc)$_2$] = 40 mM, [DAF] = 20 mM, T = -45 °C, solvent = CDCl$_3$ (0.5 mL). ^{1}H-^{15}N HMBC: o1 = 250 ppm, sw1 = 250 ppm, nt = 16, d1 = 4, ni = 256.

The integrated 1D ^{1}H NMR spectrum of **A** reveals a DAF:OAc stoichiometry of 1:4. A 1D ROESY experiment shows through-space interactions between the DAF ligand and two chemically distinct acetate ligands (Scheme 2.5, Figure A2.5). The integration of the two acetate resonances reflects three and six protons, corresponding to a DAF:OAc^1:OAc^2 ratio of 1:1:2. A third acetate peak is evident in the 1D ^{1}H NMR spectrum, but does not appear in the ROESY spectrum (Figure A2.5).

Scheme 2.5. Observed DAF to OAc ROE Correlations for **A**

ROE from **a^0$_o$** to OAc and OAc
OAc ≠ OAc
DAF:OAc:OAc = 1:1:2
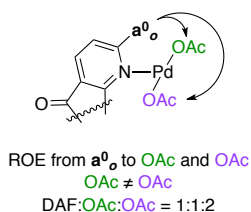
X-ray quality crystals were obtained from a 0.5:1 DAF:Pd(OAc)$_2$ mixture in CDCl$_3$, and diffraction analysis revealed a C_s-symmetric Pd^{II} dimer with a one DAF and two acetate ligands

bridging the two Pd atoms (Figure 2.4). Each of the Pd centers has an additional monodentate (κ^1) acetate ligand, which are eclipsed with respect to the Pd–Pd axis. Redissolution of the crystals in CDCl$_3$ reproduces the spectrum of **A** present in the 0.5:1 DAF:Pd(OAc)$_2$ solution.
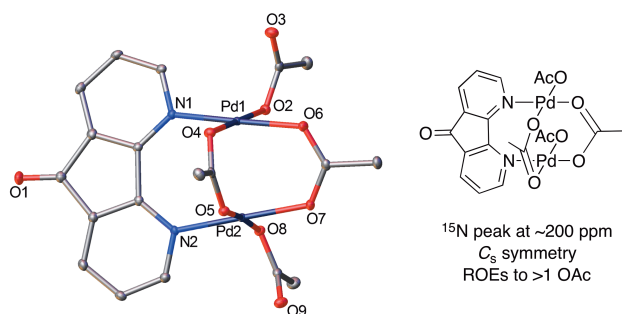
Figure 2.4. X-ray crystal structure of **A** and summary of NMR spectroscopic data supporting this structure in solution. The crystal structure is drawn with 50% probability ellipsoids and all H atoms are omitted for clarity.

This structure exhibits a mirror plane perpendicular to the Pd–Pd axis that rationalizes the chemical equivalence of two pyridyl rings of the DAF ligand evident in the 1D ^{1}H NMR spectrum. It also accounts for the ^{1}H-^{15}N HMBC data showing that both DAF pyridyl rings are coordinated to Pd. The μ-OAc and two κ^1-OAc ligands adjacent to the DAF ligand are the origin of the observed ROEs. The μ-OAc *trans* to the DAF ligand is too far from the DAF protons to be detected by the ROESY experiment.

2.2.4 Structural Assignment of B

Addition of more DAF to the solution of **A** results in conversion to **B**. Analysis of the resulting data revealed that **B** features two chemically distinct rings, **b**^{1} and **b**^{2} (Figure 2.5A). A Pd-bound pyridyl ring (**b**^{1}) is clearly evident from the ^{15}N resonance at 189 ppm, and an unbound ring (**b**^{2}) is associated with the resonance at 305 ppm (Figure 2.5B).
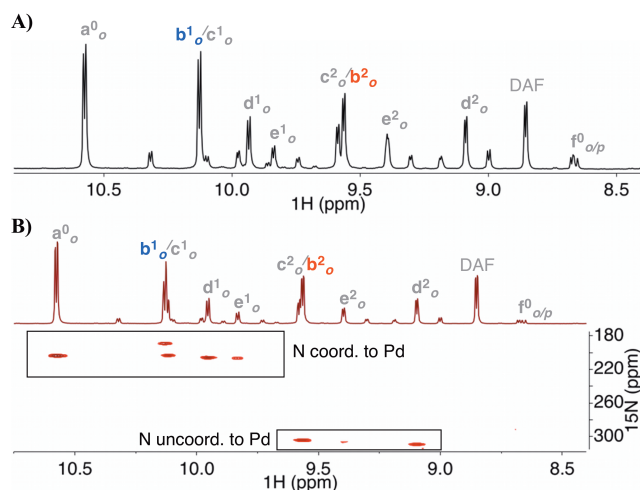
Figure 2.5. 1D ^{1}H (A) and ^{1}H-^{15}N HMBC spectra (B) of a solution of Pd(OAc)$_2$ and 1 equiv of DAF in CDCl$_3$, focusing on the aromatic spectral region. The resonances appearing at <220 ppm correspond to coordinated nitrogen atoms of DAF ligands, while those appearing at >300 ppm correspond to unbound nitrogen atoms. [Pd(OAc)$_2$] = 40 mM, [DAF] = 40 mM, T = -45 °C, solvent = CDCl$_3$ (0.5 mL). ^{1}H-^{15}N HMBC: o1 = 250 ppm, sw1 = 250 ppm, nt = 40, d1 = 6 s, ni = 256.

A 2D ROESY spectrum reveals two OAc cross-peaks for **B**, indicating that the complex contains chemically inequivalent acetate ligands (Figures A1.6 and A1.7). Furthermore, ROEs are observed from **b^1** and **b^2** to both of these acetates, confirming that **b^1** and **b^2** are present in the same complex (i.e., **B** = **b^1** + **b^2**) (Scheme 2.6). These conclusions are supported by corresponding 1D ROESY experiments in which each of the acetate resonances was selected. Integration of the DAF and OAc resonances in the 1D ^{1}H NMR spectrum reveals a DAF:OAc stoichiometry of 1:2.

Scheme 2.6. Observed DAF to OAc ROE Correlations for **B**

ROEs from **b^1_o** and **b^2_o** to OAc and OAc
OAc ≠ OAc
DAF:OAc:OAc = 1:1:1
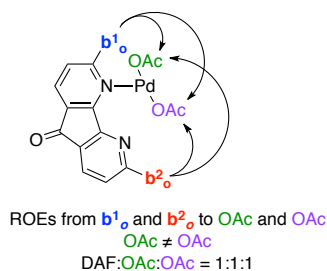
X-ray quality crystals were obtained from a 1.5:1 DAF:Pd(OAc)$_2$ mixture in CDCl$_3$, and diffraction analysis revealed a C_2-symmetric Pd^{II} dimer with two acetate ligands bridging the Pd atoms (Figure 2.6). Each Pd center is also coordinated by a κ^1-DAF and a κ^1-OAc ligand.
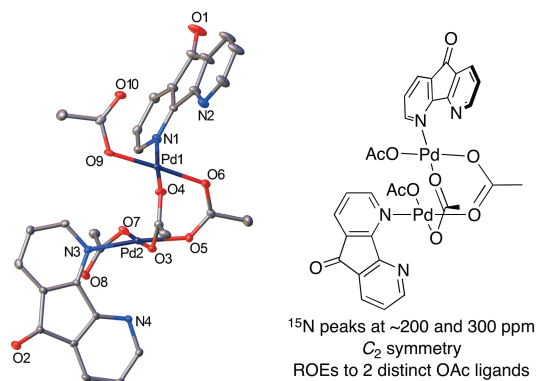
Figure 2.6. X-ray crystal structure of **B** and summary of NMR spectroscopic data supporting this structure in solution. The crystal structure is drawn with 50% probability ellipsoids and all H atoms are omitted for clarity.

A C_2 axis in this structure, perpendicular to the Pd–Pd axis and bisecting the two bridging acetate ligands, rationalizes the chemical equivalence of the two κ^1-DAF ligands and the pairs of μ- and κ^1-OAc ligands evident in the 1D ^{1}H NMR spectrum. This structure also accounts for the ^{1}H-^{15}N HMBC data showing both bound and unbound DAF pyridyl rings. The ROESY data showing through-space interactions between DAF and two chemically distinct acetate ligands are also readily rationalized by this structure.

2.2.5 Structural Assignment of C, D, and E

Addition of more DAF results in the conversion of species **A** and **B** into a mixture of four new species **C–F**. At a DAF:Pd(OAc)$_2$ ratio of 6:1, seven resonances associated with the *ortho* protons of the DAF ligand are present in the ^{1}H NMR spectrum, together with four distinct OAc peaks (Figures 2.7A, A1.9 and A1.11). Six of the seven DAF resonances correspond to three pairs of peaks with 1:1 integration, and they are assigned to species **C**, **D**, and **E**. The remaining

resonance is assigned to **F** and will be discussed separately below. The concentrations of **C**, **D**, and **E** exhibit a squared dependence on [DAF], suggesting these structures exhibit a 2:1 DAF:Pd stoichiometry (cf. Figure 2.2C). The ^{1}H-^{15}N HMBC spectrum reveals six cross-peaks for **C**, **D**, and **E** (Figure 2.7B), with c^1-e^1 corresponding to Pd-bound DAF pyridyl rings (203-207 ppm) and c^2-e^2 corresponding to unbound rings (304-310 ppm). The data indicate that each of the complexes **C**, **D**, and **E** contains DAF ligands bound in a κ^1 coordination mode.
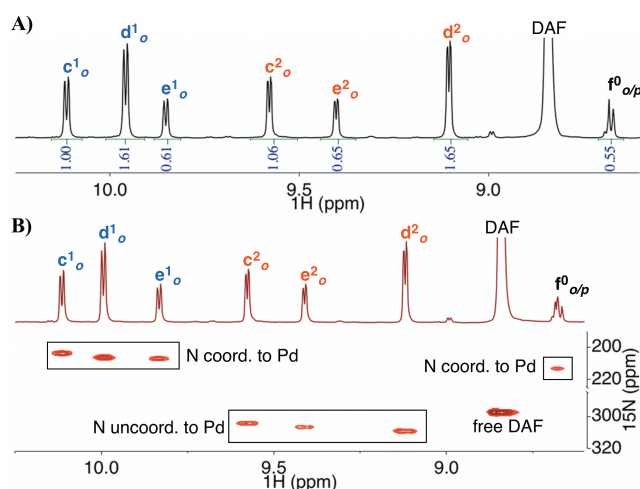
Figure 2.7. 1D ^{1}H (A) and ^{1}H-^{15}N HMBC spectra (B) of a solution of Pd(OAc)$_2$ and 6 equiv of DAF in CDCl$_3$, focusing on the aromatic spectral region. The resonances appearing at <220 ppm correspond to coordinated nitrogen atoms of DAF ligands, while those appearing at >300 ppm correspond to unbound nitrogen atoms. [Pd(OAc)$_2$] = 40 mM, [DAF] = 240 mM, T = -45 °C, solvent = CDCl$_3$ (0.5 mL). ^{1}H-^{15}N HMBC: o1 = 250 ppm, sw1 = 250 ppm, nt = 32, d1 = 4 s, ni = 256.

1D ROESY spectra for each complex reveal through-space interactions between the two (inequivalent) DAF *ortho* protons and a single acetate resonance (Scheme 2.7A and Figures A1.9 and A1.10). Furthermore, integration of the DAF and OAc resonances reveals a DAF:OAc ratio of 1:1 for each complex. The 1D ROESY experiments also reveal through-space interactions between the chemically inequivalent DAF *ortho* protons in **C** and **E** (i.e., from $c^1_o \leftrightarrow c^2_o$ and $e^1_o \leftrightarrow e^2_o$) but not in **D**. The distance between the *ortho* protons within an individual DAF ligand ($d \sim 7.0$ Å) is too large to show an ROE; however, these signals can arise from interactions between two independent DAF ligands within the same complex. Computational modeling shows that
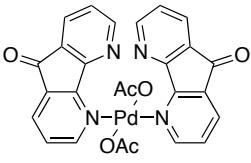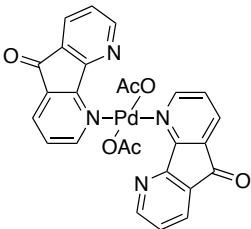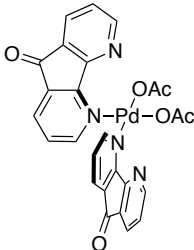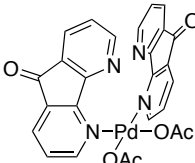
two DAF ligands with an *anti* relationship have *ortho* protons sufficiently close to exhibit an ROE (Scheme 2.7B and Figures A1.9 and A1.10). No ROE is expected for two DAF ligands with a *syn* relationship.

Scheme 2.7. Observed DAF↔DAF and DAF↔OAc ROE Correlations for **C–E**
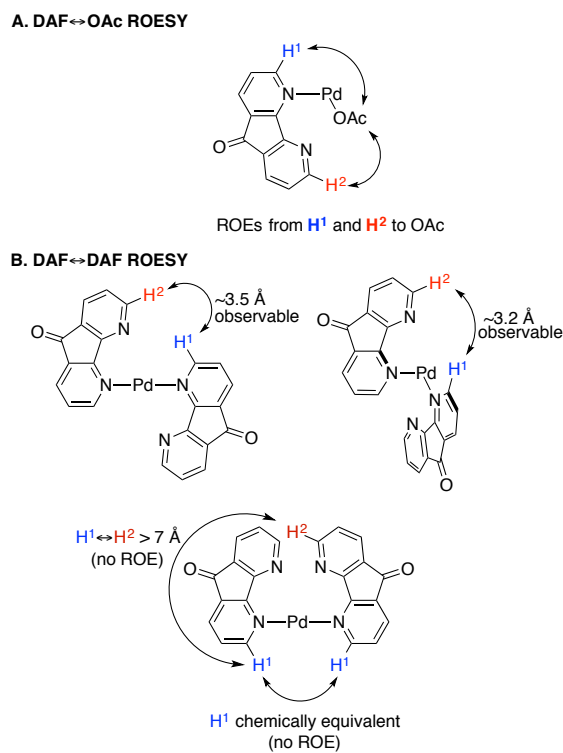
Four stereoisomers, **1**–**4**, satisfy the constraints of the NMR spectroscopic data (Table 2.1). These structures correspond to Pd(κ^1-DAF)$_2$(OAc)$_2$ complexes that are distinguished by *cis* vs. *trans* and *syn* vs. *anti* relationships between the two DAF ligands in the Pd coordination sphere. The viability of these structures is bolstered by characterization of one of these complexes by X-ray crystallography (Figure 2.8). The X-ray quality crystals were obtained from a 6:1 DAF:Pd(OAc)$_2$ mixture in CDCl$_3$.

Table 2.1. Assignments of **C**–**E** from NMR Spectroscopic and DFT Results

	1	**2**	**3**	**4**
DAF-DAF relation:	*trans/syn*	*trans/anti*	*cis/anti*	*cis/syn*
Static Point Group:	C_2	C_i	C_2	C_s
ΔG_{rel} (kcal/mol):	0.00	0.15	1.54	6.02
Assignment:	**D**	**E**	**C**	not observed
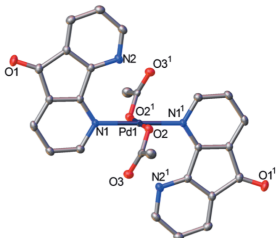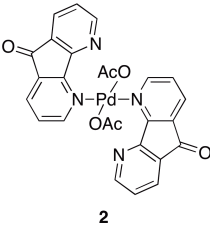
Figure 2.8. X-ray crystal structure of *trans/anti*-Pd(κ^1-DAF)$_2$(OAc)$_2$ **2**. The crystal structure is drawn with 50% probability ellipsoids and all H atoms are omitted for clarity.

The relative energies of structures **1**–**4** were assessed by performing DFT computations.[18] Structures **1**–**3** are within 1.6 kcal/mol of each other, with **1** having the lowest energy. Structure **4**, however, is significantly higher in energy (ΔG = +6.0 kcal/mol relative to **1**) and would have a population that would not be detected by NMR spectroscopy (Table 2.1). The higher energy of this complex can be rationalized by the steric clash between the *cis/syn* relationship between the two DAF ligands. These data suggest the three species detected in solution consist of a mixture of structures **1**, **2** and **3**.

The ROESY experiments reveal chemical exchange between **D** and **E** (Scheme 2.8A and Figure A2.9). The exchange process converts one of the DAF *ortho* protons in **D** ($\mathbf{d^1}_o$) into an

equal mixture of the two *ortho* protons in **E** (e^1_o and e^2_o). The temperature dependence of this exchange process was used to estimate an activation energy of $\Delta G^\ddagger = 13 \pm 0.5$ kcal/mol (Figure A2.12-13).[19] These observations can be rationalized by an intramolecular exchange process that interconverts the *trans/syn-* and *trans/anti*-bis-DAF complexes **1** and **2** (cf. Table 2.1). A mechanism for this process was identified by DFT methods, and the calculated barrier is 11 kcal/mol, which is in good agreement with the experimental value.

Scheme 2.8. Observation of and Proposed Mechanism for Chemical Exchange Between **D** & **E**

A. 1D ROESY Spectrum of Chemical Exchange Between D & E

B. Mechanism for Chemical Exchange Between D & E
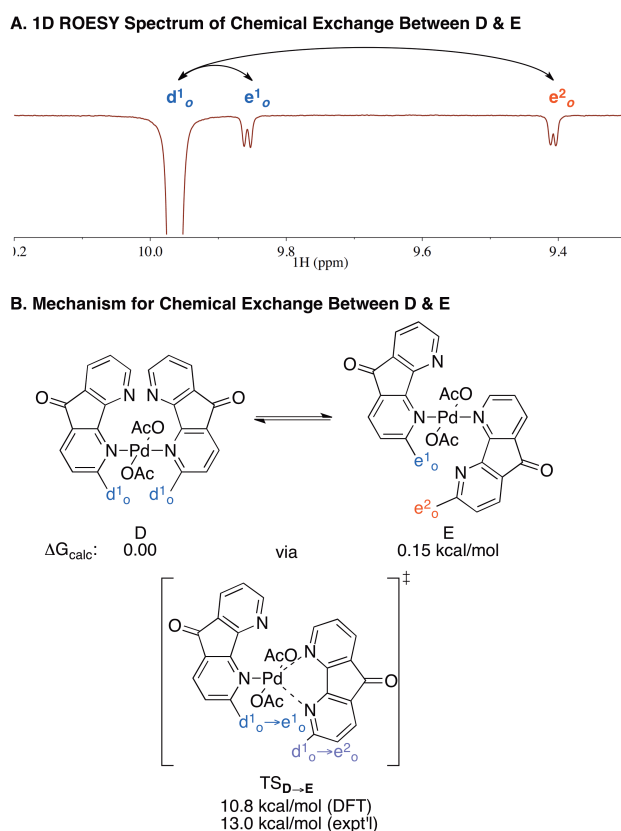
Together, the ROESY data and DFT computations enable structural assignment of complexes **C**–**E**. The DAF↔DAF ROEs observed for **C** and **E** (cf. Scheme 2.7) require an *anti* relationship between the DAF ligands and thereby limit these species to structures **2** and **3** (cf. Table 2.1). Because structure **4** has been excluded from consideration on the basis of DFT data, complex **D**

is assigned to the *trans/syn* structure **1**. The chemical exchange between **D** and **E** permits assignment of complex **E** to the *trans/anti* structure **2**. Thus, complex **C** corresponds to the *cis/anti* structure **3**.

2.2.6 Structural Assignment of F

Complex **F** appears together with **C–E** as the DAF concentration increases. Unlike **C–E**, however, its concentration increases with a linear (rather than squared) dependence on [DAF], suggesting that it exhibits a 1:1 DAF:Pd(OAc)$_2$ stoichiometry (cf. Figure 2.2C). The 1D ^{1}H NMR spectrum for **F** is consistent with a symmetrical DAF ligand, and ^{1}H-^{13}C HSQC, variable temperature and 1D TOCSY data show that the resonances at 8.66 ppm corresponds to both *ortho* and *para* protons (**f**$_{o/p}$ in Figure 2.7A; see also Figures A1.17-19). 1D ROESY data reveal a through-space interaction between the *ortho* proton of DAF and an acetate ligand. Integration of the acetate peak reveals a DAF:OAc stoichiometry of 1:2 (Figure A2.11). Finally, the ^{1}H-^{15}N HMBC spectrum (cf. Figure 2.7B) exhibits only a single cross-peak for **F** at 213.3 ppm, showing that the symmetrical pyridyl rings of the DAF ligand are coordinated to Pd. The monomeric structure in Scheme 2.9 is consistent with all of these data.

Scheme 2.9. Proposed Structure for **F**

^{15}N resonance at ~200 ppm
C_2 symmetry reflects DAF rings
ROEs to one OAc resonance
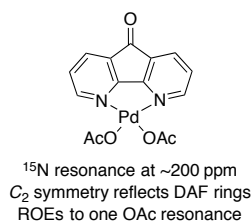
2.3 Discussion

2.3.1 Origin of Diverse Coordination Geometries with DAF

The results presented here highlight the rich coordination chemistry of DAF and Pd(OAc)$_2$. Numerous different structures have been characterized in which DAF exhibits bridging (μ), κ^1- and/or κ^2-binding modes. All but one of six structures identified here deviate from the bidentate chelating coordination mode typically associated with bipyridyl-type ligands. These results can be rationalized by the structural distortion of DAF relative to the traditional bpy framework. DAF has a carbonyl group that bridges the 3/3' positions of bpy, which increases the distance between the two nitrogen atoms and shifts the orientation of the nitrogen lone pairs (Scheme 2.10). Both of these geometrical changes contribute to DAF being a less favorable bidentate ligand relative to bpy and phen.

Scheme 2.10. Structural Comparison of Bipyridine and DAF.
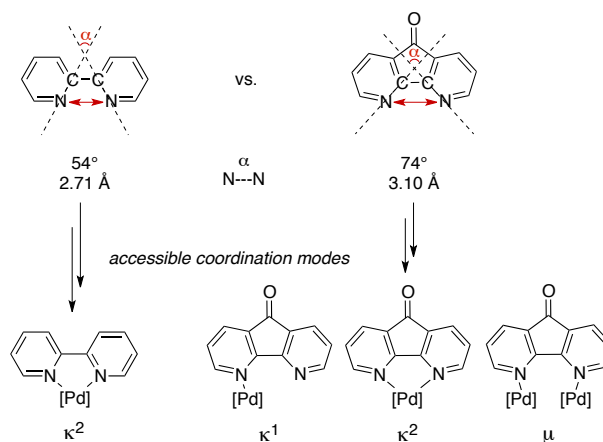
2.3.2 Relevance to Aerobic Oxidation Catalysis

The unique coordination chemistry of DAF has important implications for Pd-catalyzed aerobic oxidation reactions. The simplified mechanism of these catalytic reactions consists of two half-reactions: substrate oxidation by Pd^{II} and catalyst reoxidation by O$_2$ (Scheme 2.11). The turnover-limiting step in most (if not all) of these reactions is associated with the Pd^{II}-mediated

substrate oxidation half-reaction and corresponds to one of various fundamental steps, such as ligand substitution (i.e., substrate binding), alkene insertion (e.g., into a Pd–C or Pd–N bond), β-hydride elimination or C–H activation. Ligand steric and electronic properties influence the rate of the Pd^{II}-mediated reaction steps, and one or more ligands typically must dissociate from Pd^{II} to provide coordination sites for substrate reactivity. Steps associated with the catalyst reoxidation half-reaction are typically fast, by comparison, but ancillary ligands still play an important role.[20] Ligands not only promote the reaction of O_2 with Pd^0, but they also can minimize catalyst aggregation into inactive metallic Pd ("Pd-black").[21]

Scheme 2.11. Representative Catalytic Cycle for Pd-Catalyzed Aerobic Oxidations.
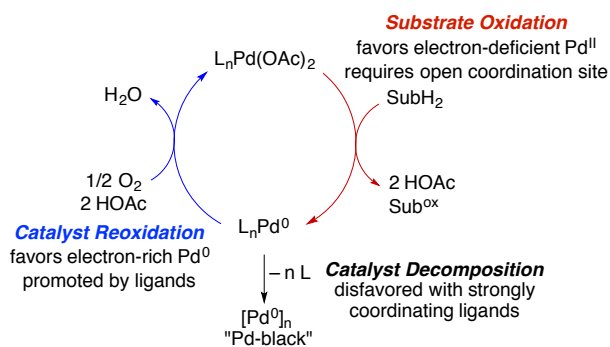
Neutral monodentate ligands, such as pyridine, triethylamine (NEt_3) and DMSO, have been widely used in Pd-catalyzed aerobic oxidation reactions,[1] and typical catalyst systems employ a 2:1 $L:Pd^{II}$ stoichiometry. Mechanistic studies have revealed that faster initial rates may be obtained with a 1:1 $L:Pd^{II}$ stoichiometry, which enhances substrate accessibility to the Pd^{II} coordination sphere.[22] The use of $\geq$ 2:1 $L:Pd^{II}$ stoichiometry in reported catalyst systems represents the optimal balance between catalyst activity and stability. At $L:Pd^{II}$ ratios < 2:1, the catalyst often decomposes before the reaction reaches full conversion.

Bidentate ligands are appealing because they enhance catalyst stability, but they often inhibit catalytic turnover. The chelate effect disfavors neutral ligand dissociation and, therefore, anionic

ligand dissociation is required to enable substrate access to the Pd^{II} coordination sphere. Formation of a charged complex has a strong solvent dependence, as illustrated by a recent study of amidopalladation of alkenes with a $(bpy)Pd^{II}(amidate)Cl$ complex (Scheme 2.12).[23] Alkene insertion does not proceed in toluene, while it proceeds readily in DMSO at room temperature. The reaction was shown to proceed via pre-equilibrium dissociation of chloride, which is strongly inhibited in a non-polar solvent.

Scheme 2.12. Solvent Effect on X-Type Ligand Dissociation

Solvent Effect
Toluene: No reaction
DMSO: Rapid reaction at rt;
Chloride inhibition
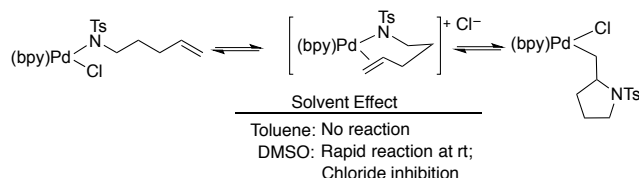
The structures of $DAF-Pd(OAc)_2$ complexes presented herein show that DAF exhibits properties of both mono- and bidentate ligands. And, the empirical success of DAF in Pd-catalyzed aerobic oxidation reactions suggests that DAF can take advantage of the beneficial features of both ligand types. The κ^1 coordination mode, evident in structures **B–E**, provides access to open coordination sites at Pd^{II} without requiring dissociation of an anionic ligand. This feature should stabilize intermediates and/or transition states associated with key substrate oxidation steps, such as C–H activation, alkene insertion or β-hydride elimination (Scheme 2.13).[7-9] On the other hand, the bidentate character of DAF evident in **F**, $Pd(DAF)(\eta^3\text{-allyl})]^{+}$[6b] and $Pd(DAF)Cl_2$[12] provides a means to enhance catalyst stability upon formation of Pd^0 in the catalytic cycle.

Scheme 2.13. Proposed Intermediates and Transition States in DAF-Promoted Catalysis
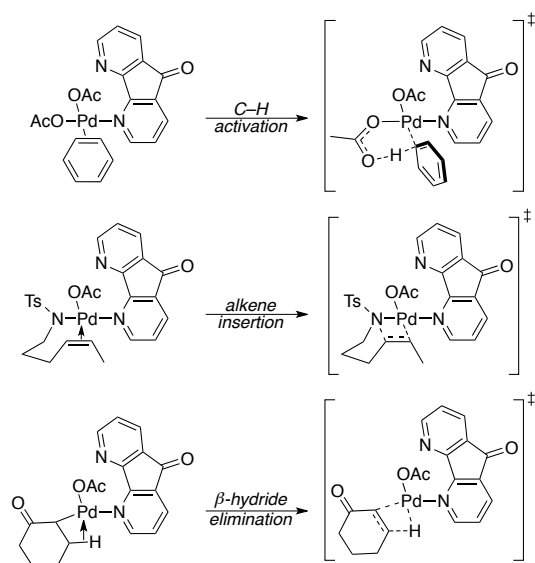
The principles discussed here have implications for other Pd-catalyzed oxidation reactions. Of particular note are the allylic and aromatic C–H oxidation reactions that employ 2,2'-bipyrimidine (bpm)-Pd[II] catalysts, reported recently by Bercaw/Labinger [24 a] and Yin,[24b] respectively (Scheme 2.14). These reactions are promoted by coordination of the bpm ligand to a second metal, Pd[II] or Al[III]. This coordination could lead to a structural distortion similar to that has been characterized for DAF in the present study.[25] Further investigation of this concept in catalytic reactions is the focus of ongoing investigation.

Scheme 2.14. Pd(bpm)(OAc)$_2$-Catalyzed C–H Oxidation Reactions Promoted by Ligand Coordination to a Second Metal.
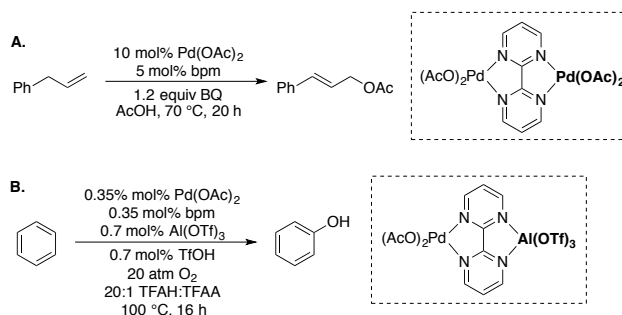
2.4 Conclusion

The rich coordination chemistry of diazafluorenone (DAF)-Pd(OAc)$_2$ has been characterized by diverse NMR spectroscopic methods, X-ray crystallography and DFT calculations. In particular, ^{1}H-^{15}N HMBC and ROESY experiments played a critical role in determining the coordination mode of the DAF ligand in solution. The data show that DAF is able to adopt bridging (μ), chelating (κ^2) and monodentate (κ^1) coordination modes in monomeric and dimeric Pd^{II} complexes. Six different structures have been characterized. The equilibrium population changes systematically as a function of [DAF], with monomeric structures favored at higher [DAF]. The hemilabile character of DAF provides a compelling rationale for the beneficial reactivity of DAF, relative to other bidentate ligands, in Pd-catalyzed aerobic oxidation reactions, and it provides a valuable foundation for future studies in this field.

Contributions: Dr. Charlie Fry assisted with the initial 1H-15N HMBC experimental set up and was a source of consulting. Dr. Ilia Guzei and Brian Dolinar were the X-ray crystallographers who obtained and solved all the X-ray diffraction patterns.

2.5 Experimental

2.5.1 General Experimental Considerations

All commercially available compounds were used as received. $CDCl_3$ for NMR spectroscopy was filtered through dry K_2CO_3 to remove residual HCl prior to use. All samples were prepared in a teflon-capped scintillation vial and placed in a dark location a day in advance to allow the species to equilibrate prior to data acquisition. ^1H and ^{15}N NMR spectra were recorded on a Varian INOVA 600 MHz or Bruker Avance-500 spectrometer. ^1H NMR chemical shifts are reported in parts per million relative to internal TMS (0.00 ppm) in $CDCl_3$. ^{15}N NMR chemical shifts are reported in parts per million and referenced using the ^1H spectrum to liquid ammonia (0.00 ppm). In cases where spectral overlap occurred, integrations were obtained by using line-fitting routines in the MestReNova v. 8.02 software package. The sample temperature was calibrated with an external 4% MeOH in MeOD-d_3 reference standard. The pw90 and longest T_1 values were computed from the pw360 and inversion recovery experiments, respectively, after each temperature change. All standard ^1H spectra were recorded quantitatively (recycle delay $\geq$ 5*T_1) and integrals referenced to an internal standard (1,3,5-trimethoxybenzene). Selective TOCSY and ROESY experiments were used as implemented in Varian ChemPack 3.1 and were performed using SEDUCE shaped pulses with spinlock frequencies of 8.5 kHz and 5.4 kHz, respectively.

Crystals of complexes **A**, **B** and **E** were grown by vapor diffusion of pentane or hexane into 20-40 mM $CDCl_3$ solutions of $Pd(OAc)_2$ with various quantities of DAF (**A**: 0.5 equiv, **B**: 1.0 equiv, **E**: 6 equiv). Optimal crystals were grown in a room held at a constant 4 °C. Complex **A** produced a nearly quantitative amount of crystals whereas **B** and **E** were significantly more challenging to grow and produced few crystals. The details of the X-ray data collection can be found below for each of the complexes.

2.5.2 General Computational Considerations.

All computations were performed with the Gaussian 09 program[26] using resources provided by University of Wisconsin–Madison Chemistry Department. Spin-restricted density functional theory (DFT) calculations were performed with the hybrid density functional, rB3LYP.[27,28] A

combination of the Stuttgart RSC 1997 ECP/triple-ζ basis[29] for Pd and the all-electron 6-31+G(d) basis set for all other atoms was used for gas-phase geometry optimizations and normal mode analyses. Full geometry optimizations were carried out in internal coordinates using the default Berny algorithm. Frequency calculations were performed at the optimized geometries to confirm that each geometry had the appropriate number of imaginary frequencies: zero for minima or one for transition states. The imaginary frequency identifying a saddle-point was visually inspected for the proper motion.

At the calculated stationary points, solvation-corrected single-point total energy calculations were carried out with the Pd basis detailed above and the 6-311+G (d,p) basis on all other atoms with electrostatic and non-electrostatic solvation effects evaluated using the polarizable-continuum model (PCM). The solvation cavity was generated using UFF radii, explicitly treating hydrogen atoms, and the radii were scaled by a factor of 1.2. The solvent chosen was chloroform.

Contributions: Dr. Charlie Fry assisted with the initial ^{1}H-^{15}N HMBC experimental setup and consultation. Dr. Ilia Guzei and Brian Dolinar acquired and solved X-ray crystallographic data.

2.6 References

1. For leading reviews, see: (a) Stahl, S. S., *Angew. Chem. Int. Ed.* **2004,** *43*, 3400-3420. (b) Gligorich, K. M.; Sigman, M. S., *Chem. Commun.* **2009,** 3854-3867.

2. For representative examples, see the following: (a) Nishimura, T.; Onoue, T.; Ohe, K.; Uemura, S., *J. Org. Chem.* **1999,** *64*, 6750-6755. (b) Fix, S. R.; Brice, J. L.; Stahl, S. S., *Angew. Chem. Int. Ed.* **2002,** *41*, 164-166. (c) Ferreira, E. M.; Stoltz, B. M., *J. Am. Chem. Soc.* **2003,** *125*, 9578-9579. (e) Iwasawa, T.; Tokunaga, M.; Obora, Y.; Tsuji, Y., *J. Am. Chem. Soc.* **2004,** *126*, 6554-6555. (f) Zhang, Y.-H.; Shi, B.-F.; Yu, J.-Q., *J. Am. Chem. Soc.* **2009,** *131*, 5072-5074. (g) Izawa, Y.; Stahl, S. S., *Adv. Synth. Catal.* **2010,** *352*, 3223-3229.

(h) Izawa, Y.; Pun, D.; Stahl, S. S., *Science* **2011,** *333*, 209-213.

3. (a) Steinhoff, B. A.; Guzei, I. A.; Stahl, S. S., *J. Am. Chem. Soc.* **2004,** *126*, 11268-11278. (b) Komano, T.; Iwasawa, T.; Tokunaga, M.; Obora, Y.; Tsuji, Y., *Org. Lett.* **2005,** *7*, 4677-4679. (c) Kubota, A.; Emmert, M. H.; Sanford, M. S., *Org. Lett.* **2012,** *14*, 1760-1763.

4. (a) Brink, G.-J. t.; Arends, I. W. C. E.; Papadogianakis, G.; Sheldon, R. A., *Appl. Catal., A* **2000**, 435-442. (b) Hu, J.; Gu, Y.; Guan, Z.; Li, J.; Mo, W.; Li, T.; Li, G., *Chem. Sus. Chem.* **2011**, *4*, 1767-1772. (c) Ye, M.; Gao, G.-L.; Yu, J.-Q., *J. Am. Chem. Soc.* **2011**, *133*, 6964-6967. (d) Ben-Yahia, A.; Naas, M.; Kazzouli, S. E.; Essassi, E. M.; Guillaumet, G., *Eur. J. Org. Chem.* **2012**, 7075-7081.

5. Ref 4b and 4c. See also: (a) Shiotani, A.; Itatani, H.; Inagaki, T., *J. Mol. Catal.* **1986,** *34*, 57-66. (b) Gasperini, M.; Ragaini, F.; Cenini, S.; Gallo, E.; Fantauzzi, S., *Applied Organomet. Chem.* **2007**, *21*, 782-787.

6. Ref 2g and the following: (a) Andappan, M. M. S.; Nilsson, P.; Larhed, M., *Chem. Commun.* **2004**, 218-219. (b) Campbell, A. N.; White, P. B.; Guzei, I. A.; Stahl, S. S., *J. Am. Chem. Soc.* **2010**, *132*, 15116-15119. (c) Zheng, C. W.; Wang, D.; Stahl, S. S., *J. Am. Chem. Soc.* **2012,** *134*, 16496-16499.

7. (a) Campbell, A. N.; Meyer, E. B.; Stahl, S. S., *Chem. Commun.* **2011**, *47*, 10257-10259. (b) Xiao, B.; Gong, T.-J.; Liu, Z.-J.; Liu, J.-H.; Luo, D.-F.; Xu, J.; Liu, L., *J. Am. Chem. Soc.* **2011,** *133*, 9250-9253.

8. (a) Gao, W.; He, Z.; Qian, Y.; Zhao, J.; Huang, Y., *Chem. Sci.* **2012**, *3*, 883-886. (b) Diao, T.; Wadzinski, T. J.; Stahl, S. S., *Chem. Sci.* **2012**, *3*, 887-891.

9. Piotrowicz, M.; Zakrzewski, J., *Organometallics* **2013**, doi: 10.1021/om400410u

10. (a) Li, B.; Li, B.; Zhu, X.; Zhang, Y., *Inorg. Chem. Commun.* **2003,** *6*, 1304-1306. (b) Siemeling, U.; Scheppelmann, I.; Neumann, B.; Stammler, H.-G.; Schoeller, W. W., *Organometallics* **2004,** *23*, 626-628. (c) Yang, H.-J.; Kou, H.-Z.; Gao, F.; Cui, A.-L.; Wang,

R.-J., *Acta Crystallogr., Sec. E: Struct. Rep. Online* **2004,** *60*, m611-m613. (d) Zhang, R.-L.; Zhao, J.-S.; Yang, S.-Y.; Ng, S. W., *Acta Crystallogr., Sec. E: Struct. Rep. Online* **2004,** *60*, m262-m263. (e) Tian, A.; Han, Z.; Peng, J.; Ying, J.; Sha, J.; Dong, B.; Zhai, J.; Liu, H., *Inorg. Chim. Acta* **2008,** *361*, 1332-1338. (f) Feng, X.-L.; Zhang, Y.-P., *Acta Crystallogr., Sec. E: Struct. Rep. Online* **2011,** *67*, m1171.

11. Klein, R. A.; Witte, P.; van Belzen, R.; Fraanje, J.; Goubitz, K.; Numan, M.; Schenk, H.; Ernsting, J. M.; Elsevier, C. J., *Eur. J. Inorg. Chem.* **1998**, 319-330.

12. Ref 6b. See also: Xu, Z.-G.; Liu, H.-Y.; Zhan, Q.-G.; Chen, J.; Xu, M.-J., *Acta Crystallogr., Sec. E* **2009**, *65*, m1166.

13. (a) Milani, B.; Alessio, E.; Mestroni, G.; Sommazzi, A.; Garbassi, F.; Zangrando, E.; Bresciani-Pahor, N.; Randaccio, L., *J. Chem. Soc,. Dalton Trans.* **1994**, 1903-1911. (b) Ragaini, F.; Gasperini, M.; Cenini, S.; Arnera, L.; Caselli, A.; Macchi, P.; Casati, N., *Chem. Eur. J.* **2009,** *15*, 8064-8077. (c) Ye, Y.; Ball, N. D.; Kampf, J. W.; Sanford, M. S., *J. Am. Chem. Soc.* **2010,** *132*, 14682-14687.

14. TOCSY = Total Correlation Spectroscopy. This technique uses scalar coupling to transfer magnetization from one nuclei to another. The extent of transfer depends on the mixing time, with longer mixing times unveiling more of the coupling network, and will proceed until a quaternary center or non-protonated heteroatom is encountered.

15. ROESY = Rotating-frame Nuclear Overhauser Effect Spectroscopy. This technique is similar to NOESY in that it detects through-space interactions between protons. The ROESY experiment holds the selected magnetization in the transverse plane (rotating frame) by a high-power spinlock rather than along the z-axis (NOESY). The sign of an ROE is always positive, whereas the sign of an NOE is dependent on the tumbling frequency of the molecule relative to the static magnetic field. At the temperature used in the experiments in this study,

NOE data cannot unambiguously distinguish between through-space interactions and chemical exchange. See the Supporting Information for more detailed discussion.

16. HMBC = Heteronuclear Multiple-Bond Correlation spectroscopy is a long-range scalar coupling experiment that involves polarization transfer from ^{1}H to X-nuclei that are 2 or 3 bonds away. It is routinely used to resolve the chemical shift of insensitive nuclei in structure determination studies.

17. This upfield shift in the ^{15}N resonance is due to the occupation of the lone-pair in bonding. The ^{15}N chemical shift is also sensitive to the oxidation state of the metal, the coordination geometry (axial vs equatorial) and the ligand *trans* to the nitrogen. See references: (a) Mason, J., *Chem. Rev.* **1981,** *81*, 205-227. (b) Pazderski, L.; Szłyk, E.; Sitkowski, J.; Kamieński, B.; Kozerski, L.; Toušek, J.; Marek, R., *Magn. Reson. Chem.* **2006,** *44*, 163-170.

18. See Supporting Information for full computational details. Optimization and frequency calculations were performed with rB3LYP/6-31+G* for all non-Pd atoms and the Stuttgart 1997 basis set/ECP was used for Pd. PCM solvation calculations were performed with $CHCl_3$ solvent parameters and with a larger basis set (6-311+G**) for all non-Pd atoms.

19. The experimental barrier was calculated from observing the lineshape of the acetate peaks for **D** and **E** variable-temperature NMR experiments (Figure A2.11-2).

20. (a) Wilke, G.; Schott, H.; Heimbach, P., *Angew. Chem. Int. Ed.* **1967,** *6*, 92-93. (b) Konnick, M. M.; Guzei, I. A.; Stahl, S. S., *J. Am. Chem. Soc.* **2004,** *126*, 10212-10213. (c) Konnick, M. M.; Stahl, S. S., *J. Am. Chem. Soc.* **2008,** *130*, 5753-5762. (d) Konnick, M. M.; Decharin, N.; Popp, B. V.; Stahl, S. S., *Chem. Sci.* **2011,** *2*, 326-330.

21. Steinhoff, B. A.; Stahl, S. S., *J. Am. Chem. Soc.* **2006,** *128*, 4348-4355.

22. See refs. 2f, 3c and the following for examples: (a) Steinhoff, B. A.; Stahl, S. S., *Org. Lett.* **2002,** *4*, 4179-4181. (b) Schultz, M. J.; Park, C. C.; Sigman, M. S., *Chem. Commun.* **2002,** 3034-3035. (c) Ye, X. A.; Liu, G. S.; Popp, B. V.; Stahl, S. S., *J. Org. Chem.* **2011,** *76*, 1031-

1044.

23. White, P. B.; Stahl, S. S., *J. Am. Chem. Soc.* **2011,** *133*, 18594-18597.

24. (a) Lin, B.-L.; Labinger, J. A.; Bercaw, J. E., *Can. J. Chem.* **2009,** *87*, 264-271. (b) Guo, H. J.; Chen, Z.; Mei, F.; Zhu, D.; Xiong, H.; Yin, G., *Chem.–Asian J.* **2013,** *8*, 888-891.

25. We thank Dr. Jay A. Labinger (Caltech) for drawing our attention to this relationship between DAF-Pd(OAc)2 and the bpm-[Pd(OAc)2]2 catalyst system.

26. Gaussian 09, Revision C.01, Frisch, M. J.; Trucks, G. W.; Schlegel, H. B.; Scuseria, G. E.; Robb, M. A.; Cheeseman, J. R.; Scalmani, G.; Barone, V.; Mennucci, B.; Petersson, G. A.; Nakatsuji, H.; Caricato, M.; Li, X.; Hratchian, H. P.; Izmaylov, A. F.; Bloino, J.; Zheng, G.; Sonnenberg, J. L.; Hada, M.; Ehara, M.; Toyota, K.; Fukuda, R.; Hasegawa, J.; Ishida, M.; Nakajima, T.; Honda, Y.; Kitao, O.; Nakai, H.; Vreven, T.; Montgomery, J. A. Jr.; Peralta, J. E.; Ogliaro, F.; Bearpark, M.; Heyd, J. J.; Brothers, E.;Kudin, K. N.; Staroverov, V. N.; Keith, T.; Kobayashi, R.; Normand, J.; Raghavachari, K.; Rendell, A.; Burant, J. C.; Iyengar, S. S.; Tomasi, J.; Cossi, M.; Rega, N.; Millam, J. M.; Klene, M.; Knox, J. E.; Cross, J. B.; Bakken, V.; Adamo, C.; Jaramillo, J.; Gomperts, R.; Stratmann, R. E.; Yazyev, O.; Austin, A. J.; Cammi, R.; Pomelli, C.; Ochterski, J. W.; Martin, R. L.; Morokuma, K.; Zakrzewski, V. G.; Voth, G. A.; Salvador, P.; Dannenberg, J. J.; Dapprich, S.; Daniels, A. D.; Farkas, O.; Foresman, J. B.; Ortiz, J. V.; Cioslowski, J.; Fox, D. J. Gaussian, Inc., Wallingford CT, 2010.

27. Becke, A.D. *J. Chem. Phys.* **1993**, *98*, 1372 –1377.

28. Lee, C.; Yang, W.; Parr, R. G. *Phys. Rev. B.* **1988**, *37*, 785 – 789.

29. a) Feller, D. *J. Comp. Chem.* **1996**, *17*(13), 1571-1586. b) Schuchardt, K.L.; Didier, B.T.; Elsethagen, T.; Sun, L.; Gurumoorthi, V.; Chase, J.; Li, J.; and Windus, T.L. *J. Chem. Inf. Model*. **2007**, *47*(3), 1045-1052

Chapter 3.

Reversible Alkene Insertion into the Pd–N Bond of Pd^{II}-

Sulfonamidates and Implications for Catalytic Amidation

Reactions

3.1 Introduction

The discovery of Pd^{II}-catalyzed oxidative coupling of ethylene and water (the Wacker Process) >50 years ago inspired extensive efforts to develop methods for the oxidative amination of alkenes (aza-Wacker reactions).[1] Early studies showed that many alkyl- and arylamine nucleophiles coordinate strongly to Pd^{II} and inhibit catalytic turnover, and therefore much of this work focused on stoichiometric reactions of nitrogen nucleophiles with preformed Pd^{II}–alkene complexes.[2] In 1982, Hegedus and McKearin demonstrated that *p*-toluenesulfonamides (tosylamides) could be used in catalytic intramolecular aza-Wacker reactions, with benzoquinone as the oxidant.[3] More recently, amide-type nucleophiles have been used in aerobic oxidative amination reactions,[4] including enantioselective[5] and intermolecular[6] applications. Mechanistic studies suggest that these aza-Wacker reactions often proceed via alkene insertion into the Pd–N bond of the amidate ligand, not attack of a nitrogen nucleophile onto a Pd^{II}–coordinated alkene.[7,8] The first fundamental studies of alkene insertion into Pd–N bonds have been reported only recently by the groups of Wolfe and Hartwig with Pd^{II}–anilide complexes.[9-11] Analogous reactions with Pd–amidates are unknown. Here, we describe well-defined Pd^{II}–sulfonamidate complexes that undergo alkene insertion into the Pd–N bond, and the reaction is shown to be reversible. The presence of O_2 influences the fate of the resulting alkyl-Pd^{II} species. These observations, elaborated below, have important implications for catalytic reactions, including oxidative and non-oxidative transformations.

A well-defined Pd^{II}–sulfonamidate complex, suitable for fundamental investigation, was prepared by adding a solution of (tBu$_2$bpy)PdCl$_2$ (**1**, tBu$_2$bpy = 4,4'-di-*tert*-butyl-2,2'-bipyridine) to a suspension of sodium tosylamidate (**2a**) in CH$_2$Cl$_2$ at room temperature. The air-stable Pd-amidate complex **3a** was obtained in good yield (eq 3.1) and was characterized by ^{1}H and ^{13}C NMR spectroscopy, mass spectrometry and X-ray crystallography (Figure 3.1, left).[12] Initial attempts to observe alkene insertion into the Pd–N bond of **3a** were carried out in benzene, THF and dichloromethane, but no reaction was observed (Scheme 3.1). In chloroform, however, **3a** reacted very slowly at room temperature, affording the alkyl-Pd^{II} amidopalladation (AP) product

4a in good yield (Figure 3.1, right). At higher temperatures, **4a** underwent further reaction via β-hydride elimination and could not be obtained cleanly from the reaction mixture. The reaction proved to be much more efficient in dimethylsulfoxide (DMSO) as the solvent, proceeding in 84% yield in 12 h.

(3.1)
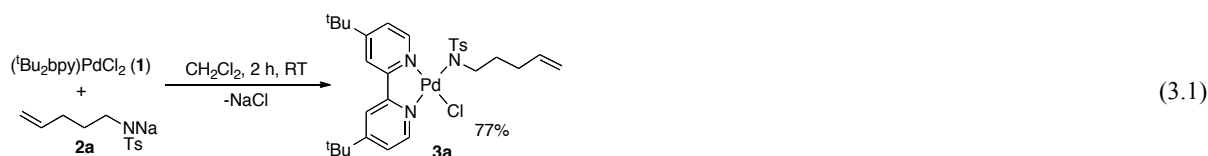
Scheme 3.1. Amidopalladation of an Alkene
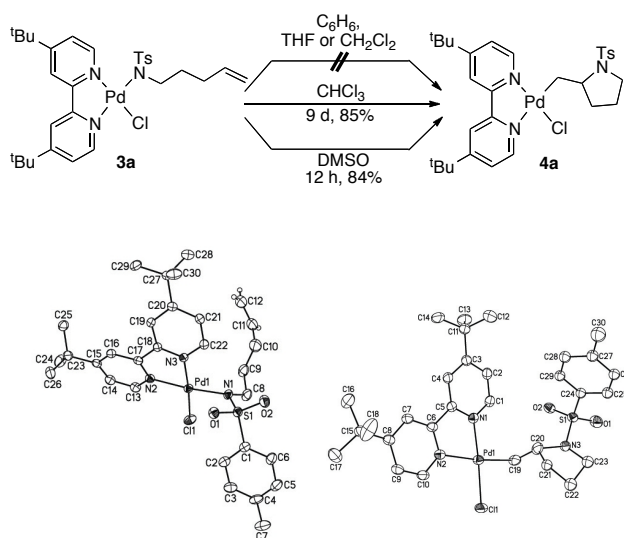
Figure 3.1. X-ray crystal structures of **3a** (left) and **4a** (right) with thermal ellipsoids shown at 40% and 50% probability level, respectively. Most hydrogen atoms have been omitted for clarity.[12]

3.2 Results and Discussion

The beneficial effect of a polar solvent (DMSO) suggested that the reaction proceeds via an ionic intermediate. At least two reasonable ionic mechanisms can be considered: (1) dissociation of the amidate, followed by alkene coordination and nucleophilic attack of the pendant amidate on the alkene (*trans*-AP), or (2) chloride dissociation, followed by alkene coordination and

insertion into the Pd–N bond (*cis*-AP), and reassociation of the chloride ligand to the Pd[II] center. Two experimental observations provide support for the latter, *cis*-AP pathway. Addition of chloride to the reaction mixture strongly inhibits the reaction (Figure 3.2), consistent with a mechanism involving pre-equilibrium dissociation of chloride prior to the AP step. In addition, we prepared a Pd-sulfonamidate complex with a stereochemically defined, deuterium-labeled substrate probe (**5**, Scheme 3.2).[13] The reaction of this complex under an atmosphere of O$_2$ led to products **6** and **7**, which arise from *cis*-AP of the alkene, followed by β-hydride elimination. No products arising from competing *trans*-AP of the alkene were observed.
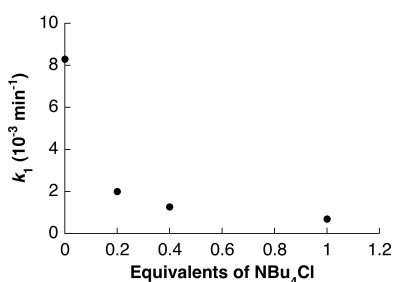
Figure 3.2. Chloride inhibition on amidopalladation for **3a**

Scheme 3.2. Isotopic Labeling Study Demonstrating that C–N Bond-Formation Proceeds via *cis*-Amidopalladation
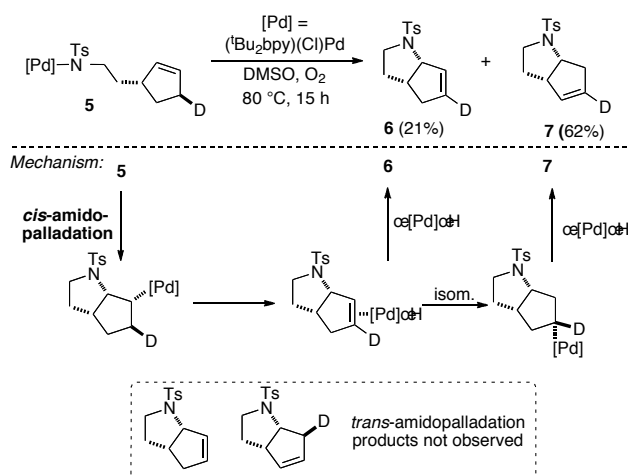
As expected from the reaction illustrated in Scheme 3.2, the alkyl-Pd^{II} complex **4a** is susceptible to β-hydride elimination. Heating a DMSO solution of **4a** to 60 °C under aerobic conditions led to a mixture of isomeric products **8a**, **8a'** and **8a"** (eq 3.2).[14] A different outcome was observed, however, when the reaction was performed under anaerobic conditions: the β-hydride elimination products **8a**–**8a"** were obtained in 50% yield, together with a 40% yield of 4-pentenyl tosylamide **9** (eq 3.3).

(3.2)

(3.3)
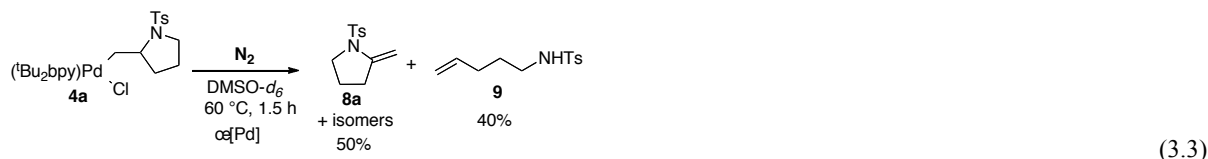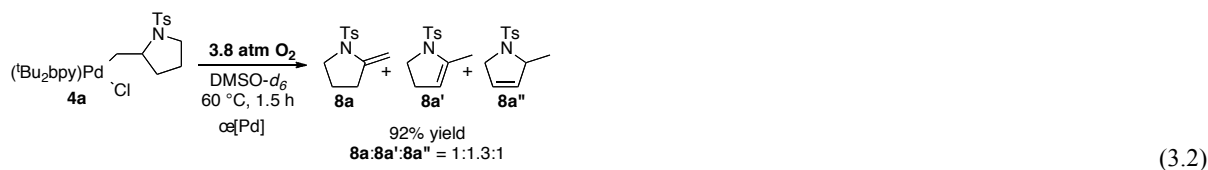
Scheme 3.3. Proposed Mechanism for the Parallel Formation of 8 and 9 under Anaerobic Conditions
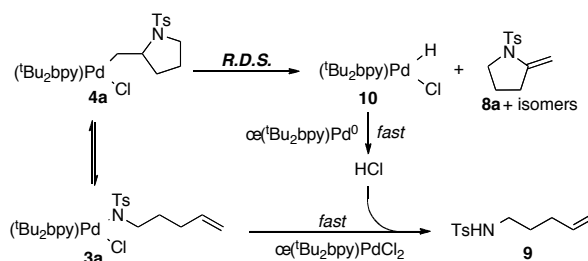
The formation of **9** in eq 3.3 was unexpected, but this result can be rationalized if alkene insertion into the Pd–N bond is reversible (i.e., **4a** ⇆ **3a**). According to the mechanism in Scheme 3.3, β-hydride elimination from **4a** forms the enamide products **8a**–**8a"** together with a Pd^{II}–hydride species **10**. In the absence of O$_2$,[15] HCl can form via reductive elimination from **10** and react with **3a** to afford the alkenyl tosylamide **9**. This proposal implies that HCl reacts much more rapidly with **3a** than with **4a**. In order to test this hypothesis, excess HCl (~60 equiv) was

added to a DMSO-d_6 solution of **4a** at room temperature. Rapid and quantitative formation of **9** was observed in this reaction, together with (tBu$_2$bpy)PdCl$_2$ (**1**, eq 3.4); pyrrolidine **11**, the product of protonolysis of the Pd–C bond of **4a**, was not observed.

(3.4)
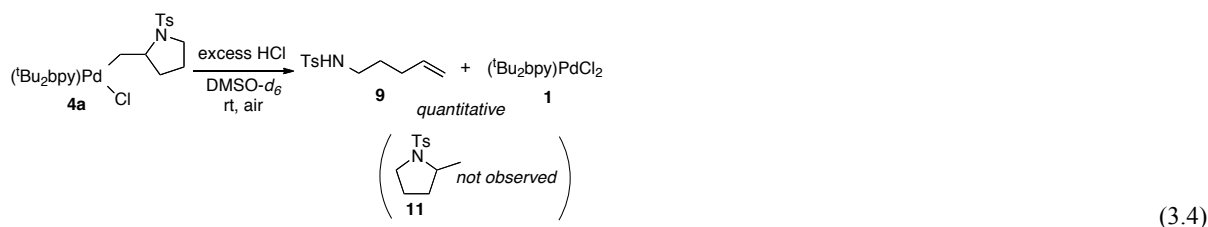
Additional, more-direct evidence for reversible amidopalladation of the alkene was obtained in the investigation of a series of substituted Pd^{II}-sulfonamidate complexes (Figure 3.3). The reactions of four different *para*-substituted benzenesulfonamidate complexes [X = Me (**3a**), OMe (**3b**), Cl (**3c**) and NO$_2$ (**3d**)] were monitored by ^{1}H NMR spectroscopy at 30 °C in DMSO-d_6 under aerobic conditions (Figure 3.3a). Each of the Pd complexes underwent clean amidopalladation of the alkene to afford an equilibrium mixture of complexes **3a–d** and the corresponding alkyl–Pd^{II} species **4a–d** (Figure 3.3b), together with slower concomitant formation of heterocycles **8–8"a–d** via β-hydride elimination from **4a–d**. The data were fit to a simplified kinetic model, **3 ⇄ 4 → 8-8"**, that enabled quantitative comparison of kinetic and thermodynamic constants associated with the two observable steps (Figure 3.3c). Electronic effects on these parameters were probed via Hammett analysis (Figure 3.3d).[16]

Alkene insertion into the Pd–N bond (i.e., *cis*-AP, k_1) is favored for electron-rich amidates. This trend is similar to that observed previously for irrreversible alkene insertion into Pd–anilides, and it is consistent with an alkene insertion mechanism that formally corresponds to intramolecular nucleophilic attack of the amidate ligand onto the coordinated alkene.[9] The reverse reaction, β-amidate elimination, (k_{-1}) is favored for electron-deficient amidates (Figures 3.3c and 3.3d). Together, these trends cause the equilibrium constant to be largest for the *p*-Me derivatives **3/4a** ($K_1 \sim 10$) and smallest for the electron-deficient *p*-NO$_2$ derivative **3/4d** ($K_1 \sim 1$) (Figure 3.3c).

a) Alkene insertion/β-hydride elimination sequence
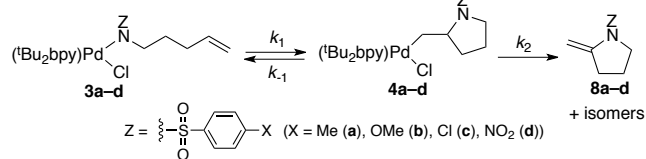
b) Kinetic profiles for alkene insertion/β-hydride elimination reactions with Pd-sulfonamidate complexes, **3a-d**
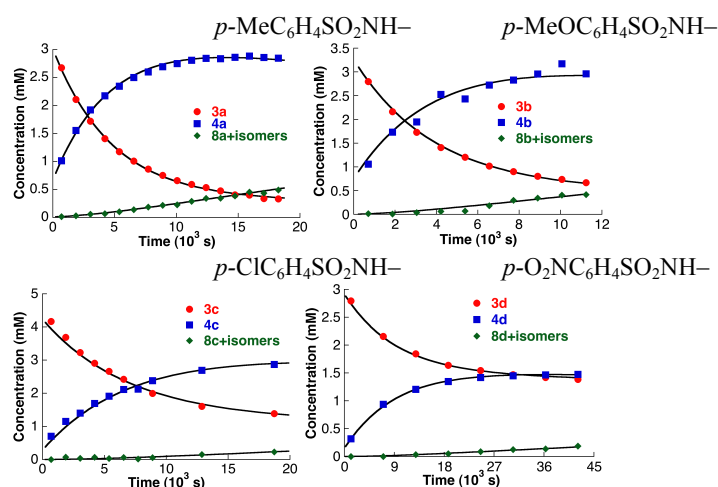
c) Kinetic parameters derived from fits of the data

X	k_1 (10^{-5} s^{-1})	k_{-1} (10^{-5} s^{-1})	K_1	k_2 (est'd) (10^{-5} s^{-1})	$K_1 \cdot k_2$ (10^{-5} s^{-1})
CH$_3$ (**a**)	19.0	1.83	10.0	1.12	11.1
OMe (**b**)	22.6	3.64	6.21	1.53	9.50
Cl (**c**)	10.3	3.56	2.89	0.59	1.71
NO$_2$ (**d**)	5.64	5.16	1.09	0.33	0.36

d) Hammett analysis of the *cis*-amidopalladation (k_1), β-amidate elimination (k_{-1}) and β-hydride elimination (k_2) steps.
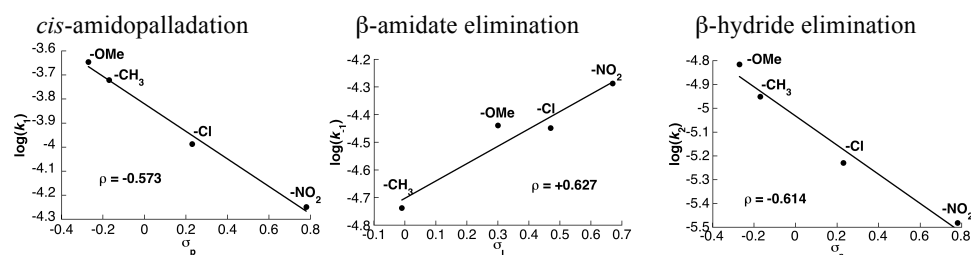
Figure 3.3. Kinetic studies of alkene insertion/β-hydride elimination reactions of four Pd^{II}–sulfonamidate complexes. Conditions: 3.68 mM **3**, 3.8 atm O$_2$, DMSO, 30 °C, 7-12 h. Note: Every fifth data point is shown to enhance clarity.

That K_1 is largest for the *p*-Me, and not the *p*-OMe derivative, appears to reflect the lack of "resonance" electronic effects in the amidate elimination step k_{-1}; the Hammett correlation for k_{-1} is best fit with the "inductive" Hammett parameter s_I, rather than s_p, which incorporates both resonance and inductive effects. The k_2 values estimated from these fits show that β-hydride elimination is favored with more-electron-rich derivatives, consistent with a formal "hydride"-transfer mechanism in which electron-donating groups stabilize the build-up of positive charge on the adjacent carbon atom in the transition state. The combined electronic effects, $K_1 \cdot k_2$, reveal that the *p*-Me (tosylamidate) derivative **3a** is the most reactive complex toward formation of the oxidative amidation products **8–8"**.

Overall, these observations have important implications for catalysis. For example, the development of enantioselective Wacker-type oxidation reactions has been a long-standing challenge in the field of asymmetric catalysis.[17] Alkene insertion into the Pd–N bond of **3a** results in formation of a new stereogenic center (Scheme 3.1), and such steps provide the basis for enantioselective oxidative amination reactions (e.g., eq 3.5).[5c] Recent work has highlighted the importance of controlling the stereochemical course of the nucleopalladation step in enantioselective reactions (i.e., *cis*- vs. *trans*-nucleopalladation).[1f] The results reported here reveal that nucleopalladation could be reversible, in which case β-hydride elimination or another termination step will be the stereochemistry-determining step of the reaction. To our knowledge, this possibility has not been considered previously in Wacker-type reactions.
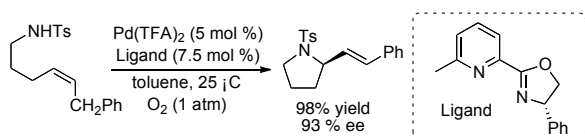
(3.5)

Reversible C–N bond formation has been observed in reactions involving *trans*-AP of an alkene,[18] but reversible insertion of an alkene into a Pd–N bond has not been observed previously. The latter observation, combined with the significantly more-facile protonolysis of Pd–N bonds

relative to Pd–C bonds (cf. eq 3.4), represents a key challenge for the development of Pd-catalyzed *hydroamination* reactions that proceed via *cis*-AP pathways.

In summary, this study has led to key insights into reactions of Pd[II]–sulfonamidates with alkenes, perhaps most notably demonstrating that alkene insertion into the Pd–N bonds of such species is facile and reversible. This work provides an important foundation for more-thorough characterization of *cis*-amidopalladation reactions relevant to important catalytic transformations.

3.3 Experimental

3.3.1 General Experimental Considerations.

All commercially available compounds were used as received. Solvents used for synthetic reactions were dried over alumina columns prior to use; solvents for NMR spectroscopy were used as received. ^{1}H and ^{13}C NMR spectra were recorded on Bruker 300 MHz, Varian 500 MHz and Varian 600 MHz spectrometers. ^{1}H NMR chemical shifts are reported in parts per million relative to internal TMS (0.00 ppm) for $CDCl_3$ or the residual protons (2.50 ppm) for DMSO-d_6. ^{13}C NMR chemical shifts are reported in parts per million relative to the solvent peak (77.23 ppm for $CDCl_3$, 39.51 ppm for DMSO-d^6). ESI- and EMM-MS experiments were performed on a Waters (Micromass) LCT[®] mass spectrometer. All exact mass measurements (EMM) for compounds containing palladium were compared against the calculated, monoistopic mass. Flash chromatography was performed using SiliaFlash[®] P60 (Silicycle, particle size 40-63 μm, 230-400 mesh) from Sigma Aldrich. All synthetic procedures were carried out under ambient conditions. ([t]Bu$_2$bpy)PdCl$_2$ (**1**) was prepared according to previously reported procedures.[19]

For kinetic studies, DMSO-d_6 was used and stored under a dry nitrogen atmosphere. ^{1}H NMR spectroscopic kinetic data were recorded using Varian INOVA-500 and INOVA-600 spectrometers. Trimethyl(phenyl)silane was used as an internal standard without purification for all kinetic studies. Ethylene glycol was used for temperature calibration of the NMR spectrometer for variable temperature measurements. Under the conditions of the NMR experiments performed in this study, mass transfer of O$_2$ from the headspace into solution is slow.

Therefore, only the dissolved O_2 concentration is relevant. In most of our experiments, we use ~3.4-3.8 atm O_2, which corresponds to a dissolved O_2 concentration of ~7-8 mM in DMSO.[20] Issues associated with O_2 solubility and mass-transfer into solution have been discussed elsewhere.[21]

3.3.2 General Procedure for the Synthesis of Substituted Benzenesulfonamides.

Synthesis of the substituted benzenesulfonamides from the corresponding 4-penten-1-ol was carried out according to a literature procedure.[22] The ^{1}H NMR spectrum of the compounds in DMSO-d^6 is provided for comparison with the corresponding sodium salts in the next section.
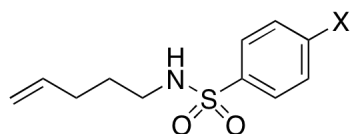
X = OMe

1.54 g, 77% yield; clear, pale yellow oil (Combiflash using hexanes/ethyl acetate; TLC conditions – 3:1 hexanes:EtOAc, R_f = 0.23). Characterization data agrees with literature report.[23]

^{1}H NMR $((CD_3)_2SO$, 300 MHz) δ 7.71 (d, J = 8.8 Hz, 2H), 7.45 (bt, J = 5.8 Hz, 1H), 7.11 (d, J = 8.8 Hz, 2H), 5.78-5.64 (m, 1H), 4.99-4.89 (m, 2H), 3.83 (s, 3H), 2.70 (q, J = 6.9 Hz, 2H), 1.97 (q, J = 6.9 Hz, 2H), 1.43 (pent, J = 6.6 Hz, 2H)

X = Me

Obtained from previous studies.[24] Characterization data agrees with literature report.[25]

^{1}H NMR $((CD_3)_2SO$, 300 MHz) δ 7.67 (d, J = 8.2 Hz, 2H), 7.52 (t, J = 5.9 Hz, 1H), 7.39 (d, J = 8.2 Hz, 2H), 5.81-5.67 (m, 1H), 4.93-4.81 (m, 2H), 2.68 (q, J = 6.6 Hz, 2H). 2.38 (s, 3H), 1.96 (q, J = 6.9 Hz, 2H), 1.45 (pent, J = 7.3 Hz, 2H)

X = Cl

1.50 g, 74% yield; clear, colorless waxy solid; mp = 30-32 °C (Combiflash using hexanes/ethyl acetate; TLC conditions – 3:1 hexanes:EtOAc, R_f = 0.49).

^{1}H NMR (CDCl$_3$, 500 MHz) δ 8.06 (d, J = 8.5 Hz, 2H), 7.49 (d, J = 8.5 Hz, 2H), 5.75-5.67 (m, 1H), 5.00-4.96 (m, 2H), 4.63 (bt, 1H), 2.97 (q, J = 6.7 Hz, 2H), 2.05 (q, J = 7.0 Hz, 2H), 1.58 (pent, J = 7.0 Hz, 2H)

^{13}C NMR (CDCl3, 126 MHz) δ 139.34 δ 138.75 δ 137.25 δ 129.62 δ 128.72 δ 115.98 δ 42.87 δ 30.81 δ 28.88

^{1}H NMR ((CD$_3$)$_2$SO, 300 MHz) δ 7.80-7.66 (m, 5H), 5.78-5.64 (m, 1H), 4.99-4.89 (m, 2H), 2.74 (q, J = 6.6 Hz, 2H), 1.97 (q, J = 7.2 Hz, 2H), 1.44 (pent, J = 7.3 Hz, 2H)

HRMS: m/z (ESI) calculated [M+Na]+ = 282.0326, measured 282.0319 (Δ = 2.5 ppm)

X = NO$_2$

1.12 g, 56% yield; yellow powder (Combiflash using hexanes/ethyl acetate; TLC conditions – 3:1 hexanes:EtOAc, R_f = 0.34). Characterization data agrees with literature report.[23]

^{1}H NMR ((CD$_3$)$_2$SO, 300 MHz) δ 8.42 (d, J = 8.7 Hz, 2H), 8.05-8.02 (m, 3H), 5.78-5.65 (m, 1H), 4.99-4.89 (m, 2H), 2.82-2.76 (m, 2H), 1.98 (q, J = 7.1 Hz, 2H), 1.45 (pent, J = 7.3 Hz, 2H)

3.3.3 General Procedure for the Synthesis of Na[*N*-arylsulfonyl-pent-4-enamide].

A scintillation vial, stir bar and septum were dried overnight in a 70 °C oven. The stir bar was added and the vial was capped with the septum. The vial was placed under vacuum and allowed to cool. Once the vial was cool, sodium hydride (60% by wt in a mineral oil suspension, 1 mole equivalent) was added to the vial and placed under N$_2$. Dry Et$_2$O (~3 mL/mmol NaH) was added via syringe to the vial to form a suspension of NaH. To the stirring suspension of NaH, a solution of amide (1.1 equiv) in dry diethyl ether (~6 mL/mmol NaH) was added at room temperature. Subsequently, 2 mL of dry diethyl ether was used to transfer the residual amide solution. The reaction mixture was stirred 2-3 h, after which 5 mL/mmol NaH of hexanes was

added to the vial to promote precipitation. The resulting precipitate was filtered, washed with hexanes (3x5mL) and Et$_2$O (1x1mL) to remove the excess amide and collected.
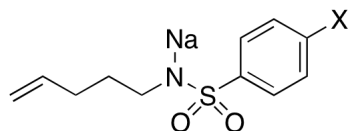
X = OMe

56.2 mg, 65% yield; white powder.

^{1}H NMR ((CD$_3$)$_2$SO, 500MHz) δ 7.51 (d, J = 8.6 Hz, 2H), 6.84 (d, J = 8.6 Hz, 2H), 5.78-5.70 (m, 1H), 4.92-4.88 (m, 1H), 4.85-4.82 (m, 1H), 3.75 (s, 3H), 2.55 (t, J = 7.0 Hz, 2H), 1.94 (q, J = 7.5 Hz, 2H), 1.30 (m, J = 7.3 Hz, 2H)

^{13}C NMR ((CD$_3$)$_2$SO, 126 MHz) δ 159.07 δ 140.73 δ 139.67 δ 127.88 δ 113.83 δ 112.65 δ 55.09 δ 45.44 δ 32.04 δ 31.49

X = Me

821.8 mg, 83% yield; white powder.

^{1}H NMR ((CD$_3$)$_2$SO, 500MHz) δ 7.51 (d, J = 7.9 Hz, 2H), 7.14 (d, J = 7.9 Hz, 2H), 5.77-5.69 (m, 1H), 4.92-4.88 (m, 1H), 4.85-4.83 (m, 1H), 2.59 (t, J = 7.1 Hz, 2H). 2.29 (s, 3H), 1.94 (q, J = 7.7 Hz, 2H), 1.35 (m, J = 7.6 Hz, 2H)

^{13}C NMR ((CD$_3$)$_2$SO, 126 MHz) δ 144.48 δ 139.40 δ 138.02 δ 128.22 δ 126.36 δ 114.01 δ 44.90 δ 31.51 δ 31.30 δ 20.79

X = Cl

61.9 mg, 90% yield; white powder.

^{1}H NMR ((CD$_3$)$_2$SO, 500MHz) δ 7.57 (d, J = 8.4 Hz, 2H), 7.35 (d, J = 8.4 Hz, 2H), 5.77-5.69 (m, 1H), 4.91-4.88 (m, 1H), 4.85-4.83 (m, 1H), 2.58 (t, J = 7.0 Hz, 2H), 1.94 (q, J = 7.5 Hz, 2H), 1.32 (m, J = 7.4 Hz, 2H)

^{13}C NMR ((CD$_3$)$_2$SO, 126 MHz) δ 147.74 δ 139.56 δ 132.42 δ 128.05 δ 127.49 δ 113.88 δ 45.40 δ 31.96 δ 31.40

X = NO$_2$

57 mg, 58% yield; yellow powder.

^{1}H NMR ((CD$_3$)$_2$SO, 300MHz) δ 8.21 (d, J = 8.8 Hz, 2H), 7.76 (bd, J = 8.8 Hz, 2H), 5.76-5.68 (m, 1H), 4.91-4.83 (m, 2H), 2.67 (t, J = 7.1 Hz, 2H), 1.94 (q, J = 7.7 Hz, 2H), 1.35 (m, J = 7.4 Hz, 2H)

^{13}C NMR ((CD$_3$)$_2$SO, 126 MHz) δ 153.91 δ 147.26 δ 139.14 δ 127.25 δ 123.42 δ 114.18 δ 44.73 δ 31.26 δ 31.11

3.3.4 General Procedure for the Synthesis of (^{t}Bu$_2$bpy)Pd(N-arylsulfonamidate)(Cl), 3a-d.

Minimal amounts of CH$_2$Cl$_2$ were added to ^{t}Bu$_2$bpyPdCl$_2$ (**1**, 1 equiv) in a scintillation vial to form a clear, yellow solution. This solution was added to another vial containing the sodium salt of the desired amide (1.1 equiv) and stir bar. Residual amounts of **1** were transferred to the reaction vial with minimal amounts of CH$_2$Cl$_2$. The reaction vial was capped with a teflon cap and the reaction mixture was stirred for 2-3 h at room temperature. Subsequently, the reaction mixture was filtered through a Celite pad to remove sodium salts and washed with CH$_2$Cl$_2$ to remove any palladium-amidate complex left on the Celite. The filtrate was collected into a round-bottom flask and the solvent was removed, either by rotovap or by blowing N$_2$ over the solution. Minimal amounts of benzene were added to the resulting glassy Pd-amidate complex and the solution was dripped slowly into a stirring round-bottom flask of hexanes (≥10 mL hexanes/1 mL benzene used to dissolve the Pd-amidate). Yellow, fluffy precipitate formed and was allowed to stir for 20 minutes. [note*: If hard, globular, orange precipitate is observed, either the benzene solution was too concentrated or not enough CH$_2$Cl$_2$ was removed. In either case, the precipitation step must be repeated.] The precipitate was then filtered through a medium-fritted funnel, washed with hexanes (2x2 mL) and Et$_2$O (2x1mL) and allowed to dry. [note:

Small amounts of product are lost in the ether wash, but this step is necessary to fully remove sulfonamide from the Pd-amidate complex.] The dried palladium complex was then transferred to a vial and stored in a glovebox.
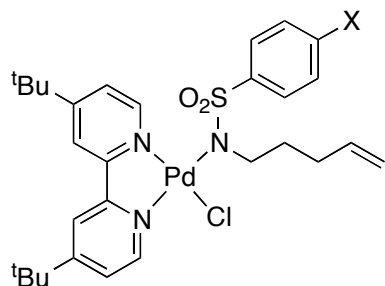
3a: X = Me

248.3 mg, 77% yield; fine yellow powder.

^{1}H NMR (CDCl$_3$, 500 MHz) δ 9.32 (d, J = 6.2 Hz, 1H), 9.17 (d, J = 6.2 Hz, 1H), 7.96 (d, J = 8.1 Hz, 2H), 7.86 (s, 1H), 7.85 (s, 1H), 7.67 (dd, J = 2.2, 6.3 Hz, 1H), 7.44 (dd, J = 2.3, 6.0 Hz), 7.24 (d, J = 8.1 Hz, 2H), 5.86-5.78 (m, 1H), 4.96 (dm, J = 16.9 Hz, 1H), 4.87 (dm, J = 10.3 Hz, 1H), 2.87-2.76 (m, 2H), 2.38 (s, 3H), 2.30-2.22 (m, 1H), 2.12 (q, J = 8.1 Hz, 2H), 1.94-1.87 (m, 1H), 1.45 (s, 9H), 1.42 (s, 9H).

^{13}C NMR (CDCl$_3$, 126 MHz) δ 165.08 δ 164.74 δ 156.28 δ 155.59 δ 151.33 δ 151.15 δ 140.70 δ 139.95 δ 139.15 δ 128.66 δ 128.39 δ 124.03 δ 123.56 δ 118.43 δ 118.31 δ 114.44 δ 49.92 δ 35.88 δ 32.42 δ 31.95 δ 30.51 δ 21.69

HRMS: m/z (ESI) calculated [M-Cl]$^+$ = 610.1876, measured 610.1890 (Δ = 2.3 ppm)

3b: X = OMe

83 mg, 75% yield; fine yellow powder.

^{1}H NMR (CDCl$_3$, 500 MHz) δ 9.32 (d, J = 6.1 Hz, 1H), 9.18 (d, J = 6.1 Hz, 1H), 8.02 (d, J = 8.9 Hz, 2H), 7.86 (s, 1H), 7.85 (s, 1H), 7.68 (dd, J = 1.9, 6.6 Hz, 1H), 7.45 (dd, J = 2.1, 6.6 Hz), 6.93 (d, J = 8.9 Hz, 2H), 5.86-5.78 (m, 1H), 4.96 (dm, J = 17.4 Hz, 1H), 4.88 (dm, J = 11.3 Hz,

1H), 3.84 (s, 3H), 2.88-2.74 (m, 2H), 2.30-2.22 (m, 1H), 2.13 (q, J = 7.1 Hz, 2H), 1.95-1.86 (m, 1H), 1.45 (s, 9H), 1.42 (s, 9H).

^{13}C NMR (CDCl$_3$, 126 MHz) δ 165.08 δ 164.74 δ 161.37 δ 156.28 δ 155.59 δ 151.30 δ 151.30 δ 139.15 δ 135.12 δ 130.27 δ 124.05 δ 123.58 δ 118.44 δ 118.32 δ 114.43 δ 113.16 δ 55.47 δ 49.89 δ 35.88 δ 32.36 δ 31.95 δ 30.51 δ 30.49

HRMS: m/z (ESI) calculated [M-Cl]$^+$ = 628.1815, measured 628.1846 (Δ = 5.0 ppm)

3c: X = Cl

116.9 mg, 83% yield; fine yellow powder.

^1H NMR (CDCl$_3$, 500 MHz) δ 9.26 (d, J = 6.1 Hz, 1H), 9.16 (d, J = 5.7 Hz, 1H), 8.01 (d, J = 8.8 Hz, 2H), 7.87 (bs, 2H), 7.67 (bd, J = 5.6 Hz, 1H), 7.47 (bd, J = 6.4 Hz), 7.39 (d, J = 8.8 Hz, 2H), 5.86-5.78 (m, 1H), 4.97 (bd, J = 17.3 Hz, 1H), 4.89 (bd, J = 10.1 Hz, 1H), 2.88-2.78 (m, 2H), 2.31-2.22 (m, 1H), 2.13 (bq, J = 7.1 Hz, 2H), 1.94-1.86 (m, 1H), 1.45 (s, 9H), 1.42 (s, 9H).

^{13}C NMR (CDCl$_3$, 126 MHz) δ 165.25 δ 164.94 δ 156.28 δ 155.64 δ 151.32 δ 151.03 δ 141.44 δ 138.97 δ 136.67 δ 129.86 δ 128.23 δ 124.10 δ 123.69 δ 118.52 δ 118.42 δ 114.58 δ 49.91 δ 35.91 δ 32.35 δ 31.88 δ 30.51 δ 30.49

HRMS: m/z (ESI) calculated [M-Cl]$^+$ = 628.1346, measured 628.1373 (Δ = 4.3 ppm)

3d: X = NO$_2$

84 mg, 79% yield; fine yellow powder.

^1H NMR (CDCl$_3$, 500 MHz) δ 9.20 (d, J = 6.2 Hz, 1H), 9.11 (d, J = 6.2 Hz, 1H), 8.27 (d, J = 9.1 Hz, 2H), 8.21 (d, J = 9.1 Hz, 2H), 7.90-7.88 (m, 2H), 7.69 (dd, J = 2.1, 6.1 Hz, 1H), 7.48 (dd, J = 1.9, 6.1 Hz), 5.86-5.77 (m, 1H), 4.98 (bdd, J = 1.5 Hz, 17.1 Hz, 1H), 4.90 (bdd, J = 1.3 Hz, 10.1 Hz, 1H), 2.94-2.84 (m, 2H), 2.33-2.24 (m, 1H), 2.15 (bq, J = 7.3 Hz, 2H), 1.95-1.86 (m, 1H), 1.46 (s, 9H), 1.43 (s, 9H).

^{13}C NMR (CDCl$_3$, 126 MHz) δ 165.47 δ 165.21 δ 156.28 δ 155.71 δ 151.32 δ 150.87 δ 148.90 δ 138.74 δ 129.37 δ 124.16 δ 123.84 δ 123.44 δ 118.66 δ 118.59 δ 114.77 δ 50.04 δ 35.97 δ 35.94 δ 32.33 δ 31.83 δ 30.43 δ 30.41

HRMS: m/z (ESI) calculated [M-Cl]$^+$ = 641.1571, measured 641.1600 (Δ = 4.5 ppm)
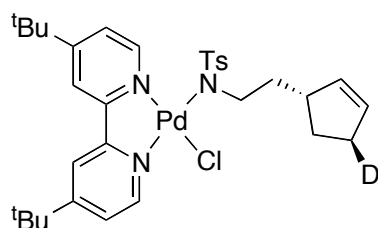
5

40.7 mg, 90% yield; fine yellow powder

^{1}H NMR (CDCl$_3$, 500 MHz) δ 9.31 (dd, *J* = 1.8, 6.2 Hz, 1H), 9.18 (d, *J* = 6.2 Hz, 1H), 7.97 (d, *J* = 8.2 Hz, 2H), 7.85 (m, 2H), 7.66 (dd, *J* = 1.8, 6.1 Hz, 1H), 7.43 (bd, *J* = 6.1 Hz, 1H), 7.24 (d, *J* = 8.0 Hz, 2H), 5.72-5.63 (m, 1H), 2.91 (m, 2H), 2.72 (m, 1H), 2.43-2.35 (m, 1H, diast.), 2.38 (s, 3H) 2.32-2.26 (m, 1H), 2.23-2.16 (m, 1H, diast.), 2.05-1.98 (m, 1H), 1.96-1.89 (m, 1H, diast.), 1.77-1.69 (m, 1H, diast.), 1.49 (m, 1H), 1.44 (s, 9H), 1.42 (s, 9H).

^{13}C NMR (CDCl$_3$, 126 MHz) δ 165.03 δ 164.68 δ 156.30 δ 155.59 δ 151.39 δ 151.17 δ 140.69 δ 140.03 δ 135.71 δ 135.65 δ 130.14 δ 128.68 δ 128.40 δ 124.06 δ 123.55 δ 118.40 δ 118.29 δ 48.97 δ 48.91 δ 43.88 δ 43.85 δ 39.46 δ 35.87 δ 31.86 (1:1:1 triplet) δ 30.53 δ 30.51 δ 29.99 δ 29.88 δ 21.71

HRMS: m/z (ESI) calculated [M-Cl]$^+$ = 635.2112, measured 635.2120 (Δ = 1.3 ppm)

3.3.5 Synthesis of Alkyl-Palladium(II) Complex 4a.
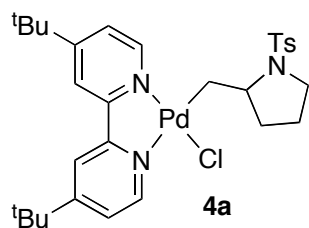
Pd^{II}-amidate complex **3a** (122 mg) was dissolved in 2 mL of CDCl$_3$ that had been passed through oven-dried K$_2$CO$_3$. The solution was capped and stored in a dark cabinet at room temperature. A small amount of the solution was used for periodic examination by ^{1}H NMR spectroscopy to the monitor reaction progress. After 9 d, **4a** had reached its maximum quantity (~85% yield) and began decomposing via β-hydride elimination into heterocyclic products **8a-a"** and byproducts **1** and **9**. The solvent was removed and crystals of **4a**, **1** and **3a** were obtained by vapor diffusion of pentanes into C$_6$H$_6$. The yellow crystals of **4a** were manually separated from the orange crystals of **3a**. Efforts to remove **1** from **4a** via recrystallization or filtration were unsuccessful. Consequently, **4a** contains 8.5 mol % **1** by ^{1}H NMR spectroscopy. Overall yield post-recrystallization for **4a** was 47% yield.

^{1}H NMR (CDCl$_3$, 500MHz) δ 9.24 (d, $J = 6.1$ Hz, 1H), 9.07 (d, $J = 5.7$ Hz, 1H), 8.02 (bd, $J = 1.9$ Hz, 2H), 7.95 (bd, $J = 1.4$ 1H), 7.73 (d, $J = 8.3$ Hz, 2H), 7.70 (dd, $J = 2.0$, 6.1 Hz, 1H), 7.49 (dd, $J = 1.5$, 5.7 Hz, 1H), 7.36 (C$_6$H$_6$), 7.24 (d, $J = 8.3$ Hz, 2H), 4.11-4.06 (m, 1H), 3.37-3.33 (m, 1H), 3.19-3.14 (m, 1H), 2.50 (bdd, $J = 8.5$, 12.0 Hz, 1H), 2.47-2.42 (m, 1H), 2.40 (s, 3H), 2.11-2.02 (m, 1H), 1.98 (bdd, $J = 3.2$, 8.2 Hz, 1H), 1.82-1.75 (m, 1H), 1.61-1.55 (m, 1H), 1.47 (s, 9H), 1.42 (s, 9H).

^{13}C NMR (CDCl$_3$, 126 MHz) δ 163.43 δ 163.39 δ 156.73 δ 153.38 δ 150.71 δ 149.09 δ 142.89 δ 136.74 δ 129.66 δ 127.41 δ 124.44 δ 123.57 δ 123.57 δ 118.97 δ 117.79 δ 62.81 δ 48.57 δ 35.74 δ 35.65 δ 33.68 δ 30.61 δ 30.53 δ 25.21 δ 23.76 δ 21.65

HRMS: m/z (ESI) calculated [M-Cl]$^+$ = 610.1876, measured 610.1876 (Δ = 0.0 ppm)

3.3.6 General Procedure for Kinetic Studies by ^{1}H NMR Spectroscopy under Aerobic and Anaerobic Conditions.

3.3.6.1 Aerobic

A pre-weighed amount of a Pd-amidate or Pd-alkyl complex along with a J-Young tube were brought into a purge-box containing a dry nitrogen atmosphere. The Pd complex was dissolved in 500 μL of a DMSO-d_6 stock solution containing phenyl trimethylsilane as an internal standard and transferred to the J-Young tube that was subsequently sealed and placed inside a dry ice/acetone bath to freeze the sample. The J-Young tube was connected to a gas manifold and its headspace was evacuated and refilled with 1 atm O_2. This step was repeated twice. After the last evacuation step, the NMR tube was backfilled with 3.4-3.8 atm O_2 by condensing O_2 into the tube using liquid nitrogen and monitoring the amount of O_2 using a manometer in a sealed vacuum line. For every tube, enough O_2 was condensed in order to have at least a 1:1 molar ratio of dissolved O_2:Pd-complex. *Warning: Pressurizing the tube beyond the standard limits, based on tube diameter and wall thickness, or warming a pressurized tube too rapidly can cause the tube to explode.* The NMR tube was left in an acetone/dry ice bath until it was warmed and inserted in the preheated NMR spectrometer.

3.3.6.2 Anaerobic

The procedure was identical to the aerobic procedure except that the evacuation of the headspace and backfilling with O_2 were omitted.

3.4 References

1. For reviews, see: (a) Bäckvall, J. E. *Acc. Chem. Res.* **1983,** *16*, 335-342. (b) Hegedus, L. S. *Tetrahedron* **1984,** *40*, 2415-2434. (c) Larock, R. C.; Zeni, G. *Chem. Rev.* **2004,** *104*, 2285-

2309. (d) Beccalli, E. M.; Broggini, G.; Martinelli, M.; Sottocornola, S. *Chem. Rev.* **2007**, *107*, 5318-5365. (e) Minatti, A.; Muñiz, K. *Chem. Soc. Rev.* **2007,** *36*, 1142-1152. (f) McDonald, R. I.; Liu, G.; Stahl, S. S. *Chem. Rev.* **2011,** *111*, 2981-3019.

2. See refs. 1a,b and the follow representative primary references: (a) Cope, A. C.; Kliegman, J. M.; Friedrich, E. C. *J. Am. Chem. Soc.* **1967**, *89*, 287-291. (b) Åkermark, B.; Bäckvall, J.-E.; Hegedus, L. S.; Zetterberg, K; Siiralah-Hansén, K; Sjöberg, K. *J. Organomet. Chem.* **1974**, *72*, 127-138. (c) Bäckvall, J. E. *Tetrahedron Lett.* **1978**, 163-166. (d) Hegedus, L. S.; Allen, G. F.; Bozell, J. J.; Waterman, E. L. *J. Am. Chem. Soc.* **1978**, *100*, 5800-5807. (e) Pugin, B.; Venanzi, L. M. *J. Organomet. Chem.* **1981**, *214*, 125-133. (f) Åkermark, B.; Zetterberg, K. *J. Am. Chem. Soc.* **1984**, *106*, 5560-5561. (g) Hegedus, L. S.; Åkermark, B.; Zetterberg, K.; Olsson, L. F. *J. Am. Chem. Soc.* **1984,** *106*, 7122-7126.

3. Hegedus, L. S.; McKearin, J. M. *J. Am. Chem. Soc.* **1982,** *104* (9), 2444-2451.

4. See, for example: (a) van Benthem, R. A. T. M.; Hiemstra, H.; Longarela, G. R.; Speckamp, W. N. *Tetrahedron Letters* **1994,** *35*, 9281-9284. (b) Rönn, M.; Bäckvall, J.-E.; Andersson, P. G. *Tetrahedron Lett.* **1995,** *36*, 7749-7752. (c) Larock, R. C.; Hightower, T. R.; Hasvold, L. A.; Peterson, K. P. *J. Org. Chem.* **1996,** *61*, 3584-3585. (d) Stahl, S. S.; Fix, S. R.; Brice, J. L. *Angew. Chem., Int. Ed.* **2002,** *41*, 164-166. (d) Trend, R. M.; Ramtohul, Y. K.; Ferreira, E. M.; Stoltz, B. M. *Angew. Chem., Int. Ed.* **2003,** *42*, 2892-2895.

5. (a) Scarborough, C. C.; Bergant, A.; Sazama, G. T.; Guzei, I. A.; Spencer, L. C.; Stahl, S. S. *Tetrahedron* **2009,** *65*, 5084-5092. (b) He, W.; Yip, K. T.; Zhu, N. Y.; Yang, D. *Org. Lett.* **2009,** *11*, 5626-5628. (c) Jiang, F.; Wu, Z. X.; Zhang, W. B. *Tetrahedron Lett.* **2010,** *51*, 5124-5126. (d) McDonald, R. I.; White, P. B.; Weinstein, A. B.; Tam, C. P.; Stahl, S. S. *Org. Lett.* **2011**, *13*, 2830-2833.

6. (a) Hosokawa, T.; Takano, M.; Kuroki, Y.; Murahashi, S. I., *Tetrahedron Lett.* **1992,** *33*, 6643-6646. (b) Stahl, S. S.; Timokhin, V. I.; Anastasi, N. R. *J. Am. Chem. Soc.* **2003,** *125*,

12996-12997. (c) Brice, J. L.; Harang, J. E.; Timokhin, V. I.; Anastasi, N. R.; Stahl, S. S. *J. Am. Chem. Soc.* **2005,** *127*, 2868-2869. (d) Kim, S. K.; Lee, J. M.; Ahn, D. S.; Jung, D. Y.; Lee, J.; Do, Y.; Chang, S. K. *J. Am. Chem. Soc.* **2006,** *128*, 12954-12962. (e) Rogers, M. M.; Kotov, V.; Chatwichien, J.; Stahl, S. S. *Org. Lett.* **2007,** *9*, 4331-4334. (f) Obora, Y.; Shimizu, Y.; Ishii, Y. *Or.g Lett.* **2009,** *11*, 5058-5061. (g) Liu, X.; Hii, K. K. *Eur. J. Org. Chem.* **2010,** *2010*, 5181-5189.

7. See ref. 1a and the following: (a) Isomura, K.; Okada, N.; Saruwatari, M.; Yamasaki, H.; Taniguchi, H. *Chem. Lett.* **1985,** 385-388. (b) Liu, G. S.; Stahl, S. S. *J. Am. Chem. Soc.* **2006,** *128*, 7179-7181. (c) Muñiz, K.; Hövelmann, C. H.; Streuff, J. *J. Am. Chem. Soc.* **2007,** *130*, 763-773. (d) Liu, G. S.; Stahl, S. S. *J. Am. Chem. Soc.* **2007,** *129*, 6328-6335.

8. For recent catalytic and fundamental studies of alkene amidation reactions with carbamate and carboxamide nucleophiles that proceed via *trans*-amidopalladation, see the following: (a) Michael, F. E.; Cochran, B. M. *J. Am. Chem. Soc.* **2008**, *130*, 2786-2792. (b) Sibbald, P. A.; Rosewall, C. F.; Swartz, R. D.; Michael, F. E. *J. Am. Chem. Soc.* **2009,** *131*, 15945-15951.

9. (a) Neukom, J. D.; Perch, N. S.; Wolfe, J. P. *J. Am. Chem. Soc.* **2010**, 132, 6276. (b) Klinkenberg, J. L.; Hartwig, J. F. *J. Am. Chem. Soc.* **2010**, 132, 11830. (c) Neukom, J. D.; Perch, N. S.; Wolfe, J. P. *Organometallics* **2011**, 30, 1269. (d) Hanley, P. S.; Hartwig, J. F. *J. Am. Chem. Soc.* **2011,** *133*, 15661-15673.

10. Prior to fundamental studies of alkene insertion, Wolfe and coworkers provided stereochemical evidence for a *cis*-amidopalladation step: (a) Wolfe, J. P.; Ney, J. E. *Angew. Chem., Int. Ed.* **2004,** *43*, 3605-3608. (b) Wolfe, J. P.; Ney, J. E. *J. Am. Chem. Soc.* **2005,** *127*, 8644-8651. (c) Wolfe, J. P.; Nakhla, J. S.; Kampf, J. W. *J. Am. Chem. Soc.* **2006,** *128*, 2893-2901.

11. For leading references to fundamental studies of alkene reactivity with other transition-metal amido complexes, see: (a) Hong, S.; Marks, T. J. *Acc. Chem. Res.* **2004,** *37*, 673-686. (b) Müller, T. E.; Hultzsch, K. C.; Yus, M.; Foubelo, F.; Tada, M. *Chem. Rev.* **2008,** *108*, 3795-3892. (c) Zhao, P.; Krug, C.; Hartwig, J. F. *J. Am. Chem. Soc.* **2005**, *127*, 12066-12073. (d) Hoover, J. M.; DiPasquale, A.; Mayer, J. M.; Michael, F. E. *J. Am. Chem. Soc.* **2010,** *132*, 5043-5053. (e) Leitch, D. C.; Platel, R. H.; Schafer, L. L. *J. Am. Chem. Soc.* **2011**, *133*, DOI: 10.1021/ja202448b.

12. See Experimental Section and Appendix 2 for further details.

13. For the synthesis and previous application of this substrate probe, see ref. 7d.

14. This reaction was carried out in an NMR tube. Because gas-liquid mixing is slow in an NMR tube, an elevated pressure of O_2 was used to ensure at least 1 equiv of O_2 was dissolved in solution.

15. The reaction of O_2 with (N-N)Pd(H)Cl complexes was the focus of a recent study: Decharin, N.; Popp, B. V.; Stahl, S. S. *J. Am. Chem. Soc.* **2011**, *133*, 13268-13271.

16. Data acquisition focused on the alkene insertion/deinsertion steps ($K_)$). Thus, the reliability of the k_2 data is constrained by the limited data obtained for the b-hydride elimination step.

17. For recent progress in this area, see refs. 1f, 4d, 5 and the following additional leading references: (a) Uozumi, Y.; Kyota, H.; Kato, K.; Ogasawara, M.; Hayashi, T. *J. Org. Chem.* **1999,** *64*, 1620-1625. (b) Sasai, H.; Arai, M. A.; Kuraishi, M.; Arai, T. *J. Am. Chem. Soc.* **2001,** *123*, 2907-2908.

18. See, for example: (a) Vitagliano, A.; Hahn, C.; Morvillo, P. *Eur. J. Inorg. Chem.* **2001**, 419-429. (b) Michael, F. E.; Cochran, B. M. *J. Am. Chem. Soc.* **2008,** *130*, 2786-2792. (c) Timokhin, V. I.; Stahl, S. S. *J. Am. Chem. Soc.* **2005,** *127*, 17888-17893.

19. Foley, S. R.; Shen, H.; Qadeer, U. A.; Jordan, R. F. *Organometallics* **2004,** *23*, 600-609.

20. Battino, R. *Solubility Data Series: Oxygen and Ozone*; Pergamon Press: Oxford, U.K.,

1981; Vol. 7

21. (a) Steinhoff, B. A.; Guzei, I. A.; Stahl, S. S *J. Am. Chem. Soc.* **2004**, *126*, 11268–11278. (b) Steinhoff, B. A.; Stahl, S. S. *J. Am. Chem. Soc.* **2006**, *128*, 4348–4355.

22. Liu, G. S.; Stahl, S.S. *J. Am. Chem. Soc.* **2007**, *129*, 6328-6335.

23. Brenzovich, W. E.; Benitez, D.; Lackner, A. D.; Shunatona, H. P.; Tkatchouk, E.; Goddard, W. A.; Toste, F. D. *Angew. Chem. Int. Ed.* **2010,** *49*, 5519-5522.

24. Fix, S. R.; Brice, J. L.; Stahl, S. S. *Angew. Chem. Int. Ed.* **2002,** *41*, 164-166.

25. Hegedus, L. S.; McKearin, J. M. *J. Am. Chem. Soc.* **1982,** *104*, 2444-2451.

Chapter 4.

Characterization of Unusual Bidentate Ligand Behavior in Pd-Catalyzed Aerobic Oxidation Reactions: A Case Study in Wacker-Type Cyclization

This work was done in collaboration with an undergraduate researcher Geyunjian Zhu at the University of Wisconsin–Madison

4.1 Introduction

The past decade has seen a rise in the prominence of nitrogen-containing ligands for oxidative palladium catalysis.[1] The role of ligands in Pd-catalyzed oxidations are two-fold: first, to tune the catalyst's reactivity and selectivity for a substrate by altering the electronics and coordination sphere at Pd^{II}, and second, to promote reoxidation of the reduced catalyst and hindering aggregation of Pd^0 ("Pd-black"). These two roles are often conflicting when developing a catalyst system since electron-deficient Pd^{II} centers form stronger oxidants while electron-rich Pd^0 centers accelerate reoxidation (Scheme 4.1). As a result, a balance between catalyst (re)activity and longevity is often necessary when optimizing a catalyst system.[2]

Scheme 4.1. Conceptual Overview of Aerobic Palladium Catalysis
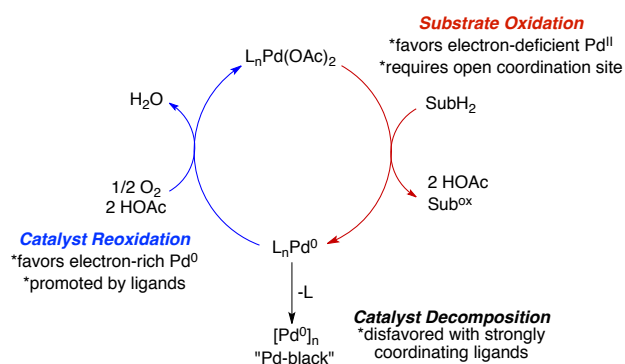
Aerobic Pd-catalyzed oxidations present additional challenges. First, the ligands must be oxidatively stable, which limits the use of phosphines. Second, the reoxidation of Pd^0 with dioxygen is slow compared to other chemical oxidants such as benzoquinone, Ag^I and Cu^{II} and can require higher ligand loadings to prevent Pd^0 aggregation. These higher ligand concentrations, in turn, can inhibit the rate of substrate oxidation by occupying coordination sites on Pd^{II}.[2] As a result, the identity and quantity of ligand are important parameters that must be considered in catalyst development.

Pyridines are aerobically stable and were observed early on by Uemura to support aerobic Pd-catalyzed alcohol oxidations.[3] Our group shortly thereafter applied the Pd(OAc)$_2$/pyridine (pyr, **L1**) catalyst system to aerobic aza-Wacker cyclizations, which form substituted pyrrolidines from olefinic amides (Scheme 4.2A).[4] The mechanism of this reaction has been extensively studied with experimental and DFT methods. These studies demonstrated that the fastest initial rates are obtained with a 1:1 pyridine:Pd stoichiometry. This can be rationalized by a need for open coordination sites at the catalyst center to which the substrate can bind during the oxidation half-reaction (Scheme 4.2B). However, the most stable catalyst was found have a ≥2:1 pyridine:Pd stoichiometry. As a result, the optimal catalyst conditions have a 2:1 pyridine:Pd stoichiometry, which sufficiently stabilizes the reduced catalyst but requires ligand dissociation during substrate oxidation.[5]

Scheme 4.2. Conditions and Proposed Mechanism for Pd(OAc)$_2$/pyridine-Catalyzed aza-Wacker Cyclization
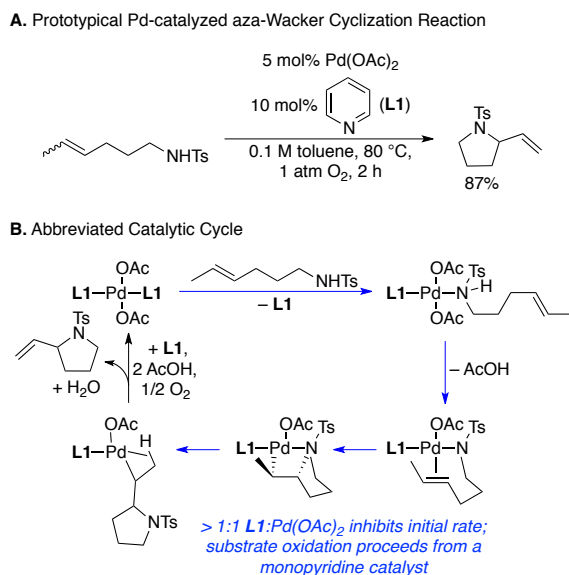
Simple bidentate pyridine analogs such as 2,2'-bipyridine (bpy) and 1,10-phenanthroline (phen) often inhibit reactivity.[6] However, a series of modified bpy and phen ligands have been

recently published that demonstrate improved activity over the parent ligand (Scheme 4.3). For example, 6,6'-dimethyl-2,2'-bipyridine (6,6'-Me$_2$bpy, **L2**) and 2,9-dimethyl-1,10-phenanthroline (neocuproine, **L3**) have seen successful application in Heck coupling of arenes and alkenes,[7] dehydrogenation of ketones to phenol[8] and carbonylation reactions.[9] Additionally, 4,5-diazafluorenone (DAF, **L4**) has promoted the aerobic Pd-catalzyed allylic acetoxylation of terminal olefins,[10] C–C coupling of indoles with benzene,[11] dehydrogenation of cyclic ketones[12] and Heck coupling of ferrocenes with electron-deficient alkenes.[13]

Scheme 4.3. Representative Aerobic Pd-Catalyzed Reactions with Neocuproine, 6,6'-Me2bpy and DAF Ligands
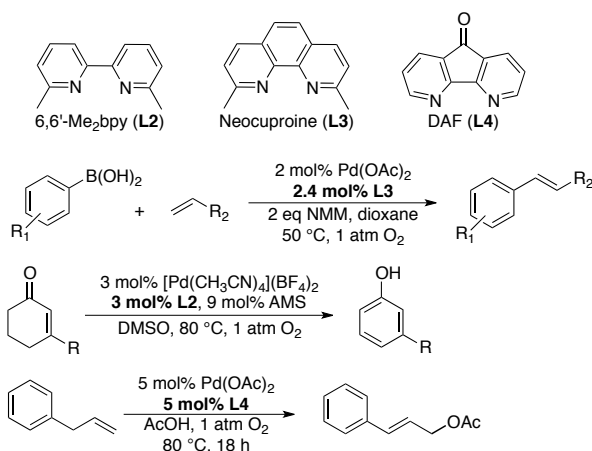
The ability of DAF, 6,6'-Me$_2$bpy and neocuproine to promote varous aerobic Pd-catalyzed oxidation reactions led us to classify these ligands as "privileged" in the sense that they support a number of distinct chemical steps in such as C–H activation, alkene insertion, reductive elimination and β-hydride elimination. Therefore, we set forth to study these and other bidentate ligands within the context of the well-characterized aza-Wacker cyclization reaction.

Herein we report that DAF and 6,6'-Me$_2$bpy demonstrate superior catalytic activity over the parent bpy ligand. A series of NMR spectroscopic, X-ray crystallographic and DFT studies reveal the weakly chelating and hemilabile nature DAF and 6,6'-Me$_2$bpy. We propose that the

origin of the observed catalytic activity is due to the ability of DAF and 6,6'-Me$_2$bpy to alternate between chelating and monodentate coordination modes, effectively acting as stoichiometric monodentate ligands for Pd(OAc)$_2$.

4.2 Results and Discussion

4.2.1 Bidentate Ligands Screened for Oxidative Amidation.

Prominent bidentate ligands were screened at 50 °C under standard oxidative amidation conditions in order to assess reactivity (Table 4.1). Particularly active ligands were reevaluated at 24 °C to compare their activity against the ligand-free condition. The ligand-free condition (entry 1) gives a low yield and poor mass balance at 50 °C due to a competing amide-to-imine oxidation side-reaction, which is considerably reduced at room temperature. The reaction proceeds smoothly with pyridine (entry 2) as the ligand, similar to our previously reported results. Sterically unhindered, chelating ligands such as phen (entry 3a), bathophenanthroline (entry 3c) and 4,4'-^{t}Bu$_2$bpy (entry 4), inhibit the reaction as expected. Among sterically encumbered ligands (entries 3b, 3d, 5, 6), only 6,6'-Me$_2$bpy supports catalytic turnover to a similar extent as pyridine. Furthermore, the yield diminishes significantly when one of the methyl groups is removed from the bpy framework (entry 5 vs 6). DAF (entry 7) exhibits a strong promoting effect, exceeding pyridine's activity at both 50 °C and 24 °C. All reactions have excellent mass balance, except the ligand-free condition, and show no sign of decomposition into Pd-black under all conditions. These results confirm our hypothesis that bidentate ligands could operate within the oxidative amidation reaction and justifies the use of this reaction for investigating the features that allow DAF and 6,6'-Me$_2$bpy to support catalysis.

Table 4.1. Assessment of Bidentate Ligands on Oxidative Amidation[a]

Entry	Ligand	Yield[b]	Entry	Ligand	Yield[b]
1	None	66% 59% (24 °C)	4		1%
2	(pyridine) 10 mol%	**86%** **47%** (24 °C)	5		38%
3			6		**81%** **40%** (24 °C)
	a: $R_1 = R_2 = H$	3%	7		**97%** **97%** (24 °C)
	b: $R_1 = Me, R_2 = H$	9%			
	c: $R_1 = H, R_2 = Ph$	1%			
	d: $R_1 = Me, R_2 = Ph$	7%			

[a]Conditions: substrate (75 μmol, 0.1 M), Pd(OAc)2 (3.75 μmol), O_2 (1 atm), toluene (0.75 mL), 50 °C, 24 h. [b]Yield determined by ^{1}H NMR spectroscopy, int. std. = $PhSiMe_3$.

4.2.2 Investigation into the Reaction Kinetics with Various Ligands.

Reaction monitoring for the oxidative cyclization was performed for DAF, 6,6'-Me2bpy and pyridine at 50 °C in order to assess catalyst activity and stability compared to the ligand-free condition.[14] The promoting effect of DAF is clearly demonstrated as the rate of substrate consumption greatly exceeds the ligand-free condition (Figure 4.1). Pyridine shows a similar rate as the ligand-free condition with 6,6'-Me2bpy performing modestly slower. The clean kinetic profiles and absence of Pd-black in the reactors point toward stable catalyst systems in the presence and absence of ligand.
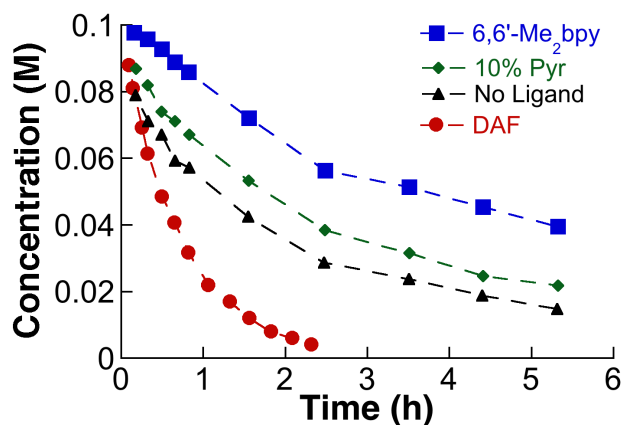
Figure 4.1. Kinetic time-course of the oxidative cyclization of **1**. Conditions: Pd(OAc)$_2$ (3.4 mg, 15 μmoles), ligand (DAF & 6,6'-Me$_2$bpy = 15 μmoles; pyridine 30 μmoles), **1** (76 mg, 300 μmoles, 0.1 M), 50 °C, 1 atm O$_2$, toluene (3 mL), int. std. = 1,3,5-trimethoxybenzene. The reaction was followed for 2.5 hours for DAF with data collected every 5 min, and the other ligands were followed for 5.5 hours with data collected every 10 min for the first 50 min and every hour for the rest.

4.2.3 Determination of the Amidopalladation Mechanism.

The mechanism of amidopalladation dictates how the C–N bond is formed and is sensitive to the identity of the solvent, substrate and ligands on palladium. The two potential pathways for amidopalladation are 1) electrophilic activation of the alkene by Pd^{II} followed by nucleophilic attack of the amide (*trans*-amidopalladation, *trans*-AP) and 2) formation of a Pd-amidate, coordination of the pendent alkene to Pd^{II} and insertion into the Pd–N bond (*cis*-amidopalladation, *cis*-AP) (Scheme 4.4A). Our group had previously developed a stereospecifically-deuterated substrate (Scheme 4.4B) capable of distinguishing between the two pathways and was applied to the present catalytic reactions where the ligand was DAF or 6,6'-Me$_2$bpy. Both ligands are observed to proceed via *cis*-AP, which agrees previous observations from our group that most Pd(OAc)$_2$ catalysts with mono- or bidentate ligands generally operate through *cis*-AP (Scheme 4.4B).
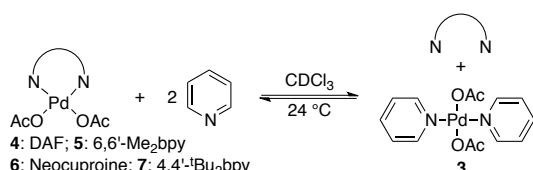
Scheme 4.4. Investigation into the Mechanism of C–N Bond Formation

A) Mechanistic Distinction Between *cis*- and *trans*-Amidopalladation

cis-amidopalladation
(***cis*-AP**)

trans-amidopalladation
(***trans*-AP**)

B) Determination of Amidopalladation Pathway for DAF and 6,6'-Me₂bpy

5% Pd(OAc)₂
5% Ligand
0.1 M toluene, 48 h
24 °C, 1 atm O₂

I

II   **III**
***cis*-AP products**

cis-**AP Only**
98% yield

cis-**AP Only**
72% yield

IV   **V**
trans-**AP products
not observed**
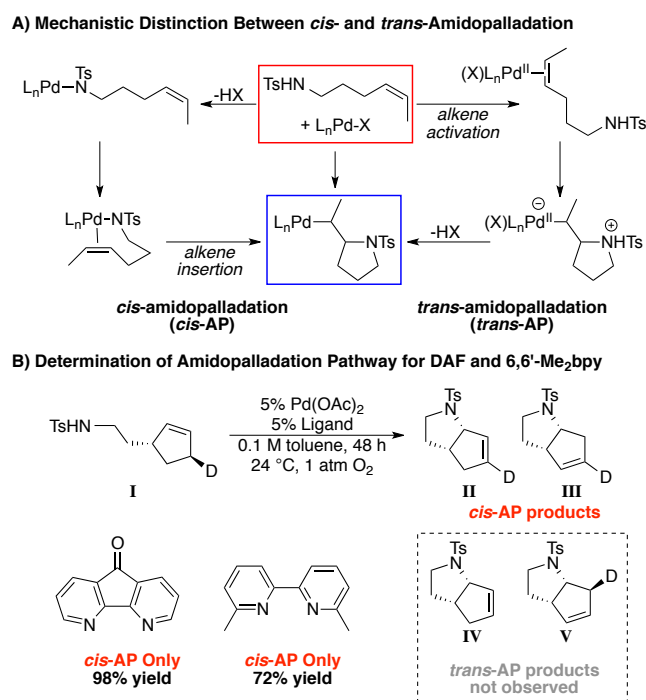
4.2.4 Assessing Ligand Coordination Strength via Titrating Pyridine.

We propose that the unusually high activity of DAF and 6,6'-Me₂bpy in the aza-Wacker reaction is due to the formation of destabilized chelates with Pd^{II}.[Error! Bookmark not defined.] To address this hypothesis, a series Pd(OAc)₂ complexes were synthesized with DAF, 6,6'-Me₂bpy, neocuproine and 4,4'-^{t}Bu₂bpy as ligands. These well-defined complexes have been observed by NMR spectroscopy and X-ray crystallography to form the 1:1 ligand:Pd adduct with a κ^2-bound ligand.[15] The only exception is DAF, which forms multiple species in solution that have been previously characterized by our group.[16] Pyridine was added into a CDCl₃ solution of each complex to compare the coordination strength of chelating ligands relative to a standard monodentate ligand. The mixtures were analyzed by ^{1}H NMR spectroscopy, looking specifically for the appearance of Pd(pyr)₂(OAc)₂ (**3**) and the dissociated bidentate ligand (Figures A4.6-A4.9).

The DAF•Pd(OAc)$_2$ mixture (**4**) completely dissociates to form **3** and free DAF after 2 equivalents of pyridine are added. Pd(κ^2-6,6'-Me$_2$bpy)(OAc)$_2$ (**5**) is also very susceptible to ligand dissociation and exhibited 85% ligand dissociation at 2 equivalents of pyridine (Table 4.2). The Pd(κ^2-neocuproine)(OAc)$_2$ complex (**6**), on the other hand, is markedly more resistant to dissociation with only 7% conversion to **3** after 2 equivalents of pyridine were added. Pd(4,4'-^{t}Bu$_2$bpy)(OAc)$_2$ (**7**) is very stable and shows no evidence of ligand dissociation even after 5 equivalents of pyridine are added. In summary, the ligand's strength of coordination to Pd(OAc)$_2$ follows 4,4'-^{t}Bu$_2$bpy >> neocuproine > pyridine >> 6,6'-Me$_2$bpy > DAF. This trend is inversely proportional to the catalytic yields in Table 4.1 and suggests that the strength of ligand chelation could be important for reactivity.

Table 4.2. Comparison of Ligand Lability with Catalytic Yields.

Ligand	Complex Dissociated (%)	Estimated K_{eq}
DAF	100	>100
6,6'-Me$_2$bpy	85	1.45
Neocuproine	7	4.11 x 10^{-5}
4,4'-^{t}Bu$_2$bpy	0	<0.01

An intriguing observation was made during the addition of pyridine to the DAF•Pd(OAc)$_2$ (**4**) solution. A rapidly exchanging species, **8**, is observed from the beginning of the titration until 2 equivalents of pyridine have been added (Figure 4.2). The intermediate is persistent and has been identified as the *trans*-(κ^1-DAF)(pyr)Pd(OAc)$_2$ (**8**) complex by X-ray crystallography. Furthermore, chemical exchange could be minimized at -35 °C and subsequent analysis with ^{1}H 1D, ^{1}H-^{13}C and ^{1}H-^{15}N 2D NMR techniques confirms the solution-phase identity of **8** to be the *trans*-Pd(κ^1-DAF)(pyr)(κ^1-OAc)$_2$ complex (Figures A4.10-A4.16).

A. Observation of Mixed Ligand Complex **8** During Addition of Pyridine to **4**
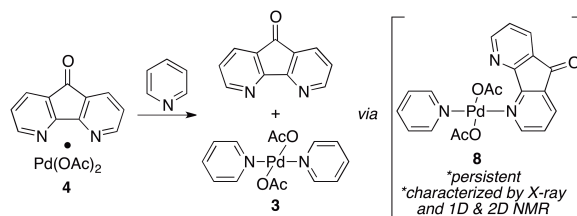
B. Crystal Structure of **8**
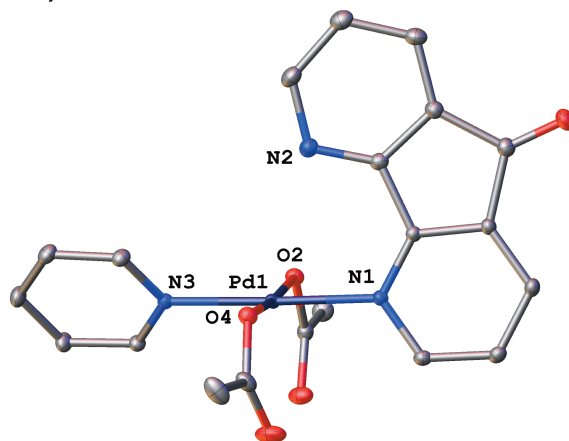
Figure 4.2. Observation of a mixed DAF/pyridine intermediate, **8**, characterized by NMR spectroscopy (**A**) and X-ray crystallography (**B**). Molecular diagram of the crystal is drawn with 50% probability ellipsoids and all H atoms are omitted for clarity.

A similar but transient intermediate, **9**, is also observed during the addition of pyridine to the Pd(6,6'-Me$_2$bpy)(OAc)$_2$ (**5**) solution; however **9** readily disproportionates to form **3**, **5** and free 6,6'-Me$_2$bpy (Figure 4.3). The disproportionation of **9** could be mitigated at temperatures <-40 °C but significant chemical exchange still occurs even at -90 °C, which prevents the application of heteronuclear 2D NMR techniques. However, ^{1}H 1D TOCSY, EXSY and ROESY experiments (Figures A4.17-A4.19), in combination with standard ^{1}H 1D integrations, reveal a 6,6'-Me$_2$bpy ligand that consists of two inequivalents rings (Figure 4.3). Through-space interactions are observed between a 6,6'-Me$_2$bpy, pyridine and two acetate ligands, and the integrations support a stoichiometry consistent with a *trans*-Pd(κ^1-6,6'-Me$_2$bpy)(pyr)(κ^1-OAc)$_2$ complex, **9** (Figure A4.19). We have recently characterized a series of DAF-Pd(OAc)$_2$ coordination complexes providing evidence for κ^1 coordination;[17] however, evidence for κ^1 coordination is unprecedented for 6,6'-Me$_2$bpy to the best of our knowledge.
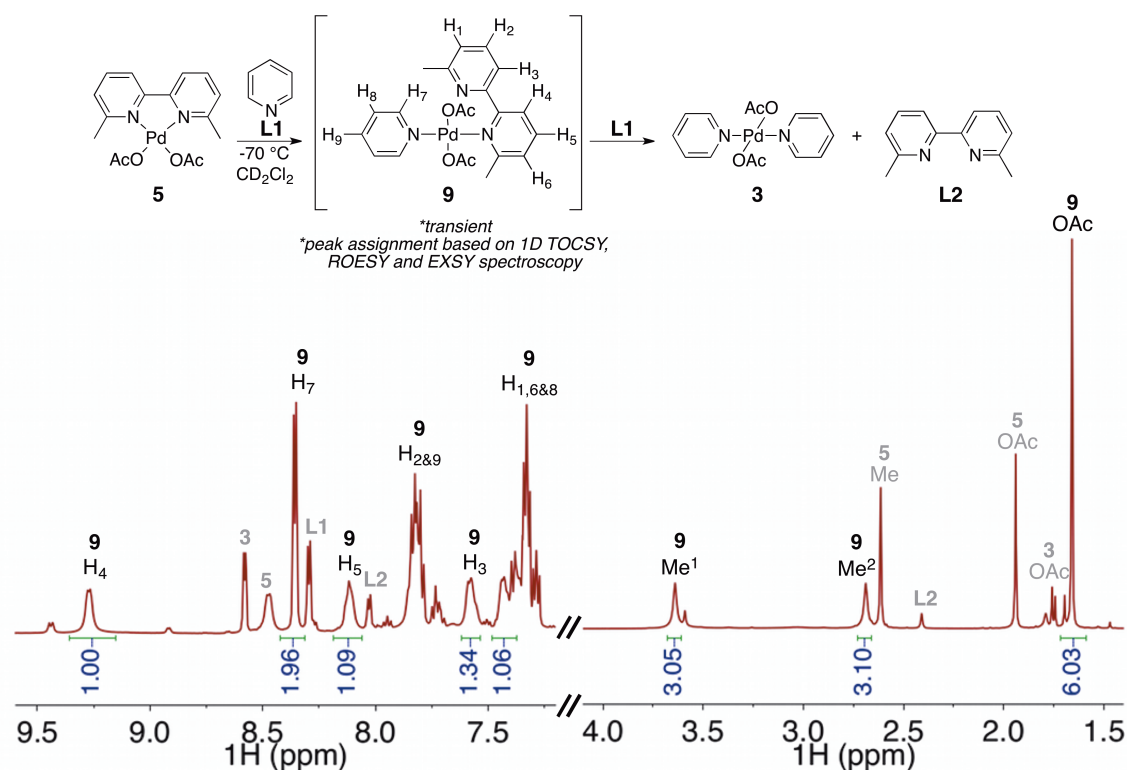
Figure 4.3. Observation of a mixed 6,6'-Me$_2$bpy/pyridine intermediate, **9**, characterized by NMR spectroscopy. The integrations of the aromatic and aliphatic protons are consistent with *trans*-Pd(κ^1-6,6'-Me$_2$bpy)(pyr)(OAc)$_2$. Correlations within and between ligands were made with 1D TOCSY and ROESY experiments (Figures A4.18-19).

4.2.5 Computational Investigation of Ligand Coordination and Viability of κ^1-Ligand Intermediates in the Reaction Coordinate.

The relative chelate strengths of each ligand was investigated by DFT methods. A similar trend is observed to form a ligated metal complex as is seen in the pyridine titration: the complexes formed with neocuproine and 4,4'-*t*Bu$_2$bpy are much stronger than those formed by DAF and 6,6'-Me$_2$bpy (Scheme 4.5).

Scheme 4.5. Assessment of Ligand Coordination Strength by DFT Methods
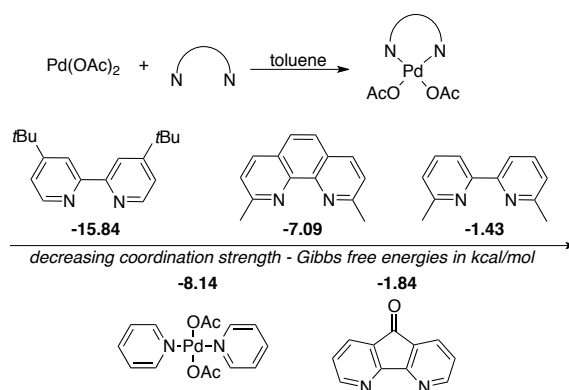
The observation of a chelating ligand forming a κ^1-ligated Pd complex prompted us to investigate the plausibility of these intermediates along the oxidative amidation catalytic cycle by DFT methods. Several boundary conditions have been created from the experimental results: 1) the *cis*-AP mech indicates that the amide and alkene must both coordinate to Pd prior to forming the C–N bond and 2) the computed barriers must reasonably match the experimental values[14] obtained from the Eyring equation (22.5 kcal/mol and 24.6 kcal/mol for DAF and 6,6'-Me$_2$bpy, respectively). The reaction coordinate for bidentate ligands is a modified version of our previously published reaction coordinate where pyridine loss has been substituted with a $\kappa^2 \rightarrow \kappa^1$ isomerism. Formation of the chelated complex was found to be the most stable Pd^{II} complex for each of the ligands and serves as the starting point for the reaction coordinate (Scheme 4.6, **A→B**).

Next, the substrate and catalyst forms a Pd-amidate complex by exchanging protons with an acetate and satisfies a requirement of the *cis*-AP pathway (**B→C**).[18] One of the pyridyl rings of the chelating ligand is then displaced by the pendent alkene in a neutral ligand exchange process (**C→D**). The C–N bond is formed via alkene insertion into the Pd–N bond (**E**), thus completing the *cis*-amidopalladation mechanism. β-Hydride elimination from the Pd-alkyl proceeds via a Pd-assisted deprotonation by the coordinated acetate that also reduces Pd^{II} to Pd^0 in the process

(**F→H**). The resulting coordinated acetic acid is then displaced by the chelating ligand to form

the κ^2-coordinated Pd^0-alkene complex (**I**). Substitution of the alkene with dioxygen and

subsequent protonolysis of the Pd^{II}-peroxo to regenerate the catalyst has been previously studied

by our group and others and is not proposed to be rate-limiting.[19]

Scheme 4.6. Computational Investigation into the Oxidative Amidocyclization Reaction Coordinates for Pd(OAc)$_2$ with DAF, 6,6'-Me$_2$bpy and neocuproine ligands
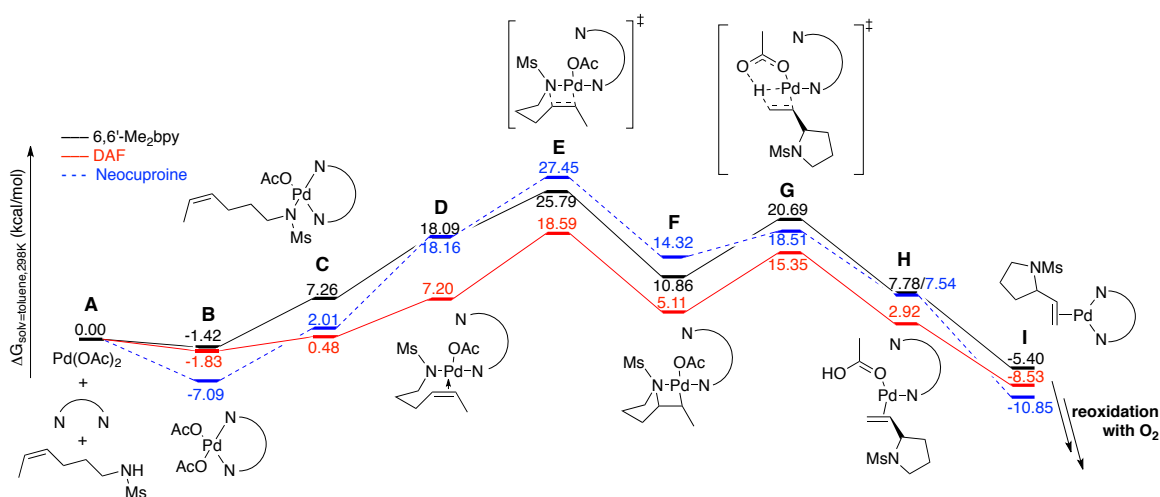
The lowest energy point for all the ligands is the chelated Pd(ligand)(OAc)$_2$ complex

(Scheme 4.6, **B**) and the highest global barrier is the amidopalladation transition state, **E**. There

is a reasonable agreement between the experimental and calculated barriers (DAF: 20.42 vs 22.5

kcal/mol; 6,6'-Me$_2$bpy: 27.21 vs 24.6 kcal/mol) and supported the plausibility of κ^1-ligated

intermediates in the catalytic cycle. The absolute energy of **E** for 6,6'-Me$_2$bpy and neocuproine is

insignificant (25.79 vs 27.45 kcal/mol) yet the overall barriers are quite different (22.71 vs 34.54

kcal/mol). This clearly demonstrates the effect of stabilizing a ground-state structure can have on

the overall barrier for a reaction, and provides an explanation for the difference in catalyst

activity between the two ligands (cf. Table 4.1).

4.2.6 Geometric Rationale for Forming Weak Chelates and κ^1-Coordinated Complexes.

DAF and 6,6'-Me$_2$bpy deviate from the inhibitory effect that is expected from simple bidentate ligands and successfully catalyze the oxidative amidocyclization reaction. The pyridine titration, NMR spectroscopic, X-ray crystallographic and DFT studies have revealed that these ligands can alternate between chelating and partially dissociated geometries. These observations suggest that these ligands act as hemilabile ligands during catalysis. We propose that the origin of this hemilabile behavior, and by extension catalytic activity, is due to the unique structural features of each ligand that differentiates it from the parent bipyridine ligand.

The carbonyl group in DAF effectively lengthens the nitrogen-nitrogen (N---N) distance between the two pyridyl rings. A comparison of crystal structures of DAF and bipyridine ligands reveal N---N distances of 3.06 Å and 2.71 Å, respectively (Scheme 4.7).[20] The large N---N distance for DAF contracts considerably to 2.78 Å upon chelating to PdCl$_2$, a difference of 0.28 Å, whereas bpy contracts only by 0.09 Å to 2.62 Å. The resulting Pd–N bond length and N-Pd-N bite angle are slightly larger for DAF but otherwise the chelated structures appear very similar (Scheme 4.7).[21] However, the significant shortening of the N---N distance for DAF upon coordination to Pd^{II} introduces strain that is spread over multiple bonds and angles within the ligand. As a result, the κ^2 geometry is destabilized while the monodentate (κ^1) coordination mode is preferred since the N---N distance (3.10 Å) is more akin to its uncoordinated value (3.06 Å).[16]

Scheme 4.7. Examination of Geometric Parameters for Chelation from Crystallographic Structures

N---N: 3.06 Å   N---N: 2.71 Å

PdCl$_2$ PdCl$_2$

N---N: 2.78 Å   N---N: 2.62 Å
Pd–N: 2.09 Å   Pd–N: 2.03 Å
N-Pd-N: 83.7°   N-Pd-N: 80.4°

large change in N---N distance upon chelating DAF
induces steric strain in ligand
chelated complex becomes destabilized
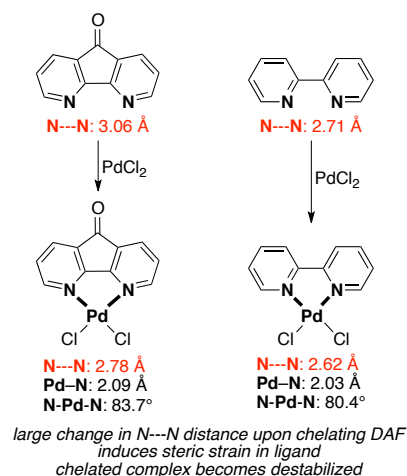
6,6'-Me$_2$bpy has two significant steric interactions that occur upon coordination and serve to counteract the energetic benefit from chelation. A minor steric interaction occurs between the protons in the 3,3' position when the ligand rotates into a *syn* conformation to coordinate to Pd, which is inherent in the 2,2'-bipyridine class of ligands (Figure 4.4A). The second and most significant steric interaction is between the two *ortho* methyl groups and acetates, which results in the 6,6'-Me$_2$bpy ligand bending 27° out of the square plane in order to alleviate this interaction (Figure 4.4B).

A. Steric Interactions Formed Upon Chelation to Pd(OAc)$_2$

2.05 Å < 2.4 Å
(van der Waals)

ligand bends
out of plane

B. Crystal Structure of Pd(κ^2-6,6'-Me$_2$bpy)(OAc)$_2$

27° bend away
from planarity
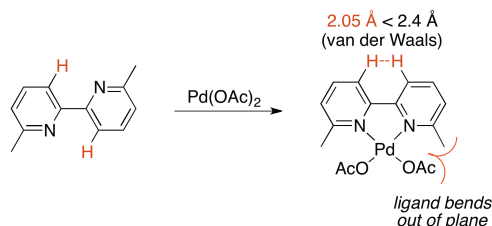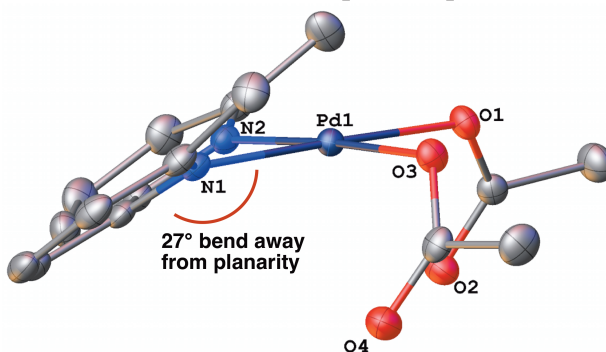
Figure 4.4. A steric clash occurs between the 3,3' protons when the ligand rotates into a syn orientation (**A**). The crystal structure of Pd(κ^2-6,6'-Me$_2$bpy)(OAc)$_2$ displays how the methyl groups that project into the square plane cause the ligand to bend 27° out of the plane to minimize steric interactions (**B**). The molecular representation of the crystal structure is drawn with 50% thermal ellipsoids and the hydrogen atoms are omitted for clarity.

Ultimately, the steric interactions in DAF and 6,6'-Me$_2$bpy introduce energetic costs upon coordination to Pd^{II}. The result is a weakly bound ligand-metal complex that *could partially dissociate in order to accommodate an incoming L-type ligand* such as an amide, alkene or arene. We propose that the ability of DAF and 6,6'-Me$_2$bpy to readily accommodate substrate coordination to Pd^{II} is the origin of the reported success of these ligands in aerobic Pd-catalyzed oxidation reactions.

4.2.7 Relevance to Aerobic Oxidation Catalysis.

In the aza-Wacker reaction, the *cis*-amidopalladation mechanism requires two open coordination sites: an X-type site for the Pd-amidate and a L-type site for the alkene. The X-site is generated from an inner-sphere proton transfer from the amide to OAc at the beginning of the mechanism. However, the second site could be generated either from ionization of an ionic

ligand, which is favored only in polar solvents, or dissociation of a neutral ligand, which competes against the chelate effect for bidentate ligands (Scheme 4.8A).

Scheme 4.8. Examples of X- and L-Type Ligand Dissociation Mechanisms for *cis*-Amidopalladation

A) Mechanisms for Alkene Coordination in *cis*-AP Pathway

B) X-type Ligand Dissociation for 4,4'-*t*Bu₂Bpy in DMSO

C) L-type Ligand Dissociation for Pyridine in Toluene
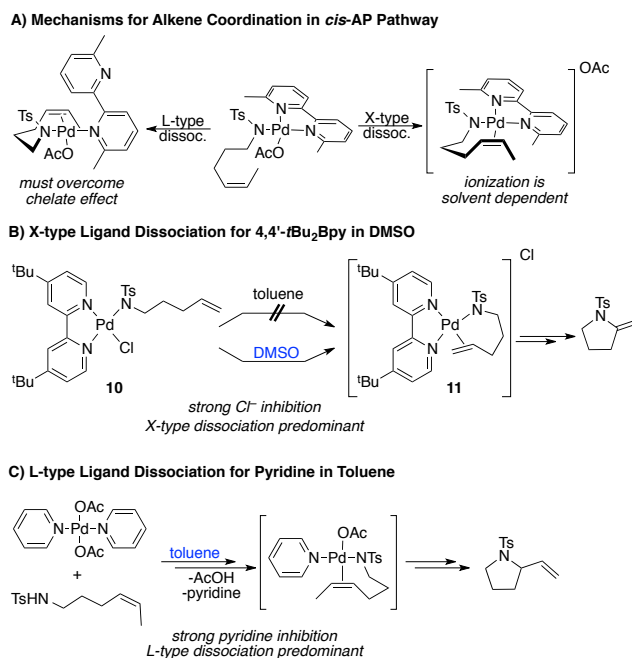
We have previously reported two mechanistic studies where each pathway for *cis*-amidopalladation is independently observed. The first example uses a well-defined Pd(4,4'-^{t}Bu₂bpy)(Cl)(*N*-tosyl-4-pentenamide), **10**, complex where amidopalladation step is strongly inhibited in nonpolar solvents such as toluene (Scheme 4.8B).[22] However, alkene insertion into the Pd–N bond is observed when the solvent is changed to DMSO, which suggests that the process occurred via a stabilized ion pair (Scheme 4.8B). A chloride inhibition study confirmed that the amidopalladation step proceeded via X-type ligand dissociation.

Alternatively, L-type dissociation is favored for monodentate ligands. Thorough mechanistic studies of the Pd(OAc)₂/pyridine catalyst system revealed that the optimal initial reaction rate was obtained from a 1:1 pyridine:Pd stoichiometry, which implied that the active catalytic

species is a Pd(pyr)(OAc)$_2$ complex (Scheme 4.8C).[1e,2a,b] Addition of more ligand inhibited the reaction; however, 4:1 or 2:1 pyridine:Pd(OAc)$_2$ stoichiometries are needed to effectively stabilize the catalyst. Therefore, under standard reaction conditions (≥2:1 pyr:Pd), the Pd(pyr)$_2$(OAc)$_2$ catalyst resting state is an off-cycle species that must dissociate a pyridine ligand for substrate oxidation to proceed. In short, monodentate ligands more easily facilitate substrate oxidation than bidentate ligands, however catalyst stability is often more effective with bidentate ligands due to the chelate effect.

Overcoming the balance between catalyst reactivity and stability has been a significant challenge for the field of oxidative Pd catalysis. Several strategies, such as the application weakly coordinating monodentate ligands or using chemical oxidants to facilitate the kinetics of reoxidation, have emerged to address this challenge.[23] However, each of these has their disadvantage: weakly coordinating ligands often do not stabilize Pd^0 above ambient temperature and chemical oxidants can require additional purification steps to remove. In this report, we have observed catalytic activity with chelating ligands and Pd(OAc)$_2$ under aerobic conditions and have characterized the hemilabile nature of both DAF and 6,6'-Me$_2$bpy. We propose that during catalysis these bidentate ligands behave as a stoichiometric monodentate ligands for substrate oxidation and chelating ligands for catalyst reoxidation (Scheme 4.9). This allows for fast initial rates to be obtained and provides long-lasting catalysts even at elevated temperature. These "masked" monodentate ligands offer a different strategy for addressing the conflict between catalyst activity and longevity.

Scheme 4.9. Mode of Action for Hemilabile Ligands
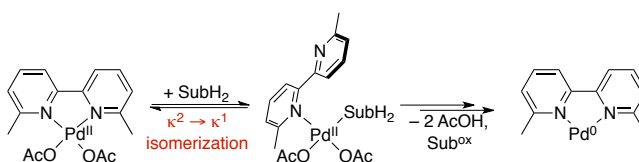
4.3 Conclusion

DAF and 6,6'-Me$_2$bpy were found to be effective ligands in the aerobic Pd-catalyzed oxidative aza-Wacker reaction where the parent bipyridine ligand has been shown to strongly inhibit catalysis. Stereochemical studies indicated that the reactions proceeded via alkene insertion into a Pd–N bond. NMR spectroscopic, X-ray crystallographic and DFT computational data supported a mechanism where the bidentate ligand partially dissociates to accommodate substrate coordination. This phenomenon is rationalized by the particularly weak chelates that are formed with Pd(OAc)$_2$ and DAF or 6,6'-Me$_2$bpy. Weakly chelating ligands are proposed to benefit catalysis by adopting monodentate ligand qualities (κ^1-coordination) during substrate oxidation while chelating and stabilizing Pd^0 for reoxidation.

Contributions: Geyunjian performed many of the early ligand screen studies under my supervision.

4.4 Experimental

4.4.1 General Experimental Considerations

All commercially available compounds were used as received. c*is-N*-Tosyl-4-hexenylamide (**1**) was used from a previously reported synthesis.[24] Aerobic Pd-catalyzed transformations of **1** with various ancillary ligands were performed using a custom 48-well reaction apparatus that enabled reactions to be performed simultaneously under a constant pressure of O$_2$ (approx 1 atm) with controlled temperature and orbital agitation. Kinetic data were obtained by removing aliquots from a scaled-up reaction using an identical but larger-well reactor. The reactions or aliquots were filtered over a plug of silica, washed with EtOAc and the solvent was removed with a centrifugal evaporator. The yield was measured by ^{1}H NMR spectroscopy after addition of either trimethyl(phenyl)silane or 1,3,5-trimethoxybenzene as external standards to the crude evaporated mixture.

4.4.1.1 Synthesis and Characterization of Well-Defined Pd(N~N)(OAc)₂ Complexes

Well-defined Pd(N~N)(OAc)₂ complexes were synthesized from a modification of a literature procedure.[25] A slight of excess of ligand (1.05 equiv) dissolved in minimal acetone was added to a concentrated solution of Pd(OAc)₂ in acetone. The mixture was stirred overnight during which the Pd(N~N)(OAc)₂ complex precipitated out of solution. The yellow precipitate was isolated by vacuum filtration, washed with acetone and dried under vacuum to afford the desired complex.

Pd(6,6'-Me₂bpy)(OAc)₂ (**5**)

90 mg, 65% yield, yellow powder

^{1}H NMR (500 MHz, CDCl₃) δ 8.48 (d, J = 8.0 Hz, 2H), 7.91 (t, J = 7.9 Hz, 2H), 7.04 (d, J = 7.7 Hz, 2H), 2.71 (s, 6H), 2.02 (s, 6H).

^{13}C NMR (126 MHz, CDCl₃) δ 178.01, 163.92, 157.42, 140.35, 126.56, 121.36, 24.32, 23.02.

Pd(neocuproine)(OAc)₂ (**6**)

118 mg, 85% yield, yellow powder

^{1}H NMR (500 MHz, CDCl₃) δ 8.33 (d, J = 8.3 Hz, 2H), 7.84 (s, 2H), 7.47 (d, J = 8.3 Hz, 2H), 2.93 (s, 6H), 2.04 (s, 6H).

^{13}C NMR (126 MHz, CDCl₃) δ 178.76, 165.60, 147.73, 138.31, 128.09, 127.05, 126.32, 24.75, 23.05.

Pd(^{t}Bu₂bpy)(OAc)₂ (**7**)

121 mg, 87% yield, yellow powder

^{1}H NMR (500 MHz, CDCl₃) δ 8.24 (d, J = 6.0 Hz, 2H), 7.83 (d, J = 2.0 Hz, 2H), 7.48 (dd, J = 6.1, 2.0 Hz, 2H), 2.13 (s, 6H), 1.42 (s, 18H).

^{13}C NMR (126 MHz, CDCl₃) δ 178.45, 165.13, 155.47, 149.95, 123.84, 118.41, 35.81, 30.29, 23.46.

4.4.2 General NMR Spectroscopy Considerations.

Routine screening data were analyzed using an automated Bruker Av400 spectrometer equipped with an inverse BBFO+ probe. Characterization of well-defined Pd complexes was performed on a Bruker Av500 spectrometer equipped with a ^{13}C sensitive DCH LHe cryoprobe. Variable temperature and multidimensional spectra were recorded on a Varian INOVA 600 MHz spectrometer equipped with a HPX probe or Bruker Av500 spectrometer equipped with an inverse BBFO+ probe. ^{1}H NMR chemical shifts are reported in parts per million relative to internal TMS (0.00 ppm) in CDCl$_3$. ^{13}C and ^{15}N NMR chemical shifts are reported in parts per million and externally referenced to TMS from the ^{1}H spectrum. The ^{15}N chemical shifts is externally referenced to the ^{1}H spectrum and calibrated to liquid ammonia (at 0.00 ppm). The sample temperature was calibrated with an external 4% MeOH in MeOD-d_3 reference standard. The pw90 and longest T$_1$ values were computed from the pw360 and inversion recovery experiments, respectively, after each temperature change. All standard ^{1}H spectra were recorded quantitatively (recycle delay $\geq$ 5*T$_1$) and integrals referenced to an internal standard (1,3,5-trimethoxybenzene). Selective TOCSY and ROESY experiments were used as implemented in Varian ChemPack 3.1 and were performed using SEDUCE shaped pulses with spinlock frequencies of 8.5 kHz and 5.4 kHz, respectively.

4.4.3 General Computational Considerations.

All computations were performed with the Gaussian 09 program[26] using resources provided by University of Wisconsin–Madison Chemistry Department. Spin-restricted density functional theory (DFT) calculations were performed with the hybrid density functional, rB3LYP.[27,28] A combination of the Stuttgart RSC 1997 ECP/triple-ζ basis[29] for Pd and the all-electron 6-31+G(d) basis set for all other atoms was used for gas-phase geometry optimizations and normal mode analyses. Full geometry optimizations were carried out in internal coordinates using the default Berny algorithm. Frequency calculations were performed at the optimized geometries to

confirm that each geometry had the appropriate number of imaginary frequencies: zero for minima or one for transition states. The imaginary frequency identifying a saddle-point was visually inspected for the proper motion.

At the calculated stationary points, solvation-corrected single-point total energy calculations were carried out with the Pd basis detailed above and the 6-311+G (d,p) basis on all other atoms with electrostatic and non-electrostatic solvation effects evaluated using the polarizable-continuum model (PCM). The solvation cavity was generated using UFF radii, explicitly treating hydrogen atoms, and the radii were scaled by a factor of 1.2. The solvent chosen was toluene.

4.5 References.

1. (a) Stahl, S. S., *Angew. Chem. Int. Ed.* **2004**, *43*, 3400-3420. (b) Stoltz, B. M., *Chem. Lett.* **2004,** *33*, 362-367. (c) Sigman, M. S.; Jensen, D. R., *Acc. Chem. Res.* **2006**, *39*, 221-229. (d) Gligorich, K. M.; Sigman, M. S., *Chem. Commun.* **2009**, 3854-3867. (e) McDonald, R. I.; Liu, G. S.; Stahl, S. S., *Chem. Rev.* **2011**, *111*, 2981-3019.

2. (a) Steinhoff, B. A.; Stahl, S. S., *Org. Lett.* **2002,** *4*, 4179-4181. (b) Steinhoff, B. A.; Guzei, I. A.; Stahl, S. S., *J. Am. Chem. Soc.* **2004,** *126*, 11268-11278. (c) Zhang, Y. H.; Shi, B. F.; Yu, J. Q., *J. Am. Chem. Soc.* **2009,** *131*, 5072-5074. (d) Emmert, M. H.; Cook, A. K.; Xie, Y. J.; Sanford, M., *Angew. Chem. Int. Ed.* **2011,** *50*, 9409-9412. (e) Ye, X. A.; Liu, G. S.; Popp, B. V.; Stahl, S. S., *J. Org. Chem.* **2011,** *76*, 1031-1044. (f) Kubota, A.; Emmert, M. H.; Sanford, M. S., *Org. Lett.* **2012,** *14*, 1760-1763.

3. (a) Nishimura, T.; Onoue, T.; Ohe, K.; Uemura, S., *Tetrahedron Lett.* **1998,** *39*, 6011-6014. (b) Nishimura, T.; Onoue, T.; Ohe, K.; Uemura, S., *J. Org. Chem.* **1999,** *64*, 6750-6755.

4. Fix, S. R.; Brice, J. L.; Stahl, S. S., *Angew. Chem. Int. Ed.* **2002,** *41*, 164-166.

5. Ye/Popp/Decharin

6. Select cases such as carbonylation have seen limited success: (a) Soro, B.; Stoccoro, S.; Agostina Cinellu, M.; Minghetti, G.; Zucca, A.; Bastero, A.; Claver, C., *J. Organomet. Chem.* **2004**, *689*, 1521-1529. (b) Gasperini, M.; Ragaini, F.; Cenini, S.; Gallo, E.; Fantauzzi, S., *Applied Organomet. Chem.* **2007**, *21*, 782-787. (c) Hu, J.; Gu, Y.; Guan, Z.; Li, J.; Mo, W.; Li, T.; Li, G., *Chem. Sus. Chem.* **2011**, *4*, 1767-1772. (c) Campos-Carrasco, A.; Estorach, C. T.; Bastero, A.; Reguero, M.; Masdeu-Bultó, A. M.; Franciò, G.; Leitner, W.; D'Amora, A.; Milani, B., *Organometallics* **2011,** *30*, 6572-6586. (d) Didgikar, M. R.; Joshi, S. S.; Gupte, S. P.; Diwakar, M. M.; Deshpande, R. M.; Chaudhari, R. V., *J. Mol. Catal. A: Chem.* **2011**, *334*, 20-28.

7. (a) Andappan, M. M. S.; Nilsson, P.; Larhed, M., *Chem. Commun.* **2004**, 218-219. (b) Andappan, M. M. S.; Nilsson, P.; von Schenck, H.; Larhed, M., *J. Org. Chem.* **2004**, *69*, 5212-5218. (c) Enquist, P. A.; Lindh, J.; Nilsson, P.; Larhed, M., *Green Chemistry* **2006**, *8*, 338-343. (d) Lindh, J.; Enquist, P. A.; Pilotti, A.; Nilsson, P.; Larhed, M., *J. Org. Chem.* **2007,** *72*, 7957-7962. (e) Zheng, C. W.; Wang, D.; Stahl, S. S., *J. Am. Chem. Soc.* **2012**, *134*, 16496-16499.

8. Izawa, Y.; Zheng, C. W.; Stahl, S. S., *Angew. Chem. Int. Ed.* **2013**, *52*, 3672-3675.

9. (a) Yasuda, H.; Watarai, K.; Choi, J. C.; Sakakura, T., *J. Mol. Catal. A: Chem.* **2005,** *236*, 149-155. (b) Ragaini, F.; Larici, H.; Rimoldi, M.; Caselli, A.; Ferretti, F.; Macchi, P.; Casati, N., *Organometallics* **2011**, *30*, 2385-2393.

10. Campbell, A. N.; White, P. B.; Guzei, I. A.; Stahl, S. S., *J. Am. Chem. Soc.* **2010**, *132*, 15116-15119.

11. Campbell, A. N.; Meyer, E. B.; Stahl, S. S., *Chem. Commun.* **2011**, *47*, 10257-10259.

12. (a) Gao, W. M.; He, Z. Q.; Qian, Y.; Zhao, J.; Huang, Y., *Chem. Sci.* **2012**, *3*, 883-886. (b) Diao, T.; Wadzinski, T. J.; Stahl, S. S., *Chem. Sci.* **2012**, *3*, 887-891.

13. Piotrowicz, M. Ç.; Zakrzewski, J., *Organometallics* **2013**, doi: 10.1021/om400410u

14. The reactions were monitored at 24 °C in order to extract rate constants for the DAF and 6,6'-Me2bpy conditions (Figure A4.4). Gibbs' free energies of activation were estimated from the Eyring equation using the extracted rate constants to be 22.5 and 24.6 kcal/mol for DAF and 6,6'-Me2bpy, respectively.

15. (a) Newkome, G. R.; Fronczek, F. R.; Gupta, V. K.; Puckett, W. E.; Pantaleo, D. C.; Kiefer, G. E., *J. Am. Chem. Soc.* **1982,** *104*, 1782-1783. (b) Milani, B.; Alessio, E.; Mestroni, G.; Sommazzi, A.; Garbassi, F.; Zangrando, E.; Brescianipahor, N.; Randaccio, L., *J. Chem. Soc. Dalton Trans.* **1994,** 1903-1911. (c) Bercaw, J. E.; Day, M. W.; Golisz, S. R.; Hazari, N.; Henling, L. M.; Labinger, J. A.; Schofer, S. J.; Virgil, S., *Organometallics* **2009,** *28*, 5017-5024.

16. Thesis Chapter 2

17. DAF has also been observed to form k1, k2 and m coordination complexes with Pd as well as other transition metals.

18. The methanesulfonyl (Ms) group was used rather than the toluenesulfonyl (Ts) protecting group used in catalysis in order to expedite computation time.

19. (a) Wilke, G.; Schott, H.; Heimbach, P., *Angew. Chem. Int. Ed.* **1967,** *6*, 92-93. (b) Konnick, M. M.; Guzei, I. A.; Stahl, S. S., *J. Am. Chem. Soc.* **2004,** *126*, 10212-10213. (c) Konnick, M. M.; Stahl, S. S., *J. Am. Chem. Soc.* **2008,** *130*, 5753-5762. (d) Konnick, M. M.; Decharin, N.; Popp, B. V.; Stahl, S. S., *Chem. Sci.* **2011,** *2*, 326-330.

20. (a) Fun, H. K.; Sivakumar, K.; Zhu, D. R.; You, X. Z., *Acta Crystallogr., Sec. C: Cryst. Struct. Commun.* **1995,** *51*, 2076-2078. (b) Figuerola, A.; Ribas, J.; Casanova, D.; Maestro, M.; Alvarez, S.; Diaz, C., *Inorg. Chem.* **2005,** *44*, 6949-6958.

21. (a) Canty, A. J.; Skelton, B. W.; Traill, P. R.; White, A. H., *Aust. J. Chem.* **1992,** *45*, 417-422. (b) Xu, Z.-G.; Liu, H.-Y.; Zhan, Q.-G.; Chen, J.; Xu, M.-J., *Acta Crystallogr. Sec. E: Struct. Rep. Online* **2009,** *65*, m1166.

22. White, P. B.; Stahl, S. S., *J. Am. Chem. Soc.* **2011,** *133*, 18594-18597.

23. Ref 2c. See also: (a) Schultz, M. J.; Park, C. C.; Sigman, M. S., *Chem. Commun.* **2002**, 3034-3035. (b) Kubota, A.; Emmert, M. H.; Sanford, M. S., *Org. Lett.* **2012,** *14*, 1760-1763.

24. McDonald, R. I.; White, P. B.; Weinstein, A. B.; Tam, C. P.; Stahl, S. S., *Org Lett* **2011,** *13*, 2830-2833.

25. Pearson, D. M.; Conley, N. R.; Waymouth, R. M., *Adv.Synth. Catal.* **2011,** *353*, 3007-3013.

26. Gaussian 09, Revision C.01, Frisch, M. J.; Trucks, G. W.; Schlegel, H. B.; Scuseria, G. E.; Robb, M. A.; Cheeseman, J. R.; Scalmani, G.; Barone, V.; Mennucci, B.; Petersson, G. A.; Nakatsuji, H.; Caricato, M.; Li, X.; Hratchian, H. P.; Izmaylov, A. F.; Bloino, J.; Zheng, G.; Sonnenberg, J. L.; Hada, M.; Ehara, M.; Toyota, K.; Fukuda, R.; Hasegawa, J.; Ishida, M.; Nakajima, T.; Honda, Y.; Kitao, O.; Nakai, H.; Vreven, T.; Montgomery, J. A. Jr.; Peralta, J. E.; Ogliaro, F.; Bearpark, M.; Heyd, J. J.; Brothers, E.;Kudin, K. N.; Staroverov, V. N.; Keith, T.; Kobayashi, R.; Normand, J.; Raghavachari, K.; Rendell, A.; Burant, J. C.; Iyengar, S. S.; Tomasi, J.; Cossi, M.; Rega, N.; Millam, J. M.; Klene, M.; Knox, J. E.; Cross, J. B.; Bakken, V.; Adamo, C.; Jaramillo, J.; Gomperts, R.; Stratmann, R. E.; Yazyev, O.; Austin, A. J.; Cammi, R.; Pomelli, C.; Ochterski, J. W.; Martin, R. L.; Morokuma, K.; Zakrzewski, V. G.; Voth, G. A.; Salvador, P.; Dannenberg, J. J.; Dapprich, S.; Daniels, A. D.; Farkas, O.; Foresman, J. B.; Ortiz, J. V.; Cioslowski, J.; Fox, D. J. Gaussian, Inc., Wallingford CT, 2010.

27. Becke, A.D. *J. Chem. Phys.* **1993**, *98*, 1372 −1377.

28. Lee, C.; Yang, W.; Parr, R. G. *Phys. Rev. B* **1988**, *37*, 785 − 789.

29. a) Feller, D. *J. Comp. Chem.*, **1996**, *17*(13), 1571-1586. b) Schuchardt, K.L.; Didier, B.T.; Elsethagen, T.; Sun, L.; Gurumoorthi, V.; Chase, J.; Li, J.; and Windus, T.L. *J. Chem. Inf. Model.*, **2007**, *47*(3), 1045-1052

Chapter 5.

Theoretical Investigation into the Origin of Enantioselectivity in

the Pd(TFA)$_2$/(Pyridine-Oxazoline)-Catalyzed aza-Wacker

Reaction: Role of the Pd^{II} Salt on the Amidopalladation

Mechanism and Enantioselectivity

5.1 Introduction

Nitrogen-containing heterocycles are important functional groups that are prolific in natural products and the pharmaceutical industry.[1] Our group has developed several aerobic Pd-catalyzed methods that form five- and six-membered nitrogen-containing heterocycles via cyclization of unactivated olefins containing tethered nitrogen nucleophiles (Scheme 5.1).[2] These "aza-Wacker" reactions are generally promoted by the presence of monodentate ligands, such as pyridine and DMSO, but are strongly inhibited in the presence of bidentate ligands such as 2,2'-bipyridine (bpy) or 1,10-phenanthroline (phen) (Scheme 5.1). However, we recently reported an enantioselective method that employs a Pd(TFA)$_2$ salt and a chiral 2-(2-pyridyl)oxazoline (pyrox) bidentate ligand.[3] Good to high yields were obtained for substrates with various extents of functionalization on the alkyl chain and ee's exceeding 92% for the majority of the examples.

Scheme 5.1. Application of Aerobic Pd Catalysts to the Synthesis of a Variety of Nitrogen-Containing Heterocycles**.**
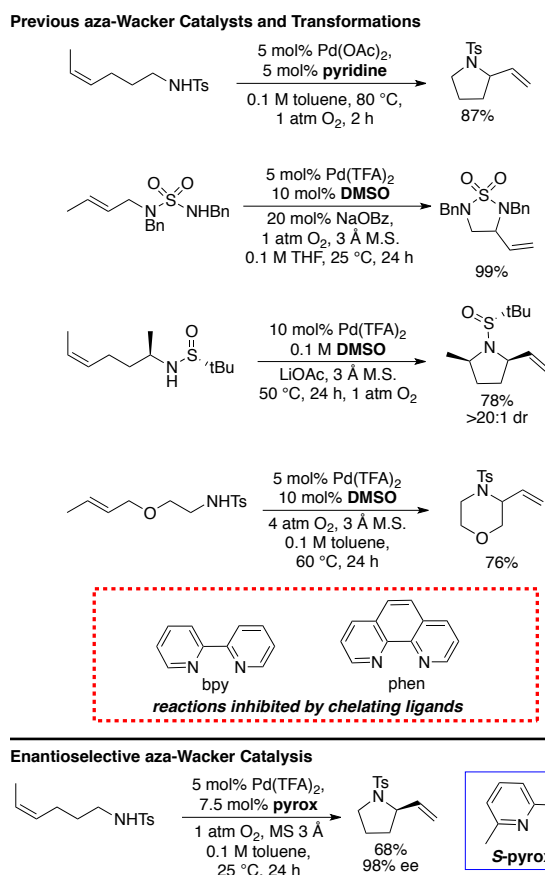
The stereocenter is formed upon addition of the nitrogen nucleophile to the alkene, known as amidopalladation. The two possible mechanisms for amidopalladation are alkene insertion into a Pd–N bond (*cis*-amidopalldation, *cis*-AP) or activation of the alkene by Pd followed by backside attacked by the nitrogen nucleophile (*trans*-amidopalladation, *trans*-AP) (Scheme 5.2). Previous mechanistic studies revealed that aza-Wacker catalysts predominantly proceed via *cis*-AP; however, electron-deficient nitrogen nucleophiles (4-nitrobenzenesulfonamide) or acidic conditions were shown switch the preferred pathway to *trans*-AP.[4]

Scheme 5.2. Mechanistic Distinction Between *Cis*- and *Trans*-Amidopalladation

cis-amidopalladation
(*cis*-AP)

trans-amidopalladation
(*trans*-AP)
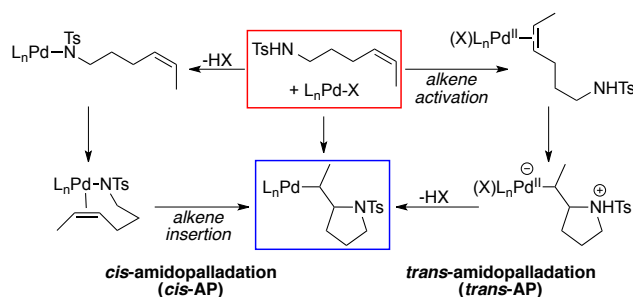
In light of historic precedent, our original report of the enantioselective method proposed that the C–N bond was formed via *cis*-AP. We hypothesized that having multiple points of contact between the substrate and catalyst (i.e amide and alkene) would impart the greatest stereocontrol (Scheme 5.3). Preliminary DFT results revealed a modest free energy of activation difference between the two enantiomers and supported this proposal.

Scheme 5.3. Previous Model for Stereocontrol with *Cis*-AP

top view

front view

quadrant representation

Major Enantiomer

Minor Enantiomer

minor steric interaction

multiple steric interactions

PG = protecting group (Ts, Ms, etc)
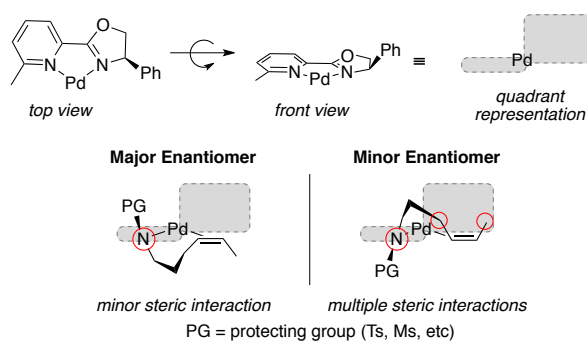
The limited literature examples of enantioselective methods and unique success of a chelating ligand for an aza-Wacker reaction prompted a follow-up mechanistic investigation into the formation of the C–N bond. The study employed an enantiopure, deuterated substrate to probe amidopalladation for the Pd(TFA)$_2$/ and Pd(OAc)$_2$/pyrox catalysts (Scheme 5.4).[5] Surprisingly, the Pd(TFA)$_2$/pyrox catalyst was determined to proceed through exclusively *trans*-

AP. When Pd(OAc)₂ was used in place of Pd(TFA)₂, the mechanism switched to predominantly

cis-AP. Furthermore, the enantioselectivity was observed to be highest (96% ee) for *trans*-AP

pathway and significantly reduced (20% ee) *cis*-AP pathway (Scheme 5.4).

Scheme 5.4. Summary of Amidopalladation Mechanism Study for Pd(TFA)₂ and Pd(OAc)₂ and *S*-Pyrox

entry	PdX₂ (5%)	% yield	% ee	*trans* : *cis* - AP
1	Pd(TFA)₂	90	96	>9 : 1
2	Pd(OAc)₂	48	20	1 : 9
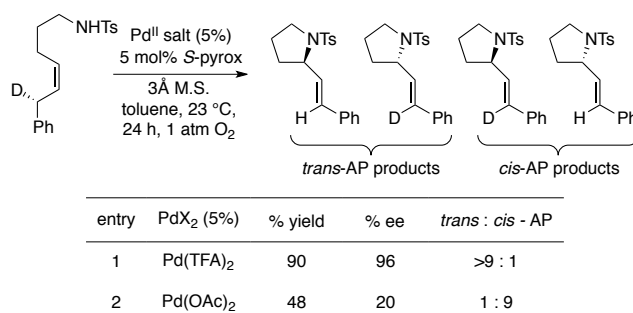
The Pd(TFA)₂/pyrox system challenged our understanding of how chirality could arise in

aza-Wacker cyclizations and prompted us to engage in a more detailed investigation with DFT

methods. Here we report a comparison between *cis*- and *trans*-amidopalladation reaction

coordinates for the Pd(TFA)₂/pyrox catalyst system. A new model for stereocontrol is introduced

for the *trans*-AP pathway that explains the observed enantioselectivity. Lastly, the origin for the

diminished enantioselectivity with the Pd(OAc)₂/system is also addressed and discussed in the

context of recent insights regarding 6,6'-substituted bipyridine ligands.

5.2 Results

5.2.1 Description of the Model System.

The majority of the calculations use an abbreviated substrate model. Specifically, the

experimentally-relevant *N*-toluenesulfonyl (Ts, tosyl) protecting group is replaced by the *N*-

methanesulfonyl (Ms, mesyl) group, which has a similar steric profile, in order to save on

computation time. The full Ts protecting group is used in cases where the subtle electronic

differences[6] play a critical (i.e barriers of *cis*- vs *trans*-AP). The *cis*-4-hexenylamide (**1**) substrate was chosen due to its simplicity and high enantioselectivity with the Pd(TFA)$_2$/pyrox catalyst system.

We propose that effective stereocontrol requires the bidentate ligand to form a rigid Pd^{II} complex. Experimentally, Pd(TFA)$_2$/pyrox displays high enantioselectivity and coordination complexes with Pd(TFA)$_2$ bearing chelating ligands have been calculated to form charge-separated species that are 2-4 kcal/mol higher in energy than the neutral complex.[7] For our purpose, we use a cationic [Pd(κ^2-pyrox)(κ^2-TFA)]$^+$ complex as the starting point for our reaction coordinate in order to effectively compare both the *cis*- and *trans*-AP pathways.[8]

5.2.2 Description of the *Cis*-AP Pathway for [Pd(κ^2-pyrox)(κ^2-TFA)]$^+$.

In our original report, we provided a reaction coordinate for *cis*-AP that terminated in the amidopalladation transition state. Here, we provide a more thorough reaction coordinate for substrate oxidation. The *cis*-AP begins with proton exchange between the TFA ligand and the mesylamide, which forms a Pd-amidate *trans* to oxazoline ring (Scheme 5.5A, **A**). The sulfonyl oxygen lone-pair serves as a neutral ligand to saturate the metal center. Next, the tethered alkene coordinates to Pd *trans* to the pyridyl ring of pyrox via displacement of the sulfonyl (**B**).[9] The C–N bond is formed via alkene insertion into the Pd–N bond (**C**) resulting in a Pd-alkyl species with a chelating amide group (**D**). The sulfonyl oxygen lone-pair then dissociates the amide and forms a new Pd-alkyl chelate (**E**). β-Hydride elimination produces the terminal olefin product and concludes the substrate oxidation (**F&G**).

Scheme 5.5. Comparison of *Cis*- and *Trans*-AP Reaction Coordinates for [Pd(κ^2-pyrox)(κ^2-TFA)]$^+$.

A. *Cis*-AP Reaction Coordinate for [Pd(TFA)/pyrox]$^+$

Bold Line: observed enantiomer (*S*)
Dotted Line: minor enantiomer (*R*)
#: Energy of *S* species
(#): Energy of *R* specoes

ΔG_{298K} (kcal/mol)

25.0
20.0
15.0
10.0
5.0
0.0
-5.0

A
(7.07)
6.32

0.00

B
(14.42)
14.04

C
(21.68)
18.70

D
(5.43)
4.27

E
-2.78
(-1.90)

F
11.51
(10.77)

G
11.09
(10.64)

‡

+ NHMs

B. *Trans*-AP Reaction Coordinate for [Pd(TFA)/pyrox]$^+$

Bold Line: observed enantiomer (*S*)
Dotted Line: minor enantiomer (*R*)
#: Energy of *S* species
(#): Energy of *R* specoes

ΔG_{298K} (kcal/mol)

25.0
20.0
15.0
10.0
5.0
0.0
-5.0

H
6.61
(6.26)

0.00

I
(22.90)
20.50

J
(22.67)
20.77

-TFAH

K
4.96
(2.54)

L
0.34
(-1.05)

M
(13.49)
11.33

N
(13.62)
9.74

‡

+ NHMs

5.2.3 Description of the *Trans*-AP Pathway for $[Pd(\kappa^2\text{-pyrox})(\kappa^2\text{-TFA})]^+$.

The *trans*-AP pathway begins with the coordination of the alkene *trans* to the pyridyl ring of pyrox (Scheme 5.5B, **H**). Next, the amide nucleophile attacks the alkene (**I**) and produces a high-energy ammonium intermediate (**J**).[9] The ammonium species is a high-energy intermediate, which is rapidly deprotonated by an equivalent of TFA⁻. A TFA ligand is then dissociated by the nitrogen lone-pair (**K**) in order to maintain the charge balance and the sulfonyl oxygen lone-pairs serves as a neutral ligand to saturate Pd (**L**). β-Hydride elimination produces the terminal olefin product and concludes the substrate oxidation (**M&N**).

5.2.4 Amidopalladation Transition States with the Tosyl-Protected Substrate.

Among the cationic reaction coordinates, the *cis*-amidopalladation pathway is the energetically preferred pathway (cf, Scheme 5.5; *cis*-AP vs *trans*-AP: 18.70 vs 20.50 kcal/mol). This computational result contradicts the experimental results which show exclusively *trans*-AP. Subtle electronic effects due to the identity of the protecting group have been observed to alter which pathway the reaction proceeds, with more electron-deficient substrates favoring *trans*-AP.[4a] Therefore, the *cis*- and *trans*-AP transition states were recalculated using the full Ts protecting group instead of the Ms group (Scheme 5.6). The preferred amidopalladation pathway subsequently switches from *cis* to *trans* with the more electron-deficient tosylamide substrate; however, the difference is small (*cis*-AP vs *trans*-AP: 20.15 vs 19.00 kcal/mol). These results highlight the delicate nature of *cis*- and *trans*-amidopalladation on substrate and catalyst identity.

Scheme 5.6. Comparison of the Protecting Group Identity on the Amidpalladation Transition State Energies for the Major Enantiomer
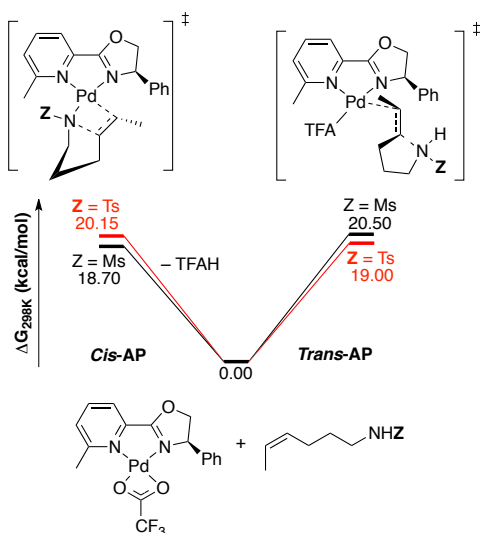
5.2.5 Description of the Neutral *Cis*-AP Pathway for Pd(OAc)₂/pyrox.

The cationic *cis*-AP pathway shown above for TFA demonstrates a modest difference in the activation energy for the two enantiomers ($\Delta\Delta G^{\ddagger}$ = 2.98 kcal/mol, Scheme 5.5). However, the cationic reaction coordinate is unsuitable for the Pd(OAc)₂/pyrox catalyst since the experimental results demonstrate a significant loss in enantioselectivity.[10] An alternative reaction coordinate for *cis*-AP is a neutral pathway where the chelating ligand partially dissociates. This could give rise to a loss of enantioselectivity since the pyrox ligand would be more flexible.

The neutral *cis*-AP reaction coordinate begins from the chelated Pd(pyrox)(OAc)₂ species, which is the lowest Pd^{II} species. Proton exchange between the Pd(κ^2-pyrox)(OAc)₂ complex and the mesylamide forms the Pd-amidate *trans* to the oxazoline (Scheme 5.7, **O**).[11] The tethered alkene coordinates to Pd via dissociation of the pyridyl ring of the pyrox ligand (**P**), which proceeds to formation of the C–N bond (**Q**). The resulting Pd-alkyl species (**R**) undergoes concomitant β-hydride elimination and reductive elimination with the coordinated acetate ligand to produce an equivalent of acetic acid and the terminal alkene product (**S**→**T**). Isomerization of the pyrox ligand from κ^1→κ^2 dissociates the coordinated AcOH, resulting in a stable Pd^0

complex (**U**). Overall, the difference in activation energy for the two enantiomers was found to be quite small (**Q**, $\Delta\Delta G^{\ddagger} = 0.20$ kcal/mol), indicating a lack of enantioselectivity for this pathway.

Scheme 5.7. Neutral Reaction Coordinate for *Cis*-AP with Pd(κ^2-pyrox)(OAc)$_2$
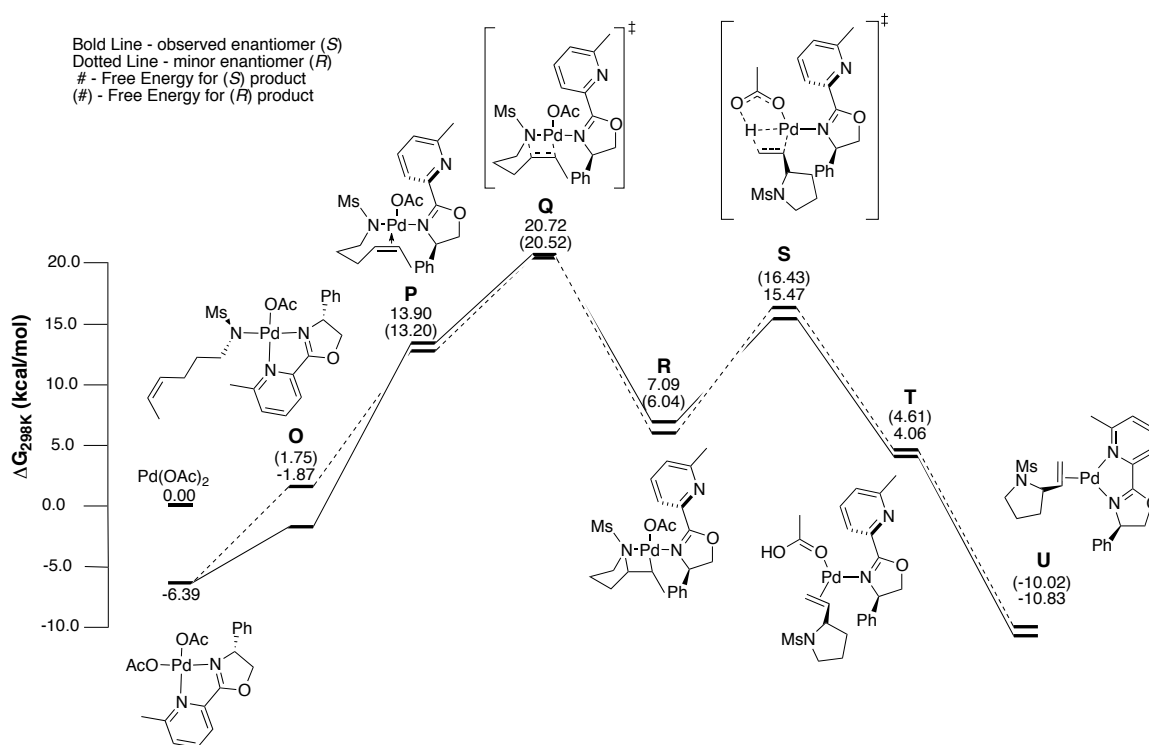
5.3 Discussion

5.3.1 Analysis of the Cationic Reaction Coordinates.

Both the *cis*- and *trans*-amidopalladation reaction coordinates reveal that the turnover-limiting step for substrate oxidation is amidopallation, which also makes it the stereodetermining step. Additionally, the pathways demonstrate a modest difference in activation energies between each enantiomer (*cis*-AP: $\Delta\Delta G^{\ddagger} = 2.98$ kcal/mol; *trans*-AP: $\Delta\Delta G^{\ddagger} = 2.40$ kcal/mol). Our previous model supports the origin for enantioselectivity in the *cis*-AP pathway where coordination of both the amide and alkene groups to Pd introduces multiple points for steric interactions with the

pyrox ligand. As a result, the conformation that minimizes these interactions becomes the favored enantiomer (cf. Scheme 5.3).

The *trans*-AP pathway only has one point of substrate contact with the catalyst center but demonstrates high enantioselectivity both experimentally and computationally. The calculated reaction coordinate provides insight into multiple factors that compound to produce this result. The first is the initial coordination of the substrate to the metal center. Similar to the *cis*-AP pathway, there is a strong electronic and steric preference for coordination of the alkene *trans* to the pyridine ring. This allows for the substrate to experience stereocontrol from the phenyloxazoline ligand due to their proximity.

Next, there is a distinction about which face of the alkene undergoes amidopalladation. The reaction coordinate reveals an insignificant energetic difference for coordinating either face of the alkene to Pd (Scheme 5.8A). The primary steric interaction that results in enantioselectivity arises when the tethered nitrogen nucleophile rearranges for amidopalladation (cf. Scheme 5.5B, **I**). For the major enantiomer, the transition state forms the pyrrolidine ring on the opposite face of the phenyl group on the oxazoline ring (Scheme 5.8B). As a result, no additional steric interactions between the substrate and catalyst occur. The minor enantiomer, however, forms the pyrrolidine ring on the same face as the phenyl group. The pyrox ligand responds by bending 11° away from the square plane in order to alleviate the steric interaction, thus a creating a higher energy transition state. The electronic asymmetry of the pyrox ligand, which dictates where the alkene coordinates, in combination with the chiral phenyloxazoline ligand allows for excellent stereocontrol in the *trans*-amidopalladation pathway.

Scheme 5.8. Investigating the Origin of Enantioselectivity in the Cationic *Trans*-AP Pathway

A. Alkene Coordination

Major Enantiomer

+6.61 kcal/mol

Minor Enantiomer

+6.26 kcal/mol

multiple degrees of freedom in substrate alkyl chain
⇓
insiginificant energetic difference for coordination

B. *trans*-Amidopalladation Transition States

Major Enantiomer

Top View

Minor Enantiomer

amide group overlaps with phenyl group

Side View

no steric clash

planar pyrox

amide/phenyl clash

bent pyrox (11°)

TFA ligand and most H's omitted for clarity

5.3.2 Analysis of the Neutral *Cis*-AP Reaction Coordinate.

The calculated barrier for the major enantiomer is 26.91 kcal/mol, which is a reasonable value for the reaction where slow reactivity is demonstrated (cf. Scheme 5.4). The neutral

reaction coordinate demonstrates a noticeable lack of enantioselectivity ($\Delta\Delta G^{\ddagger} = 0.20$ kcal/mol) unlike the cationic *cis*-AP pathway. The origin of this observation is the isomerization of the pyrox ligand from $\kappa^1 \rightarrow \kappa^2$, which increases the degrees of freedom for the chiral ligand. The 6-methylpyridine ring was found computationally to be the most labile ring. Our group has previously investigated a similar Pd(OAc)$_2$ complex with a chelating 6,6'-dimethyl-2,2'-bipyridine (6,6'-Me$_2$bpy) in the context of the aza-Wacker reaction.[4b] We demonstrated that substitution at the 6,6'-position of the bipyridine ligand destabilizes the chelated complex, which promotes the dissociation of a 6-methylpyridine ring in the presence of an exogenous L-type ligand such as pyridine. Furthermore, analysis of the reaction coordinate by DFT methods concluded that Pd(κ^1-6,6'-Me$_2$bpy) intermediates were kinetically viable in the catalytic reaction. A similar effect is likely involved with the pyrox ligand, which contributes to the low observed enantioselectivity.

5.4 Conclusions and Outlook

In conclusion, we have computationally investigated the origin of enantioselectivity of the PdX$_2$/pyrox catalyst system as a function of amidopalladation mechanism and Pd^{II} salt. We determined that when a Pd(TFA)$_2$ salt was used, a cationic reaction coordinate would give rise to high enantioselectivity for both the *cis*- and *trans*-AP pathways. The origin of the high enantioselectivity in the *cis*-AP path was determined to result from the interaction of the terminal methyl group of the substrate with the phenyl ring of the oxazoline. On the other hand, the interaction of the amide functional group with the phenyl ring of the oxazoline during amidopalladation was shown to result in the enantioselectivity for the *trans*-AP path. The energetic difference between *cis*-AP and *trans*-AP was found to be sensitive to the identity of the amide protecting group used, with the model Ms preferring *cis*-AP and the experimentally-relevant Ts preferring *trans*-AP. When Pd(OAc)$_2$ is used in place of Pd(TFA)$_2$, a loss of enantioselectivity is observed due to the pyrox ligand partially dissociating during the reaction.

These profound results allow for the understanding how electronic asymmetry, Pd^{II} salt and amide protecting group influence the accessibility of enantioselectivity.

Evidence for the pyrox ligand partially dissociating will be bolstered by thorough NMR spectroscopic evidence for a Pd/ κ^1-pyrox species. A preliminary NMR spectroscopic analysis of a solution containing a 1:1 pyridine:Pd(κ^2-pyrox)(OAc)$_2$ at -45 °C in CDCl$_3$ has identified a species consistent with a *trans*-Pd(κ^1-pyrox)(pyridine)(OAc)$_2$ complex; however a cleaner preparation of the sample needs to be performed. The *trans*-Pd(κ^1-pyrox)(pyridine)(OAc)$_2$ was observed to be transient at room temperature, however at temperatures <45 °C it is persistent and a crystal structure could likely be obtained. Furthermore, a time-course for the catalytic reaction with a Pd(OAc)$_2$/pyrox catalyst would allow for the development of experimental benchmarks to compare against the computational barriers.

5.5 Experimental

All computations were performed with the Gaussian 09 program[12] using resources provided by University of Wisconsin–Madison Chemistry Department. Spin-restricted density functional theory (DFT) calculations were performed with the hybrid density functional, rB3LYP.[13,14] A combination of the Stuttgart RSC 1997 ECP/triple-ζ basis[15] for Pd and the all-electron 6-31+G(d) basis set for all other atoms was used for gas-phase geometry optimizations and normal mode analyses. Full geometry optimizations were carried out in internal coordinates using the default Berny algorithm. Frequency calculations were performed at the optimized geometries to confirm that each geometry had the appropriate number of imaginary frequencies: zero for minima or one for transition states. The imaginary frequency identifying a saddle-point was visually inspected for the proper motion.

At the calculated stationary points, solvation-corrected single-point total energy calculations were carried out with the Pd basis detailed above and the 6-311+G (d,p) basis on all other atoms with electrostatic and non-electrostatic solvation effects evaluated using the polarizable-

continuum model (PCM). The solvation cavity was generated using UFF radii, explicitly treating hydrogen atoms, and the radii were scaled by a factor of 1.2. The solvent chosen was toluene.

5.6 References

1. For reviews see: (a) O'Hagan, D., *Nat. Prod. Rep.* **2000,** *17*, 435-446. (b) Bellina, F.; Rossi, R., *Tetrahedron* **2006,** *62*, 7213-7256.

2. (a) Fix, S. R.; Brice, J. L.; Stahl, S. S *Angew. Chem. Int. Ed.* **2002,** *41*, 164-166. (b) McDonald, R. I.; Stahl, S. S., *Angew. Chem. Int. Ed.* **2010,** *49*, 5529-5532. (c) Redford, J. E.; McDonald, R. I.; Rigsby, M. L.; Wiensch, J. D.; Stahl, S. S., *Org. Lett.* **2012,** *14*, 1242-1245. (d) Lu, Z.; Stahl, S. S., *Org. Lett.* **2012,** *14*, 1234-1237.

3. McDonald, R. I.; White, P. B.; Weinstein, A. B.; Tam, C. P.; Stahl, S. S., *Org. Lett.* **2011,** *13*, 2830-2833.

4. (a) Liu, G. S.; Stahl, S. S., *J. Am. Chem. Soc.* **2007,** *129*, 6328-6335. (b) Chapter 4

5. Weinstein, A. B.; Stahl, S. S., *Angew. Chem. Int. Ed.* **2012,** *51*, 11505-11509.

6. The reported pKa(DMSO) values for TsNH2 and MsNH2 are 15.6 and 17.5, respectively. See (a) Bordwell, F. G.; Algrim, D., *J. Org. Chem.* **1976,** *41*, 2507-2508. (b) Ludwig, M.; Pytela, O.; Vecera, M., *Collect. Czech. Chem. Commun.* **1984,** *49*, 2593-2601.

7. The solvent used in the model was AcOH (e = 6.15) and TFAH (e = 8.55). We are assuming that this process is still thermodynamically accessible in toluene (e = 2.38) but with a slightly higher energy. See ref: Munz, D.; Meyer, D.; Strassner, T., *Organometallics* **2013,** *32*, 3469-3480.

8. Attempts to model the neutral pathway via an associated outer-sphere TFA– resulted in the inability to converge upon a solution; the free TFA– anion was unable to find an ideal position within the coordination sphere.

9. Our original report highlighted that the orientation of the Pd-amidate *trans* to the oxazoline ring and alkene *trans* to the pyridyl ring provided the lowest energy path for alkene insertion. The origin of this effect was revealed to be a result from the strong *trans* effect of oxazoline ring, which disfavors the coordination of the alkene *trans* to it. Additionally, the 6-methyl group on the pyridine ring was shown to provide a steric interaction, which disfavored the coplanar orientation of the alkene required for *cis*-AP. This trend would also hold true for the *trans*-AP pathway (see Supporting Information).

10. Replacement of TFA by OAc would only shift the energy of the structures by the difference between TFA and OAc anions. As such, the relative difference in the activation energy for each enantiomers would remain the same (i.e. no effect on the enantioselectivity) since the structures would be otherwise identical.

11. Alternatively, the amidopalladation step could take place from Pd-amidate *trans* to the pyridyl ring of pyrox, which would involve dissociation of the oxazoline fragment prior to the transition state. This pathway was calculated and the barriers were found to be 4-5 kcal/mol higher than the pathway in Scheme 5.7 and demonstrated equally poor enantioselectivity.

12. Gaussian 09, Revision C.01, Frisch, M. J.; Trucks, G. W.; Schlegel, H. B.; Scuseria, G. E.; Robb, M. A.; Cheeseman, J. R.; Scalmani, G.; Barone, V.; Mennucci, B.; Petersson, G. A.; Nakatsuji, H.; Caricato, M.; Li, X.; Hratchian, H. P.; Izmaylov, A. F.; Bloino, J.; Zheng, G.; Sonnenberg, J. L.; Hada, M.; Ehara, M.; Toyota, K.; Fukuda, R.; Hasegawa, J.; Ishida, M.; Nakajima, T.; Honda, Y.; Kitao, O.; Nakai, H.; Vreven, T.; Montgomery, J. A. Jr.; Peralta, J. E.; Ogliaro, F.; Bearpark, M.; Heyd, J. J.; Brothers, E.;Kudin, K. N.; Staroverov, V. N.; Keith, T.; Kobayashi, R.; Normand, J.; Raghavachari, K.; Rendell, A.; Burant, J. C.; Iyengar, S. S.; Tomasi, J.; Cossi, M.; Rega, N.; Millam, J. M.; Klene, M.; Knox, J. E.; Cross, J. B.; Bakken, V.; Adamo, C.; Jaramillo, J.; Gomperts, R.; Stratmann, R. E.; Yazyev, O.; Austin, A. J.;

Cammi, R.; Pomelli, C.; Ochterski, J. W.; Martin, R. L.; Morokuma, K.; Zakrzewski, V. G.; Voth, G. A.; Salvador, P.; Dannenberg, J. J.; Dapprich, S.; Daniels, A. D.; Farkas, O.; Foresman, J. B.; Ortiz, J. V.; Cioslowski, J.; Fox, D. J. Gaussian, Inc., Wallingford CT, 2010.

13. Becke, A.D. *J. Chem. Phys.* **1993**, *98*, 1372 −1377.

14. Lee, C.; Yang, W.; Parr, R. G. *Phys. Rev. B* **1988**, *37*, 785 − 789.

15. a) Feller, D. *J. Comp. Chem.*, **1996**, *17*(13), 1571-1586. b) Schuchardt, K.L.; Didier, B.T.; Elsethagen, T.; Sun, L.; Gurumoorthi, V.; Chase, J.; Li, J.; and Windus, T.L. *J. Chem. Inf. Model.*, **2007**, *47*(3), 1045-1052

Appendix 1. Allylic Acetoxylation Computations

A1.1 Introduction and Results

The work contained within this appendix pertains to a computational investigation into the Pd/DAF-catalyzed allylic acetoxylation of terminal alkenes that was reported by our group in 2010 (Scheme A1.1).[1] Numerous bidentate ligands were screened but only DAF was shown to promote the reaction.

Scheme A1.1. Pd/DAF-catalyzed Allylic Acetoxylation Reaction
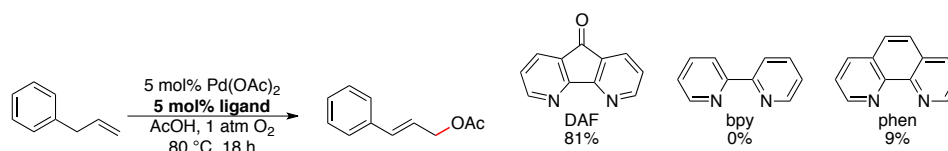
Several attempts at understanding the mechanism of this unusual DAF-promoted activity have been started; however at the time of this writing there has not been a conclusive study. The entirety of these calculations was performed under the assumption that the mechanism involved a homogeneous molecular catalyst due to preliminary mechanistic studies. However, it is likely now that the reaction proceeds via meta-stable Pd-nanoparticles in light of recent studies by Jon Jaworski. Here is a summary of the computational investigation performed and the insight gleaned into the different chemical steps involved in substrate oxidation.

The three fundamental chemical steps present in allylic acetoxylation are 1) alkene coordination, 2) C–H activation and 3) reductive elimination (Scheme A1.2). The following calculations compared the energy surface for DAF (blue), 6,6'-F$_2$bpy (green) and 4,4'-Me$_2$bpy (red) (Scheme A1.3). DAF was demonstrated to carry out the reaction both through C–H activation and reductive elimination. 6,6'-F$_2$bpy was demonstrated to enable reductive elimination but not C–H activation. Lastly, 4,4'-Me$_2$bpy inhibited both C–H activation and

reductive elimination. These three ligands provide critical insight into the factors that control different chemical steps.

Scheme A1.2. Steps Involved in Substrate Oxidation

A. Alkene Coordination

$$[Pd] \quad + \quad \diagup\!\!\diagdown\!\!\diagup Ph \quad \longrightarrow \quad [Pd]-\|$$

B. C–H Activation - Concerted Metalation Deprotonation

$$[Pd]-\| \quad \longrightarrow \quad [Pd]-\diagup\!\!\diagdown \quad + AcOH$$

C. Reductive Elimination

$$[Pd]-\diagup\!\!\diagdown \quad + [OAc] \quad \longrightarrow \quad [Pd]-\diagdown\!\!\|$$
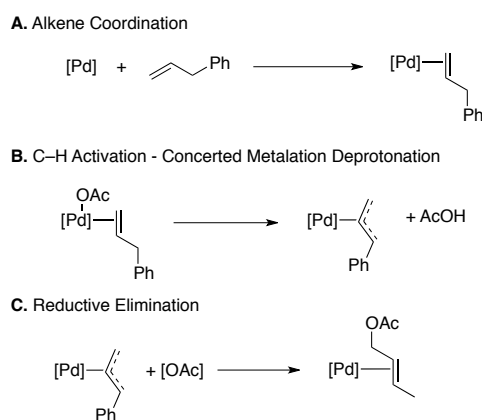
Alkene coordination was calculated both without ligand coordinated to Pd(OAc)$_2$. The alkene coordination step was calculated from a ligand-free monomeric Pd(OAc)$_2$ catalyst and found to have a relatively low barrier (Scheme A1.3).[2] A similar barrier was not calculated for the ligand-associated Pd pathway. At this point, C–H activation could occur either from a ligand-associated or ligand-free Pd(OAc)$_2$ catalyst. For the ligand-free condition a modest barrier (24.50 kcal/mol) was calculated for C–H activation to form the Pd(π-allyl)(κ^2-OAc) and an equivalent of acetic acid (Scheme A1.3). Within this pathway C–H activation is the rate-limiting step and the formation of the allyl complex is thermodyanically downhill, which makes the reverse C–H activation step kinetically irreversible (34.71 kcal/mol). These findings are consistent with experimental work performed that showed C–H activation was irreversible.

Scheme A1.3. Ligand-Free Alkene Association and C–H Activation Reaction Coordinate
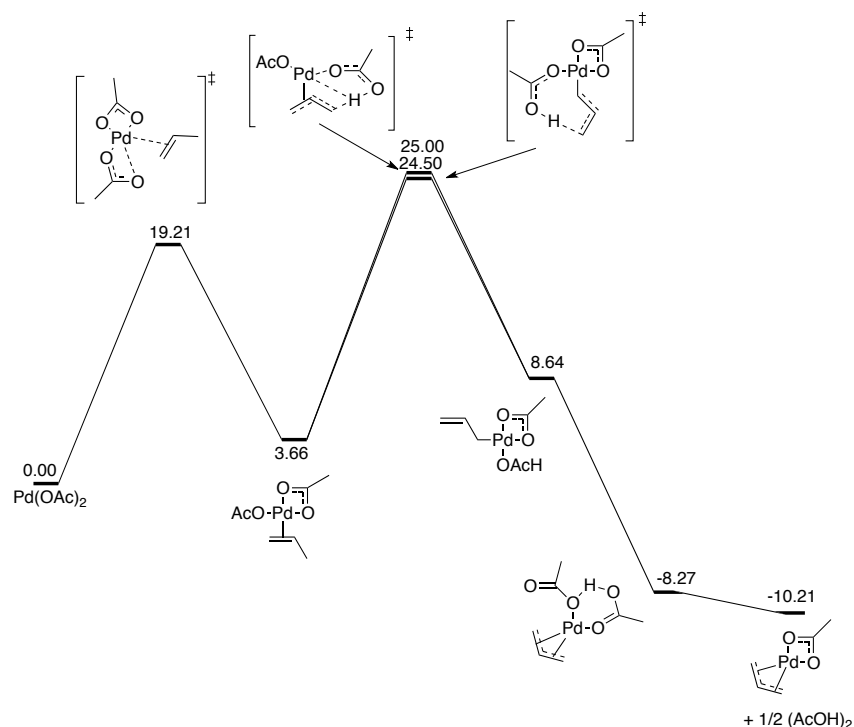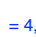
Similarly, the C–H activation pathway was also calculated from the ligand-associated complex (Scheme A1.4). Immediately evident is free energy change upon coordination of the ligand to Pd(OAc)$_2$. Coordination of DAF to Pd(OAc)$_2$ is only moderately downhill (-1.86 kcal/mol) whereas 6,6'-F$_2$bpy does not coordinate at all, which has been observed experimentally. Unlike the other ligands, 4,4'-Me$_2$bpy forms a strong coordination complex (-14.38 kcal/mol). The C–H activation step was calculated to be the lowest overall for DAF (28.96 kcal/mol). The absolute barrier energy for 4,4'-Me$_2$bpy (33.51 kcal/mol) was found to be higher but taking the ground-state stabilizing into account the overall barrier was 37.89 kcal/mol. Comparing both the ligand-free and ligand-associated pathways, it was found that C–H activation was more favorable from the ligand-free pathway. Additionally, the inhibitory effect of 4,4'-Me$_2$bpy is clearly demonstrated due to the significantly stabilized Pd(4,4'-Me$_2$bpy)(OAc)$_2$ complex (Scheme A1.4). Unfortunately, the calculations do not explain why 6,6'-F$_2$bpy does not work catalytically since

the C–H activation path is ligand-free and the experimental work shows that 6,6'-F₂bpy promotes reductive elimination.

Scheme A1.4. Ligand-Associated C–H Activation
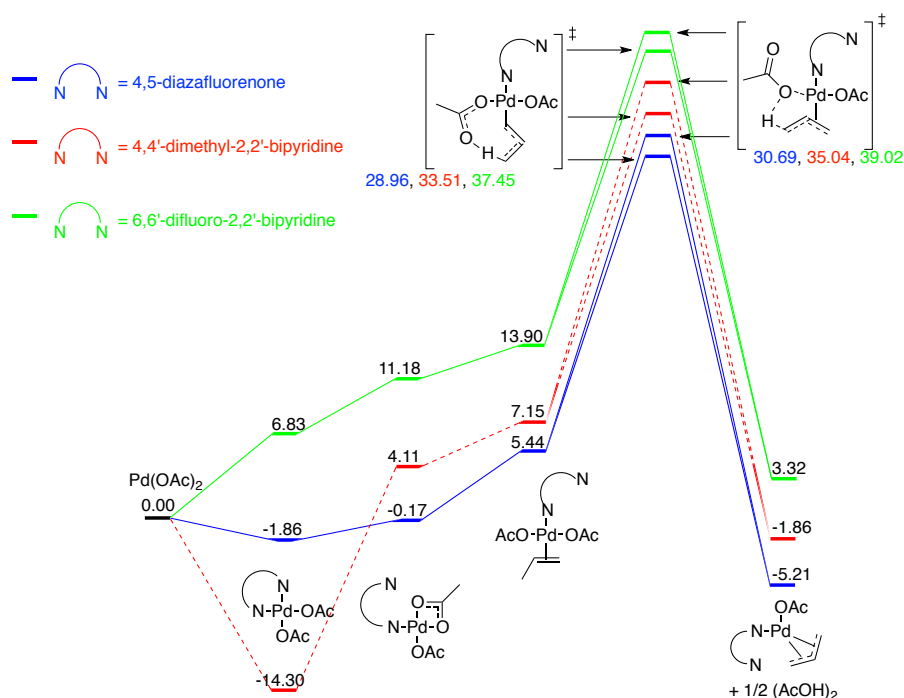
The next step in substrate oxidation is reductive elimination to form allyl acetate. Experimentally, this was demonstrated to require a ligand (DAF or 6,6'-F₂bpy) in order to occur. This can either occur from a neutral or cationic complex. Due to the difficulty in calculating solvated ions, each of these will be considered separately. The neutral pathway was calculated from Pd(π-allyl)(κ²-OAc) complex, to which the ligand coordinates (Scheme A1.5). The neutral pathway does not permit backside attack of the allyl by a nucleophile, which is commonly proposed from cationic intermediates. Instead, the η³-allyl dissociates to form the η¹-allyl complex and undergoes an intramolecular reductive elimination. There are two pairs of nucleophile and electrophile that describe this process (four total paths). The first is the carbonyl oxygen or Pd–coordinated oxygen acting as the nucleophile. The second is the dissociated alkene

or Pd-bound carbon acting as the electrophile. The lowest energy pathway for DAF was determined to be attack of the terminal alkene by the carbonyl oxygen forming a 7-membered transition state (22.79 kcal/mol). The barrier for reductive elimination for DAF was found to be lower than C–H activation, which conforms to our hypothesis that C–H activation is rate-limiting. Furthermore, the product is higher in energy than the starting material, suggesting that reductive elimination is reversible, which has been observed experimentally. Unfortunately, this path does not support 6,6'-F$_2$bpy as a ligand that would promoted reductive elimination. Therefore, the cationic pathway where reductive elimination takes place from a chelated [Pd(N~N)(η^3-allyl)]$^+$ was analyzed.

Scheme A1.5. Ligand-Associated Reductive Elimination Barriers

The cationic pathway begins at the $[Pd(N\sim N)(\kappa^2\text{-}OAc)]^+$ complex (Scheme A1.6). The DAF-ligated complex is designated as 0.00 kcal/mol. The 4,4'-Me$_2$bpy complex forms a very stable $[Pd(N\sim N)(\kappa^2\text{-}OAc)]^+$ complex compared to DAF, highlighting the weak coordination properties of DAF and significant ground-state stabilization of bpy. Interestingly, 6,6'-F$_2$bpy forms a complex of similar energy as DAF. Next, C–H activation occurs via a concerted metalation-deprotonation mechanism whereby the acetate performs an intramolecular deprotonation of the allylic C–H bond. DAF was shown to have the lowest barrier (24.09 kcal/mol) followed by 6,6'-F$_2$bpy (30.22 kcal/mol) and 4,4'-Me$_2$bpy (32.40 kcal/mol). These overall barriers for the different ligands are more closely aligned with the experimental trends: C–H activation occurs with DAF but not 6,6'-F$_2$bpy and 4,4'-Me$_2$bpy. Furthermore, the π-allyl product (-14.37 kcal/mol) is a very stable species and suggests that C–H activation is irreversible, which is in agreement with the experimental data.

Scheme A1.6. C–H Activation and Reductive Elimination via Cationic Intermediates
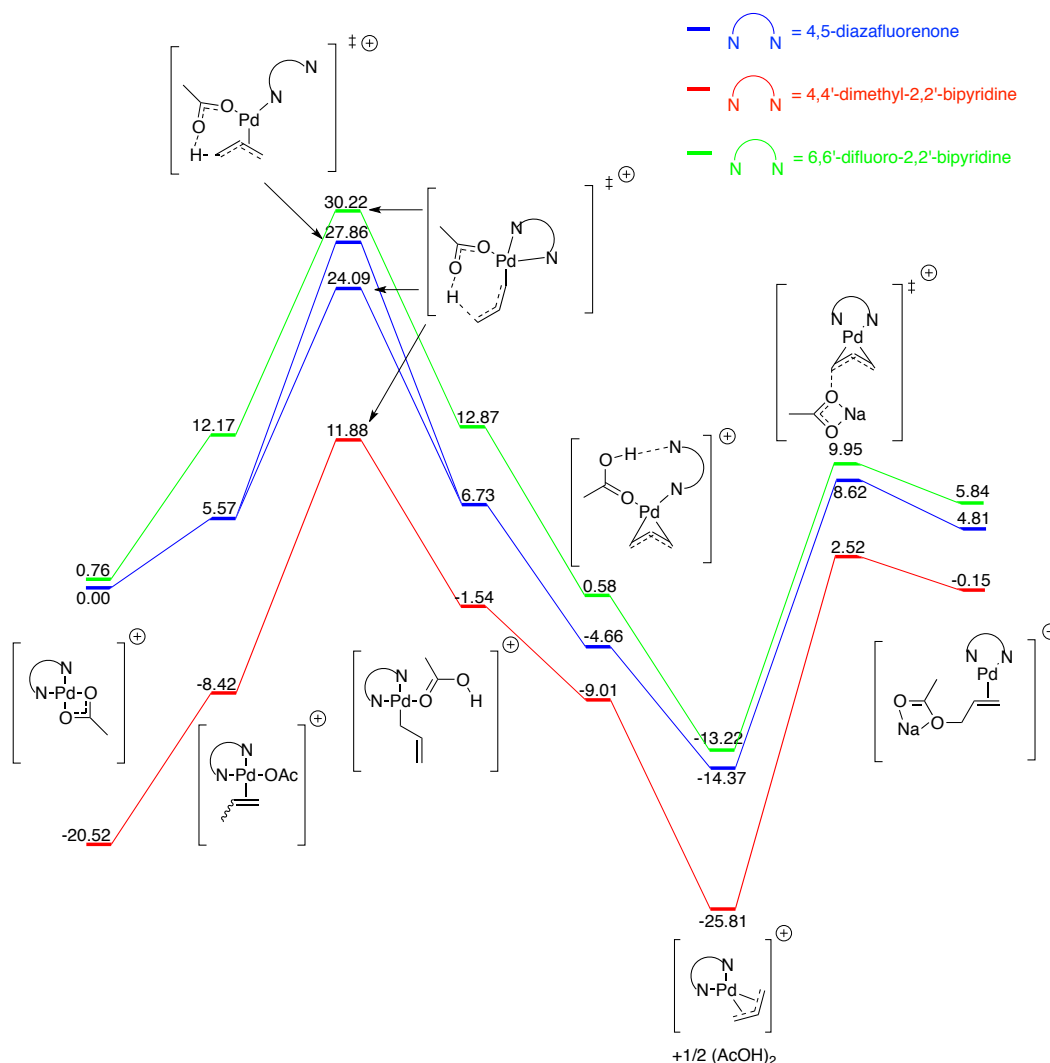
Reductive elimination takes place with a NaOAc nucleophile in order to conserve the cationic charge. The barriers for reductive elimination follow 4,4'-Me$_2$bpy (28.33 kcal/mol) > 6,6'-F$_2$bpy (24.17 kcal/mol) > DAF (22.99 kcal/mol). These values are qualitatively in agreement with the experimental data, which show that reductive elimination occurs from well-defined [Pd(N~N)(η^3-allyl)]$^+$ complexes when N~N = DAF and 6,6'-F$_2$bpy but not 4,4'-Me$_2$bpy. This contrasts the neutral pathway which shows that reductive elimination is much higher for 6,6'-F$_2$bpy than DAF. Finally, the product of reductive elimination is higher in energy than the allyl

complex, likely a result from using NaOAc as the nucleophile, and suggests that this process is reversible.

A1.2 Outlook

Overall, the neutral and cationic pathways provide interesting insight in C–H activation and reductive elimination. C–H activation likely place from a neutral species in which the DAF ligand is dissociated; however the cationic ligand-associated pathway is quite similar energetically as long as the formation of the charge-separated species is significantly thermodynamically uphill. Reductive elimination, on the other hand, most certainly takes place from a cationic intermediate since these species have been prepared under the reaction conditions and been shown to be kinetically competent. The computations between the two pathways support experimental observations that highlight the ineffectiveness of 6,6-F$_2$bpy at C–H activation and 4,4'-Me$_2$bpy at C–H and reductive elimination. However, these computations assume a homogeneous molecular catalyst and in light of Jon's results which suggest a switch from a molecular to a nanoparticle catalyst, these computations may only be valid for the first turnover. Nevertheless, it will be interesting to see how this story unfolds in the future.

A1.3 References

1. Campbell, A. N.; White, P. B.; Guzei, I. A.; Stahl, S. S., *J. Am. Chem. Soc.* **2010,** *132*, 15116-15119.
2. Bercaw has proposed that alkene association could be the rate-determining step in the Pd/bipyrimidine-catalyzed allylic acetoxylation reaction. See ref: Lin, B. L.; Labinger, J. A.; Bercaw, J. E., *Can. J. Chem.* **2009,** *87*, 264-271.

Appendix 2. Supporting Information for Chapter 2

A2.1 Compilation of All 1H and 15N Chemical Shifts for A-F

Assignment		*Ortho*	*Meta*	*Para*	^{15}N *Resonance*	*OAc*
A	a^0	10.58	7.80	8.31	203.7	1.78, 2.04, (2.05)
B	b^1	10.13	7.45	8.11	189.3	1.87, 1.95
	b^2	9.56	7.72	8.23	304.6	
C	c^1	10.12	7.37	8.00	203.7	1.85
	c^2	9.58	7.74	8.17	304.3	
D	d^1	9.96	7.59	8.16	206.3	1.66
	d^2	9.11	7.63	8.19	309.3	
E	e^1	9.85	7.63	8.16	207.1	1.52
	e^2	9.41	7.65	8.15	306.7	
F	f^0	8.66	7.93	8.66	213.3	2.27

All values are in ppm

Figure A2.1. Compilation of all ^1H and ^{15}N chemical shifts for **A-F** obtained using TOCSY, ROESY and ^1H-^{15}N HMBC experiments. The acetate resonance for **A** in parentheses is inferred from comparing relative integrations of the acetate region.

A2.2 TOCSY Spectra of A–E

A2.2.1 Structure A
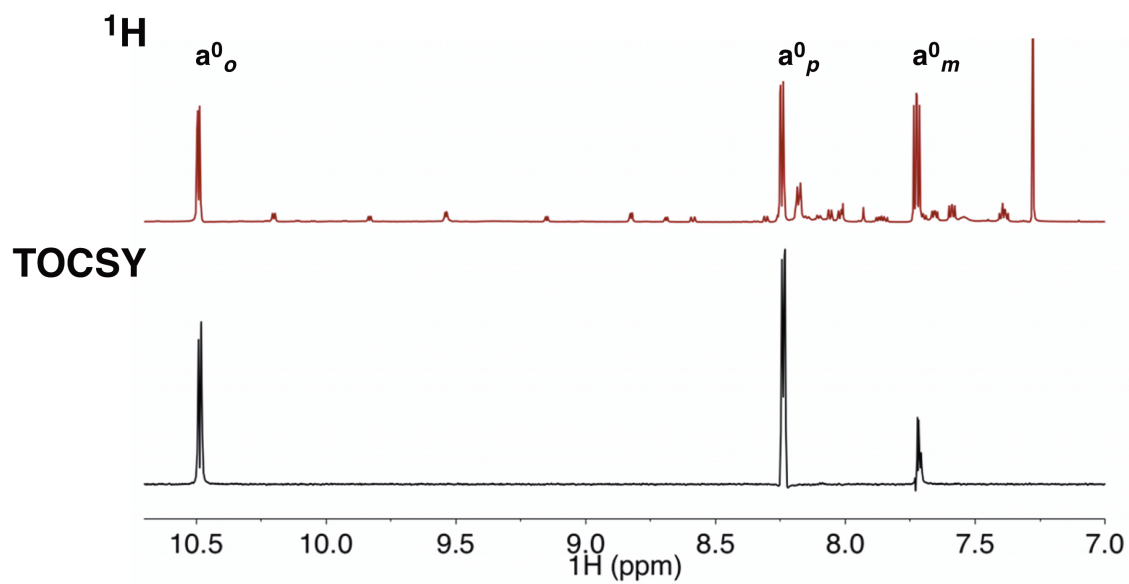
Figure A2.2. ^{1}H 1D TOCSY spectrum of 0.5 equiv DAF at 12 °C. ns = 8, d1 = 3.57 s, 8.5 kHz spinlock, mix = 0.03 s.

A2.2.2 Structure B
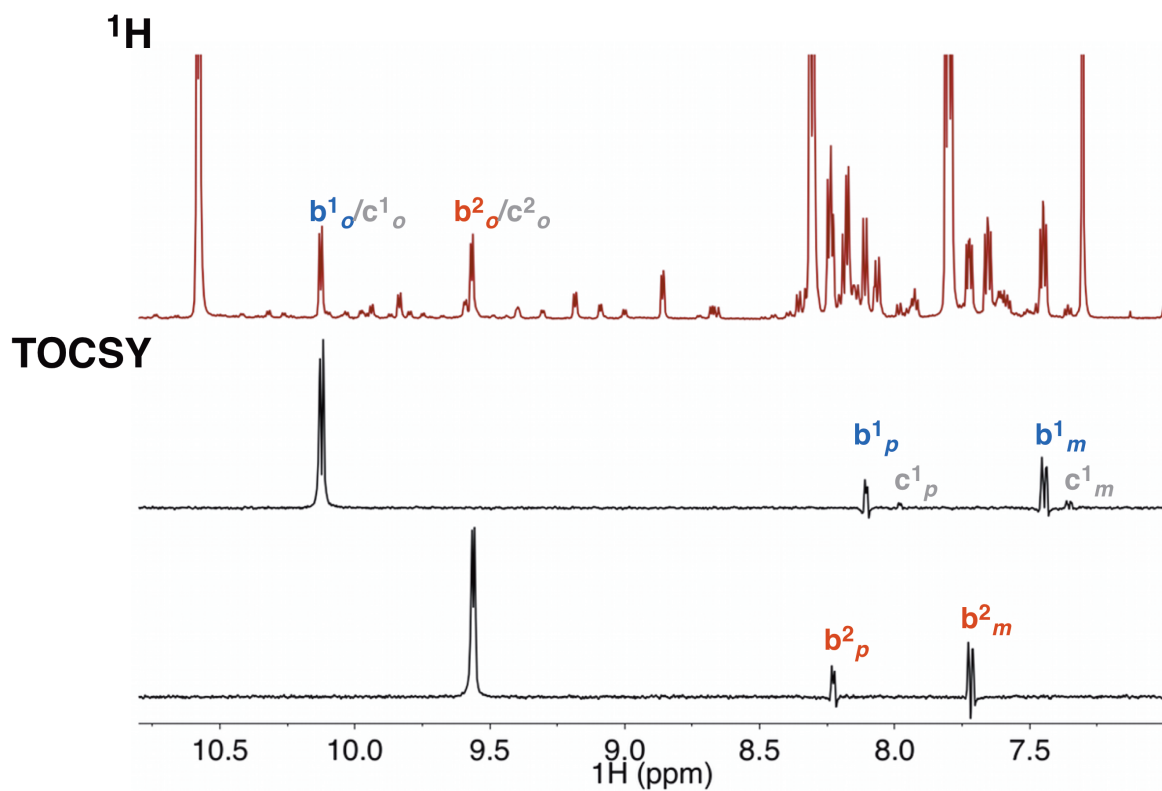
Figure A2.3. ^{1}H 1D TOCSY spectrum of 0.5 equiv DAF at -45 °C. ns = 8, d1 = 3.57 s, 8.5 kHz spinlock, mix = 0.03 s. The resonances **b^1_o** and **b^2_o** were selected in order to determine the chemical shift of the *meta* and *para* protons for each ring. Due to the significant overlap of **b^1_o** and **c^1_o**, small amounts of the *meta* and *para* protons for **C** are observed in the TOCSY.

A2.2.3 Structures C–E
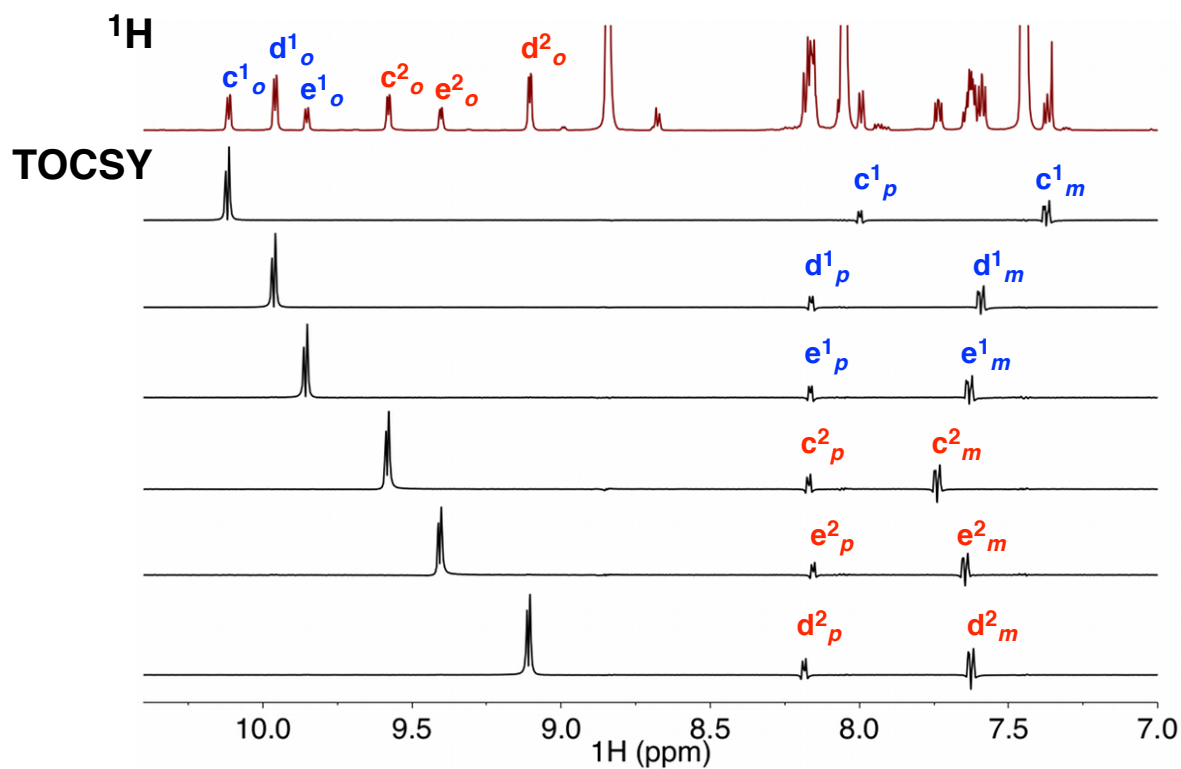
Figure A2.4. [1]H 1D TOCSY spectrum of 6 equiv DAF at -45 °C. ns = 8, d1 = 3.57 s, 8.5 kHz spinlock, mix = 0.03 s. Each resonance from c^1_o–e^2_o was selected in order to determine the chemical shift of the *meta* and *para* protons, which exhibit large amounts of chemical shift overlap in the ^{1}H spectrum.

A2.3 1D ROESY at 0.5 Equiv of DAF
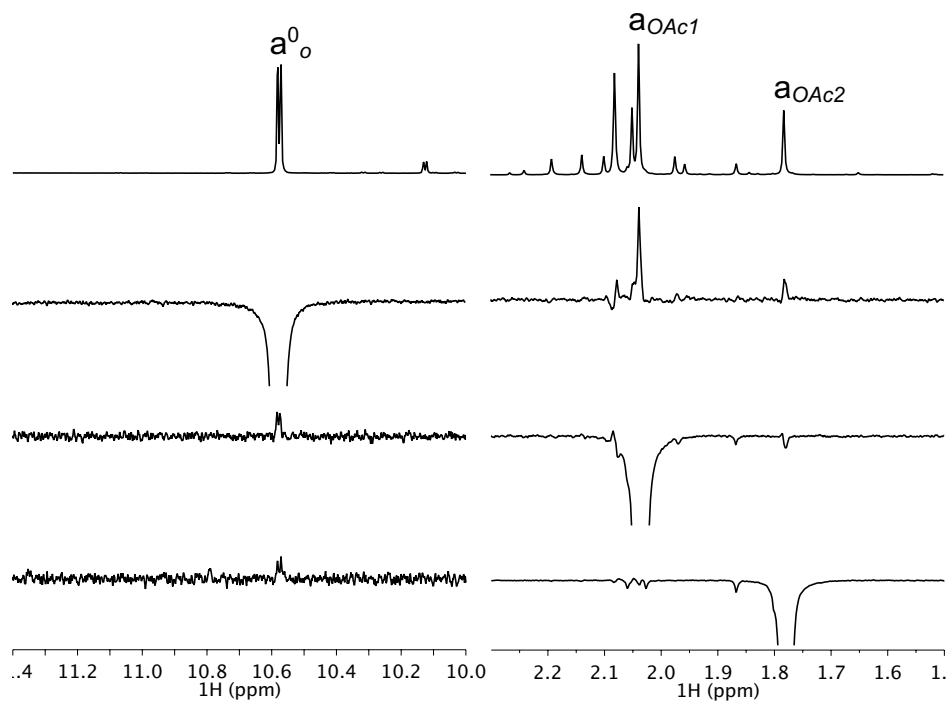
Figure A2.5. ^{1}H-^{1}H 1D ROESY spectrum of **A** at 0.5 equiv DAF at -45 °C. ns = 128, d1 = 6.3 s, 5.4 kHz spinlock, mix = 0.8 s. The extra acetate resonances represent the unobserved, by 1D ROESY, OAc resonance, free Pd(OAc)$_2$ and other minor DAF-Pd(OAc)$_2$ species.

A2.4 1D & 2D ROESY at 1 Equiv of DAF
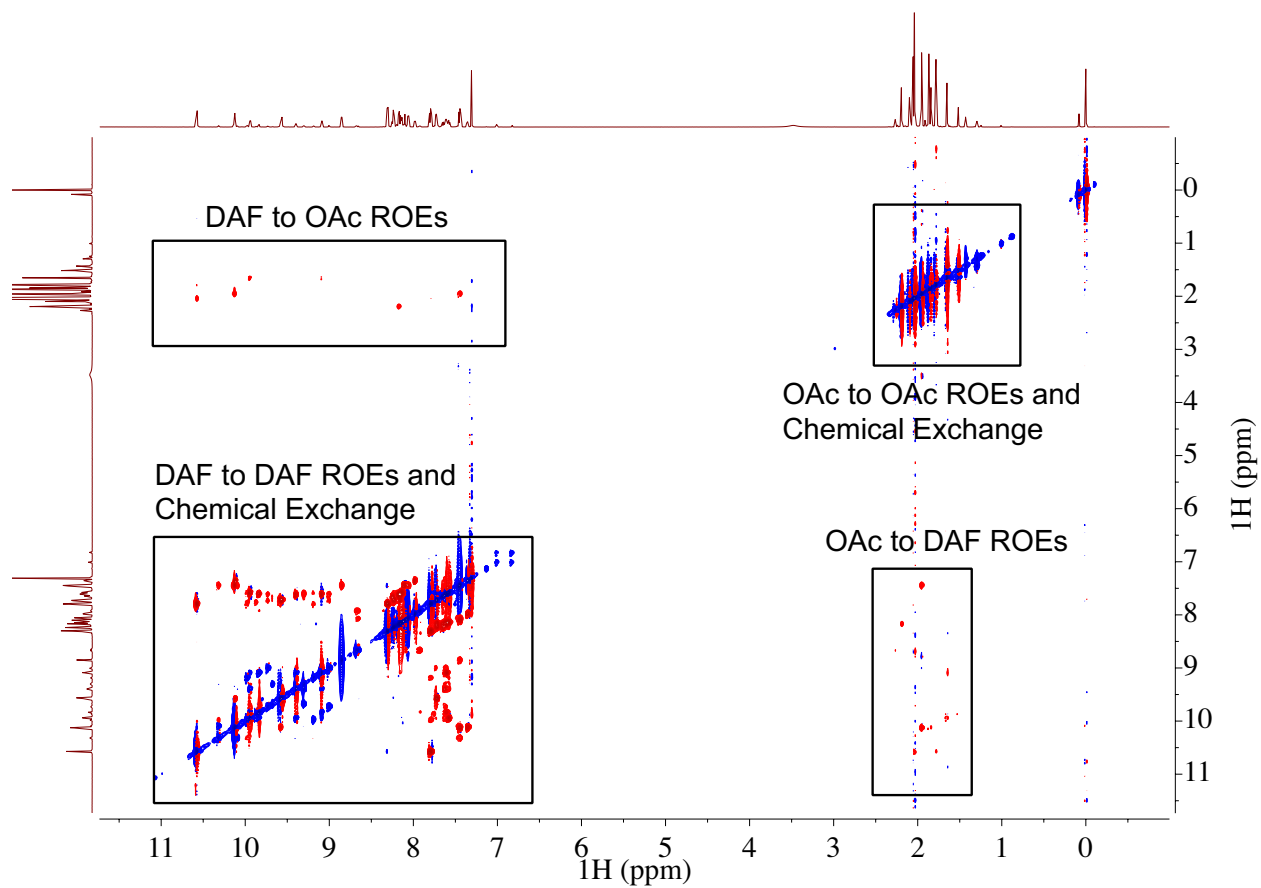
Figure A2.6. ^{1}H-^{1}H ROESY spectrum of 1 equiv DAF at -45 °C. ns = 48, d1 = 6.3 s, ni = 200, sw(f1) = sw(f2) = 12.7 ppm, 5.3 kHz spinlock, mix = 0.8 s.

A2.4.1 Zoomed-In Regions of the 2D ROESY Spectrum at 1 Equiv DAF
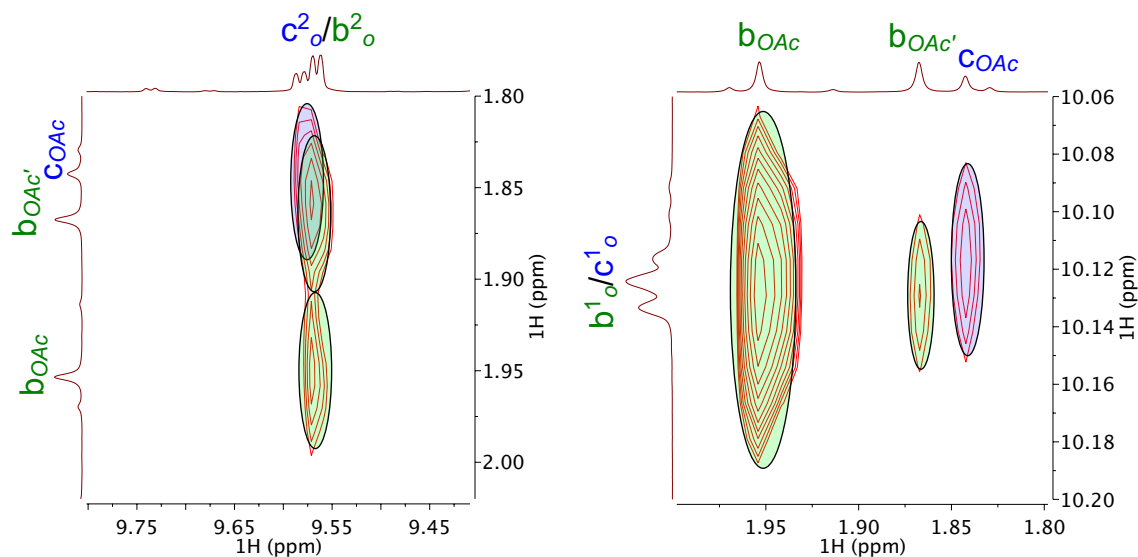
Figure A2.7. ^{1}H-^{1}H 2D ROESY at 1 Equiv of DAF. Species **B** has two acetate cross-peaks.

A2.4.2 1D ROESY Experiments on Observed Acetate Resonances
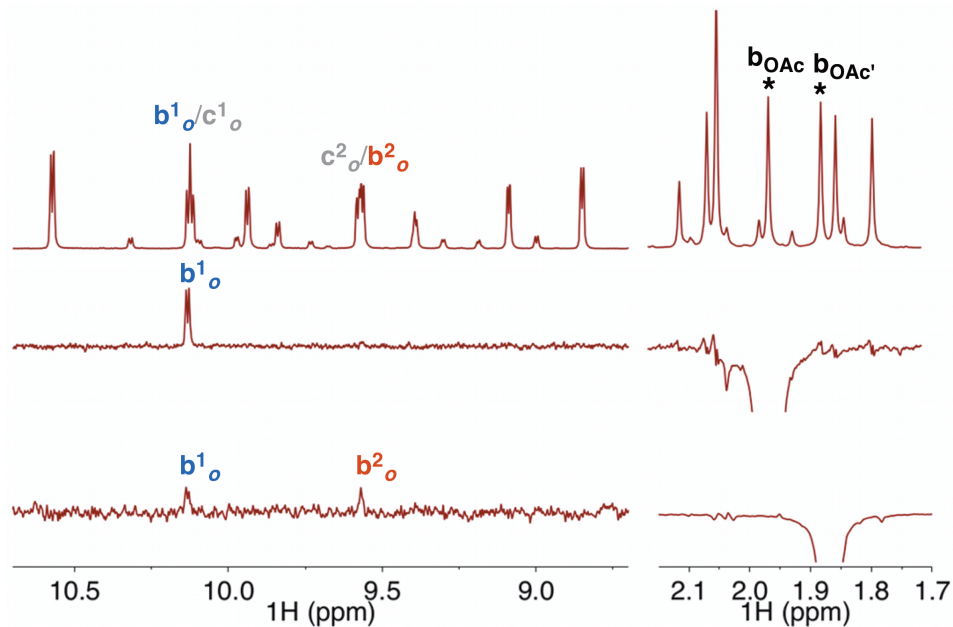
Figure A2.8. Stacked 1D ROESY experiments of $\mathbf{b_{OAc}}$ and $\mathbf{b_{OAc'}}$. The " * " indicates which peaks were irradiated. Through-space interactions are revealed between $\mathbf{b_{OAc}}/\mathbf{b_{OAc'}}$ and $\mathbf{b^1_o}/\mathbf{b^2_o}$ in the spectra. Ns = 512 (middle) and 1024 (bottom), d1 = 6.3 s, 5.4 kHz spinlock, mix = 0.8 s.

A2.5 1D ROESY Experiments on $c^1_o - d^1_o$ and $f^0_{o/p}$
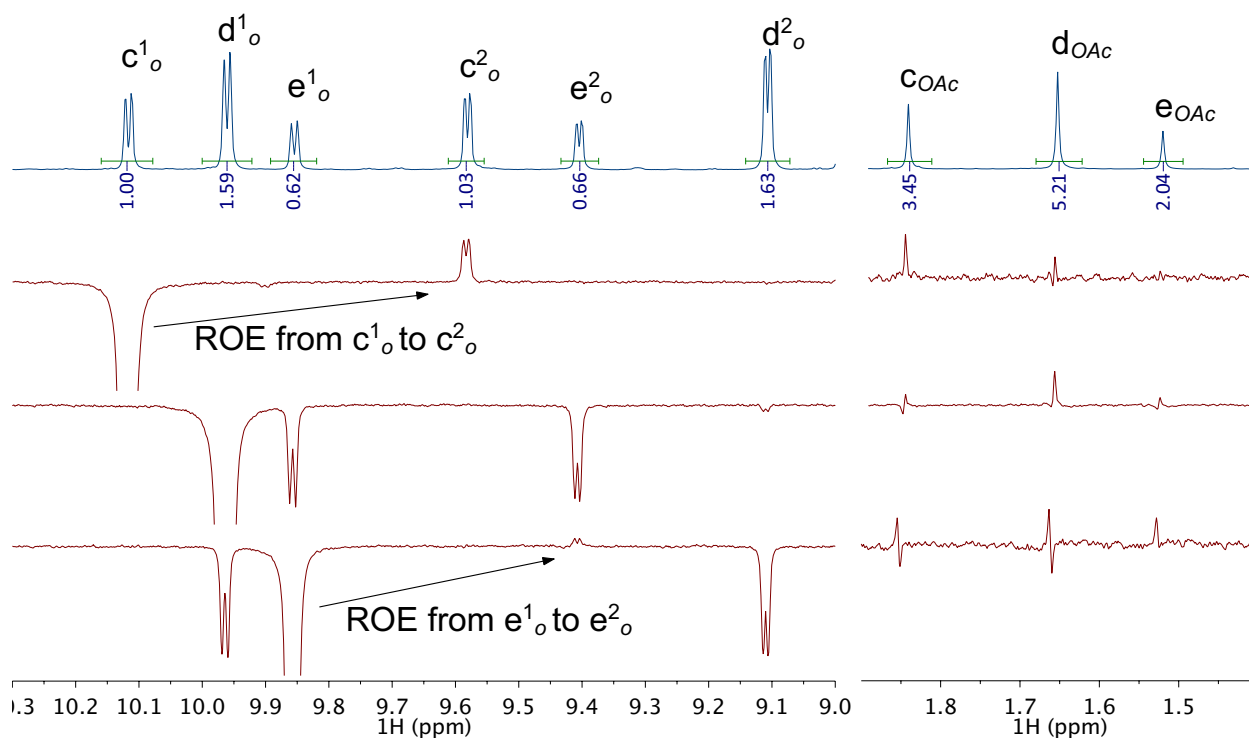
Figure A2.9. Stacked 1D ROESY experiments of $c^1_o - e^1_o$. Nearby OAc residues are identified for each complex C – E. Through-space interactions are revealed between c^1_o/c^2_o and e^1_o/e^2_o, and provide insight into the orientation of the ligands. Ns = 40, d1 = 10 s, 5.4 kHz spinlock, mix = 0.6 s.

A2.5.1 Build-Up Curves for $c_{OAc} - e_{OAC}$
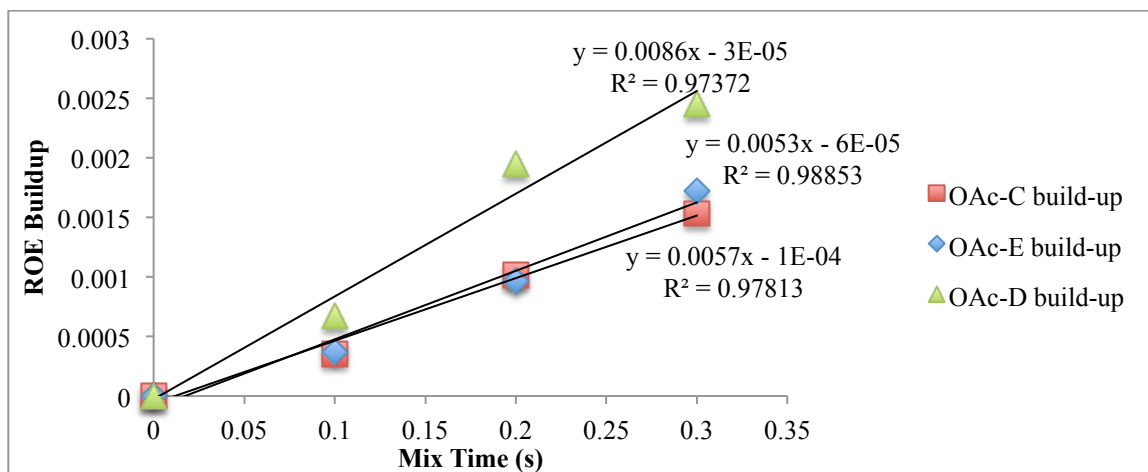
Figure A2.10. ROE build-up curves for $c_{OAc} - e_{OAc}$. These confirm that the positive peaks amidst the artifacts in S9 are indeed ROEs and not artifacts themselves.

A2.5.2 1D ROESY of $f^0_{o/p}$
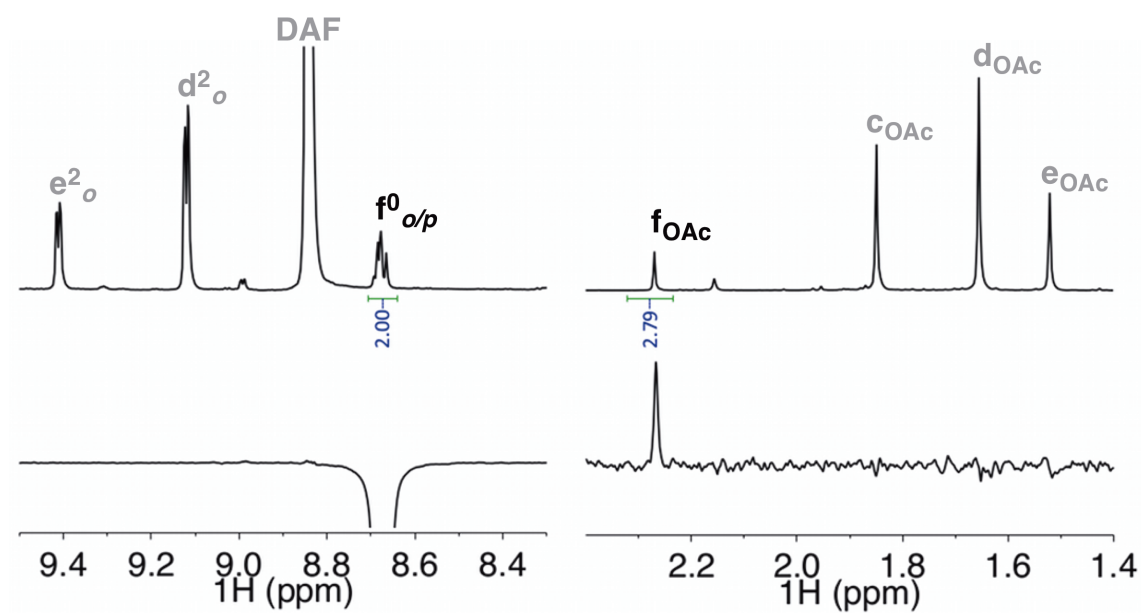
Figure A2.11. 1D ROESY experiment of $\mathbf{f^0}_{o/p}$. ns = 40, d1 = 10 s, 5.4 kHz spinlock, mix = 0.6 s.

A2.6 Measurement of $\Delta G^{\ddagger}_{exchange}$ for D and E by Lineshape Analysis
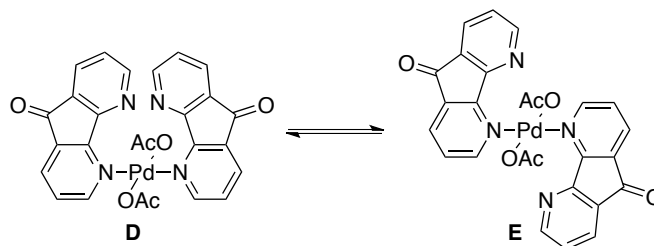
A2.6.1 Variable Temperature Spectra
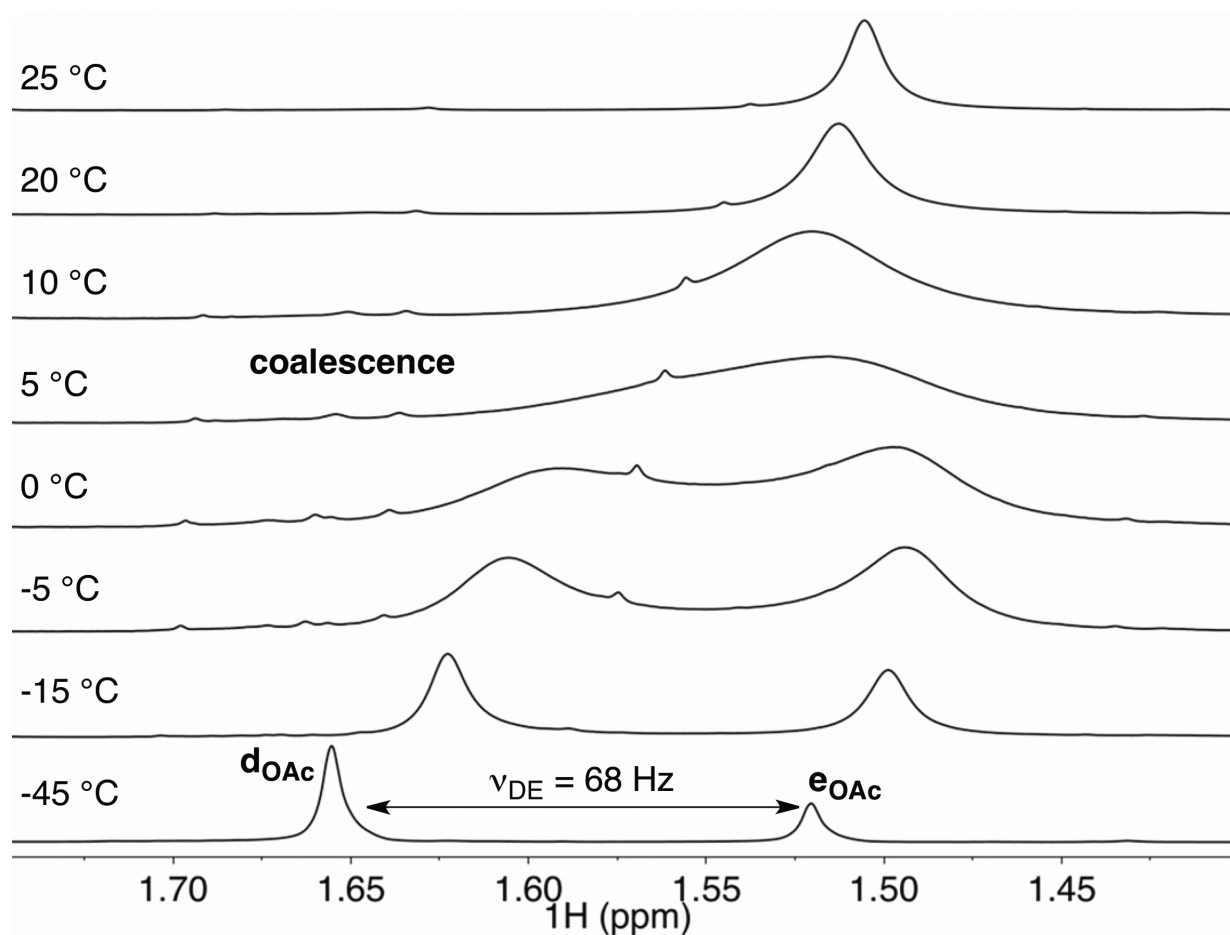
Figure A2.12. Variable-temperature spectra of a CDCl$_3$ solution of 6:1 DAF:Pd(OAc)$_2$. The spectral window is focused on the acetate resonances of **D** and **E** (**d$_{OAc}$** and **e$_{OAc}$**). These peaks were chosen for lineshape analysis due to their simple singlet nature. The resonances are sharp at -45 °C and continue to broaden until ~5 °C at which they coalesce. The single peak sharpens at higher temperatures. 1H: ns = 8, d1 = 20 s, ds =2.

A2.6.2 Determining Rate Constants of Exchange from Lineshape Analysis

The rate constants of chemical exchange between **D** and **E** were determined by lineshape analysis of the above spectra. The width at half-height was obtained from performing line-fitting routines on the peaks. Three sets of equations were used to extract out the rate constants below, at and above the coalescence point for the two acetate resonances (eq 1-3).

Below coalescence:

$$k = \pi(\nu - \nu_{ref,\mathbf{D}}) \tag{1}$$

where " ν " and " $\nu_{ref,\mathbf{D}}$ " are the line-widths at half-height for $\mathbf{d_{OAc}}$ at a given temperature and -45 °C, respectively.

At Coalescence:

$$k = (\pi/\sqrt{2})\nu_{\mathbf{DE}} \tag{2}$$

where " $\nu_{\mathbf{DE}}$ " is the difference in frequency between $\mathbf{d_{OAc}}$ and $\mathbf{e_{OAc}}$ at -45 °C

Above Coalescence:

$$k = (\pi \, \nu_{\mathbf{DE}}^{2})/(2(\nu - \nu_{ref,\mathbf{D}})) \tag{3}$$

The rate constant for the exchange process at room temperature was determined to be 1967 s^{-1}, which corresponds to a $\mathbf{\Delta G^{\ddagger}}$ = 13 kcal/mol. The rate constants at each temperature were used to construct an Eyring plot to test the quality of the analysis and provide an error for the room temperature measurement.
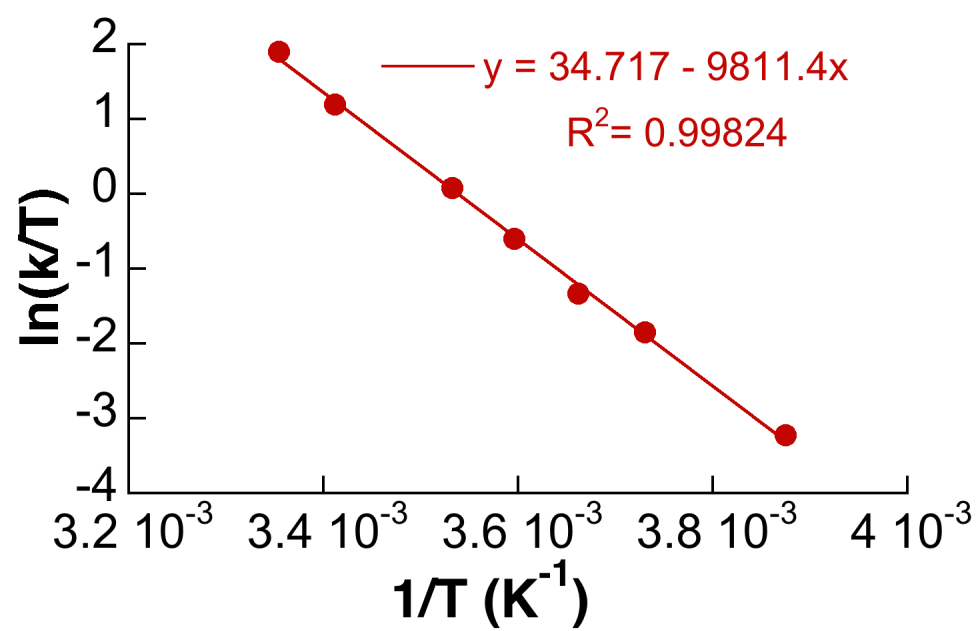
Figure A2.13. Eyring plot of the temperature-dependent rate constants obtained for exchange between **D** and **E**.

A2.7 ^{1}H-^{15}N HMBC Spectra at 0.5, 1 and 6 Equiv of DAF Relative to Pd(OAc)$_2$

A2.7.1 0.5 Equiv DAF
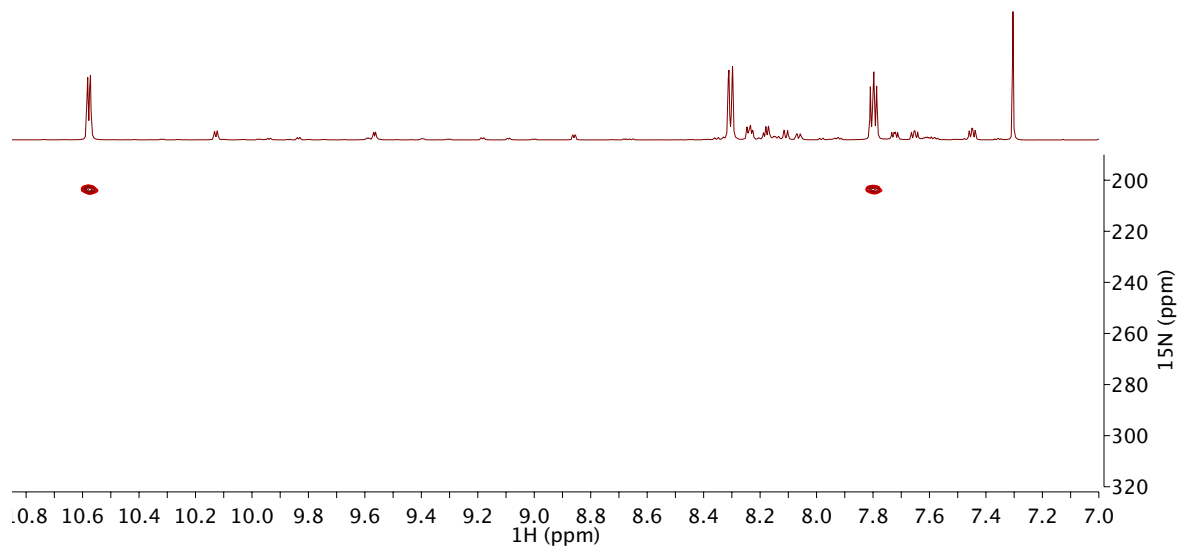
Figure A2.14. ^{1}H-^{15}N HMBC spectrum of 1:2 DAF:Pd(OAc)$_2$ at -45 °C. ns = 16, ni = 256, d1 = 4 s, sw(f1) = 250 ppm, $^1J_{NH}$ = 100 Hz and $^nJ_{NH}$ = 8 Hz. Cosine-squared window functions were applied in the f1 and f2 dimensions.

A2.7.2 1 Equiv of DAF
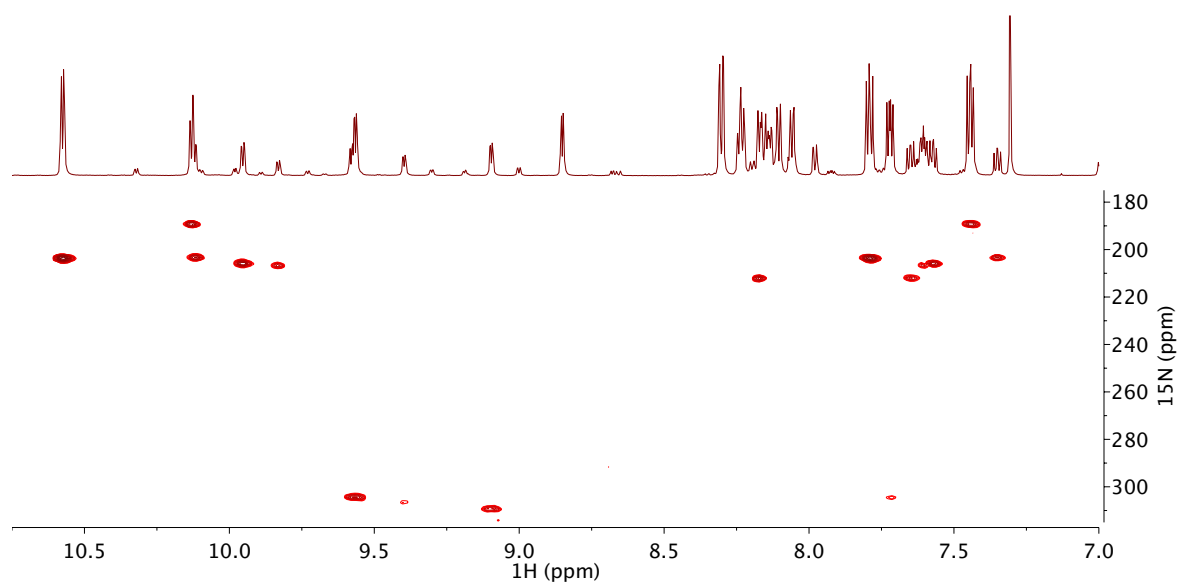
Figure A2.15. ^{1}H-^{15}N HMBC spectrum of 1:1 DAF:Pd(OAc)$_2$ at -45 °C. ns = 32, ni = 256, d1 = 4 s, sw(f1) = 250 ppm, ^{1}J$_{NH}$ = 100 Hz and ^{n}J$_{NH}$ = 8 Hz. Cosine-squared window functions were applied in the f1 and f2 dimensions.

A2.7.3 6 Equiv of DAF
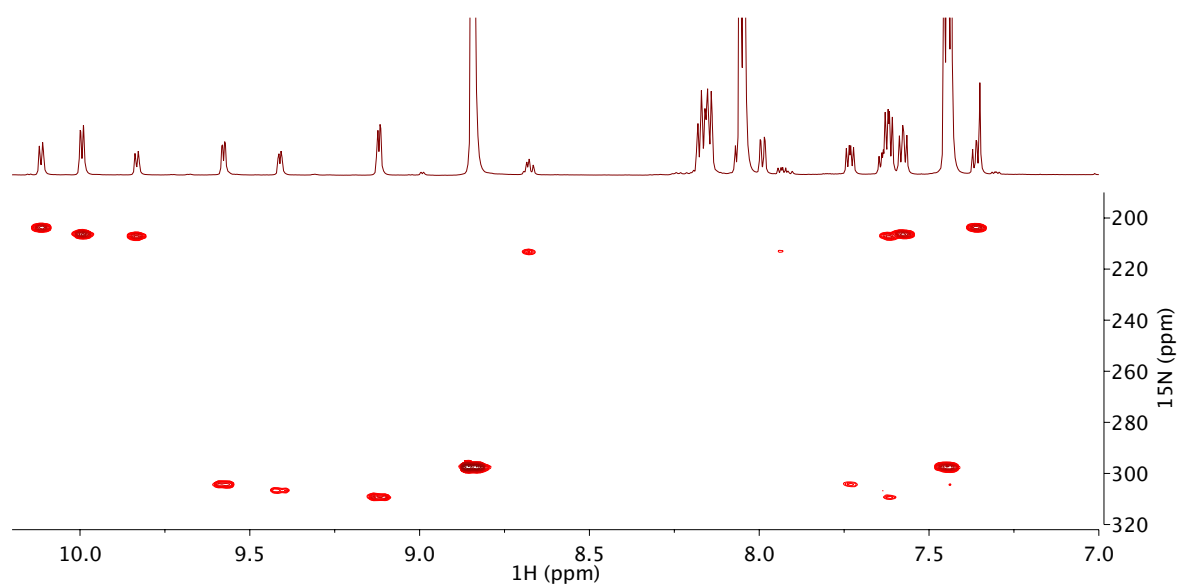
Figure A2.16. ^{1}H-^{15}N HMBC spectrum of 6:1 DAF:Pd(OAc)$_2$ at -45 °C. Ns = 32, ni = 256, d1 = 4 s, sw(f1) = 250 ppm, ^{1}J$_{NH}$ = 100 Hz and ^{n}J$_{NH}$ = 8 Hz. Cosine-squared window functions were applied in the f1 and f2 dimensions.

A2.8 Array of Temperature and 1D TOCSY Spectra of f$_{o/p}$
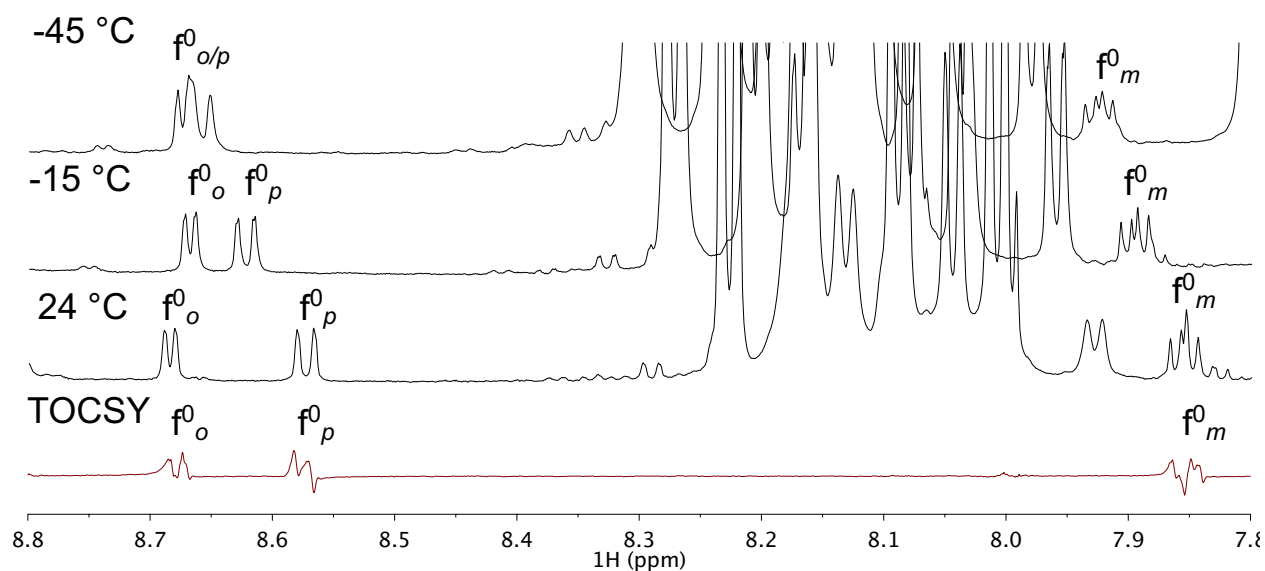
Figure A2.17. ^{1}H 1D spectra at -45, -15 and 24 °C (top three spectra) and ^{1}H 1D TOCSY at 24 °C. ^{1}H 1D: ns = 16, ds = 2, d1 = 20 s; ^{1}H 1D TOCSY: ns = 8, ds = 4, d1 = 7 s, mix = 60 ms. The **f^0_o** proton was selected in the 1D TOCSY experiment.

A2.9 ^{1}H-^{13}C HSQC Spectrum of Species f$_{o/p}$ at -45 °C

A2.9.1 Complete ortho Proton Region
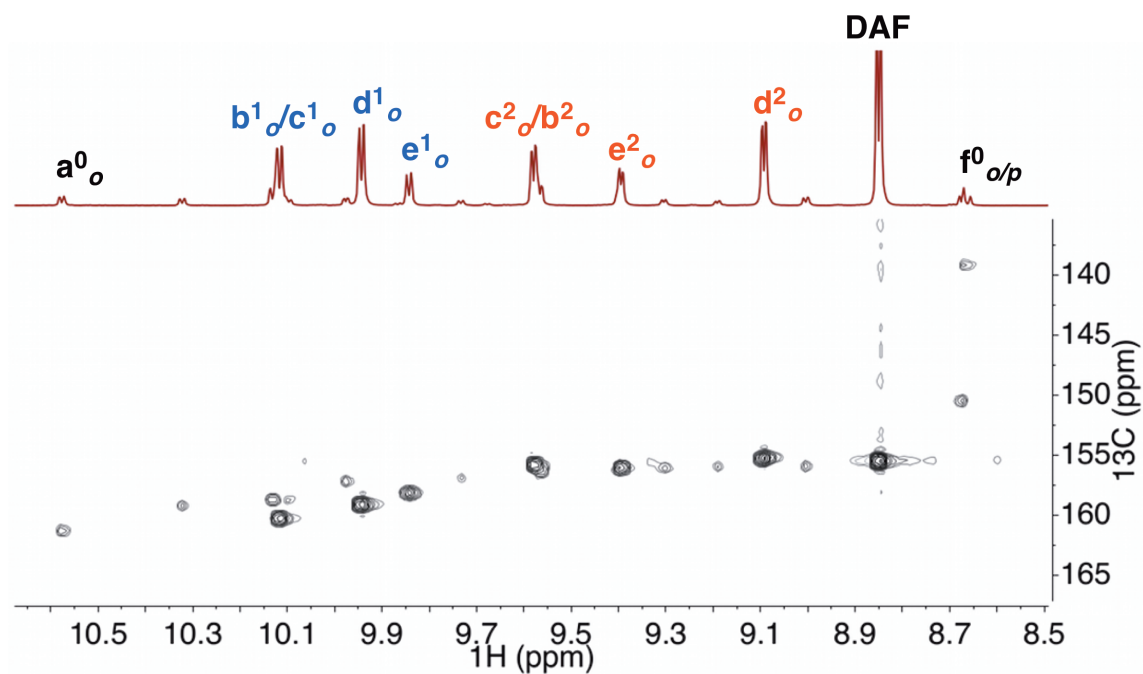
Figure A2.18. ^{1}H-^{13}C HSQC spectrum of 2:1 DAF:Pd(OAc)$_2$ -45 °C. ns = 4, ni = 256, d1 = 3.57 s, sw(f1) = 200 ppm, ^{1}J$_{CH}$ = 170 Hz. Sine-bell window functions were applied in both the f1 and f2 dimensions.

A2.9.2 Zoom-In of $f_{o/p}$ Region from S15
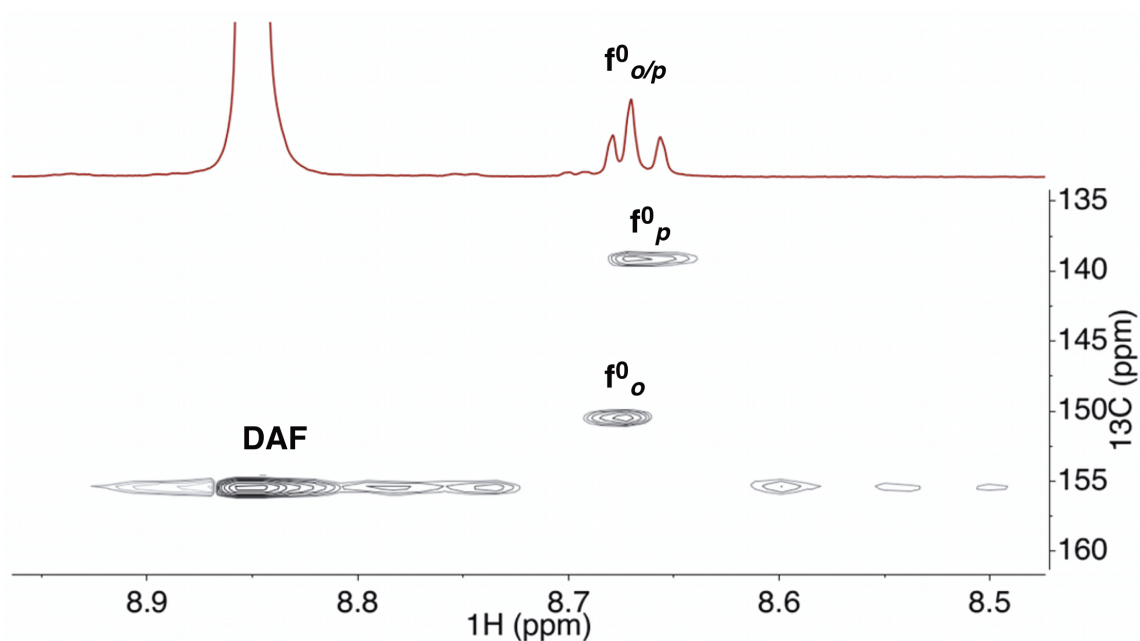
Figure A2.19. ^{1}H-^{13}C HSQC spectrum of $\mathbf{f}_{o/p}$ at -45 °C. The ^{1}H peak $\mathbf{f}_{o/p}$ clearly consisted of two different ^{1}H and ^{13}C cross-peaks. The more downfield ^{1}H resonance of $\mathbf{f}_{o/p}$ was assigned to $\mathbf{f}_o$ since the corresponding ^{13}C chemical shift was closer to the ^{13}C chemical shift of the *ortho* carbon of free DAF. The free DAF carbon exhibits t2 noise along its carbon cross-peak. ns = 4, d1 = 3.57 s, ni = 256, sw(f1) = 200 ppm, ^{1}J$_{CH}$ = 170 Hz.

Appendix 3. Supporting Information for Chapter 3

A3.1 Kinetic Profile for Reaction of 3a at 50 °C.

Figure 3.3b in the manuscript shows the approach to equilibrium **3 ⇄ 4**, starting from the various Pd-amidate complexes, **3a–d**. At temperatures suitable for monitoring this reaction, the β-hydride elimination step is quite slow. In order to monitor full conversion to the oxidative amination products, one of these reactions was carried out and monitored at 50 °C. Complex **3a** was dissolved in DMSO-d_6 and monitored by ^{1}H NMR spectroscopy at 50 °C for seven hours, revealing the equilibrium formation of **4a** and subsequent complete formation of **8a-8a"**. The kinetic profile of this reaction is shown below (every third data point is shown for clarity).
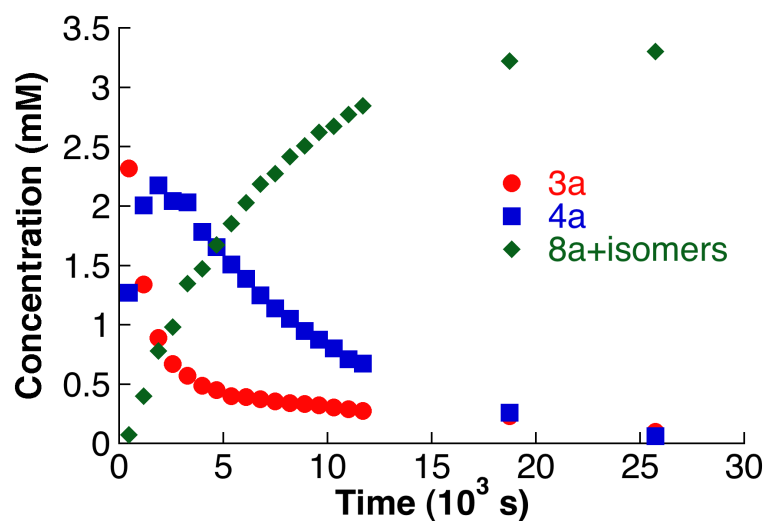
Figure A3.1. Kinetic profile for the reaction of **3a** at 50 °C in DMSO-d_6.

A3.2 Stereochemical Analysis of the Amidopalladation Step.

[Pd] = (tBu₂bpy)(Cl)Pd
Yield: 83%, **6:7** = 1:2.85
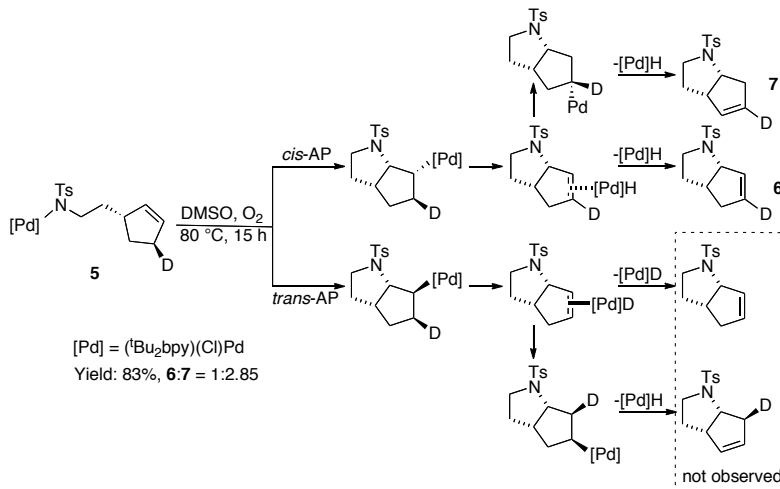
Sample preparation was identical to the experiments performed above for acyclic Pd-alkenylamidates. A ¹H NMR acquisition array was set-up at 80 °C in DMSO-d_6 and data was collected every four minutes for fifteen hours. Once the reaction was complete, the ratio of products were analyzed and quantified relative to trimethyl(phenyl)silane (PhTMS) as an the internal standard. The identities of the products were identified by comparing the ¹H NMR spectrum to the spectrum of a mixture of the known non-deuterated compounds (Figure A3.2). See ref. **Error! Bookmark not defined.** for further details of product analysis and identification.
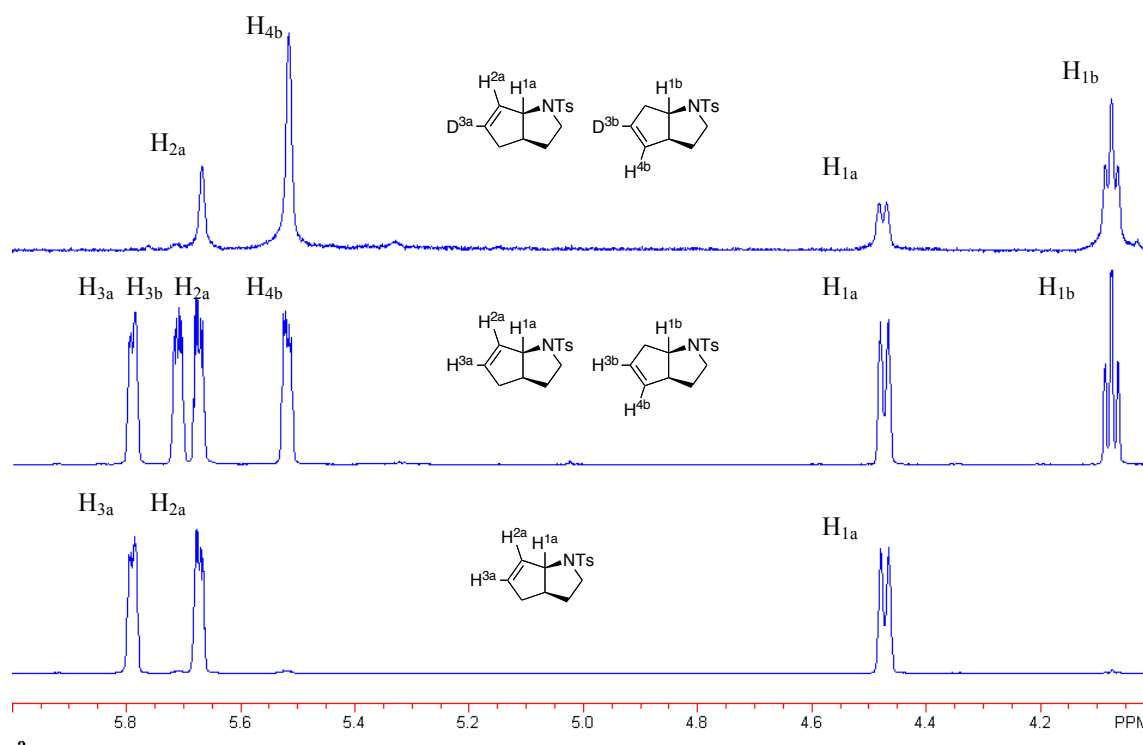
Figure A3.2. ^{1}H NMR spectra of the products of the reaction of Pd(II)-amidate complex **5** and reference compounds in DMSO-d_6.

A3.3 Addition of HCl to the Alkyl-Pd(II) Complex 4a.
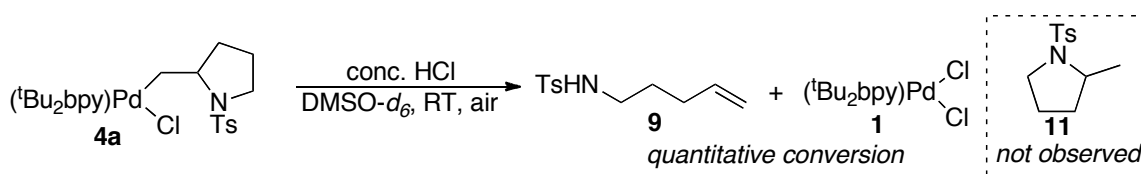
A solution of **4a** (2.70 mg, 4.16 μmol) and 1,3,5-trimethoxybenzene as an internal standard (0.44 mg, 2.62 μmol) in 600 μL of DMSO-d_6 was added to a standard 5 mm NMR tube. A ^{1}H NMR spectrum of the sample was obtained, and then a drop of concentrated HCl (~8 μL, 277 μmol HCl, ~60 equiv) was added to the side of the tube. The sample was mixed by pipetting the sample over the drop of HCl several times. Shortly after mixing, a white cloudy precipitate began to form. A ^{1}H NMR spectrum was obtained of the sample after addition of the acid. The conversion of **4a** to **9** was quantitative and proceeded with good mass balance for the aliphatic

fragments (i.e. "pyrrolidine" to amide).   Only 66% yield of **1** was observed by ^{1}H NMR, suggesting that some of the Pd was present in the precipitate or formed tetrachloropalladate in situ.

A3.4 Copies of ^{1}H and ^{13}C NMR Spectra for Isolated Compound

159.066
140.730
139.673
127.877
113.827
112.648
55.090
40.010
45.444
39.838
39.674
39.510
39.343
39.175
39.004
32.038
31.490

160   140   120   100   80   60   40   20   PPM

1:1:1 13C-2H triplet
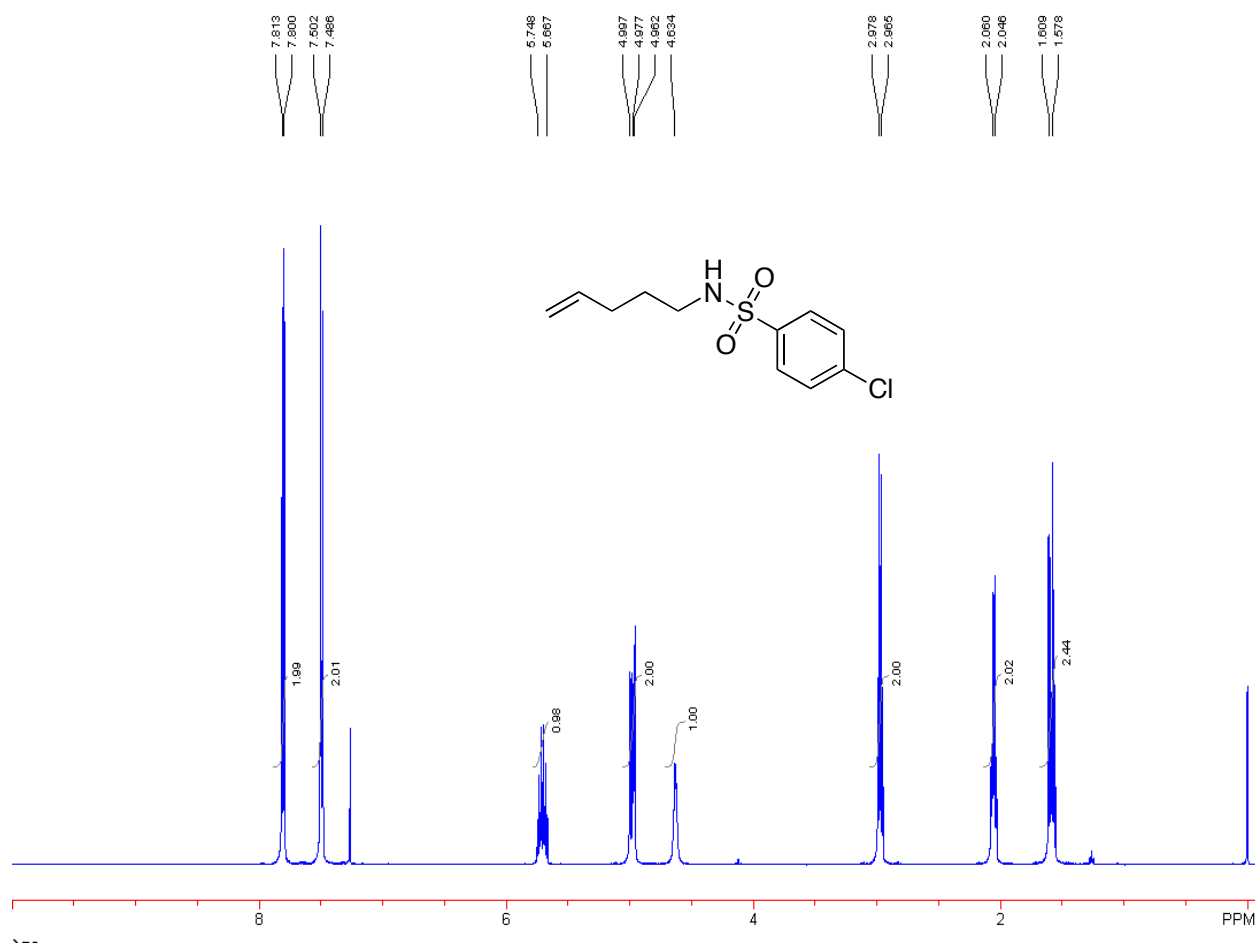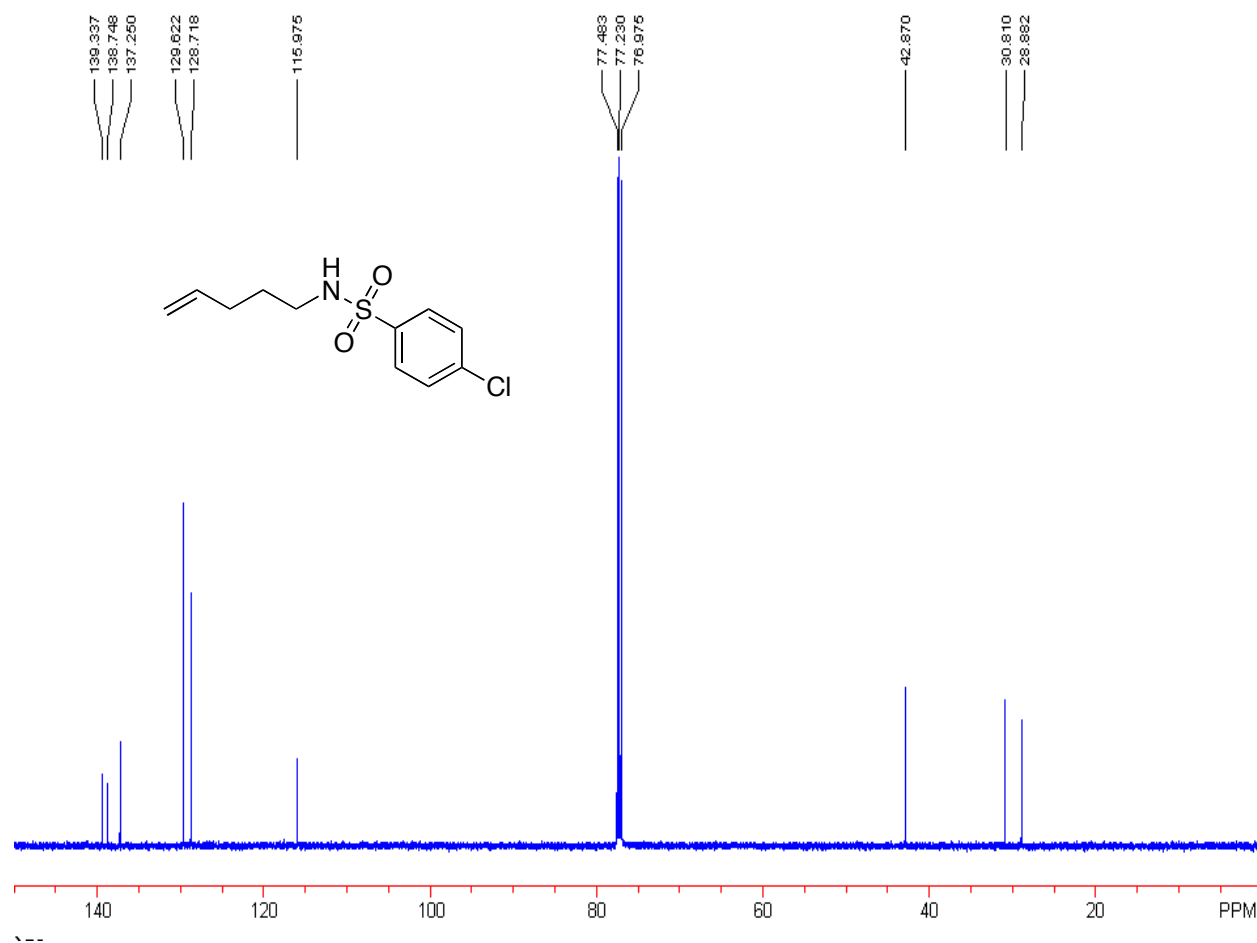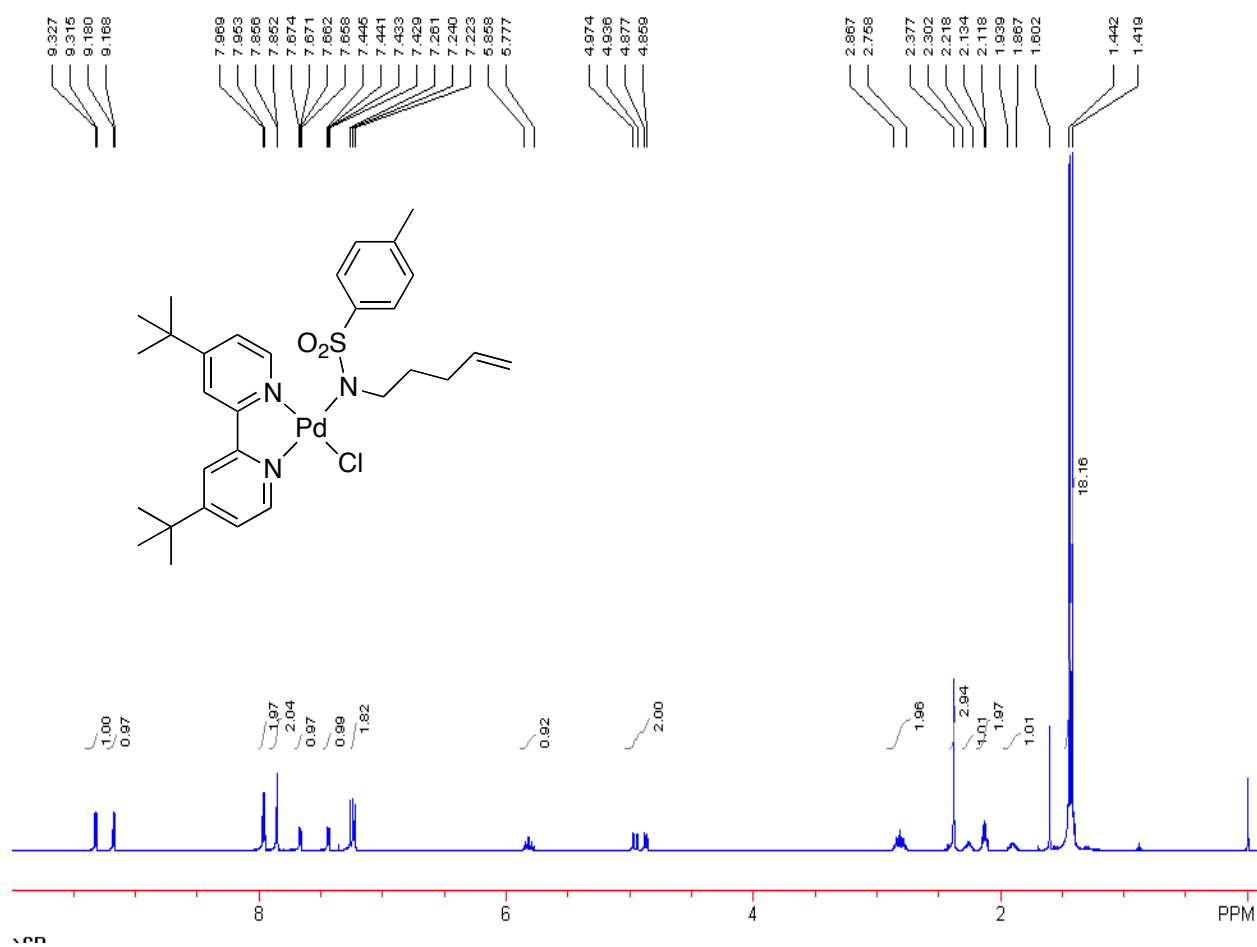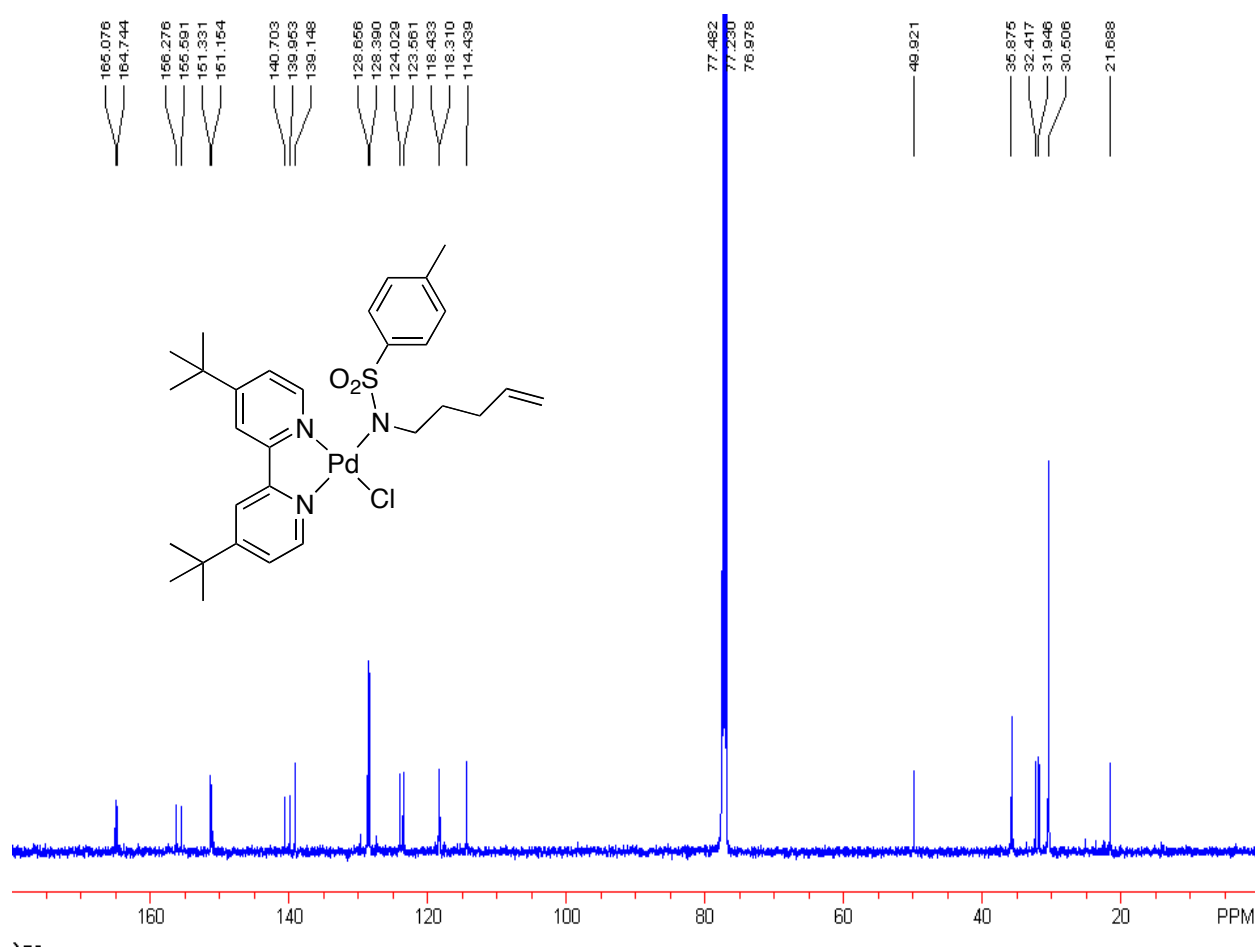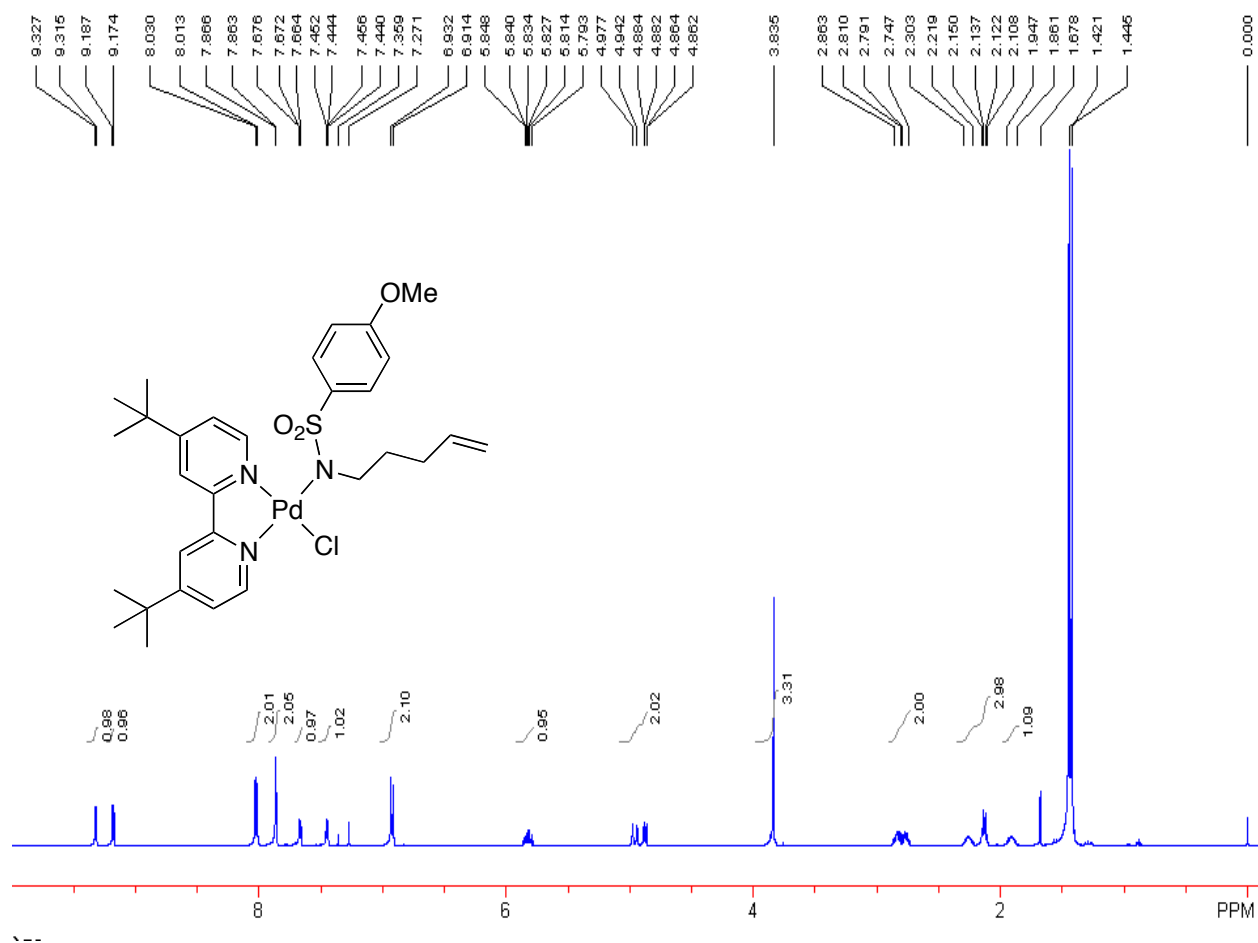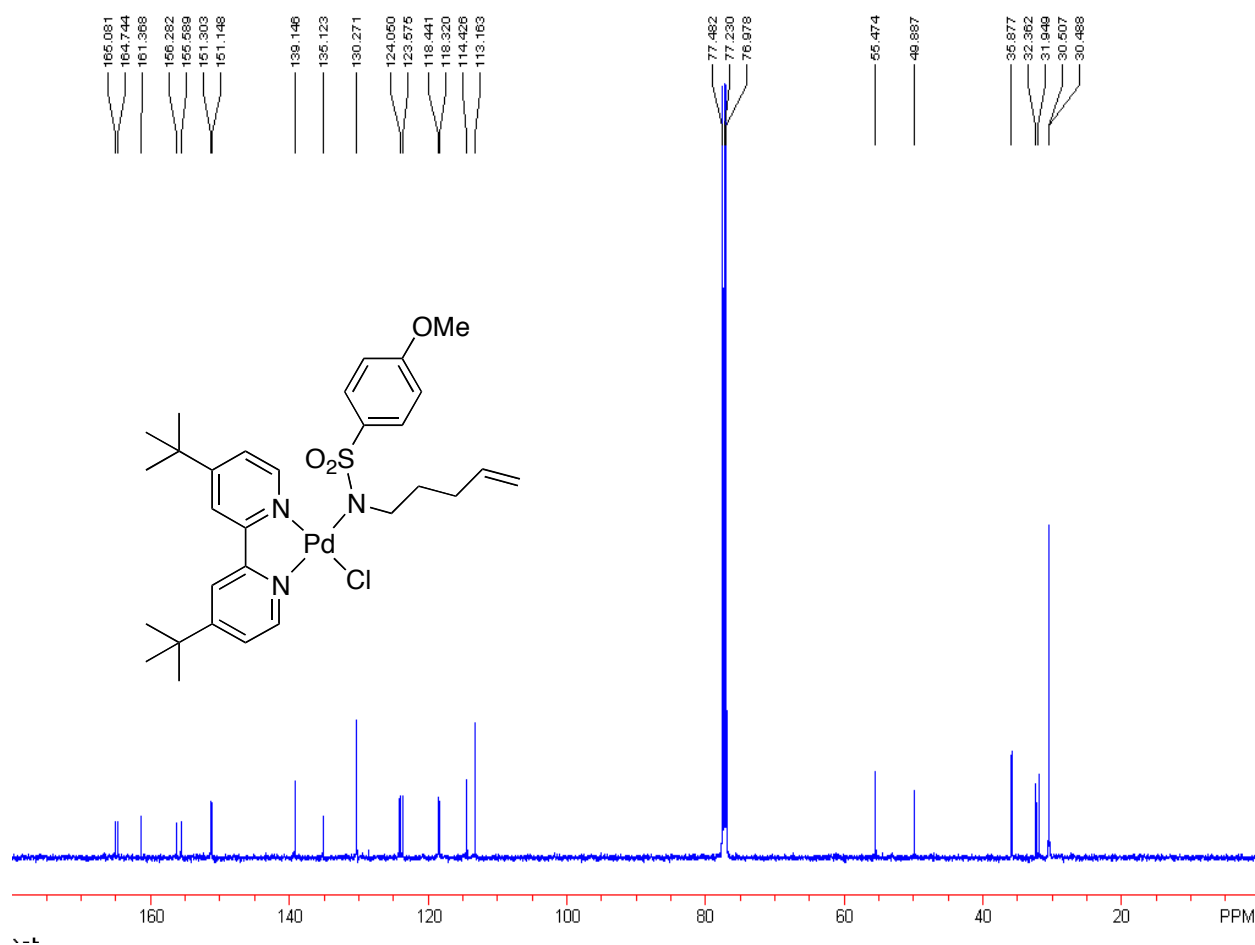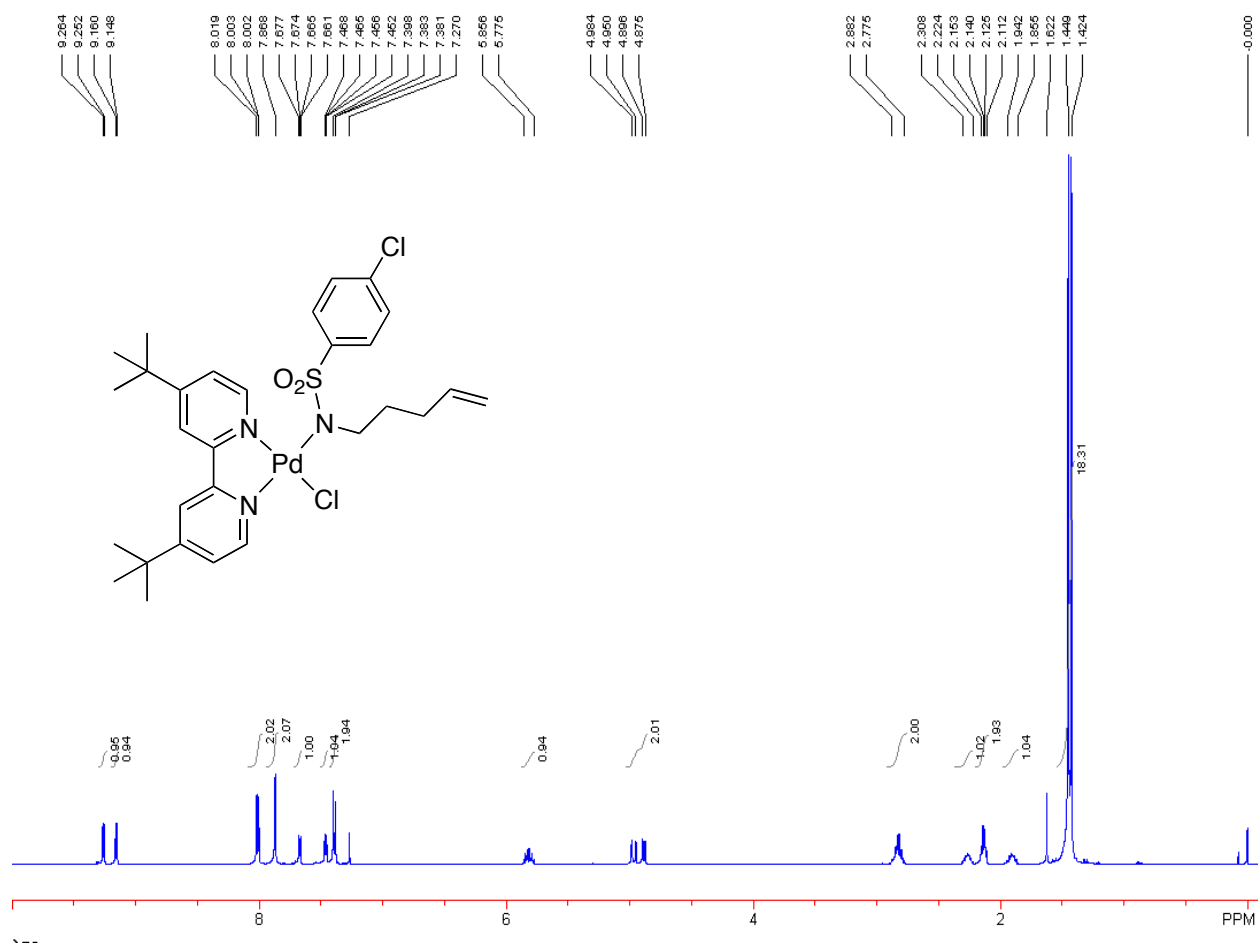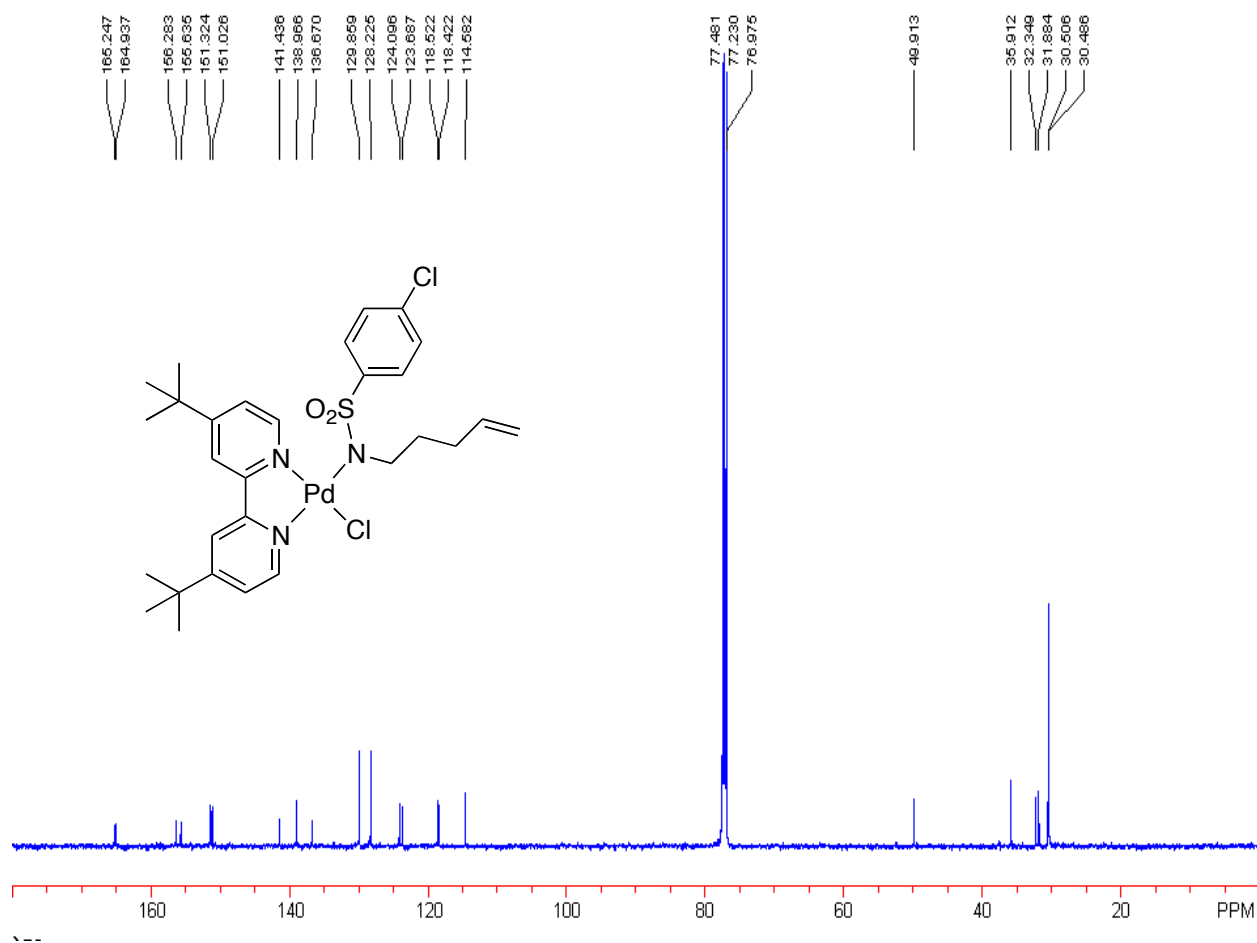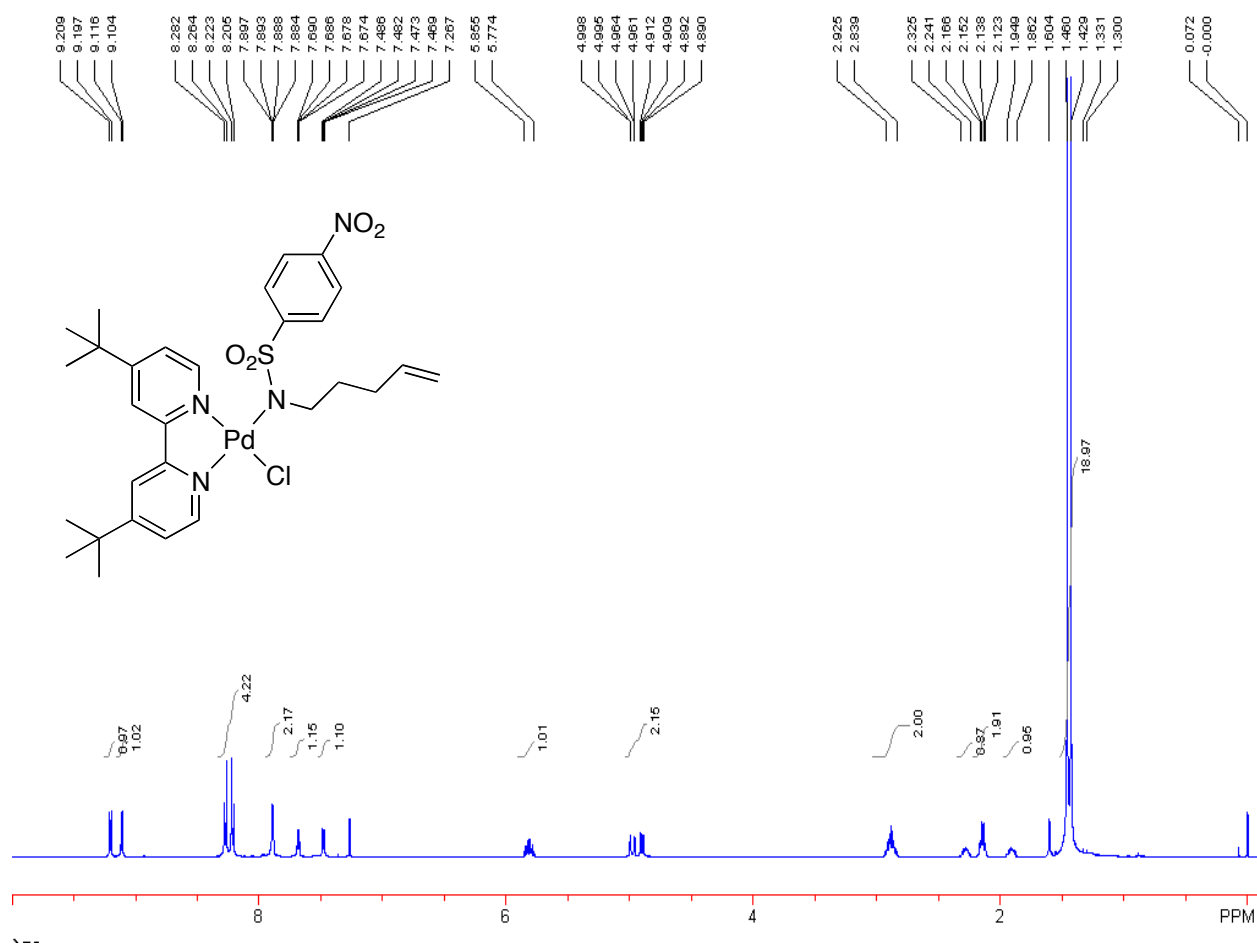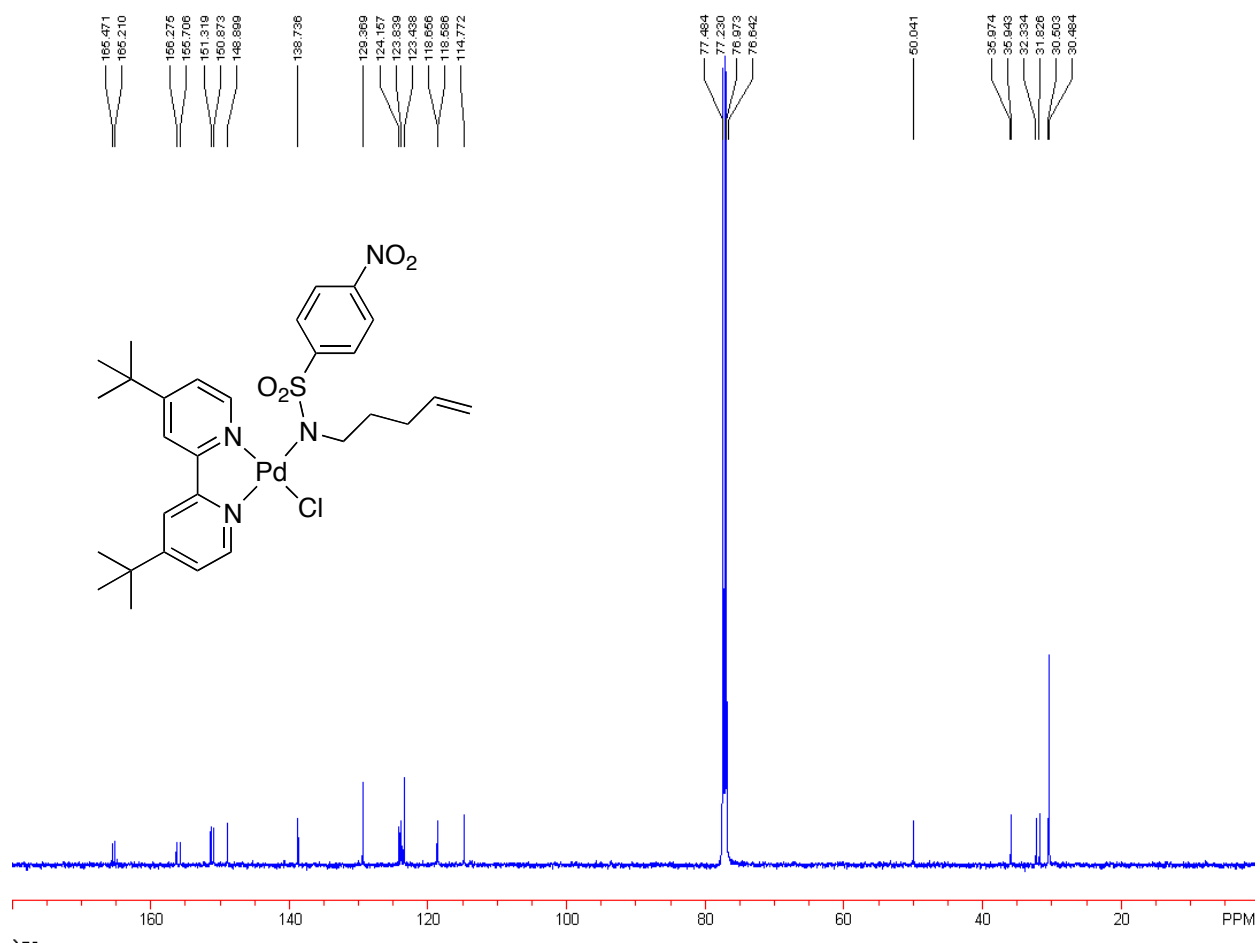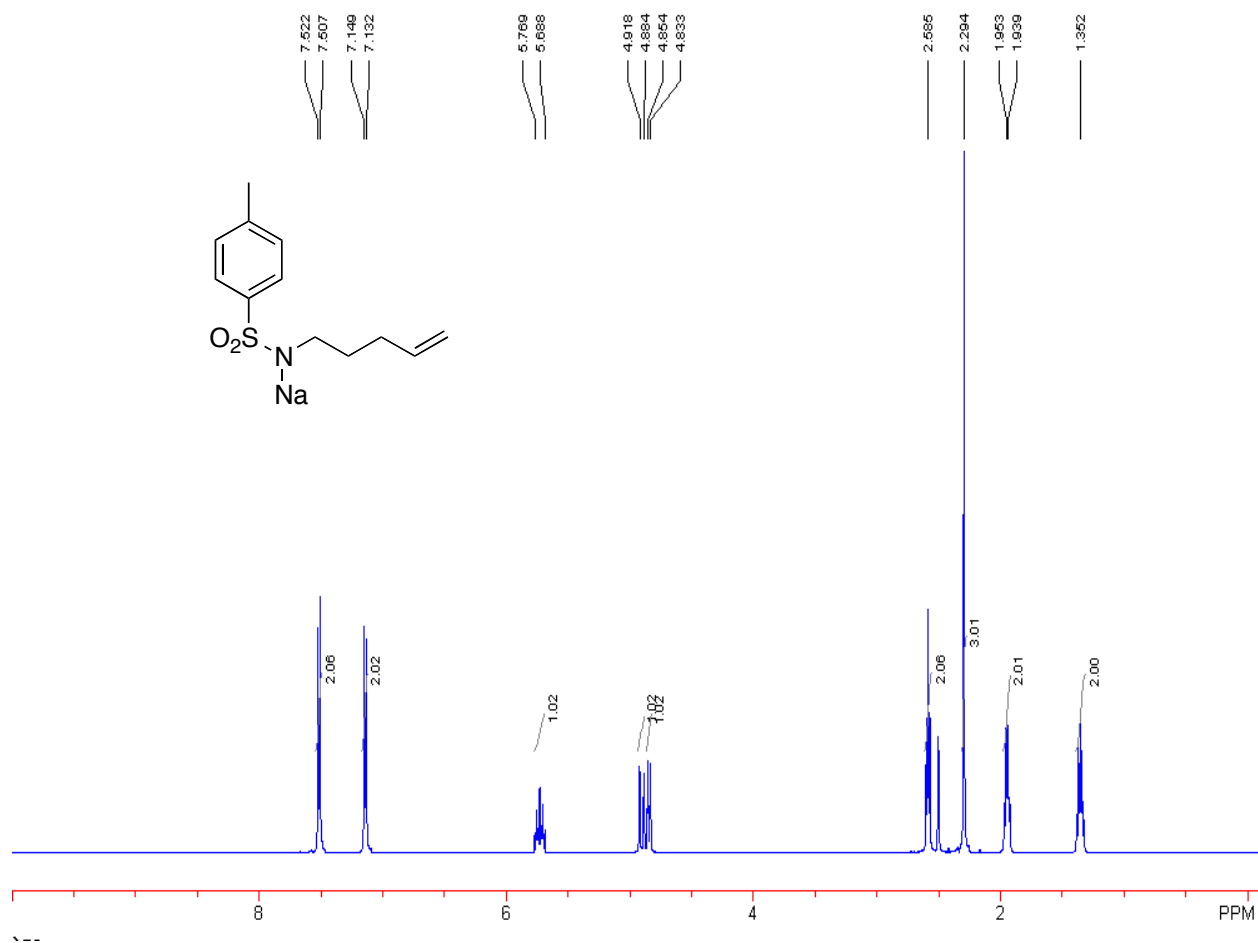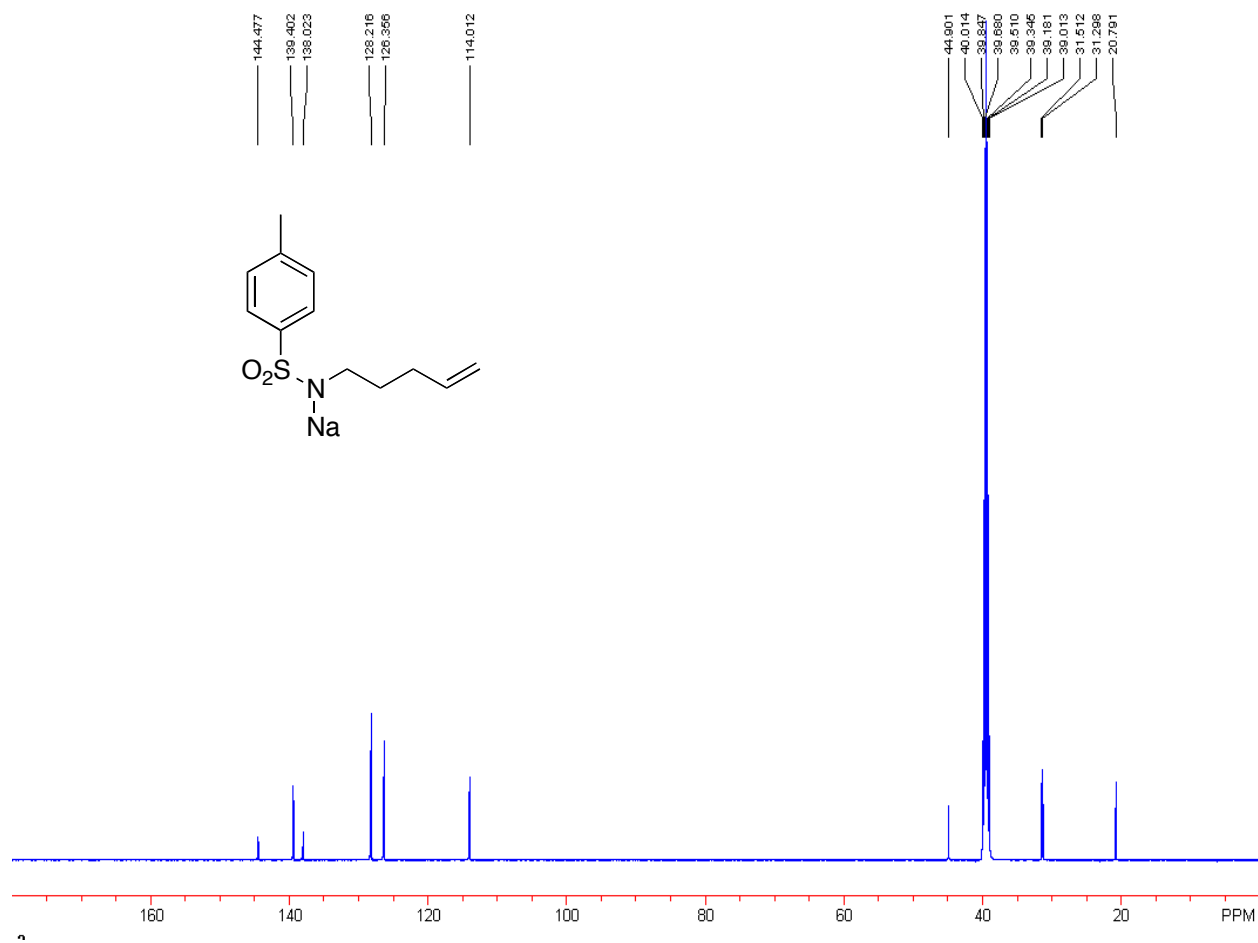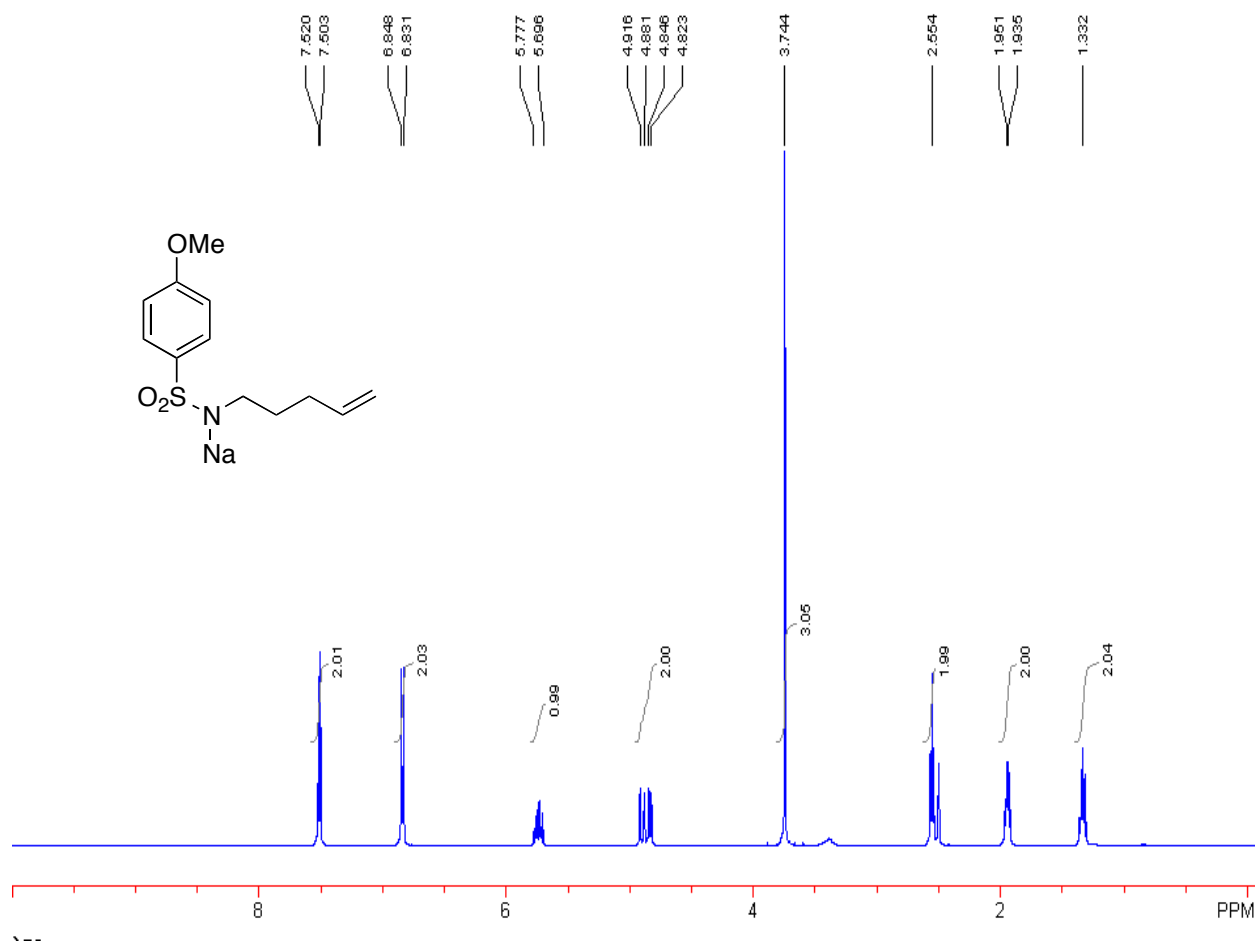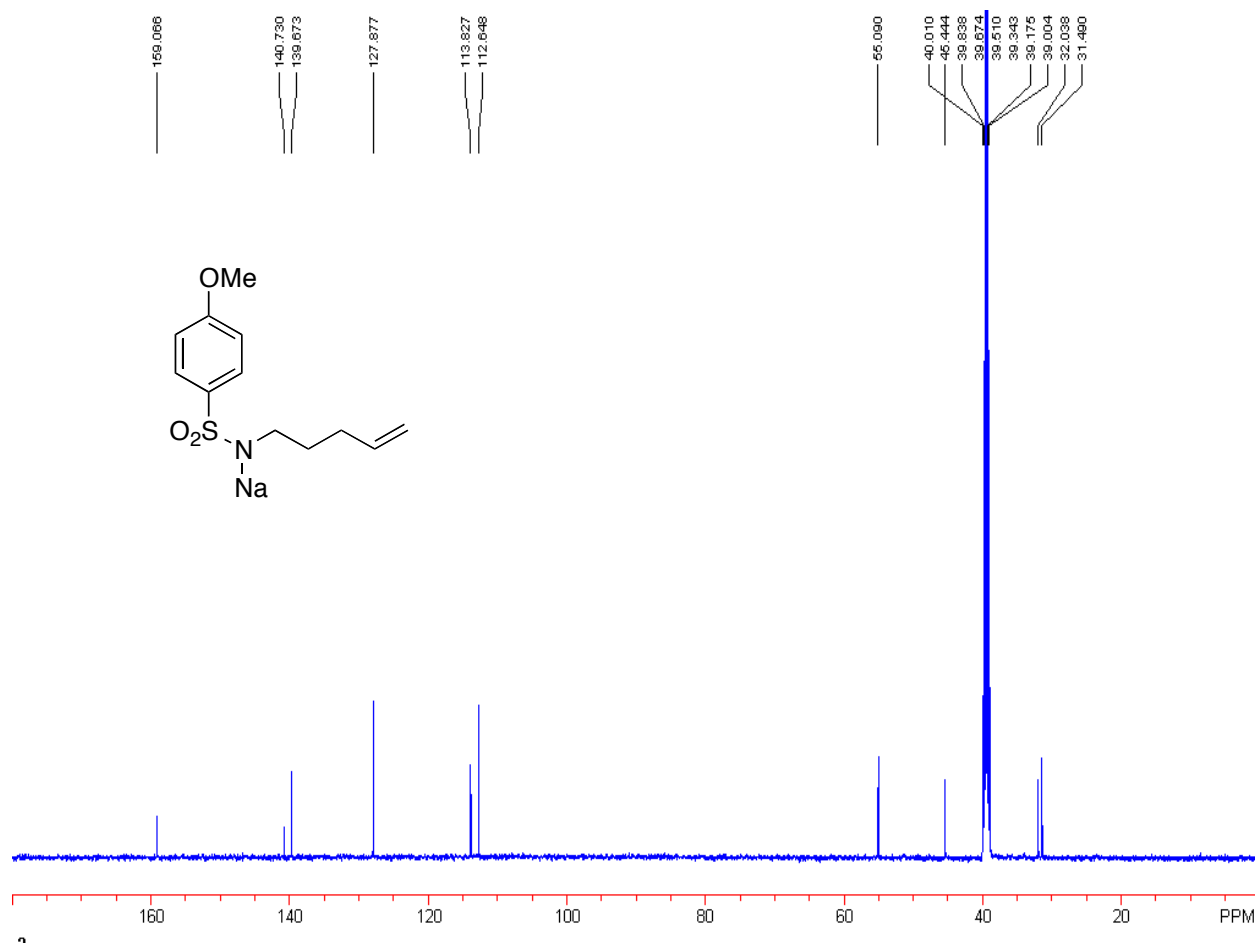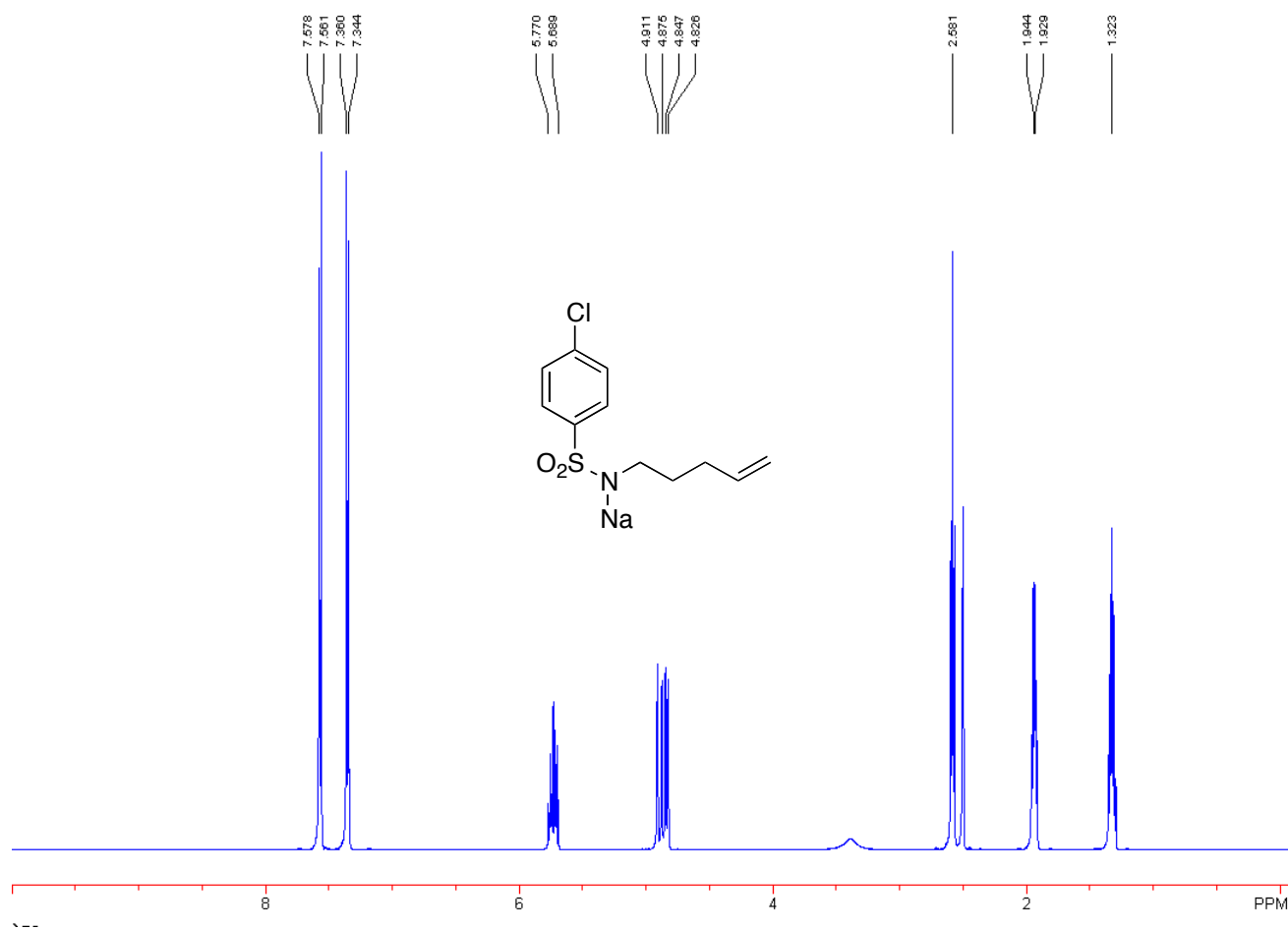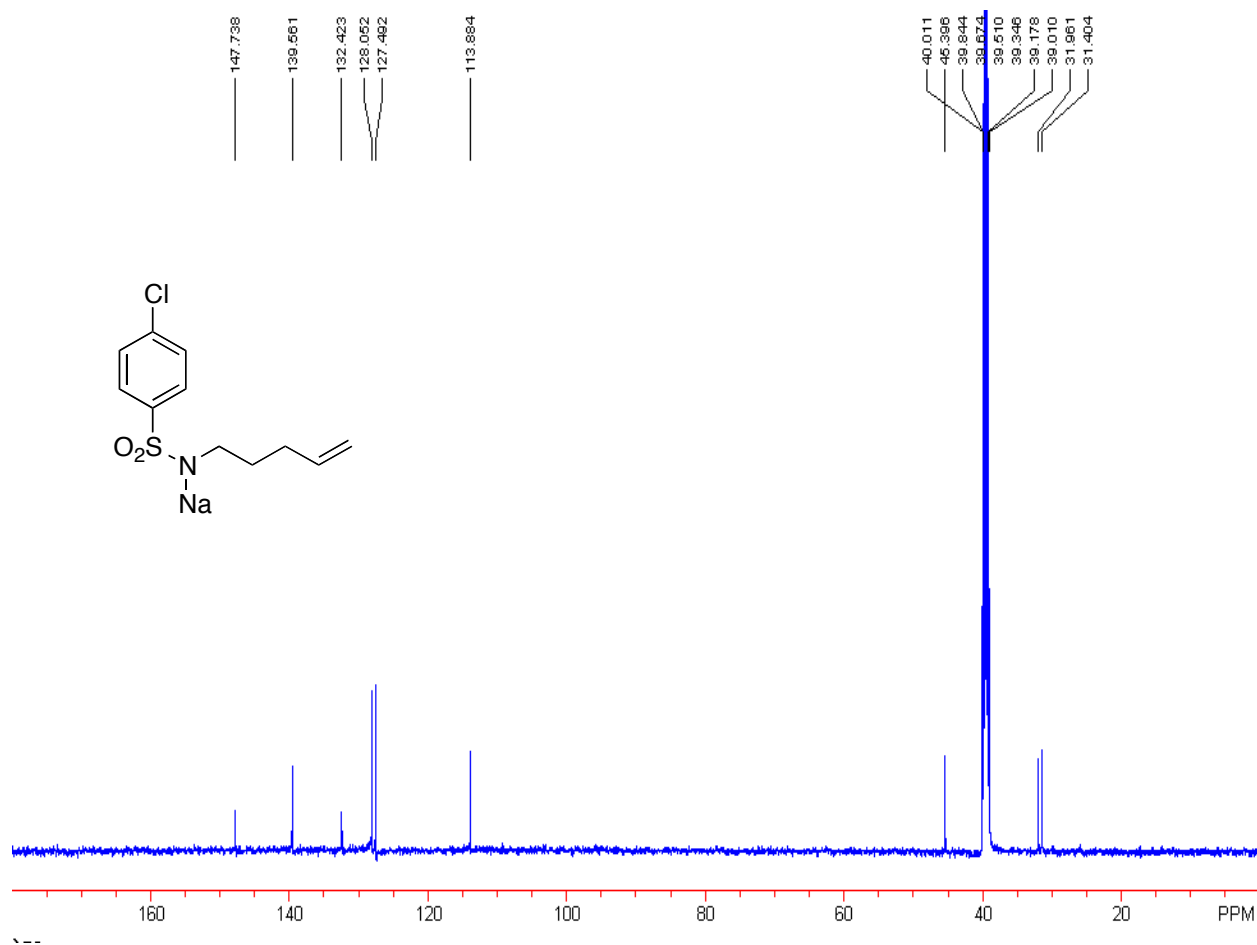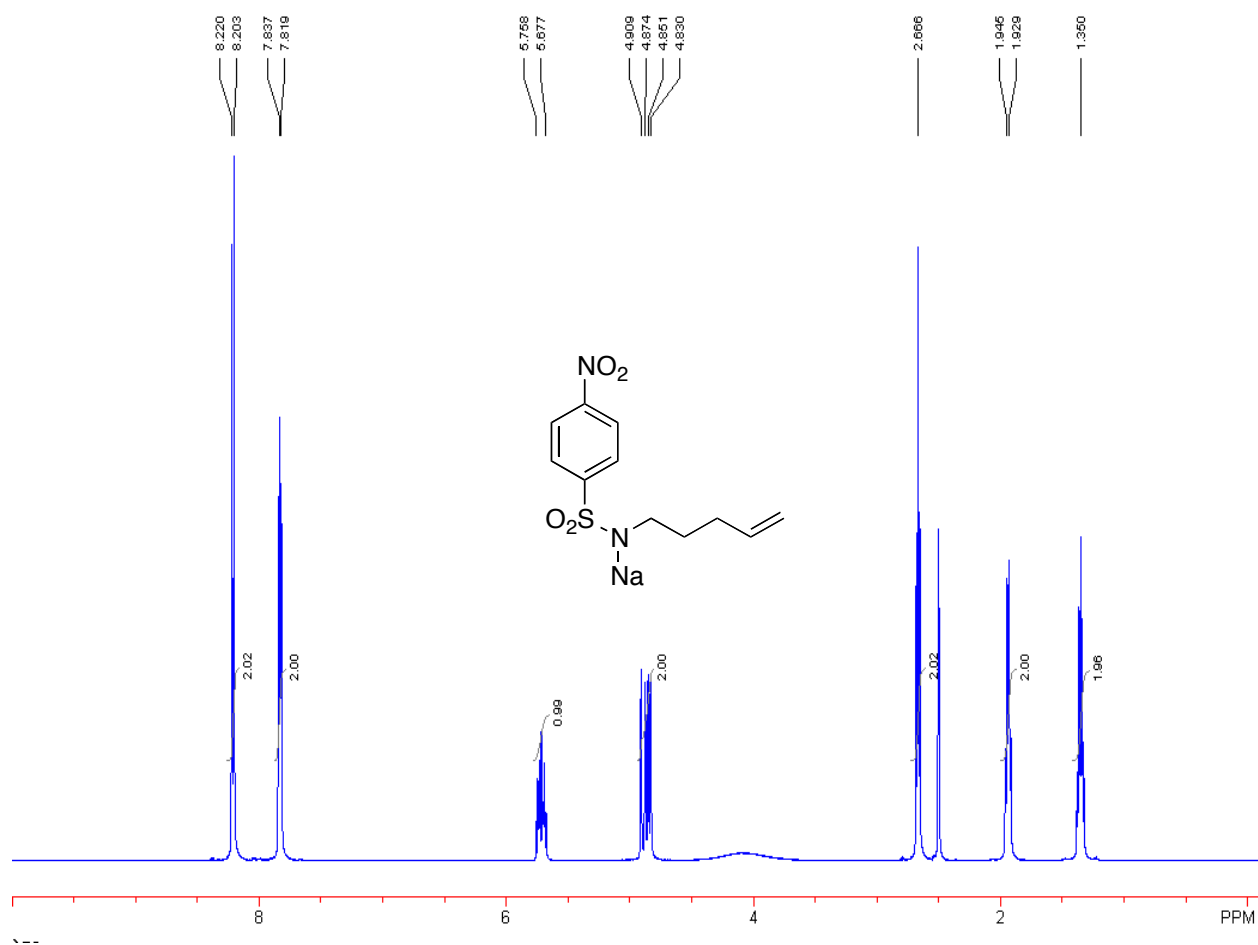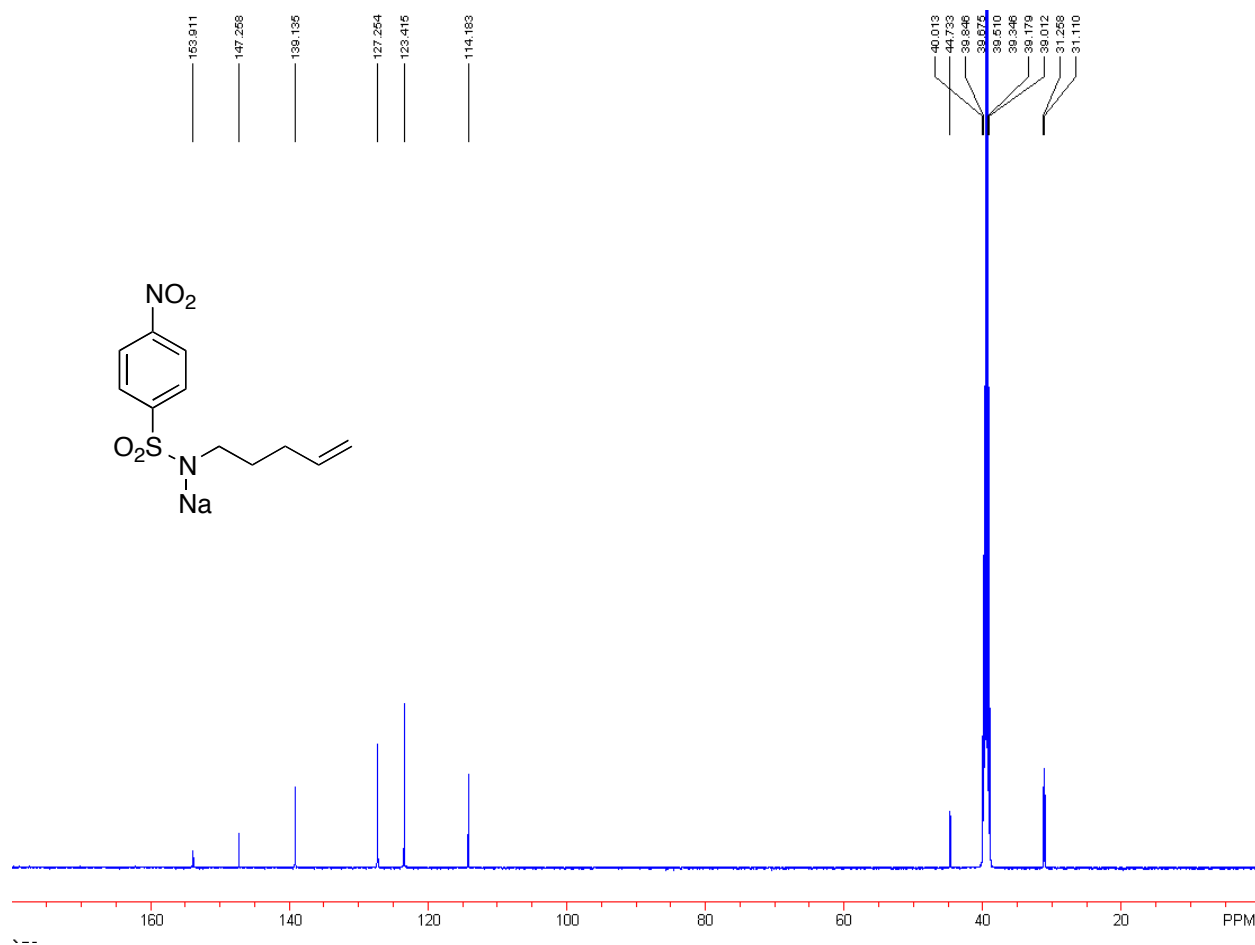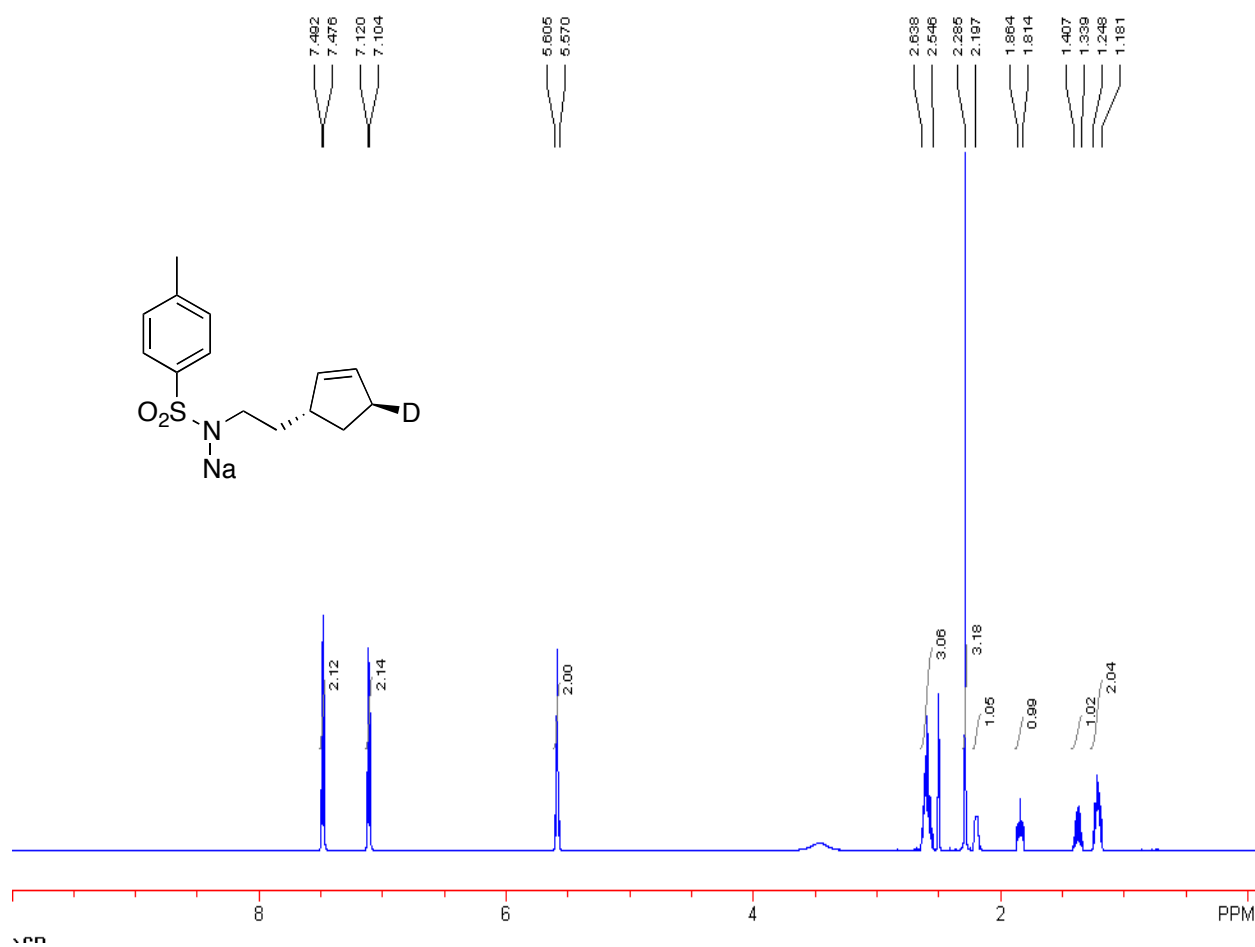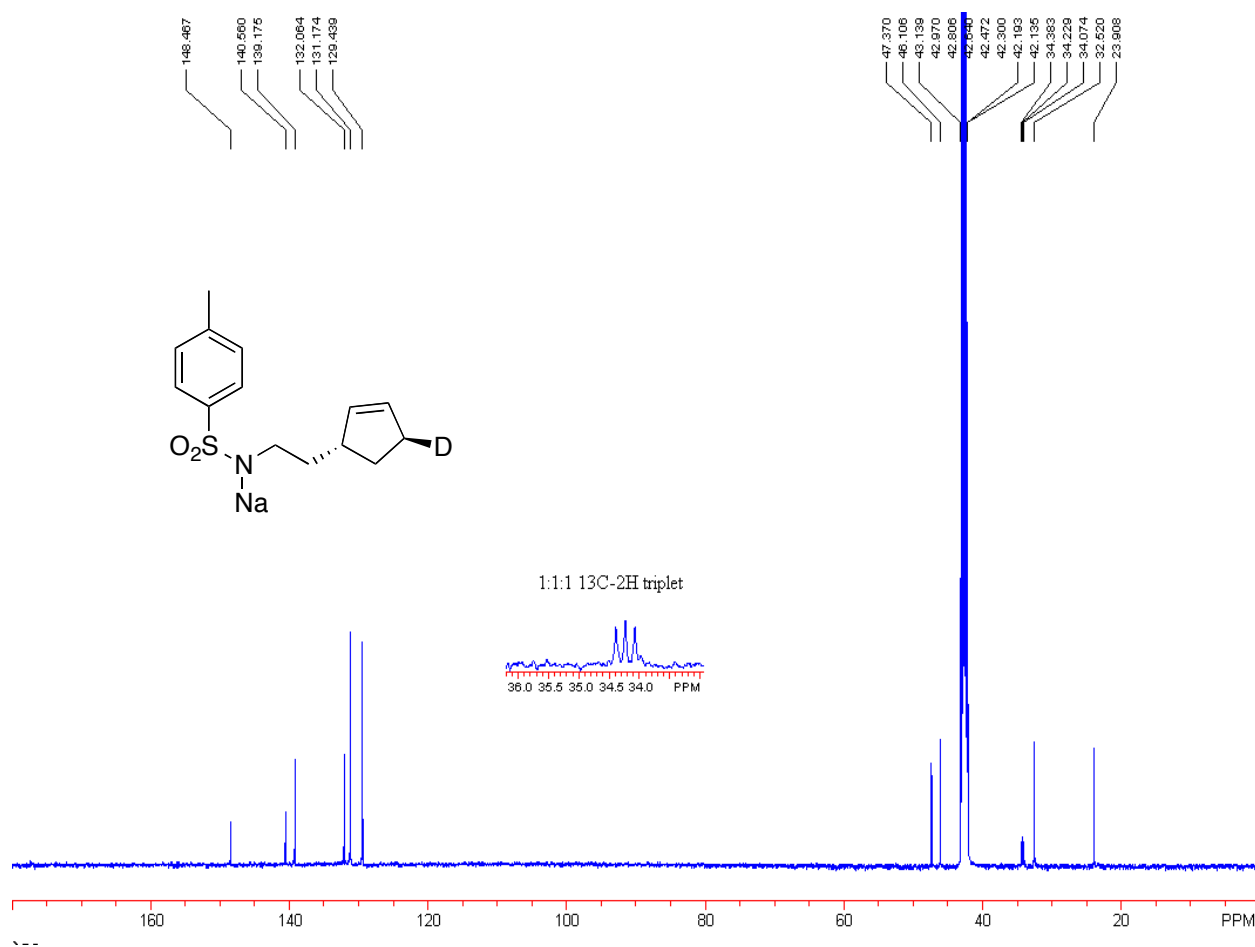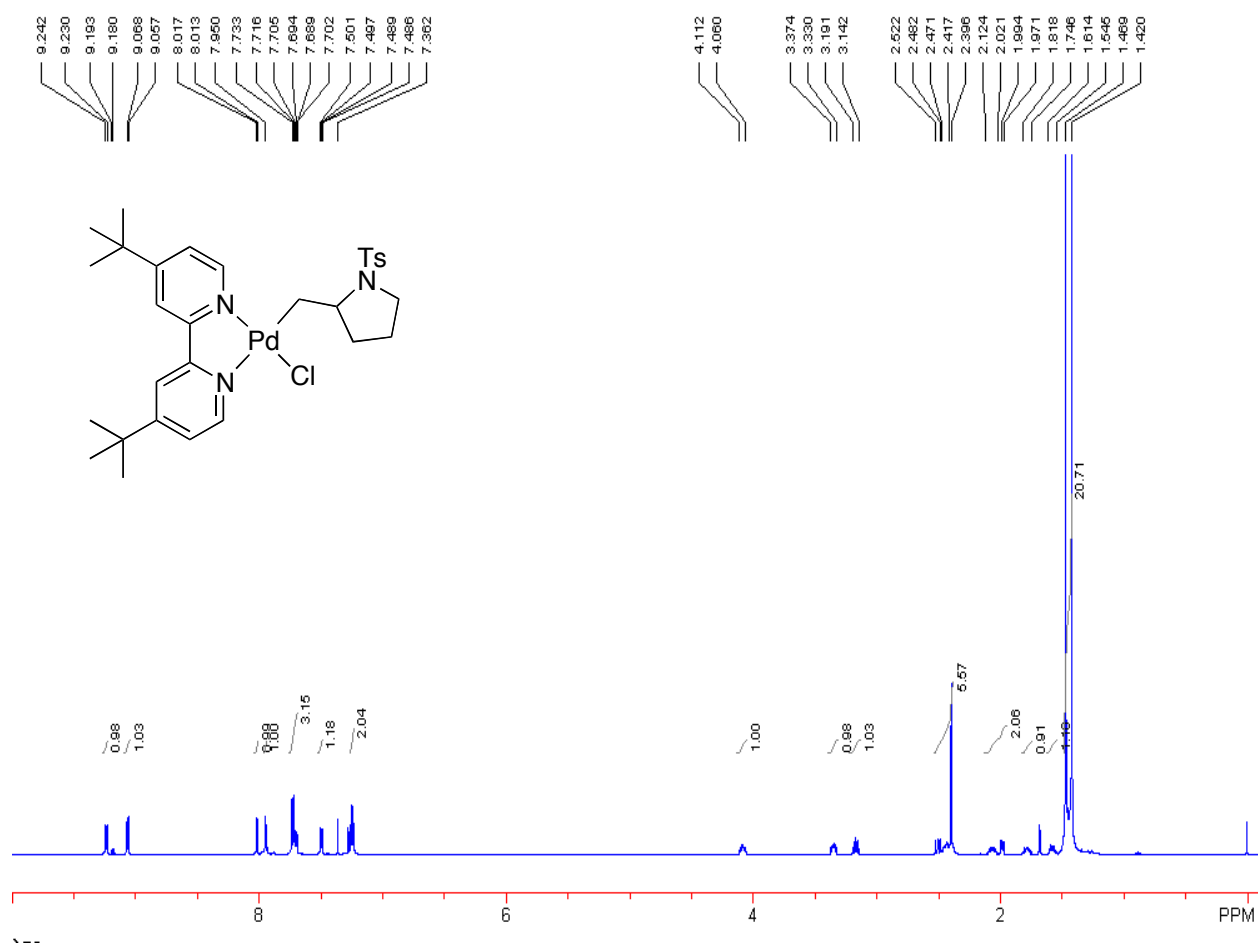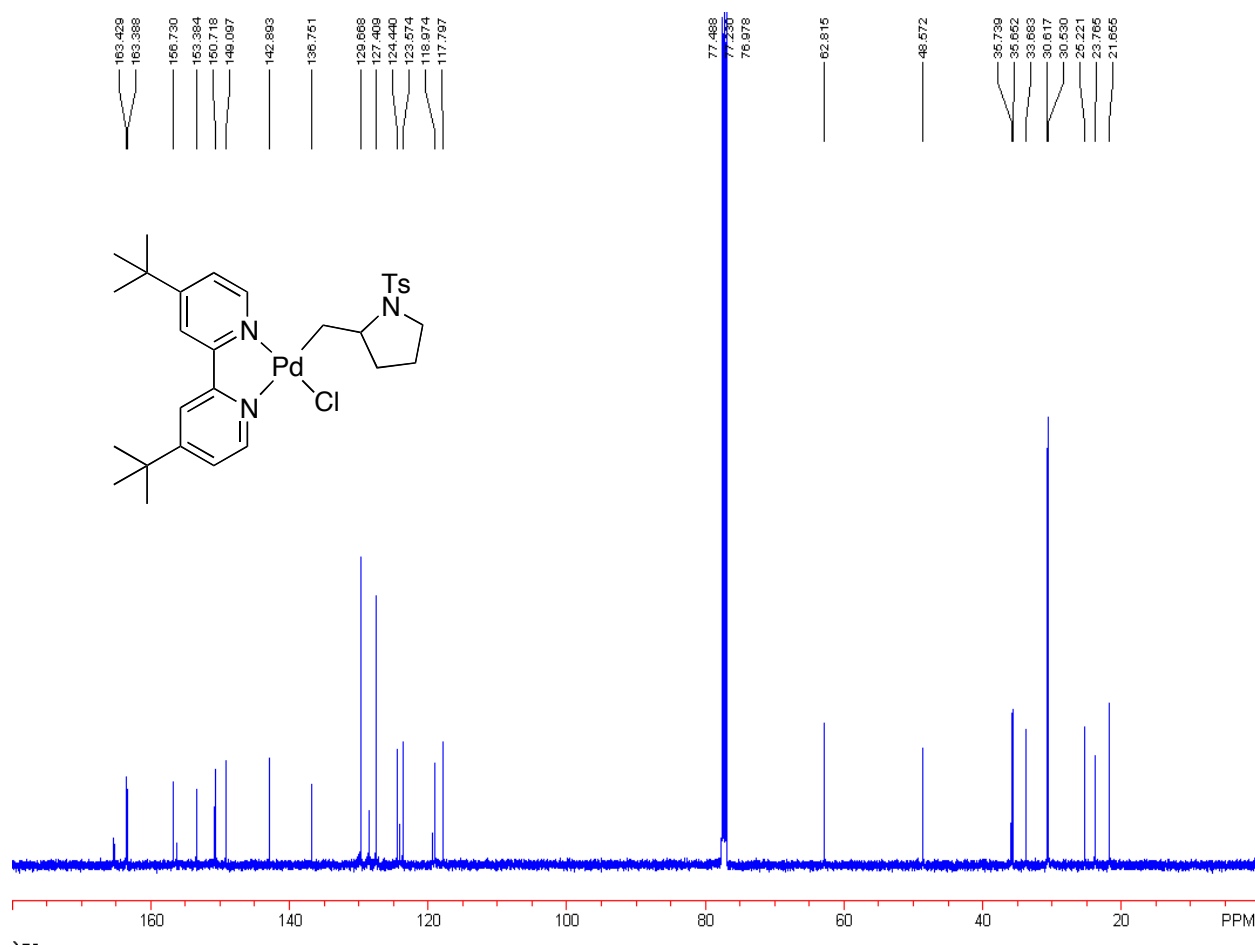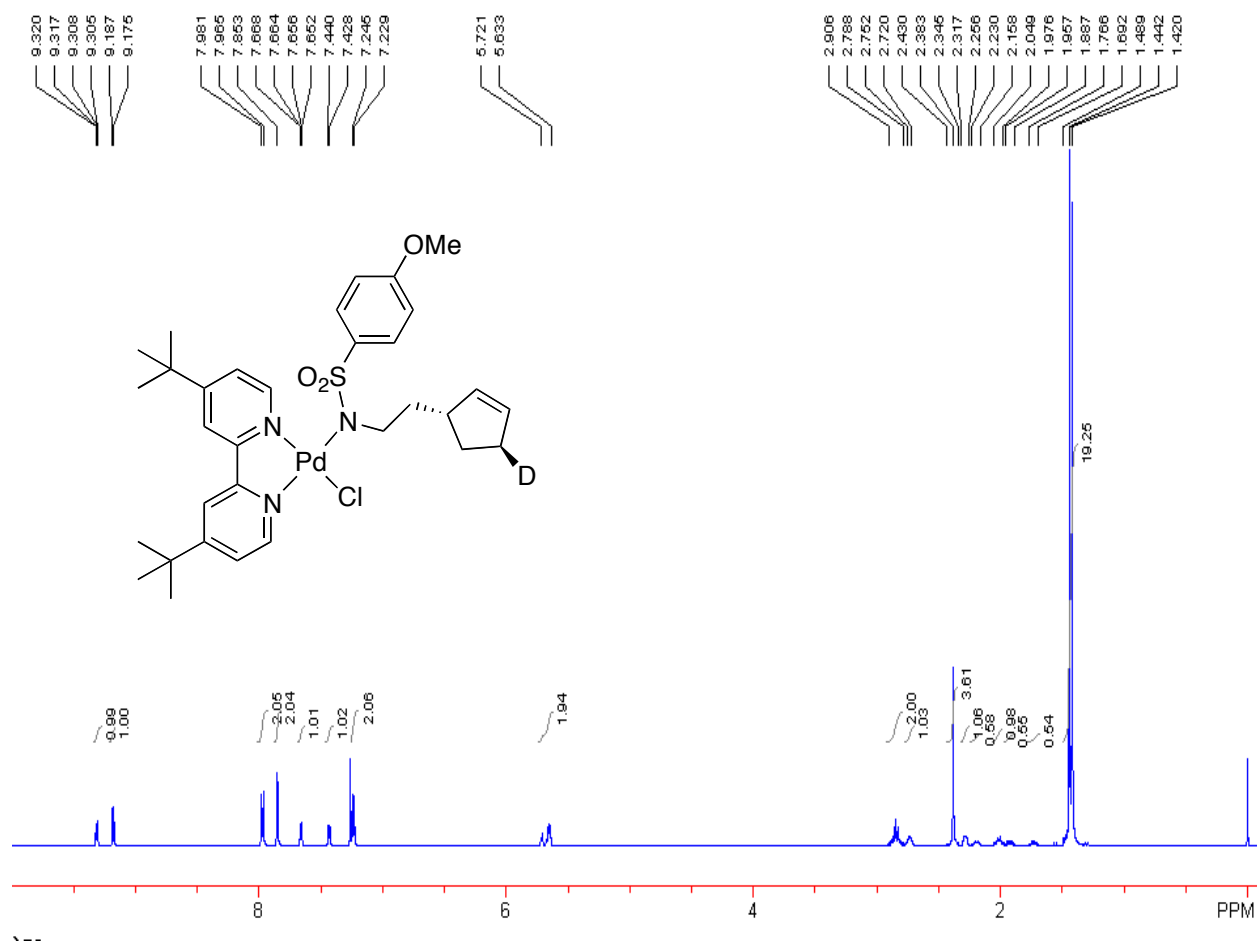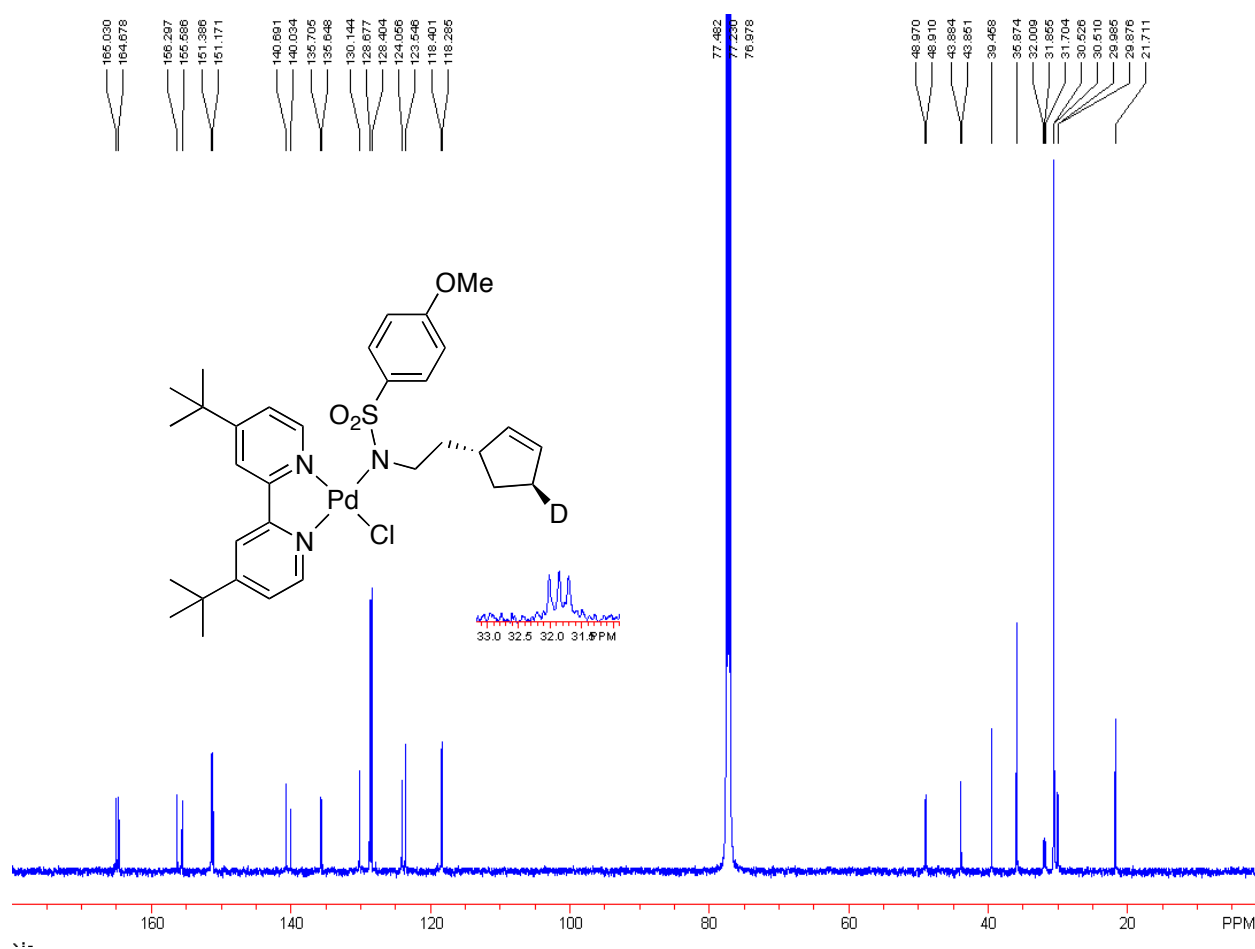
Appendix 4. Chapter 4 DAF and 6,6'-Me2bpy Amidation Study

A4.1 Determination of Amidopalladation Stereochemistry
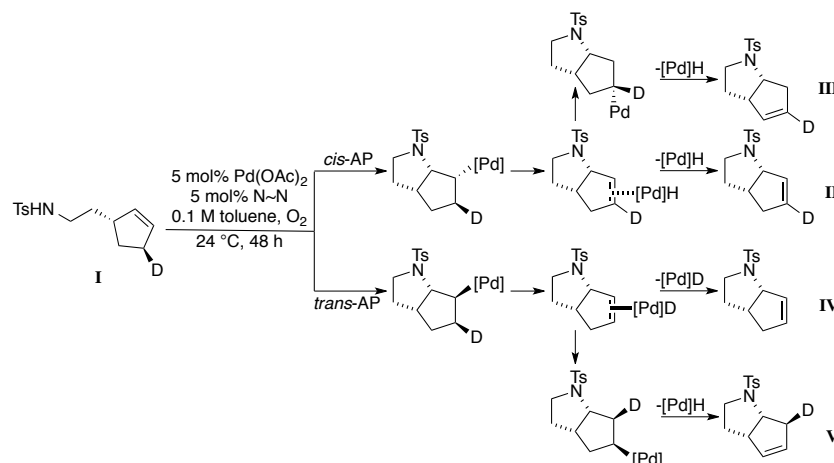
Figure A4.1. Mechanistic origin for the observation of different alkene isomers with and without the deuterium label.

A4.1.1 Reproduction of Chemical Shifts for I-V[1]

I
^{1}H NMR (CDCl$_3$) δ 7.76 (dt, J = 2.1, 9.0 Hz, 2H), 7.31 (dt, J = 2.1, 9.0 Hz, 2H), 5.71 (m, 1H), 5.56 (m, 1H), 4.58 (t, J = 6.0 Hz, 1H), 2.98 (dt, J = 6.6, 6.6 Hz, 2H), 2.65 (m, 1H), 2.44 (s, 3H), 2.28 (m, 1H), 1.98 (m, 1H), 1.63-1.38 (m, 2H), 1.32(m, 1H)

II
^{1}H NMR (CDCl$_3$) δ 7.73 (m, 2H), 7.33 (m, 2H), 5.81 (q, J = 2.1 Hz, 1H), 4.55 (dq, J = 2.1, 8.1 Hz, 1H), 3.37 (ddd,, J = 4.5, 6.9, 9.9 Hz, 1H), 3.06 (ddd, J = 6.6, 8.7, 9.9 Hz, 1H), 2.61 (m, 1H), 2.47 (m, 1H), 2.43 (s, 3H), 2.10 (dq, J = 2.1, 17.1 Hz, 1H), 1.83 (m, 1H), 1.51 (m, 1H)

III
^{1}H NMR (CDCl$_3$) δ 7.73 (m, 2H), 7.33 (m, 2H), 5.45 (q, J = 2.1 Hz, 1H), 4.18 (dt, J = 6.9, 4.2 Hz, 1H), 3.40-3.20 (m, 2H), 2.71 (m, 2H), 2.43 (s, 3H), 2.22 (m, 1H), 1.68-1.48 (m, 2H)

IV
^{1}H NMR (CDCl$_3$) δ 7.73 (m, 2H), 7.33 (m, 2H), 5.81 (m, 1H), 5.75 (m, 1H), 4.55 (dq, J = 2.1, 8.1 Hz, 1H), 3.37 (ddd,, J = 4.5, 6.9, 9.9 Hz, 1H), 3.06 (ddd, J = 6.6, 8.7, 9.9 Hz, 1H), 2.61 (m, 1H), 2.47 (m, 1H), 2.43 (s, 3H), 2.11 (dq, J = 2.1, 17.1Hz, 1H), 1.83 (m, 1H), 1.51 (m, 1H)

V
^{1}H NMR (CDCl$_3$) δ 7.73 (m, 2H), 7.33 (m, 2H), 5.72 (m, 1H), 5.45 (m, 1H), 4.18 (dt, J = 6.9, 4.2 Hz, 1H), 3.40-3.20 (m, 3H), 2.71 (m, 1H), 2.43 (s, 3H), 1.68-1.48 (m, 2H)

A4.1.2 Spectra of Reaction Mixtures in CDCl$_3$

L = DAF
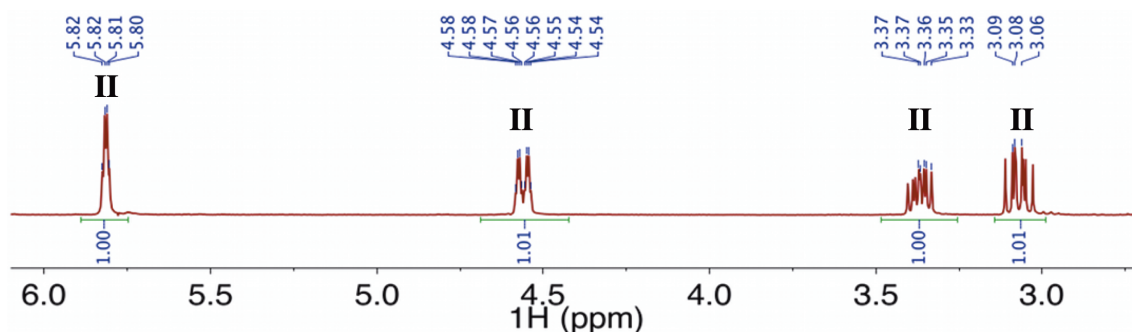
Figure A4.2. ^{1}H NMR spectrum of the crude reaction mixture of Pd(OAc)$_2$/DAF with **I**. Only a single product (**II**) is observed and corresponds to a product from the *cis*-AP pathway. Ns = 16, ds = 2, d1 = 25 s.

L = 6,6'-Me$_2$bpy
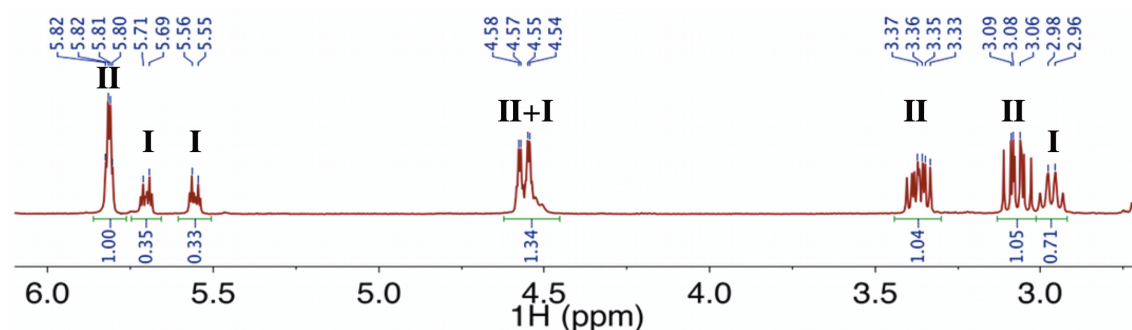
Figure A4.3. ^{1}H NMR spectrum of the crude reaction mixture of Pd(OAc)$_2$/6,6'-Me$_2$bpy with **I**. Only a single product (**II**) is observed and corresponds to a product from the *cis*-AP pathway. Ns = 16, ds = 2, d1 = 25 s.

A4.2 Kinetic Timecourse of aza-Wacker Reaction at Room Temperature
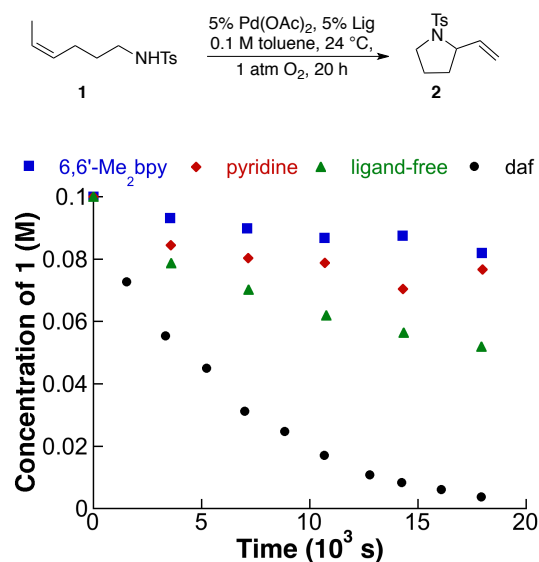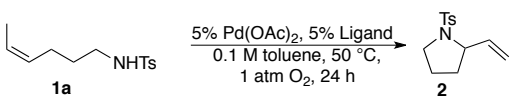
Figure A4.4. Kinetic time-course of the oxidative cyclization of **1**. Conditions: Pd(OAc)$_2$ (5.6 mg, 25 μmoles), ligand (DAF & 6,6'-Me$_2$bpy = 25 μmoles; pyridine 50 μmoles), **1** (127 mg, 500 μmoles, 0.1 M) 24 °C, 1 atm O$_2$, toluene (5 mL), int. std. = 1,3,5-trimethoxybenzene. The reaction was followed for 5 hours for DAF with data collected every 30 min, and the other ligands were followed for 21 hours with data collected every 60 min for the first 6 hours and last 3 hours (not shown). The observed catalytic rate constants for DAF and 6,6'-Me$_2$bpy were found to be $k_{obs,DAF} = 1.80 \times 10^{-4}$ M s^{-1} and $k_{obs,6,6'\text{-Me2bpy}} = 5.11 \times 10^{-6}$ M s^{-1}. Using these rate constants in the Eyring equation reveals a free energy of activation of 22.5 and 24.6 kcal/mol for DAF and 6,6'-Me$_2$bpy, respectively.

A4.3 Screening Table of Ligands at 50 °C
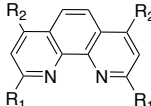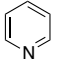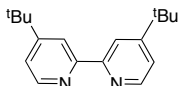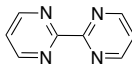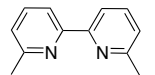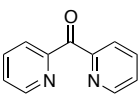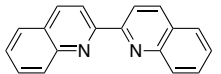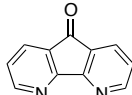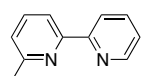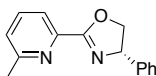
Entry	Ligand	Yield	Entry	Ligand	Yield
1	None	66% RT: 59%	7	(phenanthroline) **a:** $R_1 = R_2 = H$ **b:** $R_1 = Me, R_2 = H$ **c:** $R_1 = H, R_2 = Ph$ **d:** $R_1 = Me, R_2 = Ph$	3% 9% 1% 7%
2	(pyridine) 10 mol%	86% RT: 47%	8	(bipyrimidine)	2%
3	(tBu bipyridine)	1%	9	(di-2-pyridyl ketone)	26%
4	(6,6'-Me₂bpy)	81% RT: 40%	10	(DAF)	**97%** RT: 97%
5	(biquinoline)	35%	11	(pyridyl oxazoline, Ph)	63%
6	(6-methyl bipyridine)	38%			

Figure A4.5. Screening table of various bidentate ligands for activity in aerobic Pd-catalyzed aza-Wacker reactions. Most bidentate ligands were shown to inhibit the reaction except DAF and 6,6'-Me₂bpy, which served to promote the reaction at 50 °C. Conditions: substrate (75 mmol, 0.1 M), Pd(OAc)2 (3.75 mmol), O$_2$ (1 atm), toluene (0.75 mL), 50 °C, 24 h. Reactions were processed by filtering the mixture through silica, washing with EtOAc and removing the solvent. The resulting concentrate was dissolved in CDCl$_3$ containing an external standard (1,3,5-trimethoxybenzene) and analyzed by ^{1}H NMR spectroscopy.

A4.4 Pyridine Titration of Pd(N~N)(OAc)₂ Complexes

Increasing quantities of pyridine (0.5 equiv per 10 μL of a CDCl$_3$ stock solution) were added to solutions containing **4** and the well-defined complexes **5-7** (40 mM in CDCl$_3$, 0.5 mL). After every addition of pyridine, the sample was allowed to equilibrate at room temperature for 45 minutes prior to data acquisition. The speciation was monitored by ^{1}H NMR spectroscopy.

Intermediate complexes were identified by comparing a given spectrum against free pyridine, Pd(pyr)$_2$(OAc)$_2$ and free bidentate ligand standards.

A4.4.1 DAF
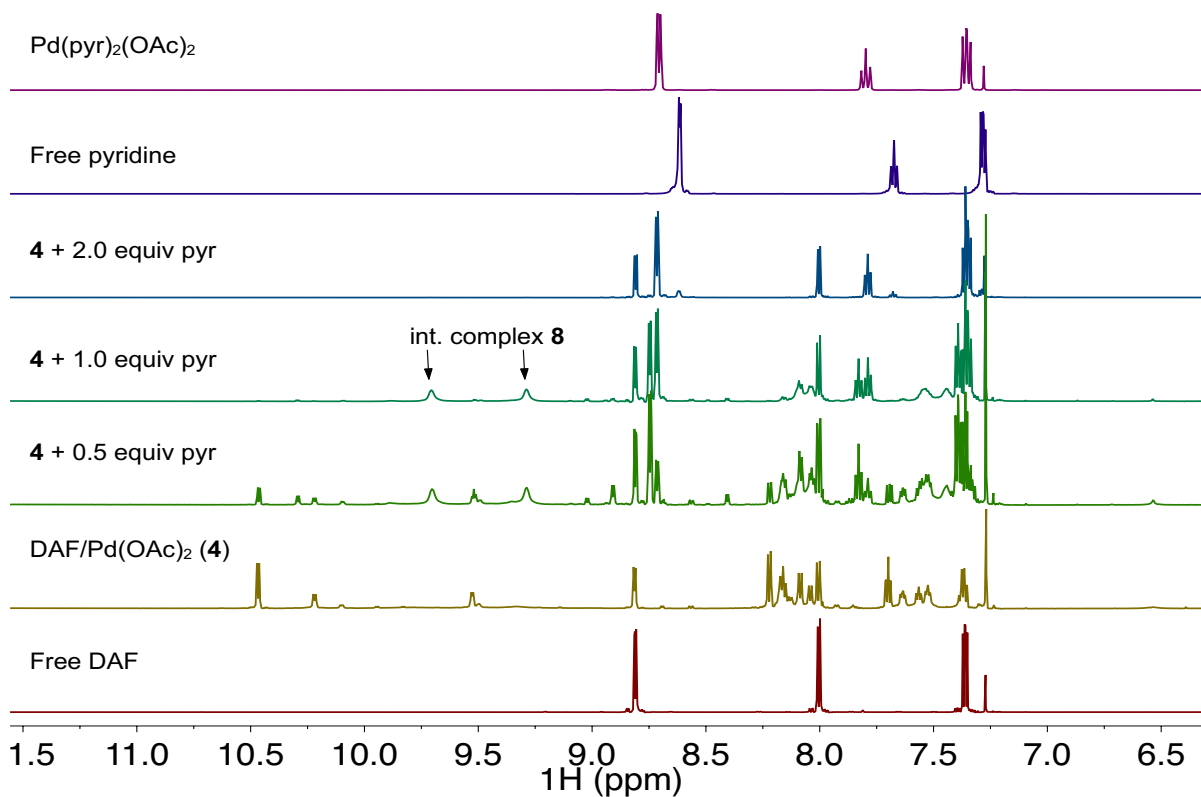
Figure A4.6. Titration of pyridine into a CDCl$_3$ solution containing a 1:1 DAF:Pd(OAc)$_2$ mixture and 1,3,5-trimethoxybenzene as an internal standard. In the absence of pyridine, multiple DAF-Pd(OAc)$_2$ complexes are present, which have been characterized previously to be a mixture of monomeric and dimeric species.[2] Addition pyridine results in the reduction of the species and appearance of Pd(κ^1-DAF)(pyridine)(OAc)$_2$ (**8**). After two equivalents of pyridine are added, DAF ligand is dissociated and all of the Pd can be account for as Pd(pyridine)$_2$(OAc)$_2$. ns = 8, ds = 2, d1 = 15.

A4.4.2 6,6'-Me₂bpy
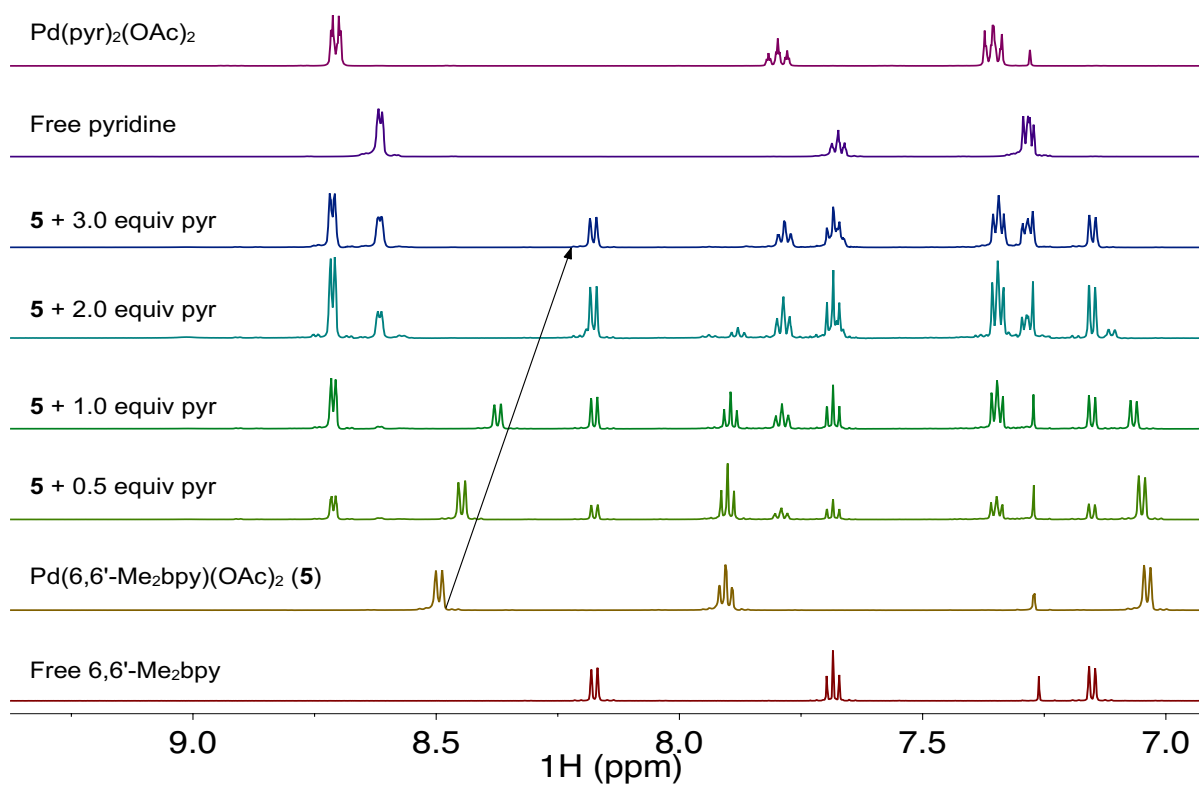
Figure A4.7. Titration of pyridine into a CDCl$_3$ solution containing Pd(κ^2-6,6'-Me$_2$bpy)(OAc)$_2$ (**5**) and 1,3,5-trimethoxybenzene as an internal standard. Addition pyridine results in the dissociation of 6,6'-Me$_2$bpy with concomitant formation of Pd(pyridine)$_2$(OAc)$_2$. Additionally, there is a change in the chemical shift of **5** signifying rapid exchange with a low-populated intermediate species that was later identified to be Pd(κ^1-6,6'-Me$_2$bpy)(pyridine)(OAc)$_2$ (**9**) (see below). After two equivalents of pyridine are added, nearly all the 6,6'-Me$_2$bpy ligand is dissociated and can be accounted for as Pd(pyridine)$_2$(OAc)$_2$. ns = 8, ds = 2, d1 = 15.

A4.4.3 Neocuproine
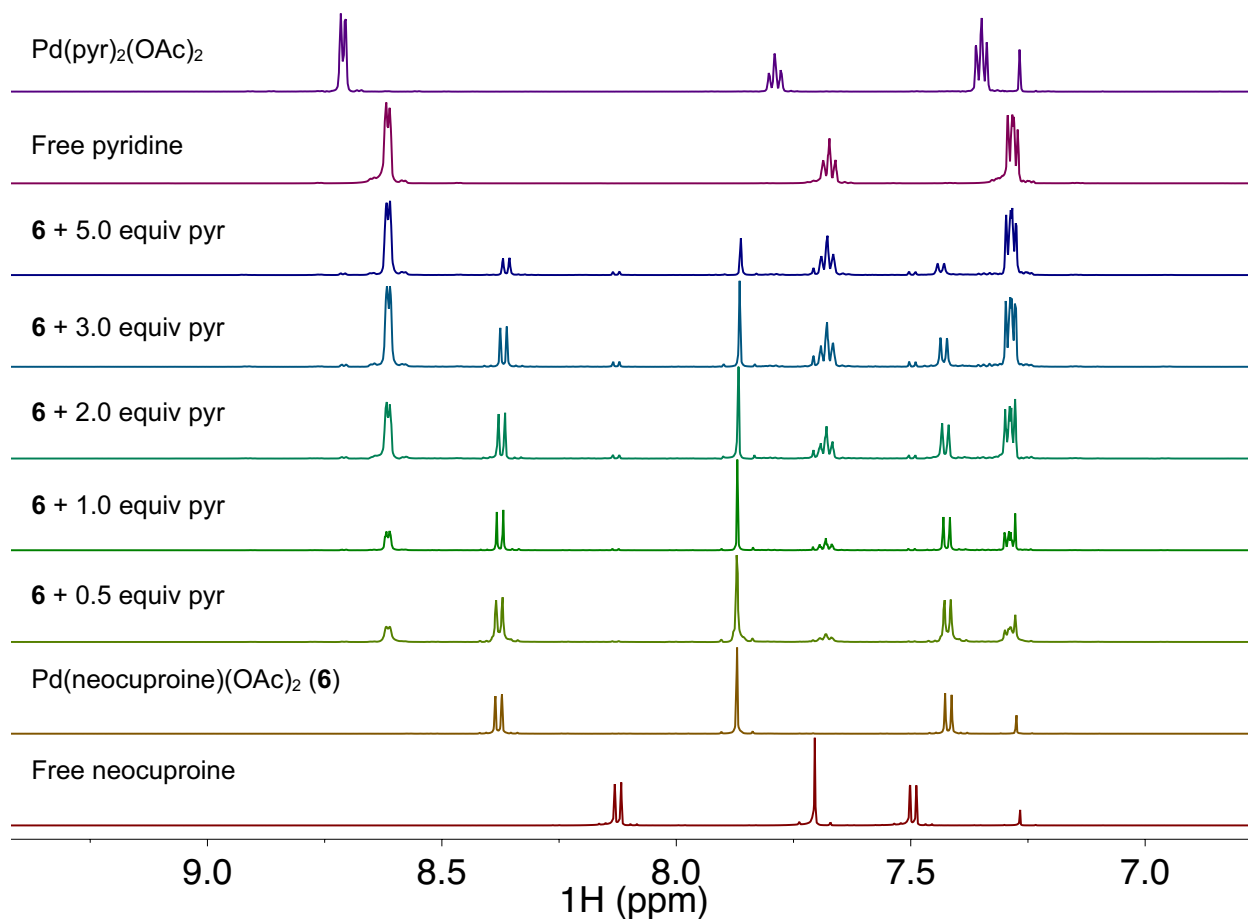
Figure A4.8. Titration of pyridine into a CDCl$_3$ solution containing Pd(κ^2-neocuproine)(OAc)$_2$ (**6**) and 1,3,5-trimethoxybenzene as an internal standard. **6** is resistant to ligand dissociation and shows only trace amounts of neocuproine and Pd(pyridine)$_2$(OAc)$_2$ after 5 equivalents of pyridine have been added. ns = 8, ds = 2, d1 = 15.

A4.4.4 4,4'-^{t}Bu$_2$bpy
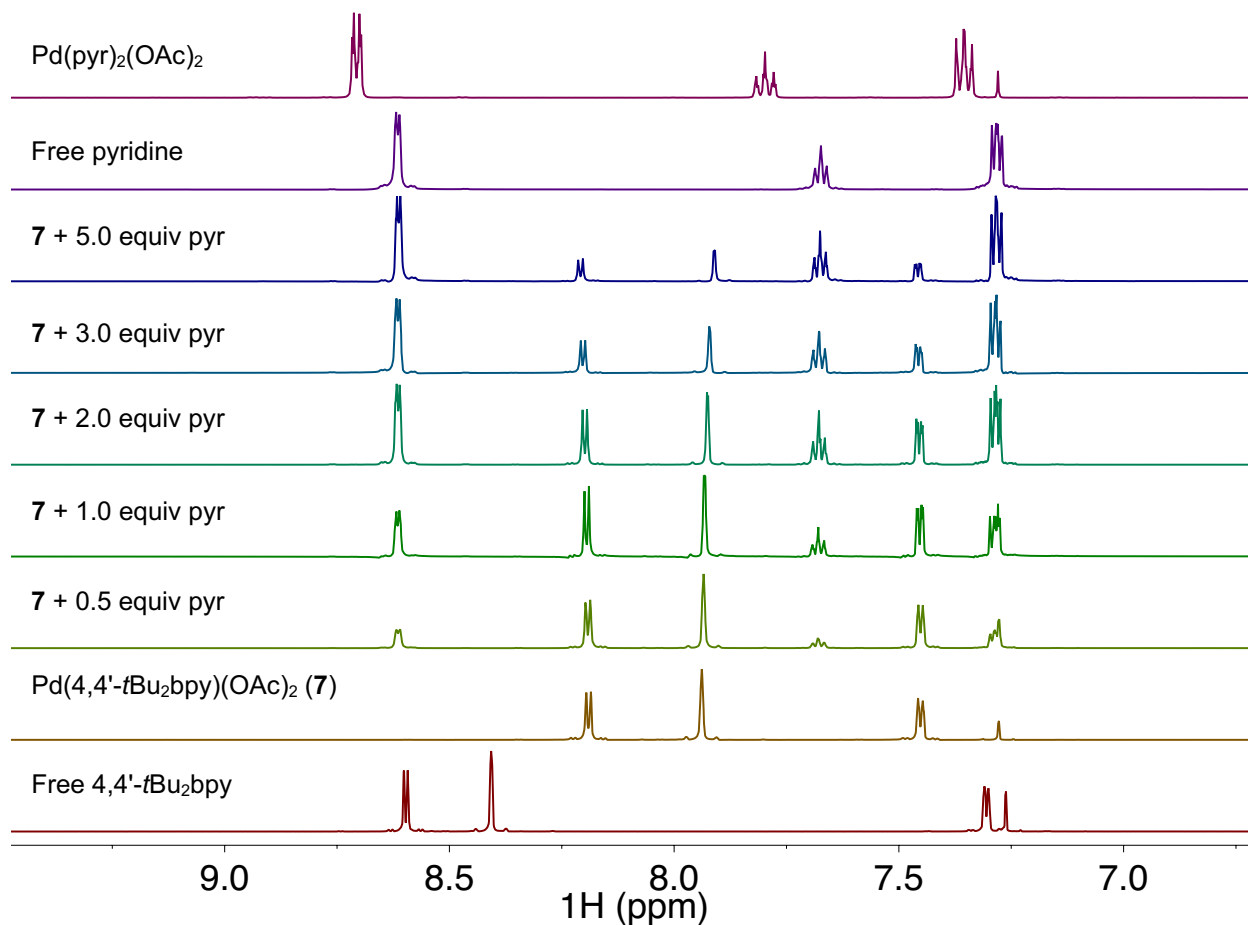
Figure A4.9. Titration of pyridine into a CDCl$_3$ solution containing Pd(κ^2-4,4'-^{t}Bu$_2$bpy)(OAc)$_2$ (**7**) and 1,3,5-trimethoxybenzene as an internal standard. **7** is resistant to ligand dissociation and shows no sign of 4,4'-^{t}Bu$_2$bpy and Pd(pyridine)$_2$(OAc)$_2$ after 5 equivalents of pyridine have been added. ns = 8, ds = 2, d1 = 15.

A4.5 Characterization of *trans*-Pd(κ^1-DAF)(pyr)(OAc)$_2$ (8) by NMR Spectroscopy.
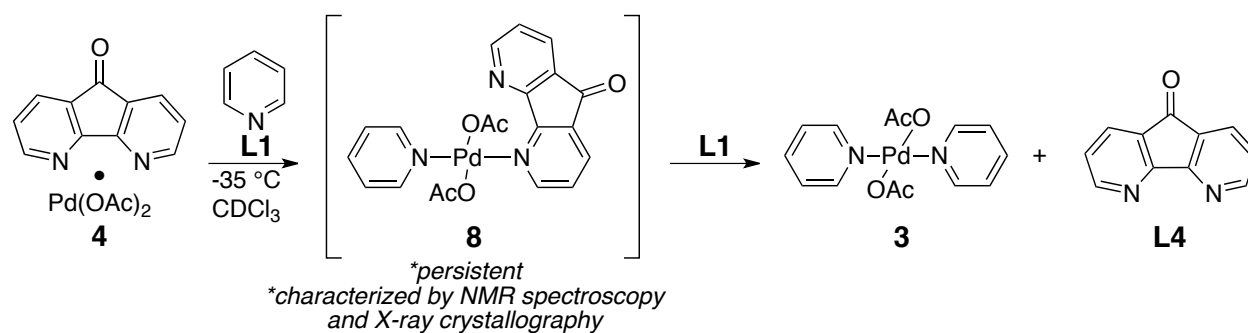
A4.5.1 ^{1}H 1D Spectrum at -35 °C
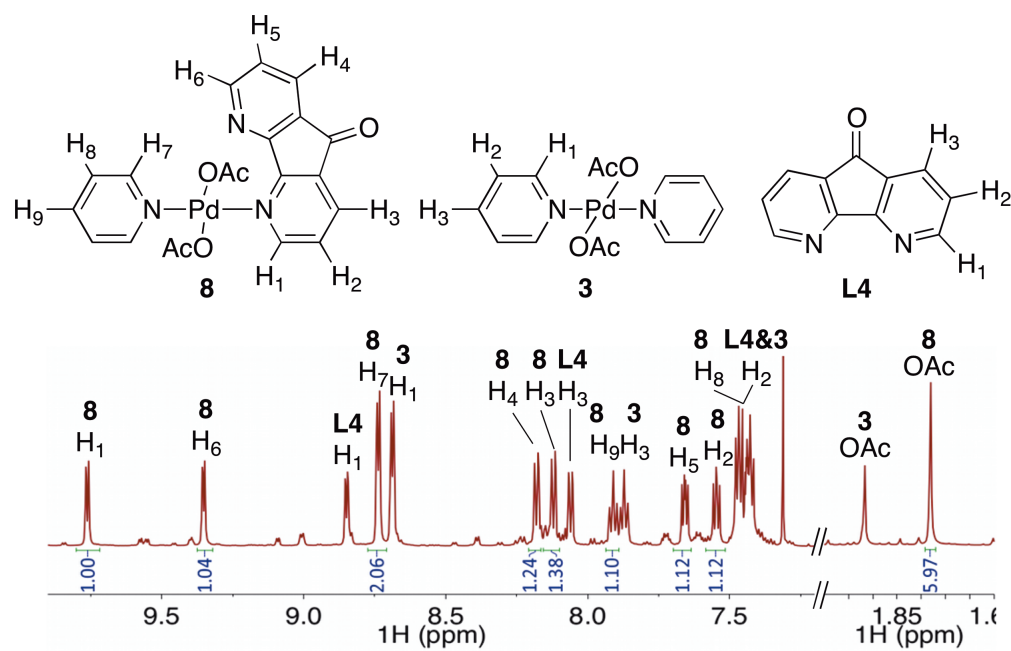
Figure A4.10. ^{1}H 1D spectrum of a 1:1:1 DAF:pyridine:Pd(OAc)$_2$ mixture in CDCl$_3$ at -35 °C. The spectrum is split between the aromatic and aliphatic region to enhance visual resolution. ns = 4, ds = 2, d1 = 7.56 s.

A4.5.2 ^{1}H 1D TOCSY Spectra at -35 °C
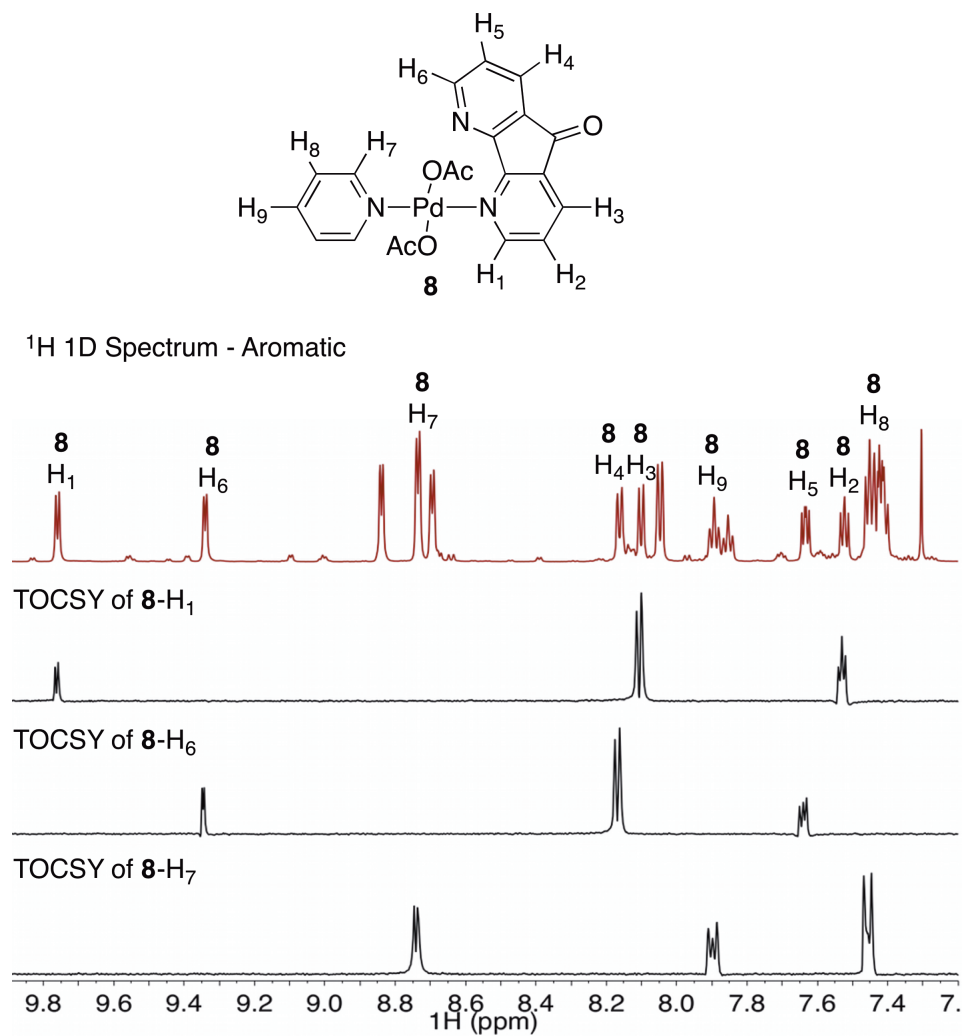
Figure A4.11. ^{1}H 1D Spectrum (top) and 1D TOCSY spectra (bottom three) of a 1:1:1 DAF:pyridine:Pd(OAc)$_2$ mixture in CDCl$_3$ at -35 °C. ^{1}H 1D: ns = 4, ds = 2, d1 = 7.56 s; ^{1}H 1D TOCSY: These are slices extracted from an array of spectra with varying mix times for each proton. ns = 16, ds = 4, d1 = 2.52 s, 8.5 kHz spinlock, mix = 30 ms.

A4.5.3 ^{1}H 1D ROESY Spectra at -45 °C
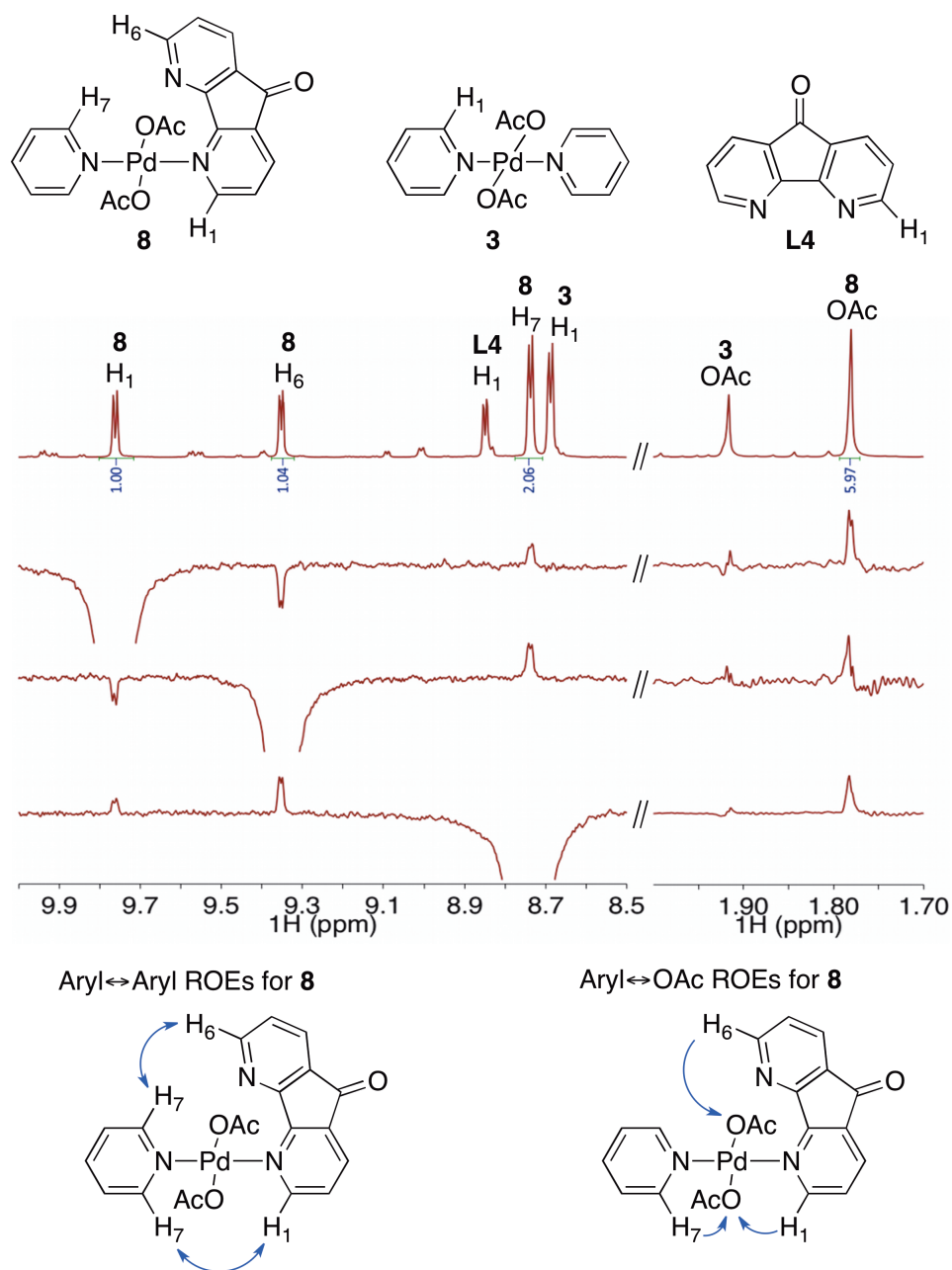
Figure A4.12. ^{1}H-^{1}H 1D ROESY Spectrum of **8-H$_1$** (top), **8-H$_6$** (middle) and **8-H$_7$** (bottom) at -45 °C. Through-space interactions between both the DAF and pyridine ligand are observed as well as to the nearby acetate. These ROEs and integration confirm a stoichiometry consistent with a Pd(κ^1-DAF)(pyr)(OAc)$_2$ complex. ns = 128-256, d1 = 5.0 s, 5.4 kHz spinlock, mix = 0.3 s.

A4.5.4 ^{1}H-^{13}C HSQC Spectrum at -35 °C
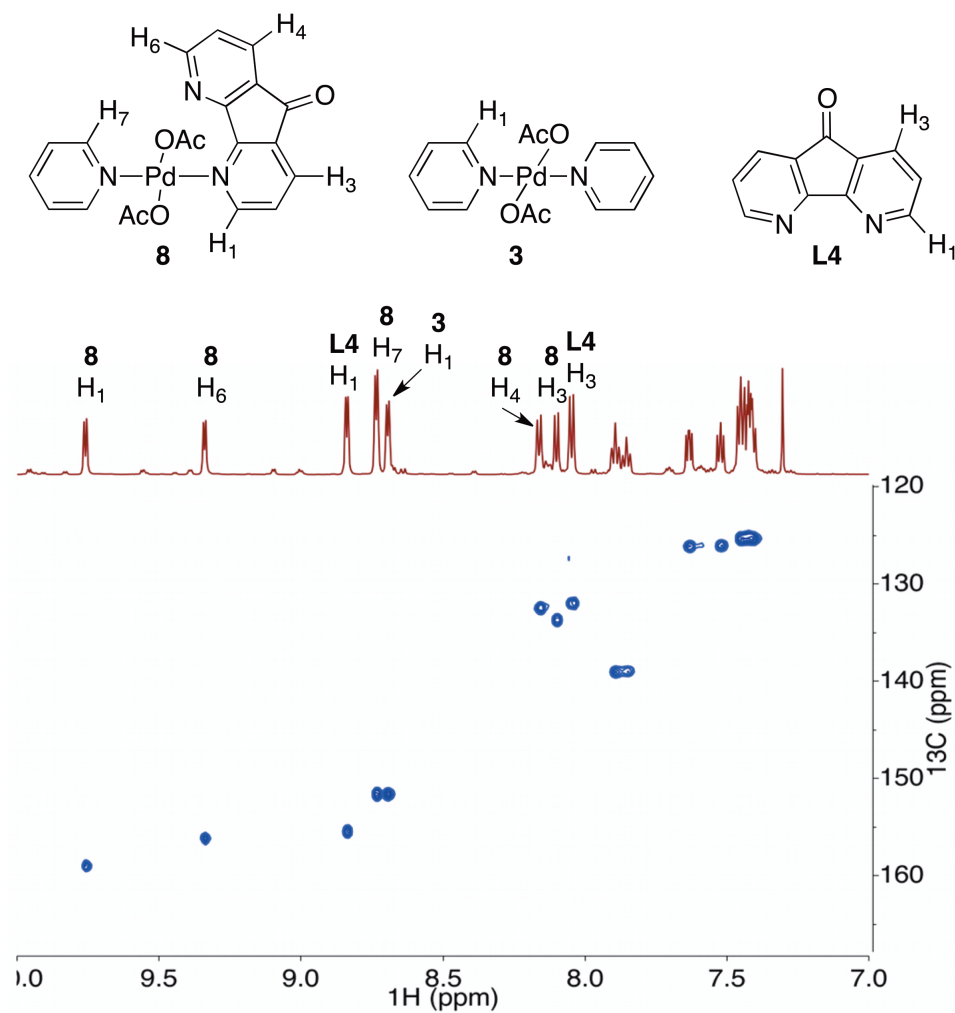
Figure A4.13. ^{1}H-^{13}C HSQC spectrum of a 1:1:1 DAF:pyridine:Pd(OAc)$_2$ mixture in CDCl$_3$ at -45 °C. ns = 8, ni = 128, d1 = 2.52 s, sw(f1) = 195 ppm, ^{1}J$_{CH}$ = 170 Hz .

A4.5.5 ^{1}H-^{13}C HMBC Spectrum at -35 °C
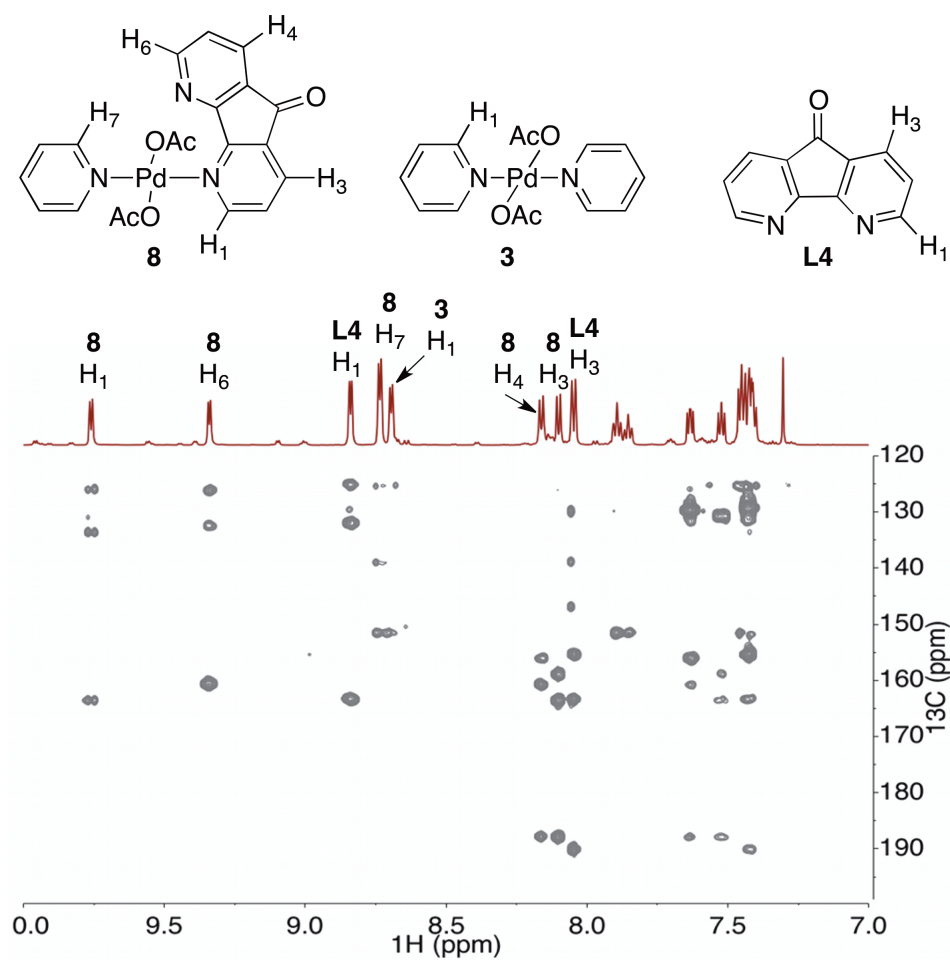
Figure A4.14. ^{1}H-^{13}C HMBC spectrum of a 1:1:1 DAF:pyridine:Pd(OAc)$_2$ mixture in CDCl$_3$ at -45 °C. ns = 8, ni = 256, d1 = 2.52 s, sw(f1) = 195 ppm, ^{n}J$_{CH}$ = 3 Hz ^{1}J$_{CH}$ = 170 Hz .

A4.5.6 Interpretation of HSQC and HMBC Spectra
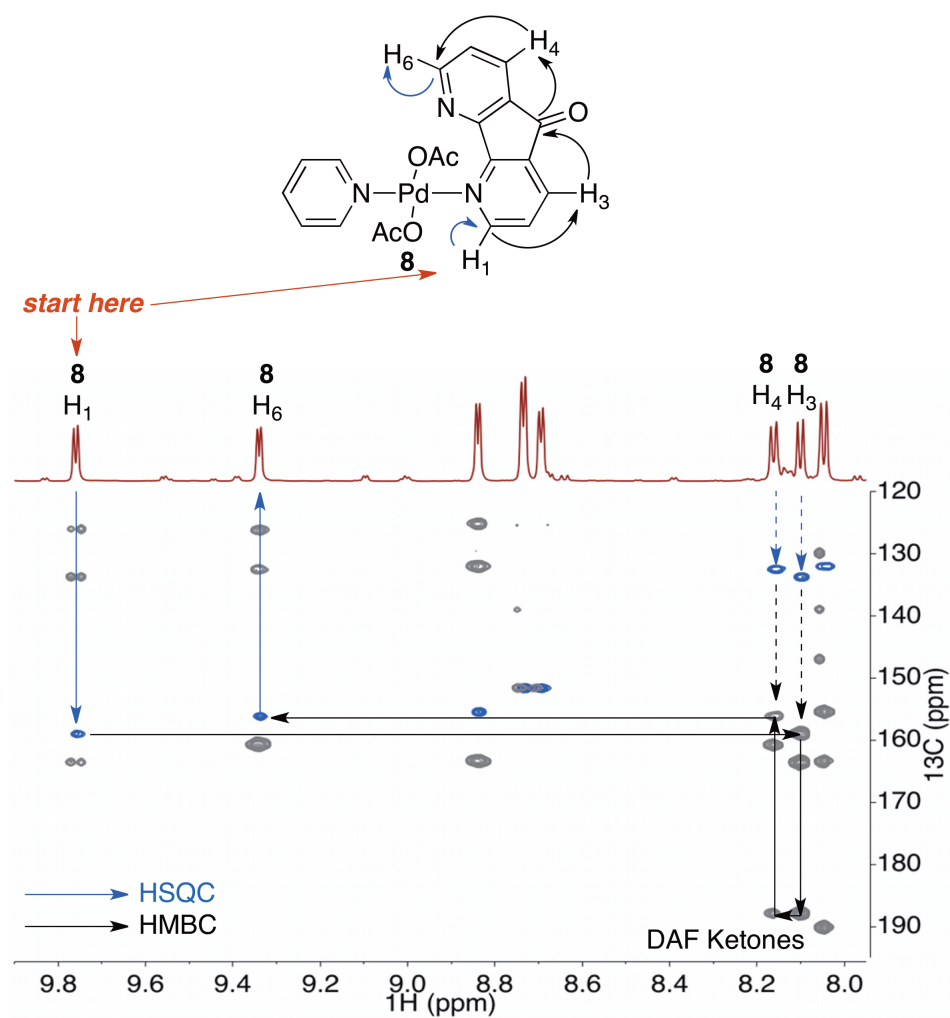
Figure A4.15. Overlay of the ^{1}H-^{13}C HSQC and HMBC spectra to facilitate interpretation. The two resonances **8**-H$_1$ and **8**-H$_6$ belong to two chemically inequivalent pyridine rings that connect to the share same DAF carbonyl. This is suggestive of a k1-DAF complex.

A4.5.7 ^{1}H-^{15}N HMBC Spectrum at -35 °C
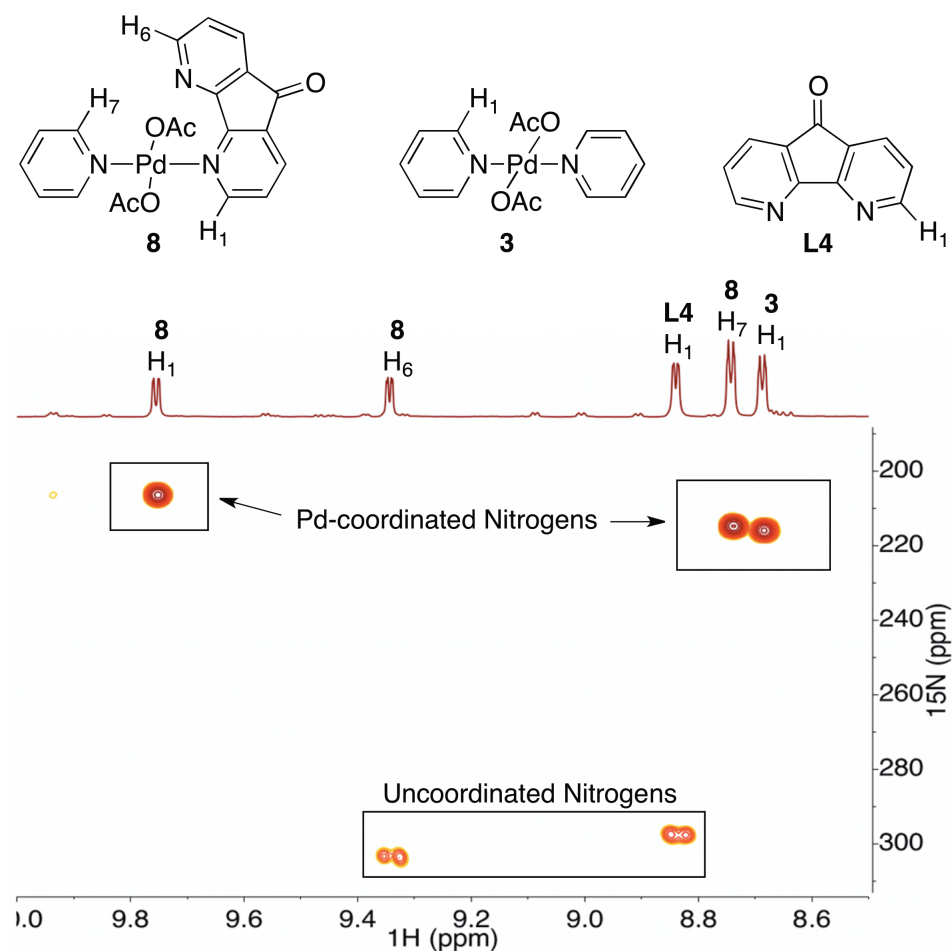
Figure A4.16. ^{1}H-^{15}N HMBC spectrum of a 1:1:1 DAF:pyridine:Pd(OAc)$_2$ mixture in CDCl$_3$ at -45 °C. The resonances near 200 ppm correspond to Pd-coordinated nitrogens while those around 300 ppm are uncoordinated nitrogens. This spectrum confirms that **8** consists of κ^1-DAF and pyridine ligand. ns = 24, ni = 256, d1 = 2.52 s, sw(f1) = 400 ppm, ^{1}J$_{NH}$ = 100 Hz and ^{n}J$_{NH}$ = 8 Hz. Cosine-squared window functions were applied in the f1 and f2 dimensions.

A4.6 Characterization of *trans*-Pd(κ^1-6,6'-Me$_2$bpy)(pyr)(OAc)$_2$ (9) by NMR Spectroscopy
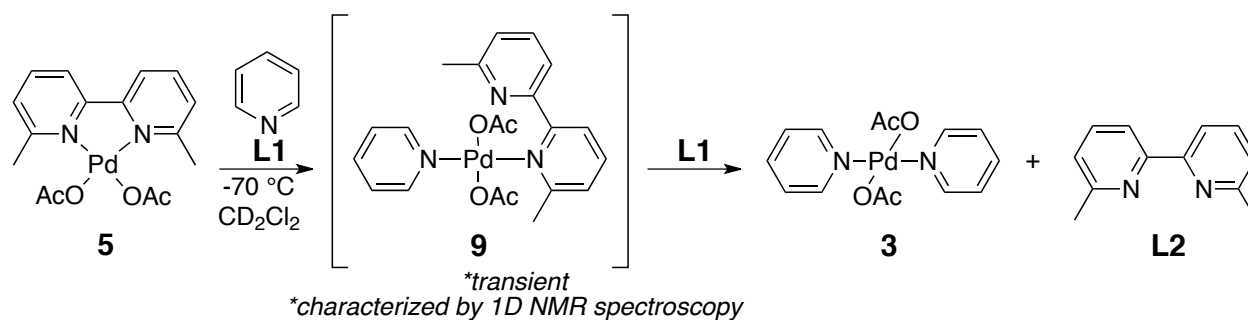
A4.6.1 ^{1}H 1D Spectrum at -70 °C
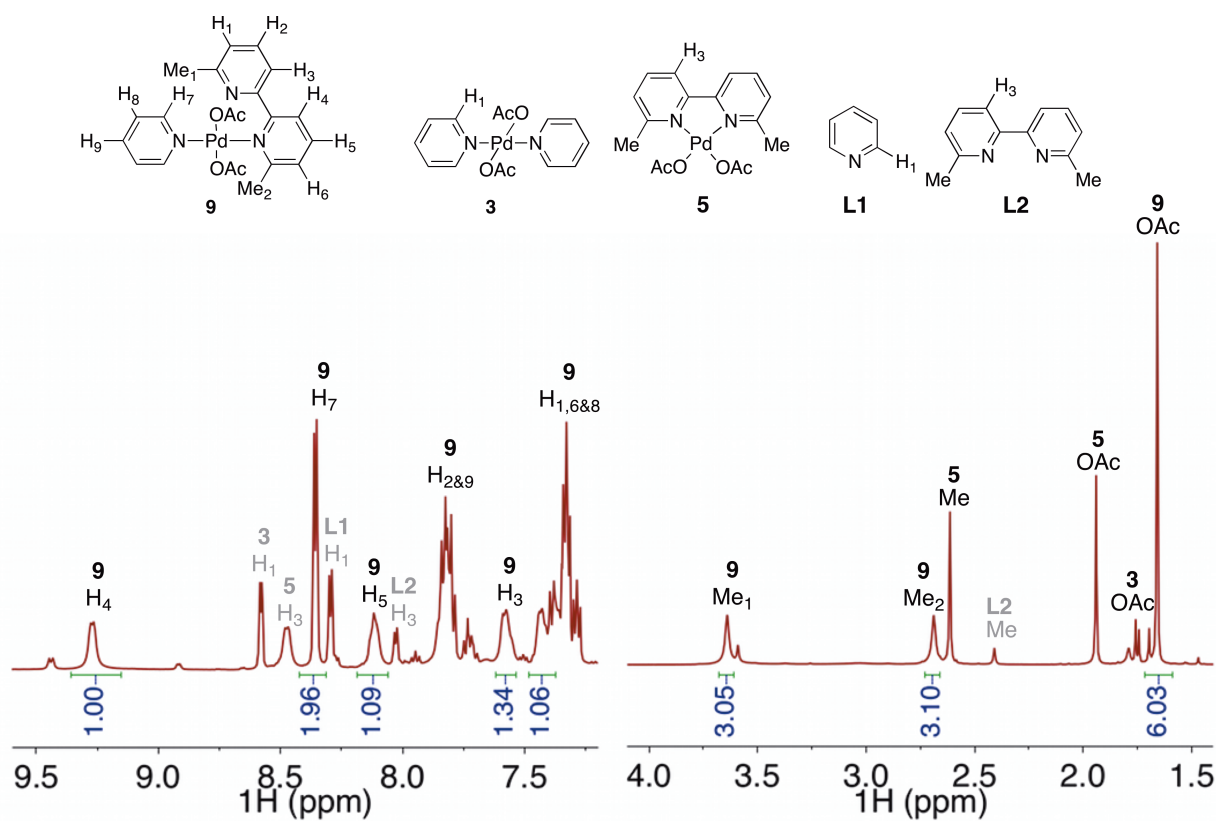
Figure A4.17. ^{1}H 1D spectrum of a 1:1 pyridine:Pd(6,6'-Me$_2$bpy)(OAc)$_2$ mixture in CD$_2$Cl$_2$ at -70 °C. An intermediate broad species, **9**, has been identified in the aromatic and aliphatic regions. ns = 8, ds = 2, d1 = 20 s.

A4.6.2 ^{1}H 1D EXSY and TOCSY Spectra at -70 °C
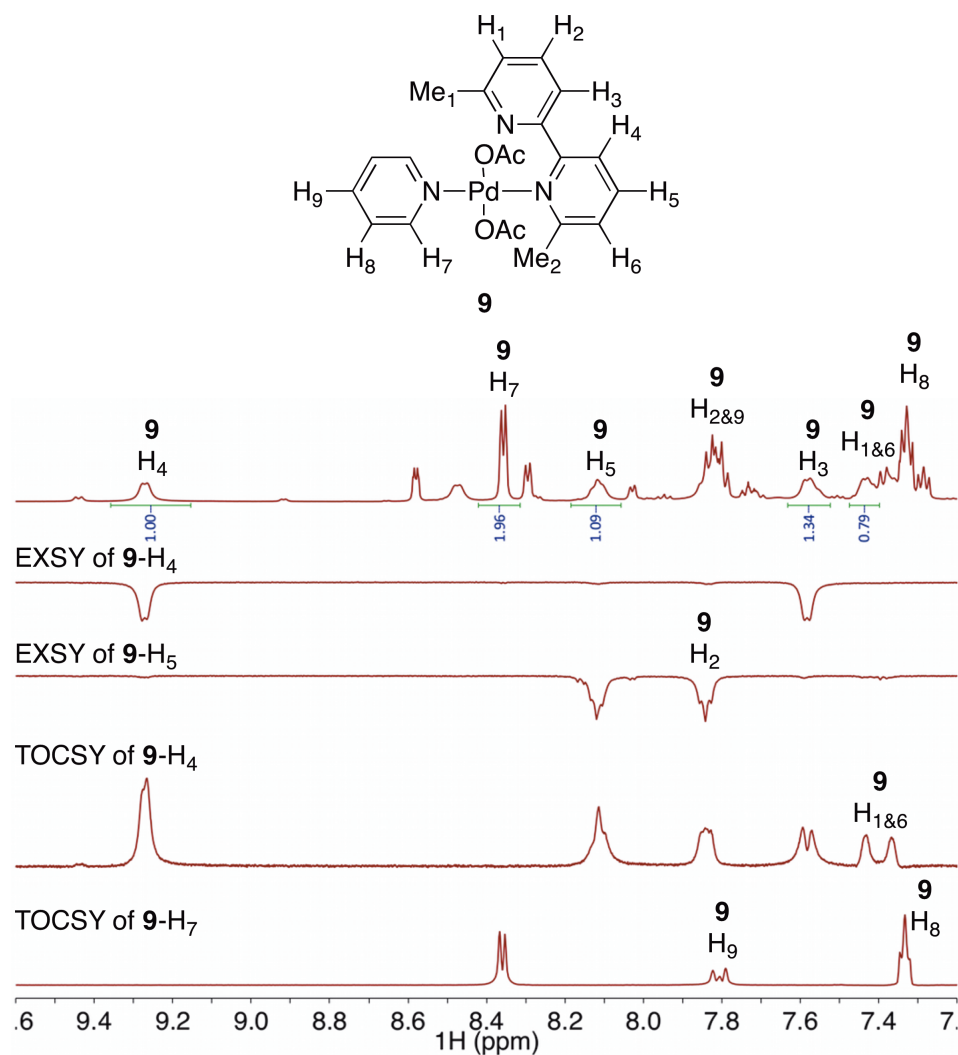
Figure A4.18. ^{1}H 1D EXSY and TOCSY spectra of a 1:1 pyridine:Pd(6,6'-Me$_2$bpy)(OAc)$_2$ mixture in CD$_2$Cl$_2$ at -70 °C. The EXSY experiments identify exchange between **9**-H$_4$ and **9**-H$_3$ as well as **9**-H$_5$ and **9**-H$_2$. The TOCSY experiment of **9**-H$_4$ reveal six resonances that are consistent with an asymmetrically coordinated 6,6'-Me$_2$bpy ligand. Furthermore, the lack of exchange within the pyridine ligand of **9** is evident from the TOCSY experiment of **9**-H$_7$. ns = 16, ds = 4, d1 = 4 s, 8.5 kHz (TOCSY) and 5.4 kHz (EXSY) spinlock, mix =0.3 s (EXSY) and 0.06 s (TOCSY).

A4.6.3 ^{1}H 1D ROESY Spectra at -70 °C
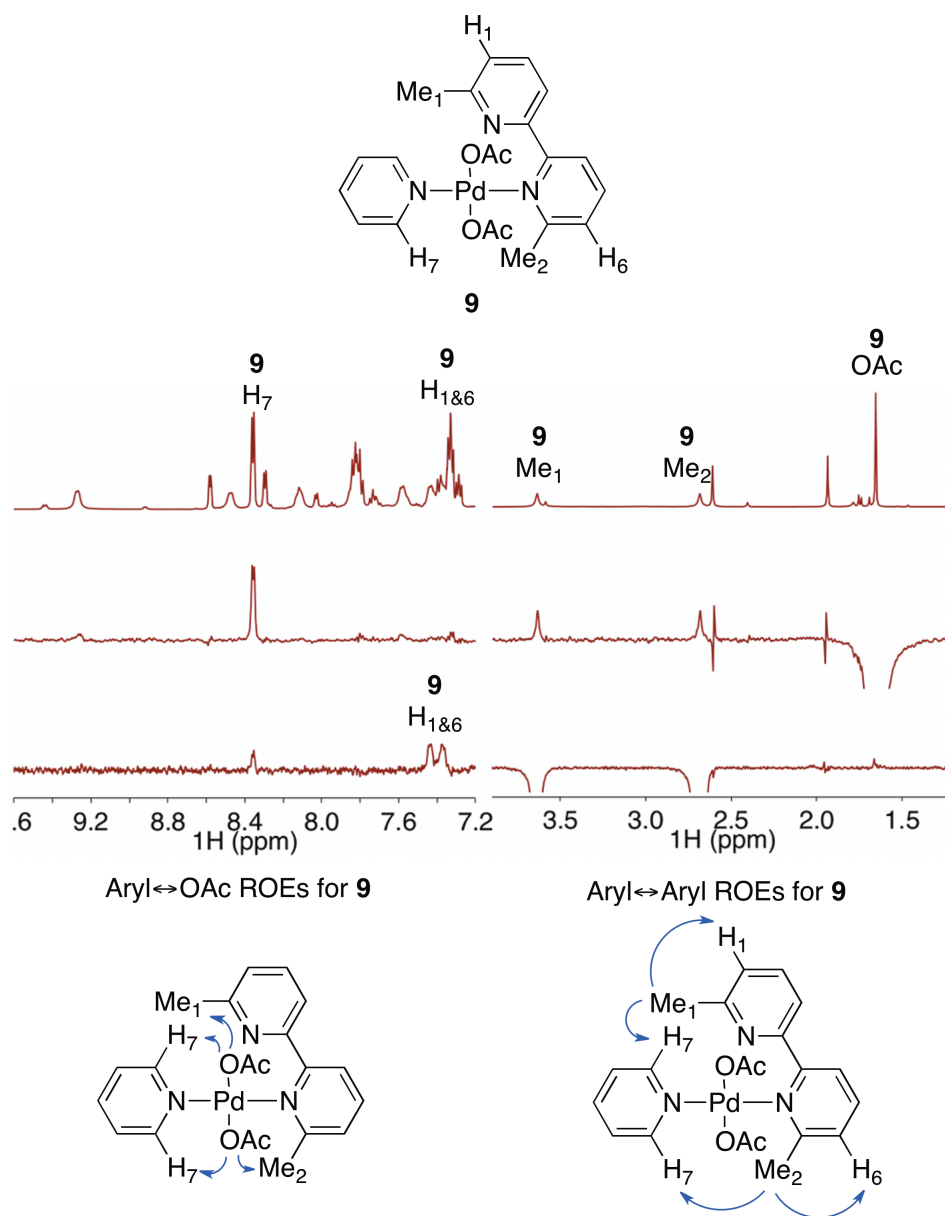
Figure A4.19. ^{1}H 1D ROESY spectra of a 1:1 pyridine:Pd(6,6'-Me$_2$bpy)(OAc)$_2$ mixture in CD$_2$Cl$_2$ at -70 °C. Through-space interactions are evident between the **9**-OAc residues and the methyl groups (**9**-Me$_1$ and **9**-Me$_2$) of the 6,6'-Me$_2$bpy ligand as well as the pyridine ligand, **9**-H$_7$ (middle). Additional through-space interactions are observed between **9**-Me$_1$ and **9**-Me$_2$ to **9**-H$_1$, **9**-H$_6$ and **9**-H$_7$. These through-space and integrations of the corresponding resonances are consistent with a Pd(κ^1-6,6'-Me$_2$bpy)(pyridine)(OAc)$_2$. ns = 256, ds = 4, d1 = 7 s, 5.4 kHz spinlock, mix = 0.6 s.

A4.6.4 Proposed Mechanism for Chemical Exchange

The ROESY, TOCSY and EXSY data suggest that the intermediate species formed upon the addition of pyridine to Pd(6,6'-Me$_2$bpy)(OAc)$_2$ is the Pd(κ^1-6,6'-Me$_2$bpy)(pyridine)(OAc)$_2$ (**9**) complex. The 6,6'-Me$_2$bpy ligand has been shown by the EXSY experiments to engage in intramolecular chemical exchange in which the two pyridyl rings interconvert with each other. Additionally, the pyridine ligand of **9** appears sharp and the TOCSY experiment reveals an absence of chemical exchange. Therefore, the pyridine ligand experiences the same chemical environment regardless of intramolecular exchange process of the 6,6'-Me$_2$bpy ligand. A possible mechanism that satisfies these observations is an intramolecular ligand substitution in which the pyridyl rings of 6,6'-Me2bpy alternate between uncoordinated and coordinated to Pd. Evidence for this mechanism of exchange has been presented previously in the context of Pd(κ^1-DAF)$_2$(OAc)$_2$ complexes interconverting between different isomers.[2]

Scheme A4.1. Proposed Mechanism for Chemical Exchange Between **9**-H$_1$ and **9**-H$_6$
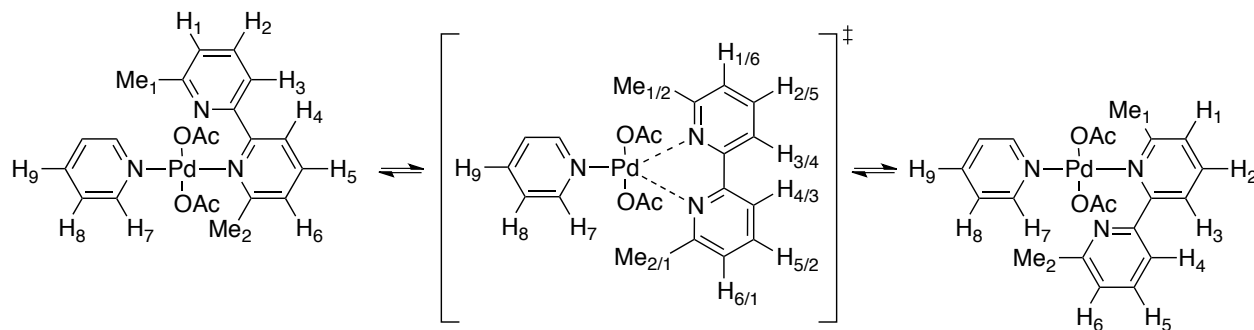
A4.7 Crystal Structure Details for Pd(6,6'-Me₂bpy)(OAc)₂ (5)
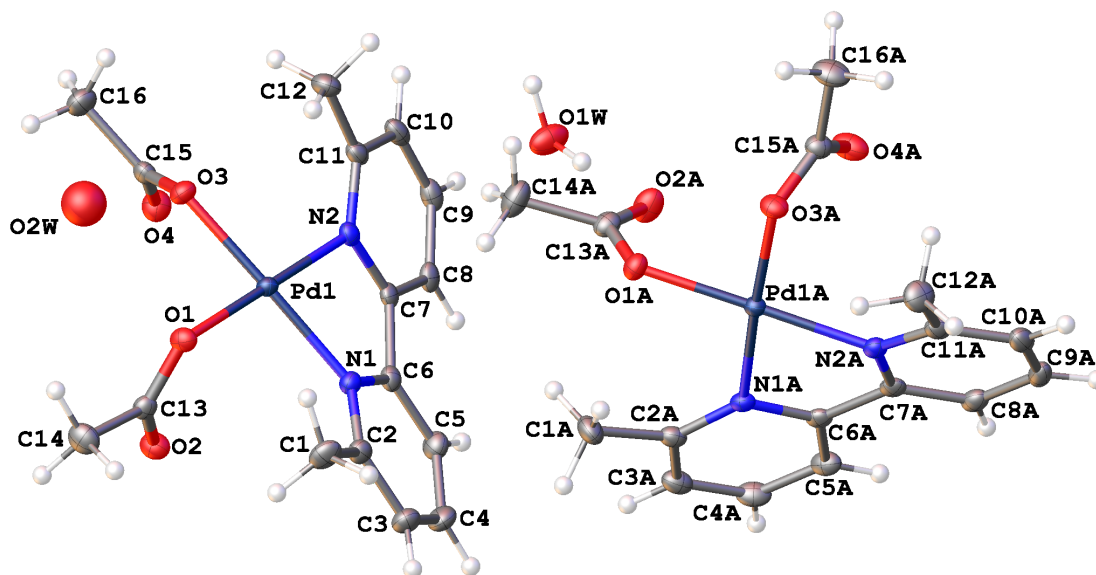
Figure A4.20. A molecular drawing of **5**. All atoms are drawn as 50% thermal probability ellipsoids. The minor component and all H atoms are omitted for clarity.

A4.7.1 Data Collection

A yellow crystal with approximate dimensions 0.513 x 0.060 x 0.054 mm³ was selected under oil under ambient conditions and attached to the tip of a MiTeGen MicroMount©. The crystal was mounted in a stream of cold nitrogen at 100(1) K and centered in the X-ray beam by using a video camera.

The crystal evaluation and data collection were performed on a Bruker SMART APEXII diffractometer with Cu K$_\alpha$ (λ = 1.54178 Å) radiation and the diffractometer to crystal distance of 4.03 cm.

The initial cell constants were obtained from three series of ω scans at different starting angles. Each series consisted of 41 frames collected at intervals of 0.6º in a 25º range about ω with the exposure time of 5 seconds per frame. The reflections were successfully indexed by an automated indexing routine built in the APEXII program. The final cell constants were calculated from a set of 9896 strong reflections from the actual data collection.

The data were collected by using the full sphere data collection routine to survey the reciprocal space to the extent of a full sphere to a resolution of 0.80 Å. A total of 50662 data were harvested by collecting 18 sets of frames with 0.7º scans in ω with an exposure time 5/10/15 sec per frame. These highly redundant datasets were corrected for Lorentz and polarization effects. The absorption correction was based on fitting a function to the empirical transmission surface as sampled by multiple equivalent measurements. [1]

A4.7.2 Structure Solution and Refinement

The systematic absences in the diffraction data were uniquely consistent for the space group $P2_1/c$ that yielded chemically reasonable and computationally stable results of refinement [2].

A successful solution by the direct methods provided most non-hydrogen atoms from the E-map. The remaining non-hydrogen atoms were located in an alternating series of least-squares cycles and difference Fourier maps. All non-hydrogen atoms were refined with anisotropic displacement coefficients. All hydrogen atoms were included in the structure factor calculation at idealized positions and were allowed to ride on the neighboring atoms with relative isotropic displacement coefficients.

There are two symmetry independent Pd complexes with very similar geometries in the asymmetric unit.

There is also one fully occupied molecule of solvent water and one ~16% occupied molecule of solvent water per two Pd complexes in the asymmetric unit. The fully occupied water molecule was refined with restraints; no H atoms were located on the partially occupied water molecule (O2w), which was refined isotropically.

The final least-squares refinement of 442 parameters against 6545 data resulted in residuals R (based on F^2 for $I{\geq}2\sigma$) and wR (based on F^2 for all data) of 0.0202 and 0.0504, respectively. The final difference Fourier map was featureless.

The molecular diagram is drawn with 50% probability ellipsoids.

A4.7.3 References

[1]   Bruker-AXS. (2007-2011) APEX2, SADABS, and SAINT Software Reference Manuals. Bruker-AXS, Madison, Wisconsin, USA.

[2]   Sheldrick, G. M. (2008) SHELXL. *Acta Cryst.* **A64**, 112-122.

[3]   Dolomanov, O.V.; Bourhis, L.J.; Gildea, R.J.; Howard, J.A.K.; Puschmann, H. "OLEX2: a complete structure solution, refinement and analysis program". *J. Appl. Cryst.* (2009) **42**, *339-341*.

[4]   Guzei, I.A. (2006-2011). Internal laboratory computer programs "G1", "ResIns", "FCF_filter", "Modicifer".

Table A4.1. Crystal data and structure refinement for **5**.

Identification code	stahl133
Empirical formula	$C_{16} H_{18} N_2 O_4$ Pd 0.58 H_2O
Formula weight	419.16
Temperature	100(1) K
Wavelength	1.54178 Å
Crystal system	Monoclinic
Space group	$P2_1/c$
Unit cell dimensions	$a = 14.136(4)$ Å $\alpha = 90°$.
	$b = 9.529(3)$ Å $\beta = 94.090(17)°$.
	$c = 25.085(8)$ Å $\gamma = 90°$.
Volume	3370.4(18) Å^3
Z	8
Density (calculated)	1.652 Mg/m^3
Absorption coefficient	9.112 mm^{-1}
F(000)	1694
Crystal size	0.51 x 0.06 x 0.05 mm^3
Theta range for data collection	3.13 to 72.43°.
Index ranges	-17<=h<=17, -9<=k<=11, -30<=l<=30
Reflections collected	50662
Independent reflections	6545 [R(int) = 0.0288]
Completeness to theta = 67.00°	99.5 %
Absorption correction	Numerical with SADABS
Max. and min. transmission	0.6389 and 0.0893
Refinement method	Full-matrix least-squares on F^2
Data / restraints / parameters	6545 / 3 / 442

Goodness-of-fit on F^2 1.024
Final R indices [I>2sigma(I)] R1 = 0.0202, wR2 = 0.0491
R indices (all data) R1 = 0.0226, wR2 = 0.0504
Largest diff. peak and hole 0.539 and -0.435 e.Å^{-3}

Table A4.2. Bond lengths [Å] and angles [°] for **5**.

Pd(1)-O(1)	2.0076(14)	C(13)-C(14)	1.509(3)
Pd(1)-O(3)	2.0092(14)	C(14)-H(14A)	0.9800
Pd(1)-N(2)	2.0215(16)	C(14)-H(14B)	0.9800
Pd(1)-N(1)	2.0300(17)	C(14)-H(14C)	0.9800
O(1)-C(13)	1.282(3)	C(15)-C(16)	1.519(3)
O(2)-C(13)	1.233(2)	C(16)-H(16A)	0.9800
O(3)-C(15)	1.291(2)	C(16)-H(16B)	0.9800
O(4)-C(15)	1.230(3)	C(16)-H(16C)	0.9800
N(1)-C(2)	1.344(3)	Pd(1A)-O(3A)	1.9977(14)
N(1)-C(6)	1.369(3)	Pd(1A)-O(1A)	2.0034(14)
N(2)-C(11)	1.345(3)	Pd(1A)-N(2A)	2.0228(17)
N(2)-C(7)	1.367(2)	Pd(1A)-N(1A)	2.0327(16)
C(1)-C(2)	1.500(3)	O(1A)-C(13A)	1.282(2)
C(1)-H(1A)	0.9800	O(2A)-C(13A)	1.236(3)
C(1)-H(1B)	0.9800	O(3A)-C(15A)	1.290(3)
C(1)-H(1C)	0.9800	O(4A)-C(15A)	1.231(2)
C(2)-C(3)	1.400(3)	N(1A)-C(2A)	1.347(3)
C(3)-C(4)	1.376(3)	N(1A)-C(6A)	1.370(2)
C(3)-H(3)	0.9500	N(2A)-C(11A)	1.350(3)
C(4)-C(5)	1.393(3)	N(2A)-C(7A)	1.363(3)
C(4)-H(4)	0.9500	C(1A)-C(2A)	1.499(3)
C(5)-C(6)	1.379(3)	C(1A)-H(1AA)	0.9800
C(5)-H(5)	0.9500	C(1A)-H(1AB)	0.9800
C(6)-C(7)	1.477(3)	C(1A)-H(1AC)	0.9800
C(7)-C(8)	1.378(3)	C(2A)-C(3A)	1.399(3)
C(8)-C(9)	1.384(3)	C(3A)-C(4A)	1.378(3)
C(8)-H(8)	0.9500	C(3A)-H(3A)	0.9500
C(9)-C(10)	1.382(3)	C(4A)-C(5A)	1.386(3)
C(9)-H(9)	0.9500	C(4A)-H(4A)	0.9500
C(10)-C(11)	1.395(3)	C(5A)-C(6A)	1.381(3)
C(10)-H(10)	0.9500	C(5A)-H(5A)	0.9500
C(11)-C(12)	1.500(3)	C(6A)-C(7A)	1.477(3)
C(12)-H(12A)	0.9800	C(7A)-C(8A)	1.386(3)
C(12)-H(12B)	0.9800	C(8A)-C(9A)	1.385(3)
C(12)-H(12C)	0.9800	C(8A)-H(8A)	0.9500

C(9A)-C(10A)	1.381(3)
C(9A)-H(9A)	0.9500
C(10A)-C(11A)	1.392(3)
C(10A)-H(10A)	0.9500
C(11A)-C(12A)	1.506(3)
C(12A)-H(12D)	0.9800
C(12A)-H(12E)	0.9800
C(12A)-H(12F)	0.9800
C(13A)-C(14A)	1.515(3)
C(14A)-H(14D)	0.9800
C(14A)-H(14E)	0.9800
C(14A)-H(14F)	0.9800
C(15A)-C(16A)	1.514(3)
C(16A)-H(16D)	0.9800
C(16A)-H(16E)	0.9800
C(16A)-H(16F)	0.9800
O(1W)-H(1WA)	0.9584(11)
O(1W)-H(1WB)	0.9583(11)

A4.8 Crystal Structure Details for Pd(κ^1-DAF)(pyridine)(OAc)$_2$ (8)
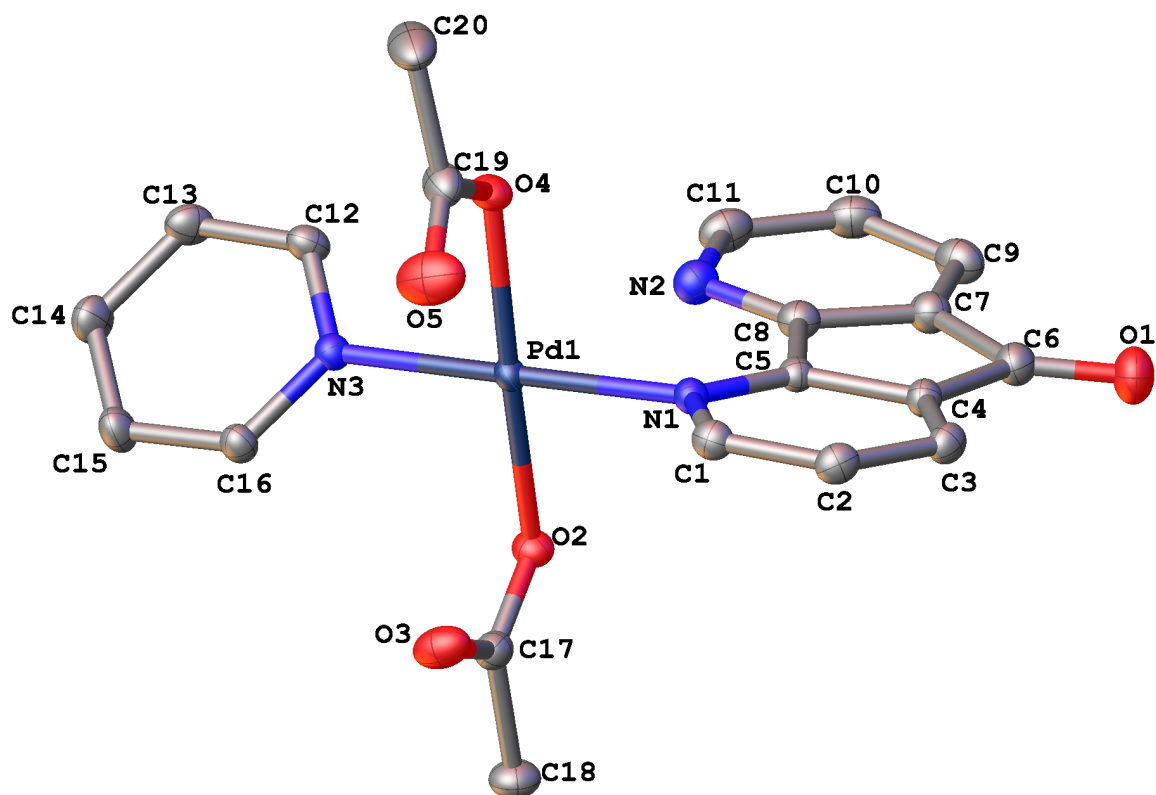
Figure A4.21. A molecular drawing of **8**. All atoms are drawn as 50% thermal probability ellipsoids. The minor component and all H atoms are omitted for clarity.

A4.8.1 Data Collection

A colorless crystal with approximate dimensions 0.258 x 0.177 x 0.046 mm^3 was selected under oil under ambient conditions and attached to the tip of a MiTeGen MicroMount©. The crystal was mounted in a stream of cold nitrogen at 100(1) K and centered in the X-ray beam by using a video camera.

The crystal evaluation and data collection were performed on a Bruker Quazar SMART APEXII diffractometer with Mo K_α ($\lambda = 0.71073$ Å) radiation and the diffractometer to crystal distance of 4.96 cm.

The initial cell constants were obtained from three series of ω scans at different starting angles. Each series consisted of 12 frames collected at intervals of 0.5º in a 6º range about ω with the exposure time of 5 seconds per frame. The reflections were successfully indexed by an automated indexing routine built in the APEXII program suite. The final cell constants were calculated from a set of 9706 strong reflections from the actual data collection.

The data were collected by using the full sphere data collection routine to survey the reciprocal space to the extent of a full sphere to a resolution of 0.70 Å. A total of 49989 data were harvested by collecting 6 sets of frames with 0.5º scans in ω and φ with exposure times of 20 sec per frame. These highly redundant datasets were corrected for Lorentz and polarization effects. The absorption correction was based on fitting a function to the empirical transmission surface as sampled by multiple equivalent measurements. [1]

A4.8.2 Structure Solution and Refinement

The systematic absences in the diffraction data were uniquely consistent for the space group $P2_1/n$ that yielded chemically reasonable and computationally stable results of refinement [2-4].

A successful solution by the direct methods provided most non-hydrogen atoms from the *E*-map. The remaining non-hydrogen atoms were located in an alternating series of least-squares cycles and difference Fourier maps. All non-hydrogen atoms were refined with anisotropic displacement coefficients. All hydrogen atoms were included in the structure factor calculation at idealized positions and were allowed to ride on the neighboring atoms with relative isotropic displacement coefficients.

There is positional disorder in the molecule in one of the acetate ligands at atoms O5 and O5A (major component = 83.6(8)%). The two atoms were constrained to have the same anisotropic displacement parameters.

The final least-squares refinement of 268 parameters against 5569 data resulted in residuals R (based on F^2 for $I \geq 2\sigma$) and wR (based on F^2 for all data) of 0.0219 and 0.0554, respectively. The final difference Fourier map was featureless.

A4.8.3 References

[1]   Bruker-AXS. (2009) APEX2, SADABS, and SAINT Software Reference Manuals. Bruker-AXS, Madison, Wisconsin, USA.

[2]   Sheldrick, G. M. (2008) SHELXL. *Acta Cryst.* **A64**, 112-122.

[3]   Dolomanov, O.V.; Bourhis, L.J.; Gildea, R.J.; Howard, J.A.K.; Puschmann, H. "OLEX2: a complete structure solution, refinement and analysis program". *J. Appl. Cryst.* (2009) **42**, *339-341*.

[4]   Guzei, I.A. (2006-2008). Internal laboratory computer programs "Inserter", "FCF_filter", "Modicifer".

Table A4.3. Crystal data and structure refinement for **8**.

Identification code	Stahl156
Empirical formula	$C_{20}H_{17}N_3O_5Pd$
Formula weight	485.76
Temperature/K	100(1)
λ/Å	0.71073
Crystal system	monoclinic
Space group	$P2_1/n$
a/Å	11.060(3)
b/Å	10.703(4)
c/Å	15.879(5)
α/°	90
β/°	102.713(11)
γ/°	90
Volume/Å^3	1833.7(10)
Z	4
ρ_{calc} mg/mm^3	1.760
μ/mm^{-1}	1.052

F(000)	976.0
Crystal size/mm^3	0.258 × 0.177 × 0.046
2Θ range for data collection	4.098 to 61.252°
Index ranges	-15 ≤ h ≤ 15, -14 ≤ k ≤ 15, -22 ≤ l ≤ 22
Reflections collected	49989
Independent reflections	5569[R(int) = 0.0264]
Data/restraints/parameters	5569/0/268
Goodness-of-fit on F^2	1.123
Final R indexes [I>=2σ (I)]	R$_1$ = 0.0219, wR$_2$ = 0.0543
Final R indexes [all data]	R$_1$ = 0.0236, wR$_2$ = 0.0554
Largest diff. peak/hole / e Å^{-3}	0.98/-0.34

Table A4.4. Bond Lengths for **8**.

Atom	Atom	Length/Å	Atom	Atom	Length/Å
Pd1	O2	2.0225(12)	C2	C3	1.394(2)
Pd1	O4	2.0176(12)	C3	C4	1.384(2)
Pd1	N1	2.0307(13)	C4	C5	1.396(2)
Pd1	N3	2.0115(14)	C4	C6	1.495(2)
O1	C6	1.207(2)	C5	C8	1.475(2)
O2	C17	1.2952(19)	C6	C7	1.496(2)
O3	C17	1.224(2)	C7	C8	1.401(2)
O4	C19	1.282(2)	C7	C9	1.388(2)
O5	C19	1.234(3)	C9	C10	1.403(3)
O5A	C19	1.241(13)	C10	C11	1.405(3)
N1	C1	1.3528(19)	C12	C13	1.382(2)
N1	C5	1.3332(18)	C13	C14	1.388(2)
N2	C8	1.325(2)	C14	C15	1.387(2)
N2	C11	1.347(2)	C15	C16	1.384(2)
N3	C12	1.3472(19)	C17	C18	1.513(2)
N3	C16	1.3434(19)	C19	C20	1.519(2)
C1	C2	1.391(2)			

Table A4.5. Bond Angles for **8**.

Atom	Atom	Atom	Angle/°	Atom	Atom	Atom	Angle/°
O2	Pd1	N1	88.73(5)	O1	C6	C7	127.46(15)
O4	Pd1	O2	174.87(4)	C4	C6	C7	104.95(13)
O4	Pd1	N1	92.12(5)	C8	C7	C6	109.19(14)
N3	Pd1	O2	90.57(5)	C9	C7	C6	131.49(15)
N3	Pd1	O4	88.44(5)	C9	C7	C8	119.31(15)
N3	Pd1	N1	178.33(5)	N2	C8	C5	126.43(14)
C17	O2	Pd1	115.93(9)	N2	C8	C7	125.71(15)
C19	O4	Pd1	116.56(10)	C7	C8	C5	107.85(13)
C1	N1	Pd1	123.47(10)	C7	C9	C10	116.57(16)
C5	N1	Pd1	119.46(10)	C9	C10	C11	118.92(16)
C5	N1	C1	116.94(12)	N2	C11	C10	124.94(16)
C8	N2	C11	114.53(14)	N3	C12	C13	121.84(14)
C12	N3	Pd1	119.21(10)	C12	C13	C14	119.07(14)
C16	N3	Pd1	121.43(10)	C15	C14	C13	118.79(15)
C16	N3	C12	119.36(13)	C16	C15	C14	119.40(15)
N1	C1	C2	122.84(14)	N3	C16	C15	121.53(14)
C1	C2	C3	120.04(14)	O2	C17	C18	114.13(13)
C4	C3	C2	116.72(14)	O3	C17	O2	124.87(14)
C3	C4	C5	120.11(13)	O3	C17	C18	120.98(15)
C3	C4	C6	131.53(14)	O4	C19	C20	114.43(16)
C5	C4	C6	108.35(13)	O5	C19	O4	124.63(16)
N1	C5	C4	123.32(13)	O5	C19	C20	120.74(17)
N1	C5	C8	127.08(13)	O5A	C19	O4	118.8(6)
C4	C5	C8	109.58(12)	O5A	C19	C20	118.6(5)
O1	C6	C4	127.59(15)				

[1]. Liu, G. S.; Stahl, S. S., *J. Am. Chem. Soc.* **2007,** *129,* 6328-6335.

[2]. Chapter 2

Appendix 5. Computational Coordinates for Ch. 2, 4 and 5

A5.1 Cartesian Coordinates for Compounds in Chapter Two

1 (D)
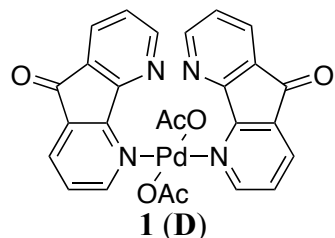
SCF Energy = -1129521.103 kcal/mol
$G_{298K,solution}$ = -1129597.829 kcal/mol
Three lowest vib. freq. (cm^{-1}): = 16.8883,
17.9130, 20.0544

N	-1.759774	2.020389	0.471802
C	-1.946669	3.267561	0.939679
C	-2.862243	1.367497	0.133186
H	-1.042499	3.800196	1.227536
C	-3.197535	3.885667	1.069810
C	-4.165894	1.898327	0.207712
C	-2.955221	-0.018231	-0.405644
H	-3.260755	4.897138	1.460024
C	-4.350259	3.187326	0.687161
C	-5.140715	0.884351	-0.299215
N	-1.975517	-0.899920	-0.623851
C	-4.305759	-0.303385	-0.677324
H	-5.341776	3.626116	0.758492
O	-6.350863	0.990770	-0.390700
C	-2.321939	-2.106470	-1.146161
C	-4.671873	-1.533796	-1.199828
C	-3.640703	-2.449264	-1.442903
H	-1.493380	-2.783672	-1.331013
H	-5.712387	-1.766673	-1.408796
H	-3.844471	-3.432379	-1.854280
Pd	-0.000941	-0.717268	-0.000907
O	-0.702861	-0.630719	1.919159
C	-0.833358	-1.740473	2.592277
O	-0.509258	-2.866750	2.193586
O	0.698925	-0.623303	-1.921291
C	0.834261	-1.731065	-2.597517
O	0.511350	-2.858969	-2.203229
C	1.471549	-1.535600	-3.970038

H	1.037660	-2.242181	-4.683271
H	1.353469	-0.509595	-4.328342
H	2.544295	-1.754700	-3.895637
C	-1.445428	-1.555910	3.977891
H	-2.395067	-2.101669	4.022858
H	-0.781875	-1.999374	4.728166
H	-1.618645	-0.503037	4.212869
N	1.973990	-0.900300	0.621107
C	2.953146	-0.017559	0.404643
C	2.321378	-2.108307	1.139531
C	2.859067	1.369807	-0.129777
C	4.304093	-0.303028	0.674038
C	3.640596	-2.451447	1.433888
H	1.493102	-2.786210	1.323409
N	1.755965	2.023389	-0.464923
C	4.162459	1.901290	-0.204214
C	5.138205	0.886131	0.298486
C	4.671196	-1.534890	1.192424
H	3.845185	-3.435735	1.842047
C	1.941886	3.272049	-0.929162
C	4.345819	3.191836	-0.679908
O	6.348447	0.992589	0.388772
H	5.712014	-1.768037	1.399582
H	1.037195	3.805309	-1.214211
C	3.192400	3.890945	-1.058997
H	5.337093	3.631201	-0.751070
H	3.254805	4.903619	-1.446206

2 (E)
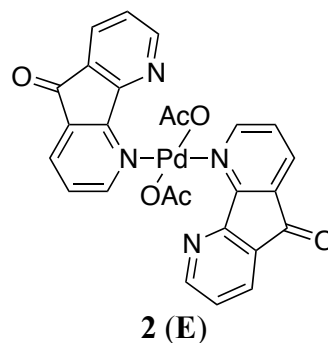
SCF Energy = -1129521.375 kcal/mol
$G_{298K,solution}$ = -1129597.678 kcal/mol

Three lowest vib. freq. (cm^{-1}): = 14.0196, 18.3965, 20.3846

N	-2.469302	1.895730	-0.055204
C	-3.067139	3.084108	-0.254852
C	-3.255372	0.833298	-0.182180
H	-2.425202	3.957328	-0.154791
C	-4.421201	3.249949	-0.572279
C	-4.631583	0.889819	-0.476560
C	-2.880637	-0.599588	-0.016527
H	-4.820839	4.248403	-0.722737
C	-5.239299	2.119541	-0.683631
C	-5.192603	-0.495111	-0.492425
N	-1.685691	-1.129000	0.253034
C	-4.031421	-1.388641	-0.181346
H	-6.297602	2.192118	-0.918926
O	-6.344598	-0.831899	-0.704211
C	-1.605625	-2.473596	0.389921
C	-3.959382	-2.767911	-0.066555
C	-2.706498	-3.314654	0.234321
H	-0.627421	-2.856541	0.650214
H	-4.841691	-3.387229	-0.202080
H	-2.571949	-4.384481	0.354971
Pd	0.042154	-0.017201	0.334577
O	-0.235257	0.373440	2.314558
C	-0.178144	-0.612371	3.174042
O	-0.007308	-1.801615	2.892707
O	0.480908	-0.251369	-1.651248
C	-0.390860	-0.205366	-2.622063
O	-1.613187	-0.073851	-2.506897
C	0.259993	-0.330090	-3.999339
H	-0.509054	-0.398126	-4.772171
H	0.889667	0.546906	-4.191758
H	0.908602	-1.212023	-4.038252
C	-0.329783	-0.149550	4.620439
H	-0.543641	-1.005157	5.265322
H	0.606974	0.315792	4.951703
H	-1.120589	0.601786	4.711328
N	1.744927	1.153930	0.424012
C	2.973200	0.762974	0.077915
C	1.566161	2.462256	0.729834
C	3.467887	-0.610282	-0.222488
C	4.049965	1.662623	-0.026071
C	2.588880	3.405441	0.658459
H	0.561589	2.731514	1.036157

N	2.781864	-1.742928	-0.150857
C	4.835232	-0.518609	-0.552172
C	5.275082	0.905497	-0.453381
C	3.871523	3.006705	0.256366
H	2.374430	4.438593	0.911614
C	3.474180	-2.857497	-0.445913
C	5.541315	-1.673475	-0.860618
O	6.383063	1.365897	-0.662885
H	4.695261	3.710621	0.176649
H	2.914618	-3.788320	-0.383430
C	4.827802	-2.876901	-0.809758
H	6.595852	-1.637435	-1.119924
H	5.310344	-3.822886	-1.036381

3 (C)
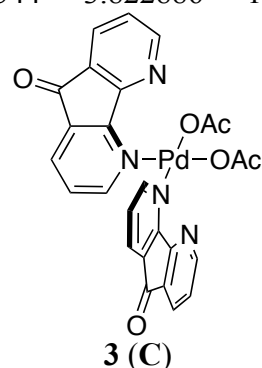
SCF Energy = -1129518.962 kcal/mol
G$_{298K,solution}$ = -1129596.284 kcal/mol
Three lowest vib. freq. (cm^{-1}): = 16.9288, 23.7605, 24.4324

N	-2.542346	-1.726233	-0.051518
C	-3.367739	-2.782705	0.077602
C	-3.049216	-0.674970	-0.681343
H	-2.953314	-3.636643	0.608902
C	-4.676138	-2.821737	-0.422050
C	-4.338960	-0.619128	-1.244100
C	-2.371824	0.625638	-0.933570
H	-5.281468	-3.710814	-0.273325
C	-5.181911	-1.714412	-1.117095
C	-4.520478	0.704135	-1.920822
N	-1.164487	1.025415	-0.523551
C	-3.233974	1.440901	-1.687928
H	-6.184264	-1.706459	-1.536522
O	-5.495978	1.102595	-2.531658
C	-0.768988	2.272846	-0.884513
C	-2.835557	2.714798	-2.063778

C	-1.561109	3.124899	-1.654757
H	0.201966	2.572179	-0.513272
H	-3.490832	3.359953	-2.642454
H	-1.182475	4.111416	-1.900963
Pd	0.000005	0.000037	0.883188
O	-1.150134	0.803972	2.345805
C	-1.072355	2.082558	2.595804
O	-0.455472	2.918225	1.923349
C	-1.827660	2.487433	3.858169
H	-2.090357	3.547643	3.814466
H	-2.722787	1.874952	4.000314
H	-1.173200	2.326852	4.723940
N	1.164470	-1.025438	-0.523496
C	2.371808	-0.625694	-0.933547
C	0.768957	-2.272885	-0.884388
C	3.049210	0.674926	-0.681408
C	3.233945	-1.441008	-1.687861
C	1.561067	-3.124990	-1.654586
H	-0.202000	-2.572185	-0.513124
N	2.542350	1.726232	-0.051649
C	4.338960	0.619031	-1.244147
C	4.520464	-0.704276	-1.920786
C	2.835517	-2.714924	-2.063635
H	1.182422	-4.111518	-1.900732
C	3.367760	2.782696	0.077428
C	5.181921	1.714315	-1.117205
O	5.495954	-1.102780	-2.531609
H	3.490784	-3.360118	-2.642276
H	2.953328	3.636685	0.608641
C	4.676155	2.821689	-0.422234
H	6.184274	1.706328	-1.536630
H	5.281490	3.710775	-0.273574
O	1.150160	-0.803823	2.345824
C	1.072376	-2.082393	2.595908
O	0.455463	-2.918096	1.923525
C	1.827728	-2.487191	3.858268
H	2.090300	-3.547437	3.814687
H	2.722939	-1.874797	4.000253
H	1.173359	-2.326412	4.724071
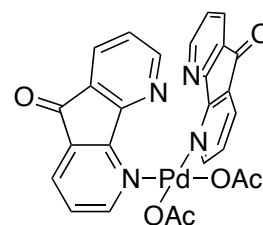
4 (unobserved)

SCF Energy = -1129513.314 kcal/mol
$G_{298K,solution}$ = -1129591.807 kcal/mol
Three lowest vib. freq. (cm^{-1}): = 15.4620, 18.9380, 24.0526

N	1.968901	0.404858	-1.726005
C	2.645607	0.740637	-2.837804
C	2.460615	0.878946	-0.589178
H	2.246040	0.340796	-3.767484
C	3.793552	1.546431	-2.853184
C	3.599608	1.704282	-0.492917
C	1.940687	0.645773	0.789469
H	4.283508	1.767708	-3.796781
C	4.290312	2.053220	-1.646123
C	3.840042	2.051690	0.940252
N	0.905309	-0.101117	1.182650
C	2.760225	1.340032	1.699524
H	5.173760	2.684568	-1.604009
O	4.716790	2.761355	1.401559
C	0.675839	-0.190888	2.515492
C	2.513713	1.274460	3.060805
C	1.433217	0.482760	3.469839
H	-0.133902	-0.847102	2.808253
H	3.142836	1.803980	3.770825
H	1.189010	0.359598	4.519700
Pd	-0.184686	-1.300589	-0.113047
O	1.489792	-2.391013	-0.444226
C	2.022919	-3.012966	0.577614
O	1.705402	-2.868735	1.762275
C	3.116439	-3.993626	0.165091
H	3.815322	-4.142263	0.992514
H	2.647718	-4.957842	-0.067454
H	3.644965	-3.652954	-0.729845
N	-2.073397	-0.433667	0.355231
C	-2.549399	0.806555	0.187942
C	-2.927078	-1.351534	0.892106
C	-1.868911	2.013279	-0.369257

C	-3.869273	1.166652	0.526224
C	-4.237338	-1.053861	1.264190
H	-2.530619	-2.361257	0.976885
N	-0.611223	2.110455	-0.778684
C	-2.795649	3.075974	-0.388336
C	-4.094840	2.606581	0.179857
C	-4.738386	0.238662	1.076040
H	-4.851978	-1.844653	1.681714
C	-0.245341	3.314198	-1.259449
C	-2.410328	4.314547	-0.879243
O	-5.118361	3.248722	0.333783
H	-5.757058	0.511410	1.337688
H	0.784340	3.389219	-1.602773
C	-1.090466	4.427364	-1.334922
H	-3.104624	5.149919	-0.905981
H	-0.715027	5.362985	-1.738161
O	-1.101605	-2.442564	-1.512768
C	-1.606702	-3.605802	-1.203626
O	-1.802195	-4.025329	-0.055910
C	-1.949494	-4.451370	-2.424759
H	-2.671108	-5.226418	-2.154903
H	-2.337806	-3.831371	-3.238548
H	-1.032974	-4.934434	-2.785391

TS$_{D \to E}$
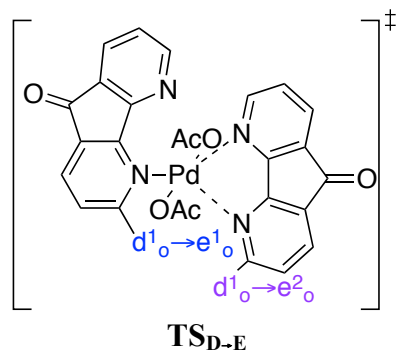
SCF Energy = -1129510.257 kcal/mol
G$_{298K,solution}$ = -1129587.056 kcal/mol
Three lowest vib. freq. (cm^{-1}): = -106.6246, 9.6790, 14.8124

N	-2.230020	2.065779	-0.223914
C	-2.647592	3.344892	-0.167624
C	-3.184189	1.149426	-0.110719
H	-1.868717	4.099733	-0.256700
C	-3.980171	3.741077	-0.006096
C	-4.555252	1.440834	0.042440

C	-3.028672	-0.335216	-0.141450
H	-4.227539	4.797727	0.031777
C	-4.975376	2.760855	0.099361
C	-5.329847	0.162151	0.101996
N	-1.913290	-1.057259	-0.263522
C	-4.304286	-0.919756	-0.027614
H	-6.025640	3.012883	0.218061
O	-6.534851	0.028938	0.226058
C	-2.042937	-2.408272	-0.293408
C	-4.446456	-2.299066	-0.047968
C	-3.276667	-3.052409	-0.192659
H	-1.119401	-2.958054	-0.422136
H	-5.425156	-2.762355	0.041985
H	-3.303890	-4.136700	-0.220964
Pd	0.057356	-0.288912	-0.136234
O	-0.229246	0.077354	1.827558
C	-0.285535	-0.946924	2.639711
O	-0.210792	-2.133526	2.304189
O	0.372780	-0.461205	-2.125104
C	0.542947	-1.646824	-2.644480
O	0.501819	-2.717066	-2.024791
C	0.777897	-1.621779	-4.151311
H	-0.179146	-1.789996	-4.661110
H	1.177248	-0.659564	-4.482982
H	1.454070	-2.434172	-4.432393
C	-0.491550	-0.551657	4.098970
H	-1.557367	-0.642257	4.343849
H	0.057899	-1.240855	4.746739
H	-0.180944	0.479247	4.288436
N	2.336478	-1.169836	0.348350
C	3.238457	-0.209272	0.262775
C	2.812749	-2.397450	0.632177
C	2.915842	1.190493	-0.035655
C	4.622101	-0.345404	0.433128
C	4.179169	-2.651000	0.823533
H	2.071057	-3.185683	0.707543
N	1.690534	1.641026	-0.248051
C	4.097370	1.943634	-0.057682
C	5.251508	1.011787	0.240541
C	5.118707	-1.610826	0.723889
H	4.500816	-3.663039	1.049092
C	1.599373	2.957701	-0.514936
C	4.002466	3.301390	-0.330315
O	6.431249	1.301492	0.308356
H	6.181005	-1.788977	0.867311

```
H    0.596656    3.333465    -0.697252
C    2.711865    3.808338    -0.564124
H    4.880043    3.941312    -0.363204
H    2.565512    4.861051    -0.78635
```

A5.2 Cartesian Coordinates for Compounds in Chapter Four

A5.2.1 Comparison of Coordination Strengths of Various Ligands

Pd(k²-OAc)₂

SCF Energy = -367052.6214 kcal/mol

$G_{298K,solution}$ = -367098.7392 kcal/mol

Three lowest vib. freq. (cm^{-1}): 35.9500, 36.7803, 57.2856

Pd	-0.000036	-0.000550	0.000219
O	1.765734	-1.088611	-0.031898
C	2.442257	-0.001290	-0.036449
O	1.766883	1.086764	-0.032520
O	-1.766991	1.086336	0.032693
C	-2.442311	-0.001745	0.036866
O	-1.765767	-1.089078	0.032499
C	-3.938314	-0.002722	0.018548
H	-4.322689	0.902841	0.494713
H	-4.281666	-0.017997	-1.023221
H	-4.321580	-0.895503	0.519348
C	3.938286	-0.001419	-0.018522
H	4.321972	0.870112	-0.555472
H	4.282094	0.058263	1.021476
H	4.321845	-0.925647	-0.457733

pyr (L1)

SCF Energy = -155807.9749 kcal/mol

$G_{298K,solution}$ = -155809.7946 kcal/mol

Three lowest vib. freq. (cm^{-1}): 383.8283, 418.8754, 613.5143

C	-1.001686	-1.214441	0.000225
C	0.396110	-1.219177	0.000127
C	1.065062	0.006053	-0.000084
C	0.308618	1.179275	-0.000208
C	-1.085116	1.072689	-0.000121
N	-1.740913	-0.096325	0.000107
H	2.151509	0.045664	-0.000157
H	-1.556401	-2.151141	0.000381
H	0.940094	-2.159629	0.000238

H	0.782591	2.156886	-0.000352
H	-1.706618	1.966471	-0.000179
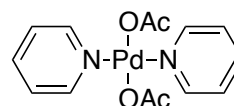
trans-Pd(pyr)₂(OAc)₂ (3)

SCF Energy = -155807.9749 kcal/mol

$G_{298K,solution}$ = -155809.7946 kcal/mol

Three lowest vib. freq. (cm^{-1}): 30.3903, 32.3537, 40.5628

Pd	-1.372657	0.387046	0.000113
N	-3.430286	0.383933	0.003731
C	-4.107606	0.170680	-1.141543
C	-4.104357	0.595114	1.151293
C	-5.500257	0.166224	-1.175372
H	-3.502761	0.001277	-2.026894
C	-5.496895	0.595298	1.189860
H	-3.497028	0.766379	2.034582
C	-6.208450	0.379671	0.008451
H	-6.010125	-0.004030	-2.118319
H	-6.004072	0.763998	2.134536
H	-7.295118	0.378003	0.010297
N	0.685250	0.390164	-0.003542
C	1.362739	0.592469	1.143700
C	1.359201	0.190036	-1.153250
C	2.755433	0.596630	1.177301
H	0.757779	0.754194	2.030511
C	2.751769	0.190369	-1.191928
H	0.751541	0.026350	-2.037853
C	3.463508	0.394649	-0.008607
H	3.265411	0.757823	2.121789
H	3.258820	0.030816	-2.138268
H	4.550180	0.396410	-0.010589
O	-1.373050	-1.556539	-0.639415
C	-1.365081	-1.794983	-1.920241
O	-1.363091	-0.927153	-2.806242
O	-1.376480	2.330620	0.639661
C	-1.364792	2.569095	1.920454

O	-1.357042	1.701291	2.806443
C	-1.342862	4.055107	2.259889
H	-1.520963	4.200253	3.327857
H	-0.363308	4.474197	1.999239
H	-2.092342	4.596316	1.673310
C	-1.339907	-3.280924	-2.259745
H	-1.520164	-3.426569	-3.327280
H	-0.358667	-3.697424	-2.001320
H	-2.086599	-3.824101	-1.671417

Pd(6,6'-Me₂bpy)₂(OAc)₂ (4)

SCF Energy = -727278.6949 kcal/mol

G$_{298K,solution}$ = -727299.7382 kcal/mol

Three lowest vib. freq. (cm^{-1}): 25.7471, 41.4355, 43.4250

6,6'-Me₂bpy (L2)

SCF Energy = -360220.8737 kcal/mol

G$_{298K,solution}$ = -360199.5691 kcal/mol

Three lowest vib. freq. (cm^{-1}): 34.1430, 64.7331, 65.9393

C	-3.446390	1.790075	0.302832
C	-2.848171	2.908266	-0.279795
C	-1.473926	2.908687	-0.499251
C	-0.738947	1.773952	-0.122144
N	-1.316701	0.697740	0.438937
C	-2.641252	0.696196	0.650964
C	0.738461	1.713861	-0.331693
N	1.316211	2.790062	-0.892802
C	2.640758	2.791598	-1.104847
C	3.445893	1.697709	-0.756737
C	2.847680	0.579533	-0.174078
C	1.473441	0.579129	0.045418
H	0.961634	-0.263683	0.494309
H	4.516509	1.726288	-0.940068
H	-0.962117	3.751503	-0.948132
H	-4.517015	1.761471	0.486105
H	-3.449258	3.770224	-0.559434
H	3.448762	-0.282436	0.105538
C	-3.219033	-0.546171	1.284608
H	-3.010655	-1.424804	0.662805
H	-2.757666	-0.726465	2.262731
H	-4.302198	-0.465120	1.420556
C	3.218570	4.034047	-1.738302
H	2.755496	4.215834	-2.715324
H	3.012289	4.912249	-1.115166
H	4.301402	3.952082	-1.876342

neocuproine (L3)

SCF Energy = -408052.7486 kcal/mol

G$_{298K,solution}$ = -408034.1533 kcal/mol

Three lowest vib. freq. (cm^{-1}): 45.6921, 45.9024, 68.8501

N	2.038456	1.522386	-0.820559
C	3.107580	0.779457	-0.446276
C	2.082599	2.840938	-0.687790
C	4.290486	1.363639	0.090067
C	3.047124	-0.670148	-0.597118
C	3.219161	3.511875	-0.162921
C	0.866703	3.625202	-1.118627
C	4.314507	2.772171	0.222392
N	1.923677	-1.229644	-1.106890
C	4.173277	-1.447496	-0.202496
H	3.215332	4.595119	-0.070330
H	0.101206	2.942284	-1.493843
H	0.448973	4.199456	-0.281297
H	1.118805	4.343522	-1.909718
H	5.200738	3.256060	0.628228
C	1.857933	-2.546395	-1.248377
C	4.080074	-2.850233	-0.362741
C	2.930848	-3.402160	-0.882433
C	0.585313	-3.122486	-1.820782
H	4.919929	-3.478530	-0.072669
H	2.837026	-4.477232	-1.014441
H	0.115323	-3.821371	-1.116475
H	-0.118634	-2.316458	-2.039690
H	0.783995	-3.679835	-2.745589
C	5.399834	0.540320	0.473821
H	6.288302	1.019024	0.880128
C	5.343332	-0.814861	0.332776

H   6.185847   -1.438371   0.624364
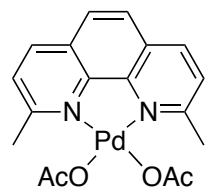
Pd(neocuproine)₂(OAc)₂ (6)

SCF Energy = -775117.179 kcal/mol

$G_{298K,solution}$ = -775139.98 kcal/mol

Three lowest vib. freq. (cm^{-1}): 24.0990, 30.7046, 39.5477

Pd	0.521719	0.091336	0.096288
N	-1.393998	0.869834	0.429218
C	-2.333147	-0.014051	-0.033949
C	-1.772716	2.090226	0.821065
C	-3.688149	0.339406	-0.223708
C	-1.914171	-1.369130	-0.260335
C	-3.120096	2.507112	0.654250
C	-0.796935	3.026593	1.472076
C	-4.059414	1.662273	0.113412
N	-0.604976	-1.682744	0.003287
C	-2.864255	-2.331565	-0.674514
H	-3.388533	3.513096	0.961780
H	0.109733	2.512963	1.788744
H	-0.508567	3.819121	0.771499
H	-1.274731	3.504548	2.335419
H	-5.086902	1.987734	-0.029049
C	-0.209083	-2.961659	-0.047211
C	-2.415326	-3.667010	-0.791613
C	-1.116670	-3.973466	-0.457922
C	1.188174	-3.335164	0.346245
H	-3.105265	-4.441937	-1.116553
H	-0.760106	-4.997646	-0.501269
H	1.874348	-3.181057	-0.493773
H	1.546445	-2.714000	1.170959
H	1.223762	-4.389778	0.636856
O	1.533489	1.840925	-0.009612
C	1.264873	2.619252	-1.027391
O	0.305422	2.497102	-1.794157
C	2.286432	3.739546	-1.197961
H	3.142504	3.347622	-1.761035
H	1.847467	4.564301	-1.765422
H	2.660341	4.091546	-0.231812
O	2.297812	-0.685886	-0.484788
C	3.215108	-0.785297	0.446565

O	3.001879	-0.751948	1.660276
C	4.621061	-0.959993	-0.115929
H	5.038077	0.033981	-0.320263
H	5.259515	-1.458910	0.617771
H	4.611401	-1.515284	-1.058779
C	-4.614863	-0.641990	-0.705899
H	-5.645801	-0.343604	-0.876965
C	-4.217652	-1.929842	-0.923437
H	-4.925830	-2.677449	-1.270950
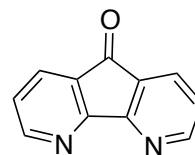
DAF (L4)

SCF Energy = -381229.0644 kcal/mol

$G_{298K,solution}$ = -381251.33 kcal/mol

Three lowest vib. freq. (cm^{-1}): 98.3572, 131.0681, 151.2322

N	-3.892371	-0.301418	-0.003418
C	-5.211401	-0.026485	-0.003193
C	-3.090539	0.758064	-0.003752
H	-5.870609	-0.892261	-0.002896
C	-5.754098	1.264288	-0.003333
C	-3.532651	2.096815	-0.003995
C	-1.597815	0.758112	-0.003689
H	-6.832117	1.395303	-0.003003
C	-4.892449	2.369247	-0.003736
C	-2.344120	3.008915	-0.003593
N	-0.795981	-0.301365	-0.003945
C	-1.155661	2.097022	-0.003317
H	-5.263694	3.390669	-0.003958
O	-2.344439	4.227956	-0.003689
C	0.522965	-0.026463	-0.003806
C	0.204177	2.369242	-0.003128
C	1.065716	1.264300	-0.003273
H	1.182097	-0.892265	-0.003847
H	0.575593	3.390614	-0.002779
H	2.143735	1.395411	-0.002890
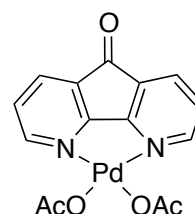
Pd(DAF)₂(OAc)₂ (5)

SCF Energy = -748286.2643 kcal/mol
$G_{298K,solution}$ = -748351.9069 kcal/mol
Three lowest vib. freq. (cm^{-1}): 16.0654, 30.7119, 40.5721

N	-3.738947	-0.188014	-0.192794
C	-5.068095	-0.045332	-0.397784
C	-3.057509	0.950545	-0.101671
H	-5.633189	-0.959575	-0.522284
C	-5.668064	1.219748	-0.484351
C	-3.546259	2.251065	-0.174986
C	-1.628193	0.956203	0.090743
H	-6.739220	1.269265	-0.650967
C	-4.914794	2.403237	-0.372186
C	-2.351426	3.181194	-0.007263
N	-0.937994	-0.176921	0.183624
C	-1.149474	2.260565	0.161977
H	-5.384218	3.380276	-0.442210
O	-2.356095	4.393226	-0.008221
C	0.390015	-0.023673	0.388299
C	0.217854	2.423590	0.358871
C	0.980231	1.246120	0.472844
H	0.962198	-0.933314	0.514100
H	0.679734	3.404328	0.427339
H	2.050983	1.304149	0.639308
Pd	-2.332326	-1.796713	-0.002969
O	-3.680948	-3.286556	-0.010016
C	-4.513186	-3.437910	-1.008527
O	-4.698854	-2.629154	-1.922880
O	-0.972168	-3.276027	0.007349
C	-0.139239	-3.418841	1.006566
O	0.039677	-2.606777	1.919317
C	0.621226	-4.738758	0.944935
H	1.517766	-4.682528	1.567114
H	-0.026901	-5.534462	1.331781
H	0.882445	-4.997922	-0.085294
C	-5.263157	-4.763681	-0.944124
H	-6.162775	-4.714143	-1.562449
H	-4.610596	-5.553994	-1.334574
H	-5.517832	-5.025523	0.087035
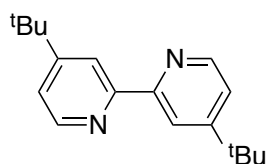
4,4'-*t*Bu₂bpy

SCF Energy = -508235.8519 kcal/mol
$G_{298K,solution}$ = -508149.6727 kcal/mol
Three lowest vib. freq. (cm^{-1}): 21.7041, 34.6370, 41.3368

N	0.636238	-1.292012	-0.181314
C	1.858378	-0.740468	-0.093857
C	0.572684	-2.614623	-0.368028
C	3.038157	-1.497324	-0.190862
C	1.923194	0.737628	0.114751
C	1.690580	-3.439385	-0.475152
H	-0.428224	-3.038647	-0.435790
C	2.977202	-2.880117	-0.386012
H	3.979166	-0.970193	-0.109100
C	0.743413	1.494471	0.211841
N	3.145332	1.289160	0.202293
H	1.546242	-4.505284	-0.626416
C	4.227244	-3.768176	-0.500825
C	0.804367	2.877258	0.407030
H	-0.197593	0.967344	0.130032
C	3.208886	2.611769	0.389028
C	2.090990	3.436534	0.496119
C	-0.445665	3.765307	0.522045
H	4.209794	3.035793	0.456783
H	2.235322	4.502442	0.647323
C	-0.442052	4.475573	1.897796
H	0.444468	5.105154	2.031121
H	-1.325770	5.118820	1.992464
H	-0.462778	3.746772	2.716673
C	-0.421722	4.828297	-0.603391
H	-1.305224	5.474671	-0.530515
H	0.465418	5.468177	-0.543341
H	-0.427838	4.354422	-1.592102
C	-1.750172	2.955732	0.397252
H	-1.824977	2.447946	-0.571244
H	-1.839382	2.200199	1.186325
H	-2.610437	3.629706	0.485213
C	4.223633	-4.479049	-1.876228
H	5.107406	-5.122256	-1.970653
H	3.337176	-5.108768	-2.009296
H	4.244282	-3.750612	-2.695442
C	4.203350	-4.830670	0.625126
H	3.316232	-5.470603	0.565319
H	5.086883	-5.477034	0.552552
H	4.209418	-4.356333	1.613610

C	5.531725	-2.958502	-0.376442
H	5.620612	-2.202985	-1.165568
H	5.606809	-2.450681	0.592014
H	6.392014	-3.632414	-0.464652
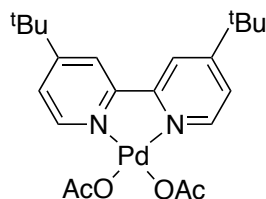
Pd(4,4'-*t*Bu₂bpy)₂(OAc)₂ (7)

SCF Energy = -875301.4164 kcal/mol

$G_{298K,solution}$ = -875264.2481 kcal/mol

Three lowest vib. freq. (cm^{-1}): 8.6468, 14.5006, 23.6714

Pd	1.805513	-0.000643	0.000489
O	3.280014	1.371793	-0.213964
C	3.563721	2.135476	0.811874
O	2.865075	2.266047	1.821310
C	4.883238	2.882504	0.648964
H	5.702479	2.208359	0.927991
H	5.044503	3.183303	-0.390756
H	4.907662	3.752843	1.309755
O	3.278591	-1.374822	0.213988
C	3.561405	-2.137457	-0.812898
O	2.862628	-2.265765	-1.822518
C	4.879931	-2.886442	-0.650928
H	4.903249	-3.755903	-1.312914
H	5.700069	-2.212988	-0.928983
H	5.040753	-3.188887	0.388385
N	0.227639	-1.306759	0.111039
C	-1.002390	-0.737420	0.059041
C	0.327192	-2.639989	0.219263
C	-2.159724	-1.519867	0.113579
C	-1.001899	0.738109	-0.058487
C	-0.791145	-3.461853	0.279885
H	1.333606	-3.035206	0.250028
C	-2.082761	-2.913780	0.224953

H	-3.123888	-1.031918	0.066809
C	-2.158752	1.521227	-0.113618
N	0.228506	1.306726	-0.109730
H	-0.635480	-4.532036	0.362753
C	-3.321075	-3.820245	0.282731
C	-2.080916	2.915110	-0.224749
H	-3.123223	1.033825	-0.067485
C	0.328882	2.639921	-0.217592
C	-0.788949	3.462442	-0.278722
C	-3.318666	3.822306	-0.283200
H	1.335513	3.034616	-0.247462
H	-0.632607	4.532553	-0.361223
C	-3.281121	4.804081	0.914520
H	-2.388866	5.438764	0.897792
H	-4.158216	5.461617	0.885603
H	-3.291348	4.264619	1.868740
C	-3.297618	4.623258	-1.608765
H	-4.173090	5.281418	-1.660898
H	-2.404540	5.251144	-1.694599
H	-3.323220	3.953903	-2.476637
C	-4.635568	3.024796	-0.217443
H	-4.734799	2.324343	-1.055582
H	-4.730095	2.463023	0.719726
H	-5.483450	3.716734	-0.268891
C	-3.301455	-4.620893	1.608494
H	-4.177299	-5.278597	1.660121
H	-2.408761	-5.249213	1.695168
H	-3.327380	-3.951323	2.476193
C	-3.283249	-4.802317	-0.914744
H	-2.391407	-5.437557	-0.897212
H	-4.160781	-5.459291	-0.886321
H	-3.292425	-4.263056	-1.869086
C	-4.637472	-3.021992	0.215815
H	-4.736927	-2.321282	1.053713
H	-4.730989	-2.460398	-0.721559
H	-5.485782	-3.713440	0.266817

A5.2.2 Oxidative aza-Wacker Reaction Coordinate for L = DAF
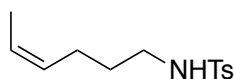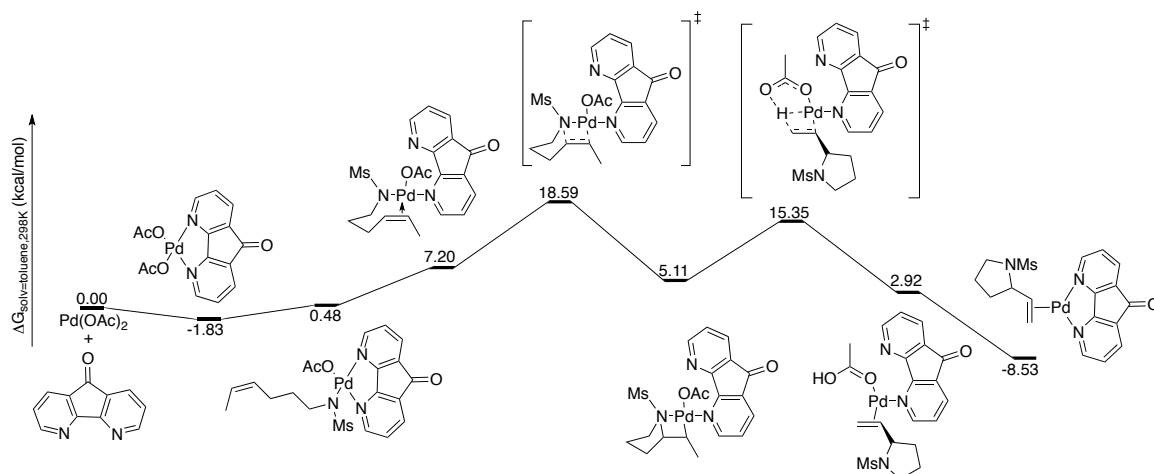
N-tosyl-*cis*-4-hexenylamide (1)
SCF Energy = -551647.7023 kcal/mol
G$_{298K,solution}$ = -551640.237 kcal/mol
Three lowest vib. freq. (cm^{-1}): 21.4478, 30.3154, 60.6082

C	-0.966341	0.357854	-0.706573
H	-0.474134	1.321985	-0.535757
H	-0.768051	0.091210	-1.756568
C	-0.327881	-0.713215	0.200432
H	-0.823323	-1.680678	0.046281
H	-0.495737	-0.437350	1.251366
C	1.172458	-0.869717	-0.058055
H	1.341467	-1.182115	-1.094624
H	1.693328	0.086858	0.080585
C	-2.455606	0.465221	-0.503326
H	-3.012067	-0.448251	-0.722178
C	-3.158136	1.529170	-0.085854
H	-4.238823	1.406876	0.001952
C	-2.647083	2.896219	0.279552
H	-2.931040	3.153346	1.309189
H	-1.559737	2.984086	0.200328
H	-3.092914	3.663320	-0.368548
N	1.721197	-1.918233	0.825244
H	1.527669	-1.756969	1.813603
S	3.369714	-2.296707	0.697544

C	3.346717	-3.749344	-0.369429
H	4.387378	-4.048623	-0.515583
H	2.779128	-4.536794	0.128205
H	2.893850	-3.479245	-1.325779
O	3.785263	-2.716827	2.043006
O	4.087139	-1.235540	-0.023783
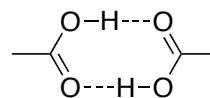
Acetic acid dimer
SCF Energy = -287536.3442 kcal/mol
G$_{298K,solution}$ = -287572.6562 kcal/mol
Three lowest vib. freq. (cm^{-1}): 41.7734, 49.9209, 67.7704

C	-3.810296	0.260355	0.010303
O	-2.626196	0.020494	0.247950
O	-4.271203	1.471678	-0.275948
H	-3.524425	2.140702	-0.267535
O	-2.243297	3.264713	-0.248799
C	-1.059252	3.025291	-0.010596
O	-0.598005	1.814040	0.275611
H	-1.344661	1.144929	0.267067
C	0.013107	4.081980	-0.015220
H	0.499821	4.119113	0.965393
H	0.782851	3.824167	-0.750691
H	-0.421525	5.053241	-0.253920

C	-4.882908	-0.796090	0.015474
H	-5.652683	-0.537758	0.750714
H	-5.369535	-0.833742	-0.965174
H	-4.448428	-1.767296	0.254680

SCF Energy = -1156170.387 kcal/mol
$G_{298K,solution}$ = -1156203.494 kcal/mol
Three lowest vib. freq. (cm^{-1}): 15.0810, 17.3517, 28.5369

N	1.531336	-1.199050	-0.447292
C	1.502761	-2.507472	-0.777602
C	2.721556	-0.614634	-0.508249
H	0.535463	-2.991519	-0.712295
C	2.664404	-3.186631	-1.172106
C	3.931002	-1.188735	-0.885847
C	2.896549	0.778523	-0.168593
H	2.585363	-4.238949	-1.424955
C	3.910987	-2.535607	-1.235707
C	4.982767	-0.091777	-0.798434
N	1.876595	1.538189	0.223074
C	4.229756	1.146989	-0.331804
H	4.808465	-3.066000	-1.540886
O	6.165572	-0.182110	-1.049017
C	2.194562	2.829482	0.473468
C	4.561528	2.469674	-0.058971
C	3.507643	3.308576	0.347255
H	1.364819	3.472526	0.742428
H	5.576715	2.843363	-0.158385
H	3.696186	4.355229	0.563884
Pd	0.107150	0.185768	0.297172
O	-1.262719	1.387513	1.187086
C	-1.405444	2.654872	0.896088
O	-0.716226	3.294062	0.095641
C	-2.559565	3.304602	1.651986
H	-2.531002	4.388318	1.518442
H	-3.509269	2.920144	1.261220
H	-2.518100	3.053815	2.716991
N	-1.304936	-1.267648	0.194927
S	-1.398416	-2.204571	1.568198

C	-2.595988	-0.897728	-0.418625
O	-0.007326	-2.456615	2.000567
O	-2.273149	-3.361014	1.284653
C	-2.204726	-1.262574	2.890022
C	-2.417280	-0.586264	-1.907750
H	-3.048185	-0.037814	0.093377
H	-3.274942	-1.753235	-0.310695
H	-1.642042	-0.344393	3.062521
H	-3.227388	-1.033709	2.582429
H	-2.207261	-1.904149	3.774892
C	-3.744577	-0.242399	-2.616817
H	-1.714223	0.250581	-2.024551
H	-1.960370	-1.456876	-2.396283
C	-4.350633	1.062559	-2.164070
H	-4.451629	-1.071613	-2.493117
H	-3.538933	-0.174651	-3.696287
C	-5.594045	1.290403	-1.712833
H	-3.677287	1.919989	-2.229336
C	-6.711499	0.298694	-1.528890
H	-5.846359	2.318431	-1.446819
H	-7.072049	0.306040	-0.490857
H	-7.572260	0.560159	-2.160476
H	-6.418682	-0.726318	-1.773866
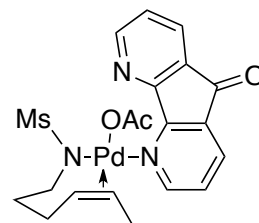
SCF Energy = -1156164.973 kcal/mol
$G_{298K,solution}$ = -1156196.777 kcal/mol
Three lowest vib. freq. (cm^{-1}): 10.6907, 24.4242, 26.7872

N	-0.825734	-0.161627	1.030733
C	-0.763599	-0.386028	2.366477
C	-1.993247	-0.368532	0.419984
H	0.197132	-0.202220	2.827106
C	-1.864685	-0.823939	3.106135
C	-3.142294	-0.802750	1.104103
C	-2.335309	-0.190657	-1.020253
H	-1.746811	-0.981387	4.173118
C	-3.092171	-1.039296	2.470671
C	-4.276413	-0.914427	0.131719
N	-1.524663	0.194181	-1.998638

C	-3.697843	-0.508394	-1.188619
H	-3.972363	-1.372127	3.013885
O	-5.420157	-1.260713	0.366923
C	-2.090485	0.286104	-3.218022
C	-4.272038	-0.413510	-2.447440
C	-3.433800	0.001985	-3.490884
H	-1.428836	0.605166	-4.020570
H	-5.320158	-0.650560	-2.608448
H	-3.810155	0.103600	-4.504291
Pd	0.891769	0.623213	0.079374
O	0.010046	2.457685	0.445269
C	0.005170	2.906221	1.675160
O	0.528671	2.343837	2.640449
C	-0.702819	4.250006	1.825606
H	-1.054769	4.370330	2.853312
H	0.011953	5.055528	1.613908
H	-1.534976	4.347168	1.122193
N	1.412360	-1.345681	-0.353142
S	2.272125	-2.166077	0.790294
C	1.656983	-1.720989	-1.754799
O	2.097970	-1.452230	2.072659
O	3.647775	-2.510978	0.360312
C	1.404825	-3.751489	0.956082
C	2.948881	-1.180609	-2.384512
H	0.787150	-1.357610	-2.315969
H	1.653408	-2.817619	-1.847024
H	0.387811	-3.558859	1.301975
H	1.397871	-4.268424	-0.006239
H	1.960936	-4.338889	1.691012
C	3.035305	0.350830	-2.336184
H	3.809496	-1.618544	-1.869630
H	2.990487	-1.507801	-3.433107
C	2.990088	0.914108	-0.936646
H	2.249022	0.795413	-2.957504
H	3.994009	0.662888	-2.780581
C	2.538682	2.167546	-0.598104
H	3.576679	0.375138	-0.194073
C	2.024455	3.210491	-1.551644
H	2.769074	2.523029	0.405624
H	1.197877	3.766034	-1.102824
H	2.837709	3.919806	-1.766119
H	1.685785	2.790424	-2.502196
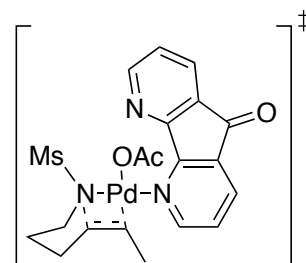
SCF Energy = -1156156.211 kcal/mol

$G_{298K,solution}$ = -1156185.386 kcal/mol

Three lowest vib. freq. (cm^{-1}): **-257.905**, 21.9669, 28.2309

N	-1.408777	-1.151419	-0.332870
C	-1.641416	-2.478673	-0.507910
C	-2.479435	-0.365050	-0.187255
H	-0.753971	-3.100397	-0.556227
C	-2.925117	-3.021395	-0.566074
C	-3.801323	-0.840984	-0.231105
C	-2.509841	1.100086	0.056075
H	-3.034164	-4.092017	-0.705713
C	-4.046261	-2.190551	-0.429323
C	-4.739937	0.316973	-0.022787
N	-1.458155	1.896761	0.169683
C	-3.852820	1.509230	0.158621
H	-5.059964	-2.579894	-0.465562
O	-5.956740	0.278241	-0.006798
C	-1.729964	3.193927	0.405393
C	-4.129759	2.848635	0.399991
C	-3.028969	3.708117	0.526602
H	-0.859957	3.839612	0.500565
H	-5.151708	3.207363	0.487601
H	-3.170781	4.767474	0.718420
Pd	0.567474	-0.451132	-0.183804
O	0.607663	-1.173799	1.805309
C	0.819268	-2.448841	1.928789
O	0.933825	-3.251706	0.986300
C	0.952055	-2.929333	3.372137
H	1.993129	-2.801358	3.695409
H	0.318769	-2.344985	4.046254
H	0.704403	-3.991882	3.440693
N	2.522900	0.219583	-0.046337
C	3.668168	-0.670234	-0.299695
S	2.812074	1.644425	0.778848
C	4.292016	-0.289109	-1.647758
H	3.292640	-1.698986	-0.305771

H	4.407244	-0.588725	0.504701
C	2.465251	1.293879	2.517106
O	1.824234	2.641556	0.322926
O	4.249757	1.971767	0.681933
C	3.140665	-0.165173	-2.663336
H	4.812103	0.668205	-1.539794
H	5.021468	-1.036892	-1.983397
H	1.454337	0.894925	2.601985
H	3.192737	0.559222	2.868686
H	2.584288	2.239104	3.053585
C	1.991901	0.635501	-2.114348
H	2.802601	-1.159877	-2.969615
H	3.492503	0.352100	-3.569101
C	0.628848	0.250408	-2.233119
H	2.186209	1.683876	-1.910128
H	-0.062164	1.094714	-2.197741
C	0.200394	-0.870376	-3.175920
H	-0.877835	-1.039278	-3.098410
H	0.412060	-0.611574	-4.224415
H	0.695037	-1.824618	-2.965827
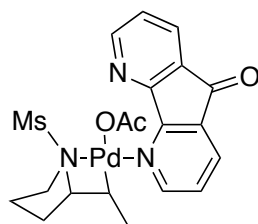
SCF Energy = -1156171.032 kcal/mol

$G_{298K,solution}$ = -1156198.869 kcal/mol

Three lowest vib. freq. (cm^{-1}): 13.8680, 24.1338, 25.9529

N	-1.390391	-1.117090	-0.337364
C	-1.515695	-2.438004	-0.637287
C	-2.520793	-0.422893	-0.177450
H	-0.580730	-2.988112	-0.690769
C	-2.749857	-3.062320	-0.814762
C	-3.799166	-0.987898	-0.339901
C	-2.680631	1.009266	0.197911
H	-2.771113	-4.120571	-1.054161
C	-3.934163	-2.326331	-0.672041
C	-4.834997	0.071204	-0.093849
N	-1.712101	1.874037	0.466338
C	-4.057693	1.304188	0.243480
H	-4.913965	-2.777295	-0.802792
O	-6.044766	-0.056374	-0.156041

C	-2.114163	3.117464	0.790612
C	-4.466286	2.586671	0.582236
C	-3.455502	3.516927	0.860679
H	-1.315966	3.824989	1.004192
H	-5.519736	2.848894	0.629232
H	-3.698251	4.539919	1.132091
Pd	0.550541	-0.378641	-0.113263
O	0.758163	-1.402802	1.801921
C	1.065315	-2.655490	1.726581
O	1.231180	-3.289178	0.663270
C	1.257283	-3.361051	3.068827
H	1.120477	-4.439949	2.956830
H	2.280909	-3.184115	3.424711
H	0.571199	-2.965564	3.824169
N	2.524850	0.374813	-0.307002
C	3.635988	-0.656266	-0.306926
S	2.895822	1.783946	0.698550
C	4.262607	-0.542769	-1.698212
H	3.175119	-1.631834	-0.135015
H	4.344031	-0.448193	0.497755
C	2.599484	1.160752	2.361195
O	1.902917	2.810946	0.369700
O	4.327572	2.091949	0.553773
C	3.052138	-0.233888	-2.590491
H	4.984256	0.282090	-1.720089
H	4.780888	-1.462941	-1.987436
H	1.591070	0.750039	2.422994
H	3.338800	0.390343	2.585710
H	2.735627	2.024549	3.017645
C	2.230113	0.783995	-1.784128
H	2.474553	-1.149365	-2.756462
H	3.330872	0.173351	-3.567911
C	0.699707	0.712697	-1.840348
H	2.626446	1.792810	-1.957055
H	0.278452	1.690869	-1.590021
C	0.070905	0.167655	-3.116461
H	-1.022478	0.204394	-3.049386
H	0.357253	0.768850	-3.995645
H	0.349628	-0.870932	-3.328055
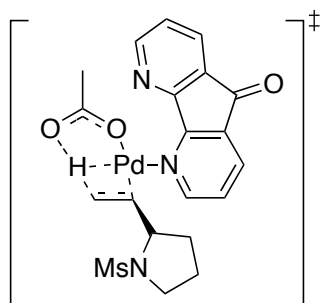
SCF Energy = -1156152.386 kcal/mol
$G_{298K,solution}$ = -1156188.625 kcal/mol
Three lowest vib. freq. (cm^{-1}): **-1041.9015**, 6.8028, 18.0480

Pd	-0.099503	1.217189	-0.044585
O	-1.170789	3.123030	-0.323734
C	-0.483896	4.068339	0.177538
O	0.641791	3.909726	0.749046
C	-1.029877	5.482017	0.090535
H	-1.097991	5.912177	1.095533
H	-0.333989	6.105708	-0.481653
H	-2.012268	5.494695	-0.385967
N	3.382415	-1.520077	0.023959
C	3.308286	-2.956464	-0.344242
S	4.890258	-0.767700	0.068974
C	2.383699	-2.969330	-1.565237
H	2.864644	-3.518201	0.489751
H	4.305951	-3.352519	-0.537294
C	5.130380	-0.404101	1.819365
O	4.800349	0.523588	-0.631388
O	5.921641	-1.748240	-0.308134
C	1.375066	-1.865193	-1.225419
H	2.954677	-2.711280	-2.465953
H	1.913801	-3.946003	-1.726982
H	4.324015	0.250664	2.153967
H	5.127234	-1.345321	2.372710
H	6.098245	0.095268	1.912580
C	2.200860	-0.755094	-0.533131
H	0.618703	-2.247550	-0.527470
H	0.847459	-1.473787	-2.100165
C	1.441086	-0.017943	0.554181
H	2.574411	-0.039798	-1.271983
H	1.085199	-0.683713	1.344713
C	1.824353	1.330695	0.960434
H	2.679771	1.773055	0.445672
H	0.974954	2.472340	0.685264
H	1.819484	1.539071	2.032816
N	-1.660311	0.185820	-1.090180
C	-2.649260	-0.522886	-0.536818
C	-1.760583	0.412482	-2.425806
C	-2.820113	-0.907708	0.892853
C	-3.740512	-1.031162	-1.267828
C	-2.806477	-0.057979	-3.217000
H	-0.962711	1.006233	-2.857918
N	-2.010193	-0.616787	1.903781
C	-4.015900	-1.644884	1.012412
C	-4.655577	-1.767501	-0.333646
C	-3.836170	-0.807855	-2.631129
H	-2.810013	0.169414	-4.278180
C	-2.399616	-1.073362	3.109659
C	-4.409798	-2.111952	2.258145
O	-5.692593	-2.338937	-0.618943
H	-4.672047	-1.193100	-3.208209
H	-1.738308	-0.831771	3.939058
C	-3.568661	-1.810305	3.337265
H	-5.327359	-2.680457	2.382772
H	-3.811141	-2.137568	4.343776
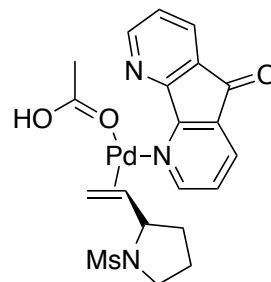
SCF Energy = -1156167.031 kcal/mol
$G_{298K,solution}$ = -1156201.063 kcal/mol
Three lowest vib. freq. (cm^{-1}): 9.8219, 18.5649, 21.7375

Pd	-0.027550	1.067079	-0.537045
O	-1.217897	2.937480	-1.400176
C	-1.902885	3.654478	-0.679978
O	-2.398999	3.260837	0.496165
C	-2.269217	5.076026	-1.021732
H	-3.358088	5.194896	-1.027321
H	-1.870834	5.752891	-0.257365
H	-1.858286	5.339353	-1.997089
N	3.763326	-1.006511	0.628068
C	3.883906	-2.475773	0.797019
S	5.161953	-0.091977	0.417950

C   3.047953   -3.042939   -0.354250
H   3.455130   -2.759901   1.768464
H   4.931326   -2.779130   0.781840
C   5.116525   1.066810   1.798884
O   5.055590   0.707160   -0.814362
O   6.324241   -0.972838   0.627510
C   1.896949   -2.033372   -0.455794
H   3.642098   -3.048837   -1.276998
H   2.707480   -4.066902   -0.161584
H   4.192267   1.643710   1.734080
H   5.161225   0.497538   2.729338
H   5.990334   1.715927   1.698882
C   2.538385   -0.650932   -0.189964
H   1.141805   -2.240655   0.314157
H   1.389634   -2.048770   -1.424932
C   1.641561   0.324629   0.545921
H   2.876355   -0.202675   -1.129103
H   1.305694   -0.053943   1.515461
C   1.730557   1.730482   0.372077
H   2.427258   2.144863   -0.357896
H   -2.193624   2.299619   0.668940
H   1.488531   2.396316   1.202411
N   -1.539452   -0.376908   -1.286174
C   -2.481365   -0.966773   -0.542943
C   -1.293846   -0.959024   -2.488785
C   -3.009066   -0.524677   0.775229
C   -3.130887   -2.165506   -0.901248
C   -1.916511   -2.123808   -2.936462
H   -0.548332   -0.459866   -3.099368
N   -2.735425   0.605693   1.424529
C   -3.917742   -1.497061   1.240275
C   -4.051947   -2.574038   0.207255
C   -2.852542   -2.771425   -2.115765
H   -1.654789   -2.523459   -3.911287
C   -3.349378   0.767160   2.615903
C   -4.545430   -1.325887   2.464403
O   -4.760821   -3.563546   0.256886
H   -3.340304   -3.695920   -2.411444
H   -3.124806   1.695020   3.136739
C   -4.233325   -0.159125   3.176583
H   -5.248430   -2.062362   2.843973
H   -4.681810   0.044171   4.144038
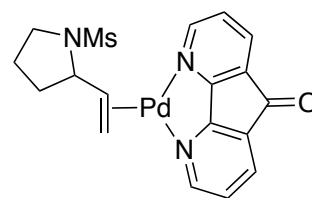
SCF Energy = -1012405 kcal/mol
$G_{298K,solution}$ = -1012426.19 kcal/mol
Three lowest vib. freq. (cm^{-1}): 11.0705, 21.7888, 23.7829

Pd   0.094544   1.003546   -0.533957
N   3.891595   -1.032404   0.649225
C   4.055674   -2.507107   0.721480
S   5.264819   -0.065902   0.527415
C   3.193887   -3.026152   -0.434403
H   3.670560   -2.863209   1.687351
H   5.108826   -2.781678   0.651257
C   5.140974   1.020280   1.961445
O   5.172715   0.790124   -0.667583
O   6.447007   -0.921505   0.730505
C   2.028348   -2.029534   -0.451716
H   3.758798   -2.975122   -1.373828
H   2.875113   -4.064168   -0.284563
H   4.205366   1.578096   1.892573
H   5.168157   0.405546   2.863157
H   6.000949   1.694146   1.925064
C   2.669862   -0.654490   -0.164484
H   1.312662   -2.271513   0.346383
H   1.479415   -2.008416   -1.398086
C   1.769098   0.316915   0.571141
H   3.010993   -0.197766   -1.099069
H   1.443356   -0.051581   1.548131
C   1.838166   1.721572   0.369157
H   2.541740   2.129130   -0.357826
H   1.580225   2.400870   1.183449
N   -1.633613   -0.406330   -1.270798
C   -2.511342   0.342856   -1.930977
C   -1.958390   -1.716216   -1.194083
C   -2.354979   1.783395   -2.127108
C   -3.696497   -0.087476   -2.537657
C   -3.120104   -2.256435   -1.761234
H   -1.256135   -2.348439   -0.659011
N   -1.324331   2.477311   -1.656138
C   -3.435660   2.278460   -2.864784
C   -4.356358   1.118249   -3.170091

```
C   -4.024285   -1.434888   -2.456862        H   -4.272285    4.085743   -3.725845
H   -3.310844   -3.320168   -1.656988        H   -2.339543    5.468471   -2.867763
C   -1.354796    3.797631   -1.943081
C   -3.463219    3.636498   -3.156876
O   -5.401501    1.147037   -3.789743
H   -4.929262   -1.834316   -2.905866
H   -0.520830    4.384034   -1.568881
C   -2.385486    4.400773   -2.676373
```

A5.2.3 Oxidative aza-Wacker Reaction Coordinate for L = 6,6'-Me₂bpy
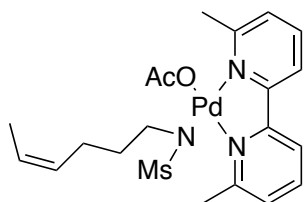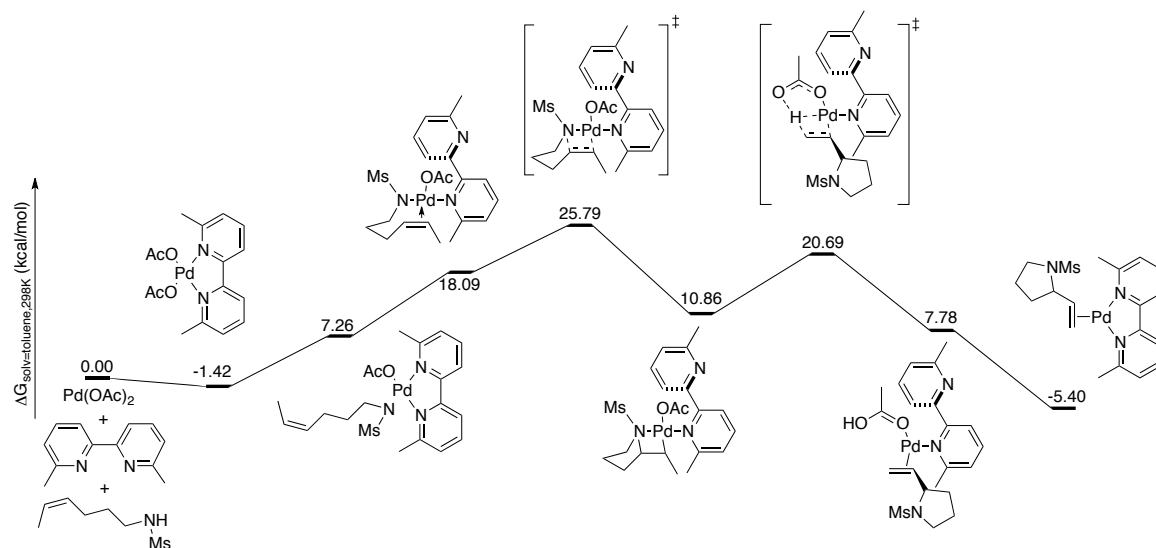
SCF Energy = -1135153.963 kcal/mol
G$_{298K,solution}$ = -1135399.402 kcal/mol
Three lowest vib. freq. (cm^{-1}): 13.3057,
17.9693, 25.6330

Pd	0.611584	-0.179593	0.519059
C	-5.472614	0.489638	-2.428002
C	-4.253302	1.048794	-2.480516
C	-2.920105	0.376422	-2.690233
C	-1.902117	0.659398	-1.563910
C	-2.300070	0.016448	-0.232615
N	-1.355123	0.386891	0.841517
S	-1.871630	-0.073151	2.362261
O	-2.626809	-1.342004	2.392877
C	-3.085247	1.204284	2.810603
O	-0.720388	0.107045	3.276167
H	-3.306005	0.366646	0.041342
H	-2.373364	-1.072764	-0.350028
H	-1.795835	1.745714	-1.426277
H	-0.924436	0.269135	-1.870865
H	-3.033343	-0.706964	-2.809567

H	-2.487776	0.742866	-3.633912
H	-4.198227	2.133885	-2.360631
C	-5.831047	-0.966027	-2.561774
H	-6.321825	1.157655	-2.272072
H	-2.589661	2.174245	2.872049
H	-3.891256	1.219942	2.073706
H	-3.481248	0.914931	3.787284
H	-6.364116	-1.318917	-1.668105
H	-6.507936	-1.123147	-3.413434
H	-4.958352	-1.609130	-2.705570
N	2.588310	-0.638901	-0.037933
C	3.065192	0.318387	-0.878197
C	3.242025	-1.807881	0.109430
C	4.158202	0.070640	-1.708038
C	2.423268	1.651519	-0.755486
C	4.362516	-2.091248	-0.688453
C	2.796966	-2.787735	1.160253
C	4.798815	-1.165797	-1.626292
H	4.517734	0.823729	-2.398412
N	1.423655	1.751824	0.168204
C	2.881176	2.769411	-1.454172
H	4.872923	-3.040973	-0.561192
H	2.112830	-2.330686	1.875021
H	2.280858	-3.640857	0.706903
H	3.676074	-3.174248	1.689342
H	5.647173	-1.385653	-2.268181
C	0.944652	2.967118	0.512790

```
C    2.338240    4.019358   -1.162874
H    3.660360    2.675981   -2.200487
C    1.391735    4.120642   -0.152287
C   -0.053347    3.076946    1.625375
H    2.675986    4.902520   -1.697839
H    0.986518    5.084617    0.138537
H   -1.057803    2.868835    1.244895
H    0.142166    2.337783    2.406704
H   -0.028940    4.085319    2.050909
O   -0.039522   -2.092950    0.567713
C   -0.136378   -2.717566   -0.577000
O    0.215949   -2.268985   -1.673307
C   -0.761683   -4.101257   -0.435257
H   -1.832818   -3.989031   -0.229788
H   -0.627448   -4.670740   -1.358024
H   -0.332003   -4.641514    0.414628
```
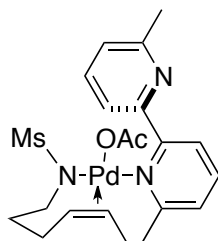

SCF Energy = -1135150.882 kcal/mol

$G_{298K,solution}$ = -1135134.127 kcal/mol

Three lowest vib. freq. (cm^{-1}): 21.1029, 26.9383, 31.2696

```
Pd  -0.455939    0.425237   -0.226775
C    0.535965   -0.145862   -2.333351
C   -0.774693   -0.555694   -2.362960
C   -1.898317    0.117914   -3.112473
C   -3.283811   -0.149095   -2.500784
C   -3.379223    0.274000   -1.028758
N   -2.361032   -0.336222   -0.165627
S   -2.599985   -1.861200    0.389201
C   -3.012496   -1.680270    2.142251
O   -1.315584   -2.600140    0.350867
O   -3.790892   -2.463798   -0.250495
H   -3.263895    1.359043   -0.919103
H   -4.376891    0.019158   -0.650707
H   -3.520890   -1.216757   -2.574169
H   -4.042137    0.392328   -3.083261
H   -2.183097   -1.172861    2.636867
H   -3.931111   -1.094367    2.220988
```

```
H   -3.162980   -2.684445    2.547419
H   -1.719196    1.197387   -3.192158
H   -1.885668   -0.273031   -4.142806
H   -0.979879   -1.557354   -1.992004
H    1.261588   -0.852399   -1.932945
C    1.123185    0.980802   -3.143331
H    1.964086    1.460414   -2.635480
H    1.515743    0.558410   -4.080130
H    0.390280    1.744722   -3.414373
N    3.614151   -1.319146   -0.004623
C    2.569994   -0.693606    0.571357
C    3.725857   -2.650467    0.122258
C    1.604538   -1.362924    1.330785
C    2.557661    0.789418    0.382341
C    2.784363   -3.401887    0.842781
C    4.914061   -3.294483   -0.549903
C    1.717738   -2.748455    1.454520
H    0.801345   -0.820916    1.815319
N    1.422418    1.434265    0.008336
C    3.756779    1.483877    0.580853
H    2.891561   -4.480425    0.917624
H    4.922168   -4.378797   -0.401421
H    4.904095   -3.090430   -1.627036
H    5.849168   -2.881766   -0.152679
H    0.968503   -3.305097    2.008079
C    1.439416    2.784120   -0.166418
C    3.783223    2.863879    0.425265
H    4.640648    0.920871    0.855801
C    2.611806    3.515762    0.050559
C    0.189090    3.481010   -0.626121
H    4.700459    3.422916    0.590190
H    2.591490    4.591953   -0.087722
H   -0.093275    3.146736   -1.631204
H   -0.660793    3.275625    0.035274
H    0.353975    4.562117   -0.666906
O   -0.734145    0.881683    1.772811
C   -1.574748    1.819472    2.125550
O   -2.165796    2.584207    1.358411
C   -1.794946    1.899869    3.634365
H   -2.010645    2.932687    3.920722
H   -2.668077    1.289161    3.896613
H   -0.933674    1.521249    4.191554
```
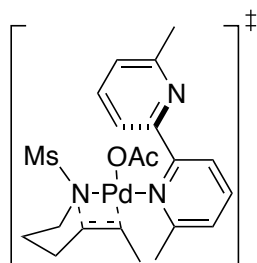
SCF Energy = -1135143.814 kcal/mol
$G_{298K,solution}$ = -1135126.427 kcal/mol
Three lowest vib. freq. (cm^{-1}): **-251.2760**, 25.0296, 28.8016

Pd	-0.350935	0.464287	-0.190095
N	3.576636	-1.418353	-0.127523
C	2.639981	-0.672821	0.485164
C	3.637288	-2.733104	0.137910
C	1.740281	-1.194010	1.422917
C	2.674032	0.781912	0.147818
C	2.758199	-3.341085	1.046749
C	4.696498	-3.520131	-0.594647
C	1.806235	-2.559901	1.697786
H	1.027181	-0.550416	1.926223
N	1.525188	1.450274	-0.132054
C	3.915823	1.426981	0.133991
H	2.824348	-4.408702	1.236829
H	4.716602	-4.565969	-0.272424
H	4.514646	-3.494540	-1.675913
H	5.686550	-3.081508	-0.424164
H	1.113824	-3.007829	2.403751
C	1.570839	2.783937	-0.398939
C	3.975117	2.789194	-0.132454
H	4.805094	0.843057	0.339454
C	2.789515	3.471039	-0.391820
C	0.297035	3.508300	-0.736125
H	4.927537	3.312670	-0.134702
H	2.792875	4.535614	-0.602877
H	-0.079149	3.187464	-1.714754
H	-0.498081	3.313654	-0.008286
H	0.478480	4.586538	-0.785788
O	-0.640532	1.057533	1.828452
C	-1.472257	2.014287	2.121286
O	-2.125461	2.674408	1.300604
C	-1.576808	2.308357	3.617364
H	-0.653432	2.794412	3.956138
H	-2.420772	2.973723	3.813842
H	-1.684449	1.383590	4.194387
N	-2.223534	-0.430893	-0.309385
C	-3.394266	0.297578	-0.826699
S	-2.502080	-1.848949	0.517330
C	-3.724037	-0.221400	-2.231270
H	-3.142777	1.362250	-0.823066
H	-4.252930	0.169650	-0.157445
C	-2.740657	-1.384397	2.247858
O	-1.266912	-2.653040	0.443401
O	-3.773295	-2.447042	0.059499
C	-2.407855	-0.261618	-3.031681
H	-4.149100	-1.226393	-2.148469
H	-4.457901	0.419302	-2.736185
H	-1.845760	-0.862021	2.587529
H	-3.618075	-0.737283	2.317233
H	-2.908232	-2.313488	2.799241
C	-1.290503	-0.888250	-2.247197
H	-2.132680	0.747437	-3.352736
H	-2.542513	-0.866736	-3.941513
C	0.024188	-0.355225	-2.169427
H	-1.411176	-1.936151	-1.990441
H	0.779891	-1.106346	-1.926471
C	0.518910	0.689215	-3.163601
H	1.500258	1.068186	-2.865653
H	0.634351	0.243801	-4.163154
H	-0.152117	1.546813	-3.266287
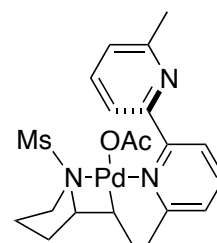
SCF Energy = -1135160.15 kcal/mol
$G_{298K,solution}$ = -1135141.361 kcal/mol
Three lowest vib. freq. (cm^{-1}): 20.5098, 22.5859, 34.8118

Pd	0.340785	-0.449784	-0.103806
N	-3.622480	1.326602	-0.260590
C	-2.729025	0.566477	0.393741
C	-3.743473	2.622194	0.072143
C	-1.938163	1.048255	1.446564
C	-2.689363	-0.867376	-0.020291
C	-2.979185	3.191413	1.100816
C	-4.746819	3.428235	-0.715955

C	-2.077271	2.390203	1.798961
H	-1.258877	0.389837	1.978424
N	-1.497105	-1.487353	-0.208985
C	-3.901268	-1.546098	-0.188823
H	-3.097224	4.242487	1.349041
H	-4.793893	4.465141	-0.368547
H	-4.484530	3.429743	-1.780529
H	-5.746266	2.985301	-0.630925
H	-1.486601	2.806491	2.610571
C	-1.469752	-2.808806	-0.528782
C	-3.886409	-2.896986	-0.515033
H	-4.826353	-0.998572	-0.052296
C	-2.657945	-3.532811	-0.674242
C	-0.139151	-3.472247	-0.752205
H	-4.815388	-3.447472	-0.638047
H	-2.604101	-4.587474	-0.924746
H	0.334365	-3.077024	-1.659224
H	0.555468	-3.291637	0.076254
H	-0.268893	-4.551556	-0.881591
O	0.566644	-0.975158	2.014462
C	1.369379	-1.929224	2.364715
O	2.088696	-2.580460	1.584514
C	1.374622	-2.250786	3.859031
H	0.458710	-2.800357	4.111066
H	2.236990	-2.870918	4.115986
H	1.375290	-1.334180	4.458886
N	2.193049	0.548491	-0.499773
C	3.457147	-0.291004	-0.440817
S	2.395235	2.119463	0.284031
C	4.004380	-0.265200	-1.868841
H	3.168384	-1.288127	-0.101167
H	4.154526	0.130194	0.286224
C	2.439106	1.673006	2.028947
O	1.178688	2.887158	0.002785
O	3.703400	2.670687	-0.103586
C	2.728809	-0.258362	-2.721986
H	4.587380	0.648140	-2.034157
H	4.648010	-1.127251	-2.073220
H	1.597796	1.012061	2.253506
H	3.389690	1.182898	2.245151
H	2.372155	2.622166	2.567533
C	1.785299	0.713114	-1.996499
H	2.297992	-1.265029	-2.747017
H	2.901741	0.060228	-3.755151
C	0.286101	0.397350	-1.966169
H	2.007880	1.740407	-2.313626

H	-0.275645	1.324583	-1.805022
C	-0.296948	-0.361326	-3.150534
H	-1.371383	-0.520058	-3.009722
H	-0.175372	0.208986	-4.086429
H	0.164156	-1.342494	-3.309062
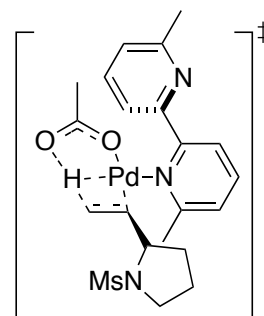
SCF Energy = -1135143.039 kcal/mol
$G_{298K,solution}$ = -1135131.529 kcal/mol
Three lowest vib. freq. (cm^{-1}): **-1073.2224**, 14.7130, 18.4937

Pd	-0.938414	-1.166733	-0.252972
N	-1.030090	3.043680	1.060333
C	-1.659876	1.870881	0.873268
C	-0.500071	3.316816	2.263809
C	-1.825624	0.923861	1.894236
C	-2.248129	1.662632	-0.482863
C	-0.602491	2.415565	3.334215
C	0.217377	4.637173	2.401908
C	-1.281126	1.212806	3.145703
H	-2.382521	0.009295	1.721240
N	-2.165626	0.441232	-1.065515
C	-2.896369	2.734390	-1.108924
H	-0.162069	2.661106	4.296453
H	0.492506	4.839811	3.441680
H	1.133805	4.641327	1.798775
H	-0.413475	5.455392	2.037118
H	-1.389416	0.506252	3.964370
C	-2.787986	0.229544	-2.252267
C	-3.512154	2.531279	-2.338415
H	-2.907840	3.698048	-0.613372
C	-3.470363	1.259307	-2.906846
C	-2.721441	-1.153121	-2.842693
H	-4.028491	3.345354	-2.840267
H	-3.956798	1.056064	-3.855797
H	-1.683680	-1.438906	-3.050833
H	-3.123290	-1.889005	-2.137438

H	-3.292820	-1.206947	-3.774767
O	-2.653841	-2.126824	0.805146
C	-2.253337	-3.194217	1.367432
O	-1.050661	-3.609707	1.334046
C	-3.262994	-4.040556	2.121069
H	-3.367776	-5.009504	1.619473
H	-2.897914	-4.239443	3.134074
H	-4.235684	-3.546141	2.162821
N	3.275687	0.010221	-0.975566
C	3.716878	1.058132	-1.929197
S	4.353993	-0.523632	0.202391
C	2.717519	2.195355	-1.701941
H	3.640751	0.666334	-2.953278
H	4.754937	1.333419	-1.738129
C	4.789873	-2.187251	-0.343690
O	3.628706	-0.662501	1.475715
O	5.585386	0.280984	0.133190
C	1.409479	1.441519	-1.425890
H	3.019182	2.784085	-0.826563
H	2.647362	2.873203	-2.560020
H	3.881306	-2.790389	-0.384784
H	5.259303	-2.118393	-1.327202
H	5.491516	-2.592591	0.389937
C	1.817071	0.191941	-0.608574
H	0.952742	1.125089	-2.373057
H	0.673982	2.043911	-0.887950
C	1.004051	-1.045062	-0.949362
H	1.757383	0.394001	0.463958
H	1.032764	-1.267024	-2.021091
C	0.959971	-2.203358	-0.062325
H	1.498711	-2.116873	0.883192
H	-0.273756	-2.655713	0.552624
H	1.084356	-3.181287	-0.534135

Pd	-0.820861	-1.158687	-0.289030
N	-1.154952	3.128998	1.010713
C	-1.711915	1.919238	0.829182
C	-0.599721	3.425161	2.197076
C	-1.770066	0.952980	1.844586
C	-2.329226	1.678773	-0.507724
C	-0.599593	2.508848	3.259108
C	0.026841	4.792157	2.325550
C	-1.201198	1.264051	3.078928
H	-2.271448	0.007376	1.675905
N	-2.265040	0.438243	-1.046842
C	-2.978700	2.738657	-1.154823
H	-0.140733	2.773327	4.207628
H	0.387431	4.976954	3.342308
H	0.873710	4.892407	1.635906
H	-0.697334	5.571703	2.062118
H	-1.228117	0.543110	3.891981
C	-2.903407	0.199331	-2.217362
C	-3.613413	2.501450	-2.368683
H	-2.973840	3.717946	-0.690846
C	-3.587038	1.212137	-2.898586
C	-2.853469	-1.202639	-2.763939
H	-4.130163	3.303644	-2.889279
H	-4.084983	0.984204	-3.836245
H	-1.814870	-1.534842	-2.878461
H	-3.334553	-1.899579	-2.068209
H	-3.360053	-1.266433	-3.732416
O	-2.754261	-2.183046	0.793999
C	-2.511608	-3.234715	1.384415
O	-1.284532	-3.743590	1.458534
C	-3.552435	-4.065236	2.086578
H	-3.575587	-5.072594	1.656670
H	-3.291812	-4.169810	3.145498
H	-4.531908	-3.595550	1.988364
N	3.406568	0.072529	-0.929197
C	3.853398	1.222347	-1.756428
S	4.467170	-0.593654	0.191845
C	2.783270	2.287572	-1.499696
H	3.863285	0.922826	-2.813931
H	4.862209	1.526945	-1.474981
C	4.736866	-2.268934	-0.420651
O	3.790596	-0.716128	1.494041
O	5.757635	0.110112	0.093730
C	1.506004	1.451962	-1.347107
H	3.007139	2.824552	-0.569121

SCF Energy = -1135156.323 kcal/mol

$G_{298K,solution}$ = -1135144.435 kcal/mol

Three lowest vib. freq. (cm^{-1}): 13.8385, 16.0347, 25.6854

H	2.721224	3.022930	-2.309779
H	3.774976	-2.783284	-0.457764
H	5.187052	-2.204623	-1.413283
H	5.415728	-2.761447	0.280472
C	1.939509	0.189024	-0.570108
H	1.126663	1.160796	-2.335926
H	0.703246	1.979575	-0.827585
C	1.171795	-1.062278	-0.951881
H	1.862795	0.356379	0.508110
H	1.205465	-1.263565	-2.026777
C	1.021774	-2.177906	-0.078261
H	1.011242	-3.181453	-0.510417
H	1.450946	-2.123562	0.923616
H	-0.680343	-3.118926	0.956077
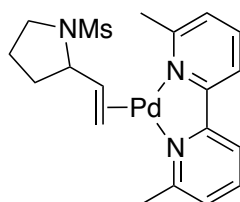
SCF Energy = -991396.2282 kcal/mol

$G_{298K,solution}$ = -991371.2873 kcal/mol

Three lowest vib. freq. (cm^{-1}): 14.0997, 19.3259, 26.5437

Pd	-0.652704	-0.144342	-0.737638
N	-2.344109	1.276202	-0.250626
C	-3.397776	0.700090	0.372104
C	-2.399140	2.586710	-0.571162
C	-4.533756	1.436643	0.735341
C	-3.321474	-0.768965	0.595034
C	-3.502282	3.377035	-0.223398
C	-1.237052	3.165467	-1.329525
C	-4.578418	2.796796	0.444369
H	-5.379928	0.950979	1.207635
N	-2.443980	-1.445003	-0.183767
C	-4.133915	-1.420157	1.531412
H	-3.511265	4.430971	-0.484095
H	-1.399787	4.224401	-1.554253
H	-0.312843	3.058500	-0.754875
H	-1.088033	2.619760	-2.267708
H	-5.447898	3.389717	0.715190
C	-2.398119	-2.791780	-0.114366
C	-4.068697	-2.808238	1.628774
H	-4.792497	-0.856813	2.183134

C	-3.208845	-3.502793	0.781992
C	-1.441027	-3.510316	-1.026747
H	-4.684063	-3.338681	2.350438
H	-3.151441	-4.586830	0.813582
H	-1.368637	-2.993685	-1.987455
H	-0.434175	-3.526162	-0.593017
H	-1.758816	-4.545639	-1.190117
N	3.661175	0.687264	0.179107
C	4.217843	1.939821	0.755751
S	4.544016	-0.736765	0.345374
C	3.099181	2.447226	1.671308
H	4.409615	2.653211	-0.058014
H	5.160937	1.744053	1.267216
C	4.800565	-1.272350	-1.357517
O	3.720920	-1.766932	1.002458
O	5.868909	-0.397423	0.894361
C	1.838972	2.032892	0.903290
H	3.146511	1.936615	2.641639
H	3.162665	3.526688	1.850506
H	3.825778	-1.413258	-1.827396
H	5.380227	-0.505521	-1.874907
H	5.354314	-2.213932	-1.314894
C	2.152816	0.627490	0.351918
H	1.675701	2.725678	0.066881
H	0.928975	2.019196	1.510453
C	1.436097	0.263639	-0.934497
H	1.929806	-0.126739	1.113762
H	1.628742	0.961028	-1.754434
C	1.129004	-1.088760	-1.247593
H	1.083256	-1.404964	-2.291957
H	1.408908	-1.877712	-0.548427

A5.2.4 Oxidative aza-Wacker Reaction Coordinate for L = Neocuproine
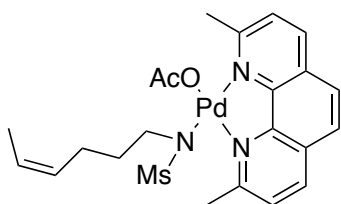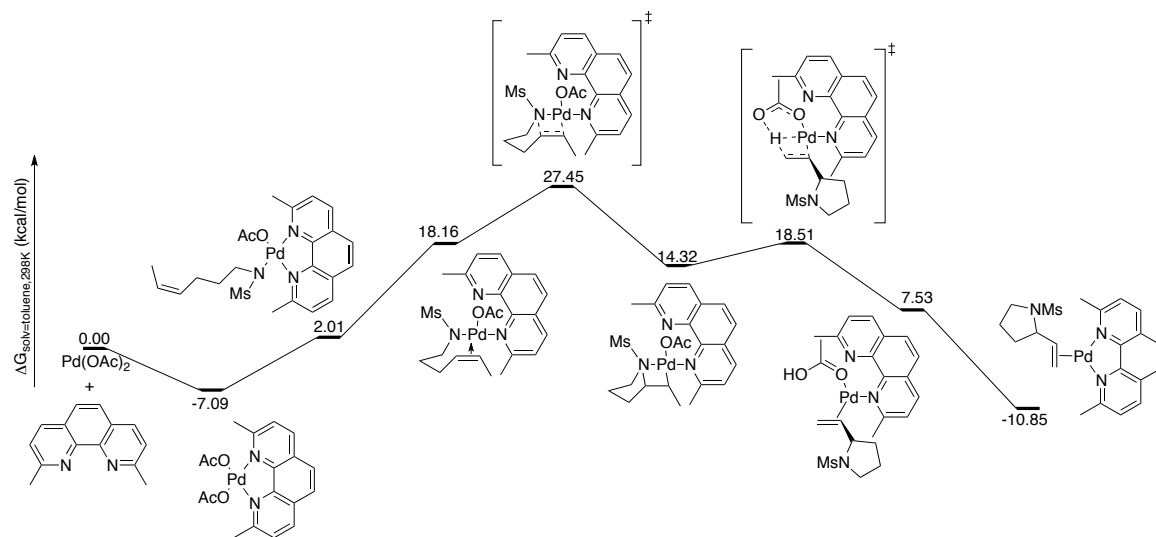
SCF Energy = -1182992.437 kcal/mol
$G_{298K,solution}$ = -1182984.791 kcal/mol
Three lowest vib. freq. (cm^{-1}): 13.7062, 16.7392, 28.9918

Pd	-0.301674	-0.339585	-0.617336
C	5.436392	1.060045	2.718916
C	4.158127	1.470194	2.709483
C	2.904348	0.641411	2.831248
C	1.942793	0.796742	1.632151
C	2.506034	0.191104	0.343206
N	1.606205	0.442916	-0.801722
S	2.276574	0.021274	-2.272507
O	3.135451	-1.179280	-2.234394
C	3.407293	1.395690	-2.644569
O	1.186199	0.096635	-3.272444
H	3.482489	0.652869	0.136471
H	2.693549	-0.881810	0.481637
H	1.725878	1.862825	1.468975

H	0.994773	0.303113	1.876780
H	3.139275	-0.420057	2.969615
H	2.364436	0.954161	3.737831
H	3.981055	2.543230	2.600400
C	5.957168	-0.345890	2.851019
H	6.207379	1.826664	2.620852
H	2.839366	2.322201	-2.739952
H	4.161086	1.475325	-1.858447
H	3.886550	1.141478	-3.593313
H	6.567851	-0.617670	1.978865
H	6.608176	-0.438875	3.731678
H	5.160066	-1.088606	2.944318
N	-2.269918	-1.021555	-0.235727
C	-2.971235	-0.030009	0.393174
C	-2.779441	-2.253724	-0.303877
C	-4.176661	-0.272935	1.090052
C	-2.485130	1.316481	0.254354
C	-3.987476	-2.565296	0.374971
C	-2.108010	-3.311902	-1.132344
C	-4.660688	-1.602788	1.089113
N	-1.354689	1.515742	-0.498651
C	-3.225112	2.379415	0.824259
H	-4.364051	-3.582217	0.319704
H	-1.300065	-2.902097	-1.736646
H	-1.689271	-4.096487	-0.490888

H	-2.852989	-3.785502	-1.783767
H	-5.575685	-1.843577	1.624721
C	-0.985048	2.765989	-0.803995
C	-2.768077	3.691986	0.565523
C	-1.683900	3.876134	-0.260145
C	0.160416	3.000631	-1.740281
H	-3.295839	4.541405	0.992351
H	-1.342574	4.874834	-0.513708
H	1.108744	2.911916	-1.200754
H	0.179833	2.246598	-2.531617
H	0.086532	4.001121	-2.178530
O	0.576830	-2.151493	-0.441765
C	0.559291	-2.717254	0.737239
O	-0.013980	-2.277185	1.739402
C	1.353487	-4.019230	0.769928
H	2.424274	-3.787572	0.725867
H	1.140702	-4.566091	1.691676
H	1.127768	-4.638305	-0.104408
C	-4.861526	0.816451	1.720991
H	-5.766281	0.606249	2.285350
C	-4.402059	2.095401	1.592452
H	-4.934332	2.924396	2.051595

SCF Energy = -1182983.544 kcal/mol

$G_{298K,solution}$ = -1182968.646 kcal/mol

Three lowest vib. freq. (cm^{-1}): 23.8561, 28.0520, 32.9746

Pd	0.571122	-0.406736	-0.192138
C	0.503486	-0.111892	-2.605186
C	1.809642	-0.047836	-2.191206
C	2.865220	-1.107396	-2.394574
C	3.982633	-1.048356	-1.338864
C	3.467176	-1.153766	0.103915
N	2.490334	-0.126268	0.496111
S	3.068831	1.383992	0.809658
C	2.238578	1.860578	2.339596
O	2.634639	2.377754	-0.210695
O	4.517582	1.301628	1.097137
H	2.972442	-2.116967	0.274896

H	4.320330	-1.102698	0.789892
H	4.541858	-0.110512	-1.447624
H	4.694371	-1.865084	-1.523630
H	1.162408	1.734988	2.214603
H	2.606623	1.213730	3.137807
H	2.503883	2.903758	2.529288
H	2.417905	-2.109359	-2.413776
H	3.310936	-0.950583	-3.390105
H	2.173779	0.925001	-1.866548
H	-0.083658	0.798802	-2.522036
C	-0.112678	-1.185771	-3.461864
H	-1.137035	-1.420539	-3.157019
H	-0.168362	-0.802517	-4.491549
H	0.469296	-2.110011	-3.493281
N	-1.417261	1.687833	-0.629363
C	-2.530603	1.055325	-0.195216
C	-1.379308	3.018621	-0.677044
C	-3.694420	1.777082	0.205083
C	-2.571650	-0.405323	-0.173924
C	-2.470646	3.809579	-0.235638
C	-0.150264	3.668908	-1.254656
C	-3.619754	3.188219	0.196560
N	-1.455891	-1.159203	-0.443758
C	-3.814412	-1.031719	0.131288
H	-2.396116	4.892767	-0.261724
H	-0.162536	4.751811	-1.094520
H	0.764415	3.253613	-0.820991
H	-0.107223	3.493947	-2.338644
H	-4.481963	3.768107	0.518496
C	-1.543607	-2.500207	-0.489382
C	-3.889018	-2.439114	0.066132
C	-2.771957	-3.163897	-0.266147
C	-0.311052	-3.333338	-0.701065
H	-4.832791	-2.933763	0.283457
H	-2.800303	-4.247166	-0.321566
H	0.348607	-2.905408	-1.457054
H	0.252329	-3.378129	0.241514
H	-0.584678	-4.349291	-1.004221
O	0.038413	-0.444340	1.799548
C	0.334937	-1.479495	2.537685
O	0.818448	-2.544111	2.139824
C	0.040566	-1.265867	4.021193
H	-0.257799	-2.212885	4.479430
H	0.961308	-0.930055	4.514633
H	-0.729307	-0.505538	4.178207
C	-4.899699	1.096537	0.567422

H   -5.763898   1.684737   0.866584
C   -4.963189   -0.260601   0.506200
H   -5.880532   -0.790394   0.750027
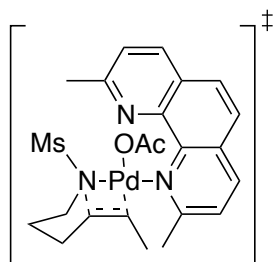
SCF Energy = -1182974.292 kcal/mol
G$_{298K,solution}$ = -1182959.328 kcal/mol
Three lowest vib. freq. (cm^{-1}): **-270.9291**, 15.6179, 26.6203

Pd   0.478474   -0.329411   -0.261804
N   -1.588443   1.739198   -0.458580
C   -2.674798   1.011991   -0.117241
C   -1.609335   3.065344   -0.338920
C   -3.870951   1.628071   0.358928
C   -2.652840   -0.440530   -0.281337
C   -2.735784   3.749301   0.184059
C   -0.404011   3.835709   -0.810644
C   -3.858645   3.030825   0.525542
N   -1.503860   -1.105596   -0.631759
C   -3.871310   -1.150157   -0.074425
H   -2.708205   4.829653   0.292319
H   -0.479620   4.893976   -0.540664
H   0.514414   3.424561   -0.383678
H   -0.322114   3.774636   -1.904289
H   -4.746878   3.528832   0.908209
C   -1.541250   -2.430903   -0.862300
C   -3.889783   -2.537573   -0.326506
C   -2.742998   -3.165813   -0.743634
C   -0.277290   -3.178037   -1.182727
H   -4.813960   -3.093433   -0.186324
H   -2.728759   -4.231232   -0.948410
H   0.317691   -2.660025   -1.936599
H   0.335781   -3.266158   -0.274057
H   -0.512793   -4.182467   -1.549815
O   0.050892   -0.843015   1.748452
C   0.457027   -1.961934   2.264391
O   1.097090   -2.848170   1.675004
C   0.050165   -2.155555   3.726177

H   0.704294   -2.888041   4.206240
H   0.068457   -1.208959   4.275083
H   -0.978600   -2.536424   3.761501
C   -5.047435   0.857316   0.622009
H   -5.936893   1.366205   0.985798
C   -5.052852   -0.481931   0.386947
H   -5.947842   -1.076512   0.552108
N   2.490224   0.015615   0.140356
C   3.456508   -1.093278   0.011491
S   2.979073   1.342990   1.022292
C   4.302572   -0.858507   -1.244696
H   2.886048   -2.024702   -0.034372
H   4.093159   -1.150820   0.900700
C   2.386142   1.095245   2.710448
O   2.274920   2.524182   0.482792
O   4.454751   1.371966   1.085280
C   3.337102   -0.509910   -2.394861
H   4.988964   -0.025672   -1.060178
H   4.901156   -1.741926   -1.500683
H   1.304268   0.961453   2.685870
H   2.875100   0.207994   3.118744
H   2.678926   1.986739   3.271636
C   2.323355   0.514161   -1.969440
H   2.841367   -1.416974   -2.754353
H   3.899273   -0.087005   -3.241534
C   0.930915   0.434419   -2.252007
H   2.715834   1.491463   -1.705597
H   0.419223   1.393024   -2.172911
C   0.389778   -0.413239   -3.396770
H   -0.686512   -0.573569   -3.285268
H   0.543235   0.108369   -4.353747
H   0.867692   -1.392222   -3.488677
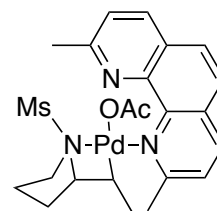
SCF Energy = -1182990.757 kcal/mol
G$_{298K,solution}$ = -1182973.587 kcal/mol
Three lowest vib. freq. (cm^{-1}): 19.3713, 31.5489, 37.3000.

N   -1.638912   1.595074   0.150760
C   -2.777423   0.914476   -0.095538

C	-1.660226	2.923094	0.225816
C	-4.024490	1.577783	-0.297049
C	-2.747728	-0.545888	-0.110093
C	-2.848715	3.662847	0.002818
C	-0.377337	3.622358	0.587369
C	-4.020776	2.989735	-0.261352
N	-1.567801	-1.226035	0.029018
C	-3.985044	-1.238201	-0.251968
H	-2.826685	4.747615	0.053353
H	-0.044977	3.287374	1.577386
H	0.416961	3.376344	-0.123593
H	-0.508248	4.708998	0.612983
H	-4.950907	3.529489	-0.425545
C	-1.575719	-2.568272	0.110985
C	-3.971612	-2.646489	-0.178848
C	-2.781373	-3.302162	0.023386
C	-0.281357	-3.312547	0.276930
H	-4.904851	-3.196352	-0.276413
H	-2.744193	-4.384052	0.098504
H	0.325704	-3.221789	-0.631476
H	0.317794	-2.914163	1.105945
H	-0.473350	-4.376590	0.451050
O	0.470932	-0.077827	2.179425
C	1.022590	-0.956499	2.945585
O	1.600527	-1.994941	2.563162
C	0.907816	-0.670761	4.444544
H	1.710452	-1.171137	4.993430
H	0.916865	0.404804	4.647894
H	-0.050213	-1.065835	4.806897
C	-5.231447	0.833936	-0.496064
H	-6.160794	1.376172	-0.653804
C	-5.212404	-0.525864	-0.459102
H	-6.126217	-1.101678	-0.583208
N	2.484956	-0.034388	-0.525507
C	3.430385	-1.125279	-0.053132
S	3.184048	1.569323	-0.318996
C	3.965997	-1.754465	-1.339847
H	2.850563	-1.812019	0.565931
H	4.219687	-0.697010	0.567877
C	3.008804	1.824316	1.454665
O	2.314069	2.500939	-1.048505
O	4.615708	1.523730	-0.657865
C	2.756040	-1.689750	-2.282380
H	4.797939	-1.159114	-1.733567
H	4.322494	-2.776874	-1.175021
H	1.983395	1.591858	1.752263

H	3.716538	1.173023	1.970398
H	3.263677	2.873624	1.625437
C	2.128715	-0.311688	-2.015287
H	2.051043	-2.489592	-2.032482
H	3.026100	-1.799561	-3.337889
C	0.601686	-0.184263	-2.022827
H	2.625272	0.438940	-2.643932
H	0.329857	0.858411	-2.226209
C	-0.168500	-1.106324	-2.958346
H	-1.242368	-0.898216	-2.900992
H	0.134007	-0.951619	-4.007640
H	-0.028822	-2.170395	-2.736987
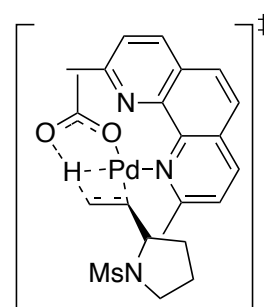
SCF Energy = -1182976.737 kcal/mol
$G_{298K,solution}$ = -1182968.296 kcal/mol
Three lowest vib. freq. (cm^{-1}): **-1084.5059**, 16.3780, 20.8403

Pd	0.474369	1.296766	-0.446991
O	1.892785	2.796709	0.398834
C	1.237033	3.785817	0.840520
O	-0.035675	3.879109	0.800460
C	1.996128	4.947662	1.457489
H	1.807118	5.856915	0.875550
H	1.628214	5.131916	2.472655
H	3.068707	4.744129	1.482585
N	-3.330318	-0.878315	-0.989980
C	-3.498190	-2.106518	-1.805613
S	-4.487242	-0.529323	0.184099
C	-2.271279	-2.950269	-1.448174
H	-3.487229	-1.829690	-2.869060
H	-4.450871	-2.587605	-1.580890
C	-5.322609	0.930921	-0.466009
O	-3.801358	-0.117613	1.422001
O	-5.487039	-1.610253	0.220342
C	-1.174056	-1.887965	-1.295909
H	-2.445987	-3.472321	-0.498987

H	-2.037950	-3.700753	-2.212041
H	-4.588587	1.729275	-0.587278
H	-5.779134	0.670394	-1.423052
H	-6.087610	1.213247	0.261881
C	-1.866450	-0.660513	-0.653680
H	-0.781006	-1.611600	-2.283157
H	-0.328193	-2.220907	-0.689024
C	-1.348754	0.663806	-1.181939
H	-1.764041	-0.689290	0.432443
H	-1.369772	0.707408	-2.275788
C	-1.610613	1.922222	-0.491892
H	-2.180012	1.864271	0.438143
H	-0.535650	2.700813	0.112037
H	-1.909095	2.767066	-1.116704
N	2.089227	-0.067292	-1.068623
C	2.535492	-1.096094	-0.286365
C	2.664219	0.158460	-2.259138
C	3.559891	-1.978638	-0.734571
C	1.975166	-1.308917	1.044500
C	3.694954	-0.671905	-2.753241
C	2.196260	1.337404	-3.068882
C	4.130453	-1.740364	-2.002470
C	3.996033	-3.073045	0.084614
N	1.045326	-0.447558	1.510296
C	2.443317	-2.405413	1.823931
H	4.128807	-0.457870	-3.724965
H	1.115967	1.284787	-3.242871
H	2.384553	2.268556	-2.522707
H	2.712975	1.380563	-4.033255
H	4.914842	-2.398457	-2.369086
H	4.773287	-3.727809	-0.301833
C	3.453878	-3.284534	1.315708
C	0.533670	-0.604306	2.727480
C	1.881380	-2.569335	3.111035
H	3.786917	-4.113467	1.935943
C	0.934670	-1.677173	3.564841
C	-0.501698	0.389805	3.186975
H	2.211769	-3.396723	3.735307
H	0.497802	-1.781709	4.554006
H	-0.528030	0.458922	4.279763
H	-0.292133	1.377373	2.767552
H	-1.503453	0.092398	2.848612
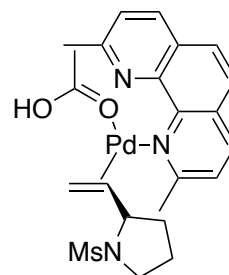
SCF Energy = -1182989.658 kcal/mol
$G_{298K,solution}$ = -1182979.264 kcal/mol
Three lowest vib. freq. (cm^{-1}): 14.7128, 18.5997, 21.4662

C	0.820177	-1.850488	3.469515
C	0.530914	-0.698739	2.693492
N	1.100017	-0.494703	1.508982
C	1.975922	-1.398508	1.013934
C	2.346754	-2.566646	1.740714
C	1.727214	-2.772575	2.994729
C	3.324462	-3.473498	1.215948
C	3.924076	-3.225059	0.018455
C	3.570962	-2.069952	-0.755897
C	2.577201	-1.159537	-0.294045
C	4.184131	-1.800845	-1.998256
C	3.808737	-0.685024	-2.712225
C	2.793298	0.159946	-2.207278
N	2.181702	-0.088602	-1.041983
Pd	0.404802	1.253939	-0.467774
C	-1.602424	1.931789	-0.475908
C	-1.486832	0.708994	-1.200220
C	-1.989866	-0.617553	-0.667169
N	-3.459176	-0.848668	-0.974304
C	-3.661359	-2.149175	-1.662921
C	-2.393030	-2.939299	-1.325668
C	-1.315400	-1.847754	-1.314440
S	-4.597859	-0.341623	0.154746
O	-5.708275	-1.309824	0.175703
C	2.384105	1.385986	-2.977818
C	-0.452703	0.331515	3.187823
O	2.085068	2.766270	0.429097
C	1.623794	3.798776	0.906617
C	2.457330	4.886558	1.531877
O	0.316108	4.059876	0.916804
C	-5.242996	1.185881	-0.554117
O	-3.919420	0.021342	1.412764
H	2.299504	5.830087	0.997868

H	2.145297	5.044065	2.570148
H	3.512318	4.611410	1.498491
H	-3.735807	-1.971600	-2.744919
H	-4.584952	-2.622168	-1.326963
H	-2.492641	-3.396536	-0.332830
H	-2.191336	-3.737185	-2.049547
H	-4.412136	1.879240	-0.695956
H	-5.720725	0.946466	-1.506219
H	-5.971967	1.586784	0.154964
H	-1.017350	-1.603318	-2.342947
H	-0.411237	-2.129044	-0.768609
H	-1.867104	-0.647327	0.417851
H	-1.513864	0.765349	-2.292465
H	-2.062766	1.921468	0.513669
H	-0.134320	3.281732	0.466120
H	-1.767386	2.854804	-1.036392
H	4.272718	-0.449501	-3.665343
H	1.293703	1.497295	-2.965252
H	2.795846	2.283867	-2.500278
H	2.745668	1.346356	-4.010960
H	4.948199	-2.476386	-2.376431
H	4.678881	-3.900813	-0.376857
H	3.587295	-4.353607	1.798402
H	1.980198	-3.656503	3.576372
H	0.334552	-1.988742	4.431619
H	-0.196438	1.317933	2.793814
H	-1.468986	0.094166	2.845031
H	-0.472743	0.370221	4.282625
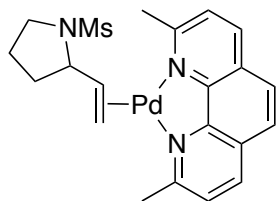
SCF Energy = -1039234.292 kcal/mol

$G_{298K,solution}$ = -1039211.32 kcal/mol

Three lowest vib. freq. (cm^{-1}): 14.2565, 22.8966, 28.6978

Pd	-0.321592	-0.311904	-0.812179
N	-1.957484	1.259643	-0.554176
C	-3.053574	0.772814	0.094553
C	-1.883986	2.566316	-0.818659
C	-4.086998	1.612948	0.584671
C	-3.171736	-0.661532	0.260338

C	-2.880560	3.468935	-0.368703
C	-0.728218	3.069375	-1.639786
C	-3.962608	3.000513	0.342740
N	-2.203567	-1.454654	-0.276426
C	-4.300831	-1.187468	0.942498
H	-2.774216	4.527595	-0.588351
H	-1.084021	3.401674	-2.624590
H	-0.242375	3.928348	-1.161743
H	0.001300	2.269474	-1.783250
H	-4.728685	3.680850	0.707605
C	-2.316394	-2.783247	-0.176869
C	-4.389147	-2.592546	1.059282
C	-3.408161	-3.381890	0.498343
C	-1.242072	-3.634681	-0.795291
H	-5.234810	-3.037454	1.578582
H	-3.462049	-4.464511	0.563385
H	-0.960631	-3.240917	-1.775989
H	-0.337587	-3.617673	-0.175461
H	-1.572138	-4.673513	-0.898116
N	3.942650	0.643333	0.197303
C	4.470267	1.967333	0.621998
S	4.815203	-0.738915	0.600534
C	3.298456	2.599607	1.380229
H	4.720963	2.555313	-0.272148
H	5.376501	1.850739	1.217540
C	5.119780	-1.521921	-0.994913
O	3.972229	-1.663117	1.379007
O	6.122996	-0.316588	1.132834
C	2.084535	2.067734	0.610080
H	3.285613	2.240451	2.417249
H	3.355779	3.694094	1.399280
H	4.157663	-1.729874	-1.465909
H	5.718533	-0.841826	-1.603695
H	5.666250	-2.447504	-0.795636
C	2.427564	0.597686	0.296684
H	1.966486	2.625796	-0.327572
H	1.141447	2.136868	1.160410
C	1.779185	0.034566	-0.953753
H	2.162416	-0.033207	1.151798
H	2.046267	0.577543	-1.864919
C	1.461359	-1.349496	-1.055630
H	1.473008	-1.834315	-2.034388
H	1.686647	-2.015323	-0.221420
C	-5.302011	-0.302370	1.463684
C	-5.202471	1.046190	1.286079
H	-6.149864	-0.730798	1.992759

H   -5.969770   1.714578   1.669158

A5.3 Cartesian Coordinates for Compounds in Chapter Five

A5.3.1 Cationic *cis*-AP

A5.3.1.1 Major Enantiomer

(TFAH)$_2$

SCF Energy = -661180.3796 kcal/mol
G$_{298K,solution}$ = -661348.2092 kcal/mol
Three lowest vib. freq. (cm^{-1}): = 15.0789, 22.3492, 29.2209

C	-1.523675	-0.661321	0.000223
O	-0.342510	-0.967447	0.000305
O	-2.033339	0.546175	0.000050
H	-1.304136	1.233518	-0.000029
O	0.038553	2.298106	-0.000115
C	1.219724	1.992009	-0.000011
O	1.729427	0.784523	0.000448
H	1.000222	0.097166	0.000457
C	2.330134	3.075377	-0.000627
C	-2.634108	-1.744665	0.000392
F	-3.410927	-1.612393	-1.092034
F	-3.409881	-1.612929	1.093656
F	-2.099661	-2.969106	-0.000160
F	1.795677	4.299809	0.000357
F	3.105282	2.943775	-1.094356
F	3.107596	2.943018	1.091328

cis-4-hexenylmesylamide

SCF Energy = -551647.7023 kcal/mol
G$_{298K,solution}$ = -551640.237 kcal/mol
Three lowest vib. freq. (cm^{-1}): = 21.4471, 30.3161, 60.6092

C	-2.420916	0.436212	0.577571
H	-2.547663	-0.579912	0.967986
H	-2.212712	1.078110	1.447930
C	-1.201028	0.476565	-0.364619
H	-1.073371	1.488102	-0.771690
H	-1.389474	-0.186205	-1.221337

C	0.088806	0.052147	0.341441
H	0.300336	0.733954	1.172721
H	-0.013437	-0.954861	0.766934
C	-3.679376	0.919930	-0.095512
H	-3.638693	1.951992	-0.449303
C	-4.815091	0.239238	-0.311457
H	-5.620808	0.767857	-0.823249
C	-5.135287	-1.180672	0.069133
H	-5.410196	-1.766889	-0.818376
H	-4.303755	-1.691320	0.563208
H	-5.999471	-1.215450	0.746792
N	1.220165	0.128114	-0.604589
H	1.069407	-0.407042	-1.459686
S	2.770063	-0.265926	-0.039161
C	3.467702	1.355757	0.324927
H	4.473755	1.184762	0.715469
H	3.499564	1.935391	-0.598590
H	2.848571	1.846530	1.078894
O	3.482627	-0.827763	-1.195032
O	2.683238	-0.999996	1.231543

[Pd(κ^2-pyrox)(κ^2-TFA)]$^+$

SCF Energy = -890273.4594 kcal/mol
G$_{298K,solution}$ = -890363.6195 kcal/mol
Three lowest vib. freq. (cm^{-1}): = 13.8018, 14.6707, 25.2473

Pd	-0.017900	-0.682326	-0.202770
N	-1.104321	0.923832	-0.719395
N	-1.935246	-1.398850	0.173030
C	-2.918584	-0.494339	-0.115536
C	-2.383248	0.776595	-0.603065
C	-2.263992	-2.621518	0.638130
C	-3.624763	-2.946184	0.818591
H	-3.874315	-3.933297	1.193237
C	-4.624669	-2.029838	0.524182
H	-5.669445	-2.289290	0.665072
C	-4.266864	-0.764709	0.042254
H	-5.004634	-0.008790	-0.204276
O	-3.148941	1.802106	-0.927926

C	-2.236384	2.873201	-1.383504
C	-0.793378	2.308771	-1.169517
H	-0.263133	2.239255	-2.123624
H	-2.452119	3.752272	-0.776654
H	-2.476420	3.062256	-2.430557
H	1.691128	3.337125	-1.567540
C	1.325968	3.530513	-0.561486
C	0.063316	3.065618	-0.174669
C	-0.391700	3.313372	1.130071
H	-1.369748	2.958599	1.451237
C	0.405571	4.019606	2.031556
H	0.045100	4.209599	3.038575
C	1.665077	4.485094	1.636655
H	2.283780	5.037681	2.337944
C	2.123915	4.240365	0.340419
H	3.100716	4.599075	0.029214
C	-1.180732	-3.611557	0.952855
H	-0.581974	-3.838884	0.064886
H	-0.494550	-3.221066	1.711316
H	-1.614540	-4.542161	1.324877
O	1.969927	-0.176484	-0.546849
C	2.322174	-1.330172	-0.149422
O	1.431046	-2.149746	0.231644
C	3.808110	-1.748764	-0.155931
F	4.112844	-2.371858	0.991191
F	4.019393	-2.596165	-1.180089
F	4.599472	-0.682373	-0.302899

A$_{\text{major}}$

SCF Energy = -1111332.2 kcal/mol

G$_{298K,solution}$ = -1111323.43 kcal/mol

Three lowest vib. freq. (cm^{-1}): = 11.5857, 13.7890, 20.6137

C	-1.771332	3.674213	1.496363
C	-1.498380	2.292303	1.398150
N	-0.494415	1.856917	0.610715
C	0.295626	2.785348	-0.016637
C	0.070509	4.150251	0.043155
C	-1.009469	4.604714	0.808896
C	1.450602	2.203575	-0.701621
N	1.667886	0.934943	-0.639293
C	2.897730	0.607735	-1.402138
C	3.364768	2.030204	-1.854121

O	2.318238	2.950975	-1.373368
Pd	0.097925	-0.134417	0.134278
C	-6.170597	0.273321	-0.542743
C	-5.046478	0.273876	-1.277610
C	-4.314110	-0.905852	-1.868201
C	-2.854693	-1.031551	-1.376109
C	-2.775496	-1.420111	0.105222
N	-1.412218	-1.452346	0.706053
S	-0.496341	-2.761324	0.342651
O	-1.114345	-3.836436	-0.427454
C	-2.323141	1.325519	2.197152
C	0.124089	-3.445298	1.884662
O	0.724708	-2.049526	-0.307394
H	-3.352834	-0.717548	0.708880
H	-3.230849	-2.406943	0.251171
H	-2.333113	-0.074882	-1.528617
H	-2.330498	-1.782172	-1.979451
H	-4.846465	-1.843805	-1.672964
H	-4.290038	-0.793248	-2.961401
H	-4.602270	1.244677	-1.511769
C	-6.997249	-0.906226	-0.108953
H	-6.561553	1.243744	-0.232045
H	2.598743	0.005177	-2.266199
H	3.422185	2.150058	-2.936400
H	4.300699	2.340356	-1.387488
H	0.731709	4.829128	-0.484223
H	-1.228968	5.665547	0.880930
H	-2.593419	3.991782	2.130278
H	-3.324159	1.226413	1.759813
H	-1.862854	0.338539	2.247761
H	-2.453989	1.710757	3.214223
H	0.562318	-2.642462	2.478911
H	-0.717210	-3.909752	2.403981
H	0.875586	-4.193754	1.619962
H	-7.125660	-0.912451	0.981912
H	-8.006036	-0.847046	-0.539309
H	-6.566298	-1.867083	-0.404006
C	3.917001	-0.166723	-0.590244
C	4.425503	-1.373773	-1.083853
C	4.381133	0.321281	0.640692
C	5.390770	-2.082728	-0.362401
H	4.065135	-1.766056	-2.032128
C	5.340575	-0.388308	1.364570
H	3.993528	1.255754	1.042366
C	5.849131	-1.591576	0.862226
H	5.781612	-3.015954	-0.758038

H	5.694434	-0.001922	2.316453
H	6.600642	-2.140371	1.422877

B_{major}

SCF Energy = -1111328.148 kcal/mol

G$_{298K,solution}$ = -1111315.707 kcal/mol

Three lowest vib. freq. (cm^{-1}): = 22.3300, 27.2091, 34.2193

O	1.690055	3.354459	0.076798
C	0.768130	2.437842	-0.198641
N	1.158407	1.318817	-0.720013
C	2.648156	1.338379	-0.772983
C	2.961590	2.823426	-0.414446
C	-0.640578	2.744925	0.057139
N	-1.496402	1.753157	-0.299900
C	-2.819702	2.001124	-0.276700
C	-3.298327	3.230439	0.221742
C	-2.420242	4.211278	0.660702
C	-1.047080	3.978418	0.548278
C	-3.788881	0.996625	-0.833179
Pd	-0.385317	-0.142083	-0.672929
N	-1.958460	-1.257631	0.092003
S	-1.541623	-1.566139	1.694604
O	-0.708436	-0.412255	2.103716
C	3.316553	0.338472	0.158220
C	1.127702	-1.418964	-1.839583
C	1.095783	-1.068545	-3.304700
C	0.330278	-2.352343	-1.205912
C	-0.695397	-3.208114	-1.892759
C	-1.896521	-3.572756	-1.016575
C	-2.685555	-2.323695	-0.613291
O	-1.015200	-2.925947	1.923139
C	-3.105554	-1.451263	2.594481
H	-3.115195	-1.856106	-1.508670
H	-3.540006	-2.628836	0.008660
H	-1.563581	-4.110774	-0.124611
H	-2.563368	-4.240015	-1.576582
H	-1.030003	-2.750472	-2.830601
H	-0.169520	-4.135246	-2.172057
H	0.632976	-2.680709	-0.211773
H	2.031979	-1.136738	-1.308462
H	2.961411	1.133589	-1.801351
H	3.246707	3.427020	-1.279623

H	3.693433	2.932267	0.385477
H	-0.310219	4.726482	0.817927
H	-2.791336	5.154001	1.051209
H	-4.370119	3.401314	0.242063
H	-3.362588	0.491113	-1.702642
H	-4.031757	0.228378	-0.094747
H	-4.712562	1.498995	-1.134520
H	-3.521016	-0.451328	2.461672
H	-3.795868	-2.222555	2.247715
H	-2.854777	-1.626460	3.643926
H	1.420149	-0.037291	-3.475172
H	1.801357	-1.721546	-3.839754
H	0.112363	-1.198172	-3.762137
C	4.549013	-0.212381	-0.226050
C	5.236009	-1.077684	0.628985
C	4.690175	-1.408182	1.873054
C	3.458670	-0.869585	2.257065
C	2.773898	0.004325	1.407368
H	4.976699	0.036050	-1.196054
H	6.190485	-1.495663	0.321399
H	5.219137	-2.085946	2.537111
H	3.021913	-1.131870	3.216405
H	1.808947	0.393641	1.719107

C_{major}

SCF Energy = -1111322.22 kcal/mol

G$_{298K,solution}$ = -1111311.052 kcal/mol

Three lowest vib. freq. (cm^{-1}): = -206.6090, 9.3615, 21.4120

N	-1.941743	-1.244557	-0.064088
C	-3.018821	-1.785841	-0.913188
C	-2.733037	-3.217809	-1.375949
C	-1.291386	-3.242941	-1.911374
C	-0.335859	-2.615304	-0.951924
C	0.700728	-1.714711	-1.317091
H	-3.112576	-1.113265	-1.773211
H	-3.973285	-1.750526	-0.370833
H	-2.839597	-3.904669	-0.533185
H	-3.435972	-3.523542	-2.159191
H	-1.235205	-2.765737	-2.893800
H	-0.965761	-4.287833	-2.036096
H	-0.246919	-3.091595	0.020464
H	1.559201	-1.752093	-0.645472

Pd	-0.325693	0.000877	-0.561299
N	1.363460	1.235730	-0.619219
C	2.833180	1.039446	-0.763655
C	1.155372	2.449305	-0.227160
C	3.391839	2.454462	-0.411288
H	3.038305	0.810598	-1.814163
O	2.210245	3.245775	-0.069195
C	-0.183509	2.999148	0.013382
H	3.882627	2.951925	-1.249821
H	4.045197	2.451167	0.462076
N	-1.202728	2.120342	-0.168929
C	-0.361394	4.337715	0.345563
C	-2.463759	2.587241	-0.093178
C	-1.669380	4.808319	0.484758
H	0.499059	4.983001	0.480823
C	-2.718217	3.930434	0.249612
C	-3.603576	1.673443	-0.442080
H	-1.859574	5.843050	0.753382
H	-3.747798	4.267659	0.318180
H	-3.754851	1.674171	-1.529974
H	-3.389527	0.650962	-0.139187
H	-4.535420	2.010121	0.020820
S	-1.928579	-1.716325	1.559142
C	-3.034355	-0.573869	2.420532
H	-2.644275	0.440885	2.330881
H	-4.041817	-0.658640	2.008011
H	-3.032704	-0.893390	3.466053
O	-0.562670	-1.460153	2.048317
O	-2.519031	-3.056653	1.702042
C	1.047073	-1.471617	-2.780316
H	1.804556	-0.690723	-2.876557
H	1.467169	-2.384370	-3.226854
H	0.187441	-1.171462	-3.386737
C	3.409083	-0.067287	0.100621
C	4.453011	-0.852938	-0.408149
C	2.966789	-0.281768	1.413841
C	5.052317	-1.835743	0.385084
H	4.802193	-0.697829	-1.427456
C	3.557451	-1.271955	2.202120
H	2.142622	0.299213	1.819011
C	4.603762	-2.047330	1.691787
H	5.863097	-2.435409	-0.019107
H	3.194517	-1.440763	3.211864
H	5.063281	-2.814780	2.308204

C$_{major,tosyl}$

SCF Energy = -1256313.14 kcal/mol

$G_{298K,solution}$ = -1256287.715 kcal/mol

Three lowest vib. freq. (cm^{-1}): = -209.6559, 15.9003, 16.8976

N	-0.975182	-1.406666	-0.831950
C	-1.688760	-2.050213	-1.945520
C	-1.202605	-3.479445	-2.209653
C	0.334272	-3.432073	-2.253338
C	0.898619	-2.697556	-1.081108
C	1.950132	-1.744907	-1.155871
H	-1.525794	-1.424590	-2.829883
H	-2.768760	-2.040807	-1.746917
H	-1.539174	-4.141631	-1.408988
H	-1.598934	-3.857867	-3.158983
H	0.679409	-2.996016	-3.195222
H	0.735365	-4.456519	-2.201475
H	0.695314	-3.130552	-0.105818
H	2.551516	-1.694260	-0.247291
Pd	0.642985	-0.076581	-0.877039
N	2.185868	1.279514	-0.479547
C	3.621724	1.183894	-0.098358
C	1.789036	2.489003	-0.258496
C	3.960502	2.661319	0.277956
H	4.188704	0.887466	-0.986194
O	2.683382	3.369005	0.188220
C	0.415240	2.939400	-0.509582
H	4.645656	3.142948	-0.422709
H	4.323904	2.772280	1.300061
N	-0.426967	1.970566	-0.949812
C	0.053198	4.273562	-0.356146
C	-1.668096	2.328471	-1.332441
C	-1.252427	4.636312	-0.693867
H	0.776948	4.995794	0.004055
C	-2.103756	3.661821	-1.197551
C	-2.570209	1.297527	-1.947337
H	-1.586547	5.663853	-0.585719
H	-3.113883	3.915740	-1.502488
H	-2.092232	0.859101	-2.829785
H	-2.780570	0.488691	-1.245533
H	-3.515949	1.749095	-2.256990
S	-1.452588	-1.817389	0.743251
O	-0.410011	-1.248354	1.614934
O	-1.765181	-3.255554	0.809402

C	2.732262	-1.536306	-2.446132
H	3.426331	-0.698253	-2.349421
H	3.332951	-2.428531	-2.674752
H	2.095230	-1.334645	-3.312292
C	3.905469	0.192774	1.016342
C	5.095118	-0.548631	0.980138
C	3.038090	0.043928	2.107793
C	5.417853	-1.422253	2.022602
H	5.773987	-0.444821	0.135532
C	3.355405	-0.837228	3.144035
H	2.098644	0.588725	2.142585
C	4.546828	-1.568494	3.105912
H	6.343643	-1.989591	1.984491
H	2.666617	-0.957569	3.975229
H	4.791913	-2.252349	3.913663
C	-2.987490	-0.942339	1.061925
C	-4.209505	-1.560863	0.774564
C	-2.946560	0.328598	1.642292
C	-5.396107	-0.882312	1.051541
H	-4.230633	-2.570107	0.376216
C	-4.144908	0.987653	1.919728
H	-1.992397	0.777642	1.897965
C	-5.386381	0.398834	1.628738
H	-6.345857	-1.365643	0.835202
H	-4.115535	1.968874	2.387762
C	-6.680101	1.099388	1.968076
H	-7.120928	0.677846	2.880950
H	-6.526610	2.169248	2.140771
H	-7.420811	0.983578	1.169039

D$_{major}$

SCF Energy = -1111339.248 kcal/mol
G$_{298K,solution}$ = -1111325.479 kcal/mol
Three lowest vib. freq. (cm^{-1}): = 14.8614, 20.8206, 25.1376

N	-2.020298	-1.206387	-0.190091
C	-3.366347	-1.023501	-0.865877
C	-3.579698	-2.292320	-1.690428
C	-2.162068	-2.592225	-2.194086
C	-1.275039	-2.339476	-0.967080
C	0.129291	-1.761040	-1.139280
H	-3.291466	-0.143188	-1.508716
H	-4.146810	-0.850883	-0.121678

H	-3.952643	-3.099586	-1.052101
H	-4.296189	-2.134723	-2.502486
H	-1.907022	-1.913503	-3.014783
H	-2.043503	-3.617306	-2.557250
H	-1.264108	-3.239943	-0.344088
H	0.810179	-2.164507	-0.386278
Pd	-0.331471	0.118232	-0.492263
N	1.561213	0.998941	-0.598793
C	2.940358	0.487222	-0.831062
C	1.642495	2.248392	-0.284004
C	3.815641	1.748777	-0.553214
H	3.014075	0.206785	-1.886488
O	2.853906	2.805077	-0.242079
C	0.479742	3.096335	0.011906
H	4.395036	2.079417	-1.416806
H	4.465734	1.634500	0.315724
N	-0.720344	2.462333	-0.013038
C	0.636201	4.455336	0.264926
C	-1.825906	3.202839	0.177363
C	-0.513505	5.216021	0.495666
H	1.626120	4.896778	0.273846
C	-1.747664	4.585020	0.442063
C	-3.173321	2.544348	0.069130
H	-0.440466	6.279597	0.701870
H	-2.664623	5.145609	0.598357
H	-3.689363	2.885001	-0.837535
H	-3.070156	1.462737	0.013759
H	-3.812552	2.804242	0.920357
S	-2.188880	-1.731218	1.519000
C	-2.603510	-0.218351	2.403508
H	-1.803737	0.509183	2.263308
H	-3.569600	0.158126	2.065573
H	-2.669397	-0.521863	3.452276
O	-0.855469	-2.166580	1.932255
O	-3.333108	-2.643816	1.589316
C	0.734269	-1.814323	-2.533885
H	1.769939	-1.468574	-2.526323
H	0.752260	-2.854214	-2.896175
H	0.185602	-1.221839	-3.272960
C	3.318277	-0.708158	0.023182
C	4.097643	-1.729702	-0.536036
C	2.964339	-0.782268	1.377735
C	4.519266	-2.809588	0.245364
H	4.380788	-1.683412	-1.585956
C	3.376785	-1.865188	2.156770
H	2.350992	-0.004389	1.825573

C	4.157021	-2.879933	1.592968
H	5.125274	-3.593873	-0.199640
H	3.085060	-1.919142	3.201806
H	4.478087	-3.721172	2.200679

E$_{major}$

SCF Energy = -1111348.663 kcal/mol
G$_{298K,solution}$ = -1111332.534 kcal/mol
Three lowest vib. freq. (cm^{-1}): = 18.4708, 19.9871, 28.5313

N	3.341071	-0.292701	-0.156824
C	4.676082	0.133630	0.384878
C	4.546937	1.660774	0.555393
C	3.348167	2.042281	-0.325090
C	2.375007	0.862746	-0.127385
C	1.232801	0.762029	-1.138607
H	5.444397	-0.136440	-0.346763
H	4.900781	-0.361062	1.335679
H	4.336678	1.903772	1.602502
H	5.468003	2.177549	0.271521
H	3.644011	2.119590	-1.377048
H	2.882826	2.986215	-0.027149
H	1.946418	0.957746	0.881841
H	0.708259	1.721052	-1.092540
Pd	-0.136423	-0.614483	-0.480529
N	-1.758943	0.646251	-0.654401
C	-1.968267	2.074246	-0.999382
C	-2.911865	0.105709	-0.429030
C	-3.523766	2.157249	-1.099289
H	-1.518162	2.263973	-1.978786
O	-3.993859	0.868229	-0.592615
C	-3.073581	-1.285553	0.012341
H	-3.886473	2.251244	-2.125536
H	-3.959163	2.934432	-0.470954
N	-1.909844	-1.964003	0.165820
C	-4.328801	-1.830695	0.263163
C	-1.959007	-3.237722	0.597330
C	-4.384099	-3.154797	0.705324
H	-5.222959	-1.235119	0.117840
C	-3.195561	-3.854101	0.874180
C	-0.667952	-3.984657	0.782505
H	-5.339214	-3.626726	0.915594
H	-3.205349	-4.882402	1.221268

H	-0.857090	-5.002254	1.133799
H	-0.110650	-4.033765	-0.157920
H	-0.026989	-3.476640	1.510721
S	2.768826	-1.766215	0.361950
C	3.932460	-2.942245	-0.336008
H	3.968634	-2.804846	-1.417431
H	4.909718	-2.782134	0.123862
H	3.556342	-3.934613	-0.075909
O	1.481235	-1.992444	-0.387435
O	2.725681	-1.931053	1.819726
C	1.624615	0.434289	-2.576601
H	0.746246	0.441223	-3.231100
H	2.328701	1.179709	-2.976635
H	2.101228	-0.546037	-2.664407
C	-1.367351	3.033461	0.015299
C	-0.810111	4.240493	-0.429495
C	-1.416755	2.770773	1.391566
C	-0.314862	5.174300	0.485468
H	-0.763795	4.455703	-1.495562
C	-0.916920	3.700883	2.306553
H	-1.837041	1.836254	1.754292
C	-0.366847	4.905349	1.856096
H	0.109244	6.108345	0.127202
H	-0.959416	3.485727	3.370807
H	0.016669	5.629807	2.569138

F$_{major}$

SCF Energy = -1111332.081 kcal/mol
G$_{298K,solution}$ = -1111321.084 kcal/mol
Three lowest vib. freq. (cm^{-1}): = 13.4292, 16.9555, 29.7246

N	3.642080	-0.382139	-0.618774
C	4.337822	0.858773	-1.071724
C	3.587688	1.998777	-0.381803
C	2.133850	1.507934	-0.428362
C	2.216583	-0.025145	-0.244751
C	1.254620	-0.808889	-1.133232
H	4.249360	0.916855	-2.163512
H	5.399231	0.825061	-0.816668
H	3.934907	2.093940	0.652788
H	3.727193	2.962487	-0.882023
H	1.693409	1.740794	-1.407035
H	1.502960	1.967234	0.334219

H	2.047996	-0.296745	0.801473
H	1.234025	-0.446725	-2.163995
Pd	-0.684638	-1.057296	-0.453516
N	-1.825894	0.712505	-0.689324
C	-1.649213	2.126174	-1.111766
C	-3.094558	0.505371	-0.539202
C	-3.108732	2.536009	-1.472813
H	-1.016459	2.150010	-2.003471
O	-3.929734	1.493119	-0.856176
C	-3.647881	-0.754536	-0.022347
H	-3.313528	2.509790	-2.546626
H	-3.415996	3.490674	-1.047576
N	-2.716181	-1.706222	0.226464
C	-5.007433	-0.930979	0.208862
C	-3.107258	-2.886300	0.741301
C	-5.421740	-2.156566	0.738381
H	-5.708250	-0.134591	-0.014698
C	-4.467576	-3.130606	1.008923
C	-2.058092	-3.927606	1.020050
H	-6.472542	-2.342138	0.939399
H	-4.760119	-4.087981	1.427867
H	-1.629044	-4.305721	0.083925
H	-1.243746	-3.509204	1.621160
H	-2.481669	-4.777703	1.560642
S	4.486851	-1.275302	0.574104
C	5.709675	-2.155430	-0.412640
H	5.192824	-2.784369	-1.138591
H	6.365336	-1.436153	-0.906864
H	6.284011	-2.762171	0.292150
O	3.519494	-2.254780	1.103160
O	5.202554	-0.395368	1.508194
C	1.192172	-2.280608	-0.977845
H	1.126241	-2.844476	-1.910081
H	1.926497	-2.689652	-0.277791
H	0.196346	-2.608549	-0.404963
C	-1.038318	3.011509	-0.035927
C	-0.364354	4.176159	-0.431808
C	-1.191841	2.743460	1.329997
C	0.147676	5.059258	0.521142
H	-0.233258	4.394041	-1.490434
C	-0.672053	3.623239	2.285034
H	-1.704080	1.842960	1.657306
C	-0.003077	4.782608	1.883891
H	0.667303	5.957934	0.200398
H	-0.790821	3.401211	3.341979
H	0.399286	5.465209	2.626952

G~major~

SCF Energy = -1111329.263 kcal/mol

$G_{298K,solution}$ = -1111318.658 kcal/mol

Three lowest vib. freq. (cm^{-1}): = 14.1780, 17.0966, 23.3975

N	2.505054	-1.762769	-0.288883
C	3.927429	-2.142252	-0.560899
C	4.682578	-0.812789	-0.618760
C	3.664657	0.110480	-1.299727
C	2.293456	-0.342075	-0.710665
C	1.194066	-0.162965	-1.737594
H	3.960252	-2.666151	-1.523787
H	4.305314	-2.816465	0.210563
H	4.902453	-0.468051	0.397705
H	5.624418	-0.885693	-1.171527
H	3.678763	-0.045863	-2.385605
H	3.840567	1.172602	-1.108978
H	2.060607	0.278819	0.158580
H	1.073181	0.871522	-2.056262
Pd	-0.866288	-0.617334	-0.994662
N	-1.283850	1.483936	-0.507152
C	-0.707833	2.843835	-0.650814
C	-2.458579	1.600667	0.007476
C	-1.848382	3.756075	-0.092900
H	-0.561399	3.035375	-1.720013
O	-2.909645	2.824720	0.290610
C	-3.324952	0.447777	0.294843
H	-2.267542	4.437925	-0.834919
H	-1.557564	4.305842	0.803560
N	-2.814284	-0.762059	-0.061588
C	-4.568787	0.608335	0.892706
C	-3.540304	-1.872478	0.185536
C	-5.328264	-0.535996	1.145137
H	-4.920030	1.601100	1.149535
C	-4.807421	-1.773191	0.791022
C	-2.986373	-3.218986	-0.186653
H	-6.305917	-0.458823	1.611174
H	-5.370689	-2.681429	0.977571
H	-2.800041	-3.279202	-1.264257
H	-2.036749	-3.397340	0.327960
H	-3.685560	-4.012806	0.088200
S	1.969247	-2.101237	1.299817

C	1.637112	-3.869281	1.208560
H	0.869053	-4.046298	0.454720
H	2.559330	-4.399937	0.964155
H	1.290201	-4.164486	2.202116
O	0.691522	-1.384177	1.460068
O	3.036245	-1.895590	2.289621
C	0.669876	-1.159486	-2.540198
H	0.148724	-0.918816	-3.463056
H	1.010187	-2.183284	-2.426437
H	-0.801256	-2.125668	-1.251076
C	0.617586	3.029611	0.065863
C	1.613596	3.819914	-0.524567
C	0.839651	2.487581	1.340458
C	2.810739	4.076005	0.151881
H	1.452919	4.245794	-1.513509
C	2.038963	2.735395	2.012744
H	0.088368	1.854563	1.805474
C	3.024879	3.533684	1.422162
H	3.570910	4.698086	-0.312751
H	2.203495	2.302327	2.995437
H	3.953720	3.730993	1.950120

cis-tosyl-4-hexenylamide

SCF Energy = -696638.8737 kcal/mol
G$_{298K,solution}$ = -696618.3583 kcal/mol
Three lowest vib. freq. (cm^{-1}): = 17.4496, 23.0210, 27.1919

C	-2.331858	0.571439	0.489878
H	-2.458669	-0.365444	1.044360
H	-2.086770	1.342147	1.237359
C	-1.143247	0.436857	-0.482549
H	-1.009123	1.370028	-1.044845
H	-1.372574	-0.345477	-1.220380
C	0.161502	0.095782	0.241369
H	0.417874	0.896792	0.944516
H	0.053281	-0.830136	0.822836
C	-3.606122	0.960454	-0.214009
H	-3.569775	1.925985	-0.722311
C	-4.750820	0.265268	-0.293920
H	-5.567885	0.716801	-0.858815
C	-5.066409	-1.077872	0.306432
H	-5.365988	-1.790462	-0.474230
H	-4.223998	-1.513374	0.851374
H	-5.913037	-1.002992	1.002812

N	1.260794	-0.004950	-0.736024
H	1.078361	-0.673157	-1.485741
S	2.817037	-0.336541	-0.149412
O	3.554095	-0.828812	-1.321838
O	2.758335	-1.128010	1.089567
C	3.419896	1.296283	0.289299
C	3.626526	1.617384	1.629654
C	3.708939	2.215691	-0.724920
C	4.122811	2.883228	1.956570
H	3.413222	0.882896	2.399473
C	4.201519	3.470846	-0.380541
H	3.555496	1.945430	-1.764959
C	4.416614	3.826116	0.963695
H	4.287202	3.134836	3.001662
H	4.429824	4.187116	-1.166949
C	4.960645	5.190796	1.315814
H	5.036861	5.324768	2.399455
H	5.960155	5.340060	0.888132
H	4.318437	5.988268	0.921719

A5.3.1.2 Minor Enantiomer

A$_{minor}$

SCF Energy = -1111331.603 kcal/mol
G$_{298K,solution}$ = -1111322.673 kcal/mol
Three lowest vib. freq. (cm^{-1}): = 9.7027, 14.5262, 20.1007

C	4.157857	1.689641	0.214890
O	3.111923	2.697747	0.462351
C	1.974605	2.156952	0.039823
N	2.010794	0.947830	-0.403246
C	3.387418	0.408946	-0.240452
C	0.717205	2.903663	0.049021
N	-0.356087	2.184645	-0.408912
C	-1.536076	2.821016	-0.560186
C	-1.664574	4.175269	-0.182382
C	-0.588811	4.881333	0.330356
C	0.646293	4.232425	0.433472
Pd	0.170544	0.157862	-0.849687
C	-5.291830	-0.092369	2.273004
C	-3.979627	-0.309960	2.458771
C	-3.201855	-1.583509	2.234974
C	-2.056084	-1.430989	1.209343
C	-2.582745	-1.227270	-0.216654

N	-1.561508	-0.932359	-1.262378
S	-0.699260	-2.216891	-1.801376
O	-1.084355	-3.545526	-1.335514
C	-2.723567	2.109707	-1.138911
C	-0.765091	-2.201481	-3.597802
O	0.735351	-1.738963	-1.436974
H	-3.286105	-0.393189	-0.240586
H	-3.140505	-2.116972	-0.532412
H	-1.425046	-0.574718	1.490392
H	-1.417832	-2.321957	1.240523
H	-3.860708	-2.403308	1.926547
H	-2.756521	-1.895792	3.190256
H	-3.384727	0.520993	2.846209
C	-6.335159	-1.061106	1.787185
H	-5.671233	0.900008	2.522664
H	-0.517682	-1.200831	-3.954834
H	-1.777066	-2.487501	-3.893334
H	-0.038086	-2.937764	-3.950439
H	1.537746	4.738199	0.787832
H	-2.630423	4.654217	-0.308900
H	-3.286600	2.794363	-1.781241
H	-2.431470	1.233702	-1.718782
H	-3.400708	1.788956	-0.337319
H	-0.694746	5.920989	0.624666
H	3.738116	0.076425	-1.221401
H	4.811451	2.097677	-0.558512
H	4.706558	1.560083	1.147450
H	-7.098623	-1.222541	2.560123
H	-6.861727	-0.659863	0.910695
H	-5.924482	-2.038010	1.516830
C	3.444557	-0.756976	0.728880
C	3.915450	-2.000783	0.293090
C	3.047792	-0.604163	2.066348
C	3.993099	-3.078569	1.179780
H	4.219337	-2.131978	-0.742845
C	3.122653	-1.679821	2.952269
H	2.679048	0.355167	2.425593
C	3.596254	-2.919913	2.509344
H	4.360976	-4.039080	0.830374
H	2.815292	-1.551143	3.986418
H	3.656597	-3.756667	3.199546

B_{minor}

SCF Energy = -1111326.942 kcal/mol

G_{298K,solution} = -1111315.336 kcal/mol

Three lowest vib. freq. (cm^{-1}): = 18.7863, 28.2387, 29.6887

C	2.807766	1.765049	-2.030559
O	1.799202	2.668439	-1.476389
C	1.026805	1.936024	-0.682078
N	1.330423	0.688860	-0.509593
C	2.548637	0.399985	-1.317756
C	-0.104093	2.571719	-0.000845
N	-0.839698	1.713642	0.749846
C	-1.791696	2.204092	1.563483
C	-2.081673	3.583991	1.550270
C	-1.381396	4.449074	0.720719
C	-0.342216	3.937387	-0.062496
Pd	-0.398140	-0.367220	0.194056
C	0.912313	-2.243061	0.080380
C	-0.357763	-2.716868	-0.189184
C	-1.164410	-3.552120	0.764976
C	-2.676829	-3.326174	0.695023
C	-3.039511	-1.887840	1.076713
N	-2.426049	-0.801933	0.298098
S	-2.993876	-0.602766	-1.279246
O	-3.194835	-1.872891	-2.002987
C	-2.507242	1.295819	2.523738
C	-4.627295	0.144292	-1.070236
O	-2.109062	0.418144	-1.883202
H	-2.765998	-1.702729	2.123523
H	-4.132254	-1.772298	1.024642
H	-3.049262	-3.553527	-0.307307
H	-3.173991	-4.008059	1.396127
H	-0.809374	-3.427466	1.793666
H	-0.952558	-4.598079	0.490802
H	-0.692262	-2.725188	-1.226571
C	1.677604	-2.440240	1.362705
H	1.517137	-1.969982	-0.780033
H	-4.521877	1.093902	-0.543837
H	-5.286125	-0.541000	-0.533424
H	-5.008904	0.305471	-2.081853
H	0.273219	4.570319	-0.691727
H	-2.856695	3.960075	2.211059
H	-2.775400	1.851385	3.427798
H	-3.423953	0.895088	2.081510
H	-1.876198	0.449778	2.802642
H	-1.614579	5.509426	0.703391
H	2.294458	-0.360587	-2.062783

H	2.648068	1.729125	-3.109804
H	3.786106	2.190025	-1.804585
H	2.245572	-3.379992	1.292346
H	2.403570	-1.638673	1.515793
H	1.034692	-2.506083	2.243240
C	3.725654	-0.084479	-0.490514
C	4.515017	-1.141544	-0.961531
C	4.078000	0.550369	0.709843
C	5.640542	-1.560981	-0.244942
H	4.255978	-1.638175	-1.894984
C	5.199044	0.129742	1.428361
H	3.474667	1.371239	1.090895
C	5.982986	-0.927090	0.951947
H	6.246475	-2.379761	-0.622760
H	5.462630	0.627228	2.357647
H	6.856687	-1.251476	1.510026

C$_{\text{minor}}$

SCF Energy = -1111321.021 kcal/mol
$G_{298K,solution}$ = -1111308.072 kcal/mol
Three lowest vib. freq. (cm^{-1}): = -208.4243, -2.0144, 15.1740

C	-0.347471	-2.209497	0.060442
Pd	0.350221	-0.203955	-0.139416
N	-1.436828	0.696633	0.512284
C	-2.632444	0.249526	1.280155
C	-1.316994	1.974703	0.667829
C	-3.107056	1.574059	1.957521
H	-2.297159	-0.462006	2.041135
O	-2.218709	2.603851	1.417596
C	-0.250045	2.757966	0.033418
H	-2.981567	1.578119	3.042080
H	-4.127744	1.851585	1.692937
N	0.687339	2.014435	-0.606498
C	-0.255907	4.148480	0.051419
C	1.624177	2.651479	-1.335170
C	0.748888	4.812854	-0.656175
H	-1.027247	4.682583	0.594670
C	1.677228	4.058755	-1.362774
C	2.577683	1.836527	-2.162395
H	0.791649	5.897797	-0.667575
H	2.451747	4.543849	-1.948433
H	2.935689	0.971382	-1.606010

H	2.064619	1.463421	-3.058488
H	3.428460	2.439277	-2.490884
C	-1.240089	-2.531409	-1.130092
H	-1.520791	-3.594781	-1.118527
H	-2.162271	-1.950930	-1.091344
H	-0.757827	-2.327264	-2.090990
C	0.958833	-2.760996	0.166766
C	1.613116	-3.579198	-0.898106
H	1.378477	-2.840821	1.165932
C	3.064495	-3.141275	-1.159479
H	1.032182	-3.554860	-1.823708
H	1.605524	-4.618828	-0.534583
C	3.055907	-1.617473	-1.312940
H	3.706785	-3.421801	-0.321905
H	3.448801	-3.624438	-2.064976
H	4.086436	-1.237767	-1.343334
H	2.578284	-1.324860	-2.254857
S	3.110781	-0.770460	1.250347
C	4.074197	0.752972	1.106139
H	3.395739	1.593374	0.954557
H	4.608236	0.858419	2.054222
H	4.788529	0.656496	0.285820
O	2.059974	-0.536084	2.256576
O	4.079262	-1.861029	1.443112
N	2.312087	-0.951431	-0.229126
H	-0.865937	-2.149381	1.020322
C	-3.702603	-0.403625	0.425471
C	-4.365305	-1.542277	0.901627
C	-4.089180	0.149127	-0.804429
C	-5.398113	-2.124417	0.160019
H	-4.076747	-1.978598	1.856090
C	-5.116356	-0.434943	-1.548649
H	-3.581722	1.030446	-1.190136
C	-5.773297	-1.573006	-1.067588
H	-5.905656	-3.006128	0.541173
H	-5.405510	-0.001731	-2.502199
H	-6.574008	-2.024630	-1.646336

D$_{\text{minor}}$

SCF Energy = -1111338.132 kcal/mol
$G_{298K,solution}$ = -1111324.319 kcal/mol
Three lowest vib. freq. (cm^{-1}): = 8.6783, 26.6784, 33.1356

C	0.157875	-2.132448	0.203835
Pd	0.371643	-0.130409	-0.090798
N	-1.503950	0.535852	0.584900
C	-2.652431	-0.088927	1.294383
C	-1.602482	1.816969	0.721876
C	-3.274729	1.128988	2.043967
H	-2.260126	-0.815370	2.011945
O	-2.612703	2.291560	1.452531
C	-0.681107	2.774105	0.093141
H	-3.049450	1.141589	3.113405
H	-4.346068	1.241620	1.879557
N	0.374057	2.211821	-0.549260
C	-0.927236	4.142636	0.128228
C	1.194965	3.016643	-1.245698
C	-0.047648	4.982822	-0.561250
H	-1.782481	4.529082	0.670832
C	1.007496	4.413255	-1.260620
C	2.301175	2.398621	-2.056256
H	-0.196768	6.058397	-0.559921
H	1.695466	5.033354	-1.827740
H	2.441817	1.352438	-1.787653
H	2.051264	2.441055	-3.124230
H	3.244937	2.939006	-1.924719
C	-0.826226	-2.749131	-0.778981
H	-0.794961	-3.847966	-0.707758
H	-1.848530	-2.438442	-0.558248
H	-0.619064	-2.484764	-1.821524
C	1.639438	-2.490886	0.049913
C	2.109940	-3.356811	-1.132523
H	2.037432	-2.899883	0.982096
C	3.439633	-2.725207	-1.568453
H	1.393539	-3.321844	-1.958230
H	2.215644	-4.402630	-0.829514
C	3.151165	-1.230256	-1.435476
H	4.255023	-3.010803	-0.897805
H	3.720523	-2.995530	-2.591100
H	4.050031	-0.614739	-1.357004
H	2.551571	-0.865777	-2.274092
S	3.301358	-0.700956	1.258973
C	3.645881	1.057720	1.079747
H	2.705801	1.608897	1.087092
H	4.249348	1.310298	1.956253
H	4.221467	1.233222	0.170197
O	2.420732	-0.894863	2.410963
O	4.563267	-1.436916	1.147077
N	2.306228	-1.096414	-0.187087
H	-0.166860	-2.262372	1.240955
C	-3.636787	-0.782202	0.367035
C	-4.308982	-1.925522	0.821470
C	-3.946635	-0.265193	-0.898228
C	-5.276900	-2.543442	0.024909
H	-4.073802	-2.339669	1.800270
C	-4.910238	-0.885684	-1.697476
H	-3.428043	0.614783	-1.270209
C	-5.578286	-2.024826	-1.237568
H	-5.789810	-3.429420	0.388646
H	-5.139309	-0.479370	-2.678863
H	-6.327905	-2.505479	-1.859771

E$_{minor}$

SCF Energy = -1111348.271 kcal/mol
G$_{298K,solution}$ = -1111331.653 kcal/mol
Three lowest vib. freq. (cm^{-1}): = 20.9221, 25.8374, 28.9703

C	-0.779943	-1.535658	-0.125366
Pd	-0.140349	0.402268	0.079613
N	1.734209	0.080277	-0.723897
C	2.512815	-1.097299	-1.186674
C	2.465076	1.136845	-0.870870
C	3.786681	-0.426788	-1.789346
H	1.944164	-1.598676	-1.975893
O	3.671190	0.983318	-1.419503
C	2.033086	2.477853	-0.456885
H	3.824998	-0.471615	-2.880179
H	4.717035	-0.802067	-1.362533
N	0.802550	2.521116	0.110436
C	2.842778	3.594169	-0.640897
C	0.325759	3.709982	0.523371
C	2.352375	4.829408	-0.210167
H	3.818001	3.492252	-1.103326
C	1.092659	4.882469	0.372931
C	-1.043429	3.761250	1.140734
H	2.946261	5.730678	-0.329278
H	0.684113	5.826701	0.718533
H	-1.128251	3.041854	1.960192
H	-1.257758	4.762452	1.523504
H	-1.808154	3.500767	0.400891
C	-0.802940	-2.217670	1.238356
H	-1.132252	-3.264175	1.152032

H	0.198907	-2.233130	1.677299
H	-1.477706	-1.718333	1.939275
C	-2.093416	-1.540092	-0.910355
C	-2.577648	-2.916094	-1.411613
H	-1.984658	-0.890531	-1.792657
C	-4.042579	-2.656929	-1.792392
H	-2.506046	-3.659588	-0.610413
H	-1.973936	-3.261280	-2.256366
C	-4.549782	-1.677767	-0.714636
H	-4.097024	-2.187080	-2.780383
H	-4.644206	-3.569596	-1.824003
H	-5.183402	-0.895600	-1.145885
H	-5.105344	-2.188516	0.078486
S	-3.358331	0.489063	0.352088
C	-4.537522	0.488016	1.706256
H	-4.202914	-0.219373	2.466099
H	-4.554422	1.508486	2.096517
H	-5.521263	0.222852	1.313685
O	-2.024571	0.779954	0.989910
O	-3.812388	1.418809	-0.688998
N	-3.296394	-1.105628	-0.116273
H	-0.034638	-2.010686	-0.772146
C	2.808784	-2.094989	-0.080567
C	2.707101	-3.467034	-0.344256
C	3.246607	-1.673137	1.183220
C	3.040002	-4.406118	0.636626
H	2.370072	-3.807009	-1.321800
C	3.575292	-2.609880	2.165549
H	3.326651	-0.612249	1.408434
C	3.473448	-3.978498	1.894158
H	2.959899	-5.467321	0.417730
H	3.911751	-2.271842	3.141843
H	3.731836	-4.705932	2.658530

F_{minor}

SCF Energy = -1111329.947 kcal/mol
G_{298K,solution} = -1111318.987 kcal/mol
Three lowest vib. freq. (cm⁻¹): = -116.6190, 14.9230, 25.9649

C	-1.297890	-0.297587	-1.547263
Pd	0.812820	-0.394193	-0.994216
N	0.786569	1.190154	0.480710
C	-0.199401	1.978319	1.257465

C	1.927492	1.303497	1.065352
C	0.714111	2.767834	2.241356
H	-0.811782	1.256026	1.809863
O	2.021486	2.117459	2.119397
C	3.118206	0.561707	0.628056
H	0.408248	2.696459	3.285174
H	0.843790	3.814042	1.953401
N	2.899844	-0.317610	-0.386147
C	4.361525	0.762288	1.214807
C	3.941947	-1.026828	-0.867556
C	5.442435	0.024669	0.727529
H	4.467441	1.474626	2.025049
C	5.227200	-0.864982	-0.317345
C	3.718648	-1.990805	-1.999774
H	6.432999	0.147585	1.154959
H	6.048144	-1.447286	-0.722462
H	3.281167	-1.480818	-2.864416
H	4.661685	-2.448352	-2.309360
H	3.031320	-2.789990	-1.701277
C	-0.706306	-1.168666	-2.465283
H	-0.394763	-0.809523	-3.441789
H	1.028226	-1.567676	-1.985260
H	-0.891897	-2.235935	-2.382807
C	-2.310692	-0.735865	-0.504136
C	-3.759201	-0.598654	-1.059190
H	-2.216269	-0.092589	0.375293
C	-4.537721	-1.706592	-0.340232
H	-3.763543	-0.773461	-2.142099
H	-4.154449	0.405626	-0.881436
C	-3.519238	-2.848197	-0.307914
H	-4.790944	-1.406773	0.682889
H	-5.461913	-1.980705	-0.858359
H	-3.714370	-3.571864	0.486315
H	-3.484316	-3.384087	-1.264029
S	-1.510755	-2.415934	1.444413
C	-0.828728	-4.076555	1.305006
H	-0.069915	-4.083134	0.521688
H	-0.388749	-4.304838	2.279124
H	-1.632495	-4.781868	1.084854
O	-0.399665	-1.452336	1.549120
O	-2.539082	-2.433991	2.494809
N	-2.195560	-2.176339	-0.103880
H	-1.404642	0.749039	-1.833105
C	-1.099611	2.863122	0.418777
C	-2.433498	3.051164	0.807019
C	-0.614341	3.543471	-0.707770

C -3.269674   3.908657   0.085089
H -2.820426   2.531050   1.681543
C -1.451639   4.393227 -1.435102
H   0.417091   3.403824 -1.022338
C -2.780533   4.579313 -1.039155
H -4.299129   4.052222   0.401827
H -1.065834   4.913442 -2.307702
H -3.428751   5.245099 -1.601996

G$_{minor}$

SCF Energy = -1111330.006 kcal/mol
G$_{298K,solution}$ = -1111319.108 kcal/mol
Three lowest vib. freq. (cm^{-1}): = 13.2932, 24.3054, 28.4029

C -1.374510 -0.229517 -1.477835
Pd 0.792561 -0.356996 -1.019152
N   0.729911   1.201695   0.497520
C -0.261179   1.981149   1.276253
C   1.864549   1.299561   1.096813
C   0.640561   2.732269   2.301435
H -0.895800   1.255062   1.797756
O   1.949336   2.087480   2.171071
C   3.062108   0.574238   0.650983
H   0.321602   2.620095   3.337802
H   0.773003   3.788822   2.056322
N   2.862931 -0.269284 -0.397967
C   4.296113   0.760173   1.261284
C   3.917493 -0.950906 -0.893799
C   5.388691   0.048482   0.761947
H   4.385932   1.442997   2.098382
C   5.193844 -0.800434 -0.319767
C   3.722860 -1.869899 -2.067723
H   6.372451   0.161342   1.207440
H   6.024578 -1.359713 -0.737084
H   3.270281 -1.336027 -2.909526
H   4.679743 -2.284813 -2.394446
H   3.060014 -2.702279 -1.806689
C -0.798249 -1.002846 -2.476004
H -0.493412 -0.556292 -3.417904
H   1.072313 -1.505797 -2.006992
H -0.940464 -2.079363 -2.473680
C -2.317924 -0.769531 -0.419263
C -3.798153 -0.634039 -0.888022

H -2.188080 -0.190021   0.498735
C -4.504704 -1.828148 -0.234145
H -3.853898 -0.712245 -1.980559
H -4.214882   0.335758 -0.601565
C -3.448262 -2.929407 -0.345866
H -4.719317 -1.626874   0.821443
H -5.442601 -2.090300 -0.733502
H -3.584255 -3.729865   0.384333
H -3.434897 -3.373397 -1.348537
S -1.395853 -2.558570   1.372512
C -0.614096 -4.150309   1.062467
H   0.115266 -4.033365   0.260073
H -0.127376 -4.437584   1.997964
H -1.378967 -4.883730   0.799291
O -0.345102 -1.537136   1.536287
O -2.388705 -2.739914   2.440822
N -2.142389 -2.228973 -0.131334
H -1.489735   0.839487 -1.655768
C -1.130973   2.900170   0.441529
C -2.469926   3.099355   0.805768
C -0.611066   3.600656 -0.656894
C -3.277100   3.987586   0.088004
H -2.883665   2.564131   1.658652
C -1.419314   4.481408 -1.380160
H   0.424455   3.452365 -0.953511
C -2.753543   4.678263 -1.008230
H -4.311039   4.139031   0.385820
H -1.006752   5.016823 -2.231018
H -3.379369   5.367548 -1.568059

C$_{minor,tosyl}$

SCF Energy = -1256311.719 kcal/mol
G$_{298K,solution}$ = -1256287.323 kcal/mol
Three lowest vib. freq. (cm^{-1}): = -204.1974, 9.2987, 10.6517

C -1.606607   2.233998 -0.218409
Pd -0.532430   0.428159   0.172214
N -2.045905 -0.861663 -0.516779
C -3.278471 -0.730358 -1.340363
C -1.645653 -2.088985 -0.591291
C -3.368949 -2.131723 -2.021728
H -3.106911   0.042672 -2.095444
O -2.346223 -2.931991 -1.347899

C	-0.478620	-2.591540	0.142998
H	-3.113616	-2.114686	-3.083796
H	-4.327211	-2.628062	-1.868744
N	0.228612	-1.633515	0.793160
C	-0.182678	-3.948806	0.203929
C	1.231512	-2.013564	1.606923
C	0.888147	-4.343962	1.009525
H	-0.781518	-4.662588	-0.350405
C	1.579987	-3.373822	1.723199
C	1.953735	-0.971682	2.412407
H	1.160257	-5.392073	1.091285
H	2.396505	-3.650740	2.382391
H	2.547211	-0.321527	1.764995
H	1.237841	-0.344014	2.952404
H	2.620550	-1.442812	3.139004
C	-2.682789	2.410121	0.845000
H	-3.153577	3.399431	0.747952
H	-3.468981	1.663292	0.731553
H	-2.292316	2.328854	1.863980
C	-0.436487	3.039336	-0.211606
C	-0.075230	3.985953	0.887239
H	0.064757	3.197353	-1.162368
C	1.404264	3.867833	1.292262
H	-0.723026	3.842990	1.756408
H	-0.269168	4.998183	0.498939
C	1.703087	2.376561	1.480503
H	2.046610	4.280887	0.511957
H	1.588387	4.422561	2.219574
H	2.780507	2.214278	1.620221
H	1.209118	1.999783	2.382803
S	2.152126	1.548050	-1.060145
O	1.306604	0.873687	-2.060993
O	2.669282	2.901838	-1.324891
N	1.223270	1.555071	0.359502
H	-1.983527	2.031982	-1.224151
C	-4.516022	-0.375120	-0.534970
C	-5.466760	0.493721	-1.087401
C	-4.764803	-0.954052	0.717655
C	-6.649118	0.782214	-0.399356
H	-5.284632	0.949929	-2.058722
C	-5.943527	-0.662480	1.408045
H	-4.034225	-1.624041	1.164435
C	-6.888541	0.205412	0.850735
H	-7.378171	1.457427	-0.838544
H	-6.124744	-1.112920	2.380096
H	-7.805520	0.429849	1.388197

C	3.579579	0.507627	-0.738758
C	3.523022	-0.852798	-1.052081
C	4.752890	1.079800	-0.232893
C	4.652602	-1.645825	-0.841691
H	2.621615	-1.271833	-1.487323
C	5.866869	0.268875	-0.020164
H	4.804312	2.147797	-0.047475
C	5.838462	-1.103930	-0.320909
H	4.618456	-2.699879	-1.106972
H	6.781325	0.714681	0.364034
C	7.069129	-1.956723	-0.125902
H	7.850556	-1.682203	-0.845906
H	7.493813	-1.822786	0.875899
H	6.849782	-3.019879	-0.264072

A5.3.2 Cationic trans-AP

A5.3.2.1 Major Enantiomer

H$_{major}$

SCF Energy = -1441924.56 kcal/mol
G$_{298K,solution}$ = -1441997.246 kcal/mol
Three lowest vib. freq. (cm^{-1}): = 12.4995, 13.3819, 15.9769

C	-0.050446	1.045839	1.541990
C	0.641714	0.830569	0.349082
H	0.458288	1.547493	-0.451030
Pd	-1.313618	-0.308443	0.238053
N	-2.295845	1.185315	-0.790658
C	-2.060903	2.612787	-1.143900
C	-3.269682	0.732213	-1.517112
C	-3.162873	2.859086	-2.223181
H	-1.069325	2.692174	-1.601930
O	-3.839682	1.566773	-2.373274
C	-3.768699	-0.636696	-1.382221
H	-2.764581	3.130059	-3.201792
H	-3.915901	3.581962	-1.906342
N	-3.141026	-1.360164	-0.410431
C	-4.828303	-1.112975	-2.137340
C	-3.619171	-2.580229	-0.101888
C	-5.287473	-2.408264	-1.869747
H	-5.279062	-0.486669	-2.899062
C	-4.695549	-3.121681	-0.841004
C	-3.052522	-3.367159	1.043474

H	-6.107261	-2.833007	-2.440909
H	-5.053184	-4.112403	-0.578276
H	-2.384180	-4.155634	0.678184
H	-2.493130	-2.741399	1.737194
H	-3.866058	-3.862600	1.583405
C	1.900153	0.023817	0.166763
H	1.853275	-0.518262	-0.785811
H	2.015078	-0.717846	0.959858
C	-2.135928	3.559424	0.038834
C	-1.179505	4.574772	0.172118
C	-3.179625	3.472852	0.973150
C	-1.262952	5.493267	1.223436
H	-0.368456	4.655062	-0.549236
C	-3.259374	4.385753	2.026741
H	-3.930481	2.690478	0.885609
C	-2.301505	5.398269	2.153090
H	-0.518862	6.279548	1.313535
H	-4.069921	4.310077	2.746159
H	-2.367708	6.110363	2.970637
H	-0.724319	1.900927	1.568973
C	0.274105	0.452629	2.881536
H	0.872600	1.188064	3.440230
H	-0.635814	0.279480	3.465751
H	0.834507	-0.480018	2.820408
O	-0.358852	-1.875920	1.090955
C	0.046679	-2.758680	0.223848
O	-0.138588	-2.759417	-0.982013
C	0.850794	-3.902525	0.913036
F	1.279371	-4.802002	0.025518
F	1.925975	-3.397431	1.561728
F	0.080061	-4.540536	1.825215
C	3.130022	0.964347	0.148891
H	3.024141	1.723741	-0.636404
H	3.192984	1.502376	1.104877
C	4.423611	0.176096	-0.094069
H	4.393522	-0.312981	-1.070750
H	4.533905	-0.616996	0.659047
S	7.040858	0.530595	-0.770823
O	8.054014	0.557865	0.290872
O	6.738575	-0.691760	-1.524477
C	7.444508	1.828613	-1.952703
H	8.388377	1.539664	-2.422016
H	6.647057	1.887278	-2.695194
H	7.557577	2.772385	-1.416091
N	5.573719	1.097273	-0.088782
H	5.796845	1.435224	0.847251

I_{major}

SCF Energy = -1441915.646 kcal/mol

$G_{298K,solution}$ = -1441983.352 kcal/mol

Three lowest vib. freq. (cm^{-1}): = -203.8353, 12.5162, 17.0804

C	-1.039873	0.568470	0.437918
H	-1.569629	-0.382661	0.502061
Pd	0.865856	-0.020010	-0.190060
N	0.289998	-1.967389	-0.545701
C	-0.898550	-2.803154	-0.236630
C	1.210769	-2.733810	-1.031881
C	-0.511826	-4.160563	-0.900319
H	-1.771626	-2.376725	-0.738491
O	0.905599	-4.015845	-1.231969
C	2.559031	-2.254039	-1.344573
H	-1.043151	-4.348612	-1.836655
H	-0.605588	-5.016071	-0.231534
N	2.783215	-0.952380	-1.022087
C	3.508115	-3.090642	-1.919585
C	4.000417	-0.432750	-1.278095
C	4.770483	-2.555105	-2.186288
H	3.258632	-4.120574	-2.148217
C	5.008292	-1.226592	-1.865784
C	4.289917	0.993830	-0.914950
H	5.547281	-3.166129	-2.636109
H	5.977115	-0.777797	-2.059709
H	3.489100	1.659634	-1.243004
H	4.376796	1.091796	0.173463
H	5.232536	1.319891	-1.361632
C	-1.058379	1.254879	1.802245
H	-2.088458	1.365557	2.189367
H	-0.526880	0.649256	2.541028
H	-0.601762	2.246425	1.797626
C	-1.186116	-2.908757	1.253476
C	-2.514677	-3.058345	1.677704
C	-0.158945	-2.925997	2.206857
C	-2.810883	-3.234076	3.032210
H	-3.320232	-3.037102	0.946462
C	-0.455948	-3.092353	3.562284
H	0.875278	-2.793450	1.901584
C	-1.781324	-3.250180	3.977977
H	-3.843486	-3.357599	3.347932

H	0.348966	-3.096264	4.291971
H	-2.009848	-3.383009	5.031741
O	1.478286	1.910308	0.144856
C	2.103724	2.144646	1.252653
O	2.466939	1.359858	2.115238
C	2.367462	3.671602	1.428888
F	3.111469	3.938507	2.506101
F	2.991098	4.197007	0.348362
F	1.181753	4.332605	1.569947
C	-1.553898	1.338951	-0.726473
C	-1.089869	2.750885	-1.054494
H	-1.663356	0.727552	-1.623315
C	-2.254179	3.473090	-1.739216
H	-0.208921	2.689040	-1.699563
H	-0.778835	3.280245	-0.151017
C	-3.464762	3.165112	-0.856703
H	-3.423254	1.583432	0.560331
H	-2.089131	4.551987	-1.812280
H	-2.423058	3.086944	-2.750489
H	-3.458907	3.758737	0.062011
H	-4.420841	3.308764	-1.365119
S	-4.355838	0.533431	-1.299382
O	-3.907701	-0.766902	-0.812345
C	-5.997371	0.884175	-0.640524
H	-6.283170	1.908384	-0.885390
H	-6.664412	0.178081	-1.144724
H	-5.998852	0.699829	0.435937
N	-3.294589	1.722579	-0.446387
O	-4.281521	0.911035	-2.703536

J$_{major}$

SCF Energy = -1441915.909 kcal/mol
G$_{298K,solution}$ = -1441983.082 kcal/mol
Three lowest vib. freq. (cm^{-1}): = 14.7277, 18.3868, 21.9659

C	-1.047737	0.536218	0.373870
H	-1.568288	-0.420092	0.457701
Pd	0.873112	-0.011936	-0.191878
N	0.355463	-1.974459	-0.561113
C	-0.824027	-2.835177	-0.293271
C	1.306034	-2.720250	-1.021400
C	-0.390852	-4.181369	-0.951361
H	-1.689561	-2.423310	-0.819941

O	1.032948	-4.008409	-1.234505
C	2.653494	-2.213633	-1.293633
H	-0.887611	-4.372949	-1.905935
H	-0.491652	-5.042973	-0.291421
N	2.840955	-0.907716	-0.967542
C	3.637005	-3.032116	-1.836847
C	4.054917	-0.364339	-1.185806
C	4.896175	-2.471567	-2.064317
H	3.416055	-4.067272	-2.071122
C	5.097183	-1.137970	-1.739082
C	4.300746	1.068675	-0.815904
H	5.699048	-3.067572	-2.487770
H	6.062668	-0.670281	-1.902763
H	3.498303	1.716011	-1.175851
H	4.343350	1.170657	0.274731
H	5.252359	1.414613	-1.227321
C	-1.105347	1.246005	1.729027
H	-2.137896	1.310338	2.125294
H	-0.544878	0.682137	2.479446
H	-0.698565	2.259418	1.707139
C	-1.157468	-2.957200	1.186185
C	-2.492107	-3.168729	1.562761
C	-0.165021	-2.933597	2.175225
C	-2.828098	-3.364837	2.905032
H	-3.271551	-3.181845	0.803384
C	-0.502288	-3.119872	3.518809
H	0.872220	-2.754245	1.906747
C	-1.832833	-3.339361	3.886824
H	-3.864402	-3.538082	3.183220
H	0.275860	-3.091945	4.276490
H	-2.092059	-3.488738	4.931243
O	1.433838	1.936302	0.152805
C	2.023719	2.196162	1.272972
O	2.384565	1.430956	2.154584
C	2.245477	3.731112	1.439624
F	2.933609	4.030851	2.545153
F	2.904978	4.256793	0.380653
F	1.039816	4.368164	1.518306
C	-1.637627	1.296837	-0.795356
C	-1.095292	2.671120	-1.201531
H	-1.733430	0.652929	-1.672910
C	-2.271038	3.426922	-1.827906
H	-0.261689	2.539676	-1.895466
H	-0.700829	3.206437	-0.335398
C	-3.428999	3.133144	-0.876008
H	-3.322954	1.562595	0.547733

H	-2.090473	4.502975	-1.902927
H	-2.505002	3.050521	-2.829820
H	-3.367575	3.728555	0.039379
H	-4.417187	3.258523	-1.322587
S	-4.382683	0.494336	-1.263795
O	-3.880867	-0.819003	-0.882662
C	-5.925937	0.829988	-0.394830
H	-6.223843	1.867338	-0.556233
H	-6.659018	0.154805	-0.847340
H	-5.799874	0.592546	0.663801
N	-3.218575	1.684158	-0.465714
O	-4.463326	0.934621	-2.647636

K$_{major}$

SCF Energy = -1111339.062 kcal/mol
G$_{298K,solution}$ = -1111324.783 kcal/mol
Three lowest vib. freq. (cm^{-1}): = 17.7169, 20.8456, 33.1560

C	-0.499580	-1.720078	-1.375843
H	-0.181850	-1.454875	-2.392015
Pd	-0.386653	0.068798	-0.391788
N	1.616393	0.510255	-0.749561
C	2.800997	-0.285335	-1.166701
C	1.996571	1.737887	-0.613465
C	3.800385	0.832915	-1.578336
H	2.531153	-0.890419	-2.037004
O	3.252609	2.035660	-0.954211
C	1.140724	2.817791	-0.106322
H	3.825759	1.014821	-2.656699
H	4.808210	0.688772	-1.190960
N	-0.118739	2.450520	0.240873
C	1.628881	4.117867	-0.011785
C	-0.946621	3.409593	0.689234
C	0.768989	5.108389	0.469622
H	2.646658	4.339487	-0.311464
C	-0.524961	4.748603	0.815956
C	-2.351965	3.039850	1.074546
H	1.105598	6.136535	0.562433
H	-1.226786	5.490352	1.185712
H	-2.605823	2.053153	0.692178
H	-2.464750	3.034025	2.166268
H	-3.069506	3.767024	0.679529
C	0.280625	-2.894996	-0.817436

H	0.029154	-3.798331	-1.397593
H	1.359739	-2.752168	-0.893500
H	0.030039	-3.095186	0.226612
C	3.342553	-1.190875	-0.069218
C	4.096192	-2.313933	-0.442598
C	3.179151	-0.901490	1.290733
C	4.679584	-3.132366	0.526621
H	4.225004	-2.555358	-1.496474
C	3.758567	-1.724049	2.261948
H	2.589530	-0.043126	1.600217
C	4.510411	-2.838884	1.883418
H	5.258530	-4.000057	0.222847
H	3.620138	-1.493099	3.314632
H	4.958640	-3.477211	2.639471
C	-2.015550	-1.832421	-1.277196
C	-2.842193	-1.501204	-2.526363
H	-2.330392	-2.797561	-0.866924
C	-4.106025	-0.828020	-1.975210
H	-3.053694	-2.405617	-3.104647
H	-2.290493	-0.808210	-3.174260
C	-3.547520	0.069476	-0.869821
H	-4.647799	-0.251584	-2.731291
H	-4.790526	-1.567904	-1.548586
H	-3.133886	0.994426	-1.278991
H	-4.285012	0.322060	-0.105022
S	-2.867396	-1.497476	1.289397
O	-1.795133	-2.438498	1.606627
C	-2.834768	-0.169360	2.503600
H	-3.605359	0.565890	2.272054
H	-3.065225	-0.664061	3.451600
H	-1.836506	0.268052	2.532928
N	-2.395710	-0.708582	-0.258204
O	-4.249530	-1.957966	1.133433

L$_{major}$

SCF Energy = -1111344.706 kcal/mol
G$_{298K,solution}$ = -1111329.382 kcal/mol
Three lowest vib. freq. (cm^{-1}): = 17.6729, 21.5789, 29.6193

C	0.617312	-1.670787	-0.307872
H	0.181933	-2.038151	0.630488
Pd	0.312962	0.357737	-0.264961
N	-1.561579	0.257258	0.654298

C	-2.389308	-0.787500	1.318091
C	-2.061083	1.413604	0.950556
C	-3.346930	0.068869	2.202488
H	-1.732934	-1.395321	1.947913
O	-3.120098	1.444082	1.761831
C	-1.534003	2.681873	0.427791
H	-3.106629	0.029037	3.267812
H	-4.401293	-0.157625	2.044360
N	-0.405166	2.558299	-0.311787
C	-2.181253	3.892045	0.657039
C	0.102281	3.654736	-0.906150
C	-1.638969	5.038471	0.070151
H	-3.077225	3.926843	1.266376
C	-0.502725	4.913758	-0.719706
C	1.298940	3.500144	-1.802536
H	-2.105185	6.007687	0.220235
H	-0.070062	5.783023	-1.204766
H	2.081468	2.904828	-1.328728
H	1.014071	2.971716	-2.721297
H	1.704928	4.474767	-2.085176
C	-0.129830	-2.208239	-1.528913
H	-0.084226	-3.308178	-1.560786
H	-1.186520	-1.935879	-1.522240
H	0.314388	-1.839034	-2.461483
C	-3.120777	-1.694842	0.344872
C	-3.162400	-3.073776	0.585868
C	-3.815098	-1.172051	-0.756028
C	-3.883742	-3.921447	-0.260400
H	-2.629555	-3.490743	1.438439
C	-4.531773	-2.017868	-1.604974
H	-3.790690	-0.104292	-0.961416
C	-4.567655	-3.394777	-1.358802
H	-3.908782	-4.989342	-0.061840
H	-5.062217	-1.603241	-2.457748
H	-5.126851	-4.051383	-2.019300
C	2.091597	-2.071753	-0.372460
C	2.374340	-3.544633	-0.001235
H	2.465490	-1.896249	-1.389853
C	3.850042	-3.544777	0.420520
H	2.170561	-4.212504	-0.842492
H	1.733370	-3.848782	0.836547
C	3.986449	-2.243012	1.220620
H	4.127155	-4.422117	1.012608
H	4.498916	-3.513000	-0.462103
H	3.733847	-2.384236	2.277123
H	4.989387	-1.812322	1.151622

S	3.498720	0.144539	0.064076
O	2.361984	0.679678	-0.773220
C	3.634135	1.139510	1.556525
H	4.365387	0.666409	2.216298
H	3.994175	2.123639	1.246846
H	2.655265	1.200645	2.033318
N	2.961387	-1.331058	0.613112
O	4.805146	0.127300	-0.594838

M$_{major}$

SCF Energy = -1111328.192 kcal/mol
G$_{298K,solution}$ = -1111318.421 kcal/mol
Three lowest vib. freq. (cm^{-1}): = -451.7016, 14.7631, 18.7352

C	-1.156005	-0.847367	-1.119597
H	-1.395837	0.208774	-1.227665
Pd	0.958573	-0.861854	-0.769909
N	1.032587	0.665764	0.722713
C	0.226805	1.837792	1.161685
C	2.165630	0.710272	1.334727
C	1.033142	2.313432	2.406306
H	-0.772294	1.502153	1.448884
O	2.334690	1.642536	2.272224
C	3.277227	-0.189186	0.990125
H	0.599487	1.978873	3.352256
H	1.222419	3.386068	2.430097
N	3.031896	-1.006574	-0.069867
C	4.482715	-0.172418	1.680351
C	4.002734	-1.843669	-0.486858
C	5.492337	-1.039627	1.254581
H	4.617383	0.501832	2.518711
C	5.248707	-1.870320	0.168017
C	3.734267	-2.742871	-1.661612
H	6.451640	-1.061049	1.762852
H	6.015898	-2.549255	-0.189313
H	2.929708	-3.450165	-1.431461
H	3.424712	-2.158781	-2.534767
H	4.627389	-3.314347	-1.926314
C	-0.619035	-1.512263	-2.239834
H	-0.440372	-0.950307	-3.153315
H	0.993304	-1.949877	-1.909665
H	-0.779044	-2.576321	-2.389370
C	0.102844	2.881494	0.060851

C	-1.134736	3.499034	-0.166589
C	1.216176	3.285315	-0.692407
C	-1.253559	4.511619	-1.124050
H	-2.006586	3.179937	0.397022
C	1.095900	4.293255	-1.651247
H	2.185113	2.816366	-0.537293
C	-0.140511	4.910652	-1.867991
H	-2.217439	4.985913	-1.287875
H	1.966175	4.598224	-2.226120
H	-0.233364	5.697394	-2.611570
C	-1.905631	-1.531928	0.021697
C	-1.698160	-3.049365	0.217992
H	-1.632984	-1.018127	0.949127
C	-3.038499	-3.538292	0.785993
H	-0.848481	-3.249781	0.877688
H	-1.502575	-3.553284	-0.735075
C	-4.050125	-2.715467	-0.015869
H	-3.182509	-4.616752	0.668725
H	-3.122419	-3.294129	1.851096
H	-4.231771	-3.150261	-1.006033
H	-5.008601	-2.603505	0.495962
S	-4.102798	-0.086992	0.643641
O	-3.086863	0.983346	0.643150
C	-5.448146	0.389226	-0.451962
H	-6.127410	-0.457617	-0.570435
H	-5.965461	1.218306	0.037552
H	-5.029126	0.697644	-1.410627
N	-3.391526	-1.386389	-0.201343
O	-4.685541	-0.521671	1.920640

N$_{major}$

SCF Energy = -1111331.288 kcal/mol
G$_{298K,solution}$ = -1111320.01 kcal/mol
Three lowest vib. freq. (cm^{-1}): = 14.9321, 15.5530, 26.9383

C	-1.243582	-0.439660	-1.041262
H	-1.369888	0.468503	-0.460776
Pd	0.963490	-0.781925	-0.817472
N	1.234228	0.926901	0.507849
C	0.489037	2.104997	1.017664
C	2.340241	0.835800	1.158312
C	1.499197	2.718859	2.038007
H	-0.399153	1.728046	1.534750

O	2.614211	1.763486	2.076264
C	3.302923	-0.254939	0.932298
H	1.105310	2.795645	3.052070
H	1.908550	3.678503	1.716319
N	2.914743	-1.187814	0.017640
C	4.512383	-0.311000	1.611594
C	3.741618	-2.219069	-0.257193
C	5.372470	-1.376935	1.335028
H	4.762291	0.459766	2.331766
C	4.983009	-2.325357	0.398987
C	3.328829	-3.252896	-1.267237
H	6.328503	-1.460656	1.843004
H	5.629977	-3.163273	0.162034
H	2.418241	-3.768703	-0.944425
H	3.119893	-2.789716	-2.236931
H	4.117861	-3.997133	-1.400787
C	-0.644925	-0.342451	-2.283532
H	-0.335511	0.630382	-2.659639
H	0.911815	-2.075614	-1.641929
H	-0.701568	-1.140451	-3.016201
C	0.053819	3.058195	-0.079706
C	-1.237070	3.602397	-0.049231
C	0.933345	3.442882	-1.103271
C	-1.642012	4.522118	-1.021842
H	-1.925978	3.305866	0.738541
C	0.527413	4.356065	-2.079001
H	1.938157	3.027820	-1.142893
C	-0.761493	4.899425	-2.038918
H	-2.643299	4.942528	-0.983945
H	1.216884	4.646782	-2.867017
H	-1.074936	5.613631	-2.795190
C	-2.026865	-1.619729	-0.487791
C	-2.290489	-2.802262	-1.434808
H	-1.507023	-1.991330	0.406394
C	-3.566514	-3.435709	-0.864899
H	-1.441514	-3.490957	-1.466000
H	-2.477070	-2.442589	-2.453925
C	-4.409174	-2.212685	-0.486059
H	-4.076122	-4.086601	-1.581481
H	-3.337010	-4.026528	0.029311
H	-4.992600	-1.842619	-1.336611
H	-5.090219	-2.421158	0.343010
S	-3.543083	-0.554384	1.478254
O	-2.373485	0.326226	1.667929
C	-5.023038	0.464328	1.367107
H	-5.880011	-0.166025	1.121861

H	-5.158950	0.907872	2.356835
H	-4.866870	1.233594	0.609671
N	-3.411475	-1.158769	-0.108602
O	-3.791751	-1.623884	2.454573

I_{major,tosyl}

SCF Energy = -1586911.05 kcal/mol
$G_{298K,solution}$ = -1586962.968 kcal/mol
Three lowest vib. freq. (cm^{-1}): = -251.1404,
12.4967, 15.1188

C	-0.161392	0.418030	0.563408
H	-0.531410	-0.600761	0.679686
Pd	1.788210	0.096637	-0.153883
N	1.442625	-1.891908	-0.566061
C	0.367191	-2.874831	-0.275797
C	2.424889	-2.517937	-1.127333
C	0.869008	-4.126820	-1.057292
H	-0.571076	-2.515029	-0.707179
O	2.256332	-3.811643	-1.400408
C	3.698134	-1.868428	-1.448739
H	0.335352	-4.288420	-1.997430
H	0.878138	-5.039926	-0.462553
N	3.777603	-0.565450	-1.069087
C	4.722257	-2.559925	-2.084603
C	4.918330	0.105484	-1.325529
C	5.906376	-1.868046	-2.350753
H	4.588130	-3.600381	-2.357960
C	5.996323	-0.536987	-1.970704
C	5.045607	1.539006	-0.902897
H	6.737046	-2.362188	-2.845644
H	6.900917	0.031121	-2.162026
H	4.178420	2.124363	-1.216420
H	5.110746	1.603047	0.189276
H	5.949449	1.985333	-1.324943
C	-0.232727	1.154387	1.896482
H	-1.254700	1.118021	2.312992
H	0.414145	0.673953	2.635428
H	0.060628	2.203744	1.831583
C	0.164986	-3.121497	1.211860
C	-1.113046	-3.477219	1.667704
C	1.226607	-3.069624	2.125302
C	-1.323153	-3.788908	3.013551
H	-1.946394	-3.505402	0.968947

C	1.013871	-3.372634	3.473046
H	2.219985	-2.777119	1.796354
C	-0.259638	-3.736746	3.919571
H	-2.316279	-4.070234	3.353786
H	1.843459	-3.321030	4.172691
H	-0.422234	-3.975365	4.966935
O	2.156166	2.082404	0.190301
C	2.765640	2.388072	1.289642
O	3.235655	1.649381	2.141461
C	2.854932	3.935277	1.463954
F	3.535243	4.283973	2.560318
F	3.454204	4.516747	0.397362
F	1.605069	4.468824	1.564744
C	-0.763119	1.043456	-0.624570
C	-0.546650	2.493257	-1.017728
H	-0.834632	0.378070	-1.484092
C	-1.817915	3.010578	-1.701190
H	0.316342	2.542726	-1.689523
H	-0.296395	3.101641	-0.145514
C	-2.965132	2.591404	-0.779989
H	-2.763458	1.065204	0.669372
H	-1.797661	4.096848	-1.831360
H	-1.948222	2.554762	-2.688845
H	-3.001633	3.212910	0.119916
H	-3.947829	2.623040	-1.257890
S	-3.513749	-0.140909	-1.154535
O	-2.951488	-1.327482	-0.508396
N	-2.638089	1.198523	-0.336907
O	-3.335600	0.134178	-2.576918
C	-5.214062	0.067254	-0.691623
C	-6.092674	0.688272	-1.586677
C	-5.648518	-0.411664	0.552598
C	-7.428009	0.839511	-1.213821
H	-5.743976	1.021794	-2.558801
C	-6.985057	-0.243686	0.901504
H	-4.962289	-0.923590	1.220547
C	-7.895862	0.382636	0.029286
H	-8.119019	1.313585	-1.905504
H	-7.332545	-0.615062	1.862124
C	-9.346109	0.527870	0.415557
H	-9.864894	-0.436111	0.331855
H	-9.450241	0.861876	1.453696
H	-9.866206	1.241827	-0.229407

A5.3.2.2 Minor Enantiomer

H_{minor}

H$_{minor}$

SCF Energy = -1441924.927 kcal/mol
G$_{298K,solution}$ = -1441997.592 kcal/mol
Three lowest vib. freq. (cm^{-1}): = 10.6315, 12.4260, 17.4741

C	0.674638	0.591883	-0.704354
C	0.058194	0.265401	-1.912730
H	-0.509870	1.059556	-2.395494
Pd	-1.389798	-0.195551	-0.225785
N	-2.382605	1.604977	-0.387089
C	-2.186484	2.910246	-1.078167
C	-3.609032	1.535715	0.028494
C	-3.584414	3.580887	-0.892850
H	-2.009328	2.708672	-2.140165
O	-4.399952	2.571023	-0.209965
C	-4.113234	0.381936	0.774012
H	-4.084824	3.819078	-1.832098
H	-3.552275	4.458855	-0.245998
N	-3.172484	-0.578264	1.009768
C	-5.414511	0.320227	1.245546
C	-3.490281	-1.612441	1.811205
C	-5.773152	-0.787058	2.023827
H	-6.114848	1.115679	1.016519
C	-4.804315	-1.731264	2.318787
C	-2.460796	-2.629212	2.209262
H	-6.783521	-0.888451	2.407966
H	-5.035606	-2.581219	2.953253
H	-2.590588	-3.555263	1.636784
H	-1.444740	-2.271377	2.051480
H	-2.591308	-2.885837	3.265662
C	0.399377	-0.882358	-2.820325
H	-0.498506	-1.311949	-3.276057
H	1.014419	-0.487716	-3.642296
H	0.961728	-1.674598	-2.325991
C	-1.034665	3.731935	-0.531107
C	-0.155312	4.366295	-1.418665
C	-0.864634	3.913176	0.850389
C	0.880480	5.172066	-0.935046
H	-0.280414	4.238164	-2.492177
C	0.173755	4.711785	1.333800
H	-1.538290	3.428136	1.553554
C	1.047680	5.343566	0.441422

H	1.552000	5.664314	-1.632781
H	0.298364	4.845360	2.404744
H	1.851224	5.969562	0.818817
H	0.534299	1.610955	-0.345345
C	1.784051	-0.164352	-0.026529
H	1.623944	-0.136928	1.059224
H	1.793084	-1.215334	-0.321801
O	-0.564505	-2.041111	-0.130645
C	-1.225872	-2.935991	-0.806653
O	-2.275827	-2.791462	-1.410727
C	-0.501713	-4.316172	-0.778330
F	-1.167525	-5.231921	-1.485046
F	0.744731	-4.204129	-1.296004
F	-0.381961	-4.765382	0.492703
C	3.147689	0.495808	-0.346976
H	3.359976	0.425778	-1.420641
H	3.107768	1.565826	-0.097638
C	4.280437	-0.169323	0.443381
H	4.076749	-0.115275	1.521326
H	4.346305	-1.230414	0.181501
S	6.969092	-0.118737	0.862367
O	7.805381	1.065139	1.090720
O	6.583966	-1.014781	1.960397
C	7.731100	-1.120643	-0.425020
H	8.647103	-1.534861	0.003687
H	7.046265	-1.925097	-0.701324
H	7.956230	-0.479015	-1.278133
N	5.559323	0.468975	0.091409
H	5.556653	1.478461	0.239668

I_{minor}

I$_{minor}$

SCF Energy = -1441914.186 kcal/mol
G$_{298K,solution}$ = -1441980.956 kcal/mol
Three lowest vib. freq. (cm^{-1}): = -237.3701, 10.0158, 18.1023

C	0.670397	-0.799646	-1.059818
H	0.996650	0.042468	-1.674251
Pd	-1.017435	0.114633	-0.270191
N	-0.409594	2.025298	-0.753282
C	0.852779	2.701346	-1.136351
C	-1.349531	2.914132	-0.726333
C	0.329639	4.082426	-1.631779
H	1.318501	2.160084	-1.964602

O	-1.040431	4.149199	-1.125883
C	-2.697780	2.628928	-0.229490
H	0.274074	4.152890	-2.721447
H	0.873499	4.932932	-1.221579
N	-2.854655	1.374626	0.272843
C	-3.695785	3.595163	-0.240370
C	-4.037836	1.053821	0.828114
C	-4.935333	3.255030	0.309554
H	-3.500927	4.575682	-0.659873
C	-5.095184	1.989205	0.852235
C	-4.236801	-0.307010	1.428910
H	-5.750378	3.972406	0.322269
H	-6.037241	1.698068	1.306327
H	-4.625688	-0.996659	0.670188
H	-3.301334	-0.718703	1.808879
H	-4.968538	-0.261271	2.240923
C	0.053954	-1.949887	-1.866466
H	-0.764603	-1.592597	-2.497051
H	0.783537	-2.396028	-2.568931
H	-0.355368	-2.747327	-1.237895
C	1.842544	2.800106	0.015936
C	3.215992	2.817523	-0.266928
C	1.418901	2.957582	1.343539
C	4.150184	2.997932	0.756656
H	3.558299	2.687006	-1.291075
C	2.353173	3.134075	2.368136
H	0.359801	2.938712	1.584905
C	3.720493	3.157298	2.077096
H	5.211094	3.009908	0.522767
H	2.011536	3.258122	3.392262
H	4.445645	3.298869	2.873635
O	-1.662817	-1.764643	0.277405
C	-2.530465	-2.369987	-0.462782
O	-3.118250	-1.969947	-1.456702
C	-2.790887	-3.815836	0.063386
F	-3.661301	-4.487815	-0.696441
F	-1.626240	-4.528253	0.082764
F	-3.268223	-3.798017	1.330535
C	1.444932	-1.004286	0.139294
C	0.845554	-1.751287	1.335055
H	1.928671	-0.076280	0.456597
C	2.039799	-2.307615	2.113890
H	0.172664	-2.545630	1.002019
H	0.246326	-1.055276	1.927788
C	3.050871	-2.938351	1.156580
H	2.822655	-2.697587	-0.936708

H	2.537564	-1.494862	2.654643
H	1.722056	-3.057373	2.843857
H	4.071236	-2.942342	1.543725
H	2.764896	-3.955008	0.873711
S	4.545702	-1.170011	-0.487863
O	4.933328	-0.584151	0.785474
C	5.675795	-2.497900	-0.947779
H	5.296000	-2.997927	-1.841471
H	6.623091	-1.997928	-1.172779
H	5.804529	-3.184046	-0.109313
N	2.994079	-2.102658	-0.117862
O	4.222317	-0.377195	-1.665078

J~minor~

SCF Energy = -1441914.805 kcal/mol
G~298K,solution~ = -1441981.182 kcal/mol
Three lowest vib. freq. (cm⁻¹): = 11.5848, 20.3684, 24.6544

C	-0.727637	0.820575	-0.878307
H	-1.204377	0.065826	-1.507749
Pd	1.004288	-0.110656	-0.213900
N	0.375392	-2.007806	-0.722623
C	-0.904683	-2.677033	-1.055657
C	1.317728	-2.892860	-0.776610
C	-0.406491	-4.039450	-1.623223
H	-1.417602	-2.111977	-1.838911
O	0.989987	-4.116064	-1.197243
C	2.690973	-2.617487	-0.347263
H	-0.411987	-4.075241	-2.715980
H	-0.924198	-4.904888	-1.210422
N	2.872447	-1.378979	0.185077
C	3.689369	-3.578451	-0.444711
C	4.084069	-1.070601	0.683108
C	4.956917	-3.250336	0.045441
H	3.473890	-4.546099	-0.883570
C	5.143597	-2.001570	0.618244
C	4.312809	0.271462	1.314732
H	5.773302	-3.964125	-0.010310
H	6.108875	-1.720724	1.027871
H	4.656656	0.986435	0.557705
H	3.399048	0.666795	1.759389
H	5.089089	0.203372	2.082619
C	-0.413181	2.047277	-1.744366

H	0.421708	1.846462	-2.421096
H	-1.260750	2.311738	-2.405030
H	-0.140492	2.931044	-1.158573
C	-1.827945	-2.816510	0.146544
C	-3.215053	-2.831097	-0.059352
C	-1.330036	-3.013922	1.442660
C	-4.089836	-3.047873	1.008707
H	-3.614651	-2.669846	-1.058054
C	-2.204852	-3.226816	2.511859
H	-0.259112	-2.997971	1.624799
C	-3.586285	-3.246921	2.297276
H	-5.162166	-3.057178	0.834350
H	-1.805942	-3.381603	3.510783
H	-4.265206	-3.416783	3.128285
O	1.674370	1.753252	0.356094
C	2.497487	2.385507	-0.411933
O	3.029624	2.019652	-1.449420
C	2.783171	3.815173	0.144476
F	3.607769	4.514661	-0.641189
F	1.619551	4.521439	0.251678
F	3.330923	3.759494	1.381691
C	-1.629836	1.085921	0.314848
C	-1.107415	1.861308	1.528503
H	-2.124766	0.167937	0.643832
C	-2.346301	2.457356	2.200957
H	-0.399745	2.635906	1.222110
H	-0.563844	1.175916	2.183946
C	-3.153162	3.019316	1.030609
H	-2.544030	2.561759	-0.947143
H	-2.926283	1.686247	2.720342
H	-2.104087	3.243786	2.921242
H	-4.226154	3.073588	1.222400
H	-2.790069	4.000490	0.713040
S	-4.362513	1.103468	-0.681914
O	-4.997758	0.655549	0.547194
C	-5.349126	2.386377	-1.477314
H	-4.795010	2.788192	-2.328465
H	-6.251134	1.873956	-1.826275
H	-5.613331	3.156505	-0.751027
N	-2.882175	2.056045	-0.120254
O	-3.846750	0.190605	-1.691685

K$_{minor}$

SCF Energy = -1111341.219 kcal/mol

G$_{298K,solution}$ = -1111327.206 kcal/mol
Three lowest vib. freq. (cm^{-1}): = 13.2650, 21.5436, 29.2763

C	-0.076462	-1.996399	-0.612778
H	0.777465	-2.321501	-0.008878
Pd	-0.298557	-0.024388	-0.129880
N	1.578267	0.654805	-0.701712
C	2.813794	-0.001594	-1.204178
C	1.768032	1.931517	-0.700599
C	3.688127	1.220943	-1.622802
H	2.554286	-0.592073	-2.085575
O	2.930060	2.387745	-1.170513
C	0.804418	2.896913	-0.154619
H	3.811772	1.315253	-2.703753
H	4.659065	1.251171	-1.127386
N	-0.284974	2.344954	0.439136
C	1.055957	4.264060	-0.201458
C	-1.136654	3.166841	1.075225
C	0.136409	5.120531	0.411435
H	1.945563	4.637452	-0.695714
C	-0.954035	4.564712	1.064542
C	-2.271792	2.573088	1.863576
H	0.284870	6.196000	0.392359
H	-1.671574	5.195403	1.581227
H	-3.223085	3.063312	1.628821
H	-2.357857	1.504477	1.675117
H	-2.093909	2.714606	2.937232
C	0.104030	-2.319424	-2.086873
H	1.065588	-1.972130	-2.474655
H	0.085102	-3.413197	-2.221938
H	-0.694827	-1.900231	-2.702873
C	3.462603	-0.910427	-0.175329
C	3.953541	-2.161737	-0.570205
C	3.633187	-0.498935	1.154800
C	4.608813	-2.989667	0.346732
H	3.827556	-2.493334	-1.598937
C	4.284088	-1.326066	2.072425
H	3.254480	0.467014	1.480738
C	4.774252	-2.573253	1.669970
H	4.987842	-3.956101	0.026259
H	4.412025	-0.996684	3.099995
H	5.283568	-3.214413	2.383910
C	-1.400874	-2.441435	-0.007841
C	-1.360401	-3.170437	1.341571
H	-2.011879	-3.006162	-0.719884

C	-2.613113	-2.677615	2.076852
H	-0.455770	-2.890635	1.896017
H	-1.344526	-4.254967	1.197862
C	-2.628113	-1.186710	1.737792
H	-3.514637	-3.161458	1.687945
H	-2.568700	-2.847224	3.157047
H	-3.617052	-0.731999	1.826061
H	-1.927869	-0.630031	2.365423
S	-3.474319	-0.889182	-0.862392
O	-4.585775	-1.720301	-0.393035
C	-3.942002	0.842075	-0.712376
H	-3.082037	1.466896	-0.954320
H	-4.734207	0.974933	-1.454799
H	-4.332038	1.038729	0.286231
N	-2.126575	-1.090812	0.307577
O	-2.892579	-1.094804	-2.187821

L$_{minor}$

SCF Energy = -1111346.552 kcal/mol
G$_{298K,solution}$ = -1111330.804 kcal/mol
Three lowest vib. freq. (cm^{-1}): = 19.8877, 23.7037, 32.0936

C	1.341255	0.455403	-1.357775
H	1.346510	1.412276	-0.822140
Pd	-0.205656	-0.592385	-0.505482
N	-1.550623	0.968603	-0.689362
C	-1.452835	2.439038	-0.884417
C	-2.786242	0.674516	-0.444498
C	-2.954390	2.847223	-0.968756
H	-0.956390	2.636020	-1.837835
O	-3.679498	1.663556	-0.507128
C	-3.238617	-0.676093	-0.087276
H	-3.288349	3.051275	-1.989231
H	-3.221734	3.673047	-0.309771
N	-2.242140	-1.583839	0.062503
C	-4.589157	-0.971437	0.071181
C	-2.570963	-2.854584	0.362481
C	-4.932623	-2.286383	0.394454
H	-5.336993	-0.197783	-0.061178
C	-3.919404	-3.226414	0.533990
C	-1.472667	-3.869512	0.516072
H	-5.972753	-2.568627	0.527208
H	-4.154077	-4.258017	0.776364

H	-1.887026	-4.874435	0.629619
H	-0.799349	-3.858175	-0.344921
H	-0.863287	-3.648683	1.399086
C	1.023066	0.633463	-2.844953
H	0.030276	1.058749	-3.015784
H	1.749351	1.308082	-3.323911
H	1.065746	-0.321997	-3.381706
C	-0.681578	3.137732	0.223032
C	0.205874	4.171091	-0.105874
C	-0.888011	2.820372	1.573276
C	0.874571	4.880490	0.896350
H	0.373355	4.428666	-1.149988
C	-0.218548	3.526124	2.575590
H	-1.570291	2.019572	1.848263
C	0.663524	4.558625	2.239538
H	1.555410	5.683235	0.626917
H	-0.389877	3.274811	3.618884
H	1.179223	5.110562	3.020371
C	2.700110	-0.224400	-1.189977
C	3.909933	0.663772	-1.563087
H	2.733083	-1.131547	-1.808390
C	5.076075	0.060806	-0.768009
H	3.722482	1.698735	-1.249101
H	4.085496	0.663179	-2.642205
C	4.437707	-0.286187	0.582541
H	5.440108	-0.850323	-1.256377
H	5.921023	0.747330	-0.659308
H	4.912620	-1.145952	1.063394
H	4.458031	0.563250	1.274072
S	2.386184	-2.032795	0.750651
O	3.308135	-3.166295	0.672502
C	1.986299	-1.747056	2.480933
H	1.251119	-0.943795	2.543978
H	1.593361	-2.687440	2.874858
H	2.907300	-1.480075	3.004743
N	3.007728	-0.579542	0.241094
O	1.097841	-2.195210	-0.018210

M$_{minor}$

SCF Energy = -1111328.599 kcal/mol
G$_{298K,solution}$ = -1111316.26 kcal/mol
Three lowest vib. freq. (cm^{-1}): = -146.4347, 20.2810, 26.4245

C	0.797949	-1.823557	-0.366065
H	0.911570	-1.566503	-1.417464
Pd	-1.269910	-1.246874	-0.012786
N	-1.113624	0.789219	-0.711402
C	-0.098768	1.813753	-1.079654
C	-2.278707	1.296290	-0.930184
C	-0.963715	2.838777	-1.870128
H	0.654017	1.357037	-1.726754
O	-2.344594	2.497604	-1.503826
C	-3.521911	0.618624	-0.533318
H	-0.885088	2.722568	-2.954359
H	-0.796923	3.876129	-1.582374
N	-3.341439	-0.587242	0.070678
C	-4.769952	1.194136	-0.734952
C	-4.420305	-1.260964	0.519395
C	-5.892834	0.498140	-0.280002
H	-4.848189	2.156403	-1.228156
C	-5.711483	-0.724991	0.352686
C	-4.228615	-2.587743	1.200145
H	-6.888787	0.909480	-0.413773
H	-6.563342	-1.283516	0.726254
H	-5.169795	-2.943130	1.627184
H	-3.873052	-3.340947	0.487281
H	-3.488565	-2.511746	2.002955
C	0.133007	-3.016804	-0.064264
H	-1.573237	-2.689493	0.483267
C	0.589455	2.413694	0.138952
C	1.940716	2.777043	0.044379
C	-0.106524	2.679451	1.328006
C	2.584169	3.400066	1.117573
H	2.498293	2.560191	-0.862583
C	0.537050	3.301277	2.401029
H	-1.152832	2.401192	1.426377
C	1.883770	3.664658	2.297571
H	3.633178	3.667897	1.029280
H	-0.013626	3.504037	3.315767
H	2.382715	4.149703	3.132060
C	1.817467	-1.126922	0.526631
C	1.851341	-1.494825	2.020134
H	1.671257	-0.046496	0.439720
C	3.308796	-1.227841	2.422758
H	1.618709	-2.554667	2.175957
H	1.127797	-0.903379	2.589124
C	4.090432	-1.760848	1.217034
H	3.483893	-0.152175	2.538024

H	3.591176	-1.722897	3.356791
H	5.059070	-1.270520	1.092950
H	4.249794	-2.843483	1.285439
S	3.839817	-0.476043	-1.166327
O	4.723266	0.559468	-0.609569
C	4.854733	-1.613784	-2.121326
H	4.214622	-2.393206	-2.536885
H	5.317802	-1.021520	-2.914655
H	5.623926	-2.037111	-1.471802
N	3.203199	-1.485878	0.043893
O	2.686776	-0.061705	-1.990548
H	0.273236	-3.514739	0.890445
H	-0.215788	-3.657645	-0.869714

N_{minor}

SCF Energy = -1111328.654 kcal/mol
$G_{298K,solution}$ = -1111316.127 kcal/mol
Three lowest vib. freq. (cm^{-1}): = 20.4719, 25.8302, 33.7561

C	0.815091	-1.793803	-0.414576
H	0.907903	-1.464283	-1.447262
Pd	-1.295736	-1.269910	-0.017341
N	-1.097858	0.773167	-0.724314
C	-0.077630	1.798639	-1.077381
C	-2.258744	1.289664	-0.943314
C	-0.931801	2.824666	-1.876648
H	0.685035	1.345458	-1.715014
O	-2.315671	2.493576	-1.512989
C	-3.508391	0.625401	-0.544878
H	-0.849897	2.701297	-2.959950
H	-0.759741	3.862594	-1.594266
N	-3.343071	-0.577510	0.071422
C	-4.749084	1.213857	-0.753033
C	-4.431382	-1.232429	0.527796
C	-5.881152	0.537220	-0.292251
H	-4.814096	2.172318	-1.255422
C	-5.715103	-0.680629	0.353982
C	-4.263665	-2.553107	1.226186
H	-6.871746	0.959616	-0.431175
H	-6.573902	-1.223862	0.733992
H	-5.212463	-2.885353	1.655014
H	-3.919787	-3.322093	0.524717
H	-3.524745	-2.479918	2.030131

C	0.155464	-2.993189	-0.177096
H	-1.673472	-2.669986	0.508695
C	0.592257	2.396806	0.152883
C	1.939044	2.780047	0.071556
C	-0.115487	2.641598	1.339402
C	2.566077	3.401784	1.155024
H	2.506099	2.578936	-0.833069
C	0.511896	3.261997	2.422923
H	-1.158203	2.347513	1.428256
C	1.853929	3.645112	2.332628
H	3.611902	3.684797	1.076925
H	-0.047949	3.447954	3.335668
H	2.340365	4.128582	3.175365
C	1.821303	-1.129495	0.515264
C	1.836511	-1.551664	1.993992
H	1.677720	-0.046358	0.464969
C	3.288661	-1.298353	2.424040
H	1.602250	-2.616376	2.107997
H	1.105411	-0.981270	2.574674
C	4.086712	-1.786610	1.210041
H	3.461071	-0.227435	2.580547
H	3.560100	-1.826609	3.342988
H	5.053645	-1.286696	1.113576
H	4.251446	-2.870042	1.243732
S	3.864048	-0.442333	-1.143493
O	4.743083	0.578675	-0.554303
C	4.886788	-1.562532	-2.110771
H	4.249310	-2.331891	-2.548551
H	5.359318	-0.955295	-2.887017
H	5.648286	-2.000586	-1.461939
N	3.211291	-1.476169	0.036749
O	2.721961	-0.007218	-1.972506
H	0.276582	-3.535305	0.755426
H	-0.226630	-3.579068	-1.008707

I_{minor,tosyl}

SCF Energy = -1586909.118 kcal/mol

G_{298K,solution} = -1586961.174 kcal/mol

Three lowest vib. freq. (cm⁻¹): = -259.5655, 9.9177, 14.4146

C	-0.145371	0.614050	-0.680866
H	-0.431255	-0.228846	-1.312377
Pd	1.850778	0.158632	-0.194510

N	1.730195	-1.795763	-0.830330
C	0.677986	-2.819597	-1.047170
C	2.872667	-2.325016	-1.129443
C	1.454457	-3.882629	-1.878283
H	-0.132393	-2.394457	-1.645379
O	2.863165	-3.547025	-1.661694
C	4.146667	-1.664163	-0.837057
H	1.268209	-3.805708	-2.953022
H	1.304794	-4.905793	-1.535262
N	4.020813	-0.508305	-0.128217
C	5.363423	-2.221048	-1.205746
C	5.139221	0.111943	0.287877
C	6.528959	-1.554749	-0.812608
H	5.390829	-3.144523	-1.773211
C	6.409991	-0.400760	-0.054317
C	5.043533	1.345347	1.137934
H	7.505929	-1.944642	-1.081962
H	7.293324	0.126354	0.292907
H	5.182078	2.240659	0.520298
H	4.074833	1.418522	1.631560
H	5.835588	1.343127	1.893656
C	-0.264650	1.919972	-1.463402
H	0.495717	1.981833	-2.246791
H	-1.237477	1.974043	-1.981545
H	-0.163388	2.809169	-0.837099
C	0.109033	-3.360154	0.257351
C	-1.224201	-3.792622	0.288416
C	0.903392	-3.516254	1.402923
C	-1.752564	-4.380915	1.440388
H	-1.855763	-3.660706	-0.586762
C	0.373597	-4.100860	2.556175
H	1.936022	-3.178397	1.404669
C	-0.954524	-4.537384	2.576557
H	-2.788812	-4.706591	1.451587
H	0.999306	-4.216416	3.437090
H	-1.364924	-4.993092	3.473385
O	2.033460	2.092035	0.464061
C	2.607692	2.949049	-0.315319
O	3.140902	2.771345	-1.399927
C	2.552625	4.381087	0.301003
F	3.158941	5.289216	-0.470447
F	1.258533	4.774871	0.464773
F	3.138911	4.411341	1.521477
C	-0.810854	0.511719	0.622752
C	-0.626410	1.495543	1.761158
H	-0.946244	-0.513625	0.967742

C	-1.923558	1.540081	2.575588
H	-0.355555	2.486665	1.389264
H	0.213081	1.151660	2.375252
C	-3.037403	1.762228	1.549935
H	-2.681470	1.452831	-0.506396
H	-2.086760	0.592693	3.101949
H	-1.911547	2.341683	3.320265
H	-4.028081	1.491304	1.922090
H	-3.069506	2.802460	1.212654
S	-3.660715	-0.548606	0.076659
O	-3.688146	-1.220510	1.371948
N	-2.675409	0.919064	0.365671
O	-3.026422	-1.129673	-1.106767
C	-5.278758	0.057558	-0.335730
C	-6.264257	0.109263	0.657283
C	-5.544913	0.450535	-1.654585
C	-7.531540	0.579686	0.316531
H	-6.049794	-0.233537	1.664389
C	-6.817990	0.919112	-1.967683
H	-4.781598	0.367578	-2.422334
C	-7.830355	0.992475	-0.993020
H	-8.303934	0.617785	1.080029
H	-7.034415	1.222035	-2.988816
C	-9.213571	1.469547	-1.357605
H	-9.804817	0.644845	-1.777543
H	-9.752324	1.848613	-0.484021
H	-9.178272	2.261633	-2.112615

I_{trans to oxazoline}

SCF Energy = -1441907.059 kcal/mol

$G_{298K,solution}$ = -1441974.622 kcal/mol

Three lowest vib. freq. (cm^{-1}): = -181.1851, 12.1748, 13.9889

C	-1.678794	-0.500132	0.873073
H	-2.247263	0.336298	1.271401
Pd	0.134819	0.375080	0.259439
N	1.803273	1.307812	-0.700013
C	2.996530	0.881415	-1.469318
C	1.503666	2.510907	-1.038418
C	3.341306	2.176149	-2.275377
H	2.684810	0.075058	-2.141574
O	2.272055	3.127481	-1.940282
C	0.384207	3.227109	-0.412686

H	3.324267	2.040266	-3.357709
H	4.284144	2.630022	-1.965832
N	-0.330876	2.488875	0.491421
C	0.161888	4.575324	-0.653644
C	-1.202278	3.140671	1.290257
C	-0.822664	5.225021	0.095892
H	0.762994	5.094820	-1.391385
C	-1.474992	4.508846	1.087676
C	-1.847743	2.438099	2.454282
H	-1.039348	6.276644	-0.065725
H	-2.196594	4.994734	1.737074
H	-2.864149	2.106613	2.212159
H	-1.255957	1.579646	2.776445
H	-1.927530	3.134916	3.295034
C	-1.513721	-1.581438	1.941414
H	-0.907299	-1.216968	2.775084
H	-2.482891	-1.884602	2.381716
H	-1.028753	-2.486068	1.568040
C	4.129131	0.377390	-0.596169
C	4.799720	-0.801571	-0.943169
C	4.545272	1.095450	0.534009
C	5.874335	-1.257420	-0.173582
H	4.477168	-1.373269	-1.810623
C	5.614824	0.638958	1.305163
H	4.024807	2.005104	0.825730
C	6.282830	-0.538180	0.951529
H	6.382938	-2.176915	-0.449494
H	5.922814	1.196519	2.185384
H	7.112680	-0.895362	1.554851
O	0.818336	-1.496381	-0.173124
C	1.574575	-2.051398	0.724626
O	1.905340	-1.635123	1.820579
C	2.016564	-3.473478	0.262103
F	2.944332	-4.002299	1.064532
F	0.935808	-4.307794	0.271172
F	2.506237	-3.471699	-0.999939
C	-2.320099	-0.911852	-0.407934
C	-1.852369	-2.100100	-1.236351
H	-2.572995	-0.058870	-1.040529
C	-3.068105	-2.625112	-2.005301
H	-1.421952	-2.878838	-0.601600
H	-1.053616	-1.770000	-1.906082
C	-4.176813	-2.710497	-0.954116
H	-3.947806	-1.752997	0.925334
H	-3.362947	-1.932188	-2.801403
H	-2.885348	-3.603285	-2.459482

H -5.181317 -2.703031 -1.382782
H -4.068408 -3.594683 -0.319492
S -5.184553 -0.171286 -0.258932
O -5.297820   0.019396 -1.697792
C -6.703753 -0.882298   0.402779
H -6.552019 -1.138369   1.453633
H -7.451017 -0.087572   0.314181
H -7.002790 -1.744967 -0.194595
N -3.973720 -1.504246 -0.068225
O -4.713500   0.876140   0.640165

A5.3.3 Neutral *cis*-AP

A5.3.3.1 Major Enantiomer – Amide

trans to Oxazoline

Pd(OAc)₂

SCF Energy = -367052.6214 kcal/mol
$G_{298K,solution}$ = -367098.7392 kcal/mol
Three lowest vib. freq. (cm^{-1}): = 35.9500, 36.7803, 57.2856

Pd -0.000036 -0.000550   0.000219
O   1.765734 -1.088611 -0.031898
C   2.442257 -0.001290 -0.036449
O   1.766883   1.086764 -0.032520
O -1.766991   1.086336   0.032693
C -2.442311 -0.001745   0.036866
O -1.765767 -1.089078   0.032499
C -3.938314 -0.002722   0.018548
H -4.322689   0.902841   0.494713
H -4.281666 -0.017997 -1.023221
H -4.321580 -0.895503   0.519348
C   3.938286 -0.001419 -0.018522
H   4.321972   0.870112 -0.555472
H   4.282094   0.058263   1.021476
H   4.321845 -0.925647 -0.457733

(AcOH)₂

SCF Energy = -287536.3442 kcal/mol
$G_{298K,solution}$ = -287572.6562 kcal/mol

Three lowest vib. freq. (cm^{-1}): = 41.7734, 49.9209, 67.7704

C -3.810296   0.260355   0.010303
O -2.626196   0.020494   0.247950
O -4.271203   1.471678 -0.275948
H -3.524425   2.140702 -0.267535
O -2.243297   3.264713 -0.248799
C -1.059252   3.025291 -0.010596
O -0.598005   1.814040   0.275611
H -1.344661   1.144929   0.267067
C   0.013107   4.081980 -0.015220
H   0.499821   4.119113   0.965393
H   0.782851   3.824167 -0.750691
H -0.421525   5.053241 -0.253920
C -4.882908 -0.796090   0.015474
H -5.652683 -0.537758   0.750714
H -5.369535 -0.833742 -0.965174
H -4.448428 -1.767296   0.254680

pyrox

SCF Energy = -479905.2632 kcal/mol
$G_{298K,solution}$ = -479888.0943 kcal/mol
Three lowest vib. freq. (cm^{-1}): = 21.5740, 25.1913, 39.5176

C   2.072983 -0.041459 -0.475296
N   2.944396 -1.056556 -0.540660
C   2.443106   1.274911 -0.163723
C   4.241189 -0.809788 -0.295643
C   3.786959   1.528711   0.092533
H   1.688916   2.053086 -0.130196
C   4.700767   0.475524   0.027028
C   5.175569 -1.990802 -0.386764
H   4.120127   2.533503   0.339453
H   5.756522   0.643655   0.221541
H   4.870137 -2.773037   0.317765
H   5.136605 -2.429956 -1.390415
H   6.210082 -1.707249 -0.168780
C   0.646915 -0.345387 -0.750444
N -0.298056   0.518688 -0.703510
C -1.107140 -1.670451 -1.167314
C -1.534554 -0.172789 -1.107607
H -1.378464 -2.175197 -2.097087

H	-1.800123	0.186062	-2.112008
H	-1.477529	-2.246875	-0.312919
O	0.338628	-1.626322	-1.085147
C	-2.714994	0.087258	-0.190521
C	-4.014822	0.108133	-0.713665
C	-2.539516	0.264294	1.188616
C	-5.120133	0.290270	0.122314
H	-4.164692	-0.011448	-1.785364
C	-3.641670	0.451665	2.026082
H	-1.534152	0.273945	1.600515
C	-4.935978	0.461834	1.496733
H	-6.121373	0.305764	-0.301208
H	-3.489122	0.594955	3.093091
H	-5.792835	0.609493	2.149225

Pd(κ²-pyrox)(OAc)₂

SCF Energy = -846966.6999 kcal/mol
$G_{298K,solution}$ = -846993.2245 kcal/mol
Three lowest vib. freq. (cm^{-1}): = 15.3530 , 20.6965, 23.4112

O	1.688152	3.229430	-0.771244
C	0.781575	2.296802	-0.459703
N	1.188024	1.086023	-0.305140
C	2.646823	1.031787	-0.550201
C	2.970231	2.522854	-0.886120
C	-0.625295	2.650577	-0.267615
N	-1.417174	1.588725	0.060385
C	-2.701601	1.825110	0.392004
C	-3.221298	3.134930	0.324896
C	-2.426597	4.200122	-0.069472
C	-1.081093	3.957794	-0.357961
C	-3.587271	0.705920	0.852445
Pd	-0.354561	-0.269364	-0.212147
C	3.432515	0.479212	0.623780
H	2.789610	0.386234	-1.420250
H	3.323600	2.665717	-1.909106
H	3.658809	2.987129	-0.177947
H	-0.394869	4.749433	-0.636887
H	-2.834736	5.204591	-0.132961
H	-4.262755	3.290063	0.589172
H	-4.167082	0.324466	0.004335
H	-3.008154	-0.124622	1.256194
H	-4.288262	1.074327	1.608856

C	4.480811	-0.417964	0.384425
C	5.256929	-0.901543	1.442094
C	4.985960	-0.496773	2.751521
C	3.935620	0.393501	2.998887
C	3.165403	0.879687	1.940549
H	4.679997	-0.749641	-0.631984
H	6.064613	-1.601005	1.242563
H	5.583461	-0.877456	3.575797
H	3.712427	0.703956	4.016451
H	2.341800	1.560259	2.144487
O	0.766099	-1.935392	-0.373707
C	1.548127	-2.152251	-1.395756
O	1.825968	-1.343980	-2.289074
C	2.112098	-3.570334	-1.400174
H	2.956225	-3.635636	-2.091011
H	2.414637	-3.875328	-0.393831
H	1.328406	-4.261910	-1.732215
O	-1.883515	-1.596540	-0.246917
C	-2.705336	-1.536935	-1.263877
O	-2.793059	-0.597014	-2.059289
C	-3.584966	-2.776721	-1.386815
H	-4.450740	-2.562131	-2.018252
H	-2.999916	-3.578861	-1.853082
H	-3.905088	-3.134973	-0.403350

O$_{major}$

SCF Energy = -1254848.8 kcal/mol
$G_{298K,solution}$ = -1254842.617 kcal/mol
Three lowest vib. freq. (cm^{-1}): = 12.4312, 14.0475, 20.1775

O	-0.100275	4.187408	-0.226338
C	0.296553	2.917745	-0.381563
N	-0.495646	1.984892	0.014898
C	-1.688527	2.604224	0.631815
C	-1.443597	4.121227	0.355401
C	1.584760	2.615511	-1.009397
N	1.849030	1.282266	-1.123204
C	2.941552	0.904189	-1.815191
C	3.829956	1.877001	-2.322787
C	3.590169	3.229334	-2.143122
C	2.418150	3.616125	-1.487715
C	3.219325	-0.542941	-2.095798
Pd	0.481305	0.144786	0.146089

C   -3.002186   2.088655   0.077471
H   -1.635474   2.384980   1.702148
H   -1.436706   4.733001   1.258823
H   -2.135621   4.539019   -0.379529
H   2.145934   4.656513   -1.350843
H   4.284045   3.973254   -2.523595
H   4.709839   1.537319   -2.860290
H   3.924427   -0.944431   -1.360326
H   2.313668   -1.142646   -2.033343
H   3.667609   -0.640550   -3.091142
C   -4.091081   1.916586   0.941675
C   -5.329954   1.495951   0.448723
C   -5.488457   1.234733   -0.914754
C   -4.402971   1.396390   -1.782154
C   -3.168449   1.824160   -1.289155
H   -3.965604   2.101272   2.006451
H   -6.165734   1.364242   1.131074
H   -6.448641   0.900481   -1.298979
H   -4.515919   1.183108   -2.842022
H   -2.325287   1.932227   -1.967168
O   -0.938124   -0.780331   1.258125
C   -1.284310   -0.321713   2.429969
O   -0.826675   0.690055   2.974647
C   -2.339056   -1.187921   3.111803
H   -2.725922   -0.678858   3.997494
H   -3.154941   -1.420180   2.420120
H   -1.887384   -2.139550   3.417206
N   1.631915   -1.530124   0.361627
S   2.881528   -1.320196   1.425482
C   0.972921   -2.848840   0.401700
O   3.460139   0.014670   1.153346
O   3.774642   -2.497746   1.360424
C   2.233653   -1.263620   3.118767
C   0.266268   -3.155477   -0.922922
H   0.238443   -2.907576   1.218033
H   1.744677   -3.606811   0.582448
H   1.545157   -0.420851   3.209130
H   1.728248   -2.208781   3.332589
H   3.093420   -1.139381   3.782300
C   -0.460594   -4.514868   -0.885346
H   -0.460411   -2.364119   -1.145838
H   1.005300   -3.154523   -1.736088
C   -1.078996   -4.878353   -2.210168
H   -1.213864   -4.499331   -0.089320
H   0.266758   -5.294736   -0.608772
C   -2.373728   -5.091991   -2.492196

H   -0.367808   -4.968639   -3.034121
C   -3.548828   -5.032180   -1.553270
H   -2.624405   -5.345999   -3.523709
H   -4.296074   -4.310236   -1.910946
H   -4.054945   -6.006442   -1.498689
H   -3.267451   -4.744052   -0.536483

P$_{major}$

SCF Energy = -1254838.815 kcal/mol
G$_{298K,solution}$ = -1254826.849 kcal/mol
Three lowest vib. freq. (cm^{-1}): = 15.5157,
24.4730, 31.6192

O   -3.099400   0.703459   1.716788
C   -2.046640   0.902634   0.907327
N   -1.321909   -0.133245   0.635230
C   -1.922258   -1.319949   1.330240
C   -2.993181   -0.654400   2.223935
C   -1.856468   2.299826   0.433142
N   -2.990518   2.960140   0.147261
C   -2.903659   4.228191   -0.278332
C   -1.663533   4.876533   -0.416914
C   -0.494034   4.186327   -0.108200
C   -0.581331   2.863845   0.330559
C   -4.205016   4.921760   -0.597428
Pd   0.690788   -0.219617   -0.029469
C   -2.443334   -2.373333   0.364218
H   -1.137123   -1.773064   1.933276
H   -2.683004   -0.585471   3.270584
H   -3.980107   -1.113517   2.162329
H   0.317103   2.307506   0.574070
H   0.480702   4.655963   -0.204297
H   -1.626328   5.906911   -0.759739
H   -4.733159   4.393661   -1.400106
H   -4.863373   4.916759   0.278823
H   -4.044440   5.958304   -0.909643
C   -1.677782   -3.525191   0.134009
C   -2.138682   -4.515903   -0.739380
C   -3.367197   -4.366584   -1.389055
C   -4.135361   -3.219169   -1.163858
C   -3.674967   -2.229346   -0.292645
H   -0.718447   -3.634407   0.635096
H   -1.537931   -5.406523   -0.905997
H   -3.727485   -5.139873   -2.062904

H -5.092772 -3.096000 -1.664007
H -4.282275 -1.340410 -0.132862
O   1.097611 -0.434257   1.989440
C   1.373448 -1.642801   2.401688
O   1.223992 -2.675385   1.738174
C   1.919236 -1.695742   3.825359
H   1.648745 -2.645927   4.293576
H   3.014284 -1.640459   3.782057
H   1.561749 -0.856040   4.427985
N   2.730178 -0.309489 -0.244377
S   3.544880   1.102218 -0.044568
C   3.358232 -1.398956 -0.999987
O   2.598046   2.234899 -0.210668
O   4.793746   1.099221 -0.837702
C   4.042156   1.134504   1.694149
C   3.235561 -1.255261 -2.521729
H   2.879767 -2.324603 -0.657712
H   4.419502 -1.462782 -0.729745
H   3.142481   1.040667   2.304103
H   4.723047   0.298770   1.871271
H   4.549986   2.086448   1.869927
C   1.776280 -1.102251 -2.976464
H   3.820509 -0.385292 -2.842506
H   3.673772 -2.138751 -3.006218
C   1.077734   0.084449 -2.362289
H   1.215838 -2.024951 -2.782979
H   1.757771 -0.954932 -4.068829
C -0.276202   0.192526 -2.160104
H   1.665072   0.996045 -2.276253
C -1.301800 -0.821541 -2.594758
H -0.658706   1.188112 -1.943649
H -2.249526 -0.680988 -2.073693
H -1.492669 -0.690393 -3.670661
H -0.980739 -1.854219 -2.438611

Q_{major}

SCF Energy = -1254832.24 kcal/mol
$G_{298K,solution}$ = -1254820.023 kcal/mol
Three lowest vib. freq. (cm^{-1}): = -249.4200, 16.9095, 24.4731

O -3.373920   0.117500   1.543795
C -2.306755   0.534353   0.841083
N -1.372501 -0.336593   0.641174

C -1.797573 -1.632620   1.258738
C -3.058421 -1.208634   2.047309
C -2.346444   1.948754   0.383940
N -3.569437   2.412802   0.080184
C -3.691078   3.681131 -0.335389
C -2.576911   4.531271 -0.445429
C -1.313423   4.045076 -0.117740
C -1.183961   2.723077   0.309467
C -5.085237   4.145699 -0.677824
Pd 0.621539 -0.081380   0.074707
C -2.021839 -2.725933   0.225047
H -0.999791 -1.949459   1.930023
H -2.871442 -1.112292   3.120873
H -3.927193 -1.845920   1.878935
H -0.211352   2.320113   0.569341
H -0.431803   4.675655 -0.189937
H -2.707692   5.556746 -0.780001
H -5.101992   5.204195 -0.955558
H -5.488422   3.560382 -1.512852
H -5.756473   3.994422   0.175083
C -1.085965 -3.762268   0.104060
C -1.283383 -4.784367 -0.830771
C -2.413425 -4.779691 -1.652762
C -3.348734 -3.745047 -1.539447
C -3.152611 -2.725106 -0.606091
H -0.196831 -3.752309   0.730317
H -0.552178 -5.584756 -0.912963
H -2.567769 -5.577004 -2.375591
H -4.230178 -3.733253 -2.175779
H -3.886838 -1.924820 -0.532500
O   1.104096 -0.308469   2.130928
C   1.530142 -1.476989   2.507015
O   1.565237 -2.491160   1.791524
C   2.025482 -1.533771   3.951413
H   3.091716 -1.273244   3.972650
H   1.493716 -0.819109   4.586467
H   1.920686 -2.547965   4.346092
N   2.614632   0.222198 -0.403292
C   3.546805 -0.867800 -0.735287
S   3.255399   1.710194 -0.021218
C   3.798490 -0.863934 -2.248037
H   3.087825 -1.802621 -0.398240
H   4.489544 -0.748188 -0.188053
C   3.623387   1.659456   1.747670
O   2.183396   2.708879 -0.217627
O   4.539586   1.896262 -0.726740

C	2.426782	-0.746577	-2.937048
H	4.427473	-0.005236	-2.504252
H	4.314943	-1.775665	-2.573058
H	2.708461	1.391594	2.278587
H	4.404278	0.914348	1.916945
H	3.983559	2.655087	2.020271
C	1.595483	0.351118	-2.337341
H	1.894227	-1.700897	-2.885435
H	2.560691	-0.504143	-4.002742
C	0.212816	0.225905	-2.037927
H	1.992716	1.357384	-2.433626
H	-0.313643	1.182547	-2.028825
C	-0.615023	-0.925387	-2.596794
H	-1.639728	-0.865901	-2.224934
H	-0.658346	-0.876170	-3.695524
H	-0.232996	-1.912385	-2.321409

R_{major}

SCF Energy = -1254847.592 kcal/mol
G_{298K,solution} = -1254833.649 kcal/mol
Three lowest vib. freq. (cm⁻¹): = 13.4355, 21.3606, 26.0108

O	3.432889	0.811049	1.379548
C	2.478421	0.074104	0.782439
N	1.320438	0.631624	0.650009
C	1.399021	2.021061	1.196147
C	2.795352	2.023978	1.861540
C	2.886329	-1.286297	0.345081
N	4.190224	-1.428030	0.057345
C	4.634711	-2.625596	-0.347888
C	3.774565	-3.730608	-0.466596
C	2.424999	-3.579073	-0.155823
C	1.960702	-2.332560	0.262684
C	6.106001	-2.723364	-0.668097
Pd	-0.563074	-0.097454	0.178311
C	1.187702	3.071640	0.116753
H	0.607138	2.124376	1.939401
H	2.742481	1.953287	2.951909
H	3.424717	2.868264	1.577288
H	0.916515	-2.177030	0.510630
H	1.735592	-4.414860	-0.236627
H	4.164645	-4.690190	-0.794702
H	6.388302	-3.737462	-0.967886

H	6.366266	-2.034105	-1.479964
H	6.704781	-2.434944	0.203435
C	-0.027628	3.768236	0.065029
C	-0.239109	4.743154	-0.915836
C	0.757400	5.027942	-1.853495
C	1.969320	4.329918	-1.810810
C	2.181613	3.357286	-0.831415
H	-0.809783	3.527168	0.781840
H	-1.183826	5.280706	-0.943214
H	0.593506	5.789004	-2.612477
H	2.748183	4.542649	-2.538899
H	3.126684	2.817715	-0.815005
O	-1.089732	-0.018904	2.308139
C	-1.768189	0.994502	2.739026
O	-2.123859	1.966738	2.044035
C	-2.156988	0.932769	4.216785
H	-3.050891	0.304615	4.328115
H	-1.361021	0.479022	4.815666
H	-2.395114	1.931311	4.592491
N	-2.410721	-0.786714	-0.606522
C	-3.630273	0.100242	-0.433603
S	-2.744090	-2.486302	-0.258372
C	-4.029362	0.489066	-1.858512
H	-3.323492	0.955305	0.173857
H	-4.418859	-0.440716	0.093866
C	-2.965957	-2.484613	1.529789
O	-1.522905	-3.227520	-0.596583
O	-4.012570	-2.855814	-0.905068
C	-2.676375	0.601038	-2.573866
H	-4.643161	-0.300283	-2.307711
H	-4.599665	1.423590	-1.878963
H	-2.150156	-1.924715	1.996962
H	-3.934013	-2.038606	1.764550
H	-2.956884	-3.539677	1.816787
C	-1.870190	-0.601109	-2.059891
H	-2.185667	1.539413	-2.295539
H	-2.763310	0.575688	-3.664957
C	-0.363133	-0.436668	-1.832592
H	-2.129304	-1.491270	-2.648074
H	0.122437	-1.414839	-1.913020
C	0.368138	0.586382	-2.690394
H	1.439564	0.570446	-2.466523
H	0.257053	0.356533	-3.763512
H	0.021537	1.612177	-2.533176

S_{major}

SCF Energy = -1254829.168 kcal/mol
G_{298K,solution} = -1254825.269 kcal/mol
Three lowest vib. freq. (cm⁻¹): = -1068.6335,
5.8691, 12.2189

Pd	-0.527748	-0.761508	0.985292
O	-1.969544	-0.828745	2.673442
C	-1.429855	-1.425778	3.657352
O	-0.242844	-1.885681	3.649839
C	-2.243135	-1.615598	4.924775
H	-2.401679	-2.686541	5.095972
H	-1.684424	-1.230559	5.784204
H	-3.208940	-1.111506	4.850535
N	3.411830	-0.361673	-0.996223
C	3.614519	0.090211	-2.396309
S	4.718008	-0.312459	0.067901
C	2.611277	1.236129	-2.555095
H	3.375791	-0.738279	-3.077693
H	4.652889	0.383311	-2.555830
C	5.079045	-2.052816	0.376133
O	4.270190	0.269454	1.344112
O	5.887171	0.246558	-0.631183
C	1.421183	0.751274	-1.717910
H	3.032775	2.158755	-2.136534
H	2.350527	1.425330	-3.602559
H	4.194632	-2.522818	0.809418
H	5.348164	-2.523743	-0.571492
H	5.918177	-2.086768	1.075784
C	2.044214	0.049079	-0.489039
H	0.828497	0.026046	-2.289822
H	0.748689	1.555860	-1.410253
C	1.241896	-1.144223	-0.001756
H	2.186400	0.761308	0.328394
H	1.072930	-1.882288	-0.791204
C	1.406467	-1.671401	1.349684
H	2.119769	-1.154252	1.994658
H	0.334908	-1.601719	2.335437
H	1.455465	-2.758527	1.447333
N	-2.022758	0.194984	-0.203590
C	-2.359371	1.431615	-0.352030
C	-3.141610	-0.648236	-0.705276
O	-3.538026	1.678551	-0.955826
C	-1.589747	2.620314	0.092531
C	-4.087065	0.396923	-1.355111

C	-2.693494	-1.755285	-1.640410
H	-3.609027	-1.102533	0.175760
N	-1.688264	3.706000	-0.690426
C	-0.834097	2.579696	1.270129
H	-5.114160	0.345007	-0.989045
H	-4.083744	0.357461	-2.448094
C	-2.978654	-3.090725	-1.332087
C	-2.007575	-1.466708	-2.829933
C	-1.014369	4.812058	-0.343563
C	-0.137231	3.732846	1.631589
H	-0.807511	1.681789	1.879164
C	-2.589947	-4.121777	-2.193746
H	-3.500763	-3.327014	-0.407494
C	-1.614435	-2.492992	-3.690338
H	-1.768652	-0.435431	-3.080456
C	-0.223911	4.860317	0.817545
C	-1.151339	5.999600	-1.263966
H	0.461805	3.748641	2.538001
C	-1.906202	-3.825108	-3.374818
H	-2.818464	-5.153347	-1.938644
H	-1.081113	-2.254836	-4.607364
H	0.307926	5.772007	1.075151
H	-0.601223	6.867985	-0.888527
H	-0.773937	5.753598	-2.263582
H	-2.206645	6.272961	-1.376646
H	-1.601400	-4.623951	-4.045932

T_{major}

SCF Energy = -1254842.882 kcal/mol
G_{298K,solution} = -1254836.679 kcal/mol
Three lowest vib. freq. (cm⁻¹): = 8.7524,
17.3873, 18.1031

Pd	0.319648	-0.805905	-0.870258
O	2.011652	-1.052796	-2.590224
C	1.587679	-1.458778	-3.670688
O	0.303667	-1.746698	-3.871217
C	2.449313	-1.676404	-4.885777
H	2.375845	-2.719503	-5.212179
H	2.090413	-1.051156	-5.710644
H	3.486529	-1.428910	-4.656530
N	-3.662144	-0.095190	0.979337
C	-3.879950	0.446159	2.345530
S	-4.923992	-0.040613	-0.132278

C	-2.767142	1.486699	2.502760
H	-3.762174	-0.366371	3.076156
H	-4.887845	0.851788	2.440814
C	-5.247231	-1.778050	-0.491935
O	-4.450797	0.577338	-1.382919
O	-6.120469	0.488750	0.544423
C	-1.604938	0.847267	1.732759
H	-3.070376	2.431359	2.033584
H	-2.528183	1.689548	3.552931
H	-4.334303	-2.225542	-0.888566
H	-5.555853	-2.269506	0.432843
H	-6.050490	-1.807533	-1.232763
C	-2.254990	0.187792	0.495820
H	-1.126961	0.073813	2.348191
H	-0.829985	1.559029	1.437016
C	-1.554768	-1.074168	0.031152
H	-2.316636	0.901618	-0.331027
H	-1.451705	-1.818874	0.825330
C	-1.613743	-1.544129	-1.313095
H	-2.171135	-0.961971	-2.049564
H	-0.171663	-1.573684	-3.004672
H	-1.618288	-2.621183	-1.493837
N	2.050726	0.066103	0.217693
C	2.523815	1.258069	0.358983
C	3.112768	-0.887987	0.625493
O	3.766866	1.374020	0.876769
C	1.851040	2.531797	-0.001359
C	4.188181	0.040346	1.250035
C	2.634157	-1.983084	1.558644
H	3.487300	-1.352824	-0.294226
N	2.338620	3.638896	0.581329
C	0.780240	2.546820	-0.904475
H	5.193379	-0.118705	0.854559
H	4.209670	-0.012292	2.343135
C	2.986490	-3.315532	1.312645
C	1.874676	-1.683580	2.699285
C	1.772199	4.820642	0.299555
C	0.191286	3.776096	-1.196047
H	0.424834	1.619063	-1.348774
C	2.593516	-4.332892	2.188398
H	3.565363	-3.561196	0.424568
C	1.476755	-2.696523	3.573178
H	1.579777	-0.655180	2.893558
C	0.689864	4.928068	-0.589758
C	2.359636	6.028086	0.988207
H	-0.644155	3.831730	-1.889029

C	1.836806	-4.025437	3.321320
H	2.874115	-5.362493	1.981184
H	0.882966	-2.450760	4.450238
H	0.252319	5.900180	-0.799943
H	1.849807	6.950575	0.693070
H	2.284940	5.920149	2.076625
H	3.424694	6.122670	0.747007
H	1.526104	-4.813649	4.002299

U$_{major}$

SCF Energy = -1111083.467 kcal/mol

G$_{298K,solution}$ = -1111065.24 kcal/mol

Three lowest vib. freq. (cm^{-1}): = 10.3356, 12.8699, 18.3945

Pd	-0.522261	-0.936769	-0.384626
N	3.852643	0.038699	-0.414234
C	4.434124	1.386608	-0.640271
S	4.794097	-1.143016	0.320346
C	3.434100	2.329192	0.036712
H	4.482729	1.579372	-1.721515
H	5.446288	1.442030	-0.237739
C	4.831237	-2.470224	-0.900474
O	4.102622	-1.674530	1.507856
O	6.169946	-0.628249	0.442115
C	2.092780	1.633690	-0.224412
H	3.639689	2.380731	1.113649
H	3.478608	3.347136	-0.367273
H	3.804520	-2.781634	-1.100421
H	5.311190	-2.092609	-1.805407
H	5.411557	-3.288422	-0.465903
C	2.379882	0.127676	-0.054045
H	1.762394	1.828403	-1.253805
H	1.290764	1.956191	0.443512
C	1.525013	-0.776353	-0.918809
H	2.270849	-0.160121	0.996469
H	1.613336	-0.555238	-1.986438
C	1.195567	-2.106014	-0.533740
H	1.535505	-2.487932	0.430190
H	1.061380	-2.872335	-1.300475
N	-2.106043	0.659424	-0.589063
C	-3.305021	0.216205	-0.477846
C	-2.183888	2.057615	-1.053839
O	-4.330521	1.042836	-0.792974

C	-3.624061	-1.144476	-0.021023
C	-3.721919	2.293194	-1.221069
C	-1.526760	3.048179	-0.107932
H	-1.678667	2.115852	-2.024376
N	-2.543493	-1.920916	0.216904
C	-4.939641	-1.572957	0.158679
H	-4.023282	2.470291	-2.256802
H	-4.108177	3.088736	-0.580191
C	-0.919212	4.199375	-0.626343
C	-1.562148	2.866177	1.281136
C	-2.737200	-3.173101	0.671138
C	-5.142477	-2.874396	0.619178
H	-5.764967	-0.902934	-0.054493
C	-0.362877	5.157953	0.225518
H	-0.870329	4.343894	-1.704212
C	-1.000752	3.819633	2.134457
H	-2.007326	1.965462	1.694580
C	-4.033770	-3.675265	0.880640
C	-1.517740	-4.009880	0.941277
H	-6.148390	-3.254272	0.774932
C	-0.402321	4.969651	1.609820
H	0.108485	6.043882	-0.192379
H	-1.024066	3.659939	3.209417
H	-4.158859	-4.690408	1.245386
H	-1.788598	-4.976267	1.377658
H	-0.960174	-4.180103	0.013881
H	-0.838553	-3.484663	1.620650
H	0.036938	5.708837	2.274617

A5.3.3.2 Minor Enantiomer – Amide

trans to Oxazoline

O_{minor}

SCF Energy = -1254843.168 kcal/mol
G_{298K,solution} = -1254838.99 kcal/mol
Three lowest vib. freq. (cm^{-1}): = 7.4875, 14.2744, 21.6241

O	2.675914	2.246777	-2.231916
C	1.724792	1.898968	-1.354970
N	1.694525	0.682350	-0.947441
C	2.772927	-0.074730	-1.616331
C	3.480034	1.040690	-2.451956

C	0.758496	2.892180	-0.883184
N	-0.144256	2.418860	0.022034
C	-1.028744	3.295254	0.546134
C	-1.043167	4.640774	0.122693
C	-0.136820	5.103413	-0.818949
C	0.802405	4.206785	-1.330521
C	-1.973701	2.843584	1.612787
Pd	0.050207	0.204541	0.226391
C	3.707448	-0.795382	-0.662823
H	2.283345	-0.806459	-2.265705
H	3.482613	0.845366	-3.525756
H	4.491871	1.258357	-2.103686
H	1.551978	4.502527	-2.055626
H	-0.150124	6.139829	-1.143591
H	-1.777503	5.310481	0.558601
H	-2.488230	1.928179	1.309846
H	-1.405563	2.582900	2.513986
H	-2.692463	3.633213	1.849171
C	4.381378	-1.938657	-1.114211
C	5.296631	-2.595702	-0.287474
C	5.537308	-2.121003	1.005122
C	4.858740	-0.988527	1.464662
C	3.951940	-0.325860	0.633897
H	4.178418	-2.325413	-2.111161
H	5.809399	-3.483694	-0.648257
H	6.238762	-2.637850	1.654780
H	5.023005	-0.626741	2.476122
H	3.408818	0.536513	1.010455
O	0.441961	-1.767693	0.257648
C	0.486617	-2.450545	-0.854447
O	0.334170	-1.992981	-1.993556
C	0.785930	-3.926221	-0.612935
H	0.554669	-4.504145	-1.511029
H	1.850552	-4.041217	-0.376092
H	0.219572	-4.302705	0.243898
N	-1.655870	-0.233375	1.318390
S	-1.279052	-0.486379	2.924169
C	-2.514949	-1.288086	0.740039
O	-0.266640	0.533895	3.285132
O	-1.033176	-1.896560	3.284257
C	-2.800613	-0.028785	3.808406
C	-3.019117	-0.879352	-0.647549
H	-3.384644	-1.438192	1.398415
H	-1.990195	-2.250202	0.690144
H	-3.048972	1.012897	3.599180
H	-3.614961	-0.692745	3.511118

H	-2.582284	-0.165654	4.870519
C	-3.967362	-1.932200	-1.256545
H	-3.538922	0.086298	-0.580025
H	-2.160654	-0.736932	-1.316454
C	-4.382531	-1.581745	-2.661585
H	-4.841010	-2.063882	-0.606537
H	-3.444595	-2.900873	-1.274809
C	-5.619718	-1.359616	-3.132383
H	-3.554294	-1.497510	-3.367615
C	-6.922849	-1.412957	-2.380006
H	-5.713524	-1.113297	-4.191551
H	-7.455918	-0.454688	-2.454865
H	-7.589480	-2.175617	-2.806783
H	-6.793427	-1.641597	-1.318010

P$_{minor}$

SCF Energy = -1254839.501 kcal/mol
G$_{298K,solution}$ = -1254827.55 kcal/mol
Three lowest vib. freq. (cm^{-1}): = 17.8830, 22.6031, 31.9861

O	-2.994169	-1.115782	1.801064
C	-2.301166	-0.351354	0.939674
N	-1.065879	-0.675126	0.750113
C	-0.760632	-1.886627	1.573972
C	-2.050630	-2.035942	2.414165
C	-3.061594	0.761041	0.309573
N	-4.312836	0.445480	-0.061283
C	-5.068988	1.392470	-0.634144
C	-4.586626	2.697708	-0.832555
C	-3.291856	3.015228	-0.428525
C	-2.492894	2.028642	0.154237
C	-6.462196	0.985206	-1.046018
Pd	0.642702	0.299018	-0.015917
C	-0.398460	-3.078295	0.701002
H	0.089948	-1.634106	2.211687
H	-1.915383	-1.719036	3.451956
H	-2.490426	-3.033615	2.388091
H	-1.488210	2.253451	0.505472
H	-2.902267	4.021876	-0.554604
H	-5.226549	3.448290	-1.288518
H	-6.421923	0.185187	-1.794811
H	-7.013554	0.592133	-0.184279
H	-7.021658	1.826624	-1.466529
C	0.946620	-3.439113	0.545383

C	1.303307	-4.512228	-0.277193
C	0.317554	-5.238175	-0.950557
C	-1.027697	-4.880908	-0.805849
C	-1.382181	-3.805670	0.012238
H	1.724542	-2.862261	1.038605
H	2.352252	-4.770151	-0.394234
H	0.593748	-6.074665	-1.587395
H	-1.800317	-5.437826	-1.330004
H	-2.431709	-3.533759	0.105742
O	0.926203	0.768197	1.983551
C	0.687975	2.001444	2.339916
O	0.194913	2.873765	1.615955
C	1.093834	2.318966	3.775848
H	0.407263	3.056532	4.200373
H	1.123272	1.421681	4.399970
H	2.097455	2.762410	3.765622
N	2.418115	1.275628	-0.321181
C	2.462198	2.471605	-1.168403
S	3.785495	0.386575	-0.110835
C	2.372496	2.184094	-2.672916
H	1.628803	3.105394	-0.841637
H	3.387982	3.023747	-0.965270
O	4.884651	0.924843	-0.942516
C	4.266369	0.656073	1.611915
O	3.449640	-1.055183	-0.212541
C	1.134013	1.353269	-3.043095
H	3.280759	1.656291	-2.986927
H	2.345320	3.135913	-3.221450
H	3.424492	0.371823	2.245074
H	4.511338	1.712951	1.739384
H	5.143128	0.032644	1.805951
C	1.073290	0.025367	-2.329827
H	0.218299	1.930859	-2.866156
H	1.159675	1.140820	-4.124387
C	-0.068199	-0.690281	-2.062051
H	2.018183	-0.500905	-2.213682
C	-1.455576	-0.320737	-2.517229
H	0.063598	-1.725423	-1.753235
H	-1.590185	-0.683079	-3.547599
H	-2.223413	-0.800083	-1.906390
H	-1.636148	0.756973	-2.520272

Q$_{minor}$

SCF Energy = -1254832.362 kcal/mol
G$_{298K,solution}$ = -1254820.227 kcal/mol

Three lowest vib. freq. (cm^{-1}): = -249.3353, 17.9670, 21.9223

O	3.172497	1.224294	1.615577
C	2.409218	0.415469	0.858780
N	1.159947	0.726126	0.766269
C	0.923141	1.979663	1.544060
C	2.282350	2.176283	2.258045
C	3.110622	-0.730415	0.222697
N	4.332838	-0.449291	-0.256658
C	5.034215	-1.432800	-0.837836
C	4.528054	-2.740544	-0.931850
C	3.264878	-3.021372	-0.415934
C	2.520399	-1.997132	0.173150
C	6.394019	-1.062999	-1.377075
Pd	-0.559206	-0.231332	0.091745
C	0.490941	3.121606	0.638233
H	0.128534	1.768258	2.264345
H	2.242025	1.918924	3.320214
H	2.710868	3.171831	2.134789
H	1.538863	-2.193802	0.599873
H	2.857470	-4.027914	-0.460653
H	5.125462	-3.521074	-1.395297
H	6.300354	-0.305752	-2.164625
H	7.012428	-0.627942	-0.583731
H	6.914416	-1.932214	-1.791319
C	-0.840192	3.555611	0.649074
C	-1.257842	4.590390	-0.193660
C	-0.345395	5.202570	-1.056094
C	0.985789	4.770814	-1.078453
C	1.399801	3.735378	-0.238156
H	-1.562292	3.066409	1.297509
H	-2.297275	4.906541	-0.179825
H	-0.667982	6.008266	-1.710626
H	1.700433	5.238858	-1.750846
H	2.435509	3.403057	-0.273536
O	-0.845323	-0.774358	2.126855
C	-0.584003	-2.002852	2.455112
O	-0.152227	-2.875595	1.683708
C	-0.819565	-2.339994	3.926432
H	-1.444097	-1.593305	4.424044
H	-1.274340	-3.331820	4.010368
H	0.149857	-2.380512	4.438827
N	-2.352779	-1.091289	-0.496354
C	-2.471564	-2.476854	-0.977530
S	-3.751483	-0.296505	-0.058946

C	-2.680671	-2.461417	-2.496598
H	-3.304916	-2.986698	-0.479657
H	-1.553934	-3.000373	-0.692077
C	-4.039133	-0.711178	1.676487
O	-3.469274	1.150512	-0.126531
O	-4.891160	-0.841224	-0.825700
C	-1.632600	-1.503649	-3.092875
H	-3.691171	-2.100790	-2.712676
H	-2.575005	-3.464127	-2.929505
H	-3.161523	-0.407903	2.248923
H	-4.937746	-0.167844	1.980923
H	-4.202185	-1.788660	1.754072
C	-1.571795	-0.204385	-2.340657
H	-0.648982	-1.982876	-3.110394
H	-1.895163	-1.261274	-4.134202
C	-0.362347	0.436750	-1.959882
H	-2.465809	0.411128	-2.373872
C	0.976615	0.019036	-2.557042
H	-0.467085	1.516097	-1.830420
H	0.997784	0.212183	-3.640345
H	1.786027	0.601075	-2.109388
H	1.210930	-1.038103	-2.402660

R$_{minor}$

SCF Energy = -1254848.046 kcal/mol
G$_{298K,solution}$ = -1254834.704 kcal/mol
Three lowest vib. freq. (cm^{-1}): = 16.3904, 20.2341, 28.5116

O	2.993811	2.202448	1.014221
C	2.339800	1.120419	0.555000
N	1.054657	1.211317	0.477352
C	0.641904	2.528506	1.038404
C	2.004260	3.246189	1.216488
C	3.180515	-0.057465	0.221115
N	4.310944	0.217765	-0.448164
C	5.124634	-0.796695	-0.773287
C	4.829892	-2.121633	-0.408379
C	3.663054	-2.390392	0.303993
C	2.800490	-1.341073	0.628777
C	6.371833	-0.440126	-1.544221
Pd	-0.415994	-0.209317	0.147290
C	-0.349652	3.282392	0.174748
H	0.173785	2.314301	2.005490
H	2.156772	3.660315	2.214716

H   2.178423   4.020558   0.464037
H   1.890235   -1.516871   1.199549
H   3.423657   -3.403879   0.615078
H   5.515618   -2.921906   -0.673514
H   6.109786   -0.013137   -2.519764
H   6.948117   0.319694   -1.004388
H   7.009318   -1.314565   -1.708475
C -1.558140   3.723719   0.726412
C -2.472990   4.445659   -0.046377
C -2.188208   4.728796   -1.383640
C -0.983782   4.288949   -1.944184
C -0.070285   3.573756   -1.168770
H -1.789631   3.489981   1.763292
H -3.409673   4.776758   0.394524
H -2.901193   5.282479   -1.988857
H -0.759151   4.499422   -2.986761
H   0.858812   3.227525   -1.616387
O -0.825894   -0.141803   2.308052
C -0.354574   -1.111297   3.020939
O   0.282877   -2.086027   2.572445
C -0.596684   -0.997105   4.525585
H -1.534195   -0.475365   4.741384
H -0.594862   -1.987197   4.989601
H   0.219133   -0.413898   4.972473
N -1.830925   -1.660981   -0.516916
C -1.673840   -3.078838   0.000583
S -3.514189   -1.115868   -0.505810
C -1.355324   -3.910121   -1.243871
H -2.590125   -3.400567   0.499937
H -0.861720   -3.069070   0.731143
C -3.808493   -0.817438   1.246035
O -3.545449   0.154245   -1.235723
O -4.365711   -2.229773   -0.952850
C -0.513647   -2.945974   -2.090743
H -2.280859   -4.179869   -1.765674
H -0.821653   -4.832386   -0.990732
H -2.999514   -0.204259   1.650416
H -4.773754   -0.305798   1.290046
H -3.864640   -1.777516   1.762040
C -1.228917   -1.593490   -1.954283
H   0.500996   -2.884769   -1.682877
H -0.439133   -3.246457   -3.140974
C -0.384039   -0.316357   -1.895132
H -2.049705   -1.540564   -2.681590
C   0.937410   -0.320373   -2.650231
H -0.995337   0.538721   -2.203921

H   0.775116   -0.473746   -3.730411
H   1.447110   0.642254   -2.536425
H   1.629916   -1.097213   -2.310215

S_{**minor**}

SCF Energy = -1254828.464 kcal/mol
G_{298K,solution} = -1254824.312 kcal/mol
Three lowest vib. freq. (cm^{-1}): = -1068.2637, 9.2418, 15.9158

Pd   0.218262   -0.887787   -1.060384
O   1.093084   -2.808744   -1.760001
C   0.343509   -3.301480   -2.661006
O   -0.731010   -2.757039   -3.071207
C   0.737319   -4.626128   -3.288549
H   0.755879   -4.528220   -4.378968
H   1.712924   -4.958115   -2.927289
H   -0.019541   -5.380478   -3.044752
C   -1.188826   0.620744   -0.956457
C   -1.687728   -0.334790   -1.940378
H   -1.708009   -0.003570   -2.981325
H   -0.930778   -1.528345   -2.300461
H   -2.575883   -0.905245   -1.660627
N   1.891703   -0.678089   0.257307
C   2.875323   0.150954   0.346422
C   2.202747   -1.861101   1.112992
O   3.904633   -0.198096   1.141400
C   3.004693   1.457272   -0.348541
C   3.625067   -1.532983   1.640812
C   1.155076   -2.082434   2.190748
H   2.217287   -2.731786   0.452368
N   3.662334   2.413779   0.323919
C   2.484546   1.635768   -1.635855
H   4.393056   -2.199991   1.240411
H   3.696281   -1.503575   2.729746
C   0.323766   -3.207932   2.134278
C   0.998238   -1.176808   3.250888
C   3.821326   3.614131   -0.252468
C   2.659581   2.881242   -2.238411
H   1.970538   0.823013   -2.139087
C   -0.646420   -3.428175   3.117200
H   0.429376   -3.907932   1.308827
C   0.031722   -1.394412   4.234491
H   1.627995   -0.291080   3.309847
C   3.331323   3.883844   -1.541404

C	4.557608	4.654724	0.554194
H	2.281573	3.062887	-3.241083
C	-0.794153	-2.522154	4.170028
H	-1.287724	-4.303474	3.055903
H	-0.078651	-0.684069	5.050164
H	3.484574	4.862742	-1.987195
H	5.553828	4.288443	0.827199
H	4.667539	5.592765	0.001266
H	4.023485	4.861012	1.489152
H	-1.548634	-2.690092	4.934134
C	-1.899905	0.804898	0.376465
N	-3.072637	1.746677	0.231159
C	-1.046722	1.522169	1.444080
H	-2.263029	-0.160308	0.733936
S	-4.629079	1.155482	0.035932
C	-2.888933	2.999343	1.005398
C	-1.380486	3.012114	1.271964
H	-1.350761	1.184023	2.441900
H	0.014535	1.295799	1.322241
C	-5.082882	1.685019	-1.629226
O	-5.526075	1.862764	0.964399
O	-4.571442	-0.314582	0.022956
H	-3.460908	2.967534	1.940034
H	-3.230718	3.865147	0.427401
H	-0.842628	3.432224	0.413199
H	-1.128434	3.614320	2.151262
H	-5.030888	2.774919	-1.676958
H	-4.392288	1.227722	-2.339893
H	-6.105863	1.343565	-1.807638
H	-0.786953	1.556722	-1.354036

T~minor~

SCF Energy = -1254841.986 kcal/mol
$G_{298K,solution}$ = -1254836.137 kcal/mol
Three lowest vib. freq. (cm^{-1}): = 7.1730, 13.6108, 19.7032

Pd	0.124709	-0.877728	-0.921695
O	1.268881	-2.997281	-1.305439
C	0.750180	-3.709957	-2.162990
O	-0.361935	-3.360166	-2.804267
C	1.294561	-5.047057	-2.589670
H	1.487617	-5.043253	-3.667857
H	2.215145	-5.265822	-2.047131
H	0.551489	-5.828223	-2.394748

C	-1.416469	0.528885	-1.131684
C	-1.715010	-0.607946	-1.937013
H	-1.615309	-0.523058	-3.021673
H	-0.639285	-2.467636	-2.439689
H	-2.498769	-1.293937	-1.609825
N	1.850819	-0.606581	0.458533
C	2.946908	0.073362	0.449769
C	1.959239	-1.621682	1.544250
O	3.903030	-0.280456	1.337599
C	3.275758	1.221170	-0.433466
C	3.438370	-1.487542	1.989878
C	0.936832	-1.390022	2.645196
H	1.777417	-2.600953	1.095471
N	4.308269	1.985176	-0.043307
C	2.540318	1.461182	-1.601353
H	4.061260	-2.315074	1.636237
H	3.570867	-1.361552	3.065970
C	-0.099784	-2.310021	2.843689
C	1.011956	-0.266380	3.482296
C	4.655326	3.038171	-0.796885
C	2.905033	2.553625	-2.385707
H	1.715537	0.805206	-1.871445
C	-1.044316	-2.117014	3.856737
H	-0.174142	-3.179918	2.195030
C	0.073529	-0.071854	4.497659
H	1.804467	0.465757	3.340079
C	3.972987	3.354382	-1.983058
C	5.817921	3.863476	-0.302419
H	2.364575	2.773523	-3.302865
C	-0.958873	-0.997332	4.687461
H	-1.846663	-2.837660	3.991766
H	0.146039	0.802943	5.139239
H	4.281136	4.210487	-2.577103
H	6.708434	3.235115	-0.186676
H	6.053123	4.683408	-0.988272
H	5.592795	4.286547	0.683680
H	-1.691234	-0.844525	5.475984
C	-2.172296	0.837444	0.151351
N	-3.403753	1.661620	-0.135395
C	-1.401502	1.749847	1.131579
H	-2.476617	-0.095772	0.629010
S	-4.890119	0.930846	-0.365073
C	-3.354706	3.000896	0.499603
C	-1.859591	3.174919	0.782334
H	-1.688120	1.507021	2.161609
H	-0.322258	1.605735	1.043277

C	-5.160678	1.035738	-2.147298
O	-5.916300	1.772485	0.272714
O	-4.782568	-0.499081	-0.032540
H	-3.942316	3.020271	1.425329
H	-3.758946	3.763965	-0.173648
H	-1.342127	3.538523	-0.114239
H	-1.678749	3.894697	1.587916
H	-5.178027	2.089135	-2.434902
H	-4.352304	0.504455	-2.652984
H	-6.125813	0.565882	-2.354319
H	-1.044327	1.423406	-1.639007

U_minor

SCF Energy = -1111083.267 kcal/mol
$G_{298K,solution}$ = -1111064.435 kcal/mol
Three lowest vib. freq. (cm^{-1}): = 14.5421, 18.6672, 24.8097

Pd	-0.511848	-0.797803	0.309944
C	1.521045	-0.340929	0.673812
C	1.237354	-1.694136	1.011256
H	1.132102	-1.980602	2.059629
H	1.584308	-2.496564	0.357452
N	-2.057547	0.618915	-0.509180
C	-3.206740	0.089387	-0.721960
C	-2.103316	2.001792	-1.021816
O	-4.172622	0.854891	-1.285786
C	-3.524474	-1.309117	-0.399325
C	-3.612382	2.196040	-1.365152
C	-1.569530	3.049140	-0.063277
H	-1.498552	2.027722	-1.938149
N	-2.497529	-2.006466	0.136010
C	-4.788391	-1.850558	-0.635680
H	-3.795429	2.576189	-2.371822
H	-4.131466	2.818297	-0.630097
C	-1.099534	4.267755	-0.573378
C	-1.584094	2.851943	1.323445
C	-2.698061	-3.295768	0.466171
C	-4.996753	-3.187915	-0.296957
H	-5.570837	-1.238230	-1.069624
C	-0.663604	5.279514	0.286278
H	-1.064936	4.424902	-1.650266
C	-1.141861	3.860791	2.183946
H	-1.912555	1.897547	1.724297
C	-3.944825	-3.911924	0.257912

C	-1.540737	-4.049154	1.060784
H	-5.963329	-3.655371	-0.463077
C	-0.685452	5.078129	1.669621
H	-0.299933	6.218105	-0.124244
H	-1.147857	3.691329	3.257742
H	-4.075630	-4.954404	0.532357
H	-1.188951	-3.550324	1.970019
H	-1.820330	-5.079521	1.301486
H	-0.695672	-4.059455	0.364339
H	-0.340795	5.860635	2.340722
C	2.352412	0.020857	-0.545571
N	3.823828	0.097754	-0.203611
C	2.090266	1.437584	-1.105226
H	2.215163	-0.741225	-1.316023
S	4.819356	-1.229248	-0.390060
C	4.389390	1.453039	-0.403161
C	3.134616	2.331259	-0.417319
H	2.255512	1.442371	-2.190675
H	1.062996	1.755187	-0.912639
C	4.947853	-1.922480	1.272047
O	6.157991	-0.735240	-0.756762
O	4.146177	-2.241963	-1.220734
H	4.934889	1.521190	-1.352537
H	5.084879	1.705601	0.403506
H	2.820504	2.566335	0.606827
H	3.305957	3.277773	-0.941458
H	5.405829	-1.175896	1.924163
H	3.944717	-2.180778	1.616307
H	5.579592	-2.811906	1.201370
H	1.602417	0.383535	1.488982

A5.3.3.3 Major Enantiomer – Amide

trans **to Pyridine**

O_pyr,major

SCF Energy = -1254846.872 kcal/mol
$G_{298K,solution}$ = -1254841.524 kcal/mol
Three lowest vib. freq. (cm^{-1}): = 12.3843, 14.6595, 18.8239

O	-1.319396	2.127602	2.664251
C	-0.758891	1.894220	1.469337
N	-0.970428	0.749338	0.922447

C	-1.903165	-0.024219	1.781402
C	-1.903276	0.842381	3.074135
C	0.041282	2.919329	0.794876
N	0.553850	2.517309	-0.402058
C	1.212067	3.418422	-1.154002
C	1.404690	4.734307	-0.684689
C	0.921112	5.123406	0.555800
C	0.207267	4.194762	1.317880
C	1.739152	3.021777	-2.501946
Pd	0.283975	0.344489	-0.657429
C	-3.271401	-0.198335	1.144779
H	-1.460197	-1.006099	1.956769
H	-1.258139	0.438916	3.859563
H	-2.899206	1.047193	3.465665
H	-0.219621	4.442902	2.283189
H	1.079670	6.133815	0.921401
H	1.941215	5.436909	-1.314838
H	2.775949	2.678190	-2.406768
H	1.158270	2.205179	-2.932225
H	1.727170	3.881737	-3.179383
C	-3.754484	-1.481500	0.869986
C	-5.023935	-1.655082	0.312083
C	-5.819769	-0.545774	0.021555
C	-5.340354	0.741876	0.286535
C	-4.072970	0.913171	0.844187
H	-3.126778	-2.348558	1.056407
H	-5.376370	-2.657616	0.086314
H	-6.803970	-0.679949	-0.419905
H	-5.950211	1.610970	0.052936
H	-3.708920	1.920811	1.037073
N	-0.112868	-1.644143	-0.512086
S	-1.106935	-2.247375	-1.696358
C	0.999031	-2.517910	-0.097856
O	-2.072811	-1.186971	-2.037217
O	-1.615070	-3.563880	-1.246749
C	-0.134154	-2.575470	-3.192055
C	1.426526	-2.228627	1.345397
H	1.868260	-2.405080	-0.764440
H	0.660657	-3.560178	-0.166407
H	0.357170	-1.649769	-3.494589
H	0.601208	-3.353673	-2.974707
H	-0.839029	-2.924952	-3.950844
C	2.671041	-3.038048	1.762366
H	1.648315	-1.159812	1.456056
H	0.588218	-2.460794	2.017533
C	3.000385	-2.876548	3.224388

H	3.517606	-2.739833	1.133713
H	2.488461	-4.104360	1.556861
C	4.040708	-2.224895	3.767752
H	2.287012	-3.340936	3.908801
C	5.148027	-1.495892	3.054895
H	4.108987	-2.214150	4.857246
H	5.214864	-0.457115	3.406227
H	6.121541	-1.961200	3.265795
H	5.012927	-1.467022	1.970364
O	1.617052	-0.078121	-2.145196
C	2.889578	0.029282	-1.858972
O	3.347977	0.467875	-0.799787
C	3.800796	-0.455499	-2.982743
H	4.826857	-0.125663	-2.803807
H	3.783935	-1.551966	-3.015265
H	3.450756	-0.096745	-3.956346

P$_{pyr,major}$

SCF Energy = -1254835.122 kcal/mol
G$_{298K,solution}$ = -1254824.79 kcal/mol
Three lowest vib. freq. (cm^{-1}): = 11.9799, 23.6506, 27.1033

O	-2.308551	2.268311	1.491851
C	-1.599512	1.717718	0.468874
N	-1.798457	0.498733	0.162232
C	-2.752620	-0.044825	1.149488
C	-3.136682	1.194155	2.018043
C	-0.629465	2.644839	-0.165427
N	0.549677	2.147724	-0.612136
C	1.489002	2.996915	-1.093585
C	1.220553	4.368449	-1.208041
C	-0.000787	4.878959	-0.782568
C	-0.933955	4.005843	-0.229606
C	2.850388	2.454788	-1.434260
Pd	1.094909	0.101087	-0.294790
C	-3.934692	-0.749033	0.510202
H	-2.190932	-0.758650	1.760313
H	-2.879825	1.068639	3.071021
H	-4.182886	1.494654	1.911287
H	-1.883249	4.354808	0.159517
H	-0.214977	5.941321	-0.858910
H	1.987639	5.022564	-1.610044
H	3.339293	2.085745	-0.525553
H	2.805863	1.609064	-2.124983

H	3.474853	3.237098	-1.875882
C	-4.376287	-1.979430	1.014199
C	-5.487880	-2.622878	0.459930
C	-6.169350	-2.043005	-0.612966
C	-5.733719	-0.816433	-1.126621
C	-4.626203	-0.175473	-0.567372
H	-3.843385	-2.439943	1.843687
H	-5.815351	-3.577926	0.862988
H	-7.030731	-2.542826	-1.048552
H	-6.255463	-0.361164	-1.964949
H	-4.287951	0.773346	-0.977582
O	1.818665	0.833347	1.501660
C	1.140294	0.624524	2.598064
O	0.024988	0.099493	2.673709
C	1.874108	1.083809	3.856808
H	1.150937	1.371282	4.624770
H	2.464059	0.243602	4.244397
H	2.558614	1.910955	3.648983
N	1.770949	-1.721076	0.336849
S	3.342077	-2.085961	0.018583
C	0.802897	-2.805935	0.532717
O	3.823329	-1.270034	-1.124245
O	3.525984	-3.553905	-0.028336
C	4.260390	-1.496336	1.460857
C	0.263048	-3.429838	-0.763093
H	-0.012817	-2.377608	1.127288
H	1.266753	-3.594124	1.138223
H	4.031023	-0.438919	1.601305
H	3.945235	-2.080160	2.328534
H	5.322672	-1.653011	1.255818
C	-0.325770	-2.394969	-1.736350
H	1.076671	-3.976495	-1.255664
H	-0.511326	-4.166667	-0.508017
C	0.682326	-1.349679	-2.142514
H	-1.218395	-1.921622	-1.312444
H	-0.650991	-2.916901	-2.651101
C	0.405587	-0.098504	-2.629946
H	1.710161	-1.688013	-2.249768
C	-0.957404	0.441158	-2.969237
H	1.243186	0.439898	-3.071752
H	-0.993352	1.532892	-2.896990
H	-1.176896	0.182678	-4.016520
H	-1.743545	0.026550	-2.337681

Q_pyr,major

SCF Energy = -1254827.795 kcal/mol

$G_{298K,solution}$ = -1254816.425 kcal/mol

Three lowest vib. freq. (cm^{-1}): = -260.3238, 13.9157, 24.6415

O	-2.390385	2.070423	1.516746
C	-1.693287	1.617839	0.438642
N	-1.873486	0.421862	0.041446
C	-2.804414	-0.214184	0.993226
C	-3.194195	0.943510	1.966315
C	-0.790427	2.625898	-0.171660
N	0.407914	2.223509	-0.662020
C	1.245120	3.144879	-1.196170
C	0.875366	4.495492	-1.267063
C	-0.353955	4.910644	-0.768699
C	-1.198093	3.960523	-0.200066
C	2.588657	2.700629	-1.709520
Pd	1.112718	0.247270	-0.302851
C	-3.989129	-0.881386	0.319959
H	-2.226317	-0.963705	1.542300
H	-2.916260	0.734844	3.000394
H	-4.246243	1.235414	1.899413
H	-2.156906	4.230150	0.227098
H	-0.645368	5.956471	-0.809605
H	1.570216	5.208528	-1.699508
H	3.268609	3.554352	-1.787800
H	3.036218	1.942855	-1.060035
H	2.494928	2.256442	-2.708172
C	-4.528628	-2.054827	0.865465
C	-5.652865	-2.659028	0.294298
C	-6.248775	-2.098873	-0.839081
C	-5.713079	-0.932681	-1.395394
C	-4.593028	-0.328607	-0.818491
H	-4.062257	-2.501515	1.741604
H	-6.057146	-3.569097	0.730603
H	-7.119771	-2.569189	-1.288329
H	-6.165730	-0.494863	-2.281858
H	-4.173024	0.570253	-1.262691
O	1.497360	0.939994	1.664863
C	0.794166	0.543837	2.681273
O	-0.157660	-0.252225	2.645861
C	1.204704	1.180379	4.010455
H	0.590488	2.074844	4.176200
H	1.014351	0.485740	4.833673
H	2.253963	1.489015	4.006218
N	1.885044	-1.627562	0.094411

C	1.060939	-2.724764	0.628338
S	3.540641	-1.777216	0.148213
C	0.702080	-3.686521	-0.512351
H	0.175295	-2.274436	1.085132
H	1.602501	-3.256606	1.419265
C	4.051379	-1.123895	1.754342
O	4.095285	-0.882450	-0.887842
O	3.907303	-3.208509	0.128087
C	0.256243	-2.837293	-1.716912
H	1.586793	-4.276829	-0.775527
H	-0.093419	-4.381285	-0.215100
H	3.695330	-0.096051	1.835961
H	3.615493	-1.749058	2.537071
H	5.142763	-1.182387	1.782418
C	1.251771	-1.752525	-2.002021
H	-0.738059	-2.413667	-1.545100
H	0.194998	-3.469107	-2.617078
C	0.916020	-0.422767	-2.367761
H	2.260937	-2.085679	-2.225691
H	1.739374	0.091396	-2.868145
C	-0.455825	-0.077052	-2.935227
H	-0.542288	1.004748	-3.080288
H	-0.594632	-0.548953	-3.920019
H	-1.276145	-0.379474	-2.282622

A5.3.3.4 Minor Enantiomer – Amide

trans to Pyridine

O$_{pyr,minor}$

SCF Energy = -1254845.407 kcal/mol
G$_{298K,solution}$ = -1254840.187 kcal/mol
Three lowest vib. freq. (cm^{-1}): = 12.6880, 15.8410, 21.5152

O	-2.027392	3.477507	-0.180088
C	-1.856030	2.193886	0.155890
N	-0.758686	1.620755	-0.196128
C	0.076287	2.588120	-0.931946
C	-0.871425	3.828811	-1.012792
C	-2.875497	1.474756	0.923031
N	-2.552621	0.175826	1.178070
C	-3.359253	-0.542248	1.980117
C	-4.546572	0.026921	2.486266
C	-4.899353	1.331315	2.174870
C	-4.032298	2.088841	1.382578

C	-2.991651	-1.946653	2.359212
Pd	-0.836062	-0.433063	-0.040485
C	1.404857	2.878755	-0.256533
H	0.246188	2.169284	-1.926745
H	-1.249590	4.009619	-2.021554
H	-0.436949	4.739000	-0.597530
H	-4.233436	3.123522	1.128619
H	-5.821664	1.762518	2.553201
H	-5.181150	-0.580986	3.123962
H	-3.558285	-2.653420	1.742854
H	-1.931648	-2.140737	2.195065
H	-3.243877	-2.127494	3.409998
C	2.497252	3.262888	-1.046391
C	3.718776	3.601215	-0.458323
C	3.863470	3.551860	0.931300
C	2.780276	3.164182	1.725268
C	1.557464	2.833570	1.134974
H	2.393594	3.291030	-2.129570
H	4.557371	3.893780	-1.085091
H	4.814614	3.806469	1.391418
H	2.888102	3.112200	2.805661
H	0.726192	2.517692	1.759540
N	0.873126	-0.689604	-1.165589
S	0.522305	-0.782018	-2.792774
C	1.752641	-1.775883	-0.682681
O	-0.406698	0.332946	-3.095692
O	0.177671	-2.134399	-3.278345
C	2.092077	-0.348437	-3.599671
C	2.297941	-1.447257	0.709904
H	2.602671	-1.879988	-1.373023
H	1.225710	-2.737108	-0.667293
H	2.431237	0.619864	-3.227620
H	2.838708	-1.122533	-3.414965
H	1.868711	-0.298027	-4.668295
C	3.265596	-2.532680	1.222596
H	2.804135	-0.473850	0.687904
H	1.456529	-1.349356	1.409440
C	3.726142	-2.275869	2.633701
H	4.119682	-2.616207	0.539763
H	2.748179	-3.504242	1.189672
C	4.978944	-2.100673	3.082430
H	2.921133	-2.223920	3.369985
C	6.259231	-2.123040	2.290767
H	5.105925	-1.923298	4.151899
H	6.809326	-1.179608	2.413570
H	6.924675	-2.922085	2.646896

H	6.096281	-2.278197	1.220275
O	-1.025499	-2.449273	-0.041219
C	-2.112905	-2.932327	-0.600801
O	-3.141947	-2.288237	-0.814791
C	-1.983345	-4.400081	-0.978560
H	-2.971566	-4.834428	-1.148593
H	-1.402511	-4.459693	-1.906999
H	-1.443880	-4.963659	-0.210385

P_{pyr,minor}

SCF Energy = -1254834.508 kcal/mol
G$_{298K,solution}$ = -1254823.16 kcal/mol
Three lowest vib. freq. (cm^{-1}): = 20.7153, 28.3701, 32.4466

O	2.232245	3.286730	0.139045
C	1.288941	2.395417	-0.293686
N	1.683868	1.281534	-0.771857
C	3.160764	1.281008	-0.724461
C	3.505857	2.603421	0.026772
C	-0.104224	2.893427	-0.179717
N	-1.143010	2.021033	-0.274268
C	-2.407676	2.482719	-0.150300
C	-2.655092	3.854947	0.031376
C	-1.601877	4.750332	0.118022
C	-0.299730	4.259770	0.020917
C	-3.582364	1.541338	-0.190073
Pd	-0.842568	-0.108611	-0.277751
C	3.756743	0.046935	-0.073303
H	3.519558	1.329026	-1.761471
H	4.193150	3.256007	-0.516511
H	3.882685	2.426185	1.038055
H	0.560339	4.912565	0.099011
H	-1.781975	5.810873	0.269807
H	-3.683926	4.189411	0.123995
H	-4.228932	1.776872	-1.046058
H	-3.284051	0.494067	-0.238985
H	-4.170380	1.665007	0.724893
C	4.956466	-0.484913	-0.565398
C	5.562508	-1.577611	0.061992
C	4.966213	-2.153547	1.187092
C	3.762535	-1.634108	1.674963
C	3.157397	-0.539454	1.051415
H	5.420212	-0.045517	-1.447178
H	6.492253	-1.980520	-0.331838

H	5.430484	-3.007065	1.674560
H	3.283029	-2.089418	2.537810
H	2.203626	-0.166607	1.418160
O	-0.161655	0.198172	1.665210
C	-0.977310	0.581344	2.605322
O	-2.191395	0.778704	2.471355
C	-0.298450	0.748198	3.963734
H	-0.935646	1.333515	4.631061
H	-0.140965	-0.242634	4.407704
H	0.682729	1.222759	3.863190
N	-0.674200	-2.111247	0.138539
C	0.454025	-2.849659	-0.445944
S	-2.081423	-2.949771	0.398753
C	0.345754	-3.141829	-1.949531
H	1.346564	-2.247531	-0.243116
H	0.570245	-3.797478	0.092268
O	-1.806424	-4.400397	0.294105
C	-2.497093	-2.609032	2.120020
O	-3.202534	-2.392069	-0.402354
C	0.124919	-1.874901	-2.790420
H	-0.478229	-3.846415	-2.117712
H	1.266857	-3.640887	-2.281156
H	-2.645835	-1.535140	2.246840
H	-1.681546	-2.974569	2.747004
H	-3.420370	-3.156274	2.327810
C	-1.133138	-1.138592	-2.407384
H	0.999150	-1.215308	-2.729740
H	0.024900	-2.165304	-3.849214
C	-1.379387	0.196788	-2.603259
H	-1.989022	-1.754382	-2.139596
C	-0.476088	1.163114	-3.323836
H	-2.412357	0.518999	-2.485363
H	-0.705676	1.120702	-4.399318
H	-0.643724	2.194705	-2.999994
H	0.581090	0.927759	-3.190069

Q_{pyr,minor}

SCF Energy = -1254827.5 kcal/mol
G$_{298K,solution}$ = -1254815.092 kcal/mol
Three lowest vib. freq. (cm^{-1}): = -257.4400, 17.9750, 24.5867

O	2.653078	3.036736	-0.156340
C	1.575440	2.249412	-0.461955
N	1.793781	1.058509	-0.861015

C	3.256774	0.860923	-0.885028
C	3.819405	2.187216	-0.285927
C	0.270333	2.943375	-0.316792
N	-0.882801	2.226183	-0.273005
C	-2.061669	2.878732	-0.115994
C	-2.100866	4.280610	-0.041943
C	-0.927378	5.017687	-0.100735
C	0.281281	4.337409	-0.228354
C	-3.326124	2.085244	0.042567
Pd	-0.914756	0.104943	-0.252602
C	3.723392	-0.377231	-0.141085
H	3.556205	0.762643	-1.937184
H	4.538447	2.695474	-0.932829
H	4.248774	2.050607	0.710607
H	1.227035	4.862921	-0.260745
H	-0.946335	6.102129	-0.037864
H	-3.061466	4.770198	0.080082
H	-3.474986	1.373038	-0.772510
H	-3.262824	1.511066	0.975299
H	-4.191595	2.753291	0.088193
C	4.841469	-1.083610	-0.605996
C	5.338260	-2.180505	0.104587
C	4.713357	-2.585188	1.287601
C	3.589499	-1.891492	1.748320
C	3.092851	-0.792432	1.041213
H	5.327149	-0.776888	-1.531094
H	6.205948	-2.718960	-0.268371
H	5.093972	-3.439711	1.841416
H	3.088358	-2.210852	2.658771
H	2.196792	-0.283220	1.390238
O	-0.084365	0.196709	1.706177
C	-0.752786	0.644189	2.722383
O	-1.954391	0.957734	2.718860
C	0.060164	0.732992	4.014971
H	0.200900	-0.275800	4.423513
H	1.054494	1.151887	3.827996
H	-0.470315	1.337840	4.754392
N	-1.064559	-1.960409	-0.172700
C	0.112214	-2.824537	-0.342502
S	-2.479820	-2.649258	0.385013
C	0.125213	-3.392282	-1.768829
H	0.100381	-3.636898	0.392096
H	1.000148	-2.214886	-0.152753
C	-2.558690	-2.307925	2.154203
O	-3.608471	-1.933662	-0.243536
O	-2.386688	-4.116205	0.226953

C	-0.167729	-2.229059	-2.734009
H	-0.653016	-4.158494	-1.855038
H	1.089768	-3.858658	-2.005643
H	-2.598938	-1.227743	2.307649
H	-3.468842	-2.793071	2.517268
H	-1.677496	-2.744126	2.629912
C	-1.382757	-1.465017	-2.299973
H	0.699737	-1.566210	-2.809878
H	-0.373168	-2.621942	-3.742433
C	-1.513450	-0.054008	-2.349395
H	-2.302771	-2.035287	-2.223003
C	-0.603707	0.798119	-3.226959
H	-2.555476	0.271240	-2.357994
H	-0.800468	0.599413	-4.291519
H	-0.796794	1.861900	-3.056739
H	0.457085	0.623618	-3.034434